PLANT PRODUCTS FOR ANTIVIRAL THERAPEUTICS

EDITED BY: Banasri Hazra, Anirban Mandal, Vijay Kumar Prajapati and Paul F. Moundipa

PUBLISHED IN: Frontiers in Pharmacology

frontiers Research Topics

ISSN 1664-8714
ISBN 978-2-83250-647-9
DOI 10.3389/978-2-83250-647-9

About Frontiers

Frontiers is more than just an open-access publisher of scholarly articles: it is a pioneering approach to the world of academia, radically improving the way scholarly research is managed. The grand vision of Frontiers is a world where all people have an equal opportunity to seek, share and generate knowledge. Frontiers provides immediate and permanent online open access to all its publications, but this alone is not enough to realize our grand goals.

Frontiers Journal Series

The Frontiers Journal Series is a multi-tier and interdisciplinary set of open-access, online journals, promising a paradigm shift from the current review, selection and dissemination processes in academic publishing. All Frontiers journals are driven by researchers for researchers; therefore, they constitute a service to the scholarly community. At the same time, the Frontiers Journal Series operates on a revolutionary invention, the tiered publishing system, initially addressing specific communities of scholars, and gradually climbing up to broader public understanding, thus serving the interests of the lay society, too.

Dedication to Quality

Each Frontiers article is a landmark of the highest quality, thanks to genuinely collaborative interactions between authors and review editors, who include some of the world's best academicians. Research must be certified by peers before entering a stream of knowledge that may eventually reach the public - and shape society; therefore, Frontiers only applies the most rigorous and unbiased reviews.
Frontiers revolutionizes research publishing by freely delivering the most outstanding research, evaluated with no bias from both the academic and social point of view. By applying the most advanced information technologies, Frontiers is catapulting scholarly publishing into a new generation.

What are Frontiers Research Topics?

Frontiers Research Topics are very popular trademarks of the Frontiers Journals Series: they are collections of at least ten articles, all centered on a particular subject. With their unique mix of varied contributions from Original Research to Review Articles, Frontiers Research Topics unify the most influential researchers, the latest key findings and historical advances in a hot research area! Find out more on how to host your own Frontiers Research Topic or contribute to one as an author by contacting the Frontiers Editorial Office: frontiersin.org/about/contact

PLANT PRODUCTS FOR ANTIVIRAL THERAPEUTICS

Topic Editors:
Banasri Hazra, Jadavpur University, India
Anirban Mandal, Department of Microbiology, Mrinalini Datta Mahavidyapith, India
Vijay Kumar Prajapati, Central University of Rajasthan, India
Paul F. Moundipa, University of Yaounde I, Cameroon

Citation: Hazra, B., Mandal, A., Prajapati, V. K., Moundipa, P. F., eds. (2022). Plant Products for Antiviral Therapeutics. Lausanne: Frontiers Media SA.
doi: 10.3389/978-2-83250-647-9

Table of Contents

frontiers | Frontiers in Pharmacology

TYPE Editorial
PUBLISHED 17 October 2022
DOI 10.3389/fphar.2022.1039183

OPEN ACCESS

EDITED BY
Javier Echeverria,
University of Santiago, Chile

REVIEWED BY
Anurag Varshney,
Patanjali Research Foundation, India
Fidele Ntie-Kang,
University of Buea, Cameroon

*CORRESPONDENCE
Banasri Hazra,
banasri@gmail.com

SPECIALTY SECTION
This article was submitted to Ethnopharmacology, a section of the journal Frontiers in Pharmacology

RECEIVED 07 September 2022
ACCEPTED 06 October 2022
PUBLISHED 17 October 2022

CITATION
Mandal A, Hazra B, Prajapati VK and Moundipa PF (2022), Editorial: Plant products for antiviral therapeutics. *Front. Pharmacol.* 13:1039183. doi: 10.3389/fphar.2022.1039183

Editorial: Plant products for antiviral therapeutics

Anirban Mandal[1], Banasri Hazra[2]*, Vijay Kumar Prajapati[3] and Paul F. Moundipa[4]

[1]Department of Microbiology, Mrinalini Datta Mahavidyapith, Kolkata, India, [2]Department of Pharmaceutical Technology, Jadavpur University, Kolkata, India, [3]Department of Biochemistry, School of Life Sciences, Central University of Rajasthan, Ajmer, India, [4]Laboratory of Pharmacology and Toxicology, Faculty of Science, AEFAS, University of Yaoundé I, Yaounde, Cameroon

KEYWORDS

viral infection, antiviral drug, plant-based antiviral therapeutics, antiviral plants, coronavirus

Editorial on the Research Topic
Plant products for antiviral therapeutics

Diseases caused by microbial infections continue to pose major public health challenges despite the enormous modernization of therapeutic strategies to alleviate human health disorders. From time to time, numerous such afflictions due to HIV, hepatitis B & C, herpes simplex, dengue, Ebola, and influenza viruses raised universal concern, underscored by the recent COVID-19 pandemic caused by SARS-CoV-2 (Mandal et al., 2021). Although some antiviral drugs or cocktails of drugs are available to combat these viruses, nevertheless, most of these medications showed side effects and other drawbacks like low antiviral activity, genotype-dependent efficacy, and the emergence of drug-resistant mutants. Therefore, the development of more suitable therapeutics in this field is certainly a need of the hour. Historically, medicinal herbs and natural products are the mainstay of general healthcare systems around the globe and are considered an integral part of the cultural heritage of mankind. Truly, the plant kingdom is an invaluable repository of countless phytochemicals with distinctive molecular frameworks, which provide clues on the core structures as templates for the development of novel drug molecules. Thus, quite a number of such traditional medicinal plants yielded a variety of drugs enlisted in the modern pharmacopeia. In fact, a substantial number of FDA-approved drugs are based on natural products or their derivatives (Atanasov et al., 2021).

Time-honoured herbal prescriptions practised worldwide, such as Traditional Chinese Medicines (TCM), Indian Ayurvedic and Middle-eastern Unani systems, and various regional folkloric treatments in Africa and elsewhere continue to fulfil basic healthcare requirements in developing countries (Mandal et al., 2020). As for the Western people, a resurgence in popularity of natural products for health promotion have been observed in the past few decades (World Health Organization, 2019). In fact, many medicinal plant extracts are now prescribed for the treatment of chronic ailments. Therefore, a strategic approach to combat viral infections would be to explore the

empirical records of medicinal practices enshrined in worldwide cultural traditions and develop this knowledge with necessary support from technological advancement achieved in the modern era. Under this context, the present volume entitled *Plant products for antiviral therapeutics* was published, comprising eight Original Research articles and seven Reviews/Mini-reviews, which will be briefly introduced in this editorial.

TCM is one of the world's classical therapeutic modalities, gaining substantial popularity worldwide. Actually, TCM is known to utilize the characteristics of its multiple components and produces a cocktail-like effect through integrated regulation of multiple biochemical targets to block viral infections (Tang et al., 2018). Ping et al. explored the efficacy of Jing Guan Fang (JGF) to prevent SARS-CoV-2 infection. The authors showed that JGF, a TCM formula comprising five commonly used herbs, effectively blocked syncytium formation and inhibited SARS-CoV-2 plaque formation. They demonstrated the underlying mechanism of JGF working *via* induction of lysosome-dependent ACE2 degradation and inhibition of TMPRSS2 expression in the lung tissue of mice. Additionally, a clinical study conducted on human volunteers recommended that JGF would be a useful preventative measure for frontline medical staff or people who have had high-risk exposure to COVID-19 cases.

Women of childbearing age are widely susceptible to common fungal infections as well as Herpes simplex virus type 2 (HSV-2). Since many years, a TCM called JieZe-1 had been used for the treatment of female lower reproductive tract infections. Hence, Duan et al. had explored a prescription of JieZe-1 composed of authenticated botanical ingredients as specified in ancient Chinese scripture and reported its preventive and therapeutic efficacy on HSV-2 patients in Chinese hospitals (Duan et al., 2020). Presently, Duan et al. could further validate the anti-HSV-2 effect of JieZe-1 in experiments conducted *in vitro*. Further, they optimized a mouse model of genital herpes to clarify the underlying mechanism of its anti-HSV-2 effect and found that JieZe-1 inhibited membrane fusion and TLR signaling pathways *in vivo*. Thus, the study by Duan et al. was an experimental corroboration of the anti-HSV-2 effect of JieZe-1. Finally, they suggested that the antiviral effect could be exerted through the synergic interaction of its herbal components, reflecting the scientific implication of TCM.

For using a complex mixture of natural products, it is crucial to identify the target proteins of TCM and evaluate the mechanism of action. Lai et al. explored a standardized composition of Ganghuo Kanggan Decoction (GHKGD) and its components for prospective activity against the influenza virus, using a series of network pharmacology involving compound screening, target prediction, and pathway enrichment analysis. Hence, a compound-target-disease network was constructed and analyzed to explore the relevant mechanism. Thus, they could identify 116 active compounds and 17 potential therapeutic targets of GHKGD. Further, they established a mouse model to study the therapeutic efficacy of this TCM against viral pneumonia caused by the H1N1 influenza virus. Thus, GHKGD treatment was found to balance the pro- and anti-inflammatory cytokine levels, thereby alleviating mouse lung inflammation due to influenza virus infection. Furthermore, they performed *in vivo* experiments to reveal the synergistic action of multi-component and multi-target characteristics of GHKGD and offered a theoretical basis for prospective drug development against this contagious respiratory viral disease.

Viral pneumonia is one of the most pernicious respiratory ailments; TCM treatments are documented to manage infected patients. The multi-target action of TCMs could be elucidated by way of proteomics (Lao et al., 2014). Hence, Wei et al. utilized this approach to precisely clarify the efficacy of Hou Yan Qing (HYQ) oral liquid, subsequent to its validation in a mouse model of pneumonia caused by influenza A virus (H1N1), *in vivo*. Experimental results indicated that HYQ treatment would cause elevation of galectin-3-binding protein and glutathione peroxidase 3 to produce distinctive effects on viral pneumonia patients. This TCM composition of four authentic plant samples as per Chinese Pharmacopoeia 2020, showed multiple effects on the complement system and inflammatory processes; hence, it could be a promising strategy for personalized management of viral pneumonia.

Indian Ayurveda is a well-documented traditional system of complementary herbal medicines recommended for chronic ailments and general wellness improvement (Sen and Chakraborty, 2015). Since SARS-CoV-2 infection targets multiple organs, a holistic approach may be an answer to the current crisis, as prescribed in Ayurveda. Balkrishna et al. explored a prospective Ayurvedic medicine called Giloy Ghanvati (GG), an oral tablet prepared from *Tinospora cordifolia* (Willd.) Hook. f. & Thomson, a well-known tropical plant widely used against various diseases in the Indian subcontinent. GG is a time-tested formulation recommended as a natural immunity booster to improve overall health, particularly to inhibit SARS-CoV-2 infection during the Covid-19 pandemic. Balkrishna et al. developed the SARS-CoV-2 spike-protein induced disease phenotype in a humanized zebrafish model. They studied several parameters to prove that the disease symptoms due to SARS-CoV-2 spike protein expression were substantially ameliorated by treatment of the afflicted fishes with aqueous extract of GG. Also, HPLC analysis of GG extract could detect the major phytoconstituents as cordifolioside A, magnoflorine, β-ecdysone, and palmatine, already known for anti-inflammatory and antiviral activities. Thus, the findings correlated well with the potential role of these constituents of GG against SARS-CoV-2 viral symptoms.

Vigna radiata (L.) R. Wilczek (mung bean legume), a common functional food in Oriental culture, is sparsely studied for its antiviral potential. Using appropriate techniques, Lo et al. prepared *Vigna radiata* extract (VRE)

from seed coats of mung beans and investigated the antiviral activity and mechanism of action of VRE against the influenza virus. They found that VRE mainly targets viral entry and release by interfering with hemagglutinin and neuraminidase activity and significantly inhibited viral replication in a concentration-dependent manner. The authors concluded that VRE is a multi-step inhibitor for both mammalian H1N1 and avian H6N1 subtypes of influenza virus and demonstrated its broad-spectrum potential as a preventive and therapeutic agent against influenza virus.

Buddleja indica Lam. is an evergreen shrub native to Madagascar, locally known as a topical antiseptic. The investigation by Youssef et al. is a rare study to establish the traditional medicinal claims on *Buddleja spp.* of plants, probably owing to its richness of phenolic acids and flavonoids with antioxidant and hepatoprotective activity. Youssef et al. prepared *Buddleja indica* Lam. leaf extract with credible anti-tubercular and anti- *Helicobacter pylori* activity and isolated caffeic acid, quercetin 7-O-β-D-glucoside and kaempferol. Further, *in silico* study on molecular docking of these compounds showed the highest fitting score in proteins implicated for bacterial infection and the occurrence and progression of SARS-CoV-2 virus.

Saha et al. used *in silico* tools to identify RNA dependent RNA polymerase (RdRp) inhibitors as prospective drug candidates against COVID-19. A collection of 248 plant-derived molecules with strong antiviral activity were subjected to molecular docking against the catalytic sub-unit of RdRp. Pharmacokinetics analysis and molecular dynamics simulation of the best-docked compounds showed that tellimagrandin I, saikosaponinB2, hesperidin & (-)-epigallocatechin gallate were the most prominent ones with a strong binding affinity towards RdRp. Overall, the study unveiled saikosaponin B2 to serve as a prospective molecule for the development of effective therapy against COVID-19, as it was one of the top inhibitors of RdRp, the crucial replication protein. Such an approach combined with biological testing can substantially speed up the drug discovery process from plant products.

Huang et al. reviewed an updated selection of phytochemicals active against MERS-CoV, SARS-CoV, or SARS-CoV-2, along with their specific molecular targets and mechanisms of action. Omrani et al. focussed on phylogenetic and taxonomic similarities of viruses, like influenza, MERS-CoV, SARS-CoV, and SARS-CoV-2, and pertinent mechanisms of action. Accordingly, they presented 130 plant-derived compounds with therapeutic potential to combat the currently relevant infections caused by these respiratory viruses. Alam et al. reviewed prospective anti-COVID plant products undergoing clinical trials to address a pandemic-like situation happening in the future. Anywar et al. enlisted medicinal plant species indigenous to Africa and Asia as potential antiviral agents, especially for HIV and SARS-CoV-2. Abubakar et al. reviewed selected medicinal plants and compounds implicated in the mitigation of viral invasion either *via* direct or indirect modulation of ACE2 activity to ameliorate COVID-19. The review article by Hu et al. focused on herbal products with reported therapeutic efficacy against experimental models of influenza, respiratory syncytial virus, and coronavirus - the three types of viruses eliciting pathologic manifestations of viral pneumonia. Severe respiratory distress and associated lung problems due to SARS-CoV-2 infection often create cardiovascular complications, leading to severe myocardial injuries. Hence, Beura et al. dealt with the significance of inhibiting platelet-mediated thrombus formation and discussed the role of anti-platelet and anti-thrombotic phytochemicals available from medicinal plants.

Taken together, it remains to carry on further research and clinical trials on plenty of plant products to get novel therapeutics suitable for clinical application against viral diseases.

Author contributions

AM and BH surveyed and designed this Research Topic. AM and BH wrote and drafted the editorial manuscript. VP and PM revised the manuscript critically. All authors contributed to the article and approved the submitted version.

Acknowledgments

We wish to thank all the authors contributing to this Frontiers Research Topic and all the reviewers who have helped to make it solid.

Conflict of interest

The authors declare that the research was conducted in the absence of any commercial or financial relationships that could be construed as a potential conflict of interest.

Publisher's note

References

Atanasov, A. G., Zotchev, S. B., Dirsch, V. M., and Supuran, C. T. The International Natural Product Sciences Taskforce (2021). Natural products in drug discovery: Advances and opportunities. *Nat. Rev. Drug Discov.* 20, 200–216. doi:10.1038/s41573-020-00114-z

Duan, Q., Liu, T., Yuan, P., Huang, C., Shao, Q., Xu, L., et al. (2020). Antiviral effect of Chinese herbal prescription JieZe-1 on adhesion and penetration of VK2/E6E7 with herpes simplex viruses type 2. *J. Ethnopharmacol.* 249, 112405. doi:10.1016/j.jep.2019.112405

Lao, Y., Wang, X., Xu, N., Zhang, H., and Xu, H. (2014). Application of proteomics to determine the mechanism of action of traditional Chinese medicine remedies. *J. Ethnopharmacol.* 155, 1–8. doi:10.1016/j.jep.2014.05.022

Mandal, A., Biswas, D., and Hazra, B. (2020). "Natural products from plants with prospective anti-HIV activity and relevant mechanisms of action," in *Studies in natural products chemistry*. Netherlands: Elsevier. doi:10.1016/B978-0-12-817907-9.00009-X

Mandal, A., Jha, A. K., and Hazra, B. (2021). Plant products as inhibitors of coronavirus 3CL protease. *Front. Pharmacol.* 12, 583387. doi:10.3389/fphar.2021.583387

Sen, S., and Chakraborty, R. (2015). Toward the integration and advancement of herbal medicine: A focus on traditional Indian medicine. *Bot. Targets Ther.* 5, 33. doi:10.2147/btat.s66308

Tang, H., Huang, W., Ma, J., and Liu, L. (2018). SWOT analysis and revelation in traditional Chinese medicine internationalization. *Chin. Med.* 13, 5. doi:10.1186/s13020-018-0165-1

World Health Organization (2019). *WHO global report on traditional and complementary medicine 2019*, 80–117. Available at: https://apps.who.int/iris/handle/10665/312342.

frontiers in Pharmacology

REVIEW
published: 16 October 2020
doi: 10.3389/fphar.2020.588508

Current Prevention of COVID-19: Natural Products and Herbal Medicine

Junqing Huang[1], Gabriel Tao[2], Jingwen Liu[2], Junming Cai[3], Zhongyu Huang[1] and Jia-xu Chen[1,4]**

[1] Formula-pattern Research Center, School of Traditional Chinese Medicine, Jinan University, Guangzhou, China, [2] Department of Pharmacological and Pharmaceutical Sciences, College of Pharmacy, University of Houston, Houston, TX, United States, [3] Department of Biomedical Engineering, Henry Samueli School of Engineering, University of California, Irvine, Irvine, CA, United States, [4] School of Traditional Chinese Medicine, Beijing University of Chinese Medicine, Beijing, China

Starting from December 2019, novel coronavirus disease 2019 (COVID-19) pandemic has caused tremendous economic loss and unprecedented health crisis across the globe. While the development of cure is at full speed, less attention and fewer effort have been spent on the prevention of this rapidly spreading respiratory infectious disease. Although so far, several vaccine candidates have advanced into clinical trials, limited data have been released regarding the vaccine efficacy and safety in human, not mention the long-term effectiveness of those vaccines remain as open question yet. Natural products and herbal medicines have been historically used for acute respiratory infection and generally show acceptable toxicity. The favorable stability for oral formulation and ease of scaling up manufacture make it ideal candidate for prophylactic. Hereby, we summarized the most recent advance in SARS-CoV-2 prevention including vaccine development as well as experimental prophylactics. Mainly, we reviewed the natural products showing inhibitory effect on human coronavirus, and discussed the herbal medicines lately used for COVID-19, especially focused on the herbal products already approved by regulatory agency with identifiable patent number. We demonstrated that to fill in the response gap between appropriate treatment and commercially available vaccine, repurposing natural products and herbal medicines as prophylactic will be a vigorous approach to stop or at least slow down SARS-CoV-2 transmission. In the interest of public health, this will lend health officials better control on the current pandemic.

Keywords: coronavirus disease 2019, severe acute respiratory syndrome coronavirus 2, prevention, prophylactic, natural product, herbal medicine

OPEN ACCESS

Edited by:
Banasri Hazra,
Jadavpur University, India

Reviewed by:
Ruchi Tiwari,
U.P. Pandit Deen Dayal Upadhyaya Veterinary University, India
Andy Wai Kan Yeung,
The University of Hong Kong, Hong Kong

****Correspondence:***
Junqing Huang
jqhuang@jnu.edu.cn
Jia-xu Chen
chenjiaxu@hotmail.com

Specialty section:
This article was submitted to Ethnopharmacology, a section of the journal Frontiers in Pharmacology

Received: *29 July 2020*
Accepted: *18 September 2020*
Published: *16 October 2020*

Citation:
Huang J, Tao G, Liu J, Cai J, Huang Z and Chen J-x (2020) Current Prevention of COVID-19: Natural Products and Herbal Medicine. Front. Pharmacol. 11:588508. doi: 10.3389/fphar.2020.588508

INTRODUCTION

The novel coronavirus disease 2019 (COVID-19) pandemic starting from December 2019 has cast unprecedented threat to public health worldwide with over 27.9 million infection cases and 905,000 death till September 10, 2020, and the case number is still soaring (Bai et al., 2020). COVID-19 is caused by severe acute respiratory syndrome coronavirus 2 (SARS-CoV-2), a member of beta-

coronaviruses family (Walls et al., 2020). Coronaviruses (CoVs) are a family of large (ranging from 27–32 kb), enveloped, signal-strand positive-sense RNA viruses, which have characteristic club-like spikes on their surface (Walls et al., 2020). Currently, seven strains of human CoVs are reported. Four of them merely produce mild symptoms: Human coronavirus OC43 (HCoV-OC43), Human coronavirus HKU1 (HCoV-HKU1), Human coronavirus 229E (HCoV-229E), and Human coronavirus NL63 (HCoV-NL63), while the other three cause more severe symptoms: Middle East respiratory syndrome-related coronavirus (MERS-CoV), Severe acute respiratory syndrome coronavirus (SARS-CoV), Severe acute respiratory syndrome coronavirus 2 (SARS-CoV-2) (Su et al., 2016).

SARS-CoV-2 initiate its infection *via* the interaction with angiotensin-converting enzyme 2 (ACE2) receptors and transmembrane protease, serine 2 (TMPRSS2) on host cell membrane (Hoffmann et al., 2020; Zhang H. et al., 2020). The mortality of COVID-19 is mainly due to acute respiratory distress syndrome and severe cytokine release syndrome (Hirano and Murakami, 2020; Mehta et al., 2020). Although over hundreds of clinical trials and preclinical studies have been set to seek cures for tackling COVID-19, up to date there are no approved therapeutics for this widely spreading disease. As for the prevention of COVID-19, several vaccine candidates are in pipelines, but due to the insufficiency of clinical evidence the efficacy of those vaccines remains arguable yet. Also, the safety issue of vaccine involves adaptive immune response which is far more complicated than small-molecule drug toxicity. Moreover, the scale-up of vaccine production is challenging, given that most vaccines are nucleotide or protein-based products which require more delicate manufacturing and storage system compared to small molecules. Those features make it extraordinarily demanding to provide a validated COVID-19 vaccine in the short term.

Besides vaccine development, great efforts have been dedicated to discovering effective prophylactics against COVID-19 for high risk population, whereas very limited studies give satisfactory outcome. Very recently, several clinical cases and *in-vivo* results suggest that some anti-inflammation and anti-virus drugs have potential to be prophylactic candidates. But risk of adverse event will come along with the deployment of those medicines to big population, not to mention their preventive effect remains controversial. Natural products and herbal medicines have been used for the prevention of virus infection for years. Those medicinal products show favorable efficacy and tolerable toxicity. It is undeniable that herbal medicine is still a promising resource for drug discovery, and its acceptable toxicity make it a prospective prophylactic candidate against COVID-19. In face of this global health crisis, exploring prophylactics from herbal medicine is probably a promising and practical strategy to contain pandemic.

In this review, we aimed to provide a new perspective regarding COVID-19 prevention. We called attention to natural products and herbal medicines as potential prophylactic against COVID-19. We summarized the most recent advances in COVID-19 vaccine development and lately reported experimental prophylactics. Then, we discussed both the natural products inhibiting human coronavirus and the herbal medicines proven effective in alleviating respiratory distress syndrome. We performed integrated network analysis upon selected herbal medicine to identify the most promising active components with the potential to be prophylactics. Ultimately, this review attempts to offer alternative conceptual framework for COVID-19 prevention and deeper insight into this unprecedented pandemic.

CURRENT PREVENTION OF COVID-19

Development of effective prevention is urged to contain the spread of current pandemic and halt the occurrence of future relapse. Vaccine, convalescent serum, monoclonal antibody, and marketed anti-viral drugs become the most promising options in the spotlight at this point. In this worldwide race to develop vaccine solution against SARS-COV-2, several candidates are standing out as the current front runners (**Table 1**) with the hope of deploying as early as the end of 2020. While vaccine development at full speed, repurposing or reinventing existing pharmaceutical solutions to meet the challenge will be also necessary. With established safety record, optimized mass-production infrastructure in place, repurposing could fast-track treatment options without compromising rigorous public health standards. To fill in the response gap between treatment and upcoming vaccine, repurposing preventative treatment, or

Abbreviations: ACE2, angiotensin-converting enzyme 2; ADMET, absorption, distribution, metabolism, excretion and toxicity; AKTI, Akt inhibitor; ALB, albumin; AR, androgen receptor; BAX, Bcl-2 Assaciated X protein; BCL2, B-cell lymphoma-2; BCL2L, bcl2-like gene; CASP3, caspases-3; CCL2, chemokine (C-C motif) ligand 2; COX-2, cyclooxygenase-2; COVID-19, coronavirus disease 2019; CoVs, coronaviruses; cPLA2, cytosolic Phospholipase A2; cPLA2α, cytosolic Phospholipase A2α; CXCL10, CXC motif chemokine 10; CXCL8, CXC motif chemokine 8; DPP4, Dipeptidyl peptidase-4; EGFR, Epidermal Growth Factor Receptor; ESR1, Estrogen Receptor 1; F10, Coagulation Factor X; FDA, food and drug administration; FRET, fluorescence resonance energy transfer; HCoV-229E, human coronavirus 229E; FOS, Fos proto-oncogene; GAPDH, glyceraldehyde-3-phosphate dehydrogenase; HCoV-HKU1, human coronavirus HKU1; HCoV-NL63, human coronavirus NL63; HCoV-OC43, human coronavirus OC43; HCS, high-content screening; HSPA5, heat shock protein A5; HSP90AA1, heat shock protein 90 kDa alpha, class A member 1; HSP90AB1, heat shock protein 90 kDa alpha, class B member 1; IL10, interleukin 10; IL-1β, interleukin 1β; IL2, interleukin 2; IL4, interleukin 4; IL6, interleukin 6; JUN, Jun proto-oncogene; LTA4H, leukotriene A4 hydrolase; MAPK1, mitogen-activated protein kinase 1; MAPK14, mitogen-activated protein kinase 14; MAPK3, mitogen-activated protein kinase 3; MAPK8, mitogen-activated protein kinase 8; MERS-CoV, middle east respiratory syndrome-related coronavirus; mPGES-1, Microsomal prostaglandin E synthase-1; NAb, neutralizing antibody; NOS2, Nitric oxide synthase 2; NOS2α, Nitric oxide synthase 2α; NHC, national health commission of the P.R. China; NHS, national health service; NHSBT, blood and transplant service; NIAID, national institute of allergy and infectious diseases; NTP, nucleotide triphosphate; PIK3CG, Phosphatidylinositol-4; PTGS1, Prostaglandin-Endoperoxide Synthase 1; PTGS2, Prostaglandin-Endoperoxide Synthase 2; PLpro, papain-like protease; RBD, receptor-binding domain; RdRp, RNA-dependent RNA polymerase; RELA, RELA proto-oncogene; S protein, Spike protein; SARS-CoV, severe acute respiratory syndrome coronavirus; SARS-CoV-2, severe acute respiratory syndrome coronavirus 2; SBDβ, substrate-binding domain β; sEH, soluble epoxide hydrolase; TMPRSS2, transmembrane protease; TNF, Tumor necrosis factor; TP53, tumor protein p53; WHO, world health organization; 3CLpro, 3-chymotrypsin-like protease; 5-LOX, 5-liopoxygenase; 12-LOX, 12-liopoxygenase.

TABLE 1 | COVID-19 vaccines in pipeline.

Lead Developer(s)	Vaccine Type	Development Status	Ref.
Moderna & NIAID	mRNA/nanoparticle	Phase III clinical trials ongoing	(Corbett et al., 2020; Moderna Inc, 2020)
AstraZeneca & University of Oxford	Plasmid edited gene materials/AdV	Phase I/II ongoing; phase II/III recruiting	(Oxford COVID-19 vaccine to begin phase II/III human trials | University of Oxford; Doremalen et al., 2020; Folegatti et al., 2020)
CanSino Biologics & Academy of Military Medical Sciences	Plasmid edited gene materials/Ad5	Phase I/II ongoing in China, phase I/II approved in Canada	(Halperin and Langley, 2020; Zhu et al., 2020; Zhu et al., 2020)
Sinovac Biotech & Wuhan Institute of Biological Products	Inactivated SARS-COV-2	Phase I/II ongoing	(Sinovac Biotech Co., Ltd, 2020)
Inovio Pharmaceuticals	SARS-COV-2 encoding DNA based	Phase I ongoing	(Inovio Pharmaceuticals, 2020; Smith et al., 2020)
BioNTech & Pfizer	mRNA vaccine	Phase II/III ongoing	(BioNTech SE, 2020; Mulligan et al., 2020a; Mulligan et al., 2020b)
Novavax	Recombinant Protein	Phase I complete, phase II ongoing	(Novavax Inc., 2020)
Johnson & Johnson	Recombinant Protein	Phase I/II ongoing, accelerating phase III	(Janssen Pharmaceutica, 2020)
Curevac	mRNA vaccine	Phase I ongoing	(CureVac Inc., 2020)
Imperial College London	RNA vaccine	Phase I/II ongoing	(ISRCTN - ISRCTN17072692: Clinical trial to assess the safety of a coronavirus vaccine in healthy men and women)
Russia Ministry of Health	Plasmid edited gene materials/AdV	Phase III ongoing, approved	(Logunov et al., 2020)

prophylactics, could reduce transmission of the virus for the public and lend health officials better control on the outbreak. Several compounds of interests with ongoing trials are highlighted.

Landscape of Global COVID-19 Vaccine Development

Most potential options can be broadly categorized three types: mRNA delivery, genetic material with viral carrier, and inactivated virus. Currently, more vaccines candidates on the most advanced timeline are in the second and third category for those methods have more responsive and rapid production scheme, suitable for emergent public health crisis of SARS-COV-2.

Two leading candidates on mRNA delivery are the mRNA-1273 by Moderna in collaboration with National Institute of Allergy and Infectious Diseases (NIAID) in the U.S., and BNT162b1 by BioNTech in collaboration with Pfizer in Germany. Both candidates use RNA motifs of encoding sequence for the Spike (S) protein. Since the commence of the vaccine, Moderna has announced FDA's permission for phase III recruitment starting July 2020, implying expedited development is currently on track to delivery optimistically by late 2020 (Moderna Inc, 2020). As of early Septermber, Moderna's phase III clinical trials has recruited more than 20,000 participants, on track with early estimate (ModernaTX. Inc, 2020). BioNTech, in similar timeline, is set to start phase III of clinical trial by the end of July 2020. To date, its global phase 2/3 trial has accumulatively enrolled more than 25,000 participants (BioNTech SE, 2020). It recently releases an interim report as preprint, showing positive response (~1.8–2.8 folds) to SARS-COV-2 when compared to convalescent human sera (Mulligan et al., 2020a). Under the class of genetic material with viral carrier, University of Oxford and Astra Zeneca have advance their candidate ChAdOx1 (AZD1222), a weakened adenovirus enclosure of SARS-COV-2 spike protein's genetic material, into phase II/III clinical trial (Oxford COVID-19 vaccine to begin phase II/III human trials | University of Oxford). However, limited disclosed data are available in public. A similar and noteworthy candidate is from CanSino Biologics, in collaboration with Academy of Military Medical Sciences in China (Zhu et al., 2020). Both candidates use a variation of adenovirus, commonly found for common cold, are also immunogenic. This carrier approach has yet to be approved in the U.S. nor in EU previously. The other substantially competitive candidate is from Inovio Pharmaceuticals, whose candidate is a DNA based vaccine, INO-4800 (Smith et al., 2020). It announced a positive interim report on its phase I result, and has phase II/III trial expecting in August 2020 (Inovio Pharmaceuticals, 2020). Additionally, Russian Ministry of Health, in collaboration with Russian Direct Investment Fund (RDIF), has developed and approved its first vaccine Sputnik V, and later published its phase 1 results. The Russian vaccine is controversially fast-tracked in absence of phase III clinical trial process (Logunov et al., 2020). For inactivated virus, Sinovac from China is the leading candidate with its phase I/II trial ongoing in China and pending phase III trial in Brazil. This technology named PiCoVacc, uses inactivated or fragmented virus without replicability as the triggering cue to illicit patient's sustained immunity, the ability to generate neutralizing antibody against SARS-COV-2 (Gao Q. et al., 2020).

Moreover, numerous contenders are collaborating with governments and philanthropic foundations to ramp up production to create stockpile once clinical trials provide evidence for their safety and efficacy, to shorten deployable timeline. NIAID also recently announce an establishment of a new clinical trial network focusing on COVID-19 vaccine and monoclonal antibody testing. However, mRNA vaccine, such as Moderna's mRNA-1273, has yet to be approved and adopted

historically. Lack of similar predecessor likely warrants more scrutiny from regulators and general publics.

Convalescent Serum Transfusion and Monoclonal Antibody

Convalescent serum transfusion, where patient received recovered patients' antibodies-contained plasma to develop the ability to fight viral infection, is currently widely trialed as treatment option for COVID-19 around the world. In April 2020, National Health Service (NHS) in the UK has established Blood and Transplant Service (NHSBT) to conduct recovery trial with Oxford University, studying the application viability of such technology on COVID treatment as well as prevention (NHS Blood and Transplant). To date, more than thousands of subjects are enrolled around the world in convalescent plasma clinical trials (Sheridan, 2020). FDA has also issue recommendation guideline for convalescent plasma investigational use (U.S. Food & Drug Administration, 2020). FDA has later issued an emergency use authorization (EUA) on August 23, while continued to encourage further clinical trials (U.S. Food & Drug Administration, 2020). Commercially, Regeneron has investigated antibodies purified human convalescent plasma and genetically humanized mice, in which the author shows an antibody cocktail of treatment potential (Hansen et al., 2020).

More recently, monoclonal antibody discovery against SARS-CoV-2 has yield valuable insight into variation of viable antibodies and their mechanisms. Wu et al. discussed the wide variation in neutralizing antibody (NAb) potency among infected patients, which was indicated with NAb titer (ID50: 200 ~ 21567) ranging across two orders of magnitudes (Wu F. et al., 2020). This highlight concerning needs for donor selection and post-processing effort (Robbiani et al., 2020). Another research group then provided example antibodies (B38 and H4) that binds with crucial target site like ACE2 and receptor-binding domain (RBD) (Wu Y. et al., 2020). Rogers et al. also revealed antibodies against both RBD and non-RBD epitopes of Spike (S) protein (Rogers et al., 2020). While Wang et al. identified 47D11 that has neutralization effect on both SARS-CoV and SARS-CoV-2, emphasized the domain conservation in SARS2-S-S1b (Wang C. et al., 2020). Zost et al. and Kreer et al. then add another collection of antibody candidate isolated from patients' plasma. Moreover, Kreer et al. identified that the broad spectrum of variable genes shared among the potent B cells exists in naïve populations (Kreer et al., 2020; Zost et al., 2020). Both treatment and prophylactics based on antibody could likely be more immediate and rapidly available for high risk populations than a vaccine, but production ramping could introduce uncertainty for its timeline.

Small Molecule Prophylactic

Remdesivir, developed by Gilead Sciences, acts as a prodrug of a nucleotide analog. When it is intracellularly metabolized, its product, analogue of adenosine triphosphate, will inhibit regular viral RNA polymerase's function. It is considered applicable in board spectrum to multiple other coronaviruses, such as Ebola, MERS-COV, and SARS-COV. Remdesivir is not only propelled as a treatment against SARS-COV-2, but also is under investigation for prevention purpose. Early experiment of remdesivir by de Wit et al. (2020) shows both prophylactic and therapeutic benefits, mirroring the recent study on SARS-COV-2 on the same animal model (Casadevall and Pirofski, 2020). WHO is currently also studying remdesivir as one of the options for its "solidarity" clinical trial (World Health Organization, 2020).

Emtricitabine/tenofovir disoproxil, also commonly known for its brand name TRUVADA® in the U.S., an HIV pre-exposure prophylactic. It is a combination of protease inhibitor and nucleotides reverse transcriptase inhibitor. It is considered to have beneficial effect on treating SARS-COV-2 with its possible inhibition of RNA-dependent RNA polymerase. A recent cohort study also suggests that AIDS patient taking antiretroviral therapy, especially tenofovir disoproxil fumarate/emtricitabine has lower risks of diagnosis, and reduced severity and fatality (del Amo et al., 2020). It is currently on track of the phase III clinical trial to prevent SARS-COV-2 high-risk healthcare workers in Spain, which sets to complete by August (Polo and Hernan, 2020).

Lopinavir/ritonavir, brand name KALETRA® in the U.S., is a combination used as an HIV aspartate protease inhibitor previously, has *in vitro* testing inhibitory effect on SARS-COV-2 as well. However, it has not yet been observed efficacy in treating SARS-COV-2 severe patients (Cao et al., 2020). It was solicited by WHO for its SOLIDARITY clinical trial until July 2020. Recently, after NHS/Oxford study finds no clinical benefit from this combination's usage, Lopinavir/ritonavir is discontinued onwards for WHO's clinical trial recommendation (Horby et al., 2020).

NATURAL PRODUCTS INHIBITING HUMAN CORONAVIRUS

Although combinatorial synthesis coupled with molecular docking help discover numerous synthetic drugs, more than one third of Food and Drug Administration (FDA)-approved drugs are natural products (Patridge et al., 2016). Plant, fungus and marine derived natural products have been rich resource of drug/nutrition discovery for many disease prevention (Tao et al., 2016; Wang et al., 2018; Lan et al., 2020). Natural products possess promising antiviral effects against human CoVs, which may guide the development of novel antiviral prophylactics. Here, we discussed updated researches focusing on natural products against MERS-CoV, SARS-CoV, or SARS-CoV-2 (**Figure 1**) and summarized their specific molecular targets and possible mechanisms of action (**Table 2**).

Natural Products Inhibiting MERS-CoV

MERS-CoV causes Middle East respiratory syndrome (MERS, also known as camel flu). It was first discovered in 2012 in Saudi Arabia. Since then, it has spread to 27 countries through air travel of infected people (Sheahan et al., 2020), causing an outbreak of 2,494 cases and 858 deaths worldwide based on World Health

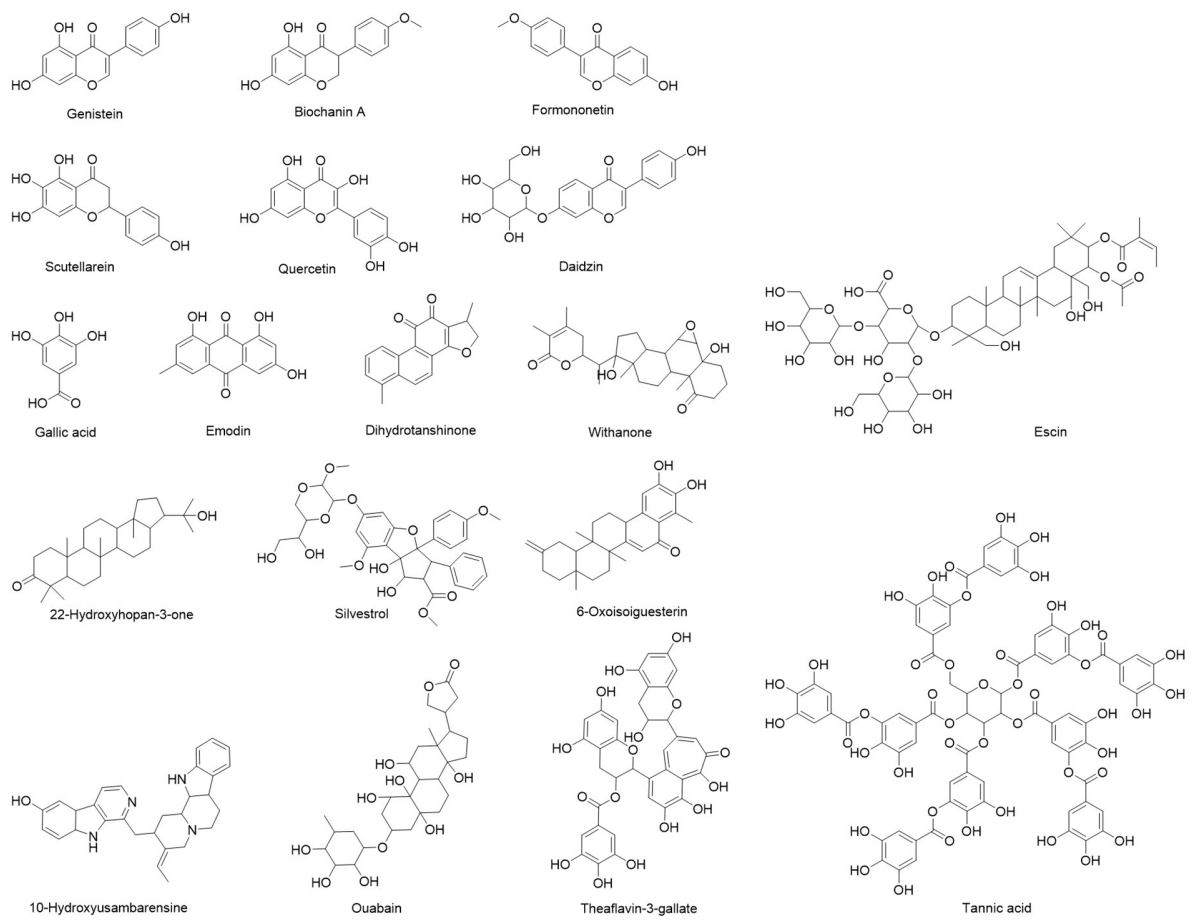

FIGURE 1 | Natural products inhibiting human coronavirus.

Organization (WHO) report (WHO | Middle East respiratory syndrome coronavirus (MERS-CoV), 2020). MERS-CoV continues infecting human, thus it has been listed as a priority pathogen with pandemic potential by WHO. The mortality rate among patients with confirmed infection is approximately 37%. So far, very few studies have investigated the natural products as potential therapeutic agents for MERS-CoV.

The envelope spike (S) protein of MERS-CoV is important for dipeptidyl peptidase 4 receptor binding and virus-cell membrane fusion, thus it is the key for virus to entry host cells (Mille and Whittaker, 2014). Kim et al. (2018) generated a pseudo-virus expressing the S protein of MERS-CoV (MERS-PV) and screened 502 compounds derived from natural products to test their ability to block MERS-CoV entry. Three compounds (Dihydrotanshinone, E-64-C, and E-64-D) met the screening criteria at a concentration of 1 μg/ml. However, only dihydrotanshinone exhibits antiviral effects on MERS-CoV in the post-attachment assay. Dihydrotanshinone is extracted from the root of *Salvia miltiorrhiza* Bunge which is commonly used in traditional Chinese medicine. However, studies to confirm antiviral efficacy against MERS-CoV infection in animal model are required.

Ouabain is from the seeds of *Strophanthus gratus* (Wall. & Hook.) Baill. It has been used in cell biology studies as standard inhibitor of the Na^+-K^+-exchanging ATPase. A study (Ko et al., 2020) screened 5,406 compounds, including about 60% of all U.S. FDA-approved drugs, utilizing a Korean MERS patient isolate. By measuring the levels of the S protein expression of infected Vero cells using immunofluorescence analysis, they identified the cardiotonic drugs ouabain had a therapeutic index greater than 100, suggesting it could be considered for anti-MERS-CoV therapy. However, further *in vitro* and *in vivo* studies are needed to illustrate the mechanism of action.

Griffithsin isolated from the *Griffithsia* genus (red marine alga) is a 121 amino acid long lectin, which is attractive anti-coronavirus candidate because it interacts with coronavirus S proteins due to their highly glycosylated nature and represses coronavirus S protein functions (Millet et al., 2016). It has antiviral activity against HIV-1 within the picomolar range (EC_{50}: 0.043 nM) (Mori et al., 2005). Milletit et al. have shown griffithsin is a potent inhibitor of MERS-CoV infection and production *in vitro* (Millet et al., 2016). In addition, Griffithsin has been shown a low systematic toxicity, hence making it a promising candidate against MERS-CoV.

TABLE 2 | Natural products potentially effective for COVID-19.

Natural Product	Inhibited Virus	Drug Targets/Relevant Signaling	Mechanism of Action	Ref.
Dihydrotanshinone	MERS-CoV	S protein of MERS-CoV	Block MERS-CoV entry using pre-and post-attachment assay	(Kim et al., 2018)
Ouabain	MERS-CoV	S protein of MERS-CoV	Block MERS-CoV entry by HCS assay, IC_{50} in Vero cells: 0.08 μM	(Ko et al., 2020)
Griffithsin	MERS-CoV	S protein of MERS-CoV	Inhibit spike protein function during entry	(Millet et al., 2016)
Silvestrol	MERS-CoV	eIF4A	Inhibit eIF4A, EC_{50}: 1.3 nM	(Müller et al., 2018)
Emodin	SARS-CoV	S protein and ACE2 interaction	Blocked the binding of S protein to ACE2 using biotinylated ELISA assay, IC_{50}: 200 μM	(Ho et al., 2007)
Scutellarein	SARS-CoV	SARS-CoV helicase protein	Inhibit the nsP13ATPase activity by FRET-based double-strand (ds) DNA unwinding assay, IC_{50}: 0.86 ± 0.48 μM	(Yu et al., 2012)
Tannic acid	SARS-CoV	3CLPro	Inhibition of 3CLPro, IC_{50}: 3 μM	(Chen et al., 2005)
Theaflavin-3-gallate	SARS-CoV	3CLPro	Blocking 3CLPro function, IC_{50}: 7 μM	(Chen et al., 2005)
Escins	SARS-CoV	NF-κB and activator protein-1 signaling pathways	Decrease levels of TNF-α and IL-6, EC_{50}: 1.5 and 2.4 μg/ml in HCLE and NHC cells	(Michelini et al., 2018)
Daidzin Genistein Formononetin Biochanin A	SARS-CoV-2	HSPA5	High binding affinity to HSPA5 SBDβ tested by virtual docking	(Elfiky, 2020)
Lead compounds from *Alpinia officinarum*	SARS-CoV-2	PL protein	High binding affinity to PLpro tested by molecular docking	(Dibakar et al., 2020)
10-Hydroxyusambarensine 6-Oxoisoiguesterin 22-Hydroxyhopan-3-one	SARS-CoV-2	3CL protein	High binding affinity to 3CLpro tested by tested by molecular docking	(Gyebi et al., 2020)
Gallic acid Quercetin	SARS-CoV-2	RdRp	High binding affinity to RdRp tested by molecular docking	(El-Aziz Abd et al., 2020)
Withanone	SARS-CoV-2	TMPRSS2	Bind and interact at the catalytic site of TMPRSS2	(Kumar et al., 2020)

Besides inhibiting MERS-CoV entry host cells, suppressing its replication is an alternative strategy. Silvestrol, a natural compound isolated from the plant *Aglaia foveolate* Pannell, is known for inhibition of the DEAD-box RNA helicase, eIF4A that participates in preparation of mRNA templates for ribosome recruitment during translation initiation (Todt et al., 2018). Thus, it suppresses the formation of virus replication. Müller and colleagues (Müller et al., 2018) investigated the inhibitory effects of silvestrol against MERS-CoV in human embryonic lung fibroblasts (MRC-5). Silvestrol was a potent antiviral molecule (EC_{50}: 1.3 nM) with no major cytotoxic effects in the primary cells and in liver or spleen. For future studies, the antiviral effects of silvestrol need to be evaluated *in vivo* infection models to consolidate its therapeutic potential.

Natural Products Inhibiting SARS-CoV

From 2002 to 2003, SARS-CoV emerged in Southern China, infecting more than 8,000 people and causing approximately 800 fatalities mostly in China and its neighboring countries. Like MRES-CoV, the envelope S protein of SARS-CoV is also essential for virus tropism and invasion into host cells, which is a potential target for the development therapeutics (Yuan et al., 2017). Angiotensin-converting enzyme 2 (ACE2) is identified as a functional receptor for SARS-CoV, which facilitates S protein-mediated infection, indicating it is also a possible target.

Emodin, an anthraquinone from *Rheum officinale* Baill and *Reynoutria multiflora* (Thunb.) Moldenke, has antibacterial and anti-inflammatory effects. Ho et al. (2007) have reported that emodin blocked the binding of S protein to ACE2 and reduced the infectivity of S protein pseudo-typed retrovirus to Vero E6 cells. Emodin effectively blocked the interaction between S protein and ACE2 in a dose-dependent manner with IC_{50} of 200 μM, indicating it might be a potential therapeutic agent for the treatment of SARS.

Scutellarein is a flavone found in *Scutellaria lateriflora* L. and other members of the genus *Scutellaria*. Yu et al. (2012) screened 64 purified natural compounds for the inhibitory effects of SARS helicase, nsP13 that possesses dsDNA unwinding activity and the ability to translocate along the nucleic acids, using fluorescence resonance energy transfer-based double-strand DNA unwinding assay. They found that scutellarein potently inhibited the SARS-CoV helicase protein *in vitro via* inhibiting the ATPase activity of nsP13. Scutellarein holds a promising potential for tackling SARS outbreaks; however, more preclinical/clinical studies to validate its efficacy are needed to evaluate their anti-viral effects.

Chymotrypsin-like protease (3CLPro) of SARS-CoV, an enzyme responsible for proteolysis, is vital to coronavirus replication, making it considered as an important target for drug discovery against SARS-CoV. Chen et al. (Doremalen et al., 2020) have screened a library with 720 compounds of natural product for inhibitory effect against 3CLPro of SARS-CoV by high-performance liquid chromatography assay and fluorogenic substrate peptide assay. Among them, two natural polyphenols found in black tea (*Camellia sinensis* (L.) Kuntze), tannic acid, IC_{50}: 3 μM; theaflavin-3-gallate, IC_{50}: 7 μM) showed

desired benefits. Black tea is common all over the world, thus this study provides a new perspective that tea-derived supplements might prevent the infection of SARS-CoV. But detailed *in vitro* and *in vivo* studies need to be conducted, SARS-CoV infection is related to the release of pro-inflammatory cytokines and uncontrolled inflammation that induce the accumulation of intra-alveolar fibrin and lead to pulmonary damage. Thus, an alternative strategy is to reduce inflammation. Escins are saponin mixtures from Japanese horse chestnut (seed of *Aesculus turbinata* Blume) that has been used as an herbal medicine. It has anti-inflammatory activities and anti-antiviral effects against SARS-CoV (an EC50 of 6.0 μM) (Wu et al., 2004). Escin has been reported to decrease the levels of TNF-α and IL-6 in J774A.1 cells infected with HSV-1 or stimulated with Toll-like receptor ligands by the inhibition of NF-κB and activator protein-1 signaling pathways (Michelini et al., 2018). However, the severe cytotoxic effects in human lung derived cells limits its potential to be a prophylactic. Usually, a more efficient or safer drug can be designed based on the original natural compound that exhibits the wanted activity. Kim et al. (2017) designed and synthesized a series of escin derivatives without the angeloyl or tigloyl groups that are important for cytotoxicity of escins and modified glycosidic linkages by hydrolysis. Those Escin derivative showed lower cytotoxicity.

Natural Products Inhibiting SARS-CoV-2

The current COVID-19 pandemic caused by SARS-CoV-2 was identified in Wuhan City, in Hubei province of China. The number of infection case is still progressively growing. The genome of SARS-CoV-2 has over 70% similarity to that of SARS-CoV (Zhang and Holmes, 2020), leading to its current name. There is an urgent need to prevent and treat SARS-CoV-2 infection. Due to the high similarity, many approved or pre-clinical anti-SARS drugs are being tested for antiviral activity against SARS-CoV-2. For example, escin (Gallelli, 2020) and sodium aescinate injection (trial filed in China with ID : ChiCTR2000029742) have been registered. As natural products has been historically used for respiratory infection, there is arising voice calling for the repurposing of natural products for COVID-19 (Wang D. et al., 2020).

Heat Shock Protein A5 (HSPA5, also known as BiP or GRP78) is one of the host-cell receptors that have been reported to be recognized by virus S protein. When infected, HSPA5 is upregulated and translocated to the cell membrane where it is recognized by the SARS-CoV-2 spike to drive the infection process. Elfiky et al. (Elfiky, 2020) have tested several compounds from natural product against the HSPA5 substrate-binding domain β (SBDβ) by molecular docking and molecular dynamics simulations. The phytoestrogens (Daidzin, Genistein, Formononetin, and Biochanin A) and estrogens have proximal binding affinities with HSPA5. Those compounds may interfere with SARS-CoV-2 attachment to the host cells. Hopefully, those medicinal plants-derived compounds may guide the drug discovery in finding the suited prophylactics for SARS-CoV-2. Detailed studies investigating the antiviral bioactivity of those compounds should be further examined.

The host enzyme transmembrane protease serine 2 (TMPRSS2) facilitates viral particle entry into host cells. Inhibiting of this enzyme blocks virus fusion with ACE2, making it a potential target to inhibit virus entry. By molecular docking and molecular dynamics simulations, Kumar et al. (2020) have shown that withanone derived from Ashwagandha leaves (*Withania somnifera* (L.) Dunal) could bind and stably interact at the catalytic site of TMPRSS2 (His296, Asp345 and Ser441). In addition, they have confirmed that withanone significantly downregulated TMPRSS2 in MCF-7 cells, suggesting its dual potential to ramp down TMPRSS2 function.

SARS-CoV-2 papain-like protease (PL pro) cleaves the viral polyproteins a/b which is essential for its survival and replication. Thus, PL pro is one of the prospective drug targets of SARS-CoV-2. Goswami et al. (Dibakar et al., 2020) established a library of small molecules found in rhizomes, Alpinia officinarum (*Alpinia officinarum* Hance), ginger (*Zingiber officinale* Roscoe), and curcuma (*Curcuma longa* L.). The compounds were docked into the solvent accessible S3-S4 pocket of PLpro. In silico results showed eight lead compounds from galangal (*Alpinia officinarum* Hance) and ginger (*Zingiber officinale* Roscoe) bound with high affinity to SARS-CoV-2 PLpro, suggesting their potential as inhibitors against SARS-CoV-2. However, subsequent *in vitro* and *in vivo* experiments are needed to elucidate their efficacy against SARS-CoV-2.

Besides S protein and PLpro, the other promising drug target for combating the infection of SARS-CoV-2 is 3-chymotrypsin-like protease (3CLpro, also known as main protease). The conserved 3CLpro controls virus replication. Gyebi et al. (2020) have screened a series of alkaloids and terpenoids derived from African plants as potential inhibitors of 3CLpro using molecular docking and absorption, distribution, metabolism, excretion, and toxicity (ADMET) virtual analysis by the SuperPred webserver. The results revealed that 10-Hydroxyusambarensine, Cryptoquindoline, 6-Oxoisoiguesterin, and 22-Hydroxyhopan-3-one might be potent inhibitors with greatest drug-likeness against SARS-CoV-2 3CLpro.

RNA-dependent RNA polymerase (RdRp) is an essential virus replicase that catalyzes the synthesis of complementary RNA strands using the virus RNA template. The molecular structure of RdRp was revealed in May 2020 (Gao Y. et al., 2020), providing a new strategy for discovering prophylactic candidates for SARS-CoV-2 inhibition. Abd El-Aziz et al. (El-Aziz Abd et al., 2020) investigated the potential of eight natural polyphenols (quercetin, naringenin, caffeine, oleuropein, ellagic acid, benzoic acid, resveratrol, and gallic acid polyphenols) as inhibitors of SARS-CoV-2 RdRp by molecular docking assay. The studied polyphenols formed hydrogen bonds with the nucleotide triphosphate (NTP) entry channel amino acids (ARG 555, ARG 555, LYS 545) in SARS-CoV-2 RdRp (except caffeine and oleuropein). Binding to NTP may inhibit the entry of the substrate and subsequently repress the enzyme activity. The results suggested that gallic acid and quercetin exhibited high binding affinity to RdRp. The NSP12 is an important RdRp for the coronavirus replicative machinery, which binds to co-factors NSP7 and NSP8 to activate its ability to replicate long RNA. A

recent study (Ruan et al., 2020) has established two homologous models for virtual screening. Cepharanthine, an alkaloid tetrandrine isolated from Stephania (*Stephania tetrandra* S.Moore), has been reported to have anti-inflammatory and antioxidant activities (Weber and Opatz, 2019). The study has shown Cepharanthine could bind to the interface active pockets of the SARS-CoV-2 NSP12-NSP8, suggesting it has therapeutic potential.

The researches mentioned above are all still in preliminary stages of drug development although they have shown great potentials against SARS-CoV-2 using computer-based screening. Further pre-clinical studies have to be performed to examine the anti-viral effects of those lead compounds. In the meanwhile, great number of clinical trials have registered to investigate the potentials of natural product to halt disease progression. For example, Koshak et al. from King Abdulaziz University will investigate the effects of Nigella sativa seed oil with immunomodulation and antiviral activity in hospitalized adult patients diagnosed with COVID-19 (Koshak et al., 2020). Corrao et al. from University of Palermo is recruiting patients to study the effectiveness of vitamin C to reduce mortality in patients (Corrao, 2020). Since the situation is uncontrollably worsening, many studies are being conducted on this topic, which may contribute to the rapid development of new prophylactics for COVID-19.

HERBAL MEDICINES ALLEVIATING ACUTE RESPIRATORY INFECTION

Herbal medicines like EPs® 7630, Sinupret®, and KanJang® have proven track record of treating acute respiratory infection due to common cold or influenza (Narimanian et al., 2005; Glatthaar-Saalmüller et al., 2011; Michaelis et al., 2011). Dating back to the beginning of COVID-19 outbreak around December 2019, herbal medicines were widely deployed across China to slow down the surge of infection cases. Its efficacy in alleviating acute respiratory distress syndrome caused by SARS-CoV-2 has been endorsed by both Chinese regulatory agency and the healthcare workers on the frontline. Recent perspectives from academics argued that the potential of herbal medicine to be an appropriate therapy for COVID-19 was open to question in the context that the pharmacological mechanism of those herbs remains unclear and hard to be fully explored (Gray and Belessis, 2020; Tao et al., 2020). That said, it is still undeniable that empirical therapy of herbal medicines contributed to the successful arrest of COVID-19 spreading in China to some extent, based on clinical observation. In addition, several preclinical studies lately proved that herbal medicines rich in flavonoid compounds had anti-virus activity in some human lung derived cell lines (Ding et al., 2017; Kong et al., 2020; Runfeng et al., 2020). Hereby, research digging into underlying mechanisms and identifying active components are urgently needed for the development of more effective herbal therapy and prophylactic.

A clinical case went public in March 2020 showed that a herbal formulation recommended by National Health Commission of the P.R. China (NHC) was effective in attenuating acute respiratory distress syndrome in a mild COVID-19 patient (Xu and Zhang, 2020). It was the first-of-its-kind to report the potential benefit of herbs in treating COVID-19. More recently several reviews systemically summarized the herbal medicines frequently used in China during COVID-19 pandemic and performed meta-analysis to illustrate its therapeutic outcome (Zhang D. et al., 2020). Xiong et al. indicated that among those herbal medicines widely distributed, Liquoric Root (*Glycyrrhiza glabra* L.), Baical Skullcap Root (*Scutellaria baicalensis* Georgi), Pinellia Rhizome [*Pinellia ternata* (Thunb.) Makino], Forsythia Fruit [*Forsythia suspensa* (Thunb.) Vahl], and Bitter Apricot Seed (*Prunus armeniaca* L.) are the most frequently prescribed herbs (Li et al., 2020). Their meta-analysis showed that herbal medicines are effective in halting the disease progression from mild to critical, decreasing hospitalization rate, shortening time of hospital stay, as well as alleviating COVID-19 associated symptoms like fever, cough, fatigue, and inflammation (Li et al., 2020).

Li et al. tested the potency of Lian-Hua-Qing-Wen, a licensed herbal formulation in inhibiting SARS-CoV-2 infection of Vero E6 cells using cytopathic effect inhibition assay and plaque reduction assay (Runfeng et al., 2020). The results showed that Lian-Hua-Qing-Wen significantly inhibited SARS-CoV-2 replication in Vero E6 cells and reduced pro-inflammatory cytokines like TNF-α, IL-6, CCL-2/MCP-1, and CXCL-10/IP-10 at mRNA level. Though its IC_{50} with over 400 μg/ml is a far cry from remdesivir efficacy, this study inspires that this herbal formulation can be validated as ideal prophylactic considering its moderate toxicity. Yang et al. performed LC-MS/MS and integrated network analysis to identify the active components of Qing-Fei-Pai-Du and Ma-Xin-Shi-Gan and their possible mechanism of action (Yang et al., 2020). The study revealed great number of compounds making up these two herbal formulations. Those chemicals mainly fall into four categories: flavonoids, glycosides, carboxylic acids, and saponins. In particular, glycyrrhizic acid isolated from Ma-Xin-Shi-Gan exhibited its anti-inflammatory effect by blocking toll-like-receptor and suppressing IL-6 production in macrophage. Huang et al. identified that quercetin, kaempferol, luteolin, isorhamnetin, baicalein, naringenin, and wogonin are probably the main active compounds responsible for the potency of herbs (Huang et al., 2020). Through *in silico* study, they hypothesized that ACE2, 3CL protein as well as intracellular signaling composed of COX-2, CASP3, MAPK, arachidonic acid, HIF-1, NF-κB, and Ras are all potential targets of herbal medicines. Most recently Ma et al. reported that Liu-Shen a herbal formulation exhibit favorable inhibitory effect against SARS-CoV-2 replication and virus-induced inflammation *in vitro* probably *via* suppressing NF-κB pathway (Ma et al., 2020).

Based on recently emerging studies, we reviewed all the herbal products both used for COVID-19 and approved by regulatory agency of which the patent numbers are identifiable. We summarized the composition and prospective drug targets of those licensed herbal products (**Table 3**) through literature search. We then ranked their ingredients based on dosage and frequency of use (**Figure 2A**). By narrowing down the sample volume, top nine

TABLE 3 | Licensed Chinese herbal medicines for acute respiratory infection.

Herbal Medicines	Affected Pathways Potential Targets	Composition		Ref.
		Herbal components	Original Species	
Lian-Hua-Qing-Wen	MAPK8, IL-6, COX-2, sEH, RELA, cPLA2α, mPGES-1, TNF, DPP4, IL-1β, CASP3, MAPK1, EGFR, BAX, BCL2, JUN, PIK3CG.	Forsythiae Fructus	*Forsythia suspensa* (Thunb.) Vahl	(Runfeng et al., 2020; Zhang D. et al., 2020)
		Lonicerae Japonicae Flos	*Lonicera Japonica* Thunb.	
		Ehedraep Herba	*Ephedra sinica* Stapf	
		Armeniacae Seman Amarum	*Prunus armeniaca* L.	
		Gypsum Fibrosum†		
		Isatidis Radix	*Isatis tinctoria* L.	
		Dryopteridis Crassirhizomatis Rhizoma	*Dryopteris crassirhizoma* Nakai	
		Houttuyniae Herba	*Houttuynia cordata* Thunb.	
		Pogostemonis Herba	*Pogostemon cablin* (Blanco) Benth.	
		Rhei Radix Et Rhizoma	*Rheum palmatum* L.	
		Rhodiolae Crenulatae Radix Et Rhizoma	*Rhodiola crenulata* (Hook.f. & Thomson) H.Ohba	
		Menthol	*Mentha* × *piperita* L.	
		Glycyrrhizae Radix Et Rhizoma	*Glycyrrhiza inflata* Batalin	
Huo-Xiang-Zheng-Qi	PTGS2, HSP90AB1, mPGES-1, LTA4H, NOS2, PTGS2.	Atractylodis Rhizoma	*Atractylodes lancea* (Thunb.) DC.	(Zhang D. et al., 2020)
		Citri Reticulatae Pericarpium	*Citrus* × *aurantium* L.	
		Magnoliae Officinalis Cortex	*Magnolia officinalis* Rehder & E.H.Wilson	
		Angelicae Dahuricae Radix	*Angelica dahurica* (Hoffm.) Benth. & Hook.f. ex Franch. & Sav.	
		Poria mushroom§	*Poria cocos* (Schw.) Wolf	
		Arecae Pericarpium	*Areca catechu* L.	
		Pinelliae Rhizoma	*Pinellia ternate* (Thunb.) Makino	
		Glycyrrhizae Radix Et Rhizoma	*Glycyrrhiza inflata* Batalin	
		Pogostemonis Herba	*Pogostemon cablin* (Blanco) Benth.	
		Perillae Folium	*Perilla frutescens* (L.) Brittonon	
Jin-Hua-Qing-Gan	COX-2, sEH, 5-LOX, PTGS2, AKTl, HSP90AA1, RELA, MAPK1, CASP3, TP53, ALB, TNF, IL6, MAPK8, MAPK14.	Lonicerae Japonicae Flos	*Lonicera Japonica* Thunb.	(Runfeng et al., 2020; Zhang D. et al., 2020)
		Gypsum Fibrosum†		
		Ehedraep Herba	*Ephedra sinica* Stapf	
		Armeniacae Seman Amarum	*Prunus armeniaca* L.	
		Scutellariae Radix	*Scutellaria baicalensis* Georgi	
		Forsythiae Fructus	*Forsythia suspensa* (Thunb.) Vahl	
		Fritillaria Thunbergii Bulbus	*Fritillaria thunbergii* Miq.	
		Anemarrhenae Rhizoma	*Anemarrhena asphodeloides* Bunge	
		Arctii Fructus	*Arctium lappa* L.	
		Artemisiae Annuae Herba	*Artemisia annua* L.	
		Menthae Haplocalycis Herba	*Mentha canadensis* L.	
		Glycyrrhizae Radix Et Rhizoma	*Glycyrrhiza inflata* Batalin	
Shu-Feng-Jie-Du	IL6, IL1B, CCL2, IL2, MAPK8, MAPK1, MAPK14, CASP3, FOS, ALB, IL4, IL1B, EGFR, FOS, AR, BCL2L, NOS2, F10, PTGS2, PTGS1, ESR1, DPP4.	Polygoni Cuspidati Rhizoma	*Reynoutria japonica* Houtt.	(Li et al., 2017; Li et al., 2020; Zhang D. et al., 2020)
		Forsythiae Fructus	*Forsythia suspensa* (Thunb.) Vahl	
		Isatidis Radix	*Isatis tinctoria* L.	
		Bupleuri Radix	*Bupleurum chinense* DC.	
		Patriniae Herba	*Patrinia scabiosifolia* Link	
		Vervain	*Verbena officinalis* L.	
		Phragmitis Rhizoma	*Phragmites australis* subsp. australis	
		Glycyrrhizae Radix Et Rhizoma	*Glycyrrhiza inflata* Batalin	
Su-He-Xiang	N/A	Styrax	*Liquidambar orientalis* Mill.	(Zhang D. et al., 2020)
		Benzoinum	*Styrax tonkinensis* (Pierre) Craib ex Hartwich	

(Continued)

TABLE 3 | Continued

Herbal Medicines	Affected Pathways Potential Targets	Composition		Ref.
		Herbal components	Original Species	
		Borneolum Syntheticumc	*Dryobalanops aromatica* C.F.Gaertn.	
		Bubali Cornu*	*Bubalus bubalis* Linnaeus	
		Moschus*	*Moschus berezovskii* Flerov	
		Santali Albi Lignum	*Santalum album* L.	
		Aquilariae Lignum Resinatum	*Aquilaria sinensis* (Lour.) Spreng.	
		Aucklandiae Radix	*Aucklandia costus* Falc.	
		Cyperi Rhizoma	*Cyperus rotundus* L.	
		Olibanum	*Boswellia carteri* Birdw.	
		Long Pepper Fruit.	*Piper longum* L.	
		Atractylodis Macrocephalae Rhizoma	*Atractylodes macrocephala* Koidz.	
		Chebulae Fructus	*Terminalia chebula* Retz.	
		Cinnabaris†		
An-Gong-Niu-Huang	N/A	Bovis Calculus* Bubali Cornu*	*Bos taurus domesticus* Gmelin *Bubalus bubalis* Linnaeus	(Zhang D. et al., 2020)
		Moschus*	*Moschus berezovskii* Flerov	
		Margarita*		
		Cinnabaris†		
		Arsenic (II) sulfide†		
		Coptidis Rhizoma	*Coptis chinensis* Franch.	
		Scutellariae Radix	*Scutellaria baicalensis* Georgi	
		Gardeniae Fructus	*Gardenia jasminoides* J.Ellis	
		Curcumae Radix	*Curcuma aromatica* Salisb.	
		Borneolum Syntheticumc	*Dryobalanops aromatica* C.F.Gaertn.	
Xi-Yan-Ping	N/A	Andrographolide sulfonatesc	*Andrographis paniculata* (Burm.f.) Nees (Burm.f.) Nees	(Zhang D. et al., 2020) (Runfeng et al., 2020; Zhang D. et al., 2020)
Xue-Bi-Jing	LTA4H, 12-LOX, IL2, cPLA2, IL6, RELA, TNF, PTGS2, IL10, NOS2α, CASP3, MAPK1.	Carthami Flos	*Carthamus tinctorius* L.	
		Paeoniae Radix Rubra	*Paeonia lactiflora* Pall.	
		Chuanxiong Rhizoma	*Conioselinum anthriscoides* 'Chuanxiong'	
		Salvia miltiorrhiza Radix Et Rhizoma	*Salvia miltiorrhiza* Bunge	
		Angelicae Sinensis Radix	*Angelica sinensis* (Oliv.) Diels	
Re-Du-Ning	COX-2, sEH, IL6, CCL2, CASP3, IL4, MAPK1, RELA, FOS, NOS2, IL1B, CXCL10, MAPK14, EGFR.	Artemisiae Annuae Herba	*Artemisia annua* L.	(Runfeng et al., 2020; Zhang D. et al., 2020)
		Lonicerae Japonicae Flos	*Lonicera Japonica* Thunb.	
		Gardeniae Fructus	*Gardenia jasminoides* J.Ellis	
Tan-Re-Qing	COX-2, sEH, LTA4H, IL6, IL1B, IL10, MAPK1, IL4, CXCL8, MAPK14, EGFR, CXCL10.	Scutellariae Radix	*Scutellaria baicalensis* Georgi	(Huang et al., 2020; Runfeng et al., 2020; Zhang D. et al., 2020)
		Saigae Tataricae Cornu*	*Saiga tatarica* Linnaeus	
		Lonicerae Japonicae Flos	*Lonicera Japonica* Thunb.	
		Forsythiae Fructus	*Forsythia suspensa* (Thunb.) Vahl	
Xing-Nao-Jing	N/A	Moschus*	*Moschus berezovskii* Flerov	
		Borneolum Syntheticum	*Dryobalanops aromatica* C.F.Gaertn.	(Runfeng et al., 2020; Zhang D. et al., 2020)
		Gardeniae Fructus	*Gardenia jasminoides* J.Ellis	
		Curcumae Radix	*Curcuma aromatica* Salisb.	
Shen-Fu	N/A	Ginseng Radix Et Rhizoma	*Panax ginseng* C.A. Mey.	(Runfeng et al., 2020; Zhang D. et al., 2020)
		Aconiti Lateralis Radix Praeparata	*Aconitum carmichaeli* Debeaux	

(Continued)

TABLE 3 | Continued

Herbal Medicines	Affected Pathways Potential Targets	Composition		Ref.
		Herbal components	Original Species	
Sheng-Mai	IL6, GAPDH, ALB, TNF, MAPK1, MAPK3, TP53, EGFR, CASP3.	Ginseng Radix Et Rhizoma	*Panax ginseng* C.A. Mey.	(Huang et al., 2020; Zhang D. et al., 2020)
		Ophiopogonis Radix	*Ophiopogon japonicus* (Thunb.) Ker Gawl.	
Pu-Di-Lan	N/A	Scutellariae Radix Traxaci Herba	*Scutellaria baicalensis* Georgi *Taraxacum mongolicum* Hand. Mazz.	(Kong et al., 2020)
		Corydalis bungeana	*Corydalis bungeana* Turcz.	
		Isatidis Radix	*Isatis tinctoria* L.	
Yin-Qiao	N/A	Forsythiae Fructus	*Forsythia suspensa* (Thunb.) Vahl	(Huang et al., 2020; Li et al., 2020)
		Lonicerae Japonicae Flos	*Lonicera Japonica* Thunb.	
		Platycodonis Radix	*Platycodon grandiflorum* (Jacq.) A. DC.	
		Menthae Haplocalycis Herba	*Mentha canadensis* L.	
		Phyllostachydis Henonis Folium	*Lophatherum gracile* Brongn.	
		Glycyrrhizae Radix Et Rhizoma	*Glycyrrhiza inflata* Batalin	
		Schizonepetae Herba	*Nepeta tenuifolia* Benth.	
		Sojae Semen Praeparatum	*Glycine max* (L.) Merr.	
		Arctii Fructus	*Arctium lappa* L.	
Yu-Ping-Feng-San	N/A	Saposhnikoviae Radix	*Saposhnikovia divaricata* (Turcz. ex Ledeb.) Schischk.	(Huang et al., 2020; Li et al., 2020)
		Astragali Radix	*Astragalus mongholicus* Bunge	
		Atractylodis Macrocephalae Rhizoma	*Atractylodes macrocephala* Koidz.	
Sang-Ju	N/A	Mori Folium	*Morus alba* L.	(Huang et al., 2020; Li et al., 2020)
		Chrysanthemi Flos	*Chrysanthemum* × *morifolium* (Ramat.) Hemsl.	
		Almond	*Prunus armeniaca* L.	
		Forsythiae Fructus	*Forsythia suspensa* (Thunb.) Vahl	
		Menthae Haplocalycis Herba	*Mentha canadensis* L.	
		Platycodonis Radix	*Platycodon grandiflorum* (Jacq.) A. DC.	
		Glycyrrhizae Radix Et Rhizoma	*Glycyrrhiza inflata* Batalin	
		Phragmitis Rhizoma	*Phragmites australis* subsp. australis	
Shuang-Huang-Lian	N/A	Lonicerae Japonicae Flos	*Lonicera Japonica* Thunb.	(Hirano and Murakami, 2020)
		Scutellariae Radix	*Scutellaria baicalensis* Georgi	
		Forsythiae Fructus	*Forsythia suspensa* (Thunb.) Vahl	
Ma-Xing-Shi-Gan	N/A	Ehedraep Herba	*Ephedra sinica* Stapf	(Li et al., 2020; Yang et al., 2020)
		Almond	*Prunus armeniaca* L.	
		Glycyrrhizae Radix Et Rhizoma	*Glycyrrhiza inflata* Batalin	
		Gypsum Fibrosum[†]		
Bai-He-Gu-Jin	N/A	Rehmanniae Radix	*Rehmannia glutinosa* (Gaertn.) DC.	(Huang et al., 2020; Li et al., 2020)
		Angelicae Sinensis Radix	*Angelica sinensis* (Oliv.) Diels	
		Paeoniae Radix Alba	*Paeonia lactiflora* Pall.	
		Glycyrrhizae Radix Et Rhizoma	*Glycyrrhiza inflata* Batalin	
		Platycodonis Radix	*Platycodon grandiflorum* (Jacq.) A. DC.	
		Scrophulariae Radix	*Scrophularia ningpoensis* Hemsl.	
		Fritillaria Thunbergii Bulbus	*Fritillaria thunbergii* Miq.	
		Ophiopogonis Radix	*Ophiopogon japonicus* (Thunb.) Ker Gawl.	
		Lilii Bulbus	*Lilium lancifolium* Thunb.	
Ren-Shen-Bai-Du	N/A	Chinese Thorawax Root. Glycyrrhizae Radix Et Rhizoma	*Bupleurum scorzonerifolium* Willd. *Glycyrrhiza inflata* Batalin	(Xian et al., 2020)

(Continued)

TABLE 3 | Continued

Herbal Medicines	Affected Pathways Potential Targets	Composition		Ref.
		Herbal components	Original Species	
		Incised Notopterygium Rhizome Root	*Hansenia forbesii* (H.Boissieu) Pimenov & Kljuykov	
		Doubleteeth Angelicae Root	*Angelica biserrata* (R.H.Shan & C.Q.Yuan) C.Q.Yuan & R.H.Shan	
		Chinese Thorawax Root	*Bupleurum scorzonerifolium* Willd.	
		Common Hogfennel Root	*Angelica decursiva* (Miq.) Franch. & Sav.	
		Chuanxiong Rhizoma	*Conioselinum anthriscoides* 'Chuanxiong'	
		Submature Bitter Orange	*Citrus* × *aurantium* L.	
		Menthae Haplocalycis Herba	*Mentha canadensis* L.	
		Poria mushroom[§]	*Poria cocos* (Schw.) Wolf	
		Platycodonis Radix	*Platycodon grandiflorum* (Jacq.) A. DC.	
		Glycyrrhizae Radix Et Rhizoma	*Glycyrrhiza inflata* Batalin	
		Ginger	*Zingiber officinale* Roscoe	

[†]*Mineral products;* [§]*Fungus-derived products; *Animal-derived products; Components without labelling are all plant-derived products.*

herbal ingredients were identified as following: Glycyrrhizae Radix Et Rhizoma (*Glycyrrhiza inflata* Batalin), Forsythiae Fructus [*Forsythia suspensa* (Thunb.) Vahl], Lonicerae Japonicae Flos (*Lonicera Japonica* Thunb.), Scutellariae Radix *(Scutellaria baicalensis* Georgi), Platycodonis Radix [*Platycodon grandiflorum* (Jacq.) A. DC.], Menthae Haplocalycis Herba (*Mentha canadensis* L.), Gardeniae Fructus (*Gardenia jasminoides* J.Ellis), Gypsum Fibrosum, and Moschus (*Moschus anhuiensis*). Furthermore, we performed integrated network analysis upon those top nine herbal ingredients to identify eighteen lead compounds with greatest drug-likeness potential (**Figures 2B, C**). It showed that ten of those compounds are flavonoid derivatives which possess either flavone

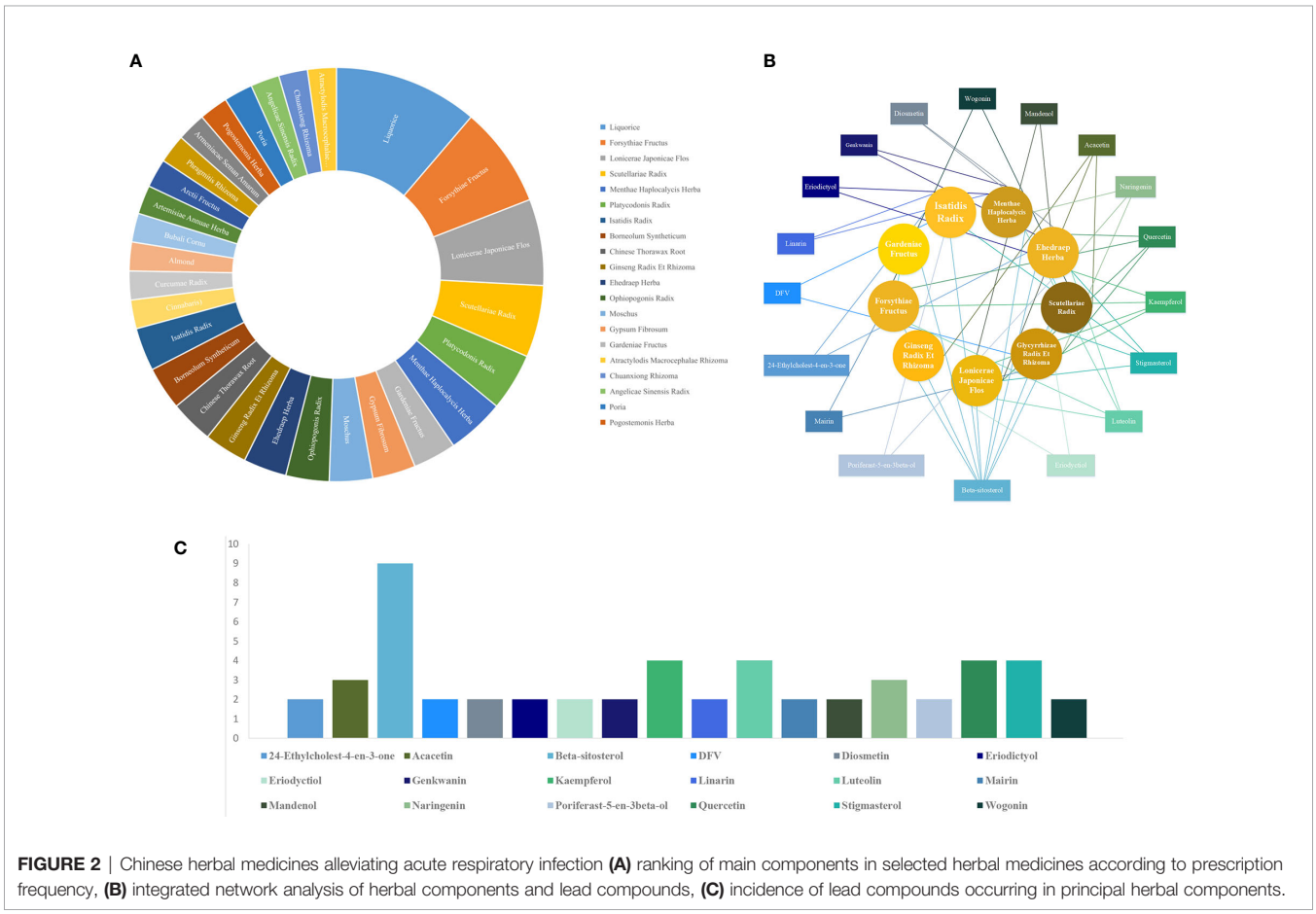

FIGURE 2 | Chinese herbal medicines alleviating acute respiratory infection **(A)** ranking of main components in selected herbal medicines according to prescription frequency, **(B)** integrated network analysis of herbal components and lead compounds, **(C)** incidence of lead compounds occurring in principal herbal components.

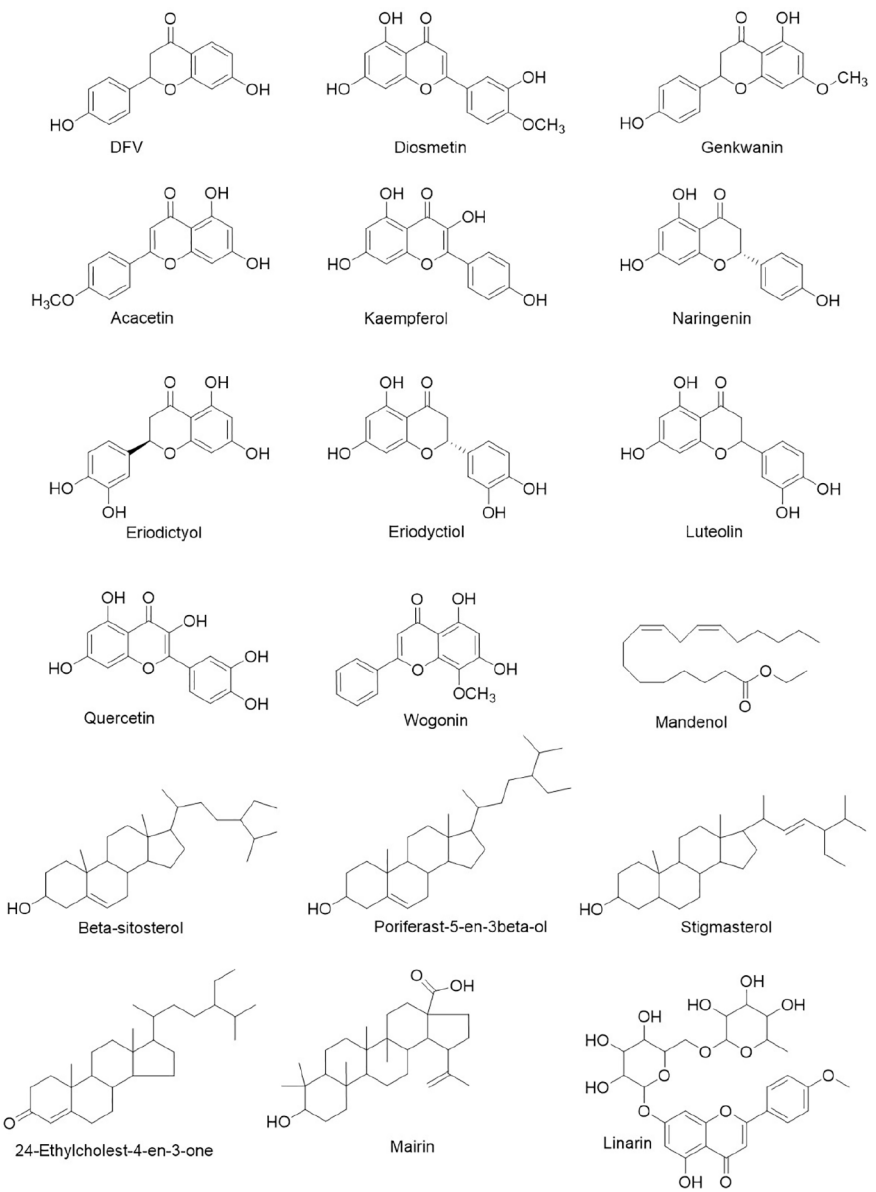

FIGURE 3 | Lead compounds with greatest drug-likeness isolated from herbs for COVID-19.

or flavanone core. It is known that many flavonoid compounds exhibit a broad spectrum of biological activities including cell membrane protective function, antioxidant activity *via* inhibition of xanthine oxidase or nitric oxide synthase as well as anti-inflammatory activity *via* inhibition of leukotriene (Verma and Pratap, 2010). Based on our integrated network analysis, COX-2 and MAPK mediated inflammatory pathways play prominent role in the therapeutic effect of these eighteen herb-derived compounds. Since many of those compounds have been historically used in dietary supplements, its toxicity is largely negligible, which makes them safe to be employed as prophylaxis against COVID-19 for large population.

CONCLUSION AND PERSPECTIVE

Since early 2020, numerous pharma companies collaborating with academics or state-sponsored research institute have joined the race of therapy development to combat wildly spreading COVID-19. As of July 2020, a range of various therapeutics has been discovered, from small molecules, neutralizing antibodies, to bioengineered products. Aided with computational chemistry and virtual screening, researchers has established a large library of novel small molecules, showing favorable binding affinity with validated drug targets (Kupferschmidt and Cohen, 2020; Tahir ul Qamar et al., 2020), but the efficacy and toxicity of those lead

compounds need further testing in both preclinical models and human subjects. Nevertheless, at this point, it seems optimizing a novel lead for COVID-19 is not a preferred option as typically the whole pipeline of new drug development takes years even if FDA grants expediated approval, and it is unimaginable for the public to endure another prolonged era of economic and public health hardship. As for neutralizing antibody, the situation is also gloomy, because establishing manufacturing infrastructure and managing supply chain of biologics are much more nuanced and demanding than small molecular drug. Thanks to the recent advances in bioengineering, several nanoengineered therapeutics have been designed to treat COVID-19. Zhang et al. recently reported novel nano-sponges made of the plasma membranes derived from human lung epithelial type II cells (Zhang Q. et al., 2020). These nano-sponges display the membrane receptors recognizable to SARS-CoV-2. They showed that, following incubation with their nano-sponges, SARS-CoV-2 lost infectability. Huo et al. produced an array of nanobodies that bind SARS-CoV-2 receptor and block its interaction with ACE2 (Huo et al., 2020). Though such studies open exciting new path for therapeutics discovery, lack of clinical data stops them from becoming relevant in the short terms. Regretfully, to date there is no approved drug for any kinds of human coronavirus infection, including SARS-CoV, MERS-CoV, or SARS-CoV-2.

Since the outcome of current therapeutics in severe/critical COVID-19 patients are still debatable, prevention rather than treatment becomes more important to restrain this pandemic. Blocking the entry of SARS-CoV-2 and suppressing infection at initial stage are considered as more practical strategy (**Figure 4**). Vaccine has been historically used to prevent influenza. Today, antibody responses and serum-neutralizing activity are standard parameters used to evaluate the short-term efficacy of vaccine (Jackson et al., 2020), whereas the long-term effectiveness cannot be truly determined until the vaccinated population show acquired immunity against infection when exposed to the virus of interest without intervention. Besides, recent clinical report pointed out that neutralizing antibody level in patients who experienced asymptomatic SARS-CoV-2 infection declined rapidly after recovery (Long et al., 2020), which leads to a concerning question how long vaccination is able to maintain its protection against COVID-19. In terms of pre-exposure/post-exposure prophylaxis, NIH recently launched trials to test the preventive effectiveness of monoclonal antibody. While the trial is ongoing, intravenous (i.v.) injection of antibody in large population brings up a lot of feasibility issues. Even the prophylactic efficacy of remdesivir was proven to be better than its therapeutic efficacy in rhesus macaque model, current administration route of remdesivir is limited to i.v. infusion that restricts its use in non-hospitalized population (Administration).

Natural products and herbal medicine have long track record to treat respiratory infection and many have been approved as drugs, over-the-counter nutrition or food additives. Those products generally have satisfactory safety profiles. The minimal toxicity makes natural product and herbal medicines ideal prophylactic candidates for long-term use. Based on recent *in silico* results, an array of natural products has been found highly potent in blocking enzyme function and membrane receptors of human coronavirus. Moderate dosing of such bioactive compounds may prevent or at least slow down SARS-CoV-2 infection process. In addition, the progression of COVID-19 is featured with uncontrolled inflammation, like cytokine release syndrome, so anti-inflammatory herbs will be a potential tool to suppress such fatal symptom. The stability of natural products and herbal medicines in human gastrointestinal tract is barely an issue. The low pH in gastric environment, digestive enzymes, and gut microbiome have less impact on the bioavailability of natural products and herbs compared to antibody and other prophylactics. This advantage makes oral dosing rather than IV administration possible. In terms of availability, the ease of production expansion realizes the mass deployment of herbal medicines to big population, while the large-scale synthesis of monoclonal antibody and remdesivir is incredibly challenging. In this day and age, a safe, effective and stable form of oral dosage

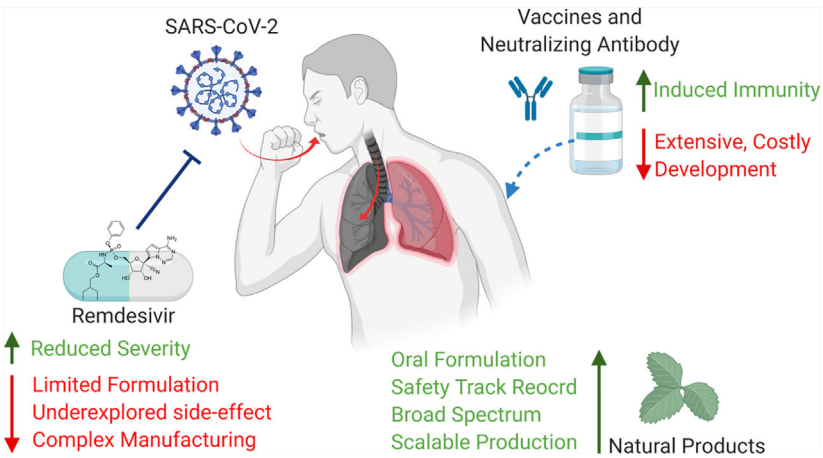

FIGURE 4 | Pros and cons of current prevention of COVID-19 (Created with BioRender.com).

prophylactics will be a strong asset for us to overcome COVID-19 pandemic.

AUTHOR CONTRIBUTIONS

Conceptualization: GT, JC, and JH. Writing—original draft preparation: GT, JL, and JC. Writing—review and editing: GT, JL, JC, and JH. Visualization: ZH, JH. Supervision: GT and JH. Funding acquisition: J-xC and JH. All authors contributed to the article and approved the submitted version.

FUNDING

This work is supported by the Huang Zhendong Research Fund for Traditional Chinese Medicine of Jinan University (No. 201911).

ACKNOWLEDGMENTS

We greatly appreciate the comments from Michael Heinrich, University College London (UCL) School of Pharmacy for manuscript preparation.

REFERENCES

Administration, D *Fact Sheet For Health Care Providers Emergency Use Authorization (EUA) of REMDESIVIR (GS-5734TM)*. Available at: https://www.fda.gov/emergency- (Accessed July 16, 2020).

Bai, Y., Yao, L., Wei, T., Tian, F., Jin, D. Y., Chen, L., et al. (2020). Presumed Asymptomatic Carrier Transmission of COVID-19. *JAMA J. Am. Med. Assoc.* 323, 1406–1407. doi: 10.1001/jama.2020.2565

BioNTech SE. (2020). *Study to Describe the Safety, Tolerability, Immunogenicity, and Potential Efficacy of RNA Vaccine Candidates Against COVID-19 in Healthy Adults ClinicalTrials.gov*. Available at: https://clinicaltrials.gov/ct2/show/NCT04368728 (Accessed July 14, 2020).

Cao, B., Wang, Y., Wen, D., Liu, W., Wang, J., Fan, G., et al. (2020). A trial of lopinavir-ritonavir in adults hospitalized with severe covid-19. *N. Engl. J. Med.* 382, 1787–1799. doi: 10.1056/NEJMoa2001282

Casadevall, A., and Pirofski, L. A. (2020). The convalescent sera option for containing COVID-19. *J. Clin. Invest.* 130, 1545–1548. doi: 10.1172/JCI138003

Chen, C.-N., Lin, C. P. C., Huang, K.-K., Chen, W.-C., Hsieh, H.-P., Liang, P.-H., et al. (2005). Inhibition of SARS-CoV 3C-like ProteaseActivity by Theaflavin–3,3'–digallate (TF3). *Evid. Based Complementary Altern. Med.* 2 (2), 209–215. doi: 10.1093/ecam/neh081

Corbett, K. S., Edwards, D., Leist, S. R., Abiona, O. M., Boyoglu-Barnum, S., Gillespie, R. A., et al. (2020). SARS-CoV-2 mRNA Vaccine Development Enabled by Prototype Pathogen Preparedness. *bioRxiv* 2020, 2020.06.11.145920. doi: 10.1101/2020.06.11.145920

Corrao, S. (2020) *Use of Ascorbic Acid in Patients With COVID 19 - Full Text View - ClinicalTrials.gov*. Available at: https://clinicaltrials.gov/ct2/show/NCT04323514 (Accessed July 14, 2020).

CureVac Inc. (2020). *CureVac Receives Regulatory Approval from German and Belgian Authorities to Initiate Phase 1 Clinical Trial of its SARS–CoV–2 Vaccine Candidate*. Available at: www.curevac.com (Accessed July 14, 2020).

de Wit, E., Feldmann, F., Cronin, J., Jordan, R., Okumura, A., Thomas, T., et al. (2020). Prophylactic and therapeutic remdesivir (GS-5734) treatment in the rhesus macaque model of MERS-CoV infection. *Proc. Natl. Acad. Sci. U. S. A.* 117, 6771–6776. doi: 10.1073/pnas.1922083117

del Amo, J., Polo, R., Moreno, S., Díaz, A., Martínez, E., Arribas, J. R., et al. (2020). Incidence and Severity of COVID-19 in HIV-Positive Persons Receiving Antiretroviral Therapy. *Ann. Intern. Med.* doi: 10.7326/M20-3689

Ding, Y., Zeng, L., Li, R., Chen, Q., Zhou, B., Chen, Q., et al. (2017). The Chinese prescription lianhuaqingwen capsule exerts anti-influenza activity through the inhibition of viral propagation and impacts immune function. *BMC Complement. Altern. Med.* 17, 1–11. doi: 10.1186/s12906-017-1585-7

El-Aziz Abd, N. M., Mohamed G., S., Awad, O. M. E., and El-Sohaimy, S. A. (2020). Inhibition of COVID-19 RNA-Dependent RNA Polymerase by Natural Bioactive Compounds: Molecular Docking Analysis. *Preprint*. doi: 10.21203/RS.3.RS-25850/V1

Elfiky, A. A. (2020). Natural products may interfere with SARS-CoV-2 attachment to the host cell. *J. Biomol. Struct. Dyn.* 1–10. doi: 10.1080/07391102.2020.1761881

Folegatti, P. M, Ewer, K. J., Aley, P. K., Angus, B., Becker, S., Belij-Rammerstorfer, S., et al. (2020) *A Study of a Candidate COVID-19 Vaccine (COV001) ClinicalTrials.gov*. Available at: https://clinicaltrials.gov/ct2/show/NCT04324606 (Accessed July 14, 2020).

Gallelli, L. (2020). *Escin in Patients With Covid–19 Infection – Full Text View – ClinicalTrials.gov*. Available at: https://clinicaltrials.gov/ct2/show/NCT04322344 (Accessed July 14, 2020).

Gao, Q., Bao, L., Mao, H., Wang, L., Xu, K., Yang, M., et al. (2020). Development of an inactivated vaccine candidate for SARS-CoV-2. *Sci. (80)* 369, eabc1932. doi: 10.1126/science.abc1932

Gao, Y., Yan, L., Huang, Y., Liu, F., Zhao, Y., Cao, L., et al. (2020). Structure of the RNA-dependent RNA polymerase from COVID-19 virus. *Sci. (80)* 368, 779–782. doi: 10.1126/science.abb7498

Glatthaar-Saalmüller, B., Rauchhaus, U., Rode, S., Haunschild, J., and Saalmüller, A. (2011). Antiviral activity in vitro of two preparations of the herbal medicinal product Sinupret® against viruses causing respiratory infections. *Phytomedicine* 19, 1–7. doi: 10.1016/j.phymed.2011.10.010

Goswami, D., Kumar, M., Ghosh, S. K., and Das, A. (2020). Natural Product Compounds in Alpinia officinarum and Ginger are Potent SARS-CoV-2 Papain-like Protease Inhibitors. *chemRxiv*. doi: 10.26434/chemrxiv.12071997.v1

Gray, P. E., and Belessis, Y. (2020). The use of Traditional Chinese Medicines to treat SARS-CoV-2 may cause more harm than good. *Pharmacol. Res.* 156:104776. doi: 10.1016/j.phrs.2020.104776

Gyebi, G. A., Ogunro, O. B., Adegunloye, A. P., Ogunyemi, O. M., and Afolabi, S. O. (2020). Potential inhibitors of coronavirus 3-chymotrypsin-like protease ($3CL^{pro}$): an *in silico* screening of alkaloids and terpenoids from African medicinal plants. *J. Biomol. Struct. Dyn.* 1–13. doi: 10.1080/07391102.2020.1764868

Halperin, S. A., Langley, J. M. Blood and Transplant, Plasma programme (2020) *Phase I/II Clinical Trial of Recombinant Novel Coronavirus Vaccine (Adenovirus Type 5 Vector) in Canada - Full Text View - ClinicalTrials.gov*. Available at: https://clinicaltrials.gov/ct2/show/NCT04398147 (Accessed July 14, 2020).

Hansen, J., Baum, A., Pascal, K. E., Russo, V., Giordano, S., Wloga, E., et al. (2020). Studies in humanized mice and convalescent humans yield a SARS-CoV-2 antibody cocktail. *Sci. (80)* 0827, eabd0827. doi: 10.1126/science.abd0827

Hirano, T., and Murakami, M. (2020). COVID-19: A New Virus, but a Familiar Receptor and Cytokine Release Syndrome. *Immunity* 52, 731–733. doi: 10.1016/j.immuni.2020.04.003

Ho, T. Y., Wu, S. L., Chen, J. C., Li, C. C., and Hsiang, C. Y. (2007). Emodin blocks the SARS coronavirus spike protein and angiotensin-converting enzyme 2 interaction. *Antiviral Res.* 74, 92–101. doi: 10.1016/j.antiviral.2006.04.014

Hoffmann, M., Kleine-Weber, H., Schroeder, S., Krüger, N., Herrler, T., Erichsen, S., et al. (2020). SARS-CoV-2 Cell Entry Depends on ACE2 and TMPRSS2 and Is Blocked by a Clinically Proven Protease Inhibitor. *Cell* 181, 271–280.e8. doi: 10.1016/j.cell.2020.02.052

Horby, P., Lim, W. S., Emberson, J. R., Mafham, M., Bell, J. L., Linsell, L., et al. (2020) *No clinical benefit from use of lopinavir-ritonavir in hospitalised COVID-19 patients studied in RECOVERY — RECOVERY Trial*. Available at: https://clinicaltrials.gov/ct2/show/NCT04381936 (Accessed July 13, 2020).

Huang, Y. F., Bai, C., He, F., Xie, Y., and Zhou, H. (2020). Review on the potential action mechanisms of Chinese medicines in treating Coronavirus Disease 2019 (COVID-19). *Pharmacol. Res.* 158:104939. doi: 10.1016/j.phrs.2020.104939

Huo, J., Le Bas, A., Ruza, R. R., Duyvesteyn, H. M. E., Mikolajek, H., Malinauskas, T., et al. (2020). Neutralizing nanobodies bind SARS-CoV-2 spikeRBD and

block interaction with ACE2. *Nat. Struct. Mol. Biol.* 27 (9), 846–854. doi: 10.1038/s41594-020-0469-6

Inovio Pharmaceuticals (2020). *Inovio Pharmaceuticals, Inc. - INOVIO"s COVID-19 DNA Vaccine INO-4800 Demonstrates Robust Neutralizing Antibody and T Cell Immune Responses in Preclinical Models. 1–5*. Available at: http://ir.inovio.com/news-releases/news-releases-details/2020/INOVIOs-COVID-19-DNA-Vaccine-INO-4800-Demonstrates-Robust-Neutralizing-Antibody-and-T-Cell-Immune-Responses-in-Preclinical-Models/default.aspx (Accessed July 13, 2020).

ISRCTN - ISRCTN17072692 *Clinical trial to assess the safety of a coronavirus vaccine in healthy men and women*. Available at: http://www.isrctn.com/ISRCTN17072692 (Accessed July 14, 2020).

Jackson, L. A., Anderson, E. J., Rouphael, N. G., Roberts, P. C., Makhene, M., Coler, R. N., et al. (2020). An mRNA Vaccine against SARS-CoV-2 — Preliminary Report. *N. Engl. J. Med*. doi: 10.1056/NEJMoa2022483. NEJMoa 2022483.

Janssen Pharmaceutica, N. V. (2020). *A Study to Evaluate the Efficacy and Safety of Sirukumab in Confirmed Severe or Critical Confirmed Coronavirus Disease (COVID)-19 – Full Text View – ClinicalTrials.gov*. Available at: https://clinicaltrials.gov/ct2/show/NCT04380961 (Accessed July 14, 2020).

Kim, J. W., Ha, T. K. Q., Cho, H., Kim, E., Shim, S. H., Yang, J. L., et al. (2017). Antiviral escin derivatives from the seeds of Aesculus turbinata Blume (Japanese horse chestnut). *Bioorg. Med. Chem. Lett.* 27, 3019–3025. doi: 10.1016/j.bmcl.2017.05.022

Kim, J. Y., Kim, Y., Park, S. J., Kim, I. K., Choi, Y. K., and Kim, S. H. (2018). Safe, high-throughput screening of natural compounds of MERS-CoV entry inhibitors using a pseudovirus expressing MERS-CoV spike protein. *Int. J. Antimicrob. Agents* 52, 730–732. doi: 10.1016/j.ijantimicag.2018.05.003

Ko, M., Chang, S. Y., Byun, S. Y., Choi, I., d'Alexandry d'Orengiani, A.-L. P. H., Shum, D., et al. (2020). Screening of FDA-approved drugs using a MERS-CoV clinical isolate from South Korea identifies potential therapeutic options for COVID-19. *bioRxiv* 2020.02.25.965582. doi: 10.1101/2020.02.25.965582

Kong, Q., Wu, Y., Gu, Y., Lv, Q., Qi, F., Gong, S., et al. (2020). Analysis of the molecular mechanism of Pudilan (PDL) treatment for COVID-19 by network pharmacology tools. *Biomed. Pharmacother.* 128:110316. doi: 10.1016/j.biopha.2020.110316

Koshak, A., Koshak, E. A., Mobeireek, A. F., Badawi, M. A., Wali, S. O., et al. (2020) *Nigella Sativa in COVID-19 – Full Text View – ClinicalTrials.gov*. Available at: https://clinicaltrials.gov/ct2/show/NCT04401202 (Accessed July 14, 2020).

Kreer, C., Zehner, M., Weber, T., Ercanoglu, M. S., Gieselmann, L., Rohde, C., et al. (2020). Longitudinal Isolation of Potent Near-GermlineSARS-CoV-2-Neutralizing Antibodies from COVID-19 Patients. *Cell* 182 (4), 843–854.e12. doi: 10.1016/j.cell.2020.06.044

Kumar, V., Dhanjal, J. K., Bhargava, P., Kaul, A., Wang, J., Zhang, H., et al. (2020). Withanone and Withaferin-A are predicted to interact with transmembrane protease serine 2 (TMPRSS2) and block entry of SARS-CoV-2 into cells. *J. Biomol. Struct. Dyn.* 1–13. doi: 10.1080/07391102.2020.1775704

Kupferschmidt, K., and Cohen, J. (2020). Race to find COVID-19 treatments accelerates. *Science* 367 (6485), 1412 LP–1413. doi: 10.1126/science.367.6485.1412

Lan, M., Li, H., Tao, G., Lin, J., Lu, M., Yan, R., et al. (2020). Effects of four bamboo derived flavonoids onadvanced glycation end products formation in vitro. *J. Funct. Foods* 71, 103976. doi: 10.1016/j.jff.2020.103976

Li, J.-P., Liu, Y., Guo, J.-M., Shang, E.-X., Zhu, Z.-H., Zhu, K. Y., et al. (2017). A Comprehensive Strategy to Evaluate Compatible Stability of Chinese Medicine Injection and Infusion Solutions Based on Chemical Analysis and Bioactivity Assay. *Front. Pharmacol.* 8:833. doi: 10.3389/fphar.2017.00833

Li, Y., Liu, X., Guo, L., Li, J., Zhong, D., Zhang, Y., et al. (2020). Traditional Chinese herbal medicine for treating novel coronavirus (COVID-19) pneumonia: Protocol for a systematic review and meta-Analysis. *Syst. Rev.* 9, 75. doi: 10.1186/s13643-020-01343-4

Logunov, D. Y., Dolzhikova, I. V., Zubkova, O. V., Tukhvatullin, A.II, Shcheblyakov, D. V., Dzharullaeva, A. S., et al. (2020). Safety and immunogenicity of an rAd26 and rAd5 vector-based heterologous prime-boost COVID-19 vaccine in two formulations: two open, non-randomised phase 1/2 studies from Russia. *Lancet* 396 (10255), 887–897. doi: 10.1016/S0140-6736(20)31866-3

Long, Q. X., Tang, X. J., Shi, Q. L., Li, Q., Deng, H. J., Yuan, J., et al. (2020). Clinical and immunological assessment of asymptomatic SARS-CoV-2 infections. *Nat. Med.* 26 (8), 1200–1204. doi: 10.1038/s41591-020-0965-6

Ma, Q., Pan, W., Li, R., Liu, B., Li, C., Xie, Y., et al. (2020). Liu Shen capsule shows antiviral and anti-inflammatory abilities against novel coronavirus SARS-CoV-2 via suppression of NF-κB signaling pathway. *Pharmacol. Res.* 158:104850. doi: 10.1016/j.phrs.2020.104850

Mehta, P., McAuley, D. F., Brown, M., Sanchez, E., Tattersall, R. S., Manson, J. J., et al. (2020). COVID-19: consider cytokine storm syndromes and immunosuppression. *Lancet* 395, 1033–1034. doi: 10.1016/S0140-6736(20)30628-0

Michaelis, M., Doerr, H. W., and Cinatl, J. (2011). Investigation of the influence of EPs® 7630, a herbal drug preparation from Pelargonium sidoides, on replication of a broad panel of respiratory viruses. *Phytomedicine* 18, 384–386. doi: 10.1016/j.phymed.2010.09.008

Michelini, F. M., Alché, L. E., and Bueno, C. A. (2018). Virucidal, antiviral and immunomodulatory activities of β-escin and *Aesculus hippocastanum* extract. *J. Pharm. Pharmacol.* 70, 1561–1571. doi: 10.1111/jphp.13002

Mille, J. K., and Whittaker, G. R. (2014). Host cell entry of Middle East respiratory syndrome coronavirus after two-step, furin-mediated activation of the spike protein. *Proc. Natl. Acad. Sci. U. S. A.* 111, 15214–15219. doi: 10.1073/pnas.1407087111

Millet, J. K., Séron, K., Labitt, R. N., Danneels, A., Palmer, K. E., Whittaker, G. R., et al. (2016). Middle East respiratory syndrome coronavirus infection is inhibited by griffithsin. *Antiviral Res.* 133, 1–8. doi: 10.1016/j.antiviral.2016.07.011

Moderna Inc. (2020). Moderna Announces Positive Interim Phase 1 Data for its mRNA Vaccine (mRNA-1273) Against Novel Coronavirus. Available at: https://www.businesswire.com/news/home/20200518005348/en/ [Accessed September 7th, 2020]

ModernaTX. Inc. (2020). *A Study to Evaluate Efficacy, Safety, and Immunogenicity of mRNA-1273 Vaccine in Adults Aged 18 Years and Older to Prevent COVID–19 ClinicalTrials.gov*. Available at: https://clinicaltrials.gov/ct2/show/NCT04470427?term=NCT04470427 (Accessed September 10, 2020).

Mori, T., O'Keefe, B. R., Sowder, R. C., Bringans, S., Gardella, R., Berg, S., et al. (2005). Isolation and characterization of Griffithsin, a novel HIV-inactivating protein, from the red alga Griffithsia sp. *J. Biol. Chem.* 280, 9345–9353. doi: 10.1074/jbc.M411122200

Müller, C., Schulte, F. W., Lange-Grünweller, K., Obermann, W., Madhugiri, R., Pleschka, S., et al. (2018). Broad-spectrum antiviral activity of the eIF4A inhibitor silvestrol against corona- and picornaviruses. *Antiviral Res.* 150, 123–129. doi: 10.1016/j.antiviral.2017.12.010

Mulligan, M. J., Lockhart, S., Neuzil, K., Raabe, V., Bailey, R., and Kena, A. (2020a). Phase 1/2 Study to Describe the Safety and Immunogenicity of a COVID-19 RNA Vaccine Candidate (BNT162b1) in Adults 18 to 55 Years of Age: Interim Report Mark. *medrxiv*, 1–16. doi: 10.1101/2020.06.30.20142570

Mulligan, M. J., Lyke, K. E., Kitchin, N., Absalon, J., Gurtman, A., Lockhart, S., et al. (2020b). Final-submission v2.0 P a g e | 1 Phase 1/2 Study to Describe the Safety and Immunogenicity of a COVID-19 RNA Vaccine Candidate (BNT162b1) in Adults 18 to 55 Years of Age: Interim Report. *medRxiv*. doi: 10.1101/2020.06.30.20142570. 2020.06.30.20142570.

Narimanian, M., Badalyan, M., Panosyan, V., Gabrielyan, E., Panossian, A., Wikman, G., et al. (2005). Randomized trial of a fixed combination (KanJang®) of herbal extracts containing Adhatoda vasica, Echinacea purpurea and Eleutherococcus senticosus in patients with upper respiratory tract infections. *Phytomedicine* 12, 539–547. doi: 10.1016/j.phymed.2004.10.001

NHS Blood and Transplant. *Plasma programme - COVID-19 research and trials - NHS Blood and Transplant*. Available at: https://www.nhsbt.nhs.uk/covid-19-research/plasma-programme/ (Accessed July 13, 2020).

Novavax Inc. (2020) *Evaluation of the Safety and Immunogenicity of a SARS-CoV-2 rS (COVID- 19) Nanoparticle Vaccine With/Without Matrix–M Adjuvant ClinicalTrials.gov*. Available at: https://clinicaltrials.gov/ct2/show/NCT04368988 (Accessed July 14, 2020).

Oxford COVID-19 vaccine to begin phase II/III human trials | University of Oxford. Available at: https://www.ox.ac.uk/news/2020-05-22-oxford-covid-19-vaccine-begin-phase-iiiii-human-trials (Accessed July 13, 2020).

Patridge, E., Gareiss, P., Kinch, M. S., and Hoyer, D. (2016). An analysis of FDA-approved drugs: Natural products and their derivatives. *Drug Discovery Today* 21, 204–207. doi: 10.1016/j.drudis.2015.01.009

Polo, R., and Hernan, M. (2020) *Randomized Clinical Trial for the Prevention of SARS-CoV-2 Infection (COVID-19) in Healthcare Personnel - Full Text View - ClinicalTrials.gov*. Available at: https://clinicaltrials.gov/ct2/show/NCT04334928 (Accessed July 13, 2020).

Robbiani, D. F., Gaebler, C., Muecksch, F., Lorenzi, J. C. C., Wang, Z., Cho, A., et al. (2020). Convergent Antibody Responses to SARS-CoV-2 Infection in Convalescent Individuals. *BioRxiv* 2020.05.13.092619. doi: 10.1101/2020.05.13.092619

Rogers, T. F., Zhao, F., Huang, D., Beutler, N., Burns, A., He, W., et al. (2020). Isolation of potent SARS-CoV-2 neutralizingantibodies and protection from disease in a small animal model. *Science* 369 (6506), 956 LP–963. doi: 10.1126/science.abc7520. eabc7520

Ruan, Z., Liu, C., Guo, Y., He, Z., Huang, X., Jia, X., et al. (2020). SARS-CoV-2 and SARS-CoV: Virtual Screening ofPotential inhibitors targeting RNA-dependent RNA polymerase activity (NSP12). *J. Med. Virol* 1–12. doi: 10.1002/jmv.26222

Runfeng, L., Yunlong, H., Jicheng, H., Weiqi, P., Qinhai, M., Yongxia, S., et al. (2020). Lianhuaqingwen exerts anti-viral and anti-inflammatory activity against novel coronavirus (SARS-CoV-2). *Pharmacol. Res.* 156:104761. doi: 10.1016/j.phrs.2020.104761

Sheahan, T. P., Sims, A. C., Leist, S. R., Schäfer, A., Won, J., Brown, A. J., et al. (2020). Comparative therapeutic efficacy of remdesivir and combination lopinavir, ritonavir, and interferon beta against MERS-CoV. *Nat. Commun.* 11, 1–14. doi: 10.1038/s41467-019-13940-6

Sheridan, C. (2020). Convalescent serum lines up as first-choice treatment for coronavirus. *Nat. Biotechnol.* 38, 655–658. doi: 10.1038/d41587-020-00011-1

Sinovac Biotech Co. Ltd. (2020). *Safety and Immunogenicity Study of Inactivated Vaccine for Prophylaxis of SARS CoV-2 Infection (COVID-19) - Full Text View - ClinicalTrials.gov*. Available at: https://clinicaltrials.gov/ct2/show/NCT04352608 (Accessed July 14, 2020).

Smith, T. R. F., Patel, A., Ramos, S., Elwood, D., Zhu, X., Yan, J., et al. (2020). Immunogenicity of a DNA vaccine candidate for COVID-19. *Nat. Commun.* 11, 1–13. doi: 10.1038/s41467-020-16505-0

Su, S., Wong, G., Shi, W., Liu, J., Lai, A. C. K., Zhou, J., et al. (2016). Epidemiology, Genetic Recombination, and Pathogenesis of Coronaviruses. *Trends Microbiol.* 24, 490–502. doi: 10.1016/j.tim.2016.03.003

Tahir ul Qamar, M., Alqahtani, S. M., Alamri, M. A., and Chen, L. L. (2020). Structural basis of SARS-CoV-2 3CLpro andanti-COVID-19 drug discovery from medicinal plants. *J. Pharm. Anal.* 10 (4), 313–319. doi: 10.1016/j.jpha.2020.03.009

Tao, G., Dagher, F., Moballegh, A., and Ghose, R. (2020). Role of Oxidative Stress in the Efficacy and Toxicity of Herbal Supplements. *Curr. Opin. Toxicol.* 20–21, 36–40. doi: 10.1016/j.cotox.2020.04.004

Tao, G. Y., Liu, J., Jung, J. H., Guo, W., Wen, X. Q., and Liu, Y. (2016). Compounds from a jellyfish-derived fungus Aspergillus fumigates. *Nat. Prod. Sci.* 22, 82–86. doi: 10.20307/nps.2016.22.2.82

Todt, D., Moeller, N., Praditya, D., Kinast, V., Friesland, M., Engelmann, M., et al. (2018). The natural compound silvestrol inhibits hepatitis E virus (HEV) replication in vitro and in vivo. *Antiviral Res.* 157, 151–158. doi: 10.1016/j.antiviral.2018.07.010

U.S. Food & Drug Administration (2020) *Recommendations for Investigational COVID-19 Convalescent Plasma | FDA*. Available at: https://www.fda.gov/vaccines-blood-biologics/investigational-new-drug-ind-or-device-exemption-ide-process-cber/recommendations-investigational-covid-19-convalescent-plasma (Accessed July 13, 2020).

van Doremalen, N., Lambe, T., Spencer, A., Belij-Rammerstorfer, S., Purushotham, J. N., Port, J. R., et al. (2020). ChAdOx1 nCoV-19 vaccination prevents SARS-CoV-2 pneumonia in rhesus macaques. *bioRxiv* 2020.05.13.093195. doi: 10.1101/2020.05.13.093195

Verma, A. K., and Pratap, R. (2010). The biological potential of flavones. *Nat. Prod. Rep.* 27, 1571–1593. doi: 10.1039/c004698c

Walls, A. C., Park, Y. J., Tortorici, M. A., Wall, A., McGuire, A. T., and Veesler, D. (2020). Structure, Function, and Antigenicity of the SARS-CoV-2 Spike Glycoprotein. *Cell* 181, 281–292.e6. doi: 10.1016/j.cell.2020.02.058

Wang, C., Li, W., Drabek, D., Okba, N. M. A., van Haperen, R., Osterhaus, A. D. M. E., et al. (2020). A human monoclonal antibody blocking SARS-CoV-2 infection. *Nat. Commun.* 11, 1–6. doi: 10.1038/s41467-020-16256-y

Wang, D., Huang, J., Yeung, A. W. K., Tzvetkov, N. T., Horbańczuk, J. O., Willschke, H., et al. (2020). The Significance of Natural Product Derivatives and Traditional Medicine for COVID-19. *Processes* 8:937. doi: 10.3390/pr8080937

Wang, W., Qin, J.-J., Li, X., Tao, G., Wang, Q., Wu, X., et al. (2018). Prevention of prostate cancer by natural product MDM2 inhibitor GS25: in vitro and in vivo activities and molecular mechanisms. *Carcinogenesis* 39, 1026–1036. doi: 10.1093/carcin/bgy063

Weber, C., and Opatz, T. (2019). "Chapter One - Bisbenzylisoquinoline Alkaloids," in *Alkaloids: Chemistry and Biology*. H.-J. B. T.-T. A. C. and B. Knölker, Eds. (Academic Press Inc) 81, 1–114. doi: 10.1016/bs.alkal.2018.07.001

WHO | Middle East respiratory syndrome coronavirus (MERS-CoV) (2020). (WHO). Available at: http://www.who.int/emergencies/mers-cov/en/ (Accessed July 13, 2020).

World Health Organization. (2020). *Solidarity clinical trial for COVID-19 treatments*. Available at: https://www.who.int/emergencies/diseases/novel-coronavirus-2019/global-research-on-novel-coronavirus-2019-ncov/solidarity-clinical-trial-for-covid-19-treatments (Accessed July 13, 2020).

Wu, C. Y., Jan, J. T., Ma, S. H., Kuo, C. J., Juan, H. F., Cheng, Y. S. E., et al. (2004). Small molecules targeting severe acute respiratory syndrome human coronavirus. *Proc. Natl. Acad. Sci. U. S. A.* 101, 10012–10017. doi: 10.1073/pnas.0403596101

Wu, F., Wang, A., Liu, M., Wang, Q., Chen, J., Xia, S., et al. (2020). Neutralizing antibody responses to SARS-CoV-2in a COVID-19 recovered patient cohort and their implications. *MedRxiv* 2020.03.30.20047365. doi: 10.1101/2020.03.30.20047365

Wu, Y., Wang, F., Shen, C., Peng, W., Li, D., Zhao, C., et al. (2020). A noncompeting pair of human neutralizing antibodies block COVID-19 virus binding to its receptor ACE2. *Science* 368, 1274–1278. doi: 10.1126/science.abc2241

Xian, Y., Zhang, J., Bian, Z., Zhou, H., Zhang, Z., Lin, Z., et al. (2020). Bioactive natural compounds against humancoronaviruses: a review and perspective. *Acta Pharm. Sin. B* 10 (7), 1163–1174. doi: 10.1016/j.apsb.2020.06.002

Xu, J., and Zhang, Y. (2020). Traditional Chinese Medicine treatment of COVID-19. *Complement. Ther. Clin. Pract.* 39:101165. doi: 10.1016/j.ctcp.2020.101165

Yang, R., Liu, H., Bai, C., Wang, Y., Zhang, X., Guo, R., et al. (2020). Chemical composition and pharmacological mechanism of Qingfei Paidu Decoction and Ma Xing Shi Gan Decoction against Coronavirus Disease 2019 (COVID-19): In silico and experimental study. *Pharmacol. Res.* 157:104820. doi: 10.1016/j.phrs.2020.104820

Yu, M. S., Lee, J., Lee, J. M., Kim, Y., Chin, Y. W., Jee, J. G., et al. (2012). Identification of myricetin and scutellarein as novel chemical inhibitors of the SARS coronavirus helicase, nsP13. *Bioorg. Med. Chem. Lett.* 22, 4049–4054. doi: 10.1016/j.bmcl.2012.04.081

Yuan, Y., Cao, D., Zhang, Y., Ma, J., Qi, J., Wang, Q., et al. (2017). Cryo-EM structures of MERS-CoV and SARS-CoV spike glycoproteins reveal the dynamic receptor binding domains. *Nat. Commun.* 8, 1–9. doi: 10.1038/ncomms15092

Zhang, D., Zhang, B., Lv, J. T., Sa, R. N., Zhang, X. M., and Lin, Z. J. (2020). The clinical benefits of Chinese patent medicines against COVID-19 based on current evidence. *Pharmacol. Res.* 157:104882. doi: 10.1016/j.phrs.2020.104882

Zhang, H., Penninger, J. M., Li, Y., Zhong, N., and Slutsky, A. S. (2020). Angiotensin-converting enzyme 2 (ACE2) as a SARS-CoV-2 receptor: molecular mechanisms and potential therapeutic target. *Intens. Care Med.* 46, 586–590. doi: 10.1007/s00134-020-05985-9

Zhang, Q., Honko, A., Zhou, J., Gong, H., Downs, S. N., Vasquez, J. H., et al. (2020). Cellular Nanosponges Inhibit SARS-CoV-2 Infectivity. *Nano Lett.* 20, 5574. doi: 10.1021/acs.nanolett.0c02278

Zhang, Y. Z., and Holmes, E. C. (2020). A Genomic Perspective on the Origin and Emergence of SARS-CoV-2. *Cell* 181, 223–227. doi: 10.1016/j.cell.2020.03.035

Zhu, F. C., Guan, X. H., Li, Y. H., Huang, J. Y., Jiang, T., Hou, L. H., et al. (2020). *A Phase II Clinical Trial to Evaluate the Recombinant Vaccine for COVID-19 (Adenovirus Vector) ClinicalTrials.gov.* Available at: https://clinicaltrials.gov/ct2/show/NCT04341389 (Accessed July 14, 2020).

Zhu, F. C., Li, Y. H., Guan, X. H., Hou, L. H., Wang, W. J., Li, J. X., et al. (2020). Safety, tolerability, and immunogenicity of a recombinant adenovirus type-5 vectored COVID-19 vaccine: a dose-escalation, open-label, non-randomised, first-in-human trial. *Lancet* 395, 1845–1854. doi: 10.1016/S0140-6736(20)31208-3

Zost, S. J., Gilchuk, P., Chen, R. E., Case, J. B., Reidy, J. X., Trivette, A., et al. (2020). Rapid isolation and profiling of a diverse panel of human monoclonal

antibodies targeting the SARS-CoV-2 spike protein. *Nat. Med.* 26 (9), 1422–1427. doi: 10.1038/s41591-020-0998-x

Conflict of Interest: The authors declare that the research was conducted in the absence of any commercial or financial relationships that could be construed as a potential conflict of interest.

frontiers in Pharmacology

ORIGINAL RESEARCH
published: 26 November 2020
doi: 10.3389/fphar.2020.584973

Vigna radiata (L.) R. Wilczek Extract Inhibits Influenza A Virus by Targeting Viral Attachment, Penetration, Assembly, and Release

Chieh-Wen Lo[1], *Chia-Chen Pi*[2], *You-Ting Chen*[1] *and Hui-Wen Chen*[1]*

[1]Department of Veterinary Medicine, National Taiwan University, Taipei, Taiwan, [2]King's Ground Biotech Co., Ltd., Pingtung, Taiwan

Vigna radiata (L.) R. Wilczek (mung bean) is a Chinese functional food with antioxidant, antimicrobial and anti-inflammatory activities. However, little is known about its antiviral activity. We aimed to investigate the antiviral activity and mechanisms of action of *Vigna radiata* extract (VRE) against influenza virus. HPLC was conducted to analyze the components of the VRE. The anti-influenza viral activity of VRE in Mardin-Darby canine kidney (MDCK) cells was evaluated by virus titration assays, hemagglutination assays, quantitative RT-PCR assays, cellular α-glucosidase activity assays and neuraminidase activity assays. Chromatographic profiling analysis identified two major flavonoids, vitexin and isovitexin, in the ethanol extract of *Vigna radiata*. Through *in vitro* studies, we showed that VRE, at concentrations up to 2,000 μg/ml, exhibited no cytotoxicity in MDCK cells. VRE protected cells from influenza virus-induced cytopathic effects and significantly inhibited viral replication in a concentration-dependent manner. A detailed time-of-addition assay revealed that VRE may act on both the early and late stages of the viral life cycle. We demonstrated that 1) VRE inhibits virus entry by directly blocking the HA protein of influenza virus; 2) VRE inhibits virus entry by directly binding to cellular receptors; 3) VRE inhibits virus penetration; 4) VRE inhibits virus assembly by blocking cellular α-glucosidase activity, thus reducing HA protein trafficking to the cell surface; and 5) VRE inhibits virus release by inhibiting viral neuraminidase activity. In summary, *Vigna radiata* extract potently interferes with two different subtypes of influenza viruses at multiple steps during the infectious cycle, demonstrating its broad-spectrum potential as an anti-influenza preventive and therapeutic agent. Continued development of *Vigna radiata*-derived products into antiviral therapeutics is warranted.

Keywords: ***Vigna radiata*** **extract, mung bean, functional foods, antiviral activity, influenza virus**

OPEN ACCESS

Edited by:
Paul F. Moundipa,
University of Yaounde I, Cameroon

Reviewed by:
Borris Rosnay Tietcheu Galani,
University of Ngaoundéré, Cameroon
Pei-Wen Hsieh,
Chang Gung University, Taiwan

***Correspondence:**
Hui-Wen Chen
winnichen@ntu.edu.tw

Specialty section:
This article was submitted to Ethnopharmacology, a section of the journal Frontiers in Pharmacology

Received: *19 July 2020*
Accepted: *19 October 2020*
Published: *26 November 2020*

Citation:
Lo C-W, Pi C-C, Chen Y-T, Chen H-W (2020) Vigna radiata *(L.) R. Wilczek Extract Inhibits Influenza A Virus by Targeting Viral Attachment, Penetration, Assembly, and Release. Front. Pharmacol. 11:584973. doi: 10.3389/fphar.2020.584973*

INTRODUCTION

Influenza A virus infection is a zoonotic infectious disease that continues to pose a pandemic threat worldwide. Epidemiological studies from 2011 to 2018 indicate that influenza A/H3N2 (39.2%) and A/H1N1 (28.3%) are the dominant strains circulating in Asian countries (Young and Chen, 2020). Influenza A virus contains eight negative-sense single-stranded viral RNA (vRNA) segments, encoding for more than 10 viral proteins. For the viral envelope-associated proteins, the

hemagglutinin (HA) interacts with the host cell receptor, and the neuraminidase (NA) plays a role in viral release. The matrix protein 1 forms a coat inside the viral envelope, and the matrix protein 2 is a proton-selective ion channel protein. For the internal proteins, polymerase basic protein 1 and 2 (PB1, PB2), polymerase acidic protein (PA) and nucleoprotein (NP) are members of the viral ribonucleoprotein (vRNP), responsible for vRNA replication. Non-structural protein 1 and 2 (NS1, NS2) have roles in host immunity modulation and vRNP transportation, respectively (Bouvier and Palese, 2008). The influenza A virus life cycle begins with the attachment between viral HA protein and host sialic acid. After that, the virus penetrates into the host cell through cellular endocytic machinery. Followed by endosomal acidification, the vRNP is released from the endosome into the cytosol. The vRNP then traffics into the nucleus and initiates the vRNA replication. The newly synthesized RNA is transported back to the cytosol for viral protein translation. After post-translational glycosylation of viral HA and NA, these proteins traffic to the cell membrane together with newly synthesized vRNP to form viral particles. Finally, the viral NA with sialidase activity cuts the linkage of viral HA and host sialic acid, leading to the release of viral particles (Dou et al., 2018).

Due to its high mutation and genomic recombination rates, new strains of influenza A virus occur frequently, and some of these strains are associated with high morbidity and mortality. In addition to the seasonal H1N1 or H3N2 strains, highly pathogenic avian influenza H5N1 viruses with human adaptive mutations in the PB2, PA, NP and M genes were found in 18 human infected cases in Hong Kong and led to one third of the infected people died (Zhou et al., 1999). Although a vaccine for seasonal influenza is available, the protective effect varies annually depending on the coverage of the vaccine formulation (Wei et al., 2020). A small number of antiviral drugs have been approved, including oseltamivir, zanamivir, and peramivir, which target viral NA to inhibit virus release from host cells (Moscona, 2008). However, drug-resistant strains have already been reported (Lampejo, 2020). Recently, baloxavir, a novel viral PA protein inhibitor, was approved in 2018 (Abraham et al., 2020). However, strains with reduced susceptibility have already emerged (Sato et al., 2020). Thus, there is an urgent need for development of new antiviral drugs.

Herbal medicines have been proven to be applicable to combat various viral infectious diseases (Li and Peng, 2013). In contrast to single-compound-based medicines, one of the advantages of herbal medicines is that they contain several active components that may simultaneously act on viruses or hosts, interfering with the viral life cycle at different stages. For example, the extract of *Houttuynia cordata* has multiple inhibitory effects on SARS-CoV by enhancing host IL-2 and IL-10 secretion and inhibiting the viral protease and RNA-dependent RNA polymerase (Lau et al., 2008). Therefore, herbal medicine-based treatment is a prominent strategy to protect people from drug-resistant viruses. Mung bean (*Vigna radiata* (L.) R. Wilczek) is one of the most important crops grown in countries of south, east and southeast Asia (Nair et al., 2013), and it is commonly used as a folk medicine in Taiwan and China due to its anti-inflammatory effects and ability to relieve heat stress (Cao et al., 2011; Zhang et al., 2013). The composition of mung bean has been reported (Ganesan and Xu, 2018). The crude extract of mung bean has been shown to have antioxidant, antidiabetic and immunoregulatory activities (Randhir and Shetty, 2007; Bai et al., 2016; Hashiguchi et al., 2017). Furthermore, extracts of mung bean sprouts exhibit the ability to protect against respiratory syncytial virus and herpes simplex virus 1 (Hafidh et al., 2015). However, whether mung bean has an inhibitory effect on influenza virus has not yet been investigated. In this study, we demonstrated that mung bean exerts anti-influenza A virus effects by blocking viral attachment, entry, glycoprotein membrane trafficking and neuraminidase activity, with no cytotoxic effects.

MATERIALS AND METHODS

Materials and Preparation of *Vigna radiata* Extract

Vigna radiata (L.) R. Wilczek (mung bean) was provided by King's Ground Biotech Co., Ltd. (Pingtung, Taiwan) with a batch number NTU01. *Vigna radiata* extract (VRE) was prepared from the seed coats of mung bean via physical, chemical and biological processes. After mixing with organic acids under high temperature and pressure, the seed coats of mung beans were dried by hot air and ground to a powder. The VRE product contained 13% crude protein, 70% carbohydrate, and 4% ash. The VRE powder was then extracted with 95% ethanol (1:10 w/v) and sonicated for 1 h. The filtered solvent of the extract was concentrated using a rotary evaporator (Eyela, Japan). The recovery of the dried extract was approximately 15–25% (w/w). The dried extract was stored at −20°C until use.

High Performance Liquid Chromatography Analysis

All solvents used were HPLC grade, and all reagents were analytical grade. The analysis was performed using a high-performance liquid chromatography system (Hitachi D2000), which consisted of an L-2130 HTA Pump, an L-2200 autosampler, and an L-2455 diode array detector. The extracted compound was separated using an Inertsil ODS-2 C18 column (250 mm × 4.6 mm, 5 μm) with a gradient mobile phase of 0.3% *ortho*-phosphoric acid (Scharlab) in ddH_2O (solvent A) and acetonitrile (Fisher Chemical) (solvent B). HPLC was performed at a flow rate of 0.8 ml/min with detection at 220 nm. The column temperature was maintained at 30°C. All samples were diluted in methanol (Honeywell) before analysis. Chromatographic peaks were identified on the basis of retention time.

Cells and Viruses

Mardin-Darby canine kidney (MDCK) cells (ATCC #CCL-34) were maintained in DMEM supplemented with 10% FBS and 1% penicillin/streptomycin/amphotericin B and cultured at 37°C

with 5% CO_2. For influenza virus infection in MDCK cells, infection medium (RPMI containing 0.75% BSA, 0.05 mM 2-mercaptoethanol, 1% PSA, and 2 μg/ml L-1-*p*-tosylamino-2-phenylethyl chloromethyl ketone-treated trypsin) was used. All the reagents for cell culture were purchased from Invitrogen. Influenza A viruses, A/Puerto Rico/8/1934 (PR8-H1N1) and A/Chicken/Taiwan/3937/2012 (3937-H6N1) (Zhu et al., 2020), were propagated in MDCK cells and titrated with as previous described (Hu et al., 2018). All types of influenza viruses were propagated in MDCK cells. Viruses were titrated by 50% tissue culture infective dose ($TCID_{50}$) assays, hemagglutination test and quantitative RT-PCR (qRT-PCR) as previously described (Chen et al., 2013). For the $TCID_{50}$ assay, in brief, MDCK cells in the 96 well plate (2×10^4 cells per well) were infected with 100 μl of 10-fold serially diluted virus-containing sample and incubated at 37°C for 3 days. Following incubation, viral infection in each well was determined by a hemagglutination assay using 1% chicken red blood cells. Viral titers were calculated by the Reed-Muench method (Reed and Muench, 1938).

Cytotoxicity Test

The cytotoxicity of VRE in MDCK cells was examined. Briefly, 2×10^4 cells were seeded in 96-well plates overnight. Then, VRE serially diluted in medium was applied to the cells and incubated for 24, 48, or 72 h. The culture medium was removed, and 100 μl of 0.5 mg/ml 3-(4,5-dimethylthiazol-2-yl)-2,5-diphenyltetrazolium bromide (MTT) solution was added, followed by incubation at 37°C for 3 h. The supernatants were removed, and 100 μl of dimethyl sulfoxide was added to each well. The absorbance value of each well was determined spectrophotometrically at 570 nm in a microplate reader (Synergy H1, BioTek, Winooski, VT, United States).

Antiviral Activity Test

MDCK cells (2×10^5) were seeded in 24-well plates overnight. PR8-H1N1 (multiplicity of infection, MOI = 0.1) was treated with serially diluted VRE at 37°C for 1 h. At the same time, MDCK cells were incubated with serially diluted VRE in medium at 37°C for 1 h. After incubation, the VRE-virus mixture was used to infect cells for 1 h. The cells were washed after supernatant removal and then incubated with serially diluted VRE for 24 h. The supernatants were collected for the $TCID_{50}$ assay to determine the viral titer. The viral titers of each group relative to the vehicle control were calculated.

Time-of-Addition Assay

MDCK cells (2×10^5) were seeded in 24-well plates overnight. PR8-H1N1 (MOI = 2) was incubated with 2,000 μg/ml VRE under six different conditions. 1) For the "pretreated virus" group, the virus was incubated with VRE in medium for 1 h before infecting MDCK cells for 1 h. After infection, the medium containing virus and VRE was removed, fresh medium was added, and the cells were incubated for an additional 11 h. 2) For the "pretreated cell" group, MDCK cells were incubated with VRE for 1 h before infection. One hour later, the virus was added and allowed to infect the cells for another 1 h. After infection, the VRE- and virus-containing medium was changed to fresh medium, and the cells were incubated for an additional 11 h. 3) For the "pretreated cell + wash" group, MDCK cells were incubated with VRE for 1 h,

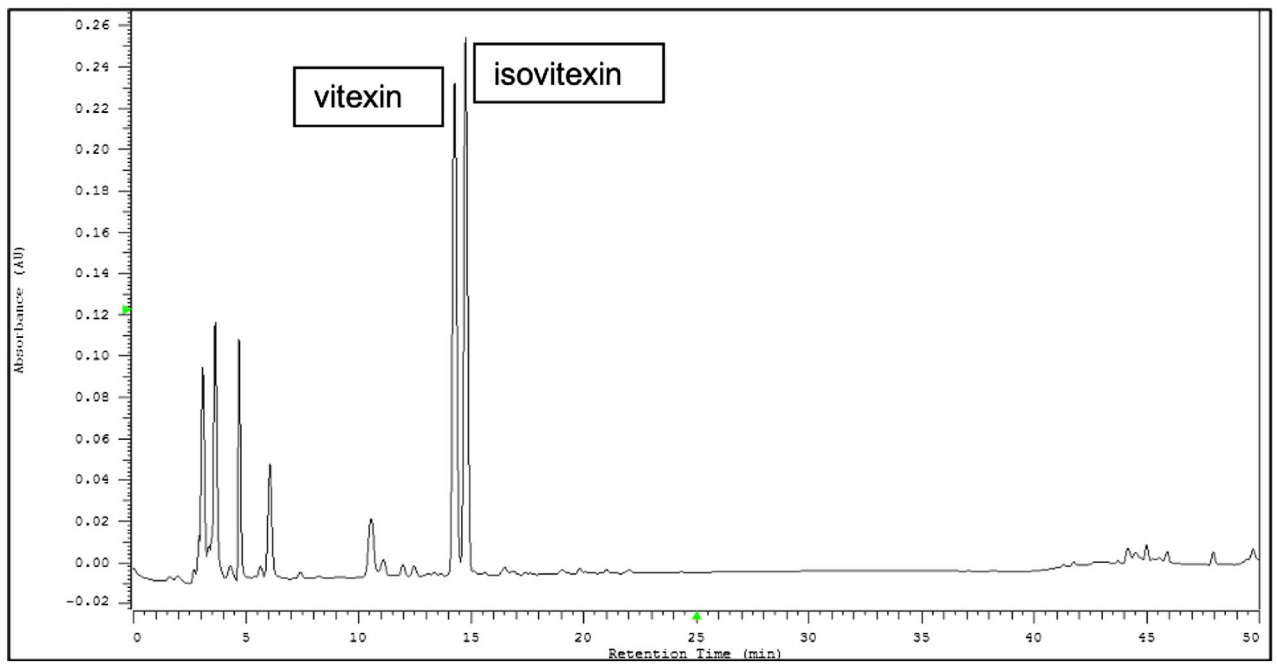

FIGURE 1 | Representative HPLC chromatograms from the seed coats of *Vigna radiata* (L.) R. Wilczek (mung bean). Vitexin and isovitexin were found to be two major components of *Vigna radiata* extract (VRE).

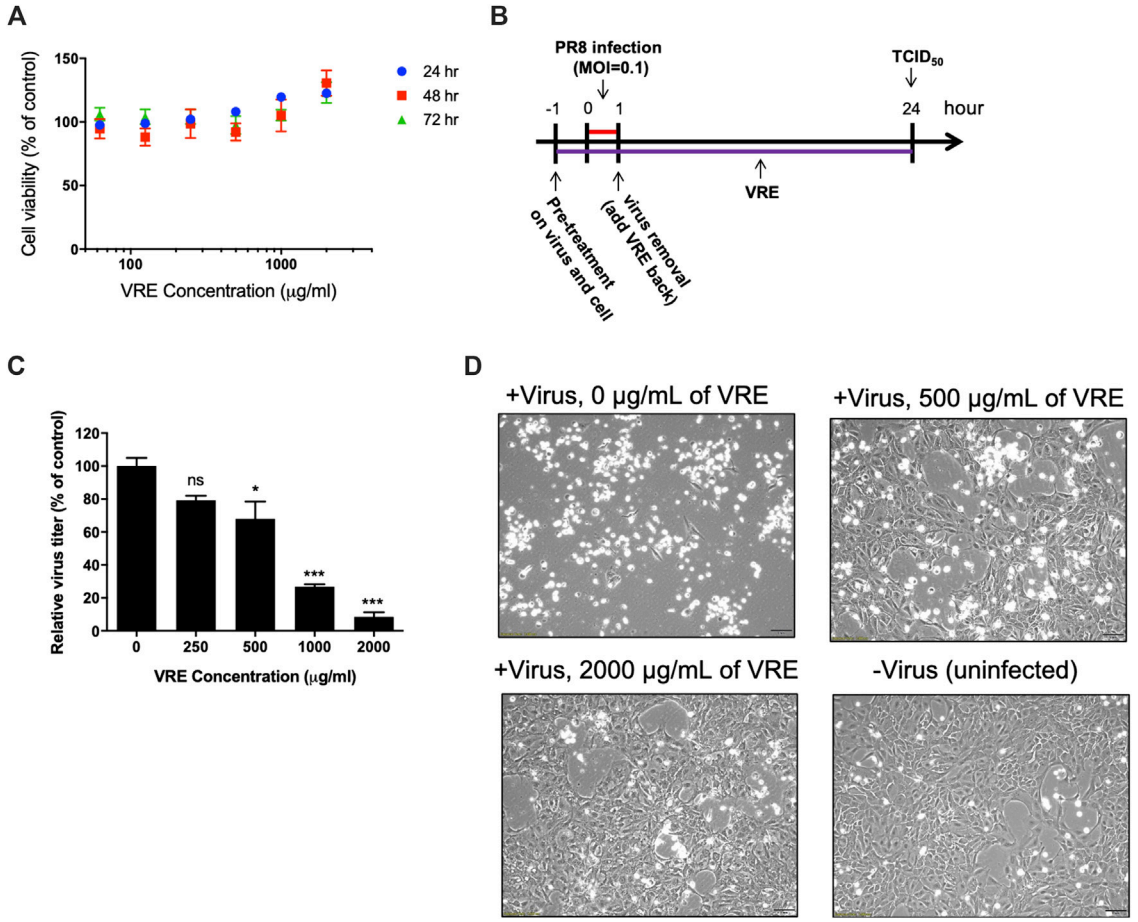

FIGURE 2 | Cytotoxicity and virus inhibitory activity of VRE in MDCK cells. **(A)** MDCK cells were treated with various concentrations of VRE at 37°C for 24, 48, and 72 h. Cell viability was evaluated by MTT assays. Data in the plot present the mean ± SEM of four replicates. **(B)** Schematic diagram of the experimental design. PR8-H1N1 (MOI = 0.1) was treated with VRE at 37°C for 1 h. At the same time, MDCK cells were incubated with VRE in medium at 37°C for 1 h. After incubation, the VRE-virus mixture was used to infect cells for 1 h. The cells were washed after supernatant removal and then incubated with VRE for 24 h. The supernatants were collected for the $TCID_{50}$ assay. **(C)** The viral titers of each group are indicated. Data in the plot present the mean ± standard error of the mean (SEM) of three replicates. Data were compared by one-way ANOVA followed by Dunnett's multiple comparisons test (ns, non-significant; $^{*}p < 0.05$, $^{***}p < 0.001$). **(D)** Images of MDCK cell were observed at 12 h post infection and compared with those of the uninfected control cells.

and the medium was replaced with fresh medium before virus infection. After 1 h of virus infection, the medium that contained the virus was removed, fresh medium was added, and the cells were incubated for an additional 11 h. 4) For the "treated infection + wash" group, virus-infected MDCK cells were treated with VRE for 1 h. After 1 h of virus infection, the medium was removed, fresh medium was added, and the cells were incubated for an additional 11 h. 5) For the "after infection" group, MDCK cells were treated with VRE after virus infection for 11 h. 6) For "all", the virus was preincubated with VRE in medium for 1 h. At the same time, MDCK cells were preincubated with VRE for 1 h. After incubation, the VRE-virus mixture was used to infect cells for 1 h. The cells were washed after supernatant removal and then incubated with VRE for 11 h. The supernatants were collected for the $TCID_{50}$ assay to determine the viral titers. To further dissect the time course of VRE's mechanism of action, another time-of-addition assay was also performed. VRE was added at 0, 2, 4, 6, and 8 h post virus infection. The supernatant was collected at 12 h post infection for the $TCID_{50}$ assay to determine the viral titer. Viral RNA in the cells was extracted and detected by qRT-PCR (Chen et al., 2013).

Hemagglutination Assay Using *Vigna radiata* Extract-Treated Red Blood Cells or Viruses

Chicken RBCs (1%) were mixed with various concentrations of VRE in a U-bottomed microplate and incubated at room temperature (RT) for 30 min. The hemagglutination activity of VRE was observed by eye. To determine VRE binding to the surface receptor of RBCs and its inhibition of virus-induced hemagglutination, 500 μl of 1% RBCs were treated with various concentrations (0, 125, 500, and 2,000 μg/ml) of VRE at RT for 30 min. The unbound VRE was removed by

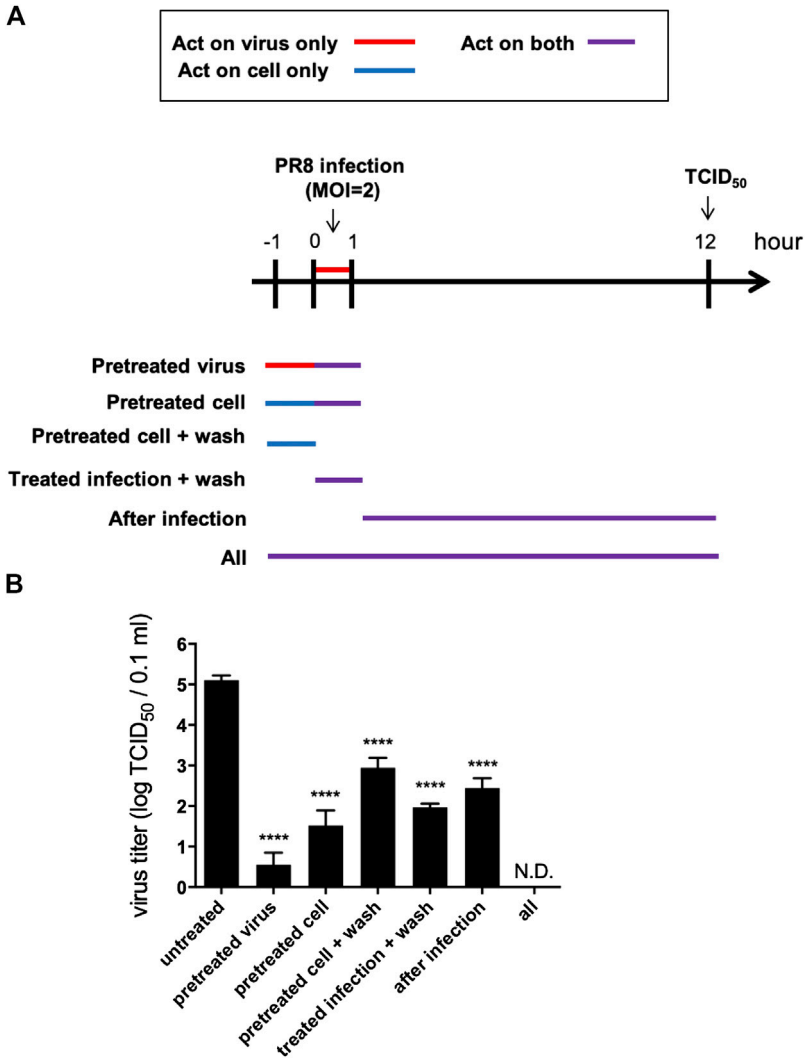

FIGURE 3 | VRE interferes with the viral life cycle under different treatment conditions. **(A)** Schematic diagram of the experimental design. MDCK cells were infected with PR8-H1N1 (MOI = 2) under six different treatment conditions. At 12 hpi, the virus titers were determined by a $TCID_{50}$ assay. **(B)** The viral titers of each group relative to the vehicle control are indicated. Data in the plot present the mean ± SEM of three replicates. Data were compared by one-way ANOVA followed by Dunnett's multiple comparisons test (****$p < 0.0001$, N.D., not detectable).

centrifugation at 1,000 ×g for 5 min, and the treated RBC pellet was washed and resuspended in 500 μl of PBS. Next, 2,000 hemagglutination unit (HAU) of PR8-H1N1 virus was added to treated RBCs and incubated at RT for 30 min. Then, the RBC pellet was washed and resuspended in 100 μl of PBS. The amount of RBC-bound virus was determined by qRT-PCR. To determine VRE binding to the viral surface and its inhibition of virus-induced hemagglutination, 2,000 HAU of PR8-H1N1 virus was treated with various concentrations (0, 125, 500, and 2,000 μg/ml) of VRE or 2 μg of polyclonal antibody against H1N1 hemagglutinin (SinoBiological #11684-T56) at RT for 30 min. Next, 500 μl of 1% RBCs was added to the treated virus solution and incubated at RT for 30 min, and then the RBC pellet was washed and resuspended in 100 μl of PBS. The amount of RBC-bound virus was determined by qRT-PCR.

Penetration Inhibition Assay

MDCK cells (2×10^5) were seeded in 12-well plates overnight before being infected with PR8-H1N1 (MOI = 2) at 4°C for 1 h. After virus binding, VRE was applied to cells for a 1 h incubation at 37°C. Unpenetrated viruses were inactivated by incubation with PBS (pH 2) for 1 min and then neutralized with PBS (pH 11). After incubation for an additional 6 h, the cells were washed and fixed with 4% paraformaldehyde (Sigma) for 20 min at room temperature. The cells were permeabilized with 0.3% Triton X-100 (Sigma) in 0.1% BSA for 30 min and then blocked with 1% BSA for 30 min at room temperature. The primary antibody, anti-NP (1:1,000, HyTest #3IN5), was diluted in 1% BSA and incubated with cells overnight at 4°C. The secondary antibody, FITC-conjugated goat anti-mouse IgG (1:1,000, Jackson ImmunoResearch), was diluted with 1% BSA and incubated with the cells for 1 h at room temperature. Nuclei were stained

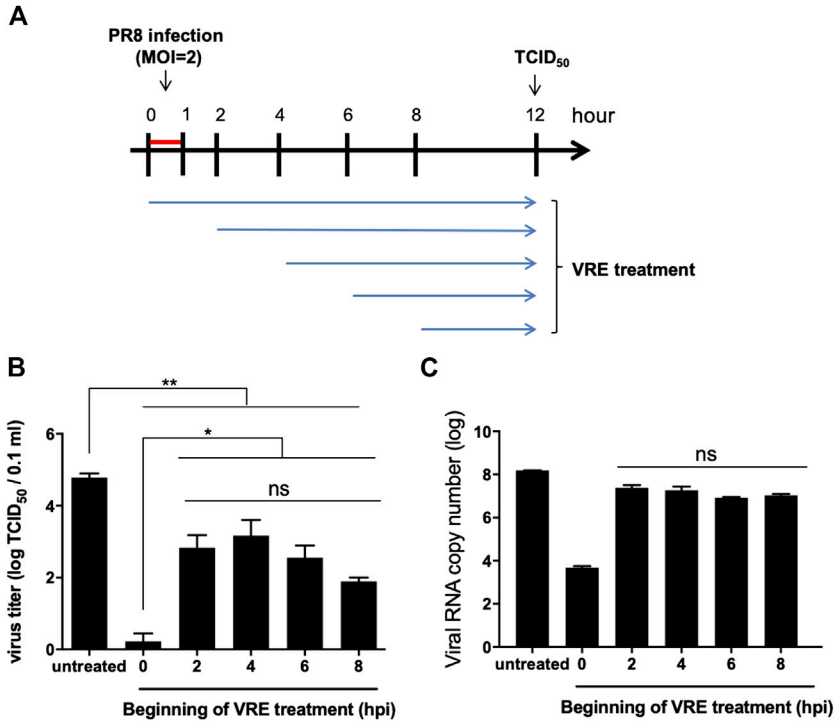

FIGURE 4 | Virus inhibition by VRE treatment. **(A)** Schematic diagram of the experimental design. Different initial time points of VRE treatment of MDCK cells relative to PR8-H1N1 (MOI = 2) infection were tested to evaluate the viral inhibition effect of VRE. **(B)** At 12 hpi, the extracellular virus titers were determined by $TCID_{50}$. **(C)** At 12 hpi, intracellular viral RNA was quantitated by qRT-PCR. The untreated cell group was used as a control. Data in the plot present the mean ± SEM of three replicates. Data were compared by one-way ANOVA followed by Dunnett's multiple comparisons test (ns, non-significant; $^{*}p < 0.05$, $^{**}p < 0.01$).

with DAPI (1:1,000, Invitrogen) in PBS for 10 min at room temperature. Fluorescence images were recorded with a microscope (Olympus IX-83), and the fluorescence signal was measured using a microplate reader (Synergy H1, BioTek). The NP expression levels relative to the nuclear signal were determined.

α-Glucosidase Inhibition Assay

The α-glucosidase inhibition assay was performed according to a previous study (Pullela et al., 2006) with some modifications. Briefly, 0.8 μl of various concentrations of VRE was mixed with 69.2 μl of phosphate buffer (100 mM, pH 6.8) and 10 μl of α-glucosidase (1 U/ml, Sigma) and incubated for 15 min at 37°C. After incubation, 20 μl of substrate, *p*-nitrophenyl-α-D-glucopyranoside (5 mM, Sigma), was added and incubated for 20 min at 37°C. The reaction was stopped by adding 50 μl of Na_2CO_3 (0.1 M). The absorbance at 450 nm was recorded before and after substrate addition, and an increase in the absorbance was observed. Relative α-glucosidase inhibition was determined as a percentage of the control.

Detection of Viral Hemagglutinin Surface Expression

The HA trafficking inhibition assay was performed as previously described (Saito and Yamaguchi, 2000) with some modifications. Briefly, 2×10^5 MDCK cells were seeded in 12-well plates overnight before being infected with PR8-H1N1 (MOI = 10) for 1 h. After the virus was removed, the cells were treated with various concentrations of VRE for 2–5 h post infection. The virus signal was then detected with immunofluorescence. For HA staining in the entire cell (surface and intracellular HA protein), the cells were fixed with 4% paraformaldehyde and then permeabilized with 0.3% Triton X-100 in 0.1% BSA. For HA staining on the cell surface, the cells were fixed with 4% paraformaldehyde before staining without permeabilization. The cells were then blocked with 1% BSA for 30 min at room temperature. The primary antibody anti-HA (1:500, SinoBiological #11684-T56) was diluted in 1% BSA and incubated with cells overnight at 4°C. The secondary antibody, FITC-conjugated goat anti-rabbit IgG (1:1,000, Jackson ImmunoResearch), was diluted with 1% BSA and incubated with cells for 1 h at room temperature. Nuclei were stained with DAPI (1:1,000, Invitrogen) in PBS for 10 min at room temperature. Fluorescence images were recorded with a microscope (Olympus IX-83), and the fluorescence signal was measured using a microplate reader (Synergy H1, BioTek). The HA expression levels relative to the nuclear signal were determined from the two different types of staining methods.

Neuraminidase Inhibition Assay

The neuraminidases from mammalian influenza virus PR8-H1N1 and avian influenza 3937-H6N1 were utilized to

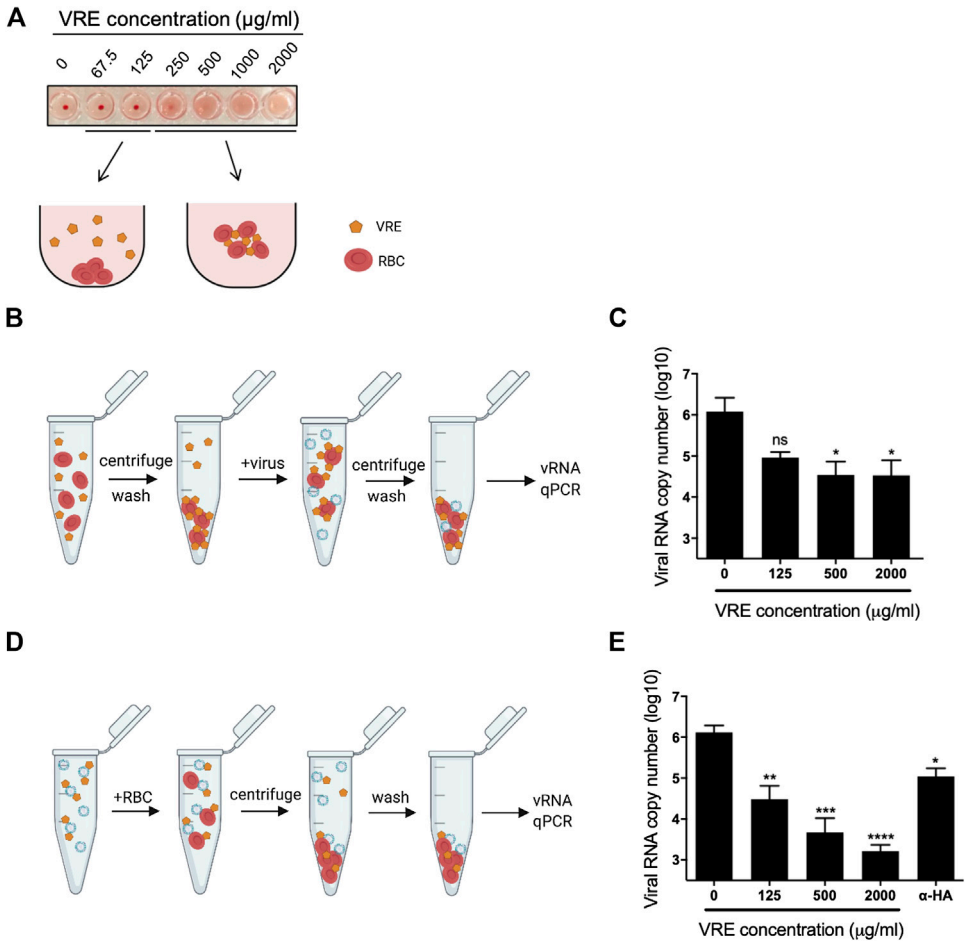

FIGURE 5 | Hemagglutination assay using VRE-treated RBCs or viruses. **(A)** VRE-induced hemagglutination was illustrated. **(B)** Schematic diagram of the experimental procedures. RBCs were treated with various concentrations of VRE at RT for 30 min. The unbound VRE was removed, and the treated RBC pellet was washed and resuspended. A total of 2,000 HAU of PR8-H1N1 virus was added to the treated RBCs and incubated at RT for 30 min. Then, the RBC pellet was washed again and resuspended in PBS. **(C)** The amount of RBC-bound virus was determined by qRT-PCR. **(D)** Schematic diagram of the experimental procedures. A total of 2,000 HAU of PR8-H1N1 virus was treated with various concentrations of VRE or 2 μg of polyclonal antibody against the H1N1 HA protein at RT for 30 min. Then, 500 μl of 1% RBCs was added to the treated virus solution and incubated at RT for 30 min, and the RBC pellet was washed and resuspended in PBS. **(E)** The amount of RBC-bound virus was determined by qRT-PCR. Data are presented as the mean ± SEM of three replicates and compared by one-way ANOVA followed by Dunnett's multiple comparisons test (ns, non-significant; *$p < 0.05$, **$p < 0.01$, ***$p < 0.001$, ****$p < 0.0001$).

investigate the inhibition ability of VRE. The neuraminidase inhibition assay was performed according to Zhu et al. (2015) with some modifications. Briefly, 1 μl of various concentrations of VRE or oseltamivir (Sigma) was mixed with 25 μl of virus (32 HAU of 3937-H6N1 virus or PR8-H1N1 virus) and 1× assay buffer (33 mM MES, 4 mM $CaCl_2$, pH 6.5) to a total of 50 μl and then incubated for 20 min at 37°C. Fifty microliters of fluorogenic substrate (50 μM 4-methylumbelliferyl-N-acetylneuraminic acid, Sigma) was added and incubated for 60 min at 37°C. The reaction was then terminated by adding 100 μl of 0.2 M Na_2CO_3. Fluorescence was measured with an excitation wavelength of 355 nm and an emission wavelength of 460 nm. Relative fluorescence units were obtained by subtracting the background value.

Transmission Electron Microscopy

A total of 10^6 MDCK cells were seeded onto a sterile plastic sheet in a 6-well plate overnight before infection with PR8-H1N1 (MOI = 5) for 1 h. The cells were treated with VRE (2,000 μg/ml) or oseltamivir (5 μg/ml) for 6–12 h post infection. The cells were then washed and fixed with 2.5% glutaraldehyde for TEM imaging. Standard operating procedures were performed for imaging via transmission electron microscopy (FEI Tecnai TF20).

Statistical Analysis

Data were analyzed by an unpaired *t* test or ANOVA with Dunnett's multiple comparison test using Prism (GraphPad, San Diego, CA, United States). *p* Values smaller than 0.05 were considered significant.

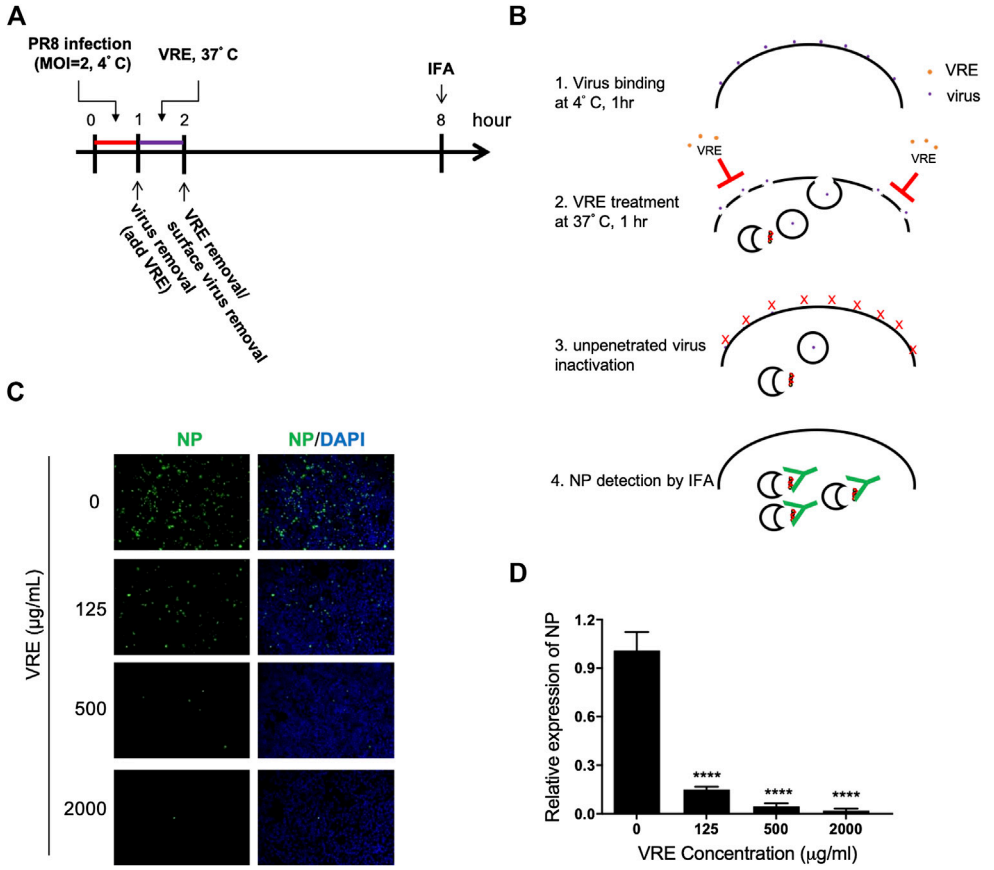

FIGURE 6 | VRE blocks virus penetration. **(A,B)** Schematic diagram of the experimental procedures. **(C)** MDCK cells were infected with PR8-H1N1 (MOI = 2) at 4˚C for 1 h for virus attachment. One hour later, VRE was applied to the cells for 1 h to inhibit virus penetration. The unpenetrated virus was inactivated with PBS at pH 2 for 1 min and neutralized with PBS at pH 11. The cells were then incubated in fresh medium for an additional 6 h. The virus signal was detected via immunofluorescence staining with an NP antibody. **(D)** The fluorescence intensity was measured with a microplate reader. Relative NP expression levels were determined. Data are presented as the mean ± SEM of three replicates and were compared by one-way ANOVA followed by Dunnett's multiple comparisons test (****$p < 0.0001$).

RESULTS

HPLC Profile of *Vigna radiata* Extract

Representative HPLC chromatograms from the seed coats of *Vigna radiata* (mung bean) are shown in **Figure 1**. Vitexin and isovitexin were found to be two major ingredients in VRE. The active compounds contain 22.153 mg/g vitexin and 24.171 mg/g isovitexin.

Vigna radiata Extract Shows No Cytotoxicity in Mardin-Darby Canine Kidney Cells

The cytotoxicity of VRE was evaluated in MTT assays. The results showed that VRE exhibited no cytotoxicity in MDCK cells, even at 2,000 μg/ml, the highest concentration used in this study (**Figure 2A**).

Vigna radiata Extract Has Concentration-Dependent Anti-Influenza Virus Activity

The antiviral activity of VRE was demonstrated in a cellular infection model (**Figure 2B**). The results showed that 500, 1,000, and 2,000 μg/ml VRE significantly ($p < 0.05$) inhibited PR8-H1N1 virus infection by 68.0%, 26.9% and 8.5%, respectively, comparing with the vehicle control in MDCK cells, as determined by a $TCID_{50}$ assay (**Figure 2C**). With images of uninfected cells as a reference, VRE treatment protected against the cytopathic effect induced by virus infection in a concentration-dependent manner (**Figure 2D**). These data suggested that VRE has potent antiviral activity against influenza virus.

Vigna radiata Extract Exhibits Antiviral Activity in the Early and Late Stages of the Viral Life Cycle

To verify the antiviral mechanism of VRE, various time points during a single infectious cycle were used to determine the stages at which VRE exerted its inhibitory effect. MDCK cells were infected with PR8-H1N1 (MOI = 2) under six different treatment conditions: pretreatment of viruses and treatment during inoculation (pretreated virus), pretreatment of cells and treatment during inoculation (pretreated cells), pretreatment of

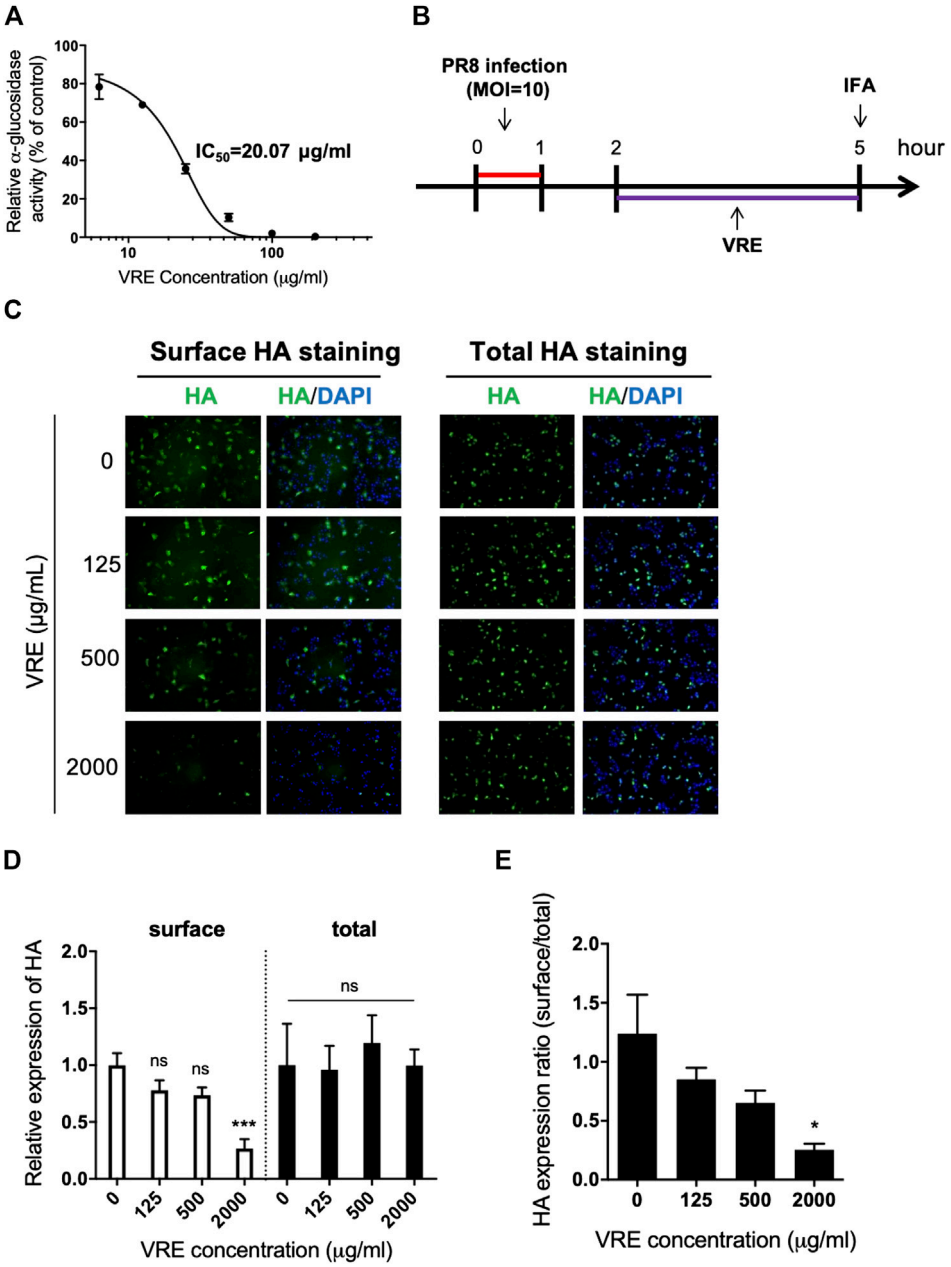

FIGURE 7 | VRE inhibits α-glucosidase activity in a concentration-dependent manner and interferes with the surface expression of HA. **(A)** α-Glucosidase activity was measured by detecting the absorbance at 450 nm and normalized to the control. The IC_{50} of VRE in inhibiting α-glucosidase is indicated. **(B)** Schematic diagram of the experimental procedures. MDCK cells were infected with PR8-H1N1 (MOI = 10) and then treated with various concentrations of VRE at 2–5 h post infection. The cells were then washed and fixed with or without permeabilization. HA expression was detected via immunofluorescence staining with an HA antibody. **(C)** HA expression on the surface (left, cells were fixed only) or in the entire cell (right, cells were fixed and permeabilized) was imaged and merged with DAPI-stained images. **(D)** Fluorescence intensity was measured. The HA expression levels relative to the nuclear signal were determined from the two different types of staining methods. **(E)** The ratio of surface/total HA expression under various VRE treatments is shown. Data are presented as the mean ± SEM of three replicates and compared by one-way ANOVA followed by Dunnett's multiple comparisons test (ns, non-significant; $^{*}p < 0.05$, $^{***}p < 0.001$).

cells (pretreated cells + wash), treatment during inoculation (treated infection + wash), treatment after inoculation (after infection), or all of the above time points (all) (**Figure 3A**). At 12 hpi, the antiviral activity was determined by a $TCID_{50}$ assay. As shown in **Figure 3B**, "pretreated virus" significantly reduced virus titers (a reduction of 4.6 $\log_{10}$, $p < 0.0001$) compared to those of the vehicle control, suggesting that VRE may block viral HA or its host receptor, sialic acid, to interfere with the entry step. In line with this finding, "pretreated cells" and "pretreated cells + wash" significantly reduced virus titers (a reduction of 3.6

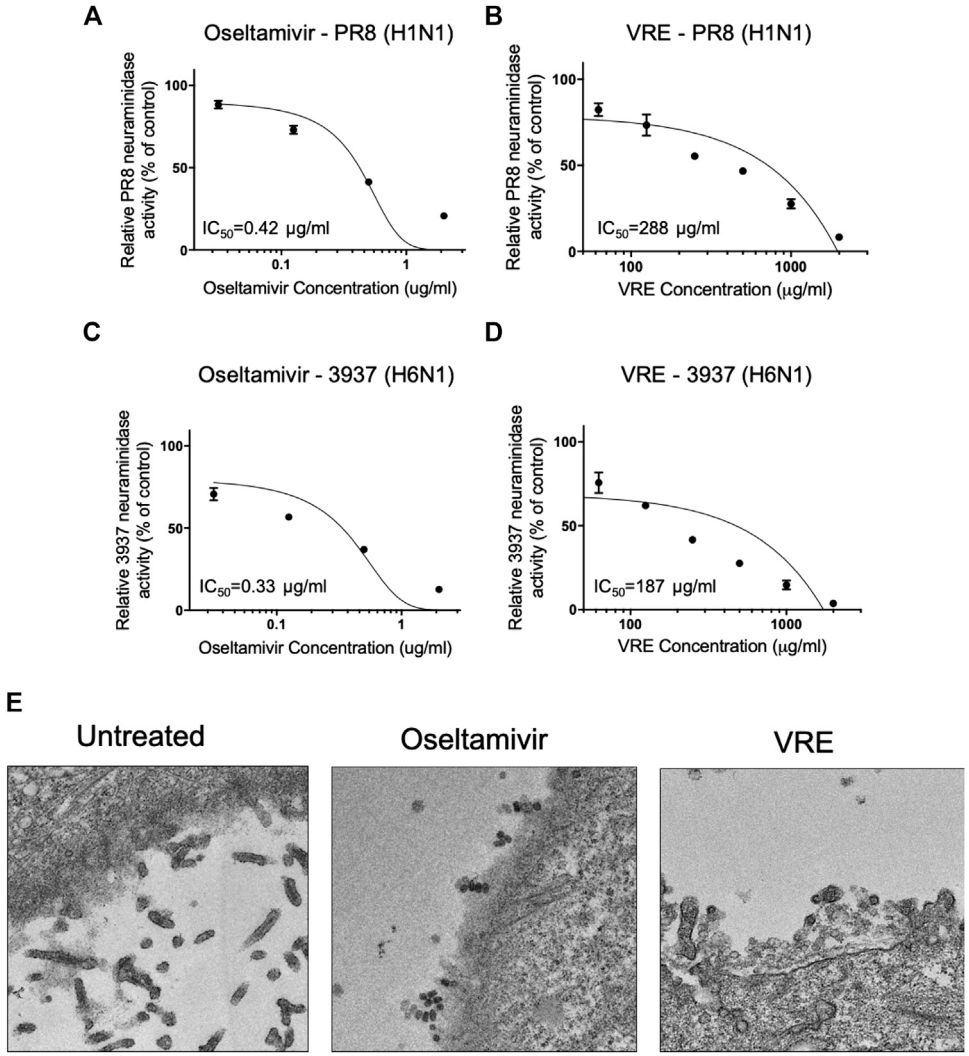

FIGURE 8 | VRE inhibits viral neuraminidase activity in a concentration-dependent manner. The PR8-H1N1 neuraminidase inhibition activity of oseltamivir **(A)** and VRE **(B)** was measured by detecting fluorescence and normalized to the control. The 3937-H6N1 neuraminidase inhibition activity of oseltamivir **(C)** and VRE **(D)** was measured by detecting fluorescence and normalized to the control. The IC_{50} for inhibiting neuraminidase is indicated. Data are presented as the mean ± SEM of three replicates. **(E)** MDCK cells were infected with PR8-H1N1 (MOI = 5) for 1 h, and the cells were treated with VRE (2,000 μg/ml) or oseltamivir (5 μg/ml) for 6–12 h post infection. TEM images demonstrated different levels of virus release from infected MDCK cells.

and 2.2 $\log_{10}$, respectively, $p < 0.0001$), indicating that VRE may block the cell surface receptor to inhibit viral entry. Similar results were found in the "treated infection + wash" group (a reduction of 3.2 $\log_{10}$, $p < 0.0001$). In the "after infection" group, VRE significantly decreased the virus titers (a reduction of 2.7 $\log_{10}$, $p < 0.0001$), suggesting that VRE may act on later stages of the viral life cycle, e.g., viral release. The "all" group showed complete elimination of virus infection, as VRE was able to act on the virus itself and on the host at multiple steps of viral replication in this experimental condition.

Another addition assay was performed at five different times in a single infectious cycle to investigate which stage of the viral life cycle is inhibited by VRE (**Figure 4A**). The results indicated that VRE treatment at 8 hpi, the late stage of the infectious cycle, significantly reduced the virus titers (a reduction of 2.9 $\log_{10}$, $p < 0.0001$), suggesting that VRE could inhibit the viral release process (**Figure 4B**). However, VRE treatment at 2, 4, and 6 hpi had similar antiviral effects as treatment at 8 hpi, suggesting that VRE mainly inhibits viral release but does not interfere with other infectious stages after viral entry. Treatment at 0 hpi exhibited the greatest ability to inhibit viral replication, suggesting that VRE could also inhibit viral entry, which is consistent with the findings obtained for the "pretreated virus" and "pretreated cell" groups in **Figure 3B**. To further confirm the antiviral mechanism of VRE, intracellular viral RNA was detected in parallel, and the results showed that VRE treatment at 2, 4, 6, and 8 hpi affected viral RNA

replication only slightly; in contrast, treatment at 0 hpi strongly decreased the viral RNA level (**Figure 4C**). Taken together, these data show that VRE mainly inhibits the viral entry and release processes.

Vigna radiata Extract Blocks Both the Hemagglutinin Protein and Cellular Receptors

To study the anti-entry activity of VRE, an RBC virus binding assay was performed to test whether VRE can directly block the viral HA protein or block cellular receptors. In the HA test of VRE, we found that VRE treatment at concentrations of 250 μg/ml and higher directly hemagglutinated chicken RBCs, indicating that VRE can interact with the sialic acid receptor on the RBC surface (**Figure 5A**). In the VRE pretreatment group (**Figure 5B**), VRE concentration-dependently inhibited virus-mediated RBC hemagglutination, suggesting that VRE could block cell receptors (**Figure 5C**). Next, to dissect the ability of VRE to bind to the viral HA protein, hemagglutination was performed using the VRE-treated virus (**Figure 5D**). In the VRE pretreatment group, similar to the anti-hemagglutination activity induced by the anti-HA antibody, VRE inhibited virus binding with RBCs in a concentration-dependent manner, suggesting that VRE is able to block the viral HA protein (**Figure 5E**).

Vigna radiata Extract Inhibits Viral Penetration

We next tested whether VRE can interfere with the penetration process. Virus was first absorbed on the cell surface before treatment with VRE. The penetrated virus was detected via immunofluorescence (**Figures 6A,B**). Viral NP expression was decreased in the presence of VRE treatment (**Figure 6C**), indicating that VRE inhibited viral penetration in a concentration-dependent manner (**Figure 6D**). Further studies are warranted to investigate the detailed mechanism by which VRE interferes with endocytosis, endosomal acidification or membrane fusion.

Vigna radiata Extract Inhibits α-Glucosidase Activity and Viral Assembly

It has been reported that inhibition of α-glucosidase leads to a reduction in viral assembly and release because the viral glycoprotein cannot be modified before transport to the cell membrane. Therefore, we sought to investigate whether VRE has anti-α-glucosidase activity. VRE inhibited α-glucosidase activity in a concentration-dependent manner with an IC_{50} of 20.07 μg/ml (**Figure 7A**). We further investigated viral HA expression in MDCK cells in the presence of VRE (**Figure 7B**). In line with the observed enzyme-inhibiting activity, cells treated with VRE exhibited less HA expression on the cell surface than did the cells in the untreated group; in contrast, the amount of total intracellular HA expression remained unaffected (**Figures 7C,D**). The ratio of surface HA to total intracellular HA was calculated, and treatment with 2,000 μg/ml VRE resulted in a significant difference (**Figure 7E**). These results indicated that VRE can affect glycoprotein modification and trafficking onto the cell surface and thus inhibit viral assembly.

Vigna radiata Extract Inhibits Neuraminidase Activity and Viral Release

To determine the antiviral release-associated mechanisms of VRE, we tested whether VRE inhibits viral neuraminidase. Neuraminidase from the mammalian influenza virus PR8-H1N1 and the avian influenza virus 3937-H6N1 were utilized to investigate the inhibition ability of VRE. As shown in **Figures 8A,B**, similar to the well-known neuraminidase inhibitor oseltamivir, which showed a low IC_{50} of 0.42 μg/ml, VRE inhibited the neuraminidase activity of the H1N1 virus in a concentration-dependent manner and had an IC_{50} of 288 μg/ml. In **Figures 8C,D**, while oseltamivir showed an IC_{50} of 0.33 μg/ml in inhibiting the neuraminidase activity of 3937-H6N1, an avian influenza strain, VRE also effectively inhibited the neuraminidase activity of the 3937-H6N1 virus, with an IC_{50} of 187 μg/ml. Furthermore, TEM imaging clearly showed that treatment of MDCK cells with 2,000 μg/ml VRE blocked virus release from infected cells, similar to what was observed in the oseltamivir-treated group (**Figure 8E**).

DISCUSSION

In this study, VRE's antiviral activity against the influenza virus was discovered. We confirmed that VRE protected cells from influenza virus-induced cytopathic effects and significantly inhibited viral replication, with effects on both the mammalian H1N1 and avian H6N1 viruses, in a concentration-dependent manner. In addition, VRE was safe in cells. Until 72 h of incubation, VRE showed no toxicity in cells, indicating that VRE has potential for development into a safe and effective pharmaceutical compound.

The detailed time-of-addition assay revealed that VRE may act on both the early and late stages of the viral life cycle. Therefore, we further dissected the role of VRE in inhibiting viral entry. For influenza virus, the HA protein is the entry determinant and can agglutinate RBCs; this process is known to be mediated by crosslinking sialic acid on the surface of RBCs. From the RBC masking assay, we showed that VRE is able to trigger RBC agglutination and mask the cell surface in a concentration-dependent manner, thus preventing the subsequent attachment of influenza virus. However, whether VRE acts directly on the viral receptor, namely, sialic acid, or on other molecules and influences receptor activity through steric hindrance remains to be explored. On the other hand, in the hemagglutination-inhibition test, we also showed that VRE directly attached to the virion and blocked the subsequent attachment of the virus to RBCs. More importantly, similar inhibition of virus binding could be further validated in susceptible cells. In light of its dual mechanisms of action in blocking viral entry, VRE shows prominent antiviral activity in the early stage. Furthermore, as VRE is able to mask the RBC surface, similar

inhibition of binding for other RBC-agglutinating viruses, such as adenoviruses, paramyxoviruses and coronaviruses, is possible and should be investigated in future studies.

Endosomal delivery of influenza virus is one of the critical steps in establishing viral infection and can become an attractive target mechanism for antivirals. In this study, after successful binding of the virus to cellular receptors, VRE was shown to influence the cellular endocytosis machinery and viral uncoating/fusion, thereby achieving significant antiviral activity. Other antiviral drugs involved in inhibiting endosomal acidification include vacuolar ATPase blockers (Chen et al., 2013), chloroquine (Yan et al., 2013), and fusion inhibitors (Kadam and Wilson, 2017). These drugs have demonstrated broad-spectrum activity against multiple types of viruses, as many viruses adopt similar endocytosis-dependent infection processes.

Considering the known anti-α-glucosidase activity of vitexin and isovitexin (He et al., 2016), two active components of VRE, we first confirmed that VRE showed anti-α-glucosidase activity, although it had a higher IC_{50} (20.07 μg/ml) than the pure compounds of vitexin and isovitexin. Then, we demonstrated that VRE significantly influences HA protein surface presentation in a concentration-dependent manner. α-Glucosidase plays a pivotal role in the glycosylation process of several biological molecules, including viral surface proteins. Previous studies have shown that altering the glycosylation of the HA protein may severely impact viral infectivity. To our knowledge, this is the first report of an influenza-inhibiting mechanism mediated by anti-α-glucosidase activity in a natural product.

Previous studies have shown that flavonoids such as apigenin, a flavonoid commonly found in natural plants, have neuraminidase-inhibiting activity (Liu et al., 2008). In a docking study, vitexin was shown to have binding affinity with influenza A virus neuraminidase (Sadati et al., 2019). Similarly, the anti-influenza A virus H1N1 ability of isovitexin, with an IC_{50} of 14 μg/ml, has been reported (Ye et al., 2011), and the potential mechanism is through the viral neuraminidase inhibition (Luo et al., 2020). In this study, we confirmed that VRE showed anti-neuraminidase activity against two different subtypes of influenza virus. Nevertheless, the IC_{50} of VRE is far higher than that of oseltamivir, a pure neuraminidase inhibitor (Bassetti et al., 2019). While many identified influenza viruses exhibit anti-oseltamivir resistance, VRE's neuraminidase-inhibitory activity deserves further study.

In summary, VRE potently interferes with influenza virus infection at multiple steps during the infectious cycle (**Supplementary Figure S1**), demonstrating its broad-spectrum potential as an anti-influenza prevention and treatment agent. Continued development of VRE to generate antiviral therapeutics is warranted.

DATA AVAILABILITY STATEMENT

The raw data supporting the conclusions of this article will be made available by the authors, without undue reservation, to any qualified researcher.

AUTHOR CONTRIBUTIONS

H-WC conceived and designed the experiments. C-WL, C-CP, and Y-TC performed the experiments and analyzed the data. C-WL drafted the manuscript. H-WC edited the manuscript. All authors read and approved the final manuscript.

FUNDING

This work was supported by King's Ground Biotech Co., Ltd. (06HT617007 to H-WC) and National Taiwan University. The funders had no role in the study design, data collection and analysis, decision to publish, or preparation of the manuscript.

ACKNOWLEDGMENTS

The authors acknowledge support from the Imaging Core Facilities at the Institute of Cellular and Organismic Biology of Academia Sinica for assistance on TEM image acquisition.

SUPPLEMENTARY MATERIAL

The Supplementary Material for this article can be found online at: https://www.frontiersin.org/articles/10.3389/fphar.2020.584973/full#supplementary-material

REFERENCES

Abraham, G. M., Morton, J. B., and Saravolatz, L. D. (2020). Baloxavir: a novel antiviral agent in the treatment of influenza. *Clin. Infect. Dis.* 71 (7), 1790–1794. doi:10.1093/cid/ciaa107

Bai, Y., Chang, J., Xu, Y., Cheng, D., Liu, H., Zhao, Y., et al. (2016). Antioxidant and myocardial preservation activities of natural phytochemicals from mung bean (*Vigna radiata* L.) seeds. *J. Agric. Food Chem.* 64 (22), 4648–4655. doi:10.1021/acs.jafc.6b01538

Bassetti, M., Castaldo, N., and Carnelutti, A. (2019). Neuraminidase inhibitors as a strategy for influenza treatment: pros, cons and future perspectives. *Expert Opin. Pharmacother.* 20 (14), 1711–1718. doi:10.1080/14656566.2019.1626824

Bouvier, N. M., and Palese, P. (2008). The biology of influenza viruses. *Vaccine* 26 (Suppl. 4), D49–D53. doi:10.1016/j.vaccine.2008.07.039

Cao, D., Li, H., Yi, J., Zhang, J., Che, H., Cao, J., et al. (2011). Antioxidant properties of the mung bean flavonoids on alleviating heat stress. *PLoS One* 6 (6), e21071. doi:10.1371/journal.pone.0021071

Chen, H. W., Cheng, J. X., Liu, M. T., King, K., Peng, J. Y., Zhang, X. Q., et al. (2013). Inhibitory and combinatorial effect of diphyllin, a v-ATPase blocker, on influenza viruses. *Antivir. Res.* 99 (3), 371–382. doi:10.1016/j.antiviral.2013.06.014

Dou, D., Revol, R., Ostbye, H., Wang, H., and Daniels, R. (2018). Influenza A virus cell entry, replication, virion assembly and movement. *Front. Immunol.* 9, 1581. doi:10.3389/fimmu.2018.01581

Ganesan, K., and Xu, B. (2018). A critical review on phytochemical profile and health promoting effects of mung bean (*Vigna radiata*). *Food Sci. Human Wellness* 7 (1), 11–33. doi:10.1016/j.fshw.2017.11.002

Hafidh, R. R., Abdulamir, A. S., Abu Bakar, F., Sekawi, Z., Jahansheri, F., and Jalilian, F. A. (2015). Novel antiviral activity of mung bean sprouts against respiratory syncytial virus and herpes simplex virus-1: an *in vitro* study on virally infected vero and MRC-5 cell lines. *BMC Compl. Altern. Med.* 15, 179. doi:10.1186/s12906-015-0688-2

Hashiguchi, A., Hitachi, K., Zhu, W., Tian, J., Tsuchida, K., and Komatsu, S. (2017). Mung bean (*Vigna radiata* (L.)) coat extract modulates macrophage functions to enhance antigen presentation: a proteomic study. *J. Proteomics* 161, 26–37. doi:10.1016/j.jprot.2017.03.025

He, M., Min, J. W., Kong, W. L., He, X. H., Li, J. X., and Peng, B. W. (2016). A review on the pharmacological effects of vitexin and isovitexin. *Fitoterapia* 115, 74–85. doi:10.1016/j.fitote.2016.09.011

Hu, C. J., Chen, Y. T., Fang, Z. S., Chang, W. S., and Chen, H. W. (2018). Antiviral efficacy of nanoparticulate vacuolar ATPase inhibitors against influenza virus infection. *Int. J. Nanomed.* 13, 8579–8593. doi:10.2147/IJN.S185806

Kadam, R. U., and Wilson, I. A. (2017). Structural basis of influenza virus fusion inhibition by the antiviral drug arbidol. *Proc. Natl. Acad. Sci. U.S.A.* 114 (2), 206–214. doi:10.1073/pnas.1617020114

Lampejo, T. (2020). Influenza and antiviral resistance: an overview. *Eur. J. Clin. Microbiol. Infect. Dis.* 39 (7), 1201–1208. doi:10.1007/s10096-020-03840-9

Lau, K. M., Lee, K. M., Koon, C. M., Cheung, C. S., Lau, C. P., Ho, H. M., et al. (2008). Immunomodulatory and anti-SARS activities of *Houttuynia cordata*. *J. Ethnopharmacol.* 118 (1), 79–85. doi:10.1016/j.jep.2008.03.018

Li, T., and Peng, T. (2013). Traditional Chinese herbal medicine as a source of molecules with antiviral activity. *Antivir. Res.* 97 (1), 1–9. doi:10.1016/j.antiviral.2012.10.006

Liu, A. L., Wang, H. D., Lee, S. M., Wang, Y. T., and Du, G. H. (2008). Structure-activity relationship of flavonoids as influenza virus neuraminidase inhibitors and their *in vitro* anti-viral activities. *Bioorg. Med. Chem.* 16 (15), 7141–7147. doi:10.1016/j.bmc.2008.06.049

Luo, S., Guo, L., Sheng, C., Zhao, Y., Chen, L., Li, C., et al. (2020). Rapid identification and isolation of neuraminidase inhibitors from mockstrawberry (*Duchesnea indica* Andr.) based on ligand fishing combined with HR-ESI-Q-TOF-MS. *Acta Pharm. Sin. B* [Epub ahead of print]. doi:10.1016/j.apsb.2020.04.001

Moscona, A. (2008). Medical management of influenza infection. *Annu. Rev. Med.* 59, 397–413. doi:10.1146/annurev.med.59.061506.213121

Nair, R. M., Yang, R. Y., Easdown, W. J., Thavarajah, D., Thavarajah, P., Hughes, J., et al. (2013). Biofortification of mungbean (*Vigna radiata*) as a whole food to enhance human health. *J. Sci. Food Agric.* 93 (8), 1805–1813. doi:10.1002/jsfa.6110

Pullela, S. V., Tiwari, A. K., Vanka, U. S., Vummenthula, A., Tatipaka, H. B., Dasari, K. R., et al. (2006). HPLC assisted chemobiological standardization of alpha-glucosidase-I enzyme inhibitory constituents from *Piper longum* Linn-An Indian medicinal plant. *J. Ethnopharmacol.* 108 (3), 445–449. doi:10.1016/j.jep.2006.06.004

Randhir, R., and Shetty, K. (2007). Mung beans processed by solid-state bioconversion improves phenolic content and functionality relevant for diabetes and ulcer management. *Innovat. Food Sci. Emerg. Technol.* 8 (2), 197–204. doi:10.1016/j.ifset.2006.10.003

Reed, L. J., and Muench, H. (1938). A simple method of estimating fifty per cent endpoints. *Am. J. Hyg.* 27, 493–497. doi:10.1093/oxfordjournals.aje.a118408

Sadati, S. M., Gheibi, N., Ranjbar, S., and Hashemzadeh, M. S. (2019). Docking study of flavonoid derivatives as potent inhibitors of influenza H1N1 virus neuraminidase. *Biomed. Rep.* 10 (1), 33–38. doi:10.3892/br.2018.1173

Saito, T., and Yamaguchi, I. (2000). Effect of glycosylation and glucose trimming inhibitors on the influenza A virus glycoproteins. *J. Vet. Med. Sci.* 62 (6), 575–581. doi:10.1292/jvms.62.575

Sato, M., Takashita, E., Katayose, M., Nemoto, K., Sakai, N., Hashimoto, K., et al. (2020). Detection of variants with reduced baloxavir marboxil susceptibility after treatment of children with influenza A during the 2018-2019 influenza season. *J. Infect. Dis.* 222 (1), 121–125. doi:10.1093/infdis/jiaa061

Wei, C. J., Crank, M. C., Shiver, J., Graham, B. S., Mascola, J. R., and Nabel, G. J. (2020). Next-generation influenza vaccines: opportunities and challenges. *Nat. Rev. Drug Discov.* 19 (4), 239–252. doi:10.1038/s41573-019-0056-x

Yan, Y., Zou, Z., Sun, Y., Li, X., Xu, K. F., Wei, Y., et al. (2013). Anti-malaria drug chloroquine is highly effective in treating avian influenza A H5N1 virus infection in an animal model. *Cell Res.* 23 (2), 300–302. doi:10.1038/cr.2012.165

Ye, W. Y., Li, X., and Cheng, J. W. (2011). Screening of eleven chemical constituents from *Radix isatidis* for antiviral activity. *Afr. J. Pharm. Pharmacol.* 5 (16), 1932–1936. doi:10.5897/Ajpp11.559

Young, B. E., and Chen, M. (2020). Influenza in temperate and tropical Asia: a review of epidemiology and vaccinology. *Hum. Vaccines Immunother.* 16 (7), 1659–1667. doi:10.1080/21645515.2019.1703455

Zhang, X. W., Shang, P. P., Qin, F., Zhou, Q., Gao, B. Y., Huang, H. Q., et al. (2013). Chemical composition and antioxidative and anti-inflammatory properties of ten commercial mung bean samples. *LWT Food Sci. Technol.* 54 (1), 171–178. doi:10.1016/j.lwt.2013.05.034

Zhou, N. N., Shortridge, K. F., Claas, E. C., Krauss, S. L., and Webster, R. G. (1999). Rapid evolution of H5N1 influenza viruses in chickens in Hong Kong. *J. Virol.* 73 (4), 3366–3374. doi:10.1128/JVI.73.4.3366-3374.1999

Zhu, Q., Bang, T. H., Ohnuki, K., Sawai, T., Sawai, K., and Shimizu, K. (2015). Inhibition of neuraminidase by *Ganoderma* triterpenoids and implications for neuraminidase inhibitor design. *Sci. Rep.* 5, 13194. doi:10.1038/srep13194

Zhu, W. Z., Wen, Y. C., Lin, S. Y., Chen, T. C., and Chen, H. W. (2020). Anti-influenza protective efficacy of a H6 virus-like particle in chickens. *Vaccines (Basel)* 8 (3). doi:10.3390/vaccines8030465

Conflict of Interest: C-CP is a current employee of King's Ground Biotech Co., Ltd. This does not alter our adherence to the policies set forth by the journal on data and material sharing.

The remaining authors declare that the research was conducted in the absence of any commercial or financial relationships that could be construed as a potential conflict of interest.

frontiers in Pharmacology

ORIGINAL RESEARCH
published: 10 December 2020
doi: 10.3389/fphar.2020.607027

Ganghuo Kanggan Decoction in Influenza: Integrating Network Pharmacology and *In Vivo* Pharmacological Evaluation

Yanni Lai[1†], Qiong Zhang[2†], Haishan Long[2†], Tiantian Han[1], Geng Li[2], Shaofeng Zhan[3], Yiwei Li[2], Zonghui Li[2], Yong Jiang[4] and Xiaohong Liu[3]**

[1]The First Clinical Medical College, Guangzhou University of Chinese Medicine, Guangzhou, China, [2]Laboratory Animal Center, Guangzhou University of Chinese Medicine, Guangzhou, China, [3]The First Affiliated Hospital of Guangzhou University of Chinese Medicine, Guangzhou, China, [4]Shenzhen Hospital of Integrated Traditional Chinese and Western Medicine, Shenzhen, China

OPEN ACCESS

Edited by:
Paul F. Moundipa, University of Yaounde I, Cameroon

Reviewed by:
Qingjun Li, Shandong University of Traditional Chinese Medicine, China
Arunachalam Karuppusamy, Federal University of Mato Grosso, Brazil

***Correspondence:**
Yong Jiang
jiangyongszzxy@163.com
Xiaohong Liu
drlxh@foxmail.com

[†]These authors have contributed equally to this work and share co authorship

Specialty section:
This article was submitted to Ethnopharmacology, a section of the journal Frontiers in Pharmacology

Received: *16 September 2020*
Accepted: *09 November 2020*
Published: *10 December 2020*

Citation:
Lai Y, Zhang Q, Long H, Han T, Li G, Zhan S, Li Y, Li Z, Jiang Y and Liu X (2020) Ganghuo Kanggan Decoction in Influenza: Integrating Network Pharmacology and In Vivo *Pharmacological Evaluation. Front. Pharmacol. 11:607027. doi: 10.3389/fphar.2020.607027*

Background: Ganghuo Kanggan decoction (GHKGD) is a clinical experience prescription used for the treatment of viral pneumonia in the Lingnan area of China, and its clinical effect is remarkable. However, the mechanism of GHKGD in influenza is still unclear.

Objective: To predict the active components and signaling pathway of GHKGD and to explore its therapeutic mechanism in influenza and to verified it *in vivo* using network pharmacology.

Methods: The potential active components and therapeutic targets of GHKGD in the treatment of influenza were hypothesized through a series of network pharmacological strategies, including compound screening, target prediction and pathway enrichment analysis. Based on the target network and enrichment results, a mouse model of influenza A virus (IAV) infection was established to evaluate the therapeutic effect of GHKGD on influenza and to verify the possible molecular mechanism predicted by network pharmacology.

Results: A total of 116 candidate active compounds and 17 potential targets were identified. The results of the potential target enrichment analysis suggested GHKGD may involve the RLR signaling pathway to reduce inflammation in the lungs. *In vivo* experiments showed that GHKGD had a protective effect on pneumonia caused by IAV-infected mice. Compared with the untreated group, the weight loss in the GHKGD group in the BALB/c mice decreased, and the inflammatory pathological changes in lung tissue were reduced ($p < 0.05$). The expression of NP protein and the virus titers in lung were significantly decreased ($p < 0.05$). The protein expression of RIG-I, NF-kB, and STAT1 and the level of MAVS and IRF3/7 mRNA were remarkably inhibited in GHKGD group ($p < 0.05$). After the treatment with GHKGD, the level of Th1 cytokines (IFN-γ, TNF-α, IL-2) was increased, while the expression of Th2 (IL-5, IL4) cytokines was reduced ($p < 0.05$).

Conclusion: Through a network pharmacology strategy and *in vivo* experiments, the multi-target and multi-component pharmacological characteristics of GHKGD in the treatment of influenza were revealed, and regulation of the RLR signaling pathway

during the anti-influenza process was confirmed. This study provides a theoretical basis for the research and development of new drugs from GHKGD.

Keywords: ganghuo kanggan decoction, influenza, network pharmacology, RIG-I-like receptors signal pathway, pneumonia, type I interferon

INTRODUCTION

Influenza is an acute infectious respiratory disease caused by the influenza virus. It has high morbidity, strong infectivity, widespread epidemic potential and high mortality (Cordova-Villalobos et al., 2017). Influenza virus pandemics, which are also common causes of death, are mainly caused by IAV. In 2009, a new type of H1N1 influenza virus caused the "Mexican influenza pandemic," which affected 214 countries and regions worldwide and caused more than 290,000 deaths, 201,000 of which were from respiratory failure (Buchholz et al., 2016). Death from severe influenza due to respiratory failure is closely related to increased permeability of the alveolar epithelial-vascular endothelial barrier and excessive release of inflammatory factors (Herold et al., 2015). Severe viral infections can induce the release of a large amount of cytokines in the body, causing a severe imbalance between the body's pro-inflammatory and anti-inflammatory cytokines, inducing cytokine storm and targeting the lungs, thus triggering acute lung injury (ALI) and even acute respiratory distress syndrome (ARDS) (Chen et al., 2018). With the rapid mutation of influenza viruses and the emergence of resistance to antiviral drugs, current vaccines and drugs still cannot effectively control the widespread spread of influenza viruses. As a result, an increasing number of scientists are focusing on the development of drugs against host targets (Hsieh et al., 2018). Therefore, how to effectively control inflammation before the inflammatory factor storm occur is an effective means to reduce the progression of influenza to ALI or ARDS.

Innate immunity is the first line of defense against pathogen invasion. Retinoic acid-inducible gene I (RIG-I), one of the main members of the RIG-I-like receptor (RLRs) family, plays an important role in the identification of intracellular influenza viruses and triggering antiviral and inflammatory responses (Liu et al., 2019). After RIG-I recognizes the 5′-triphosphate influenza virus single-stranded RNA (ssRNA), its helicase domain binds to ATP to activate the mitochondrial antiviral signal protein. The interaction between mitochondrial antiviral signaling protein (MAVS) and the stimulator of interferon genes (STING) on the endoplasmic reticulum further activates NF-κB and interferon regulatory factor 3/7 (IRF3/7), which promotes the production of pro-inflammatory factors and type I and type III interferons (Liu et al., 2019). This causes the infected cells and surrounding tissues enter an antiviral state (Lin et al., 2019).

Traditional Chinese medicine (TCM) has achieved substantial results in the treatment of viral diseases (Pleschka et al., 2009; Ge et al., 2010). Modern studies have shown that TCM can not only directly inhibit viral replication but also regulate cellular and humoural immunity, improve pulmonary circulation, and eliminate and reduce respiratory inflammatory exudates (Ma et al., 2017; Shi et al., 2020), suggesting that TCM has the advantages and characteristics of multiple components, multiple targets, and integrated regulation. GHKGD is a clinical experience formula based on clinical characteristics and its performance in treating viral pneumonia in the Lingnan area (Zhao et al., 2018). This prescription is based on the initial formula Yin Qiao San for febrile disease, with the addition of *Ilex asprella* Champ. ex Benth., *Pogostemon cablin* (Blanco) Benth., *Notopterygium incisum* K.C.Ting ex H.T.Chang and other heat-reducing and damp-releasing drugs, including *Lonicera japonica* Thunb., *Forsythia suspensa* (Thunb.) Vahl, *Saposhnikovia divaricata* (Turcz.) Schischk., *Notopterygium incisum* K.C.Ting ex H.T.Chang., *Bupleurum chinense* DC., *Atractylodes lancea* (Thunb.) DC., *Nepeta tenuifolia* Benth. *and Calculus bovis.* It has the functions of Shufeng Jiebiao, Qingre Jiedu, and Qushi Hezhong and is targeted for the treatment of wind, heat and wet invasion of lung-type influenza in Lingnan, with significant clinical effects (Yang et al., 2017a; Lyv et al., 2017).

In our previous studies, GHKGD could remarkly reduce the exudation of inflammatory mediators in mice with H1N1 (A/FM1/1/47) influenza virus pneumonia by improving anti-inflammatory cytokine levels (IL-10, IFN-γ), lowering pro-inflammatory cytokines (IL-6, TNF-α, MCP-1) (Chen et al., 2015). In addition, GHKGD could significantly prolong the average survival time of mice, and at the same time increase the oxygen content and blood oxygen saturation in the arterial blood of virus-infected mice, and reduce the partial pressure of carbon dioxide (Liu et al., 2015). However, the specific mechanism of GHKGD reducing the severity of pneumonia caused by influenza virus is not clear. Therefore, in this study, we try to use the strategy of network pharmacology, a recently developed discipline that combines holistic network analysis and pharmacology (Yue et al., 2017; Liu et al., 2020), to reveal its mechanism.

In this study, we used a network pharmacology method to analyse the interaction between active molecules, potential targets and target diseases of GHKGD. According to the preliminary analysis results, we studied the mechanism of GHKGD regulating the RLR signaling pathway in the treatment of influenza in a mouse model of IAV infection. The detailed technical strategy of the current study was shown in **Figure 1**.

MATERIALS AND METHODS

Candidate Compound Screening

All of the chemical ingredients of GHKGD were collected from the Traditional Chinese Medicine Systems Pharmacology database and Analysis Platform (TCMSP, http://tcmspw.com) (Ru et al., 2014), Bioinformatics Analysis Tool for Molecular Mechanism of Traditional Chinese Medicine (BATMAN-TCM) (http://bionet.ncpsb.org/batman-tcm/index.php/Home/Index/index)

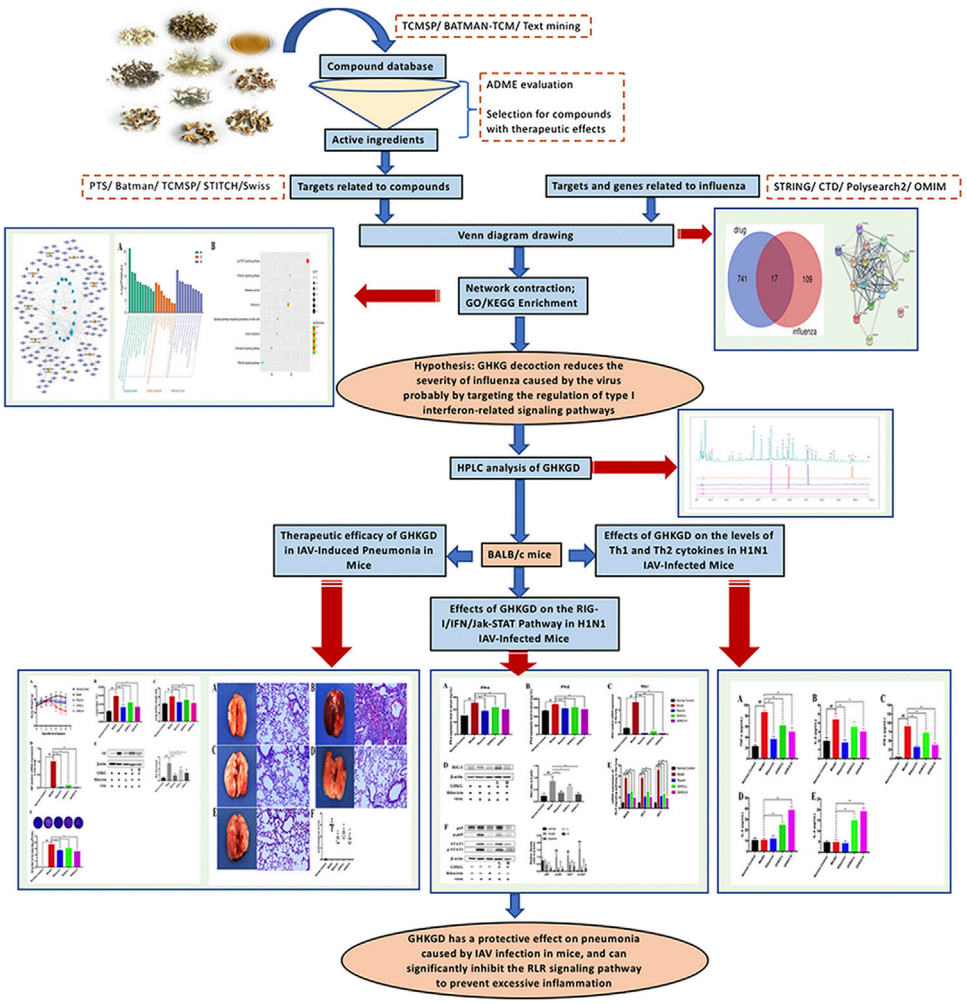

FIGURE 1 | The technical strategy of the current study.

(Liu et al., 2016) and wide-scale searches of the literature, including the Web of Science, PubMed, China BioMedical Literature (CBM) and China National Knowledge Infrastructure (CNKI) databases. Collectively, 714 compounds were identified. Here, we selected the ingredients that met the criteria of oral bioavailability (OB) ≥30% and drug-likeness (DL) ≥0.14 as candidate compounds for further analyses. OB is an important parameter to measure the pharmacokinetics and druggability of drugs *in vivo*. It represents the convergence of the processes of absorption, distribution, metabolism, and excretion (ADME) (Xu et al., 2012). DL is a qualitative principle used in drug design to accurately predict the "drug-like" nature of a compound (Lipinski et al., 2001).

Identification of Drug Targets

To obtain as many drug compound targets as possible, we searched and predicted targets from multiple databases, including the Pharmaceutical Target Seeker (http://www.rcdd.org.cn/PTS/search) (Ding et al., 2017), TCMSP, BATMAN-TCM (http://bionet.ncpsb.org/batman-tcm/), Swiss Target Prediction (Swiss, http://www.swisstargetprediction.ch/) (Gfeller et al., 2014) and STITCH (http://stitch.embl.de/). All targets were restricted to human origin. Next, we retrieved the protein targets of influenza virus from several databases, such as the CTD database (http://ctdbase.org), OMIM database (https://omim.org/), Polysearch2 database (http://polysearch.cs.ualberta.ca/) and STRING database (https://string-db.org/cgi/input.pl). Then, all target names were converted into the corresponding official gene names in the UniProt database. The Venny2.1.0 online tool (http://bioinfogp.cnb.csic.es/tools/venny/index.html) was used to obtain the overlapping targets from the two sources to identify potential drug targets for the treatment of influenza.

Gene Ontology Enrichment Analysis of Targets

To systematically understand the biological processes of GHKGD in the treatment of influenza, we performed gene ontology (GO) enrichment analysis of potential targets. The terms with a p value of less than 0.05 were selected for functional annotation and

signaling pathway clustering. The above analysis was completed using the functional annotation tool of Metascape (https://metascape.org/gp/index.html#/main/step1).

Protein-Protein Interaction Data

The Draw Venn Diagram tool (http://bioinformatics.psb.ugent.be/webtools/Venn/) was used to obtain the target genes for the interaction between the drug (Ganghuo Kanggan decoction) and the disease (influenza). The STRING search tool (version 11.0) (https://string-db.org/cgi/input.pl) was employed to show the interactions in the PPI data, with the species limited to "*Homo sapiens*."

Network Construction and Analysis

To comprehensively analyse the molecular mechanism of GHKGD in the treatment of influenza, two network diagrams, drug-target-disease and target-biological process diagrams, were constructed using Cytoscape 3.7.1 software. The NetworkAnalyzer tool in the software was used to analyse the network topology properties, and the Cytoscape plugin cytohubba was used to analyse the core nodes of the network.

Preparation and HPLC Analysis of Ganghuo Kanggan Decoction

GHKGD is composed of 19 g *Ilex asprella* Champ. ex Benth., 6 g *Pogostemon cablin* (Blanco) Benth., 9 g *Forsythia suspensa* (Thunb.) Vahl, 6 g *Saposhnikovia divaricata* (Turcz.) Schischk., 5.5 g *Notopterygium incisum* K.C.Ting ex H.T.Chang, 9 g *Lonicera japonica* Thunb., 5 g *Bupleurum chinense* DC., 5 g *Atractylodes lancea* (Thunb.) DC., 5 g *Nepeta tenuifolia* Benth., 0.2 g artificial bezoar. All crude herbs were provided from the dispensary of the First Affiliated Hospital of Guangzhou University of Chinese Medicine. Firstly, all crude drugs except artificial bezoar powder were soaked in 1.5 L water for 2 h, then they were decocted to boiling for 1.5 h. The drugs were boiled once again for 1 h with 1 L water and the decoction was merged and filtered through a four-layer gauze. Next, the filtrates were concentrated to a concentration of 2.31 g crude drug/mL as the high dose and a concentration of 0.58 g crude drug/mL as the low dose. Finally, an artificial bezoar and volatile oil were added and mixed well. The decoction was stored at −4°C and sealed for later use *in vivo*. The positive drug ribavirin was purchased from Jiangxi Huiren Pharmaceutical Co., Ltd. (production batch number: 180401, specification: 100 mg/tablet).

HPLC-GHKGD analysis was performed at 246 nm for Prim-O-glucosylcimifugin, 5-O-methylvisammioside, Amygdalin, and Notopterol, using a Thermo Scientific U3000 HPLC system. Chromatographic separation was achieved with a Phenomenon® Luna-C18 analytical column (4.6 mm × 250 mm, 5 μm). Forsythin (lot numbers: 110821–201213, purity: 95.3%), Prim-O-glucosylcimifugin (lot numbers: 111522–201209, purity: 93.7%), 5-O-Methylvisammioside (lot numbers: 111523–201509, purity: 95.8%), Notoperol (lot numbers: 111820-201504, purity: 99.9%) were purchased from National Drug Reference Standards database. Took appropriate amounts of Prim-O-glucosylcimifugin, 5-O-Methylvisammioside, forsythin and Notoperol, and then added methanol to prepare solutions of 0.16, 0.20, 0.30, 0.20, 0.12 mg/mL, respectively. Took 10 mL of the GHKGD filtrate after decoction and filtration, evaporated it to dryness, added 1.5 g of neutral alumina, stirred evenly, passed through a column of neutral alumina column (100–200 mesh, 1.5 cm in diameter), and eluted with 100 mL of 70% ethanol. Collected the eluate, evaporated to dryness, and dissolved the residue with 50% methanol to 10 mL. Chromatographic condition: Phenomenon Luna C18 2) 100R (4.6 mm × 250 mm, 5 μm). Acetonitrile (A)- 0.2% glacial acetic acid (b) was taken as a mobile phase. The flow rate was 1.0 ml min^{-1}, and the column temperature was 30°C. The detection wavelength was 246 nm. The injection volume was 10 μL.

Animals and Experimental Groups

Sixty SPF BALB/c mice (30 males and 30 females) weighing between 16 g and 18 g were purchased from the Experimental Animal Center of Guangzhou University of Traditional Chinese Medicine (GZUCM). Animal experiments were approved by the Animal Care and Use Committee of the Experimental Animal Center of GZUCM. After 24 h quarantine, the mice were randomly divided into the normal control (NC) group, model (IAV-C + sterile saline, suspended in 0.5% Tween 80) group, positive control ribavirin group, GHKG high-dose group, and GHKG low-dose group, with 12 mice in each group. Standard mouse chow and tap water were provided ad libitum during the study. The mice were housed in the Guangdong Association for the Accreditation of Laboratory Animal Care-accredited GZUCM Laboratory Animal Research Center.

All mice except those in the normal control group were infected with two LD_{50} H1N1 (PR8) virus by intranasal instillation under mild anaesthesia using ether. Mice in the normal control group were administered an equal volume of 0.9% sodium chloride solution by intranasal instillation. Two hours after infection, drugs were administered orally to the treatment groups. The ribavirin was administered at 75 mg/kg/day, and the GHKGD was administered to the high-dose and low-dose groups at 46.2 g/kg/day and 11.6 g/kg/day, respectively. The normal control and model groups were given an equal volume of 0.9% sodium chloride solution. Dosing was continued once daily for 5 days. The disease status of the mice was observed daily, and the body weight was recorded. On day 5 after infection, mice were sacrificed to collect relevant samples, and the body weight, wet lung weight, and extent of lung pathological changes were measured.

Viruses and Cells

Influenza A/Puerto Rico/8/34 (H1N1) virus was maintained at the Laboratory Animal Center, Guangzhou University of Chinese Medicine, and propagated in embryonated chicken eggs. The viruses were aliquoted and stored at −80°C. Madin-Darby canine kidney (MDCK) cells were maintained in minimum essential medium (MEM) containing 10% foetal bovine serum and antibiotics (penicillin and streptomycin).

Plague Reduction Assay

MDCK cells were seeded in 6-well tissue culture plates (6×10^5 cells/well) and were then incubated at 37°C in 5% CO_2 for 24 h. The cells were washed once with PBS and were then infected with the collected mouse lung tissue supernatant and incubated at 37°C

for 2 h. After washing three times with PBS, the cell monolayers were covered with agar overlay medium (MEM supplemented with 1% low melting point agarose and 2.5 μg/mL TPCK-treated trypsin) and incubated at 37°C for 3–4 days. The cell monolayers were fixed with 4% paraformaldehyde for 1 h. The covering was then removed, and the cell monolayers were stained with 2% crystal violet solution containing 10% ethanol.

Histopathological Staining

Mouse lung tissue was stored in a 5 mL EP tube filled with 4% paraformaldehyde solution, and after fixation for 48 h, sections were stained with haematoxylin and eosin (HE) and then tested under a microscopy in a double-blinded manner. The following scoring criteria were used to classify the degree of lung injury into five levels: the presence of necrotic bronchiole and bronchial epithelium; exudate of plasma cells in the bronchiole and bronchial lumen; inflammatory cells in the bronchiolar, peribronchiolar and alveolar interstitium (predominantly lymphocytes and neutrophils); collapse of the alveoli or bronchi (atelectasis); and diffuse or multifocal interstitial edema. No damage is marked as 0, mild damage is 1, moderate damage is 2, severe damage is 3, and severe histological change is 4 (Parsey et al., 1998).

ELISA

The IFN-α and IFN-β levels in mouse serum were measured using ELISA according to the manufacturer's instructions. Each treatment was analysed in triplicate. A Mouse IFN-α SimpleStep ELISA® Kit (Cat. Number: ab252352) and a Mouse IFN-β SimpleStep ELISA® Kit (Cat. Number: ab252363) were purchased from Abcam (Burlingame, CA, USA).

Real-Time QPCR Analysis

The mRNA expression levels of the NP, RIG-I, MAVS, IRF3, IRF7 and STAT1 genes in lung homogenates were detected by real-time quantitative PCR. Total RNA from mouse lungs was extracted using an Ultrapure RNA kit (CoWin Biotech, Beijing, China), and cDNA was then synthesized from the total RNA using a M-MLV Reverse transcriptase kit (Promega, Madison, WI, United States).

Western Blot Analysis

Western blot analysis was performed according to standard procedures. In brief, tissues were lysed in radio-immunoprecipitation assay (RIPA) buffer containing 1% PMSF and were then centrifuged at 10,000 rpm for 10 min to remove insoluble matter. The protein concentration was determined using a BCA protein concentration assay kit. Equal amounts of protein (30 μg) were separated via 10% SDS-PAGE and transferred to a PVDF membrane (Mannheim, Germany). The membrane was incubated with 5% skim milk to block non-specific binding sites, incubated with the primary antibody overnight at 4°C, and then incubated with the corresponding horseradish peroxidase (HRP)-conjugated secondary antibody at room temperature for 1–2 h. ECL reagent (Rockford, IL, USA) was used to detect antigen-antibody complexes. The protein expression levels were normalized to that of β-actin in the same sample.

BD Cytometric Bead Arry Analysis

The levels (pg/ml) of tumor necrosis factor-α (TNF-α), interferon-γ (IFN-γ), interleukin-2 (IL-2), interleukin-4 (IL-4) and interleukin-5 (IL-5) in serum samples were determined using a BD™ Cytometric Bead Array Mouse Th1/Th2 Cytokine Kit (CBA) (lot: 9073921, BD Biosciences Pharmingen, San Diego, USA), according to the manufacturer's instructions. Fluorescence was determined using a flow cytometer (FACS Calibur, Becton-Dickinson Bio-sciences, Heidelberg, Germany) and cytokine level was analyzed using a BD CBA Software.

Statistical Analysis

All data in this experiment are expressed as the mean ± SEM values. Multiple statistical analyses were conducted by one-way analysis of variance (ANOVA). Comparisons between two groups were performed using Dunnett's *t*-test. A probability value of $p < 0.05$ was defined as significant. GraphPad Prism 7.0 was used for statistical analyses.

RESULTS

Compound Information

The compounds comprising the 11 kinds of Chinese medicine in Gangzhi Kanggan Decoction were obtained from the TCMSP database and the BATMAN-TCM database. A total of 182 candidate compounds were obtained after screening with ADME parameters (OB ≥ 30%, DL ≥ 0.14). Certain compounds with significant pharmacological effects and high levels were also considered. The final candidate compounds are listed in **Supplementary Table S1**.

Compouds in GHKGD Active Against Influenza

Based on the CTD, Polysearch2, OMIM and STRING databases, a total of 126 (**Supplementary Table S2**) targets directly and indirectly associated with influenza were obtained. By employing three available resources, namely, the PTS, BATMAN, and TCMSP databases, we obtained 798 GHKGD-related targets (**Supplementary Table S3**). After determination of the overlapping targets obtained from these two sources, a total of 17 potential target gene-associated compounds were obtained. Furthermore, 116 compounds in GHKT decoction active against influenza were retrieved. Detailed information on the potential protein targets and active compounds in GHKGD obtained are presented in **Tables 1**,**2**, respectively.

Protein-Protein Interaction Network of Target Genes

As shown in **Figure 1A**, there were 17 active components of GHKGD acting on influenza-related targets: MPL, EIF2AK2, PTPN1, PTPN11, EGFR, TYK2, ISG20, IKBKE, PTPN6, PTPN2, JAK3, JAK1, JAK2, STAT3, CTSA, JUN, and STAT1. The PPI relationships among these 17 target genes were obtained by the STRING tool (**Figure 1B**). The PPI relationship network had 17 nodes and 77 edges, and the average node degree was 9.06.

TABLE 1 | Information on 17 potential target gene-associated compounds.

Uniprot ID	Protein name	Gene name	Degree
P00533	Epidermal growth factor receptor	EGFR	132
P52333	Tyrosine-protein kinase JAK3	JAK3	39
P18031	Tyrosine-protein phosphatase non-receptor type 1	PTPN1	16
O60674	Tyrosine-protein kinase JAK2	JAK2	11
Q96AZ6	Interferon-stimulated gene 20 kDa protein	ISG20	11
P17706	Tyrosine-protein phosphatase non-receptor type 2	PTPN2	8
P40763	Signal transducer and activator of transcription 3	STAT3	7
Q06124	Tyrosine-protein phosphatase non-receptor type 11	PTPN11	7
P42224	Signal transducer and activator of transcription 1-alpha/beta	STAT1	7
P23458	Tyrosine-protein kinase JAK1	JAK1	7
P29597	Non-receptor tyrosine-protein kinase TYK2	TYK2	6
P19525	Interferon-induced, double-stranded RNA-activated protein kinase	EIF2AK2	6
P10619	Lysosomal protective protein	CTSA	5
P40238	Thrombopoietin receptor	MPL	4
Q14164	Inhibitor of nuclear factor kappa-B kinase subunit epsilon	IKBKE	4
P05412	Transcription factor AP-1	JUN	3
P29350	Tyrosine-protein phosphatase non-receptor type 6	PTPN6	2

Gene Ontology Enrichment Analysis for Potential Targets in Influenza

To explore the molecular mechanism of GHKGD in influenza, GO enrichment analysis and KEGG enrichment were performed on the 17 candidate targets. A total of 81 biological processes, 10 cellular components, and 30 molecular functions were obtained by GO analysis, from which the top 10 terms were selected ($p < 0.05$) (**Figure 2A**). In addition, eight pathways were obtained by KEGG analysis, which were ralated to influenza ($p < 0.05$) (**Figure 2B**). These biological processes might be important for the occurrence and development of influenza and included terms such as regulation of type I interferon-mediated signaling pathway, regulation of interferon-gamma-mediated signaling pathway, negative regulation of cell proliferation, type I interferon signaling pathway, Jak-STAT signaling pathway, Chemokine signaling pathway, and PI3K-Akt signaling pathway. These preliminary results support the hypothesis that GHKGD reduces the severity of influenza caused by the virus, at least in part through targeting the regulation of type I interferon-related signaling pathways and the Jak-STAT signaling pathway.

Interaction Network Contruction and Network Analysis

To reveal the synergistic multi-component and multi-target effects of GHKGD in the treatment of influenza as well as to explore its mechanism of action, a compound-target-disease (C-T-D) network was constructed and analysed. This network was composed of 151 nodes (116 compounds and 17 target genes) and 22,650 edges (**Figure 3**). The network degree of heterogeneity was 1.862, and the network centrality was 0.682. Analysing the topological parameters of the network helps identify core nodes, which are compounds and targets that play an important role in the network. Here, we used the node degree to identify important components and kernel targets. The size of a node is directly proportional to its degree. The larger the node, the higher is the degree, and the more important it is in the network. As shown in **Figure 1**, the top 10 target genes ranked by node degree were EGFR (106), JAK3 (35), PTPN1 (16), JAK2 (9), ISG20 (9), PTPN2 (8), STAT3 (7), PTPN11 (7), STAT1 (7), and JAK1 (7). In addition, the core compounds (degree ≥ 8) included MOL003358 (14), MOL011980 (13), MOL017746 (9), MOL11754 (9), MOL001789 (9), MOL011755 (8), MOL000358 (8) and MOL001944 (8). Some compounds, such as compound MOL003358, can act on multiple targets simultaneously, while some targets, such as EGFR, JAK3, and ISG20, can be acted on by multiple compounds simultaneously. This pattern explains the multi-component and multi-target characteristics of TCMs. Some compounds, such as compounds MOL001789 (isoliquiritigenin), MOL000098 (quercetin), MOL000006 (luteolin) and MOL000422 (kaempferol), have been reported to exhibit activity against the influenza virus (Traboulsi et al., 2015; Zhang et al., 2017; Yan et al., 2019).

HPLC Analysis of Ganghuo Kanggan Decoction

The results of representative HPLC analysis were shown in **Figure 4**.

Therapeutic Efficacy of Ganghuo Kanggan Decoction in IAV-Induced Pneumonia in Mice

We evaluated the therapeutic effect of the drug in murine pneumonia caused by IAV at doses not inducing significant clinical symptoms and weight changes (high dose, 46.2 g/kg; low dose, 11.6 g/kg). As shown in **Figure 5A**, administration

TABLE 2 | 116 active compounds in GHKG decoction related to influenza.

Mol ID	Molecule name	MW	OB (%)	DL	Herb	Degree
MOL008838	Methyl (4R)-4-[(3R,5S,7S,8R,9S,10S,12S,13R,14S,17R)-3,7,12-trihydroxy-10,13-dimethyl-2,3,4,5,6,7,8,9,11,12,14,15,16,17-tetradecahydro-1H-cyclopenta[a]phenanthren-17-yl]pentanoate	422.67	32.32	0.76	*Calculus bovis*	3
MOL008839	Methyl desoxycholate	406.67	34.63	0.73	*Calculus bovis*	3
MOL008845	Deoxycholic acid	392.64	40.72	0.68	*Calculus bovis*	2
MOL008846	ZINC01280365	330.51	46.38	0.49	*Calculus bovis*	2
MOL000953	CLR	386.73	37.87	0.68	*Calculus bovis*	2
MOL001645	Linoleyl acetate	308.56	42.1	0.2	*Bupleurum chinense* DC.	3
MOL001789	Isoliquiritigenin	256.27	85.32	0.15	*Bupleurum chinense* DC.;	9
MOL002776	Baicalin	446.39	40.12	0.75	*Bupleurum chinense* DC. *Lonicera japonica* thunb.; *Bupleurum chinense* DC.;	3
MOL000449	Stigmasterol	412.77	43.83	0.76	*Nepeta tenuifolia* benth.	4
MOL000354	Isorhamnetin	316.28	49.6	0.31	*Bupleurum chinense* DC. *Lonicera japonica* thunb.; *Forsythia suspensa* (thunb.) vahl;	2
MOL000422	Kaempferol	286.25	41.88	0.24	*Bupleurum chinense* DC.	4
MOL004609	Areapillin	360.34	48.96	0.41	*Bupleurum chinense* DC.	2
MOL013187	Cubebin	356.4	57.13	0.64	*Bupleurum chinense* DC.	3
MOL004624	Longikaurin	348.48	47.72	0.53	*Bupleurum chinense* DC.	2
MOL004628	Octalupine	264.41	47.82	0.28	*Bupleurum chinense* DC.	2
MOL004644	Sainfuran	286.3	79.91	0.23	*Bupleurum chinense* DC.	2
MOL004648	Troxerutin	346.56	31.6	0.28	*Bupleurum chinense* DC.	3
MOL004653	(+)-anomalin	426.5	46.06	0.66	*Bupleurum chinense* DC.	3
MOL004683	Methyl (2E,4E)-octadeca-2,4-dienoate	294.53	38.77	0.17	*Bupleurum chinense* DC.	2
MOL004702	Saikosaponin c_qt	472.78	30.5	0.63	*Bupleurum chinense* DC.	3
MOL004718	α-spinasterol	412.77	42.98	0.76	*Bupleurum chinense* DC. *Bupleurum chinense* DC.; *Pogostemon cablin* (blanco) benth.; *Lonicera japonica* thunb.; *Forsythia suspensa* (thunb.) vahl;	2
MOL000098	Quercetin	302.25	46.43	0.28	*Nepeta tenuifolia* benth.	6
MOL000181	Atractylenolide III	248.35	31.15	0.17	*Atractylodes lancea* (thunb.) DC.	2
MOL000085	Beta-daucosterol_qt	414.79	36.91	0.75	*Atractylodes lancea* (thunb.) DC.	3
MOL000088	Beta-sitosterol 3-O-glucoside_qt	414.79	36.91	0.75	*Atractylodes lancea* (thunb.) DC.	2
MOL000092	daucosterin_qt	414.79	36.91	0.76	*Atractylodes lancea* (thunb.) DC.	2
MOL000094	daucosterol_qt	414.79	36.91	0.76	*Atractylodes lancea* (thunb.) DC.	2
MOL000043	Atractylenolide i	230.33	37.37	0.15	*Atractylodes lancea* (thunb.) DC.	5
MOL000184	NSC63551	412.77	39.25	0.76	*Atractylodes lancea* (thunb.) DC.	2
MOL000188	3β-acetoxyatractylone	274.39	40.57	0.22	*Atractylodes lancea* (thunb.) DC.	2
MOL000186	Stigmasterol	412.77	43.83	0.76	*Atractylodes lancea* (thunb.) DC.	2
MOL000179	2-Hydroxyisoxypropyl-3-hydroxy-7-isopentene-2,3-dihydrobenzofuran-5-carboxylic	306.39	45.2	0.2	*Atractylodes lancea* (thunb.) DC.	4
MOL000180	Aractylenolide II	232.35	46.2	0.15	*Atractylodes lancea* (thunb.) DC.	4
MOL000044	atractylenolideII	232.35	47.5	0.15	*Atractylodes lancea* (thunb.) DC.	3
MOL000011	AIDS-227003	386.38	68.83	0.66	*Saposhnikovia divaricata* (turcz.) schischk.	2
MOL011730	11-hydroxy-sec-o-beta-d-glucosylhamaudol_qt	292.31	50.24	0.27	*Saposhnikovia divaricata* (turcz.) schischk.	2
MOL011732	Anomalin	426.5	59.65	0.66	*Saposhnikovia divaricata* (turcz.) schischk.	2
MOL011737	Divaricatacid	320.32	87	0.32	*Saposhnikovia divaricata* (turcz.) schischk.	2

(Continued on following page)

TABLE 2 | (*Continued*) 116 active compounds in GHKG decoction related to influenza.

Mol ID	Molecule name	MW	OB (%)	DL	Herb	Degree
MOL011740	Divaricatol	334.35	31.65	0.38	*Saposhnikovia divaricata* (turcz.) schischk. *Saposhnikovia divaricata* (turcz.) schischk.;	2
MOL001941	Ammidin	270.3	34.55	0.22	*Notopterygium incisum* K.C.Ting ex H.T.Chang.	3
MOL011746	Isopimpinellin	246.23	43.14	0.17	*Saposhnikovia divaricata* (turcz.) schischk.	9
MOL011747	Ledebouriellol	374.42	32.05	0.51	*Saposhnikovia divaricata* (turcz.) schischk.	2
MOL011749	Phelloptorin	300.33	43.39	0.28	*Saposhnikovia divaricata* (turcz.) schischk.	2
MOL011754	4-hydroxy-9-methoxyfuro[3,2-g]chromen-7-one	232.2	31.78	0.15	*Saposhnikovia divaricata* (turcz.) schischk.	9
MOL011755	5-methoxy-8-hydroxypsoralen	232.2	48.4	0.15	*Saposhnikovia divaricata* (turcz.) schischk.	8
MOL001944	Marmesin	246.28	50.28	0.18	*Saposhnikovia divaricata* (turcz.) schischk.; *Notopterygium incisum* K.C.Ting ex H.T.Chang.	8
MOL002644	Phellopterin	300.33	40.19	0.28	*Saposhnikovia divaricata* (turcz.) schischk.; *Notopterygium incisum* K.C.Ting ex H.T.Chang.	4
MOL000359	Sitosterol	414.79	36.91	0.75	*Saposhnikovia divaricata* (turcz.) schischk.; *Nepeta tenuifolia* benth.; *Notopterygium incisum* K.C.Ting ex H.T.Chang. *Saposhnikovia divaricata* (turcz.) schischk.; *Lonicera japonica* thunb.; *Forsythia suspensa* (thunb.) vahl;	4
MOL000358	Beta-sitosterol	414.79	36.91	0.75	*Notopterygium incisum* K.C.Ting ex H.T.Chang.	6
MOL001494	Mandenol	308.56	42	0.19	*Saposhnikovia divaricata* (turcz.) schischk.; *Lonicera japonica* thunb.	4
MOL001889	Methyl linolelaidate	294.53	41.93	0.17	*Saposhnikovia divaricata* (turcz.) schischk. *Saposhnikovia divaricata* (turcz.) schischk.;	2
MOL001942	Isoimperatorin	270.3	45.46	0.23	*Notopterygium incisum* K.C.Ting ex H.T.Chang.	4
MOL003588	Prangenidin	270.3	36.31	0.22	*Saposhnikovia divaricata* (turcz.) schischk. *Saposhnikovia divaricata* (turcz.) schischk.;	2
MOL004793	Marmesine	246.28	84.77	0.18	*Notopterygium incisum* K.C.Ting ex H.T.Chang.	3
MOL007514	Methyl icosa-11,14-dienoate	322.59	39.67	0.23	*Saposhnikovia divaricata* (turcz.) schischk.	3
MOL011648	METHYL 10-OCTADECENOATE	296.55	31.9	0.17	*Saposhnikovia divaricata* (turcz.) schischk.	2
MOL013077	Decursin	328.39	39.27	0.38	*Saposhnikovia divaricata* (turcz.) schischk.	2
MOL002707	Phytofluene	543.02	43.18	0.5	*Lonicera japonica* thunb.	3
MOL002773	Beta-carotene	536.96	37.18	0.58	*Lonicera japonica* thunb.	3
MOL000432	Linolenic acid	278.48	45.01	0.15	*Nepeta tenuifolia* benth. *Lonicera japonica* thunb.; *Forsythia suspensa* (thunb.) vahl;	
MOL000006	Luteolin	286.25	36.16	0.25	*Nepeta tenuifolia* benth.	4
MOL002523	()-Cyclosativene	204.39	33.43	0.15	*Pogostemon cablin* (blanco) benth.	2
MOL002879	Diop	390.62	43.59	0.39	*Pogostemon cablin* (blanco) benth.	2
MOL005884	Patchoulan 1,12-diol	262.43	38.17	0.25	*Pogostemon cablin* (blanco) benth.	2
MOL005890	Pachypodol	356.4	75.06	0.4	*Pogostemon cablin* (blanco) benth.	2
MOL005907	ZINC02090576	220.39	77.74	0.16	*Pogostemon cablin* (blanco) benth.	2
MOL005921	Quercetin 7-O-β-D-glucoside	300.28	49.57	0.27	*Pogostemon cablin* (blanco) benth.	2
MOL005922	Acanthoside B	580.64	43.35	0.77	*Pogostemon cablin* (blanco) benth.	3
MOL005923	3,23-dihydroxy-12-oleanen-28-oic acid	518.56	30.86	0.86	*Pogostemon cablin* (blanco) benth.	2
MOL000695	Patchouli alcohol	222.41	101.96	0.14	*Pogostemon cablin* (blanco) benth.	2
MOL003062	, 5′-retro-beta,beta-carotene-3,3′-dione, 4′,5′-didehydro-	562.9	31.22	0.55	*Lonicera japonica* thunb.	3
MOL003044	Chryseriol	300.28	35.85	0.27	*Lonicera japonica* thunb.	2
MOL002914	Eriodyctiol (flavanone)	288.27	41.35	0.24	*Lonicera japonica* thunb.	2
MOL003103	Methyl octadeca-8,11-dienoate	294.53	41.93	0.17	*Lonicera japonica* thunb.	2

(Continued on following page)

TABLE 2 | (*Continued*) 116 active compounds in GHKG decoction related to influenza.

Mol ID	Molecule name	MW	OB (%)	DL	Herb	Degree
MOL003036	ZINC03978781	412.77	43.83	0.76	*Lonicera japonica* thunb.	2
MOL001495	Ethyl linolenate	306.54	46.1	0.2	*Lonicera japonica* thunb.	3
MOL003101	7-epi-vogeloside	432.47	46.13	0.58	*Lonicera japonica* thunb.	3
MOL003059	Kryptoxanthin	552.96	47.25	0.57	*Lonicera japonica* thunb.	2
MOL003014	Secologanic dibutylacetal_qt	384.57	53.65	0.29	*Lonicera japonica* thunb.	3
MOL003006	(-)-(3R,8S,9R,9aS,10aS)-9-ethenyl-8-(beta-D-glucopyranosyloxy)-2,3,9,9a,10,10a-hexahydro-5-oxo-5H,8H-pyrano[4,3-d]oxazolo[3,2-a]pyridine-3-carboxylic acid_qt	281.29	87.47	0.23	*Lonicera japonica* thunb.	2
MOL003315	3beta-acetyl-20,25-epoxydammarane-24alpha-ol	502.86	33.07	0.79	*Forsythia suspensa* (thunb.) vahl	2
MOL000522	Arctiin	534.61	34.45	0.84	*Forsythia suspensa* (thunb.) vahl	3
MOL003305	PHILLYRIN	534.61	36.4	0.86	*Forsythia suspensa* (thunb.) vahl	2
MOL003281	20 (S)-dammar-24-ene-3β,20-diol-3-acetate	486.86	40.23	0.82	*Forsythia suspensa* (thunb.) vahl	2
MOL003365	Lactucasterol	426.75	40.99	0.85	*Forsythia suspensa* (thunb.) vahl	2
MOL003344	β-amyrin acetate	468.84	42.06	0.74	*Forsythia suspensa* (thunb.) vahl	2
MOL003347	hyperforin	536.87	44.03	0.6	*Forsythia suspensa* (thunb.) vahl	2
MOL003348	Adhyperforin	550.9	44.03	0.61	*Forsythia suspensa* (thunb.) vahl	2
MOL003290	(3R,4R)-3,4-bis[(3,4-dimethoxyphenyl)methyl]oxolan-2-one	386.48	52.3	0.48	*Forsythia suspensa* (thunb.) vahl	2
MOL003295	(+)-pinoresinol monomethyl ether	372.45	53.08	0.57	*Forsythia suspensa* (thunb.) vahl	2
MOL000211	Mairin	456.78	55.38	0.78	*Forsythia suspensa* (thunb.) vahl	2
MOL003308	(+)-pinoresinol monomethyl ether-4-D-beta-glucoside_qt	372.45	61.2	0.57	*Forsythia suspensa* (thunb.) vahl	2
MOL003283	(2R,3R,4S)-4-(4-hydroxy-3-methoxy-phenyl)-7-methoxy-2,3-dimethylol-tetralin-6-ol	360.44	66.51	0.39	*Forsythia suspensa* (thunb.) vahl	2
MOL003370	Onjixanthone I	302.3	79.16	0.3	*Forsythia suspensa* (thunb.) vahl	2
MOL003322	FORSYTHINOL	372.45	81.25	0.57	*Forsythia suspensa* (thunb.) vahl	2
MOL003306	ACon1_001697	372.45	85.12	0.57	*Forsythia suspensa* (thunb.) vahl	2
MOL003358	Euxanthone	228.21	92.98	0.16	*Forsythia suspensa* (thunb.) vahl	14
MOL003330	(–)-Phillygenin	372.45	95.04	0.57	*Forsythia suspensa* (thunb.) vahl	2
MOL001941	Ammidin	270.3	34.55	0.22	*Notopterygium incisum* K.C.Ting ex H.T.Chang.; *Saposhnikovia divaricata* (turcz.) schischk.	3
MOL011962	6′-feruloylnodakenin	584.62	32.02	0.67	*Notopterygium incisum* K.C.Ting ex H.T.Chang.	3
MOL011963	8-geranoxy-5-methoxypsoralen	368.46	40.97	0.5	*Notopterygium incisum* K.C.Ting ex H.T.Chang.	3
MOL011968	Coumarin, glycoside	534.61	33.07	0.78	*Notopterygium incisum* K.C.Ting ex H.T.Chang.	4
MOL011969	Demethylfuropinnarin	270.3	41.31	0.21	*Notopterygium incisum* K.C.Ting ex H.T.Chang.	2
MOL011971	diversoside_qt	332.43	67.57	0.31	*Notopterygium incisum* K.C.Ting ex H.T.Chang.	2
MOL011975	Notoptol	354.43	62.97	0.48	*Notopterygium incisum* K.C.Ting ex H.T.Chang.	3
MOL011976	2-(4-hydroxyphenyl)ethyl 4-methoxybenzoate	272.32	36.63	0.17	*Notopterygium incisum* K.C.Ting ex H.T.Chang.	7
MOL011980	Pterostilbene	256.32	77.54	0.14	*Notopterygium incisum* K.C.Ting ex H.T.Chang.	13
MOL001951	Bergaptin	338.43	41.73	0.42	*Notopterygium incisum* K.C.Ting ex H.T.Chang.	3
MOL001956	Cnidilin	300.33	32.69	0.28	*Notopterygium incisum* K.C.Ting ex H.T.Chang.	2
MOL003609	(8S)-8-(2-hydroxypropan-2-yl)-8,9-dihydrofuro[2,3-h]chromen-2-one	246.28	32.11	0.17	*Notopterygium incisum* K.C.Ting ex H.T.Chang.	2
MOL004792	Nodakenin	408.44	57.12	0.69	*Notopterygium incisum* K.C.Ting ex H.T.Chang.	2
MOL002881	Diosmetin	300.28	31.14	0.27	*Nepeta tenuifolia* benth.	
MOL011849	Schizonepetoside B	330.42	31.02	0.28	*Nepeta tenuifolia* benth.	2
MOL011856	Schkuhrin I	420.5	54.45	0.52	*Nepeta tenuifolia* benth.	3
MOL005100	5,7-dihydroxy-2-(3-hydroxy-4-methoxyphenyl)chroman-4-one	302.3	47.74	0.27	*Nepeta tenuifolia* benth.	
MOL001506	Supraene	410.8	33.55	0.42	*Nepeta tenuifolia* benth.	3
MOL005043	Campest-5-en-3beta-ol	400.76	37.58	0.71	*Nepeta tenuifolia* benth.	2
MOL1	19-Dehydroursolic acid	—	—	—	*Ilex asprella* champ. ex benth.	3
MOL2	Oblonganoside B	—	—	—	*Ilex asprella* champ. ex benth.	3

(Continued on following page)

TABLE 2 | (*Continued*) 116 active compounds in GHKG decoction related to influenza.

Mol ID	Molecule name	MW	OB (%)	DL	Herb	Degree
MOL3	Ilexolic acid	—	—	—	*Ilex asprella* champ. ex benth.	3
MOL000263	Oleanic acid	456.78	29.02	0.76	*Ilex asprella* champ. ex benth.	3
MOL000414	Caffeic acid	180.17	54.97	0.05	*Ilex asprella* champ. ex benth.	3
MOL000511	Ursolic acid	456.78	16.77	0.75	*Ilex asprella* champ. ex benth.	3
MOL004550	Pomolic acid	472.78	16.85	0.73	*Ilex asprella* champ. ex benth.	3

of GHKGD effectively protected the infected mice from weight loss caused by IAV infection. Although initial weight loss occurred in each group beginning on day 3 of infection, the weight reduction trend over the next 3 days observed for mice treated with GHKG was similar to that observed for mice in the ribavirin group, while untreated mice (model group) showed significant weight loss over the next 3 days. These results indicated that treatment with GHKG effectively protected mice against weight loss caused by IAV infection.

The lung index and lung wet/dry weight ratio were calculated to assess the severity of influenza viral pneumonia. The pulmonary index is an indicator of the severity of pneumonia, and it increases significantly in the early stages of IAV infection (Barnard, 2009; Dai et al., 2014). As shown in **Figures 5B,C**, the lung index of the model group was significantly higher than that of the normal control group ($p < 0.01$). The lung index of the model group was 0.1466 ± 0.0022. In the groups treated with 46.2 and 11.6 g/kg GHKGD, the lung indices were 0.00840 ± 0.0012 and 0.00842 ± 0.0007, respectively, and were similar to that of the ribavirin group (0.00824 ± 0.0019). The lung wet/dry weight ratio showed a similar change trend. Both the high and low doses of GHKGD significantly reduced the lung wet/dry weight ratio of H1N1-infected mice ($p < 0.01$).

To further study the efficacy of GHKGD against H1N1, we measured the mRNA and protein levels of NP genes and their viral titers in mouse lung tissues on the fifth day after infection (**Figures 5D–F**). The NP mRNA expression level in the lung tissue of the model group (1 ± 0.11373) was 5555 times higher than that of the normal control group (0.00018 ± 0.00002), indicating that the model was successfully established. Both ribavirin and GHKGD showed excellent effects on reducing viral NP mRNA expression. It is worth noting that the therapeutic effect of high-dose GHKGD (0.01972 ± 0.001470) was similar to that of ribavirin (0.02401 ± 0.00222) and was 50 times lower than that observed in the model group. The change in NP protein expression was consistent with the change in mRNA expression. The virus titer reflects the threshold level of virus required to cause infection and the ability to resist the virus (Ma et al., 2018). The virus titer in lung tissue in the model group was 3.66 ± 0.31 $\log_{10}$ PFU/mL. Compared with that in the model group, the virus titers in the lungs of virus-infected mice treated with GHKGD (46.2 or 11.6 g/kg/day) and ribavirin were significantly reduced ($p < 0.01$) (**Figure 5F**). This result was consistent with the results of lung histological changes.

Similarly, the lungs of infected mice were harvested on day 5 post-infection, and pathological changes were assessed (**Figure 6**). As shown in **Figure 5B**, extensive bronchial epithelial cell necrosis, alveolar damage, and significant cellular infiltration were observed in the lungs of mice in the model group. In contrast, in mice treated with GHKGD, lung hyperaemia was decreased and histopathological changes were reduced in a dose-dependent manner (**Figures 5D**,E). These results indicated that GHKGD ameliorated lung damage in virus-infected mice.

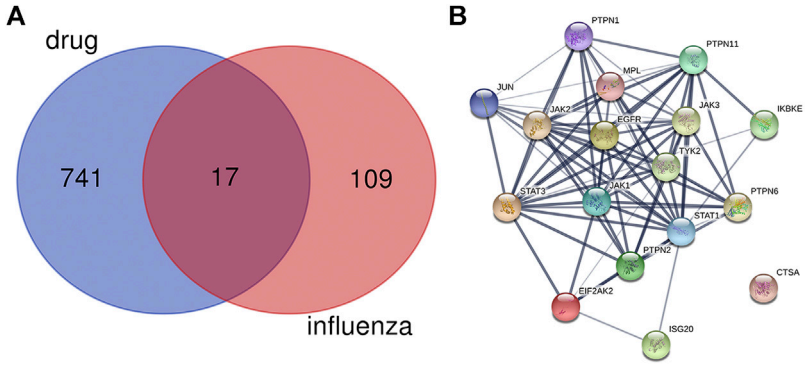

FIGURE 2 | Protein-protein interaction (PPI) networks of ingredients of GHKGD with activity against influenza. **(A)** The intersection of the drug (GHKGD) targets and influenza-related targets. There were 17 relevant overlapping targets, and all are shown on the right. **(B)** Each node represents the relevant gene, and the line thickness of the edges indicates the strength of data support.

Effects of Ganghuo Kanggan Decoction on the RIG-I-like Receptors Pathway in H1N1 IAV-Infected Mice

The RLR signaling pathway is a well-known innate immune pathway (Chen et al., 2018). As a member of the RIG-I-like receptor (RLR) family, retinoic acid-induced gene I (RIG-I) can recognize influenza virus RNA, activate the production of type I interferon (IFNs) and regulate the corresponding immune responses (Iwasaki and Pillai, 2014; Long et al., 2019; Yoneyama et al., 2015). Therefore, we measured the levels of IFN-α and IFN-β in mouse serum (**Figures 7A,B**). The results showed that the production of IFN-α and IFN-β was inhibited by GHKGD. In addition, the expression of RIG-I was measured at the mRNA and protein levels in mouse lung tissues. The expression of RIG-I was markedly increased in the model group compared with the normal control group (**Figures 7C,D**). Ribavirin and GHKGD inhibited RIG-1 expression at the mRNA and protein levels compared with that in the model group. In addition, the expression of mitochondrial antiviral-signaling protein (MAVS), interferon regulatory factor 3 (IRF3) and interferon regulatory factor 7 (IRF7) was inhibited by GHKGD (**Figure 7E**). The nuclear factor kappa-B (NF- κB) pathway, which is important for the regulation of inflammation and apoptosis, is one of the signal cascades induced by influenza virus infection (Ding et al., 2017; Yan et al., 2018). As shown in **Figure 7F**, compared to that in the normal control group, the expression of NF-κB p65 was significantly increased in the model group. Ribavirin and GHKGD markedly reduced the level of NF-κB p65 after IAV infection compared with that in the model group. STAT1 also participates in the regulation of various inflammatory mediators, and plays an important role in the production of pro-inflammatory cytokines (Meraz et al., 1996). Our results showed that the STAT1 expression was inhibited by GHKGD, thereby avoiding the excessive secretion of inflammatory factors (**Figure 7F**). These results indicated that GHKGD downregulated the expression of RIG-1, MAVS, IRF3, IRF7, NF-κB p65 and STAT1 in the RLR signaling pathway, thereby inhibiting excessive inflammatory responses.

Effects of Ganghuo Kanggan Decoction on the Levels of TH1 and TH2 Cytokines in H1N1 IAV-Infected Mice

The serum levels of Th1 (IL-2, TNF-α, and IFN-γ) and Th2 (IL-4 and IL-5) cytokines were tested by a flow cytometer. The results showed that, compared with the normal control group, the model group exhibited higher levels of TNF-α, IL-2, and IFN-γ cytokines, while the changes in the levels of IL-5 and IL-4 were not statistically significant. In addition, Ribavirin and GHKGD groups exhibited lower levels of IL-2, TNF-α, and IFN-γ cytokines compared with that in the model group (**Figures 8A–C**). The IL-5 and IL-4 levels were markedly increased in GHKGD group, while the Ribavirin group changed without statistically significant (**Figures 8D,E**). These findings suggest that the differentiation of Th1 and Th2 cytokines exert critical functions during the occurrence of influenza virus pneumonia, and the GHKGD could played an immunomodulatory role by downgrading Th1 (IL-2, TNF-α, and IFN-γ) cytokines, while raising Th2 (IL-4 and IL-5) cytokines.

DISCUSSION

ARDS and respiratory failure are the main causes of death from influenza virus infection. Drug resistance and adverse reactions to antiviral drugs have prompted scientists to consider searching for host target-based drugs to reduce viral damage to the respiratory system. Many TCMs have been used to treat influenza, and TCMs may be a potential source of alternative compounds for drug design and discovery. GHKGD is a clinical experience prescription used for the treatment of viral pneumonia in the Lingnan area (Zhao et al., 2018). In our previous clinical study, GHKGD was found to be not only effective but also safe. Compared with oseltamivir, Ganghuo Kanggan decoction shortened the antipyretic time of patients, improved their cold symptoms, inhibited the dominant response of influenza virus Th1 cell subsets, reversed the Th1/Th2 imbalance, and reduced

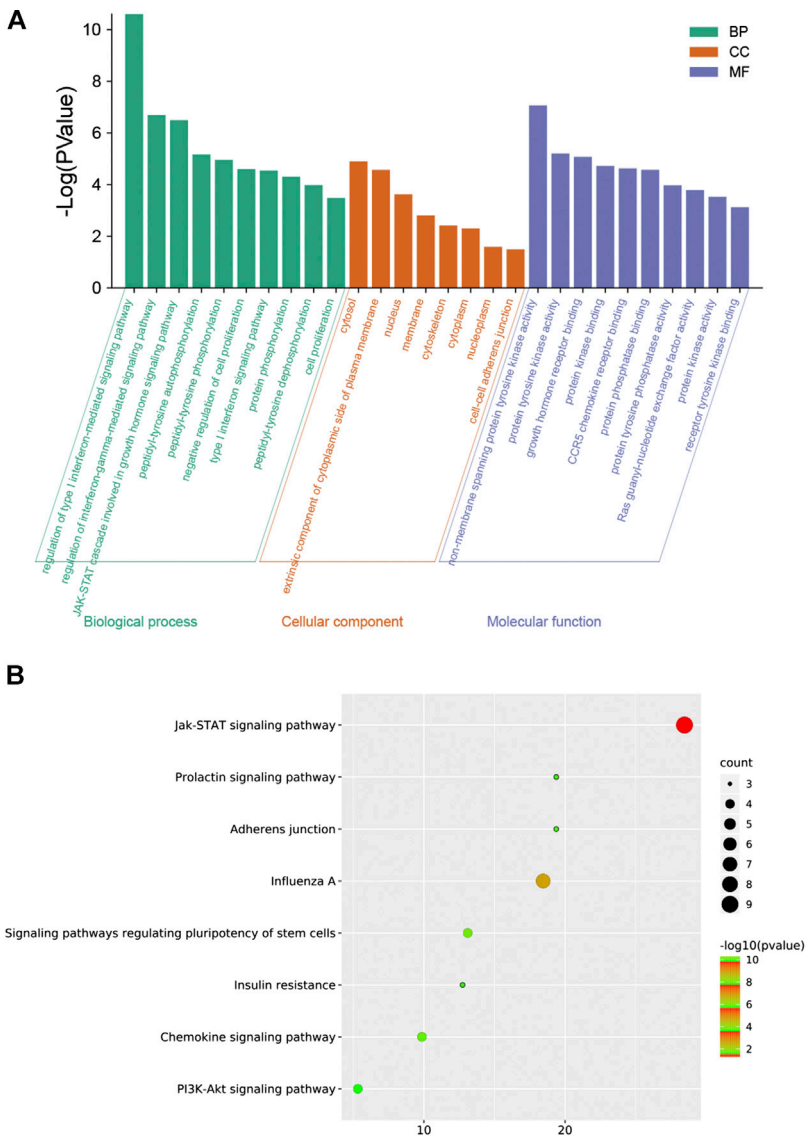

FIGURE 3 | GO enrichment analysis by Metascape database. **(A)** Heatmap of GO enrichment. **(B)** GO-genes chord.

immunoinflammatory damage (Yang et al., 2017b). The combination of oseltamivir and Ganghuo Kanggan decoction had a more obvious clinical effect than either alone (Lyv et al., 2017). In addition, *in vivo* studies have shown that GHKGD could significantly reduce the exudation of inflammatory mediators from influenza virus-induced viral pneumonia in mice and improve the survival rate of mice (Chen et al., 2015; Liu et al., 2015). Based on this, we adopted the strategy of network pharmacology (Xu et al., 2017) to predicted its possible pharmacological mechanism, and carried out *in vivo* experiments to confirm it.

Through a network pharmacology approach, we identified 116 potential active components and 17 targets. Some of the main active ingredients have been reported to have direct antiviral effects or to reduce pneumonia by suppressing inflammation; for example, isoliquiritigenin reduced influenza virus-induced lung inflammation and mortality in mice (Traboulsi et al., 2015), luteolin suppressed coat protein I complex expression to decrease the yield of IAV *in vitro* (Yan et al., 2019), and kaempferol exhibited a protective effect on H9N2 virus-induced inflammation via the suppression of the TLR4/MyD88-mediated NF-κB and MAPK pathways (Zhang et al., 2017). These results show that the strategy of applying network pharmacology to find potential active compounds is reliable and feasible. Therefore, in future work, we will further study whether other potential active ingredients have direct antiviral or anti-inflammatory effects.

Enrichment analysis of the 17 potential targets showed that GHKGD mainly regulated type I interferon-related signaling pathways to play an anti-influenza role in the body. These

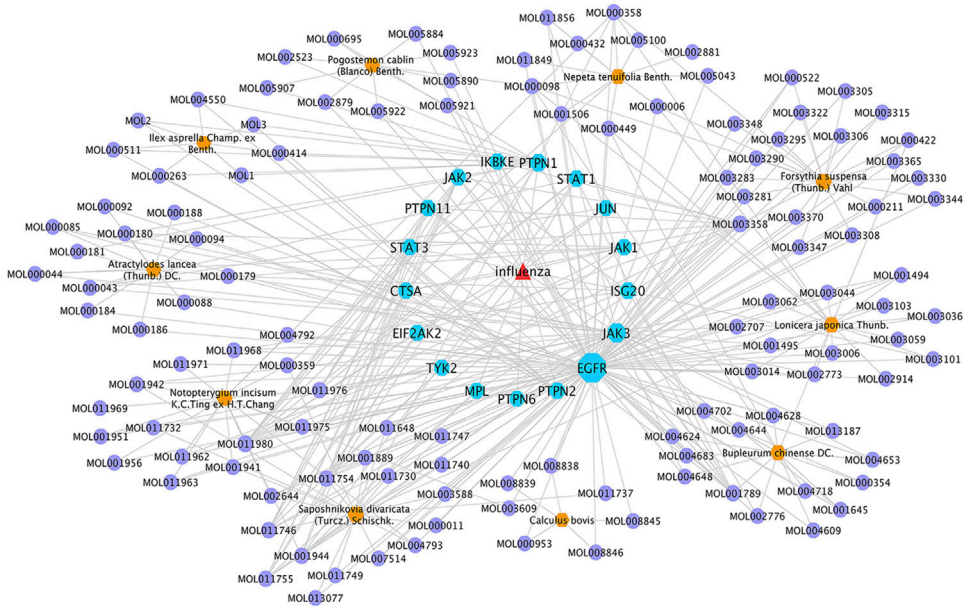

FIGURE 4 | GHKGD component-target-disease network. The network was constructed to reveal interactions between active compounds and potential targets of GHKGD. Red triangular nodes represent the disease, blue octagonal nodes represent genes, yellow hexagonal nodes represent Chinese medicines, and purple circular nodes represent active ingredients. The size of each target is positively related to its degree in the network.

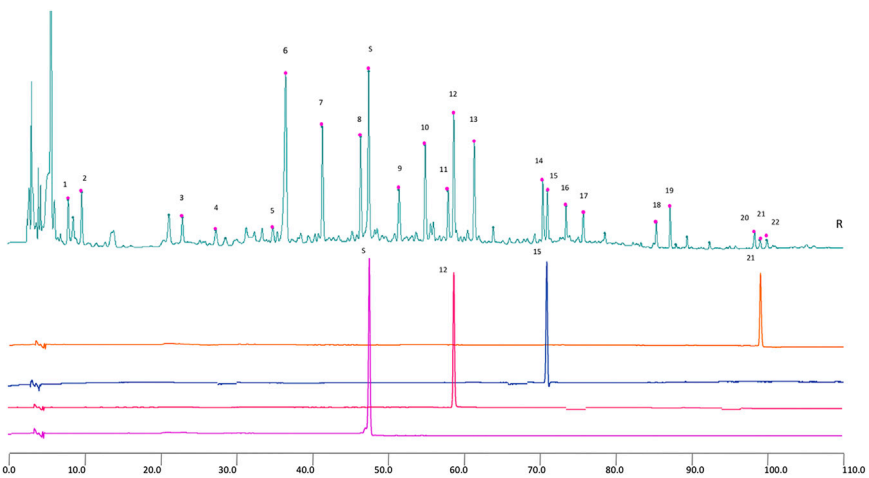

FIGURE 5 | 2D HPLC chromatograms of MHT water extract used in the trial. X-axis is the retention time, and Y-axis is the absorbance unit. S. Prim-O-glucosylcimifugin, 12. 5-O-methylvisammioside, 15. Amygdalin, and 21. Notopterol.

findings suggested that GHKGD may prevent the overexpression of inflammatory mediators in IAV-infected BALB/c mice by inhibiting the RLR signaling pathway. Then we designed *in vivo* experiments to confirm this hypothesis.

First, it can be seen that, in the BALB/c mouse model, on the fifth day after IAV infection, the body weight of the mice decreased, the lung index and lung wet/dry weight ratio increased significantly, and extensive bronchial epithelial cell necrosis, alveolar injury and obvious cellular infiltration were observed in lung tissues. However, the ribavirin group and GHKGD groups (high and low dose) of mice exhibited a significant improvement in the lung index and lung wet/dry weight ratio, reductions in NP protein expression in lung tissue and virus titers in the lung, and amelioration of lung tissue injury. These results indicated that GHKGD was an effective oral drug to control the inflammation caused by influenza A virus infection.

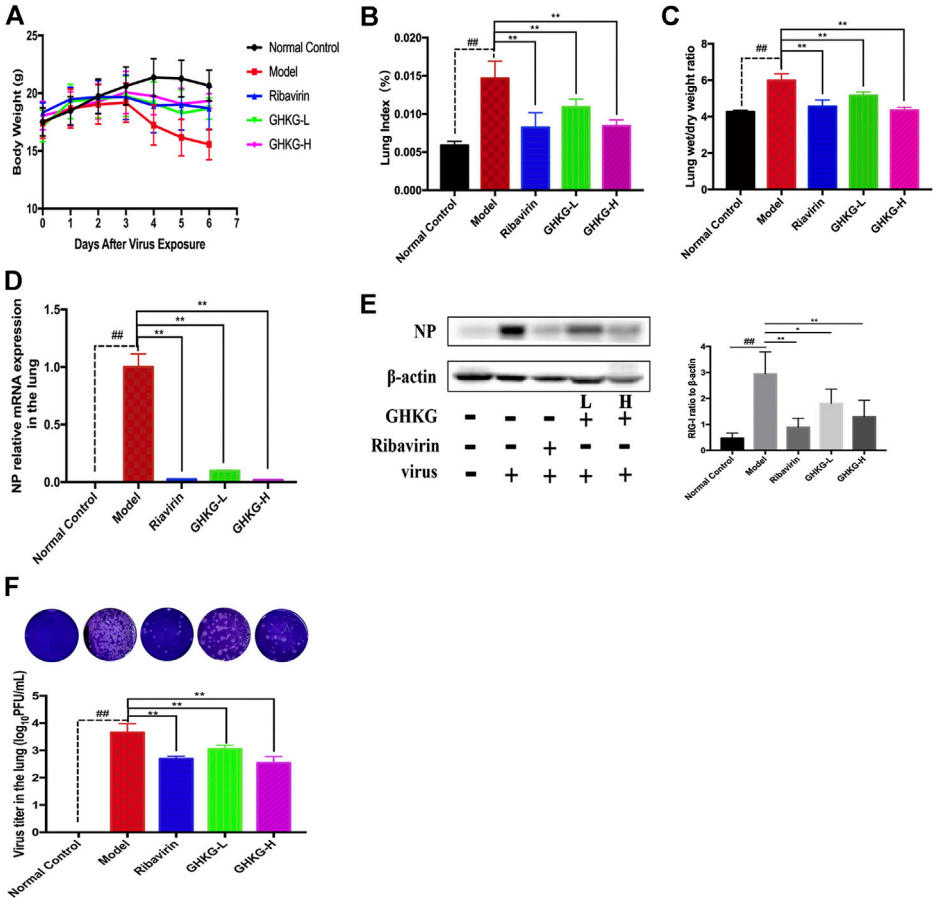

FIGURE 6 | Evaluation of the therapeutic effect of GHKGD in H1N1-infected mice. **(A)** Body weight change (mean ± SD). Mice were infected with influenza A/Puerto Rico/8/34 (H1N1) virus (2 LD 50) and treated with GHKGD high (46.2 g/kg/d) or low (11.6 g/kg/d) dose or ribavirin (75 mg/kg/d) once a day for 5 days. Clinical signs were observed for 6 days (n = 6). Mice were sacrificed at 5 dpi. The lungs were removed and rinsed with sterile PBS. The effect of GHKGD on the **(B)** lung index and **(C)** lung wet/dry weight of mice was assessed (n = 6). Inhibition of NP expression at the mRNA and protein levels by GHKGD in mice following influenza virus infection was detected: **(D)** mRNA level; **(E)** protein level. **(F)** Plaque reduction assay. MDCK cells were infected with mouse lung tissue supernatant, and the infected cells were then cultured and overlaid with MEM supplemented with 1% low melting point agarose and 2.5 μg/mL TPCK-treated trypsin. The number of plaques was calculated. The data are presented as the means ± SDs of the results from three independent experiments, and were analyzed by ANOVA. #$p < 0.05$, ##$p < 0.01$ compared to the normal control group, *$p < 0.05$, **$p < 0.01$ compared to the model group. GHKG-L, Ganghuo Kanggan Decoction with low dose; GHKG-H, Ganghuo Kanggan Decoction with high dose.

Second, we investigated whether the antiviral role of GHKGD involves the RLR signaling pathway in the lungs. After influenza virus infects the host, RIG-I, a member of the RIG-I-like receptor (RLR) family, can recognize intracellular viral RNA, leading to the activation of interferon type I and the entry of NF-κB and STAT1 into the nucleus and promoting the production of pro-inflammatory factors and pro-inflammatory chemokines (Zhu et al., 2014). An excessive immune response is considered to be a predictor of influenza-mediated death (Nimmerjahn et al., 2004). In this study, the expression of RIG-I, NF-κB and STAT1 proteins, the level of MAVS and IRF3/7 mRNA and the content of IFN-α/β in lung tissue of the model group were significantly increased, indicating that the RIG-I/NF-κB/STAT1 signaling pathway was activated. After oral administration of GHKGD to mice, pulmonary inflammation was alleviated, RIG-I, NF-κB and STAT1 protein overexpression was inhibited, and the content of IFN-α/β was decreased. These effects suggested that GHKGD might inhibit excessive inflammatory reactions by regulating the RLR signaling pathway.

It is well known that, influenza virus, a strict intracellular pathogenic microorganism, mainly stimulates Th cells to differentiate into Th1 cells and releases their signature cytokines (IFN-γ, TNF-α, IL-2) after infecting the host, while the differentiation of Th2 cells and their cytokine expression (IL-4, IL-5) were obviously suppressed (Yan et al., 2018). The balance between pro-inflammatory factors and anti-inflammatory factors mediates the process of immune damage and immune regulation after influenza virus infection. In the present study, we investigated the effect of GHKGD on Th1/Th2 imbalance in IAV-infected mice. The results demonstrated that GHKGD could significantly increase the expression of Th1 ((IL-2, TNF-α, and IFN-γ)) cytokines, and reduced the secretion of Th2 (IL-5 and IL4) cytokines, which was crucial for reducing the inflammatory factors overexpression and avoiding the production of inflammatory factor storms.

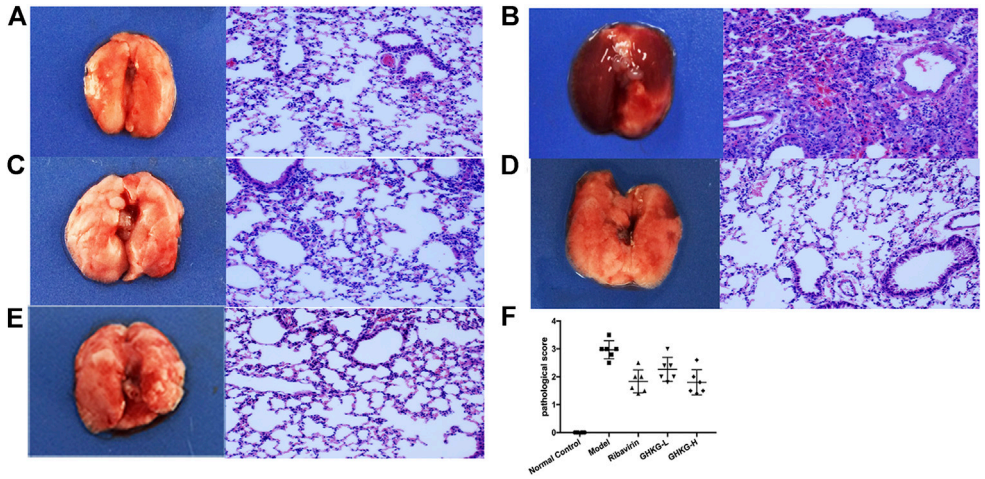

FIGURE 7 | Histological observations of lung tissues formice sacrificed at the fifth d.p.i. (HE, × 200) (n = 6) **(A)** Mock-infected mice treated with PBS (normal control, NC); **(B)** IAV-infected mice treated with PBS (viral control); **(C)** IAV-infected mice treated with ribavirin (75 mg/kg/d); **(D-E)** IAV-infected mice treated with GHKGD (46.2 and 11.6 g/kg/day, respectively); **(F)** pathological scores. The data are presented as the means ± SDs (n = 6) and were analyzed by ANOVA. #$p < 0.05$, ##$p < 0.01$ compared to the normal control group, *$p < 0.05$, **$p < 0.01$ compared to the model group. GHKG-L, Ganghuo Kanggan Decoction with low dose; GHKG-H, Ganghuo Kanggan Decoction with high dose.

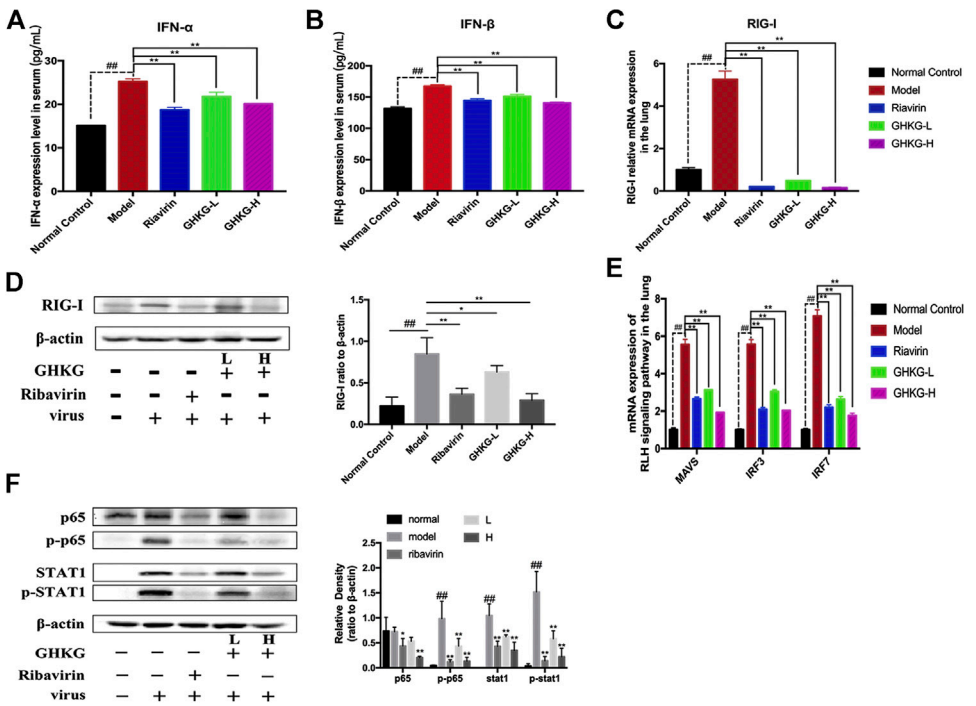

FIGURE 8 | Inhibitory effect of GHKGD on IFN-α and IFN-β levels in serum in mice following influenza virus infection (n = 6). **(A)** IFN-α level; **(B)** IFN-β level. Inhibition of RIG-1 expression at the mRNA and protein levels by GHKGD in mice following influenza virus infection. **(C)** mRNA level; **(D)** protein level. Mice were infected with influenza A/Puerto Rico/8/1934(H1N1) virus (2 LD 50) and treated with GHKGD (46.2 and 11.6 g/kg/day, respectively) or ribavirin (70mg/kg/d) once a day for 5 days. The expression of RIG-1 was measured by RT-PCR and Western blot assays. **(E)** Relative mRNA expression levels of MAVS, IRF3, and IRF7 in the RLR signaling pathway. The data are presented as the means ± standard deviations of the results from three independent experiments. **(F)** Relative protein expression levels of p65, p-p65, STAT1, p-STAT1 and β-actin in the RLR signaling pathway. The data are presented as the means ± SDs of the results from three independent experiments, and were analyzed by ANOVA. #$p < 0.05$, ## $p < 0.01$ compared to the normal control group, *$p< 0.05$, **$p < 0.01$ compared to the model group. GHKG-L, Ganghuo Kanggan Decoction with low dose; GHKG-H, Ganghuo Kanggan Decoction with high dose.

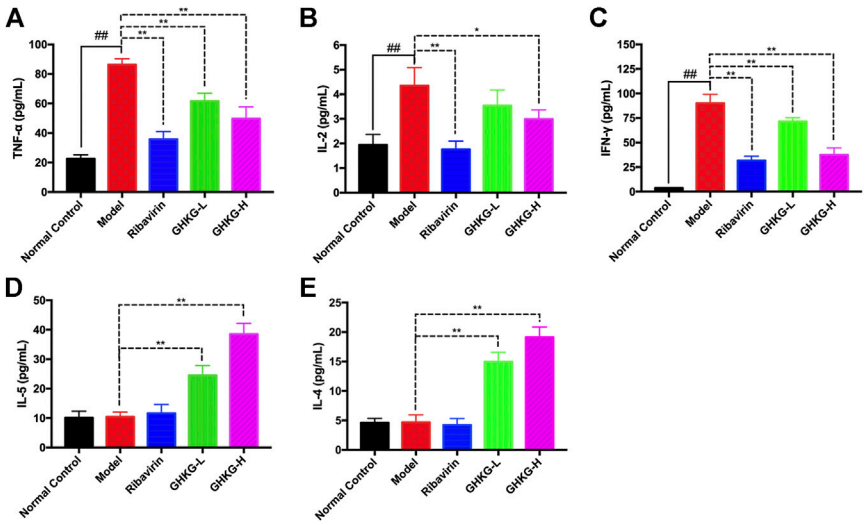

FIGURE 9 | Effect of the GHKGD on serum cytokine levels. The serum levels of TNF-α **(A)**, IL-2 **(B)**, IFN-γ **(C)**, IL-5 **(D)**, and IL-4 **(E)** were detected by BD cytometric bead array (CBA) mouse Th1/Th2 cytokine kit. The data are presented as the means ± SDs of the results from three independent experiments, and were analyzed by ANOVA. $^{\#}P < 0.05$, $^{\#\#}P < 0.01$ compared to the normal control group, $^{*}P < 0.05$, $^{**}P < 0.01$ compared to the model group. GHKG-L, Ganghuo Kanggan Decoction with low dose; GHKG-H, Ganghuo Kanggan Decoction with high dose.

CONCLUSION

In conclusion, the network pharmacological analysis of GHKGD identified 116 compounds and 17 target genes associated with influenza virus infection. EGFR, JAK3, PTPN1, JAK2, ISG20, PTPN2, STAT3, PTPN11 and STAT1 were recognized as hub genes. According to the results of pathway enrichment analysis, we verified the protective effect of GHKGD against pneumonia in mice infected with IAV and determined that GHKGD can prevent excessive inflammation by downregulating the RLR signaling pathway and regulating the balance of Th1/Th2. Our findings confirmed that network pharmacology strategies can match candidate compounds with potential targets via the construction of multi-component networks. These findings provide both a new option for the treatment of IAV infection and information to further reveal the mechanisms of GHKGD.

DATA AVAILABILITY STATEMENT

The original contributions presented in the study are included in the article/**Supplementary Material**, further inquiries can be directed to the corresponding authors.

AUTHOR CONTRIBUTIONS

YaL, SZ, YJ, GL, and XL conceived and designed the experiments. YaL, QZ, HL, TH, and ZL participated in the specific experimental process. YaL, QZ, HL, and ZL performed the research and analyzed the data. YaL wrote the paper. YaL, GL, YiL, and XL drafted the manuscript. YaL, YJ, SZ, and XL revised the manuscript. All authors approved and agreed to be responsible for all aspects of the work.

FUNDING

This work was supported by the National Natural Science Foundation of China (Grant No. 81973814) and Key-Area Research and Development Program of Guangdong Province (Grant No. 2020B1111100002).

SUPPLEMENTARY MATERIAL

The Supplementary Material for this article can be found online at: https://www.frontiersin.org/articles/10.3389/fphar.2020.607027/full#supplementary-material.

REFERENCES

Barnard, D. L. (2009). Animal models for the study of influenza pathogenesis and therapy. *Antivir. Res.* 82, A110–A122. doi:10.1016/j.antiviral.2008.12.014

Buchholz, U., Buda, S., Reuß, A., Haas, W., and Uphoff, H. (2016). Todesfälle durch Influenzapandemien in Deutschland 1918 bis 2009. Schätzwerte auf Basis der Literatur und ergänzende eigene Berechnungen [Influenza pandemic deaths in Germany from 1918 to 2009. Estimates based on literature and own calculations]. *Bundesgesundheitsblatt—Gesundheitsforsch.—Gesundheitsschutz* 59 (4), 523–536. doi:10.1007/s00103-016-2324-9

Chen, C. R., Liu, J. X., Li, G., Liu, J. B., Hu, Q. P., Lai, X. P., et al. (2015). Effects of Ganghuo Kanggan Decoction on viral pneumonia mice caused by H1N1 influenza virus. *CJTCMP* 30, 3318–3321.

Chen, X., Liu, S., Goraya, M. U., Maarouf, M., Huang, S., and Chen, J.-L. (2018). Host immune response to influenza A virus infection. *Front. Immunol.* 9, 320. doi:10.3389/fimmu.2018.00320

Cordova-Villalobos, J. A., Macias, A. E., Hernandez-Avila, M., Dominguez-Cherit, G., Lopez-Gatell, H., Alpuche-Aranda, C., et al. (2017). The 2009 pandemic in Mexico: experience and lessons regarding national preparedness policies for seasonal and epidemic influenza. La pandemia de 2009 en México: experiencia y lecciones acerca de las políticas nacionales de preparación contra la influenza estacional y epidémica. *Gac. Med. Mex.* 153 (1), 102–110.

Dai, W.-p., Li, G., Li, X., Hu, Q.-p., Liu, J.-x., Zhang, F.-x., et al. (2014). The roots of Ilex asprella extract lessens acute respiratory distress syndrome in mice induced by influenza virus. *J. Ethnopharmacol.* 155, 1575–1582. doi:10.1016/j.jep.2014.07.051

Ding, P., Yan, X., Liu, Z., Du, J. W., Du, Y. F., Lu, Y. T., et al. (2017). PTS: a pharmaceutical target seeker. *Database bax095*. doi:10.1093/database/bax095

Ding, Y., Chen, L., Wu, W., Yang, J., Yang, Z., and Liu, S. (2017). Andrographolide inhibits influenza A virus-induced inflammation in a murine model through NF-κB and JAK-STAT signaling pathway. *Microb. Infect.* 19, 605–615. doi:10.1016/j.micinf.2017.08.009

Ge, H., Wang, Y. F., Xu, J., Gu, Q., Liu, H. B., Xiao, P. G., et al. (2010). Anti-influenza agents from traditional Chinese medicine. *Nat. Prod. Rep.* 27, 1758–1780. doi:10.1039/c0np00005a

Gfeller, D., Grosdidier, A., Wirth, M., Daina, A., Michielin, O., and Zoete, V. (2014). SwissTargetPrediction: a web server for target prediction of bioactive small molecules. *Nucleic Acids Res.* 42, W32–W38. doi:10.1093/nar/gku293

Herold, S., Becker, C., Ridge, K. M., and Budinger, G. R. (2015). Influenza virus-induced lung injury: pathogenesis and implications for treatment. *Eur. Respir. J.* 45, 1463–1478. doi:10.1183/09031936.00186214

Hsieh, M. J., Lee, W. C., Cho, H. Y., Wu, M. F., Hu, H. C., Kao, K. C., et al. (2018). Recovery of pulmonary functions, exercise capacity, and quality of life after pulmonary rehabilitation in survivors of ARDS due to severe influenza A (H1N1) pneumonitis. *Influenza Other Respi Viruses* 12, 643–648. doi:10.1111/irv.12566

Iwasaki, A. and Pillai, P. S. (2014). Innate immunity to influenza virus infection. *Nat. Rev. Immunol.* 14, 315–328. doi:10.1038/nri3665

Lin, J. P., Fan, Y. K., and Liu, H. M. (2019). The 14-3-3η chaperone protein promotes antiviral innate immunity via facilitating MDA5 oligomerization and intracellular redistribution. *PLoS Pathog.* 15, e1007582. doi:10.1371/journal.ppat.1007582

Lipinski, C. A., Lombardo, F., Dominy, B. W., and Feeney, P. J. (2001). Experimental and computational approaches to estimate solubility and permeability in drug discovery and development settings. *Adv. Drug Deliv. Rev.* 46, 3–26. doi:10.1016/s0169-409x(00)00129-0

Liu, G. Q., Lu, Y., Liu, Q., and Zhou, Y. (2019). Inhibition of ongoing influenza A virus replication reveals different mechanisms of rig-I activation. *J. Virol.* 93, e02066-18. doi:10.1128/JVI.02066-18

Liu, J. X., Chen, C. R., Li, G., Liu, J. B., Dai, W. P., Lai, X. P., et al. (2015). Study on the protective effect of *Ganghuo kanggan* decoction on acute lung injury induced by influenza virus in mice. *Lishizhen Medicine and Materia Medica Research* 26, 1613–1615.

Liu, W., Zhang, X., Mao, B., and Jiang, H. (2020). Systems pharmacology-based study of Tanreqing injection in airway mucus hypersecretion. *J. Ethnopharmacol.* 249, 112425. doi:10.1016/j.jep.2019.112425

Liu, Z., Guo, F., Wang, Y., Li, C., Zhang, X. L., Li, H. L., et al. (2016). BATMAN-TCM: a bioinformatics analysis tool for molecular mechANism of traditional Chinese medicine. *Sci. Rep.* 6, 21146. doi:10.1038/srep21146

Long, J. S., Mistry, B., Haslam, S. M., and Barclay, W. S. (2019). Host and viral determinants of influenza A virus species specificity. *Nat. Rev. Microbiol.* 17, 67–81. doi:10.1038/s41579-018-0115-z

Lyv, X. X., Liu, X. H., Liu, J. B., and Li, G. (2017). Clinical observation of gang huo kanggan decoction combined with oseltamivir phosphate for treatment of viral pneumonia. *J. of Guangzhou University of TCM* 34, 16–21.

Ma, Q., Liang, D., Song, S., Yu, Q. T., Shi, C. Y., Xing, X. F., et al. (2017). Comparative study on the antivirus activity of shuang-huang-lian injectable powder and its bioactive compound mixture against human adenovirus III in vitro. *Viruses* 9, 79. doi:10.3390/v9040079

Ma, Q., Yu, Q., Xing, X., Liu, S., Shi, C., and Luo, J. (2018). San Wu huangqin decoction, a Chinese herbal formula, inhibits influenza a/PR/8/34 (H1N1) virus infection in vitro and in vivo. *Viruses* 10, 117. doi:10.3390/v10030117

Meraz, M. A., White, J. M., Sheehan, K. C., Bach, E. A., Rodig, S. J., Dighe, A. S., et al. (1996).Targeted disruption of the Stat1 gene in mice reveals unexpected physiologic specificity in the JAK-STAT signaling pathway. *Cell* 84, 431–442. doi:10.1016/s0092-8674(00)81288-x

Nimmerjahn, F., Dudziak, D., Dirmeier, U., Hobom, G., Riedel, A., Schlee, M., et al. (2004). Active NF-κB signaling is a prerequisite for influenza virus infection. *J. Gen. Virol.* 85, 2347–2356. doi:10.1099/vir.0.79958-0

Parsey, M. V., Tuder, R. M., and Abraham, E. (1998). Neutrophils are major contributors to intraparenchymal lung IL-1 beta expression after hemorrhage and endotoxemia. *J. Immunol.* 160, 1007–1013.

Pleschka, S., Stein, M., Schoop, R., and Hudson, J. B. (2009). Anti-viral properties and mode of action of standardized Echinacea purpurea extract against highly pathogenic avian influenza virus (H5N1, H7N7) and swine-origin H1N1 (S-OIV). *Virol. J.* 6, 197. doi:10.1186/1743-422X-6-197

Ru, J. L., Li, P., Wang, J., Zhou, W., Li, B. H., Huang, C., et al. (2014). TCMSP: a database of systems pharmacology for drug discovery from herbal medicines. *J. Cheminf.* 13. doi:10.1186/1758-2946-6-13

Shi, Y., Xu, H., Xiao, Y., Liu, P., Pang, P., Wu, S. Z., et al. (2020). Gegen qinlian decoction downregulates the TLR7 signalling pathway to control influenza A virus infection. *Biomed. Pharmacother.* 121, 109471. doi:10.1016/j.biopha.2019.109471

Traboulsi, H., Cloutier, A., Boyapelly, K., Bonin, M. A., Marsault, É., Cantin, A. M., et al. (2015). The flavonoid isoliquiritigenin reduces lung inflammation and mouse morbidity during influenza virus infection. *Antimicrob. Agents Chemother.* 59, 6317–6327. doi:10.1128/AAC.01098-15

Xu, T., Li, S., Sun, Y., Pi, Z. F., Liu, S., Song, F. G., et al. (2017). Systematically characterize the absorbed effective substances of Wutou Decoction and their metabolic pathways in rat plasma using UHPLC-Q-TOF-MS combined with a target network pharmacological analysis. *J. Pharmaceut. Biomed. Anal.* 141, 95–107. doi:10.1016/j.jpba.2017.04.012

Xu, X., Zhang, W., Huang, C., Li, Y., Yu, H., Wang, Y. H., et al. (2012). A novel chemometric method for the prediction of human oral bioavailability. *Int. J. Mol. Sci.* 13, 6964–6982. doi:10.3390/ijms13066964

Yan, H., Ma, L., Wang, H., Wu, S., Huang, H., Gu, Z., et al. (2019). Luteolin decreases the yield of influenza A virus *in vitro* by interfering with the coat protein I complex expression. *J. Nat. Med.* 73, 487–496. doi:10.1007/s11418-019-01287-7

Yan, H., Wang, H., Ma, L., Ma, X., Yin, J., Wu, S., et al. (2018). Cirsimaritin inhibits influenza A virus replication by downregulating the NF-κB signal transduction pathway. *Virol. J.* 15, 88. doi:10.1186/s12985-018-0995-6

Yan, Y. Q., Fu, Y. J., Wu, S., Qin, H. Q., Zhen, X., Song, B. M., et al. (2018). Anti-influenza activity of berberine improves prognosis by reducing viral replication in mice. *Phytother Res.* 32, 2560–2567. doi:10.1002/ptr.6196

Yang, L. L., Liu, X. H., and Feng, L. Z. (2017b). Study on the effect of gang huo anti sense soup and its influence on Th1/Th2 balance of anti-influenza virus. *J. Emerg. Tradit. Chin. Med.* 26, 685–687.

Yang, L. L., Liu, X. H., Feng, L. Z., and Zhang, G. (2017a). Clinical curative effect of Ganghuo kanggan decoction to treat influenza and its effect on Th1/Th2 and RIG-I, *J. of Liaoning Univ. of TCM*, 19, 83–86.

Yoneyama, M., Onomoto, K., Jogi, M., Akaboshi, T., and Fujita, T. (2015). Viral RNA detection by RIG-I-like receptors. *Curr. Opin. Immunol.* 32, 48–53. doi:10.1016/j.coi.2014.12.012

Yue, S. J., Xin, L. T., Fan, Y. C., Li, S. J., Tang, Y. P., Duan, J. A., et al. (2017). Herb pair Danggui-Honghua: mechanisms underlying blood stasis syndrome by system pharmacology approach. *Sci. Rep.* 7, 40318. doi:10.1038/srep40318

Zhang, R., Ai, X., Duan, Y., Xue, M., He, W., Wang, C., et al. (2017). Kaempferol ameliorates H9N2 swine influenza virus-induced acute lung injury by inactivation of TLR4/MyD88-mediated NF-κB and MAPK signaling

pathways. *Biomed. Pharmacother.* 89, 660–672. doi:10.1016/j.biopha.2017.02.081

Zhao, Y., Zhang, L., Zhang, G. F., and Yan, X. J. (2018). Efficacy of Ganghuo Kanggan decoction combined with Tamiflu in the treatment of viral pneumonia and its effect on the levels of inflammatory cytokines and IFN-γ. *Modern J. of Int. Trad. Chin. and West. Med.* 27, 3245–3247.

Zhu, H., Shi, X., Ju, D., Huang, H., Wei, W., and Dong, X. (2014). Anti-inflammatory effect of thalidomide on H1N1 influenza virus-induced pulmonary injury in mice. *Inflammation* 37, 2091–2098. doi:10.1007/s10753-014-9943-9

Conflict of Interest: The authors declare that the research was conducted in the absence of any commercial or financial relationships that could be construed as a potential conflict of interest.

frontiers in Pharmacology

REVIEW
published: 17 February 2021
doi: 10.3389/fphar.2020.586993

Potential Natural Products Against Respiratory Viruses: A Perspective to Develop Anti-COVID-19 Medicines

Marzieh Omrani[1†], *Mohsen Keshavarz*[2†], *Samad Nejad Ebrahimi*[1], *Meysam Mehrabi*[3], *Lyndy J. McGaw*[4*], *Muna Ali Abdalla*[5] *and Parvaneh Mehrbod*[6*]

[1]Department of Phytochemistry, Medicinal Plants and Drugs Research Institute, Shahid Beheshti University, Tehran, Iran, [2]Department of Medical Virology, The Persian Gulf Tropical Medicine Research Center, The Persian Gulf Biomedical Sciences Research Institute, Bushehr University of Medical Sciences, Bushehr, Iran, [3]Shafa Hospital, Qazvin University of Medical Sciences, Qazvin, Iran, [4]Phytomedicine Programme, Department of Paraclinical Sciences, Faculty of Veterinary Science, University of Pretoria, Onderstepoort, South Africa, [5]Department of Food Science and Technology, Faculty of Agriculture, University of Khartoum, Khartoum North, Sudan, [6]Influenza and Respiratory Viruses Department, Pasteur Institute of Iran, Tehran, Iran

OPEN ACCESS

Edited by:
Paul F. Moundipa, University of Yaounde I, Cameroon

Reviewed by:
Shiv Bahadur, GLA University, India
Pei-Wen Hsieh, Chang Gung University, Taiwan

***Correspondence:**
Lyndy McGaw
lyndy.mcgaw@up.ac.za
Parvaneh Mehrbod
mehrbode@yahoo.com

[†]*These authors have contributed equally to this work*

Specialty section:
This article was submitted to Ethnopharmacology, a section of the journal Frontiers in Pharmacology

Received: *24 July 2020*
Accepted: *17 November 2020*
Published: *17 February 2021*

Citation:
Omrani M, Keshavarz M, Nejad Ebrahimi S, Mehrabi M, McGaw LJ, Ali Abdalla M and Mehrbod P (2021) Potential Natural Products Against Respiratory Viruses: A Perspective to Develop Anti-COVID-19 Medicines. Front. Phys. 11:586993. doi: 10.3389/fphar.2020.586993

The emergence of viral pneumonia caused by a novel coronavirus (CoV), known as the 2019 novel coronavirus (2019-nCoV), resulted in a contagious acute respiratory infectious disease in December 2019 in Wuhan, Hubei Province, China. Its alarmingly quick transmission to many countries across the world and a considerable percentage of morbidity and mortality made the World Health Organization recognize it as a pandemic on March 11, 2020. The perceived risk of infection has led many research groups to study COVID-19 from different aspects. In this literature review, the phylogenetics and taxonomy of COVID-19 coronavirus, epidemiology, and respiratory viruses similar to COVID-19 and their mode of action are documented in an approach to understand the behavior of the current virus. Moreover, we suggest targeting the receptors of SARS-CoV and SARS-CoV-2 such as ACE2 and other proteins including 3CLpro and PLpro for improving antiviral activity and immune response against COVID-19 disease. Additionally, since phytochemicals play an essential role in complementary therapies for viral infections, we summarized different bioactive natural products against the mentioned respiratory viruses with a focus on influenza A, SARS-CoV, MERS, and COVID-19.Based on current literature, 130 compounds have antiviral potential, and of these, 94 metabolites demonstrated bioactivity against coronaviruses. Interestingly, these are classified in different groups of natural products, including alkaloids, flavonoids, terpenoids, and others. Most of these compounds comprise flavonoid skeletons. Based on our survey, xanthoangelol E (**88**), isolated from *Angelica keiskei* (Miq.) Koidz showed inhibitory activity against SARS-CoV PLpro with the best IC_{50} value of 1.2 μM. Additionally, hispidulin (**3**), quercetin (**6**), rutin (**8**), saikosaponin D (**36**), glycyrrhizin (**47**), and hesperetin (**55**) had remarkable antiviral potential against different viral infections. Among these compounds, quercetin (**6**) exhibited antiviral activities against influenza A, SARS-CoV, and COVID-19 and this seems to be a highly promising compound. In addition, our report discusses the obstacles and future perspectives to highlight the importance of developing screening programs to investigate potential natural medicines against COVID-19.

Keywords: antiviral potential, coronavirus, COVID-19, epidemiology, mode of action, 2019-nCoV, phylogenetic, phytochemicals

INTRODUCTION

The emergence of viral pneumonia caused by a novel coronavirus (CoV), known as the 2019 novel coronavirus (2019-nCoV), resulted in a contagious acute respiratory infectious disease in December 2019 in Wuhan, Hubei Province, China (Zhu et al., 2020). Its alarmingly rapid transmission to many countries across the world and the high level of morbidity and mortality prompted the World Health Organization (WHO) to recognize it as a pandemic on March 11, 2020 (Hui et al., 2020). As of November 2, 2020, the number of total confirmed COVID-19 infections in the world is over 46 million, and the number of deaths is reportedly more than one million individuals. These numbers are continually increasing with no sign of respite (WHO Coronavirus Disease, 2020). Additionally, the WHO announced that the disease has led to disruptions in medical services, including many hospitals and clinics for the treatment of non-communicable diseases in countries throughout the world (WHO April 17th, 2020). Moreover, the global outbreak of the pandemic coronavirus has disturbed social, religious, economic, financial and political structures across the world (Mahar 2020).

SARS-CoV and MERS-CoV broke out in 2003 and 2012 respectively, and each resulted in approximately 800 deaths. SARS-CoV and MERS-CoV are both zoonotic pathogens originating from animals, and can cause life-threatening disease with potential to cause pandemics (Ksiazek et al., 2003; Zaki et al., 2012). Recent studies have proven that the SARS-CoV-2 shares 89.1% nucleotide similarity, and 79.5% sequence identity, to a group of SARS-like coronaviruses and it falls into the genus Betacoronavirus (Harapan et al., 2020; Wu et al., 2020; Zhou et al., 2020).

The insights provided in this study indicate that natural products (or secondary metabolites) isolated from plants and microorganisms with activity against respiratory viruses support further exploration of such sources for anti-COVID-19 agents. Additionally, our review focuses on the importance of respiratory viruses similar to COVID-19 and their mode of action. This serves not only to understand the mechanism of COVID-19, but also to promote the fundamental concept of structure-based drug design, which might assist in discovering promising anti-COVID-19 drugs.

EPIDEMIOLOGY

Transmission routes, infection sources and susceptible hosts are three major conditions that influence transmission of infectious diseases. According to the latest statements of the National Health Commission of China, SARS-CoV-2 is transmitted to humans by respiratory droplets, close contact and contamination of surfaces, while transmission through aerosols is highly possible (Zhu et al., 2020).

Previous epidemics caused by SARS (2003) and MERS (2012) showed that these family members potentially cause widespread hospital outbreaks. Studies on SARS have shown that management of patients inside and outside the hospital is one of the most important steps in controlling the disease. For instance, the management and diagnosis of several imported cases to Vancouver (Canada) led to the rapid disease control and prevention of secondary transmission in the city. In return, unsuccessful control of the disease in Toronto (Canada) and Taipei (Taiwan) led to significant spread of the disease and hospitalization (Raoult et al., 2020).

The World Health Organization (WHO) declared SARS-CoV-2 as the sixth international public health concern and as a pandemic on March 11, 2020 (Zhang et al., 2020). Until now (November 2020) according to current laboratory tests, more than 46 million confirmed cases and one million deaths have been recorded around the world. According to the WHO report on 2 November, the most prevalent cases were recorded in America (20,807,415), Asia (13,626,009), Europe (10,324,515), Africa (1,796,748) and Oceania (including Australia, French Polynesia, Guam, New Zealand and Papua New Guinea) (41,916) (WHO Coronavirus Disease, 2020).

The mortality rate of SARS-CoV-2 has been reported in various studies and is estimated to be around 6.9% of confirmed cases but it may vary substantially (Zhu et al., 2020), for example ~0.1% and ~15.4% in Singapore and Belgium respectively (Johns Hopkins University). Accumulated results have revealed that the mortality rate of SARS-CoV-2 is lower than that of SARS-CoV or MERS-CoV, with rates of 10% and 37.1% respectively, but SARS-CoV-2 is ten times more contagious than the other viral infections (Bouadma et al., 2020). Statistical methods have determined that the infectious rate of SARS-CoV-2, which is presented as R0, is approximately between 1.3 and 6.5, with an average of 3.3 (Sen-Crowe et al., 2020).

Many reports indicate that SARS-CoV-2 has a long incubation period (between 2 and 14 days) with high asymptomatic transmission capability, and this feature may well be a contributing factor to the rapid spreading of the virus (Ahn et al., 2020). The pattern of the outbreak shows that all races and ages are susceptible to the infection. However, the rates of severe disease and mortality are more prevalent in the elderly and individuals with underlying disease such as cardiovascular diseases, diabetes and high blood pressure (Chen et al., 2020).

PHYLOGENY AND TAXONOMY OF COVID-19 CORONAVIRUS

The latest classification divides the Coronaviridae family into two subfamilies, the Coronavirinae and the Letovirinae (García 2020; Scagliarini and Alberti, 2020). There are four genera in the Coronavirinae subfamily including Alpha, Beta, Gamma and Delta-coronavirus. Thus far, seven human pathogenic coronaviruses have been identified, with the NL63 and 229 E in the Alpha genus, and OC43, HKU1, SARS, MERS and SARS-CoV-2 belonging to the Beta genus (Wang et al., 2020).

SARS-CoV-2 is an enveloped RNA virus possessing a positive sense, single-stranded genome around 29.9 Kb. A large part (about two-thirds) at the 5′ end of viral genome encodes the pp1ab and pp1a polyproteins, fractured into 15 non-structural proteins which consist of nsp1-16. On the opposite side (3′ end),

the virus genome encodes four structural proteins including surface spike (S), matrix (M), envelope (E), nucleocapsid (N) and also eight accessory proteins. Structural and accessory proteins participate in virus morphogenesis and immune system interference, while non-structural proteins are involved in virus replication. The spike glycoprotein is necessary for the attachment to the host cell receptors and determines tissue tropism (Zhang et al., 2020).

Analysis of phylogenetic results has shown that SARS-CoV-2 is genetically related to bat-SL-CoVZC45 and bat-SL-CoVZXC21 (89% identity), but has less similarity to SARS-CoV (79%) and MERS-CoV (50%) (Lai et al., 2020). In this regard, analysis of protein sequences showed that SARS-CoV-2 was evolutionarily most related to SARS-CoV. Evaluation of structural proteins indicated that the envelope, nucleocapsid and spike protein have 96%, 89.6%, and 77% sequence identity, respectively, compared to SARS-CoV (Lan et al., 2020).

Other research has shown SARS-CoV-2 to have the highest level of genetic similarity with Malaya pangolin coronaviruses such as *Pan*_SL-CoV_GD (91.2%) and *Pan*_SL-CoV_GX (85.4%). As an intermediate host, it seems that pangolins may have played an important role in transmitting the virus to humans (Forster et al., 2020).

In a recent study by Forster et al. (Forster et al., 2020) genetic characterization of 160 positive samples of SARS-CoV-2 were evaluated from across the world. Phylogenetic analysis showed that three variants (A, B, C) are available according to amino acid changes. Variant A is ancestral type and exists with C variant in European and American patients. The B variant is most common in Asian patients (Forster et al., 2020).

RESPIRATORY VIRUSES SIMILAR TO COVID-19 AND THEIR MODE OF ACTION

Viral respiratory infections cause life-threatening disease in many people worldwide and affect the lives of millions of people worldwide each year. Global interest in respiratory viruses has recently increased substantially owing to the emergence of some new viruses including SARS-CoV, avian influenza A H5N1, H7N9, H1N1v2009, and Mers-CoV (Visseaux et al., 2017). This review will therefore exclusively focus on influenza viruses and coronaviruses, both of which are known to cause respiratory infections.

Influenza Virus

Influenza virus belongs to the Orthomyxoviridae family, which contains three genera of influenza viruses, namely influenza A, B and C viruses. These are classified according to antigenic differences between their nucleoprotein (NP) and matrix 1 (M1) proteins. Types A and B are responsible for seasonal flu epidemics each year. Influenza virus infection remains one of the most serious threats to human health and causes epidemics or pandemics. Influenza viruses are responsible for acute contagious respiratory infections (Memoli et al., 2008). Influenza A viruses cause the most virulent disease among the three influenza types and, based on the antibody responses to these viruses, they may be divided into different serotypes (Zowalaty et al., 2011). Influenza A viruses contain seven or eight pieces of single-stranded, segmented negative-sense RNA. The genomes of influenza A viruses encode eleven proteins including HA, NA, NP, PB1, PB1-F2, PB2, NS1, NEP, PA, M1, and M2. The main antigenic factors of influenza A and B viruses are the hemagglutinin (HA) and neuraminidase (NA) *trans*-membrane glycoprotein knobs (Kampus et al., 2006). The A virus can be divided into subtypes based on the antigenic nature of their HA (16 subtypes) and NA (9 subtypes) glycoproteins (Klenk et al., 2008).

HA is the main influenza virus antigen and its antigenic sites (A, B, C, D, and E) are presented at the head of the molecule, while the feet are fixed in the viral membrane. HA influences the extent of infection into the host organism. The HA protein attaches to sialic acid-containing glycoprotein and glycolipid receptors on the cell surface (Kollerova and Betakova 2006). NA (also called sialidase) releases progeny virions from infected cells by cleaving sialic acid from the HA molecule, from other NA molecules and from receptors at the cell surface. NA may promote the movement of viruses through respiratory tract mucus, in this way enhancing viral infectivity. When the influenza virus is deficient in NA activity, this results in aggregation of virus progeny at the surface of the infected cell, which will severely impair further spread of viruses to other cells (Zhang et al., 2006). Also, NA mutations can result in the ability of influenza A viruses to adapt to novel environments, enabling the virus to jump host species barriers (Suzuki 2005). These two proteins are targets for antiviral drugs (Wilson and Von 2003) and are capable of exciting subtype-specific immune responses. M1 and M2 are matrix proteins. The M1 protein coats inside the viral envelope and has several regulatory actions, performed by interaction with host cell components. M2 is a proton-selective ion channel which only passes the proton ions. It causes hydrogen ions to enter the viral particle, lowering the pH inside of the virus and causing dissociation of M1 from RNP, finally uncoating the virus. PA encodes an RNA polymerase. PB1 encodes an RNA polymerase, while PB1-F2 protein induces apoptosis using different reading frames from the same RNA segment and PB2 encodes an RNA polymerase (Kampus et al., 2006).

The currently-approved classes of small molecule drugs for treating influenza viral infections include neuraminidase inhibitors (zanamivir and oseltamivir), as well as M2 channel blockers (amantadine and rimantadine), and viral polymerase inhibitors (favipiravir and baloxavir marboxi) (Lagoja and De Clercq 2008; Furuta et al., 2017). The efficacy of favipiravir in influenza treatment has lately been questioned owing to a lack of efficacy in primary human airway cells (Yoon et al., 2018). In 2010, two new neuraminidase inhibitors (NAIs) known as peramivir and laninamivir were licensed in Japan (Shetty and Peek 2012).

Studies have also shown that influenza infections result in the uncontrolled increase of pro-inflammatory cytokines, which makes this infection a strong risk factor for severe complications which may be terminal (De Jong et al., 2006; Rothberg and Haessler 2010). Influenza infection can induce a cytokine storm. The cytokine storm or 'hypercytokinemia' is a

systemic expression of a healthy and strong immune system, and is potentially lethal, consisting of positive feedback between cytokines and immune cells with high levels of various cytokines (Osterholm 2005). These cytokines activate guanosine triphosphatase (GTPase) proteins by isoprenylation, which adds the isoprenyl groups such as farnesyl pyrophosphate (FPP) or geranylgeranyl pyrophosphate (GGPP) to the GTPase proteins. This causes Nuclear Factor Kappa Beta (NF-κB) movement to the nucleus, recruiting Toll Like Receptor-7 (TLR-7) in the endosomal compartment which recognizes ssRNA (Kawai and Akira 2006) to express the target genes for cytokines such as TNFα/β, IL-1α/β, IFNα/γ, IL-6, MIP-1α and IL-8. This in turn enables the attraction of different immune effectors and finally leads to inflammation (Osterholm 2005; Piqueras et al., 2006). The assembly of prostaglandins, especially E2, triggers complex thermoregulatory mechanisms to increase the temperature of the body (Brydon et al., 2005). Some anti-inflammatory drugs can block or decrease influenza virus infection by a reduction in protein isoprenylation in membrane structures and continuing pathways (Blanco-Colio et al., 2003). Some effective alternative therapeutics to vaccines and conventional antiviral drugs can be based on anti-inflammatory and immunomodulatory agents (Fedson 2006).

Coronaviruses

The classification of CoVs has been based on genomic organization, similarities in the genomic sequence, replication strategies, antigenic properties of viral proteins, as well as structural characteristics of virions, cytopathogenic, pathogenic and physicochemical properties (Lai and Cavanagh, 1997). Four subgroups of CoVs (Alpha, Beta, Gamma, and Delta) contain pathogens of veterinary or human importance. Common cold symptoms in immunocompetent individuals are caused by AlphaCoVs and the BetaCoVs (HCoV-OC43 and HKU1) (Chiu et al., 2005; Jean et al., 2013). The unique mechanism of viral recombination and an inherently high mutation rate combined with a high frequency of recombination, results in the diversity of hosts and genomic features amongst CoVs (Lai and Cavanagh 1997). A different genus of CoVs can infect birds, whales, swine, cats, dogs, bats, rodents and humans (Abolnik, 2015).

There are four main structural proteins in genomes of coronaviruses including the Spike (S), Membrane (M), Envelope (E) glycoproteins, and Nucleocapsid (N) protein. Besides these structural proteins, different CoVs encode special structural and accessory proteins, such as Hemagglutinin Esterase (HE) protein, 3a/b protein, and 4a/b protein. HE can only be found in some Beta coronaviruses but envelope proteins and nucleocapsid protein are present in all virions (Lissenberg et al., 2005).

S proteins, located outside the virion, bind to the virion membrane via the C-terminal transmembrane regions and they also interact with M proteins (Consortium, 2004). Also, the attachment of virions to surface receptors in the plasma membranes of host cells can happen through the N-terminus of the S proteins (Lewicki and Gallagher, 2002). Additionally, the S proteins form homotrimers, which allow sun-like morphologies to form, giving the name to coronaviruses (Bárcena et al., 2009).

The M protein forms a complex in the absence of the S protein (Vennema et al., 1996). Glycosylation of M proteins in the Golgi apparatus is vital for the virion to fuse into the cell and to make protein antigenic (de Haan et al., 2003). By binding genomic RNA, the N protein forms a complex and the formation of interacting virions in this endoplasmic reticulum-Golgi apparatus intermediate compartment (ERGIC) with this complex is triggered by the M protein (Narayanan and Makino, 2001).

E Glycoproteins are small transmembrane proteins which play an essential role in the assembly and morphogenesis of virions within the cell. Also, the N-terminus of the E proteins allows attachment to the membrane of viruses. E Glycoproteins and the membrane glycoprotein (M) are expressed together with mammalian expression vectors to form virus-like structures within the cell (Baudoux et al., 1998).

N proteins, with a flexible structure, are capable of binding to a helix. They are localized in both the replication/transcriptional region of the coronaviruses and the ERGIC region where the virus is collected so it plays an essential role in virion structure, replication and transcription of coronaviruses (Stertz et al., 2007).

Coronavirus infection initiates following recognition of a specific receptor on the host cell surface by the coronaviral S protein and subsequent internalization of the virion core, which occurs either by direct fusion of the viral membrane with the plasma membrane or via endocytosis (Blau and Holmes, 2001). Some species (eg, SARS and CoV) use the N-terminus, while others use the C-terminus of the S1 site of the receptor-binding domains (RBD) (Islam et al., 2020). Attaching to specific cellular receptors triggers a conformational change in the spike which subsequently mediates fusion between the viral and cell membranes, causing release of the nucleocapsid into the cell (Brian and Baric, 2005). The trimeric S protein is cleaved into an amino (N)-terminal S1 subunit and a carboxyl (C)-terminal S2 subunit (Belouzard et al., 2012). The S1 subunit contains a receptor-binding domain (RBD), which binds the cellular receptor angiotensin-converting enzyme 2 (ACE2), while S2 is responsible for membrane fusion (Li et al., 2005a; Li et al. 2005b; Li et al. 2005c). Different host cell receptors are recognized by different coronaviruses such as Heparan Sulfate Proteoglycans, ACE2, Aminopeptidase N, Heat Shock Protein A5 (HSPA5), furin, and O-Acetylated Sialic Acid (Belouzard et al., 2012; Huang et al., 2015; Hasan et al., 2020; Ibrahim et al., 2020). ACE2 is an analogue of the angiotensin converting enzyme type I (ACE) and part of the renin–angiotensin system responsible for blood pressure regulation (da Silva Antonio et al., 2020). Some analysis suggested that SARS-CoV-2 recognizes human ACE2 more efficiently than SARS-CoV, increasing the capacity of SARS-CoV-2 to transmit from human to human (Wan et al., 2020). Different studies have proven that the affinity between the viral RBD and host ACE2 in the initial SARS-CoV attachment step can determine if a host is susceptible to SARS-CoV infection (Li et al., 2004; Li et al., 2005a; Li et al., 2005b; Li et al., 2005c; McCray et al., 2007). In 2007, it was demonstrated that overexpression of human ACE2 caused an enhancement in

disease severity in a mouse model of SARS-CoV infection, showing that ACE2 is essential for viral entry into the cell (Yang et al., 2007). ACE2 also functions to protect against lung injury, thus, because the virus deregulates the lung protective pathway, SARS-CoV has the potential to become highly lethal (Kuba et al., 2005). ACE2 acts as the entry receptor, and the host enzyme transmembrane protease serine 2 (TMPRSS2) is essential for S protein priming. This enzyme facilitates viral particle entry into the host cells, and its inhibition blocks virus fusion with ACE2 (Cheng et al., 2020a; Cheng et al., 2020b). After entering the cytoplasm, the virus particle releases a single-stranded, non-segmented RNA virus with the largest known RNA genome (gRNA) (Wege et al., 1978). The genome comprises seven genes. These are organized into 5' non-structural protein-coding regions containing the replicase genes (gene 1), comprising two-thirds of the genome, and 3' structural and nonessential accessory protein coding regions which in turn comprises the genes 2–7 (Weiss and Navas-Martin, 2005). Two large open reading frames, ORF1a and 1b, which translate into two large polypeptides (pp1a and pp1b), are encoded by the replicase gene 1. Pp1a and pp1b mediate all the functions necessary for viral replication and transcription (Thiel et al., 2001). Sixteen non-structural proteins (nsp) are converted with the contribution of pp1a and pp1b (Baranov et al., 2005; Tok and Tatar 2017). A Double-Membrane Vesicle (DMV), which is a virus Replication and Transcription Complex (RTC), is formed by these nsp proteins. The role of these 16 proteins, especially nsp3, in the virion structure, as well as the replication and transcription of CoV is notable (Denison 2008; Tok and Tatar 2017). Also, the major viral structural proteins and the accessory proteins are encoded by genes 2 to 7. The accessory proteins have been proven to be essential for virus-cell receptor binding (Goldsmith et al., 2004; Stertz et al., 2007).

All coronaviruses encode one main proteinase. This main proteinase is commonly referred to as '3C-like'. Thus, the coronavirus enzyme is called coronavirus 3C-like proteinase, or 3CLpro. The 3CLpro is analogous to the main picornaviral protease 3Cpro. Coronaviruses also encode one (group 3) or two (groups 1 and 2) papain-like proteases, termed PLP1pro and PLP2p (Ziebuhr et al., 2000). Upon transcription of the genome, a polypeptide is produced by BetaCoVs. The proteolytic cleavage of the polypeptide results in the generation of various proteins. Proteolytic processing is mediated by papain-like protease (PLpro) and 3-chymotrypsin-like protease (3CLpro). The protease 3CLpro cleaves the polyprotein at 11 distinct sites to result in various non-structural proteins critical for viral replication. Thus, the role of 3CLpro in the replication is substantial. The 3CLpro is located at the 3' end, which is characterized by excessive variability (Anand et al., 2003). The papain-like protease (PLpro) is an important cysteine protease in SARS-CoV virus replication. It cleaves ubiquitin chains and affects deISGylation and is responsible for processing the viral polyprotein, as well as processing the viral polypeptide into functional proteins (Lenschow et al., 2007).

In the next section, we are going to discuss natural products with efficacy against some HCoVs, including SARS-CoV, MERS-CoV, and SARS-CoV-2, which belong to BetaCoVs. The genomic organization of BetaCoVs consists of a 5′-untranslated region (UTR), a replicase complex (orf1ab), encoding non-structural proteins (nsps), S protein gene, E protein gene, an M protein gene, an N protein gene, 3'-UTR, as well as several unidentified non-structural open reading frames (Zhu et al., 2020).

The viral main proteinase (3CLpro) controls the activities of the coronavirus replication complex. It can be an attractive target for therapy. Also, due to the key role of PLpro it can be considered as an important target for antiviral agents (Anand et al., 2003). ACE2 is a functional receptor for SARS coronavirus (SARS-CoV) and SARS-CoV-2 to enter the host target cells (Hoffmann et al., 2020), and thus ACE2 inhibition can be considered for development of antiviral agents against SARS-CoV and SARS-CoV-2. These three proteins therefore provide attractive targets for drug development.

NATURAL PRODUCTS AGAINST RESPIRATORY VIRUSES

The failure of many conventional drugs against viral infections combined with the onset of specific viral resistance has led to an increasing interest in plants as promising antiviral agents (Lin et al., 2014). Nature provides an immense library of novel chemicals to explore for the development of drugs to treat various ailments including viral diseases (Denaro et al., 2020). Since natural compounds, including phenolic acids, terpenes, flavonoids, coumarins, lignans, alkaloids and proteins play an essential role in inhibiting viruses and acting as complementary therapies against viral infections (Daglia 2012), we reviewed active natural products against respiratory viruses with a focus on influenza A, SARS-CoV, MERS, and SARS-CoV-2, the cause of the current pandemic of COVID-19.

Natural Products Against Influenza Virus

Resistance to some drugs for the treatment of influenza viral infections is an ongoing problem that has been reported in several cases (Baz et al., 2009; Moscona 2009) and the efficacy of favipiravir in influenza treatment has been doubted because of a lack of efficacy in primary human airway cells (Yoon et al., 2018). Therefore, there exists a significant unmet medical need for novel effective antiviral drugs to combat this disease, and natural products can be considered as an important source of antiviral drugs against influenza.

Although favipiravir, oseltamivir, zanamivir, and peramivir are synthetic compounds, they are inspired by nature with the original active compound of natural origin (Langeder et al., 2020). Additionally, natural-based agents are used most frequently for the treatment of acute respiratory tract infection, especially in children, because of the lack of specific antiviral drugs, easy access and low cost (Lucas et al., 2018). This section provides an overview of natural products affecting the influenza A virus.

Flavonoids are phenolic substances which are one of the most numerous and widespread groups of natural constituents. There are ten major sub-groups of flavonoids, i.e. aurones, biflavonoids, catechins, chalcones, flavanones, flavanonols, flavans, flavones, flavonols and isoflavones (Harborne et al., 2013). Some

flavonoids are reported to have antiviral effects against different types of influenza viruses. In 2018 three flavonoids including 6-hydroxyluteolin 7-O-β-d-glucoside, nepitrin (**1**) and homoplantaginin were isolated from the methanol extract of *Salvia plebeia* R. Br. These compounds were found to be active against influenza virus H1N1A/PR/9/34 neuraminidase (Bang et al., 2018). Matteflavoside G (**2**), a flavonoid isolated from the rhizomes of *Matteuccia struthiopteris* (L.) Tod (currently accepted name Onoclea struthiopteris Roth), showed significant inhibitory activity against the H1N1 influenza virus neuraminidase with an EC50 value of 6.8 ± 1.1 μM and an SI value of 34.4 (Li et al., 2015). In 2016, three flavonoids (**3**–**5**) were isolated from the methanol extract of aerial part of *Salvia plebeia* R. Br. These compounds showed activity against H1N1 neuraminidase in dose-dependent manners with IC_{50} values ranging from 11.18 ± 1.73 to 19.83 ± 2.28 μM. Also, compounds 3 and 4 reduced cytopathic effects of the H1N1 virus during replication (Bang et al., 2016). Flavonoids including quercetin (**6**), isoquercetin (**7**), and rutin (**8**), isolated from the methanol extract of *Capparis sinaica* Veill (accepted scientific name Capparis spinosa var. aegyptia (Lam.) Boiss.), demonstrated a reduction in the virus titer by 68.13%, 79.66% and 73.22% inhibition at a concentration of 1 ng/ml, respectively (Ibrahim et al., 2013). Quercetin (**6**) and rutin (**8**) are reported to inhibit the viral neuraminidase activities *in vitro* and the influenza infection in animal models (Savov et al., 2006; Liu et al., 2008). Quercetin (**6**) and rutin (**8**) were isolated from the hydroalcoholic extract of *Humulus lupulus* L. This extract was found to inhibit replication of various viral strains, at a different time from infection (Di Sotto et al., 2018). Moreover, Mehrbod et al. studied *in vitro* anti-influenza virus a potential of extracts of five South African medicinal plants, including *Clerodendrum glabrum* E. Mey (current name Volkameria glabra (E.Mey.) Mabb. & Y.W.Yuan), *Cussonia spicata* Thunb., *Rapanea melanophloeos* (L.) Mez (current name *Myrsine melanophloeos* (L.) R. Br. ex Sweet), *Pittosporum viridiflorum* Sims and *Tabernaemontana ventricosa* Hochst. ex A. DC., species which are known in traditional medicine to manage several diseases such as inflammatory and respiratory diseases (Mehrbod et al., 2018). The study indicated that in all types of combined treatments such as pre- and post-penetration combined treatments, the methanol leaf extracts of *Rapanea melanophloeos* had an EC50 value of 113.3 μg/ml and the methanol, 100% and 30% ethanol and acetone leaf extracts of *P. viridiflorum* had EC50 values of 3.6, 3.4, 19.2, and 82.3 μg/ml, respectively, with highly significant effects against viral titer ($p \leq 0.01$).

Additionally, the authors found that quercetin-3-o-α-L-rhamnopyranoside (**9**) isolated from *R. melanophloeos* inhibited the viral titre by 6 logs ($p < 0.01$) in the simultaneous procedure at a concentration of 150 μg/ml (Mehrbod et al., 2018). Also, further experiments on quercetin-3-o-α-L-rhamnopyranoside (**9**) showed that the compound in combination with H1N1 was able to induce apoptosis and showed an immunomodulatory effect on some selected pro- and anti-inflammatory cytokines (Mehrbod et al., 2019) (−)-Epigallocatechin-3-gallate (EGCG) (**10**) is one of the major flavonoid components of green tea. Kim and co-workers proved that it damaged the viral membrane and blocked viral penetration into cells and marginally suppressed the viral and nonviral neuraminidase (NA) activity in an enzyme-based assay system (Kim et al., 2013). The association of influenza A virus infections with secondary complications caused by bacterial pathogens, mostly *Streptococcus pneumoniae,* has been reported (McCullers 2014). Two prenylated flavonoid derivatives named sanggenon G (**11**) and sanggenol A (**12**) were found to act as dual inhibitors of both viral and bacterial NAs. Interestingly in contrast to the approved NA inhibitor oseltamivir, these compounds inhibited planktonic growth and also biofilm formation of pneumococci (Grienke et al., 2016).

According to the results (E)-4, 2′, 4′-trihydroxy-6′-methoxy-3′,5′-dimethylchalcone (**13**) and 2.2′,4′-trihydroxy-6′- methoxy-3′,5′-dimethylchalcone (**14**) possessed the strongest effects against NA (Dao et al., 2010). In the screening of natural products for anti-influenza potential, two chalcones named echinantin (**15**) and isoliquiritigenin (**16**) revealed strong inhibitory action against various neuraminidases originating from the influenza viral strains H1N1, H9N2, novel H1N1 (WT), and oseltamivir-resistant novel H1N1 (H274Y) expressed in 293T cells. Echinantin was identified as the most active compound against NA derived from the novel H1N1 influenza with an IC_{50} of 2.49 ± 0.14 μg/ml. Additionally, the efficacy of oseltamivir was increased against H274Y neuraminidase in the presence of compound **15** (5 L μM) (Dao et al., 2011). Also, isoliquiritigenin (**16**) was among eighteen polyphenols isolated from methanol extracts of the roots of *Glycyrrhiza uralensis* Fisch. ex DC. with neuraminidase inhibitory activity (Ryu et al., 2010). Some biflavonoids like ginkgetin (**17**), hinokiflavone (**18**), and 4′-*O*-methylochnaflavone (**19**) were successfully identified as potential NA inhibitors (Miki et al., 2007; Mercader and Pomilio 2010; Kirchmair et al., 2011). Fourteen C-methylated flavonoids including chalcones, flavanones, isoflavones, and one flavanonol were isolated from the methanol extract of *Cleistocalyx operculatus* (Roxb.) Merr. and L.M.Perry (current name Syzygium nervosum A.Cunn. ex DC.).

Coumarins are a very large family of natural products. Many coumarin derivatives have been isolated from plants (Cao et al., 2019). Some coumarins have been reported to possess antiviral effects against influenza A virus. Glycyrol (**20**) is a coumarin isolated from *G. uralensis* with a strong inhibitory effect (IC_{50} = 3.1 μM) (Ryu et al., 2010). Bioassay-guided fractionation of the extract of *Ferula assa-foetida* L (also known as Ferula foetida (Bunge) Regel) afforded twenty sesquiterpene coumarins. Among the isolated compounds, nine compounds were more potent against influenza A virus (H1N1) with IC_{50} between 0.26–0.86 μg/ml than amantadine with an IC_{50} of 0.92 μg/ml. Between all isolated sesquiterpene coumarins, methyl galbanate (**21**) was the most potent (IC_{50} = 0.26 μg/ml) (Lee et al., 2009).

Ten xanthone derivatives were isolated from the ethyl acetate-soluble extract of *Polygala karensium* Kurz. The inhibitory effect of five compounds (**22**–**26**) with a hydroxy group at C-1 against neuraminidases from various influenza viral strains, notably H1N1, H9N2, novel H1N1 and oseltamivir-resistant novel

H1N1, was reported. Moreover, the cytopathic potential of H1N1 swine influenza virus in MDCK cells was reduced by these compounds (Dao et al., 2012).

Rosmarinic acid methyl ester (methyl rosmarinate) (**27**) isolated from the methanol extract of erial parts of *Salvia plebeia* R. Br was active against H1N1 neuraminidase with an IC_{50} value of 16.65 ± 0.91 μM. Also, this compound reduced cytopathic effects of the H1N1 virus during replication (Bang et al., 2016). Inotilone (**28**) and 4-(3, 4-dihydroxyphenyl)-3-buten-2-one (**29**), isolated from the mushroom *Phellinus linteus*, were effective against H1N1 neuraminidase and the influenza A/WS/33 virus. They had neuraminidase inhibitory activity with IC_{50} values of 29.1 and 125.6 μM, respectively (Hwang et al., 2014).

Embeline (**30**) is an alkyl-benzoquinone isolated from the ethyl acetate extract of fruits of *Embelia ribes* Burm. f.. This compound demonstrated antiviral activity against the H1N1 influenza virus, with an IC_{50} of 0.3 μM and an SI of 10, which provides support for further research on this molecule. It was proved that embelin (**30**) was most effective when added at the early stages of the viral life cycle (Hossan et al., 2018).

Four diarylheptanoids out of six isolated constituents from the ethanol extract of the seed of *Alpinia katsumadai* K. Schum (current name Alpinia hainanensis K.Schum.). exhibited inhibitory activities *in vitro* at low micromolar levels against human influenza virus A/PR/8/34 of subtype H1N1. Katsumadain A (**31**) was the most potent compound (IC_{50} = 1.05 ± 0.42 μM) and the most active inhibitor of the NA of four H1N1 swine influenza viruses, with IC_{50} values from 0.9 to 1.64 μM, and also had antiviral effects in plaque reduction assays (Grienke et al., 2010).

Chang et al. (Chang et al., 2016) screened a library of natural components and identified a novel anti-influenza compound with broad-spectrum activity against seasonal influenza A and B viruses. The compound 1,3,4,6-tetra-O-galloyl-b-D-glucopyranoside (TGBG) (**32**) obtained from *Euphorbia humifusa* Willd. was the most active compound against two seasonal influenza A strains, A/California/07/2009 (H1N1) and A/Perth/16/2009 (H3N2), as well as seasonal influenza B strain B/Florida/04/2006. It was proven that the mode of action of TGBG (**32**) was different from the FDA-approved anti-influenza drugs. It significantly inhibited the nuclear export of influenza nucleoproteins (NP) and suppressed the Akt signaling pathway in a dose-dependent manner (Chang et al., 2016).

In 2017, cynanversicoside A (**33**) was isolated from the ethyl acetate extract of *Cynanchum paniculatum* (Bunge) Kitag. ex H. Hara (current name *Vincetoxicum mukdenense* Kitag.). It showed potent anti-inflammatory and antiviral effects on influenza A virus -infected MPMEC by the regulation of NF-κB and MAPK signaling pathways (Wei et al., 2017). Forsythoside A (**34**) was isolated from the methanol extract of *Forsythia suspensa* (Thunb.) Vahl fruit. It increased the survival rate of infected mice in an influenza virus infection model and reduced the viral titers of different influenza virus subtypes in cell cultures. Forsythoside A (**34**) caused a reduction in the influenza M1 protein, which limited the virus spread (Law et al., 2017).

In 2016, the influenza virus NA inhibitory activities of some naturally occurring chlorogenic acids against NAs from *Clostridium perfringens*, H5N1, and recombinant H5N1 (N-His)-Tag were investigated. According to the findings, all chlorogenic acids isolated from *C. perfringens* and selected derivatives demonstrated considerable activities against NAs (Karar et al., 2016).

It is beneficial for a plant-based natural antiviral remedy to have multiple useful activities such as treating secondary infections as well as symptoms associated with influenza and other viral infections.

Fructus Gardeniae, the dry ripe fruits of *Gardenia jasminoides* J. Ellis, is widely used as a traditional medicine in several Asian countries. Bioassay-guided fractionation of the methanol extract from *Fructus Gardeniae* led to the discovery of bioactive natural products with antiviral potential against influenza virus strain A/FM/1/47-MA. The target fraction was administered orally to rats, blood was collected, and the compounds in rat serum after oral administration were separated and characterized. Thirteen compounds including iridoid glycosides, phenylpropanoids, and their derivatives were confirmed or tentatively identified (Yang et al., 2012). The characteristics of natural products against influenza virus have been summarized in **Table 1**. Structures of natural products against influenza virus are depicted in **Figure 1**.

Natural Products Against Coronaviruses

Human coronaviruses are responsible for worldwide epidemic outbreaks and infections, and their rapid spread globally is of major concern. SARS-CoV, MERS-CoV and SARS-CoV-2 are considered as the most emergent CoVs. Although several drugs, such as ribavirin, lopinavir-ritonavir, interferon, and corticosteroids, have been used as treatment with some efficacy in patients infected with SARS-CoV or MERS-CoV (Shalhoub et al., 2015; Shen et al., 2019), no specific treatments or vaccines are available against HCoVs.

In the absence of effective treatments for HCoV infections, natural products might be potential alternative therapies. Many natural products have been tested in terms of their activity against coronaviruses and showed much potential in coronavirus treatment (Adem et al., 2020). Bioactive compounds use different mechanisms to inhibit coronaviruses, and inhibition of ACE2, 3CLpro, and PLpro are most common. Here we mention some of these natural products which have been proven to be active against coronaviruses.

HCoV-229E, an α-CoV, is an important cause of respiratory viral infections in high-risk infants (Sizun et al., 2001). Saikosaponins are a group of oleanane derivatives that have been isolated from some medicinal plants such as *Heteromorpha* spp. (Recio et al., 1995). Saikosaponins (A (35), D (36), B2 (37) and C (38)) were found to possess antiviral activity on HCoV-229E at concentrations of 0.25–25 μM. Saikosaponin B2 (**37**) possessed strongest activity (IC_{50} = 1.7 ± 0.1 μM). Saikosaponin B2 (**37**) inhibited HCoV-229E viral infection by inhibiting attachment of viruses to cells, blocking viral penetration into cells, and also interfering with the early stages of viral replication (Cheng et al., 2006). Also, the efficacy of aqueous and hydromethanolic extracts from stem bark and leaves of three

TABLE 1 | Characteristics of some natural products against influenza virus.

Influenza subtype	Plant/Solvent	Compounds	Effect	Ref
H1N1/PR8	*Salvia plebeia* R.Br/methanol	6-Hydroxyluteolin 7-O-β-d-glucoside, Nepitrin (**1**) and homoplantaginin	NA inhibitor	Bang et al. (2018)
H1N1/PR8	*Matteuccia struthiopteris* (L.) Tod. (Onoclea struthiopteris Roth)/ ethanol	Matteflavoside G (**2**)	NA inhibitor	Li et al. (2015)
H1N1/PR8	*Salvia plebeian* R.Br/methanol	Hispidulin (**3**), Nepetin (**4**), Methyl ester (**5**)	NA inhibitor	Bang et al. (2016)
H5N1	*Capparis sinaica* Veill. (Capparis spinosa var. aegyptia (Lam.) Boiss.) /methanol	Quercetin **(6)**, Isoquercetin (**7**), Rutin (**8**)	NA inhibitor	Ibrahim et al. (2013)
H1N1/PR8 H1N1/ NWS H7N1	*Humulus lupulus* L./hydroalcoholic	Quercetin (**6**), Rutin (**8**)	Interference with redox-sensitive pathways	Di Sotto et al. (2018)
H1N1/PR8	*Rapanea melanophloeos* (L.) Mez (*Myrsine melanophloeos* (L.) R.Br. ex Sweet) and *Pittosporum viridiflorum* Sims /methanol	Crude	HA inhibitor	Mehrbod et al. (2018)
H1N1/PR8	*Rapanea melanophloeos* (L.) Mez *(Myrsine melanophloeos* (L.) R.Br. ex Sweet)/methanol	Quercetin-3-o-α-L-rhamnopyranoside (**9**)	Blocking the virus receptor	Mehrbod et al. (2018)
H1N1/PR8	*Rapanea melanophloeos* (L.) Mez *(Myrsine melanophloeos* (L.) R.Br. ex Sweet)/methanol	Quercetin-3-o-α-L-rhamnopyranoside (**9**)	Interaction with M2, NA and RhoA	Mehrbod et al., (2019)
H1N1/PR8, H3N2	green tea/ND	Epigallocatechin-3-gallate **(10)**	NA inhibitor	Kim et al. (2013)
H1N1	White mulberry root/methanol	Sanggenon G **(11)**, Sanggenol A **(12)**	NA inhibitor	Grienke et al. (2018)
H1N1, H9N2	*Cleistocalyx operculatus* (Roxb.) Merr. & L.M.Perry (Syzygium nervosum A.Cunn. ex DC.) /methanol	(E)-4, 2′, 4′-trihydroxy6′-methoxy-3′,5′-dimethylchalcone (**13**), 2.2′,4′-trihydroxy-6′- methoxy-3′,5′-dimethylchalcone **(14)**	NA inhibitor	Dao et al. (2010)
H1N1, H9N2, H1N1 (H274Y4Y)	*Glycyrrhiza inflata* Batalin/acetone	Echinantin **(15)**, Isoliquiritigenin **(16)**	NA inhibitor	Dao et al. (2011)
H1N1/PR8 H3N2	*Ginkgo biloba* L./ND	Ginkgetin (**17**), Hinokiflavone (**18**), 4′-O-methylochnaflavone (**19**)	NA inhibitor	Miki et al. (2007)
H1N1	*Glycyrrhiza uralensis* Fisch. ex DC./methanol	Isoliquiritigenin, glycyrol **(20)**	NA inhibitor	Ryu et al. (2010)
H1N1	*Ferula assa-foetida* L. (Ferula foetida (Bunge) Regel)/methanol	Methyl galbanate **(21)**	ND	Lee et al. (2009)
H1N1, H9N2	*Polygala karensium* Kurz/ethyl acetate	1,7-Dihydroxyxanthone, 1,7-dihydroxy-4-methoxyxanthone, 1,3,7-trihydroxyxanthone, 1.2,3,5-tetrahydroxyxanthone **(22–26)**	NA inhibitors	Dao et al. (2012)
H1N1/PR8	*Salvia plebeian* R.Br/methanol	Rosmarinic acid methyl ester (**27**)	NA inhibitor	Bang et al. (2016)
H1N1	*Phellinus linteus*/ethyl acetate	Inotilone **(28)**, 4-(3, 4-dihydroxyphenyl)-3-buten-2-one **(29)**	NA inhibitor	Hwang et al. (2014)
H1N1,H5N2, H3N2	*Embelia ribes* Burm.f./ethyl acetate	Embeline **(30)**	HA inhibitor	Hossan et al. (2018)
H1N1	*Alpinia katsumadai* K.Schum. (Alpinia hainanensis K.Schum.) /ethanol	Katsumadain A **(31)**	NA inhibitor	Grienke et al. (2010)
H1N1, H3N2, flu B	*Euphorbia humifusa* Willd./ND	1,3,4,6-tetra-O-galloyl-b-D-glucopyranoside **(32)**	Inhibits the nuclear export of NP	Chang et al. (2016)
H1N1	*Cynanchum paniculatum* (Bunge) Kitag. ex H.Hara (*Vincetoxicum mukdenense* Kitag.)/ethyl acetate	Cynanversicoside A **(33)**	Suppressing NF-κB and MAPKs activation	Wei et al. (2017)
H5N1	*Sonchus oleraceus* L. and *Armeria maritima* (Mill.) Willd./Methanol	Chlorogenic acid derivatives	NA inhibitor	Karar et al. (2016)
H1N1, H9N2, H3N2	*Forsythia suspense* (Thunb.) Vahl /Methanol	Forsythoside A **(34)**	Reduction in the M1 protein	Law et al. (2017)
H1N1	*Gardenia jasminoides* J.Ellis/methanol	Iridoids glycosides and phenylpropanoid derivatives	ND	Yang et al. (2012)

NA, neuraminidase; ND, not-determined; NP, nuclear protein; HA, hemagglutinin; M1, matrix protein; RhoA, Ras homolog family member A; MAPKs, Mitogen-activated protein kinases.

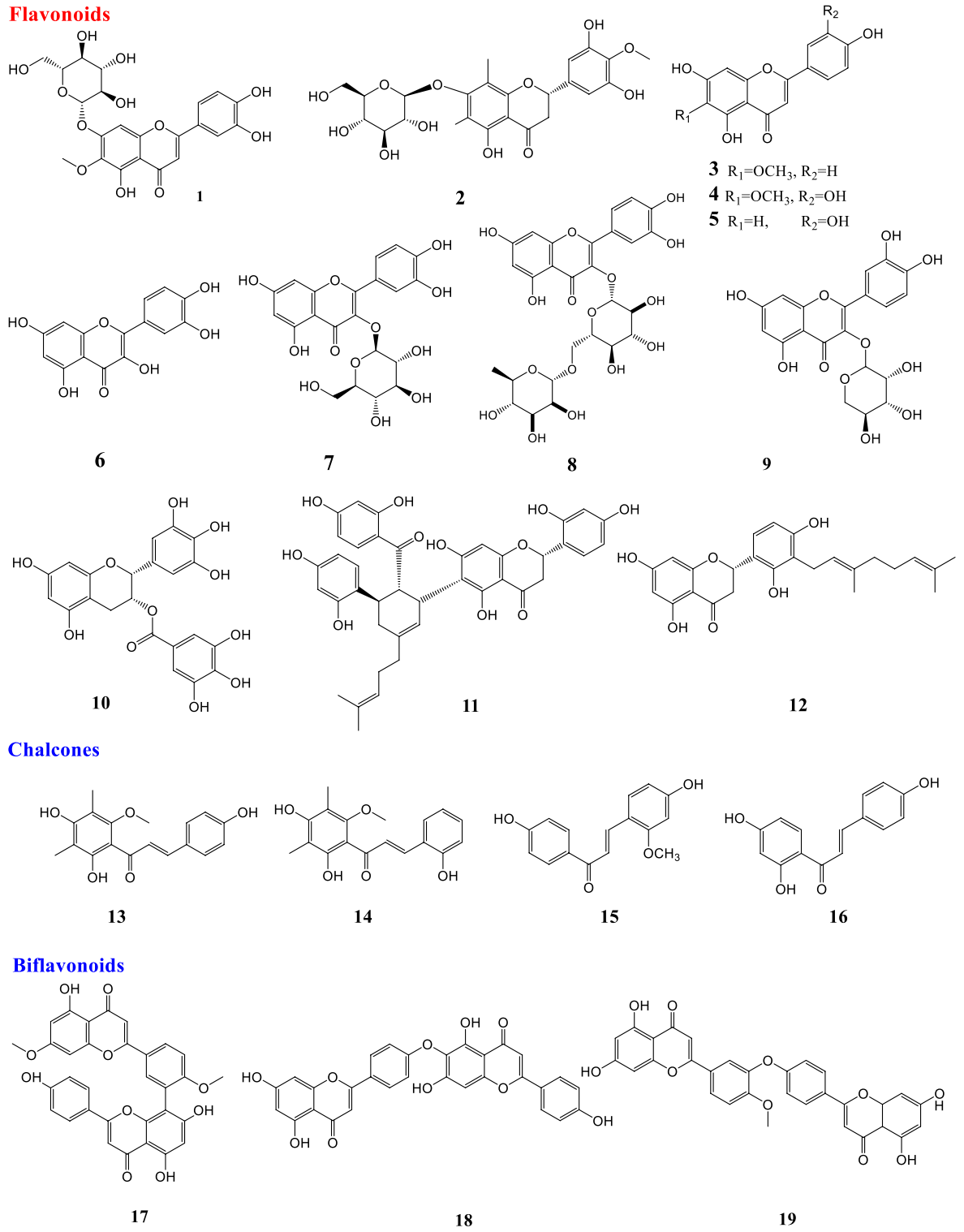

FIGURE 1 | Structures of natural products against influenza virus.

mulberry species (*Morus alba* L. var. *alba, Morus alba* L. var. *rosa* and *Morus rubra* L.) against HCoV-229E has been investigated. Leaf water-alcohol extracts had the best antiviral activity against human coronavirus 229E (Thabti et al., 2020). The structures of natural products against HCoV-229E are shown in **Figure 2**.

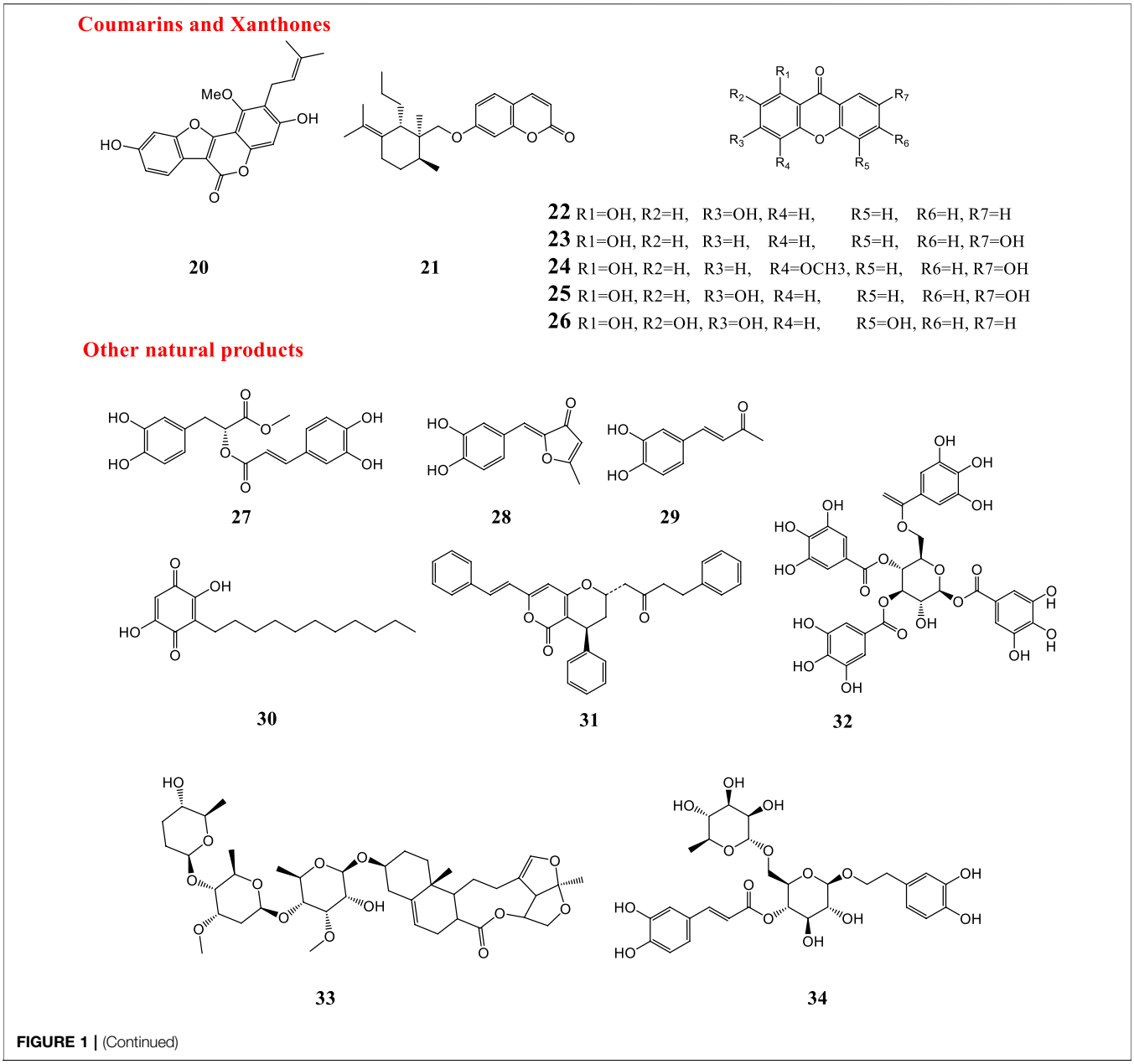

FIGURE 1 | (Continued)

Natural Products Against SARS-CoV-2

As mentioned before, SARS-CoV-2 can cause severe respiratory illness and even death. An in silico investigation revealed that some Indian herbal plant extracts inhibited the SARS-CoV-2 main protease. Highly promising inhibition was shown by extracts of harsingar, *Aloe vera* (L.) Burm. f., and giloy (*Tinospora cordifolia* (Willd.) Hook. f. & Thomson) (Srivastava et al., 2020).

Currently, there is no vaccine or effective antiviral treatment available for COVID-19. In this regard traditional medicine and natural compounds can be taken into consideration as one of the treatment modalities. Lianhuaqingwen (LH) is a traditional Chinese medicine. The antiviral effect of the LH Capsule (LHC) against influenza has been reported. It can reduce the duration of the illness and the duration of viral shedding (Duan et al., 2011). Recently the antiviral and anti-inflammatory activity of LHC against SARS-CoV-2 was investigated *in vitro*. Results showed that LHC significantly inhibited the replication of SARS-COV-2, affected virus morphology, and exhibited anti-inflammatory activity *in vitro* (Runfeng et al., 2020). These multiple beneficial effects are promising and indicate that further intensive research on this preparation is needed.

Terpenoids are a structurally diverse group of plant secondary metabolites (Cheng et al., 2007) and several such compounds have been proven to be effective against SARS-CoV-2. Some

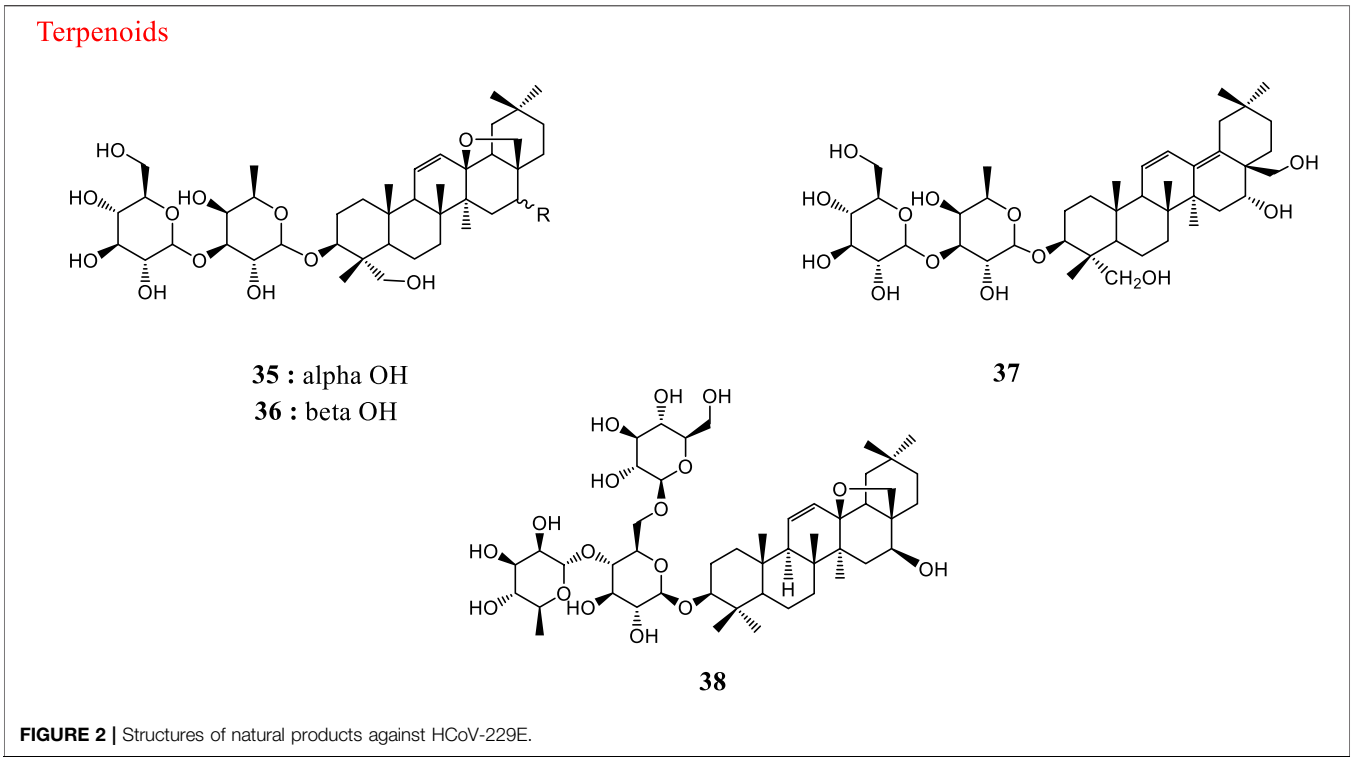

FIGURE 2 | Structures of natural products against HCoV-229E.

terpenoids, namely ursolic acid (**39**), oleanolic acid (**40**) and carvacrol (**41**) were shown to be potential inhibitors of the main protease of SARS-CoV-2 using integrated molecular modeling approaches (Kumar et al., 2020). According to another computational investigation, three natural compounds, digitoxigenin (**42**), β-eudesmol (**43**), and crocin (**44**), had good activity against the main protease of coronavirus and can be proposed as inhibitors of the COVID-19 main protease (Aanouz et al., 2020). Artemisin (**45**) and a limonoid, 6-α-acetoxygedunin (**46**), as well as glycyrrhizin (**47**) are terpenoids which showed potential inhibition against the COVID-19 main protease active site and ACE2 in an *in silico* study (Chen and Du, 2020; Khandelwal and Sharma, 2020; Omaret al., 2020) Also, among the several natural products screened by docking analysis, glycyrrhizin (**47**) and some other natural products including tryptanthrine, rhein and berberine were found to exhibit a higher degree of interaction with the COVID-19 main protease (Narkhede et al., 2020).

Recently over 180,000 natural product-based compounds from different species of animals and plants were screened against the COVID-19 main protease and the ADME properties evaluated (unpublished data). According to the results, twenty compounds were selected and introduced as new potential inhibitors. Compound (48), comprising an alkaloid structure, showed a strong binding affinity to the crucial residues of COVID-19 main protease. Additionally, the excellent ADME properties strengthened the potential of this compound to be a promising drug for the treatment of COVID-19, but this is still under evaluation. Monajjemi and co-workers investigated interactions between four natural compounds, extracted from plants of the province Gillan in Iran, and three receptors including human ACE2, COVID-19 main protease, and SARS-CoV nsp12 polymerase. Results showed that cytarabine (**49**), a compound obtained from Chuchaq (*Eryngium planum* L.), and matrine (**50**) from Trshvash (*Oxalis corniculata* L.), bind to those receptors with lower energies compared to the respective reference compounds (Monajjemi et al., 2020). Khandelwal and Sharma (2020) reported that an alkaloid named echitamine (**51**) had a strong inhibitory effect on ACE2. Another alkaloid named nicotianamine (**52**), seemed to have the potential to block the entry of 2019-nCoV into host cells by binding to ACE2 (Chen and Du, 2020). Hydroxy-chloroquine and chloroquine, synthetic derivatives of quinine, showed positive activities against SARS-CoV-2 *in vitro* and *in vivo*. Quinine is an alkaloid extract from the bark of *Remija* and *Cinchona* (Rubiaceae) species (Gautret et al., 2020). Moreover, some flavonoids including baicalin (**53**), scutellarin (**54**) and hesperetin (**55**) exhibited promising anti-2019-nCoV effects. They have the potential to bind to ACE2 and block the entry of 2019-nCoV into host cells (Chen and Du, 2020).

A computational *in vitro* and *in vivo* study on citrus peels showed that naringin (**56**) could have potential activity in preventing cytokine storms of COVID-19 and naringin (**56**) and hesperetin (**55**) had strong binding affinity to the ACE2 (Cheng et al., 2020a; Cheng et al., 2020b). Additionally, among all the flavonoids available in the traditional Chinese herb, *Exocarpium Citri grandis,* naringin (**56**) possessed the greatest potential for application in reducing the respiratory symptoms caused by COVID-19. In this study some notable features of

naringin (**56**) were revealed, namely that it could improve lung function, alleviate acute lung injury, have effects in attenuating pulmonary fibrosis, and enhance the antiviral immune response through its catabolite HPPA (Su et al., 2020).

An *in silico* study proved that quercetin (**6**), hispidulin (**3**), and cirsimaritin (**57**) exhibited better potential inhibition than hydroxy-chloroquine potential inhibition against the COVID-19 main protease active site and ACE2 (Omar et al., 2020). Moreover, according to the results of another *in silico* study in which 8,000 small molecule candidates of known drugs and natural products were screened, quercetin (**6**) was among the top five most potent compounds for binding strongly to the S-protein ACE2 (Smith and Smith, 2020). Based on the results of a computational study in which a library of phenolic natural compounds (comprising 80 flavonoids) was investigated against SARS-CoV-2 main protease, some other flavonoids including hesperidin (**58**), rutin (**8**), diosmin (**59**) and apiin (**60**) were found to have the potential to bind to the active site. Hesperidin was reported to have the best binding affinity to the main protease (Adem et al., 2020). Also, in another *in silico* study, rutin (**8**) showed notable inhibitory activity against SARS-CoV-2 main protease (Das et al., 2020).

Despite the notable effects of quercetin (**6**) and its derivatives, there are some issues which should be considered. Quercetin and its glucosides found in plants were preferred for interaction with proteins (Day et al., 2000). It has been proven that, despite administration of a high oral dose of quercetin, plasma contained traces of the glycoside due to biotransformation in the gastrointestinal tract (Mullen et al., 2004). Thus, the required concentration for quercetin to perform as an inhibitor of the SARS-CoV-2, Viral Spike Protein/ACE is not reachable by oral administration. However, by using a nasal spray containing quercetin glucosides in a suitable form, the appropriate concentration can be delivered to the active sites (Zhao et al., 2019). Later in 2020, administration of quercetin was recommended to be done directly through alternative routes such as a nasal or throat spray to be effective in clinical trials (Williamson and Kerimi, 2020).

As mentioned earlier, there is more than one host-cell receptor which has been reported to be recognized by the viral spike protein. HSPA5, also termed GRP78 or BiP, is one of these receptors in the cell-surface. Some active components found in some natural products have been tested against HSPA5 *in silico*. Based on the obtained results, some phytoestrogens (diadiazin, genistein, formontein, and biochanin A) and estrogens have the best binding affinities to HSPA5 (Elfiky, 2020). According to the results of a computational study there are several natural molecules like δ-viniferin (**66**), myricitrin (**61**), taiwanhomoflavone A, lactucopicrin 15-oxalate, nympholide A, afzelin, biorobin, hesperidin, and phyllaemblicin B that strongly bind to the SARS-CoV-2 M^{Pro}. The flavonoid myricitrin (**61**) showed strong binding with SARS-CoV-2 M^{Pro} and also high solubility and bioavailability. Interestingly, this compound also showed strong binding with other potential targets of SARS-CoV-2 infection like viral receptor ACE-2 and RNA dependent RNA polymerase (RdRp) (Joshi et al., 2020). An *in silico* study with a focus on three target proteins important in the life cycle of SARS-CoV-2, namely Spike glycoprotein, main protease and RNA-dependent RNA-polymerase was performed. The results showed that silybin (**62**), an active constituent found in *Silybum marianum*, showed binding affinity with targets in SARS-CoV-2. Also, withaferin A from *Withania somnifera* showed significant binding to the target proteins (Pandit and Latha, 2020). According to many studies, PLpro and 3CLpro can be considered as important targets for antiviral drugs against coronaviruses. About 38 drugs and analogues with antiviral activity and 55 of natural origin were screened for inhibitory activities against PLpro and 3CLpro. The results showed that saikosaponin D (**36**) possessed the highest affinity to 3 CL-PRO; Conversely, amentoflavone (**63**) seemed to be a promising inhibitor of PLpro (Contreras-Puentes and Alvíz-Amador, 2020). Molecular docking studies of 32,297 potential anti-viral phytochemicals/traditional Chinese medicinal compounds against $3CL^{pro}$ of SARS-CoV-2 were performed. The results showed that two flavonoids including 5,7,3′,4′-tetrahydroxy-2'-(3,3-dimethylallyl) isoflavone (**64**) and myricitrin (**61**) and a compound named methyl rosmarinate (27) had inhibitory effects against $3CL^{pro}$ of SARS-CoV-2 (Tahir ul Qamar et al., 2020).

A combination of the HPLC-Q-Exactive-MS/MS method with molecular docking showed that active alkaloids of the dried roots and rhizomes of *Veratrum nigrum* L (Agsirga) could block the binding of 2019-nCoV S-protein and ACE2. Agsirga is a traditional Mongolian medicine commonly used to treat tumor and cancer (Cheng et al., 2020a; Cheng et al., 2020b).

Curcumin (**65**), the principal curcuminoid in the rhizome of *Curcuma longa* L., has been reported to be active against the COVID-19 main protease and ACE2 (Omar et al., 2020). This compound has been proven to bind to the active site of SARS-CoV-2 main protease (Das et al., 2020). Also, δ-viniferin (**66**) showed strong binding with the SARS-CoV-2 main protease and strong binding affinity to ACE-2 and RNA dependent RNA polymerase (RdRp) (Joshi et al., 2020).

As mentioned before¸ TMPRSS2 is essential for viral spread and pathogenicity and a TMPRSS2 inhibitor might constitute a treatment option. A virtual screening of natural products against TMPRSS2 indicated that among compounds with promising features, geniposide (**67**) can be considered as the best drug candidate for drug development. Geniposide (**67**) is an iridoid found in the *Gardenia* genus (Rubiaceae) and is endemic in Central America and China (Rahman et al., 2020).

Eight compounds found in rhizomes of *Alpinia officinarum* and ginger were identified as potential inhibitors of SARS-CoV-2 PLpro. Binding affinities to closed and open conformer of PLpro were evaluated. Based on the obtained results, five compounds from the rhizome of *Alpinia officinarum* were identified. Compound **68** binds with the highest affinity to the open conformer of SARS-Cov-2 PLpro and three compounds including 8-gingerol, 10-gingerol and 6-gingerol from ginger were identified to be potent inhibitors of PLpro (Goswami et al., 2020).

Resveratrol (**69**) is a stilbenoid commonly found in *Vitis* species (grapes), red wine and some other plants (Akinwumi

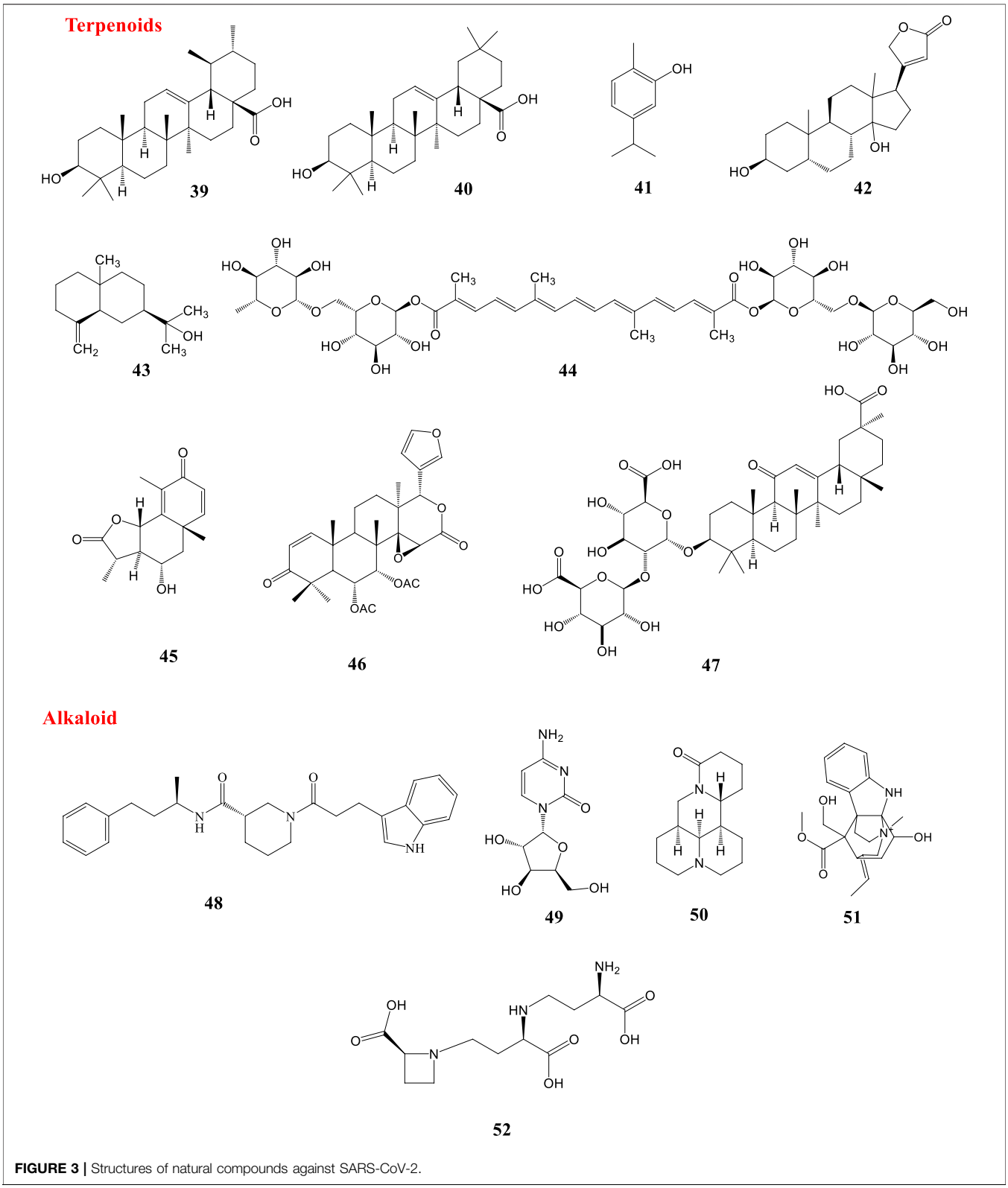

FIGURE 3 | Structures of natural compounds against SARS-CoV-2.

et al., 2018). There have been some studies assessing the impact of resveratrol on SARS-CoV-2 ACE2 activity. An *in silico* study revealed that resveratrol showed significant binding with ACE2 over other tested stilbenoids in the study (Wahedi et al., 2020). Also, resveratrol (**69**) and pterostilbene (**70**) inhibited SARS-CoV-2 infection in a

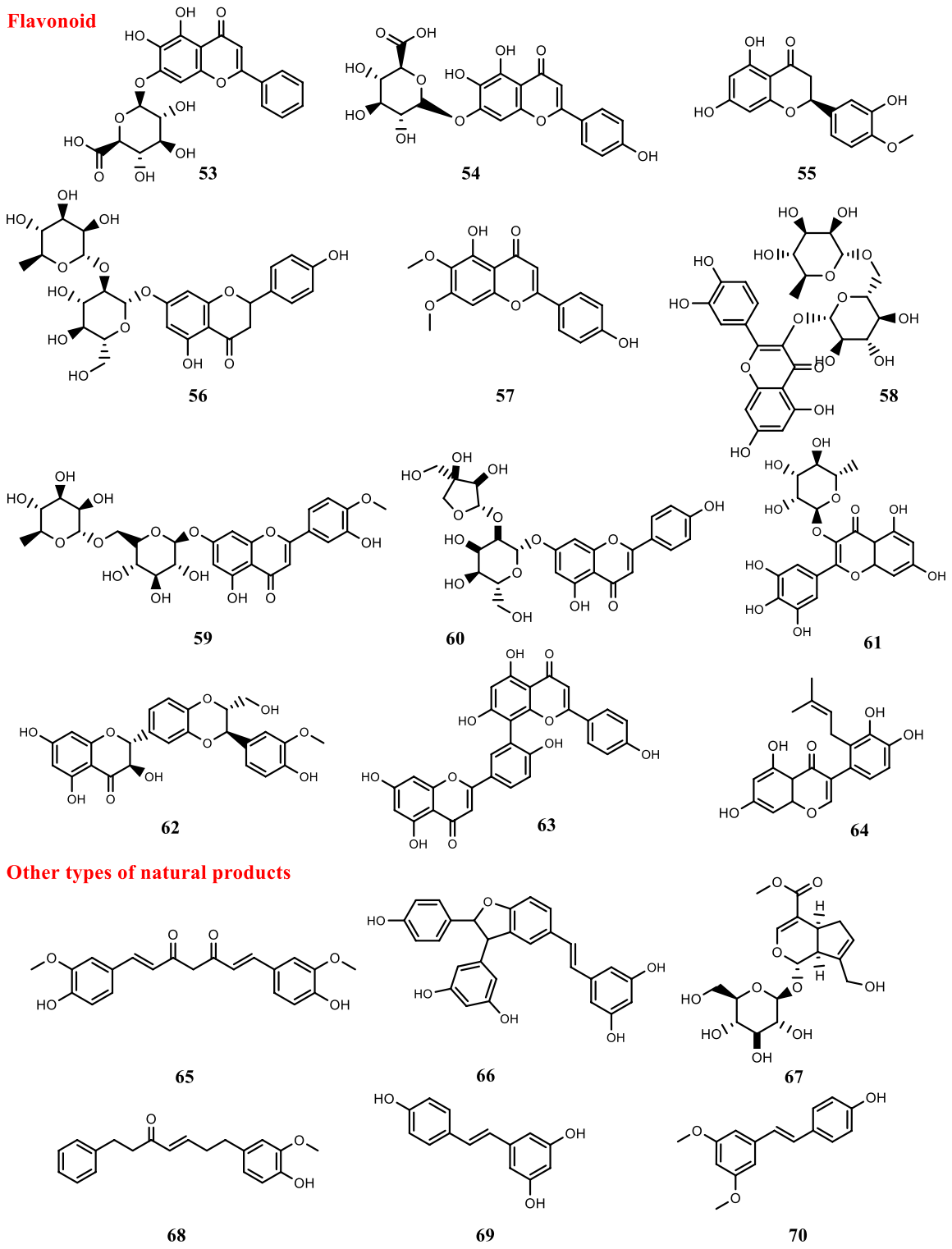

FIGURE 3 | (Continued)

Vero-E6 model. The compounds interfered with the viral infectious cycle and significantly inhibited COVID-19 infection in primary human bronchial epithelial cells cultured under air liquid interface conditions (ter Ellen et al., 2020). The structures of natural products against SARS-CoV-2 are demonstrated in **Figure 3**.

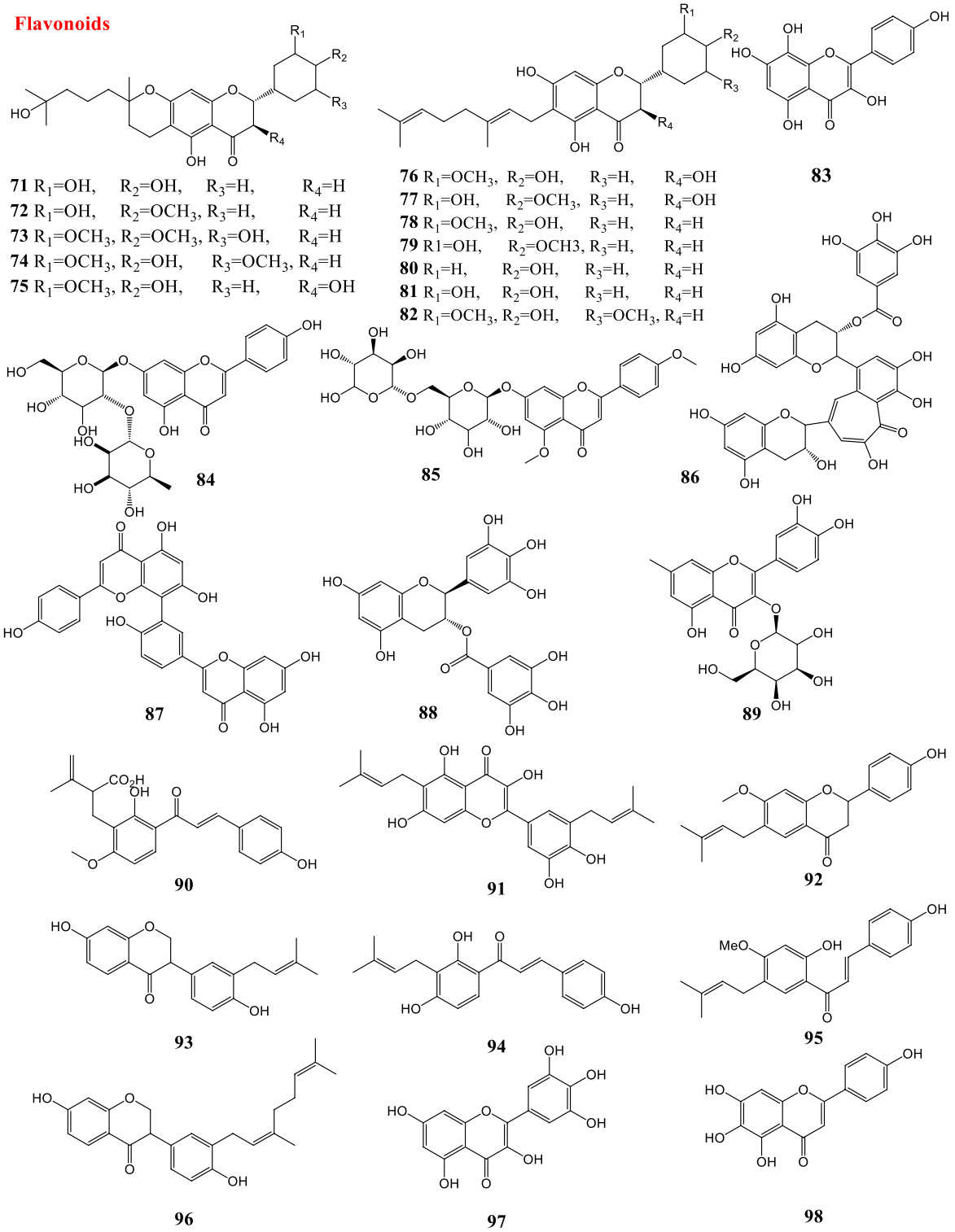

FIGURE 4 | Structures of natural products against SARS-CoV.

The efficacy of some natural compounds and medicinal plants has been tested clinically. Based on biological therapeutic activities, resveratrol (**69**) has been suggested as a potential treatment adjunct for COVID-19 (Filardo et al., 2020; Marinella, 2020). Resveratrol (**69**) can reduce copper (II) to copper (I) thereby generating highly unstable free-radicals

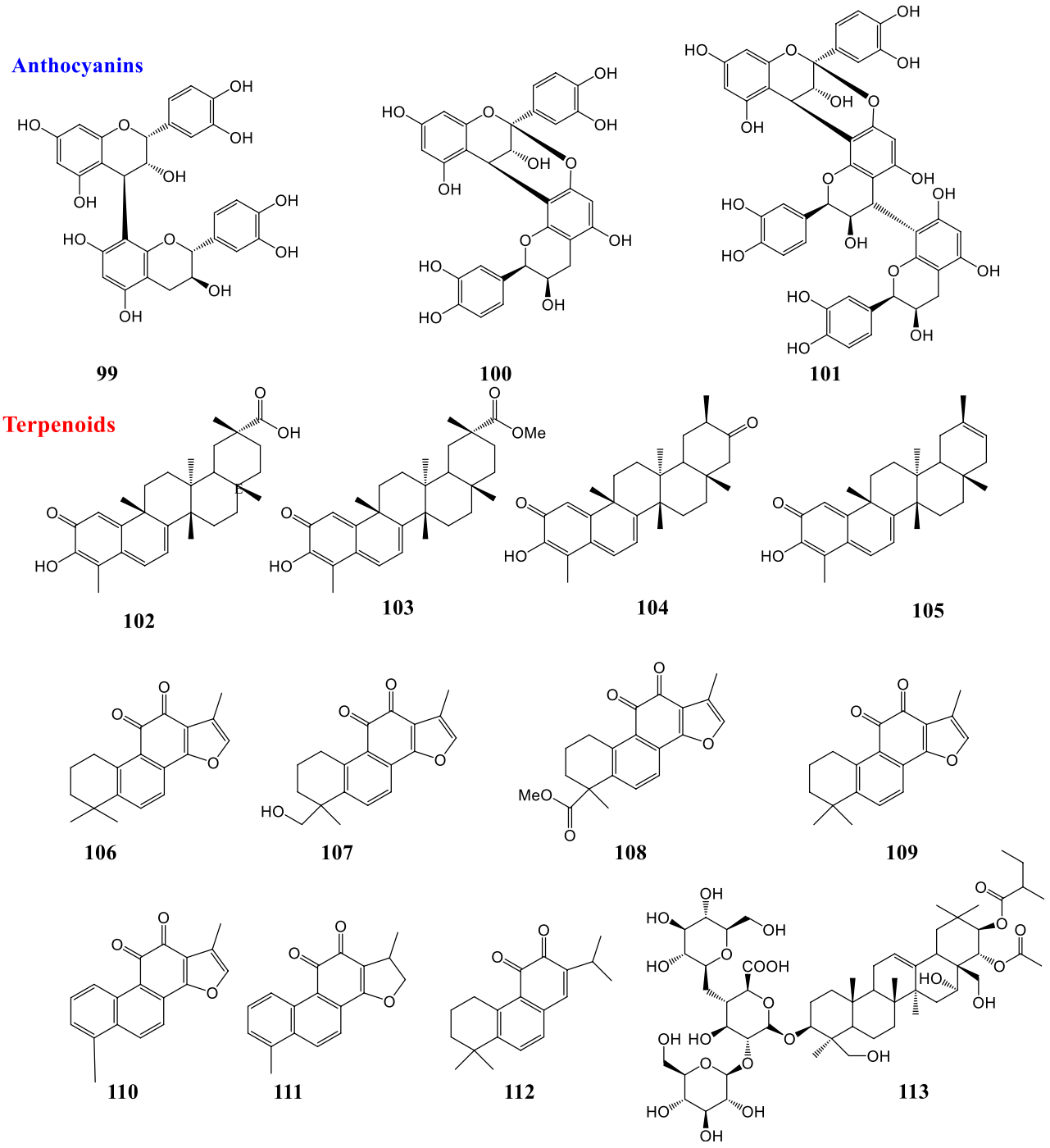

FIGURE 4 | (Continued)

which can degrade cell-free chromatin and can lead to prevention of endotoxin sepsis in mice. In one study, a nearly two-fold reduction in mortality following treatment with resveratrol-copper was observed. In this study thirty patients with severe COVID-19 received, in addition to standard care, resveratrol (**69**) and copper at doses of 5.6 mg and 560 ng, respectively orally, once every 6 h, until discharge or death (Mittra et al., 2020). Lianhua Qingwen prescription (capsules or granules) is an innovative patented Chinese medicine that is composed of 11 herbs with gypsum and menthol, and this preparation had antiviral activities against viral respiratory infections. It includes *Forsythia suspensa*

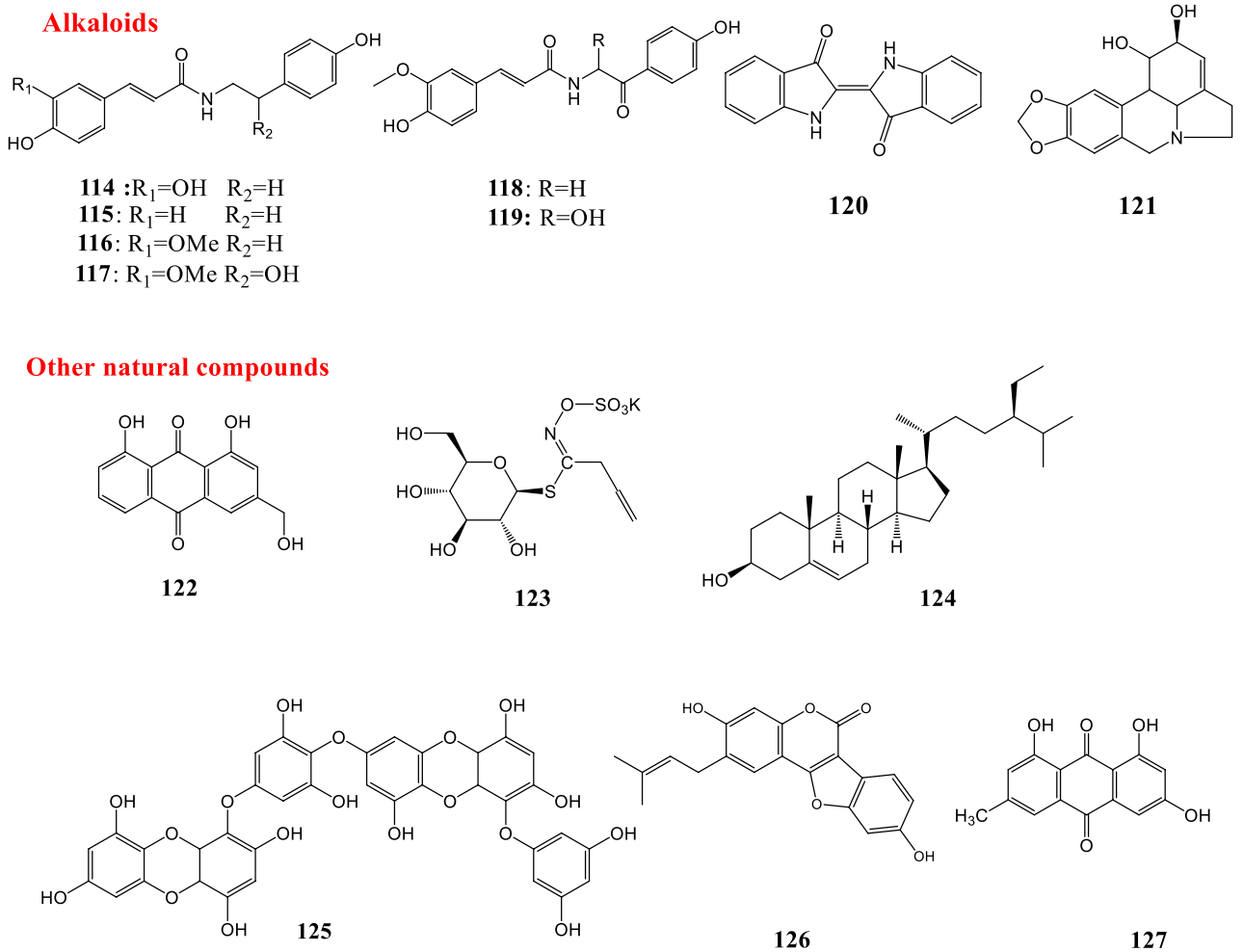

FIGURE 4 | (Continued)

(Thunb.) Vahl (Lianqiao), *Lonicera japonica* Thunb (Jinyinhua), *Ephedra sinica* Stapf (Mahuang), Armeniacae Amarum Semen (Kuxingren), Gypsum Fibrosuum (Shigao), *Isatis tinctoria* L (Banlangen), Dryopteridis Crassirhizomatis Rhizoma (Mianmaguanzhong), *Houttuynia cordata* Thunb (Yuxingcao), *Pogostemon cablin* (Blanco) Benth (Guanghuoxiang), *Rheum palmatum* L (Dahuang), *Rhodiola rosea* Linn (Hongjingtian), *Mentha haplocalyx* Briq (Bohe), *Glycyrrhiza uralensis* Fisch (Gancao) with a herbal ratio of 170 g: 170 g: 57 g: 57 g: 170 g: 170 g: 170 g: 170 g: 57 g: 34 g: 57 g: 5 g: 57 g, which is recorded in the Chinese Pharmacopeia. A study of 284 patients who received Lianhua Qinwen Capsules in combination with basic treatment showed the recovery rate in treatment group was significantly higher than the control group. Time of recovery of symptoms, fever, fatigue, and coughing was remarkably shorter in treatment (Hu et al., 2020). Also, another study reported that Lianhua Qingwen Granules could inhibit fever and cough, reduce their duration and improve individual symptoms (Yao et al., 2020). Also, some other traditional Chinese medicines were found to improve patient recovery (Luo et al., 2020). Results showed that a quadruple combination Ribavirin, Lopinavir/ritonavir, Umifenovir, and Lianhua Qingwen capsule could result in an improvement in abnormal coagulation and leukocytes, with a better prognosis (Li et al., 2020).

Natural Products Against SARS-CoV

SARS is a respiratory illness caused by severe acute respiratory syndrome coronavirus (SARS-CoV) (Drosten et al., 2003). There is evidence that supports medicinal plants and natural products in having beneficial effects in the treatment or prevention of SARS. In 2005, a study revealed that taking a modified formula of two Chinese herbal medicines (Yupingfeng Powder and Sangju Decoction) resulted in the prevention of SARS-CoV (Lau et al., 2005). None of the health care workers using the supplement contracted SARS, in comparison to 0.4% of health care workers who did not use the supplement. Improvements in influenza-like symptoms in addition to quality of life measurements were also noted among herbal supplement users (Lau et al., 2005).

TABLE 2 | Natural products against coronaviruses.

Virus type	Plant/solvent	Compounds	Effect	Ref
HCOV-229E	*Heteromorpha* spp.	Saikosaponins A, D, B_2, C **(35–38)**	Inhibiting viral attachment, blocking viral penetration, interfering with viral replication	Cheng et al. (2006)
HCOV-229E	*Morus alba* L. var. *alba, Morus alba* L. var. *rosa, Morus rubra* L., water/methanol	Crude extract	Reducing the viral titer and cytopathogenic effects	Thabti et al. (2020)
SARS-CoV-2	—	Ursolic acid (**39**), Oleanolic acid (**40**), Carvacrol (**41**)	Inhibiting the main protease	Kumar et al. (2020)
SARS-CoV-2	*In silico*	Digitoxigenin **(42)**, β-cudesmol **(43)**, Crocin **(44)**	Inhibiting SARS-CoV-2 main protease	Aanouz et al., (2020)
SARS-CoV-2	*In silico*	Artemisin (**45**)	Inhibition against COVID-19 main protease active site and ACE2	Omar et al. (2020)
SARS-CoV-2	*In silico*	6-α-acetoxygedunin (**46**)	Inhibiting ACE2	Khandelwal and Sharma (2020)
SARS-CoV-2	—	Glycyrrhizin **(47)**	Bind to ACE2 and block the entry	Chen and Du (2020)
SARS-CoV-2	*(In silico)*	An alkaloid **(48)**	Inhibiting SARS-CoV-2 main protease	Under evaluation
SARS-CoV-2/ SARS- CoV	*Eryngium planum* L	Cytarabine **(49)**	Binding to SARS-CoV-2 main protease and SARS-CoV nsp12 polymerase	Monajjemi et al. (2020)
SARS-CoV-2/ SARS- CoV	*Oxalis corniculata* L	Matrine **(50)**	—	Monajjemi et al. (2020)
SARS-CoV-2	*In silico*	Echitamine (**51**)	Inhibiting ACE2	Khandelwal and Sharma (2020)
SARS-CoV-2	—	Nicotianamine **(52)**, Baicalin **(53),** Scutellarin **(54)**, Hesperetin **(55)**	Bind to ACE2 and block the entry	Chen and Du (2020)
SARS-CoV-2	*Citrus wilsonii Tanaka*	Hesperetin **(55),** Naringin (**56**)	Inhibiting ACE2	Cheng et al. (2020a); Cheng et al. (2020b)
SARS-CoV-2	*In silico, Exocarpium Citri grandis*	Naringin (**56**)	Binding affinity to ACE2 and main protease	Su et al. (2020)
SARS-CoV-2	*In silico*	Phytoestrogens and estrogens	Binding affinity to HSPA5	Elfiky (2020)
SARS-CoV-2	*In silico*	Quercetin (**6**), Hispidulin (**3**), Cirsimaritin (**57**)	Inhibition against COVID-19 main protease active site and ACE2	Omar et al. (2020)
SARS-CoV-2	*In silico*	Hesperidin (**58**), Rutin (**8**), Diosmin (**59**), Apiin **(60)**	Inhibiting main protease	Adem et al. (2020)
SARS-CoV-2	*In silico*	Myricitrin **(61)**	Strong binding affinity to ACE-2 and RNA dependent RNA polymerase	Joshi et al. (2020)
SARS-CoV-2	*In silico Silybum marianum*	Silybin **(62)**	Inhibitory effect on spike glycoprotein, main protease and RNA-dependent RNA-polymerase	Pandit and Latha (2020)
SARS-CoV-2	*In silico*	Amentoflavone **(63)**	Inhibiting PL^{pro}	Contreras-Puentes and Alvíz-Amador (2020)
SARS-CoV-2	*In silico*	5,7,3′,4′-tetrahydroxy-2′-(3,3-dimethylallyl) isoflavone **(64)**, Myricitrin **(61),** Methyl rosmarinate **(27)**	Inhibiting $3CL^{pro}$	Tahir ul Qamar et al. (2020)
SARS-CoV-2	*In silico*	Curcumin **(65)**	Inhibition against COVID-19 main protease active site and ACE2	Omar et al. (2020)
SARS-CoV-2	*In silico*	δ-Viniferin **(66)**	Strong binding affinity to ACE-2 and RNA dependent RNA polymerase	Joshi et al. (2020)
SARS-CoV-2	*In silico*	Geniposide **(67)**	Inhibitory effect on TMPRSS2	Rahman et al. (2020)
SARS-CoV-2	*In silico Alpinia officinarum* and ginger	8-Gingerol, 10- Gingerol and 6-Gingerol and Compound **(68)**	Inhibitors of PLpro	Goswami et al. (2020)
SARS-CoV-2	*In silico*	Saikosaponin D **(36)**	Inhibiting $3CL^{Pro}$	Contreras-Puentes and Alvíz-Amador (2020)
SARS-CoV-2	*In cilico*	Resveratrol **(69)**	Inhibiting ACE2	Wahedi et al. (2020)
SARS-CoV-2	*Vitis* species (grapes), red wine	Resveratrol (**69**) and pterostilbene (**70**)	Interfere with the COVID-19 infection in Vero-E6 model	ter Ellen et al., (2020)
SARS-CoV	*Paulownia tomentosa* (Thunb.) Steud./methanol	Tomentin A-E **(71–75)**	Inhibiting PL^{pro}	Cho et al. (2013)
SARS-CoV	*Tribulus terrestris* L./ethyl acetate, methanol, water	Cinnamic amides **(76–82)**	Inhibiting PL^{pro}	Song et al. (2014)
SARS-CoV	*(In silico)*	Herbacetin **(83)**, Rhoifolin **(84)**, Pectolinarin **(85)**	Binding to S1 S and S2 sites of 3CLpro	Jo et al. (2020)
SARS-CoV	*(In silico)*	Theaflavin-3,3′-digallate (TF3) **(86)**	Inhibiting $3CL^{Pro}$	Chen et al., (2005)
SARS-CoV	Torreya nucifera (L.) Siebold & Zucc	Amentoflavone **(87)**	Inhibiting $3CL^{Pro}$	Ryu et al. (2010)

(Continued on following page)

TABLE 2 | (*Continued*) Natural products against coronaviruses.

Virus type	Plant/solvent	Compounds	Effect	Ref
SARS-CoV	*Pichia brastoris*	Quercetin **(6)**, Epigallocatechin gallate **(10)**, Gallocatechin gallate **(88)**	Inhibiting $3CL^{pro}$	Nguyen et al. (2012)
SARS-CoV	*(In silico)*	Quercetin-3-β-galactoside **(89)**	Inhibitor of SARS-CoV $3CL^{pro}$	Chen et al., (2006)
SARS-CoV	*Angelica keiskei* (miq.) koidz./ethanol	Xanthoangelol E **(90)**	Inhibitor of SARS-CoV $3CL^{pro}$ and PL^{pro}	Park et al. (2016)
SARS-CoV	*Broussonetia papyrifera* (L.) L'Hér. ex Vent /ethanol	Papyriflavonol A **(91)**	Inhibitor of PL^{pro}	Park et al. (2017)
SARS-CoV	*Psoralea corylifolia* L. (Cullen corylifolium (L.) Medik.)/ethanol	Bavachinin **(92)**, Neobavaisoflavone **(93)**, Isobavachalcone **(94)**, 4′-O-Methylbavachalcone **(95)**, Corylifol A **(96)**	Inhibiting PL^{pro}	Kim et al. (2014)
SARS-CoV	—	Myricetin **(97)**, scutellarein **(98)**	Inhibiting the SARS-CoV helicase protein by affecting the atpase	Yu et al. (2012)
SARS-CoV	Cinnamon cortex, cinnamon cortex/methanol	Procyanidin B1 (**99**), procyanidin A2 (**100**), cinnamtannin B1 **(101)**	Inhibitory activity against SARS-CoV	Zhuang et al., (2009)
SARS-CoV	Tripterygium regelii Sprague & Takeda/ethanol	Celastrol **(102)**, Pristimerin **(103)**, tingenone **(104)**, Iguesterin **(105)**	Inhibitor of SARS-CoV $3CL^{pro}$	Ryu et al. (2010)
SARS-CoV	Salvia miltiorrhiza Bunge/ethanol	Tanshinone IIA **(106)**, Tanshinone IIB **(107)**, Methyl tanshinonate **(108)**, Cryptotanshinone **(109)**, Tanshinone I **(110)**, Dihydrotanshinone I **(111)**, Rosmariquinone **(112)**	Inhibition in preincubation with the PL^{pro}	Park et al. (2012)
SARS-CoV	*Aesculus hippocastanum* **L**	Aescin **(113)**	Inhibitory activity in a cell based assay	Wu et al. (2004)
SARS-Cov	*Tribulus terrestris* L. fruits	Cinnamic amides **(114–119)**	Inhibiting PL^{Pro}	Song et al. (2014)
SARS-CoV	Isatis indigotica Fortune ex Lindl	Indigo **(120)**	Inhibits cleavage activity of the $3CL^{pro}$	Lin et al. (2005)
SARS-CoV	Lycoris radiata (L'Hér.) Herb. / ethanol	Lycorine **(121)**	Inhibits SARS-CoV in CPE inhibition assays	Li et al. (2005a), Lin et al. (2005b), Lin et al. (2005c)
SARS-CoV	Isatis indigotica Fortune ex Lindl	Aloeemodin **(122)**, Hesperetin **(55)**, Sinigrin **(123)**, Beta-sitosterol **(124)**	Inhibits cleavage activity of the $3CL^{pro}$	Lin et al. (2005)
SARS-CoV	Glycyrrhiza glabra L	Glycyrrhizin **(47)**	Inhibitor of replication	Cinatl et al. (2003)
SARS-CoV	*(In silico)*	Dieckol **(125)**	Inhibiting $3CL^{pro}$	Park et al. (2013)
SARS-CoV	*Psoralea corylifolia* L/ethanol	Psoralidin **(126)**	Inhibiting PL^{pro}	Kim et al. (2014)
SARS-CoV	Rheum officinale Baill., Polygonum multiflorum Thunb. (Reynoutria multiflora (Thunb.) Moldenke)	Emodin **(127)**	Blocking the S protein and ACE2 interaction	Ho et al. (2007)
SARS-CoV	Cimicifuga rhizoma, Phellodendron cortex, Sophora subprostrata/methanol	—	Inhibitor of RNA synthesis and N and S expression *in vitro*	Kim et al. (2008)
MERS-CoV	*(In silico)*	Dihydrotanshinone **(128)**	Block virus entry, inhibit S proteins	Kim et al. (2018)
MERS-CoV	*(In silico)*	Dodecana **(129)**	Binding affinity to MERS-CoV	Rao et al. (2018)
MERS-CoV	*(In silico)*	Emetine **(130)**	Inhibiting the replication of MERS-CoV	Shen et al. (2019)

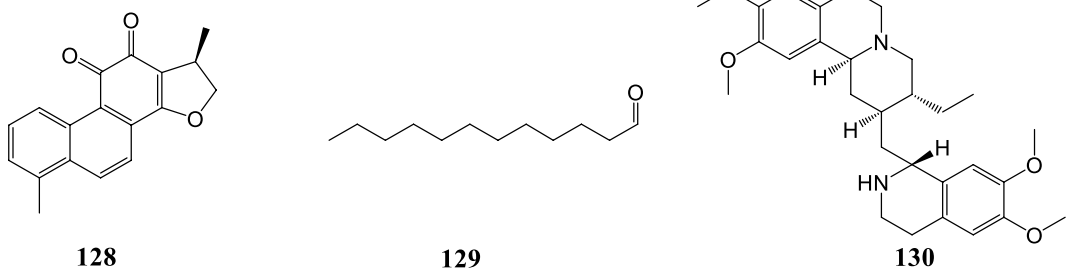

FIGURE 5 | Structures of natural products against MERS-CoV.

As mentioned before, PLpro can be considered as an important target for antiviral agents (Lenschow et al., 2007). *Paulownia tomentosa* (Thunb.) Steud., a traditional Chinese medicine, is a polyphenol-rich plant (Šmejkal et al., 2007). Flavonoids possess hydrophobic aromatic rings and hydrophilic hydroxyl groups, so they have a wide range of binding affinity to SARS-CoV 3CLpro. The binding affinity and mode of the chromen-4-one moiety depends on the presence of carbohydrate groups (Jo et al., 2020). Many small molecules capable of targeting PLpro have been isolated from the methanol extracts of the fruits of the *Paulownia* tree (*P. tomentosa*). Five new geranylated flavonoids, including tomentin A-E (**71–75**) were among these compounds. They all contain a 3,4-dihydro-2H-pyran group. Most isolated compounds (**71–82**) were evaluated as PLpro inhibitors with IC_{50} values ranging between 5.0 and 14.4 μM. All new compounds with a dihydro-2H-pyran group in their structure showed better inhibition than their parent compounds (Cho et al., 2013). According to the results of an induced-fit docking experiment, the presence of an additional 8-hydroxyl group of herbacetin (**83**) was anticipated to be critical for its high binding affinity around the S1 and S2 sites. The occupation of the S1 and S2 sites by carbohydrate groups of rhoifolin (**84**) and pectolinarin (**85**) was expected to be an additional way to achieve a high affinity to SARS-CoV 3CLpro in glycosylated flavonoids (Jo et al., 2020). In 2005, a natural product library comprising 720 compounds was screened for inhibitory activity against 3CLPro. Also the 3CLPro-inhibitory activity of extracts from different types of teas, including green tea, oolong tea, Puer tea and black tea was further investigated. Two types of tea, including Puer and black tea, showed inhibitory activities against 3CLPro. Theaflavin-3,3′-digallate (TF3) (**86**), a known ingredient in teas, was found to be a 3CLPro inhibitor (Chen et al., 2005). Moreover, some biflavonoids from *Torreya nucifera* (L.) Siebold & Zucc. are reported to be active against the 3CLpro. The biflavone amentoflavone (**87**) was the most potent inhibitor of the 3CLpro (Ryu et al., 2010). Also, quercetin (**6**), epigallocatechin gallate (**10**), and gallocatechin gallate (GCG) (**88**) isolated from the yeast *Pichia pastoris* displayed good inhibition of 3CLpro (Nguyen et al., 2012). Quercetin-3-β-galactoside (**89**) (IC_{50} = 42.79 ± 4.97 μM) was identified as a potent inhibitor of SARS-CoV 3CLpro by molecular docking studies and enzymatic inhibition assays. Additionally, the structure–activity relationship of eight new derivatives of quercetin (**6**) was investigated with the help of molecular modeling. Results revealed that the bioactivity of the derivatives was reduced by the removal of the 7-hydroxy group of the quercetin (**6**) moiety and acetoxylation of the sugar moiety (Chen et al., 2006). Xanthoangelol E (**88**), isolated from *Angelica keiskei* (Miq.) Koidz., is a chalcone with a perhydroxyl group in its structure. Compound **90** showed 3CLpro and PLpro inhibitory activity with IC_{50} values of 11.4 and 1.2 μM. Further protein-inhibitor mechanistic analysis revealed that inhibition properties of chalcones to the SARS-CoV 3CLpro seem to be competitive, whereas non-competitive inhibition was observed with the SARS-CoV PLpro (Park et al., 2016). Papyriflavonol A (**91**) is a polyphenol isolated from *Broussonetia papyrifera* (L.) L'Hér. ex Vent. It acted as an inhibitor of PLpro with an IC_{50} value of 3.7 μM (Park et al., 2017). Additionally, six polyphenols, bavachinin (**90**), neobavaisoflavone (**93**), isobavachalcone (**94**), 4′-O-methylbavachalcone (**95**), and corylifol A (**96**), were isolated from *Psoralea corylifolia* L (current scientific name Cullen corylifolium (L.) Medik.). These phytochemicals were identified as replication inhibitors of SARS-CoV by inhibiting PLpro in a dose-dependent manner with IC_{50} ranging between 4.2 and 38.4 μM (Kim et al., 2014). Myricetin (**97**) and scutellarein (**98**) are two naturally-occurring flavonoids. Both compounds act as potent inhibitors of the SARS-CoV helicase protein *in vitro* by affecting the ATPase activity (Yu et al., 2012).

Some natural products showed moderate inhibitory activity against SARS-CoV, for instance procyanidin B1 (**99**), procyanidin A2 (**100**), and cinnamtannin B1 (**101**) extracted from Cinnamon cortex (dried bark of *Cinnamomum verum* J. Presl) and the ethanol extract of Cinnamon cortex have been reported with a low or moderate anti-SARS-CoV activity (Zhuang et al., 2009).

Moreover, some terpenoids named quinone-methide triterpenes including celastrol (**102**), pristimerin (**103**), tingenone (**104**), and iguesterin (**105**) isolated from *Tripterygium regelii* Sprague & Takeda exerted inhibitory activity against SARS-CoV 3CLpro (Ryu et al., 2010). The abietane type diterpenoids isolated from the ethanol extract of *Salvia miltiorrhiza* Bunge such as tanshinone IIA (**106**), tanshinone IIB (**107**), methyl tanshinonate (**108**),

cryptotanshinone (**109**), tanshinone I (**110**), dihydrotanshinone I (**111**), and rosmariquinone (**112**)) were identified as inhibitors of the SARS-CoV 3CLpro and PLpro. The inhibitory activity of all seven compounds (**106**–**112**) was considerable (ranging from 0.8 to 30.0 μM) and an improvement in the inhibition was observed with preincubation with the PLpro. Interestingly, the inhibition was selective because no inhibitory effects against other proteases were observed (Park et al., 2012).

According to the results of an investigation on 224 phytocompounds in 2017, 20 compounds including ten diterpenoids, two sesquiterpenoids, two triterpenoids, five lignoids and one curcumin were identified to be active against SARS-CoV in a cell-based assay of cytopathogenic effect on Vero E6 cells. All compounds exhibited significant inhibition on SARS-CoV 3CLpro (Wen et al., 2007). Glycyrrhizin (**47**) is the principal triterpenoid isolated from licorice (*Glycyrrhiza glabra* L.) roots. In 2003, the results of an investigation showed that glycyrrhizin (**47**) acted as a potent inhibitor of SARS-CoV replication in Vero cells with a selectivity index of 67. Although glycyrrhizin (**47**) had a low selectivity index, it was a significantly potent inhibitor of replication of all the viruses tested and few toxic effects of glycyrrhizin (**47**) were reported (Cinatl et al., 2003). In 2004, some commercial antiviral agents and purified compounds extracted from traditional Chinese medicinal herbs were screened against SARS-CoV. Glycyrrhizin (**47**) and some other compounds including interferon-beta-1a, leukocytic interferon-alpha, ribavirin, rimantadine, lopinavir and baicalin showed antiviral activity against SARS-CoV. The two interferons were only effective when the cells were pre-incubated with the drugs 16 h before viral inoculation, and antiviral activity depended on the cell lines used. Vero, Vero E6, and fRhK-4 cell lines were used in this investigation. Inhibitory activities were not observed for artesunate, glycyrrhizin (**47**) and chlorogenic acid in fRhK-4 cell line. Ribavirin, baicalin and lopinavir were less active in the Vero-E6 cell line while glycyrrhizin, rimandatine, leukocytic interferon-alpha and interferon-beta were more active. Since antiviral activity could be shown for most of the agents in Vero cells, Vero cells were used instead of Vero E6 or fRhK-4 cells for the plaque reduction assay (Chen et al., 2004). Aescin (**113**), the major active principle from the *Aesculus hippocastanum* L (horse chestnut), was reported to have inhibitory activity against SARS-CoV with EC50 value of 6 μM and CC_{50} value of 15 μM (SI = 2.5) in a cell based assay (Wu et al., 2004).

Some alkaloids have been reported to be active against SARS-CoV. Six cinnamic amides (**114**–**119**) were isolated from *Tribulus terrestris* L. fruits. These compounds were proven to be active against SARS-CoV PLpro with IC_{50} values in the range 15.8–70.1 μM (Song et al., 2014). Indigo (**120**) is an alkaloid isolated from *Isatis indigotica* with the ability to block the cleavage processing of the 3CLpro (Lin et al., 2005). In 2005, antiviral activities of more than 200 Chinese medicinal herb extracts against SARS-CoV were evaluated. Among all extracts, the ethanol extract of *Lycoris radiata* (L'Hér.) Herb. had the most potent antiviral activity against SARS-CoV. The process of further purification in order to identify the active compound led to the isolation and identification of an alkaloid, lycorine (**121**), as a potent antiviral compound against SARS-CoV with EC50 ranging from 2.4 ± 0.2 to 88.2 ± 7.7 μg/ml. In the cytotoxicity assay, this compound had a CC50 value of 14,980.0 ± 912.0 nM, and a selective index (SI) greater than 900 (Li et al., 2005a; Li et al., 2005b; Li et al., 2005c).

Aloeemodin (**122**) and hesperetin (**55**) are two phenolic compounds, isolated from *Isatis indigotica* Fortune ex Lindl. root extract, that inhibit cleavage activity of the 3CLpro in dose-dependent manners. Sinigrin (**123**), and beta-sitosterol (**124**) are other isolated compounds with the ability to block the cleavage processing of the 3CLpro in cell-free and cell-based assays (Lin et al., 2005). The inhibitory action of dieckol (**125**), a phlorotannin isolated from the algal species *Ecklonia cava*, against SARS-CoV 3CLpro was investigated. Dieckol (**125**) (IC_{50} = 2.7 μM) showed remarkable inhibitory activity against (**125**) SARS-CoV 3CLpro cell-free cleavage. Additionally, in silico molecular docking simulation of dieckol (**125**) was performed to evaluate its interactions with protein residues in the original ligand-binding site. The findings from docking experiments confirmed the important inhibitory effect of this compound against SARS-CoV 3CLpro (Park et al., 2013). Psoralidin (**126**) is a natural phenolic compound isolated from *Psoralea corylifolia* L. which has been proved to inhibit PLproof SARS-CoV (Kim et al., 2014). Emodin (**127**) is an anthraquinone which significantly blocked the S protein, and also ACE2 interaction, in a dose-dependent manner. It was derived from the genera *Rheum officinale* Baill. and *Polygonum multiflorum* Thunb (current scientific name Reynoutria multiflora (Thunb.) Moldenke). which were identified to be active against SARS-CoV with IC_{50} values ranging from 1 to 10 μg/ml. Emodin (**127**) inhibited the infectivity of S protein-pseudotyped retrovirus to Vero E6 cells (Ho et al., 2007).

Wu and co-workers highlighted potential inhibitors against SARS-CoV and identified numerous potent SARS-CoV inhibitors through screening of a library of natural products. These compounds showed inhibitory activity against viral replication. Some active compounds were able to inhibit the 3CL protease and viral entry (Wu et al., 2004). Moreover, the potential activity of the extracts of some plants against SARS-CoV has been studied. *Houttuynia cordata* Thunb. water extract exhibited significant inhibitory effects on SARS-CoV 3CLpro (Lau et al., 2008). There is evidence of *H. cordata* protecting cells against other coronaviruses as well (Yin et al., 2011). Methanol extracts of Cimicifuga rhizoma, Phellodendron cortex, and Sophora subprostrata radix have been identified as inhibitors of RNA synthesis and N and S expression *in vitro* (Kim et al., 2008). The structures of mentioned natural compounds against SARS-CoV are shown in **Figure 4**.

Natural Products Against Middle East Respiratory Syndrome-Coronavirus

MERS-CoV, belonging to β-CoVs, is mainly endemic in the Middle East but it can also spread outside this region. MERS-

CoV causes severe human respiratory disease with a case fatality rate close to 40% (Arabi et al., 2017). In 2018, 502 compounds derived from natural products, either animal or plant, were screened for their ability to block MERS-CoV entry. Of all tested compounds, dihydrotanshinone (**128**) exhibited antiviral activity against MERS-CoV in the post-attachment assay. Also, it showed antiviral activities in the pre-attachment assay. Therefore dihydrotanshinone (**128**) may have dual inhibitory effects that block virus entry and inhibit S proteins (Kim et al., 2018).

The binding affinity of four compounds isolated from *Coriandrum sativum* L. with six proteins of MERS-CoV was evaluated via in silico methods. Virtual screening and molecular docking results showed that dodecanal (**129**) had the highest binding affinity with all the selected proteins (Rao et al., 2018).

In 2019, a high-throughput screening of potential inhibitors of CoVs *in vitro* resulted in the identification of seven compounds as inhibitors of the replication of CoVs. Among the seven inhibitors, the alkaloid emetine (**130**) exhibited the strongest anti-MERS-CoV activity with an EC50 value of 0.34 μM and SI of 9.06. It acted as an entry inhibitor blocking MERS-CoV-S-mediated infection (Shen et al., 2019). Natural products against coronaviruses are summarized in **Table 2** and their structures are shown in **Figure 5**.

CONCLUSION AND FUTURE PERSPECTIVES

At the present time no specific anti-COVID-19 drugs are available and research communities, countries, and public health organizations are investigating all means to combat this globally transmitted pandemic. Early implementation of strict physical distancing and sanitation protocols has played a role in reducing the incidence of COVID-19 in many parts of the world (Islam et al., 2020; Petersen et al., 2020). Evaluation of current promising antiviral agents is a necessary strategy to discover efficient treatments against this disease.

Natural compounds are widely recognized as complex structures, crafted by evolutionary processes to interact with macromolecular targets. Over the past years, investigations all over the world have generated renewed interest in the search for novel antiviral agents from plant origin. With consideration of the provided information on influenza viruses, SARS-CoV, and Mers-CoV, the new SARS-CoV-2 virus, which shows a broad clinical spectrum and dramatic expansion, might be controlled based on genomic organization similarities.

In this survey we summarized recently reported discoveries of natural compounds with activity against respiratory viruses. We introduced 130 natural compounds as possible therapies to fight against respiratory viruses, including influenza virus, SARS-CoV, MERS-CoV and SARS-CoV-2. Different groups of natural products have antiviral activities but the majority of these compounds belong to the alkaloid, flavonoid and terpenoid families. Although most of the natural compounds listed in this assay are potential inhibitors of COVID-19, the results are mostly based on theoretical or *in vitro* research. Most current research does not present analytical validation. Some natural products, including xanthoangelol E (**88**), hispidulin (**3**), quercetin (**6**), rutin (**8**), saikosaponin D (**36**), glycyrrhizin (**47**), methyl rosmarinate (**27**) and hesperetin (**55**) showed antiviral activities against different respiratory viruses *in vitro* and *in vivo*. These compounds can be recommended as potential lead candidates to prioritise for investigation. Additionally, resveratrol (**69**) is a natural compound which showed promising activity against COVID-19 in the clinical setting. In some cases the maximal suppression of virus infection and replication can be obtained by using a combination of drugs with different mechanisms of action. Natural products and herbal medicine can be considered as important drugs which can be used in combination with basic antiviral treatment.

Despite several existing reports about natural products and their antiviral activities, working with phytochemicals requires expertize and there are many challenges in working with natural compounds. For instance, the isolation, purification, and identification of the structures of these compounds might be paved with challenges. Also, the bioavailability of natural products should be considered before embarking on expensive clinical trials. Other issues include difficulties in prediction of a suitable dosage for these compounds, modes of drug delivery, and the outcome of the combination of two or more of these natural products. The flavonoid quercetin (**6**) is a highly promising compound on the basis of its antiviral activity against influenza A, SARS-CoV, and COVID-19. Future studies should focus on appropriate methods of delivery to combat respiratory viruses, such as nasal or throat sprays, and *in vivo* efficacy.

The structure-based drug design approach is recommended to allow synthetic chemists to develop effective anti-COVID-19 agents. In this regard, the relationship between structure and activity of the compound can be a viable strategy and guidance to create a broad range of anti-respiratory viral compounds. Some previously mentioned studies have given different perspectives, such as activity-guided fractionation, which can be used as a tactic to discover anti-COVID-19 medicines. Accordingly, screening programs may be a rational way to test traditionally used plants all over the world by working on a pseudovirus of COVID-19. Medicinal plants are known as a key natural resource for therapeutic agents. Whilst the future evolution of the current coronavirus pandemic remains unpredictable, beside the public health strategies there is an urgent need for global interdisciplinary cooperation between chemists, microbiologists, botanists and biochemists in order to find natural medicines against COVID-19 and to combat the current challenges, even during inter-epidemic periods.

AUTHOR CONTRIBUTIONS

MAA and PM co-defined the research theme. MO, MK, and MM carried out in-depth study on the research papers, collaborated on the associated data collection and drafted the manuscript. MAA, PM, SNE, and LJM revised the manuscript critically for editorial and important intellectual content. All authors have seen and approved the manuscript.

REFERENCES

Aanouz, I., Belhassan, A., El-Khatabi, K., Lakhlifi, T., El-ldrissi, M., and Bouachrine, M. (2020). Moroccan medicinal plants as inhibitors against SARS-CoV-2 main protease: computational investigations. *J. Biomol. Struct. Dyn.* 10, 1–9. doi:10.1080/07391102.2020.1758790

Adem, S., Eyupoglu, V., Sarfraz, I., Rasul, A., and Ali, M. (2020). *Identification of potent COVID-19 main protease (Mpro) inhibitors from natural polyphenols: an in silico strategy unveils a hope against CORONA*.

Akinwumi, B. C., Bordun, K.-A. M., and Anderson, H. D. (2018). Biological activities of stilbenoids. *Int. J. Mol. Sci.* 19 (3), 792. doi:10.3390/ijms19030792

Bang, S., Li, W., Ha, T. K. Q., Lee, C., Oh, W. K., and Shim, S. H. (2018). Anti-influenza effect of the major flavonoids from *Salvia plebeia* R.Br. via inhibition of influenza H1N1 virus neuraminidase. *Nat. Prod. Res.* 32 (10), 1224–1228. doi:10.1080/14786419.2017.1326042

Bang, S., Quy Ha, T. K., Lee, C., Li, W., Oh, W. K., and Shim, S. H. (2016). Antiviral activities of compounds from aerial parts of *Salvia plebeia* R. Br. *J. Ethnopharmacol.* 192, 398–405. doi:10.1016/j.jep.2016.09.030

Belouzard, S., Millet, J. K., Licitra, B. N., and Whittaker, G. R. (2012). Mechanisms of coronavirus cell entry mediated by the viral spike protein. *Viruses* 4 (6), 1011–1033. doi:10.3390/v4061011

Cao, D., Liu, Z., Verwilst, P., Koo, S., Jangjili, P., Kim, J. S., and Lin, W. (2019). Coumarin-based small-molecule fluorescent chemosensors. *Chem. Rev.* 119 (18), 10403–10519. doi:10.1021/acs.chemrev.9b00145

Chang, S. Y., Park, J. H., Kim, Y. H., Kang, J. S., and Min, J. Y. (2016). A natural component from Euphorbia humifusa Willd displays novel, broad-spectrum anti-influenza activity by blocking nuclear export of viral ribonucleoprotein. *Biochem. Biophys. Res. Commun.* 471 (2), 282–289. doi:10.1016/j.bbrc.2016.01.123

Chen, C. N., Lin, C. P., Huang, K. K., Chen, W. C., Hsieh, H. P., Liang, P. H., et al. (2005). Inhibition of SARS-CoV 3C-like protease activity by theaflavin-3,3'-digallate (TF3). *Evid. Based Complem. Alternat. Med.* 2, 209. doi:10.1093/ecam/neh081

Chen, F., Chan, K., Jiang, Y., Kao, R., Lu, H., and Fan, K. (2004). *In vitro* susceptibility of 10 clinical isolates of SARS coronavirus to selected antiviral compounds. *J. Clin. Virol.* 31 (1), 69–75.doi:10.1016/j.jcv.2004.03.003

Chen, H., and Du, Q. (2020). *Potential natural compounds for preventing SARS-CoV-2 (2019-nCoV) infection*. Preprints.

Chen, L., Li, J., Luo, C., Liu, H., Xu, W., and Chen, G. (2006). Binding interaction of quercetin-3-beta-galactoside and its synthetic derivatives with SARS-CoV 3CL(pro): structure-activity relationship studies reveal salient pharmacophore features. *Bioorg. Med. Chem.* 14 (24), 8295–8306. doi:10.1016/j.bmc.2006.09.014

Cheng, A. X., Lou, Y. G., Mao, Y. B., Lu, S., Wang, L. J., and Chen, X. Y. (2007). Plant terpenoids: biosynthesis and ecological functions. *J. Integr. Plant Biol.* 49 (2), 179–186. doi:10.1111/j.1744-7909.2007.00395.x

Cheng, J., Tang, Y., Bao, B., and Zhang, P. (2020a). *Exploring the active compounds of traditional Mongolian medicine agsirga in intervention of novel coronavirus (2019-nCoV) based on HPLC-Q-exactive-MS/MS and molecular docking method.*

Cheng, L., Zheng, W., Li, M., Huang, J., Bao, S., Xu, Q., and Ma, Z. (2020b). *Citrus fruits are rich in flavonoids for immunoregulation and potential targeting ACE2.*

Cheng, P. W., Ng, L. T., Chiang, L. C., and Lin, C. C. (2006). Antiviral effects of saikosaponins on human coronavirus 229E *in vitro*. *Clin. Exp. Pharmacol. Physiol.* 33 (7), 612–616. doi:10.1111/j.1440-1681.2006.04415.x

Cho, J. K., Curtis-Long, M. J., Lee, K. H., Kim, D. W., Ryu, H. W., Yuk, H. J., et al. (2013). Geranylated flavonoids displaying SARS-CoV papain-like protease inhibition from the fruits of *Paulownia tomentosa*. *Bioorg. Med. Chem.* 21 (11), 3051–3057. doi:10.1016/j.bmc.2013.03.027

Cinatl, J., Morgenstern, B., Bauer, G., Chandra, P., Rabenau, H., and Doerr, H. (2003). Glycyrrhizin, an active component of liquorice roots, and replication of SARS-associated coronavirus. *Lancet* 361 (9374), 2045–2046. doi:10.1016/s0140-6736(03)13615-x

Contreras-Puentes, N., and Alvíz-Amador, A. (2020). Virtual screening of natural metabolites and antiviral drugs with potential inhibitory activity against 3CL-PRO and PL-PRO. *Biomed. Pharmacol. J.* 13 (2), 933–941. doi:10.13005/bpj/1962.33851

da Silva Antonio, A., Wiedemann, L. S. M., and Veiga-Junior, V. F. (2020). Natural products' role against COVID-19. *RSC Adv.* 10 (39), 23379–23393. doi:10.1039/D0RA03774E

Dao, T. T., Dang, T. T., Nguyen, P. H., Kim, E., Thuong, P. T., and Oh, W. K. (2012). Xanthones from *Polygala karensium* inhibit neuraminidases from influenza A viruses. *Bioorg. Med. Chem. Lett.* 22 (11), 3688–3692. doi:10.1016/j.bmcl.2012.04.028

Dao, T. T., Nguyen, P. H., Lee, H. S., Kim, E., Park, J., Lim, S. I., et al. (2011). Chalcones as novel influenza A (H1N1) neuraminidase inhibitors from *Glycyrrhiza inflata*. *Bioorg. Med. Chem. Lett.* 21 (1), 294–298. doi:10.1016/j.bmcl.2010.11.016

Dao, T. T., Tung, B. T., Nguyen, P. H., Thuong, P. T., Yoo, S. S., Kim, E. H., et al. (2010). C-methylated flavonoids from *Cleistocalyx operculatus* and their inhibitory effects on novel influenza A (H1N1) neuraminidase. *J. Nat. Prod.* 73 (10), 1636–1642. doi:10.1021/np1002753

Das, S., Sarmah, S., Lyndem, S., and Singha Roy, A. (2020). An investigation into the identification of potential inhibitors of SARS-CoV-2 main protease using molecular docking study. *J. Biomol. Struct. Dyn.* 10, 1–18.

Day, A. J., Bao, Y., Morgan, M. R., and Williamson, G. (2000). Conjugation position of quercetin glucuronides and effect on biological activity. *Free Radic. Biol. Med.* 29 (12), 1234–1243. doi:10.1016/s0891-5849(00)00416-0

Di Sotto, A., Checconi, P., Celestino, I., Locatelli, M., Carissimi, S., De Angelis, M., et al. (2018). Antiviral and antioxidant activity of a hydroalcoholic extract from *Humulus lupulus* L. *Oxid. Med. Cell Longev.* 2018, 5919237. doi:10.1155/2018/5919237

Elfiky, A. A. (2020). Natural products may interfere with SARS-CoV-2 attachment to the host cell. *J. Biomol. Struct. Dyn.* 8, 1–10. doi:10.1080/07391102.2020.1761881

Filardo, S., Di Pietro, M., Mastromarino, P., and Sessa, R. (2020). Therapeutic potential of resveratrol against emerging respiratory viral infections. *Pharmacol. Therapeut.* 2020, 107613. doi:10.1016/j.pharmthera

Gautret, P., Lagier, J. C., Parola, P., Hoang, V. T., Meddeb, L., and Mailhe, M. (2020). Hydroxychloroquine and azithromycin as a treatment of COVID-19: results of an open-label non-randomized clinical trial. *Int. J. Antimicrob. Agents* 56 (1), 105949. doi:10.1016/j.ijantimicag.2020.105949

Goswami, D., Kumar, M., Ghosh, S. K., and Das, A. (2020). *Natural product compounds in Alpinia officinarum and ginger are potent SARS-CoV-2 papain-like protease inhibitors*.

Grienke, U., Mair, C. E., Kirchmair, J., Schmidtke, M., and Rollinger, J. M. (2018). Discovery of bioactive natural products for the treatment of acute respiratory infections—an integrated approach. *Planta Med.* 84 (09/10), 684–695. doi:10.1055/a-0590-5153

Grienke, U., Richter, M., Walther, E., Hoffmann, A., Kirchmair, J., and Makarov, V. (2016). Discovery of phenylated flavonoids with dual activity against influenza virus and Streptococcus pneumoniae. *Sci. Rep.* 6 (1), 27156–27211. doi:10.1038/srep27156

Grienke, U., Schmidtke, M., Kirchmair, J., Pfarr, K., Wutzler, P., and Dürrwald, R. (2010). Antiviral potential and molecular insight into neuraminidase inhibiting diarylheptanoids from Alpinia katsumadai. *J. Med. Chem.* 53 (2), 778–786. doi:10.1021/jm901440f

Harborne, J. B., Marby, H., and Marby, T. (2013). *The flavonoids*. New York, NY: Springer.

Hasan, A., Paray, B. A., Hussain, A., Qadir, F. A., Attar, F., Aziz, F. M., et al. (2020). A review on the cleavage priming of the spike protein on coronavirus by angiotensin-converting enzyme-2 and furin. *J. Biomol. Struct. Dyn.*, 22, 1–9. doi:10.1080/07391102.2020.1754293

Ho, T. Y., Wu, S. L., Chen, J. C., Li, C. C., and Hsiang, C. Y. (2007). Emodin blocks the SARS coronavirus spike protein and angiotensin-converting enzyme 2 interaction. *Antivir. Res.* 74 (2), 92–101. doi:10.1016/j.antiviral.2006.04.014

Hoffmann, M., Kleine-Weber, H., Schroeder, S., Krüger, N., Herrler, T., Erichsen, S., et al. (2020). SARS-CoV-2 cell entry depends on ACE2 and TMPRSS2 and is blocked by a clinically proven protease inhibitor. *Cell*. 181 (2), 271–280. doi:10.1016/j.cell.2020.02.052

Hossan, M. S., Fatima, A., Rahmatullah, M., Khoo, T. J., Nissapatorn, V., Galochkina, A. V., et al. (2018). Antiviral activity of Embelia ribes Burm. f. against influenza virus *in vitro*. *Arch. Virol.* 163 (8), 2121–2131. doi:10.1007/s00705-018-3842-6

Hu, K., Guan, W. J., Bi, Y., Zhang, W., Li, L., Zhang, B., et al. (2020). Efficacy and safety of Lianhuaqingwen capsules, a repurposed Chinese herb, in patients with coronavirus disease 2019: a multicenter, prospective, randomized controlled trial in patients with Coronavirus disease 2019: a multicenter, prospective, randomized controlled trial. *Phytomedicine*, 2020, 153242. doi:10.1016/j.phymed.2020.153242

Huang, X., Dong, W., Milewska, A., Golda, A., Qi, Y., Zhu, Q. K., et al. (2015). Human coronavirus HKU1 spike protein uses O-acetylated sialic acid as an attachment

receptor determinant and employs hemagglutinin-esterase protein as a receptor-destroying enzyme. *J. Virol.* 89 (14), 7202–7213. doi:10.1128/JVI.00854-15

Hwang, B. S., Lee, M. S., Lee, S. W., Lee, I. K., Seo, G. S., Choi, H. J., and Yun, B. S. (2014). Neuraminidase inhibitors from the fermentation broth of Phellinus linteus. *Mycobiology* 42 (2), 189–192.doi:10.5941/MYCO.2014.42.2.189

Ibrahim, A. K., Youssef, A. I., Arafa, A. S., and Ahmed, S. A. (2013). Anti-H5N1 virus flavonoids from Capparis sinaica Veill. *Nat. Prod. Res.* 27 (22), 2149–2153. doi:10.1080/14786419.2013.790027

Ibrahim, I. M., Abdelmalek, D. H., Elshahat, M. E., and Elfiky, A. A. (2020). COVID-19 spike-host cell receptor GRP78 binding site prediction. *J. Infect.*

Islam, N., Sharp, S. J., Chowell, G., Shabnam, S., Kawachi, I., Lacey, B., et al. (2020). *Physical distancing interventions and incidence of coronavirus disease 2019: natural experiment in 149 countries.*

Jo, S., Kim, S., Shin, D. H., and Kim, M. S. (2020). Inhibition of SARS-CoV 3CL protease by flavonoids. *J. Enzym. Inhib. Med. Chem.* 35 (1), 145–151. doi:10.1080/14756366.2019.1690480

Joshi, R. S., Jagdale, S. S., Bansode, S. B., Shankar, S. S., Tellis, M. B., Pandya, V. K., et al. (2020). Discovery of potential multi-target-directed ligands by targeting host-specific SARS-CoV-2 structurally conserved main protease. *J. Biomol. Struct. Dyn.*, 28, 1–16. doi:10.1080/07391102.2020.1760137

Gamaleldin Elsadig Karar, M., Matei, M. F., Jaiswal, R., Illenberger, S., and Kuhnert, N. (2016). Neuraminidase inhibition of Dietary chlorogenic acids and derivatives—potential antivirals from dietary sources. *Food Funct.* 7 (4), 2052–2059. doi:10.1039/c5fo01412c

Khandelwal, A., and Sharma, T. (2020). *Computational screening of phytochemicals from medicinal plants as COVID-19 inhibitors.*

Kim, D. W., Seo, K. H., Curtis-Long, M. J., Oh, K. Y., Oh, J. W., Cho, J. K., et al. (2014). Phenolic phytochemical displaying SARS-CoV papain-like protease inhibition from the seeds of Psoralea corylifolia. *J. Enzym. Inhib. Med. Chem.* 29 (1), 59–63.doi:10.3109/14756366.2012.753591

Kim, H. Y., Shin, H. S., Park, H., Kim, Y. C., Yun, Y. G., Park, S., et al. (2008). *In vitro* inhibition of coronavirus replications by the traditionally used medicinal herbal extracts, Cimicifuga rhizoma, Meliae cortex, Coptis *rhizoma*, and Phellodendron cortex. *J. Clin. Virol.* 41 (2), 122–128. doi:10.1016/j.jcv.2007.10.011

Kim, J. Y., Kim, Y. I., Park, S. J., Kim, I. K., Choi, Y. K., and Kim, S. H. (2018). Safe, high-throughput screening of natural compounds of mers-cov entry inhibitors using a pseudovirus expressing mers-cov spike protein. *Int. J. Antimicrob. Agents* 52 (5), 730. doi:10.1016/j.ijantimicag.2018.05.003

Kim, M., Kim, S. Y., Lee, H. W., Shin, J. S., Kim, P., Jung, Y. S., et al. (2013). Inhibition of influenza virus internalization by (-)-epigallocatechin-3-gallate. *Antivir. Res.* 100 (2), 460–472. doi:10.1016/j.antiviral.2013.08.002

Kuba, K., Imai, Y., Rao, S., Gao, H., Guo, F., Guan, B., et al. (2005). A crucial role of angiotensin converting enzyme 2 (ACE2) in SARS coronavirus-induced lung injury. *Nat. Med.* 11 (8), 875–879. doi:10.1038/nm1267

Kumar, A., Choudhir, G., Shukla, S. K., Sharma, M., Tyagi, P., Bhushan, A., et al. (2020). Identification of phytochemical inhibitors against main protease of COVID-19 using molecular modeling approaches. *J. Biomol. Struct. Dyn.*, 12, 1–21. (just-accepted)

Law, A. H., Yang, C. L., Lau, A. S., and Chan, G. C. (2017). Antiviral effect of forsythoside A from Forsythia suspensa (Thunb.) Vahl fruit against influenza A virus through reduction of viral M1 protein. *J. Ethnopharmacol.* 209, 236–247. doi:10.1016/j.jep.2017.07.015

Lee, C. L., Chiang, L. C., Cheng, L. H., Liaw, C. C., Abd El-Razek, M. H., Chang, F. R., et al. (2009). Influenza A (H(1)N(1)) antiviral and cytotoxic agents from Ferula assa-foetida. *J Nat Prod* 72 (9), 1568–1572. doi:10.1021/np900158f

Li, W., Greenough, T. C., Moore, M. J., Vasilieva, N., Somasundaran, M., Sullivan, J. L., et al. (2004). Efficient replication of severe acute respiratory syndrome coronavirus in mouse cells is limited by murine angiotensin-converting enzyme 2. *J. Virol.* 78 (20), 11429–11433.doi:10.1128/JVI.78.20.11429-11433.2004

Li, F., Li, W., Farzan, M., and Harrison, S. C. (2005a). Structure of SARS coronavirus spike receptor-binding domain complexed with receptor. *Science* 309 (5742), 1864–1868.doi:10.1126/science.1116480

Li, S. Y., Chen, C., Zhang, H. Q., Guo, H. Y., Wang, H., Wang, L., et al. (2005b). Identification of natural compounds with antiviral activities against SARS-associated coronavirus. *Antivir. Res.* 67 (1), 18–23.doi:10.1016/j.antiviral.2005.02.007

Li, W., Zhang, C., Sui, J., Kuhn, J. H., Moore, M. J., Luo, S., et al. (2005c). Receptor and viral determinants of SARS-coronavirus adaptation to human ACE2. *EMBO J.* 24 (8), 1634–1643.doi:10.1038/sj.emboj.7600640

Li, B., Ni, Y., Zhu, L. J., Wu, F. B., Yan, F., Zhang, X., et al. (2015). Flavonoids from matteuccia struthiopteris and their anti-influenza virus (H1N1) activity. *J. Nat. Prod.* 78 (5), 987–995. doi:10.1021/np500879t

Li, X., Yang, Y., Liu, L., Yang, X., Zhao, X., Li, Y., et al. (2020). Effect of combination antiviral therapy on hematological profiles in 151 adults hospitalized with severe coronavirus disease 2019. *Pharmacol. Res.* 160, 105036. doi:10.1016/j.phrs.2020.105036

Lin, C. W., Tsai, F. J., Tsai, C. H., Lai, C. C., Wan, L., Ho, T. Y., et al. (2005). Anti-SARS coronavirus 3C-like protease effects of Isatis indigotica root and plant-derived phenolic compounds. *Antivir. Res.* 68 (1), 36–42. doi:10.1016/j.antiviral.2005.07.002

Luo, E., Zhang, D., Luo, H., Liu, B., Zhao, K., Zhao, Y., et al. (2020). Treatment efficacy analysis of traditional Chinese medicine for novel coronavirus pneumonia (COVID-19): an empirical study from Wuhan, Hubei Province, China. *Chin. Med.* 15, 1–13.

Marinella, M. A. (2020). Indomethacin and resveratrol as potential treatment adjuncts for SARS-CoV-2/COVID-19. *Int. J. Clin. Pract.*, 74, e13535. doi:10.1111/ijcp.13535

McCray, P. B., Pewe, L., Wohlford-Lenane, C., Hickey, M., Manzel, L., Shi, L., et al. (2007). Lethal infection of K18-hACE2 mice infected with severe acute respiratory syndrome coronavirus. *J. Virol.* 81 (2), 813–821.doi:10.1128/JVI.02012-06

Mehrbod, P., Abdalla, M. A., Fotouhi, F., Heidarzadeh, M., Aro, A. O., Eloff, J. N., et al. (2018). Immunomodulatory properties of quercetin-3-O-α-L-rhamnopyranoside from Rapanea melanophloeos against influenza a virus. *BMC Compl. Alternative Med.* 18 (1), 184–210.doi:10.1186/s12906-018-2246-1

Mehrbod, P., Ebrahimi, S. N., Fotouhi, F., Eskandari, F., Eloff, J. N., McGaw, L. J., et al. (2019). Experimental validation and computational modeling of anti-influenza effects of quercetin-3-O-α-L-rhamnopyranoside from indigenous south African medicinal plant Rapanea melanophloeos. *BMC Compl. Alternative Med.* 19 (1), 1–11. doi:10.1186/s12906-019-2774-3

Miki, K., Nagai, T., Suzuki, K., Tsujimura, R., Koyama, K., Kinoshita, K., et al. (2007). Anti-influenza virus activity of biflavonoids. *Bioorg. Med. Chem. Lett* 17 (3), 772–775.doi:10.1016/j.bmcl.2006.10.075

Mittra, I., de Souza, R., Bhadade, R., Madke, T., Shankpal, P., Joshi, M., et al. (2020). Resveratrol and Copper for treatment of severe COVID-19: an observational study (RESCU 002). medRxiv.

Monajjemi, M., Mollaamin, F., and Shojaei, S. (2020). An overview on coronaviruses family from past to COVID-19: introduce some inhibitors as antiviruses from Gillan's plants. *Biointerface Res. Appl. Chem.* 10 (3), 5575–5585. doi:10.33263/BRIAC103.575585

Mullen, W., Boitier, A., Stewart, A. J., and Crozier, A. (2004). Flavonoid metabolites in human plasma and urine after the consumption of red onions: analysis by liquid chromatography with photodiode array and full scan tandem mass spectrometric detection. *J. Chromatogr. A* 1058 (1–2), 163–168.

Narkhede, R. R., Pise, A. V., Cheke, R. S., and Shinde, S. D. (2020). Recognition of natural products as potential inhibitors of COVID-19 main protease (Mpro): in-silico evidences. *Nat. Prod. Bioprospect.* 15, 1–10.

Nguyen, T. T., Woo, H. J., Kang, H. K., Nguyen, V. D., Kim, Y. M., Kim, D. W., et al. (2012). Flavonoid-mediated inhibition of SARS coronavirus 3C-like protease expressed in Pichia pastoris. *Biotechnol. Lett.* 34 (5), 831–838. doi:10.1007/s10529-011-0845-8

Omar, S., Bouziane, I., Bouslama, Z., and Djemel, A. (2020). In-silico identification of potent inhibitors of COVID-19 main protease (Mpro) and angiotensin converting enzyme 2 (ACE2) from natural products: quercetin, hispidulin, and cirsimaritin exhibited better potential inhibition than hydroxy-chloroquine against COVID-19 main protease active site and ACE2.

Pandit, M., and Latha, N. (2020). In silico studies reveal potential antiviral activity of phytochemicals from medicinal plants for the treatment of COVID-19 infection.

Park, J. Y., Kim, J. H., Kim, Y. M., Jeong, H. J., Kim, D. W., Park, K. H., et al. (2012). Tanshinones as selective and slow-binding inhibitors for SARS-CoV cysteine proteases. *Bioorg. Med. Chem.* 20 (19), 5928–5935. doi:10.1016/j.bmc.2012.07.038

Park, J. Y., Kim, J. H., Kwon, J. M., Kwon, H. J., Jeong, H. J., Kim, Y. M., et al. (2013). Dieckol, a SARS-CoV 3CL(pro) inhibitor, isolated from the edible brown algae Ecklonia cava. *Bioorg. Med. Chem.* 21 (13), 3730. doi:10.1016/j.bmc.2013.04.026

Park, J. Y., Ko, J. A., Kim, D. W., Kim, Y. M., Kwon, H. J., Jeong, H. J., et al. (2016). Chalcones isolated from Angelica keiskei inhibit cysteine proteases of SARS-CoV. *J. Enzym. Inhib. Med. Chem.* 31 (1), 23–30. doi:10.3109/14756366.2014.1003215

Park, J. Y., Yuk, H. J., Ryu, H. W., Lim, S. H., Kim, K. S., Park, K. H., et al. (2017). Evaluation of polyphenols from *Broussonetia papyrifera* as coronavirus protease inhibitors. *J. Enzym. Inhib. Med. Chem.* 32 (1), 504–515. doi:10.1080/14756366.2016.1265519

Petersen, E., Koopmans, M., Go, U., Hamer, D. H., Petrosillo, N., Castelli, F., et al. (2020). Comparing SARS-CoV-2 with SARS-CoV and influenza pandemics. *Lancet Infect. Dis.*

Rahman, N., Basharat, Z., Yousuf, M., Castaldo, G., Rastrelli, L., and Khan, H. (2020). Virtual screening of natural products against type II transmembrane serine protease (TMPRSS2), the priming agent of coronavirus 2 (SARS-CoV-2). *Molecules* 25 (10), 2271. doi:10.3390/molecules25102271

Rao, S. V., Tulasi, D., Pavithra, K., Nisha, R., and Taj, R. (2018). In silico studies on dengue and MERS coronavirus proteins with selected Coriandrum sativum l. herb constituents. *World J. Pharm. Pharmaceut. Sci.* 7 (12), 1–20. doi:10.1371/journal.pntd.0006618

Ryu, Y. B., Kim, J. H., Park, S. J., Chang, J. S., Rho, M. C., Bae, K. H., et al. (2010). Inhibition of neuraminidase activity by polyphenol compounds isolated from the roots of Glycyrrhiza uralensis. *Bioorg. Med. Chem. Lett* 20 (3), 971–974. doi:10.1016/j.bmcl.2009.12.106

Ryu, Y. B., Park, S. J., Kim, Y. M., Lee, J. Y., Seo, W. D., Chang, J. S., et al. (2010). SARS-CoV 3CLpro inhibitory effects of quinone-methide triterpenes from *Tripterygium regelii*. *Bioorg. Med. Chem. Lett* 20 (6), 1873–1876. doi:10.1016/j.bmcl.2010.01.152

Shen, L., Niu, J., Wang, C., Huang, B., Wang, W., Zhu, N., et al. (2019). High-throughput screening and identification of potent broad-spectrum inhibitors of coronaviruses. *J. Virol.* 93 (12), e00023–00019. doi:10.1128/JVI.00023-19

Smith, M., and Smith, J. C. (2020). *Repurposing therapeutics for COVID-19: supercomputer-based docking to the SARS-CoV-2 viral spike protein and viral spike protein-human ACE2 interface*.

Song, Y. H., Kim, D. W., Curtis-Long, M. J., Yuk, H. J., Wang, Y., Zhuang, N., et al. (2014). Papain-like protease (PLpro) inhibitory effects of cinnamic amides from Tribulus terrestris fruits. *Biol. Pharm. Bull.* 37 (6), 1021–1028. doi:10.1248/bpb.b14-00026

Su, W.-W., Wang, Y.-G., Li, P.-B., Wu, H., Zeng, X., Shi, R., et al. (2020). The potential application of the traditional Chinese herb Exocarpium Citri grandis in the prevention and treatment of COVID-19. *Traditional Medicine Research* 5 (3), 160–166.

Tahir ul Qamar, M., Alqahtani, S. M., Alamri, M. A., and Chen, L. L. (2020). Structural basis of SARS-CoV-2 3CLpro and anti-COVID-19 drug discovery from medicinal plants. *J Pharm Anal* 10 (4), 313–319 doi:10.1016/j.jpha.2020.03.009

ter Ellen, B., Kumar, N. D., Bouma, E., Troost, B., van de Pol, D., van der Ende-Metselaar, H., and Nawijn, M. (2020). *Resveratrol and pterostilbene potently inhibit SARS-CoV-2 infection in vitro*. bioRxiv.

Thabti, I., Albert, Q., Philippot, S., Dupire, F., Westerhuis, B., Fontanay, S., et al. (2020). Advances on antiviral activity of Morus spp. plant extracts: human coronavirus and virus-related respiratory tract infections in the spotlight. *Molecules* 25 (8), 12. doi:10.3390/molecules25081876

Wahedi, H. M., Ahmad, S., and Abbasi, S. W. (2020). Stilbene-based natural compounds as promising drug candidates against COVID-19. *J. Biomol. Struct. Dyn.*, 5, 1–10.doi:10.1080/07391102.2020.1762743

Wan, Y., Shang, J., Graham, R., Baric, R. S., and Li, F. (2020). Receptor recognition by the novel coronavirus from Wuhan: an analysis based on decade-long structural studies of SARS coronavirus. *J. Virol.* 94 (7), 12. doi:10.1128/JVI.00127-20

Wei, P., Zhang, T., Dong, H., Chen, Q., Mu, X., and Hu, G. (2017). Anti-inflammatory and antiviral activities of cynanversicoside A and cynanversicoside C isolated from *Cynanchum paniculatum* in influenza A virus-infected mice pulmonary microvascular endothelial cells. *Phytomedicine* 36, 18–25. doi:10.1016/j.phymed.2017.09.009

Wen, C. C., Kuo, Y. H., Jan, J. T., Liang, P. H., Wang, S. Y., Liu, H. G., Lee, C. K., et al. (2007). Specific plant terpenoids and lignoids possess potent antiviral activities against severe acute respiratory syndrome coronavirus. *J. Med. Chem.* 50 (17), 4087–4095.doi:10.1021/jm070295s

WHO, WHO Coronavirus Disease (2020). *COVID-19) dashboard*. Available at: https://covid19.who.int/table. Data accessed: 2020/11/2, 9:37am CET

Williamson, G., and Kerimi, A. (2020). Testing of natural products in clinical trials targeting the SARS-CoV-2 (Coved-19) viral spike protein-angiotensin converting enzyme-2 (ACE2) interaction. *Biochem. Pharmacol.* 178, 114123. doi:10.1016/j.bcp.2020.114123

Wu, C. Y., Jan, J. T., Ma, S. H., Kuo, C. J., Juan, H. F., Cheng, Y. S., Hsu, H. H., et al. (2004). Small molecules targeting severe acute respiratory syndrome human coronavirus. *Proc. Natl. Acad. Sci. U.S.A.* 101 (27), 10012–10017. doi:10.1073/pnas.0403596101

Yang, Q., Wu, B., Shi, Y., Du, X., Fan, M., Sun, Z., et al. (2012). Bioactivity-guided fractionation and analysis of compounds with anti-influenza virus activity from Gardenia jasminoides Ellis. *Arch Pharm. Res. (Seoul)* 35 (1), 9–17. doi:10.1007/s12272-012-0101-3

Yang, X. H., Deng, W., Tong, Z., Liu, Y. X., Zhang, L. F., Zhu, H., et al. (2007). Mice transgenic for human angiotensin-converting enzyme 2 provide a model for SARS coronavirus infection. *Comp. Med.* 57 (5), 450–459.

Yao, K.-t., Liu, M., Li, X., Huang, J., and Cai, H. (2020). Retrospective clinical analysis on treatment of novel coronavirus-infected pneumonia with traditional Chinese medicine Lianhua Qingwen. *Chin. J. Exp. Tradit. Med. Form.* 2020, 1–7. doi:10.1016/j.biopha.2020.110641

Yu, M. S., Lee, J., Lee, J. M., Kim, Y., Chin, Y. W., Jee, J. G., et al. (2012). Identification of myricetin and scutellarein as novel chemical inhibitors of the SARS coronavirus helicase, nsP13. *Bioorg. Med. Chem. Lett.* 22 (12), 4049–4054. doi:10.1016/j.bmcl.2012.04.081

Zhao, J., Yang, J., and Xie, Y. (2019). Improvement strategies for the oral bioavailability of poorly water-soluble flavonoids: an overview. *Int. J. Pharm.* 570, 118642. doi:10.1016/j.ijpharm.2019.118642

Zhuang, M., Jiang, H., Suzuki, Y., Li, X., Xiao, P., Tanaka, T., et al. (2009). Procyanidins and butanol extract of Cinnamomi Cortex inhibit SARS-CoV infection. *Antivir. Res.* 82 (1), 73–81. doi:10.1016/j.antiviral.2009.02.001

Conflict of Interest: The authors declare that the research was conducted in the absence of any commercial or financial relationships that could be construed as a potential conflict of interest.

frontiers in Pharmacology

ORIGINAL RESEARCH
published: 26 February 2021
doi: 10.3389/fphar.2021.634047

Discovering Potential RNA Dependent RNA Polymerase Inhibitors as Prospective Drugs Against COVID-19: An in silico Approach

Satabdi Saha[1†], *Rajat Nandi*[1†], *Poonam Vishwakarma*[2], *Amresh Prakash*[3] *and Diwakar Kumar*[1*]

[1]*Department of Microbiology, Assam University, Silchar, India,* [2]*School of Computational and Integrative Sciences, Jawaharlal Nehru University, New Delhi, India,* [3]*Amity Institute of Integrative Sciences and Health, Amity University Haryana, Gurgaon, India*

OPEN ACCESS

Edited by:
Vijay Kumar Prajapati, Central University of Rajasthan, India

Reviewed by:
Amrendra Kumar Ajay, Harvard Medical School, United States
Shashank Gupta, National Institutes of Health, United States

***Correspondence:**
Diwakar Kumar
diwakar11@gmail.com

[†]*These authors have contributed equally to this work*

Specialty section:
This article was submitted to Ethnopharmacology, a section of the journal Frontiers in Pharmacology

Received: *26 November 2020*
Accepted: *29 January 2021*
Published: *26 February 2021*

Citation:
Saha S, Nandi R, Vishwakarma P, Prakash A and Kumar D (2021) Discovering Potential RNA Dependent RNA Polymerase Inhibitors as Prospective Drugs Against COVID-19: An in silico Approach. Front. Pharmacol. 12:634047. doi: 10.3389/fphar.2021.634047

COVID-19, caused by Severe Acute Respiratory Syndrome Corona Virus 2, is declared a Global Pandemic by WHO in early 2020. In the present situation, though more than 180 vaccine candidates with some already approved for emergency use, are currently in development against SARS-CoV-2, their safety and efficacy data is still in a very preliminary stage to recognize them as a new treatment, which demands an utmost emergency for the development of an alternative anti-COVID-19 drug *sine qua non* for a COVID-19 free world. Since RNA-dependent RNA polymerase (RdRp) is an essential protein involved in replicating the virus, it can be held as a potential drug target. We were keen to explore the plant-based product against RdRp and analyze its inhibitory potential to treat COVID-19. A unique collection of 248 plant compounds were selected based on their antiviral activity published in previous literature and were subjected to molecular docking analysis against the catalytic sub-unit of RdRp. The docking study was followed by a pharmacokinetics analysis and molecular dynamics simulation study of the selected best-docked compounds. Tellimagrandin I, SaikosaponinB2, Hesperidin and (-)-Epigallocatechin Gallate were the most prominent ones that showed strong binding affinity toward RdRp. All the compounds mentioned showed satisfactory pharmacokinetics properties and remained stabilized at their respective binding sites during the Molecular dynamics simulation. Additionally, we calculated the free-binding energy/the binding properties of RdRp-ligand complexes with the connection of MM/GBSA. Interestingly, we observe that SaikosaponinB2 gives the best binding affinity ($\Delta G_{binding}$ = −42.43 kcal/mol) in the MM/GBSA assay. Whereas, least activity is observed for Hesperidin ($\Delta G_{binding}$ = −22.72 kcal/mol). Overall our study unveiled the feasibility of the SaikosaponinB2 to serve as potential molecules for developing an effective therapy against COVID-19 by inhibiting one of its most crucial replication proteins, RdRp.

Keywords: COVID-19, RdRp, plant product, inhibitors, admet, free energy

INTRODUCTION

The widespread impact of COVID-19 has undoubtedly attained singular importance in the mind of international consciousness. The situation precipitated by the COVID-19 pandemic was certainly extraordinary in its rampant spread and impact across all walks of life. WHO had declared the Wuhan borne COVID-19 virus as a public health emergency of International Concern (PHEIC) (Ibrahim et al., 2020), and later, it was recognized as 2019-nCoV/SARS-CoV-2 (Zhou et al., 2020). It is a painful reflection of the rough times we live in and equally a reminder of how important it is for us to take precise, mature, and proactive action for an effective solution or therapy. Even though more than 180 vaccine candidates with some already approved for emergency use, are currently in development against the COVID-19 worldwide (Lythgoe and Middleton, 2020), the search for specific and effective small-molecule drugs for the treatment of COVID-19 would additionally provide another treatment strategy.

SARS-CoV-2 is an RNA virus belonging to the subgenus *Sarbecovirus* (beta-CoV lineage B). This strain has been reported to vary from the other beta-coronavirus, including the MERS-CoV and SARS I virus (Walls et al., 2020). SARS-CoV-2 codes for around 16 non-structural proteins (nsp), including RNA-dependent RNA polymerase (RdRp). RdRps share multiple sequence motifs and tertiary structures with all RNA viruses, making it one of the most lucrative targets for developing potential inhibitors. RdRps play a significant role in facilitating viral gene transcription and replication related to other viral and host factors (Gorbalenya et al., 2002). The RdRp is mainly composed of palm, thumb and finger domains, which resembles the typical right-hand RNA polymerase shape. Among the seven RdRp catalytic motifs, five (A–E) are present within the most conserved palm domain, while the other two (F and G) are within the finger domains (Gorbalenya et al., 2002; Venkataraman et al., 2018; Gao et al., 2020). The catalytic site of RDRp is conserved among different organisms and has two successive, surface-exposed aspartate residues projecting out from a beta-turn motif (Doublie and Ellenberger, 1998; Elfiky and Ismail, 2018; Elfiky and Azzam, 2020).

In this study, the SARS-CoV-2 RdRp homology model was built; it was subjected to Molecular docking, molecular dynamic simulation (MDS), MD Trajectory analysis, and MM-GBSA analysis. A structure-based virtual screening was employed in search of promising compounds as RdRp inhibitors from the PubChem database (https://pubchem.ncbi.nlm.nih.gov/). Two hundred forty-eight plant compounds comprised of flavonoids, alkaloids, lactones, and terpenes with antiviral activity against single-stranded RNA viruses were selected (**Supplementary Table S1**). Additionally, two nucleoside analogs, favipiravir, and remdesivir which, were recently approved for emergency COVID-19 treatment, have been taken as control. The molecular docking and binding affinity estimation process was used to screen all the natural compounds, including the controls, to compare its results with the hit molecules. The selected compounds were further examined through pharmacokinetics analysis.

The RdRp protein with its hit-molecules and inhibitors was subjected to a more in-depth analysis to extract its bio-molecules' flexible nature, protein conformational changes, protein-ligand interactions, and structural perturbation, atomic detailing in context to time were thoroughly studied. These studies were carefully accomplished through an efficient and well-established computational method, namely MD simulation (Luthra et al., 2009; Mishra et al., 2018; Majewski et al., 2019; Wang et al., 2020). The further implication of MM-GBSA helped us to evaluate the various aspects of molecular interactions, such as the free binding energy estimation, effect of solvation, and thermodynamic integration (Wang et al., 2019; Kumar et al., 2020).

An extensive in-silico evaluation consisting of molecular docking, pharmacokinetics evaluation, MD simulation, and MM-GBSA were used to explore RdRp-hit molecules interactions' various aspects, leading to the selection of potential lead molecules for the development of promising RdRp inhibitors.

MATERIALS AND METHODS

Homology Modeling

The structure of the SARS-CoV-2 RdRp protein (PDB ID: 6m71.1 A) was downloaded from the swiss-model webserver (Waterhouse et al., 2018) in a PDB format, which was further validated using PROCHECK at the EBI server (Laskowski et al., 1993).

Energy Minimization and Model Validation

Energy minimization was performed to obtain a highly stable protein structure using the YASARA Energy minimization server (Krieger et al., 2009) and further validated using PROCHECK (Laskowski et al., 1993). Further ProSa were used to check the authenticity and the structural quality of the SARS-CoV-2 RdRp protein (Wiederstein and Sippl, 2007).

Binding Site Prediction

A literature survey was done to predict the protein's binding site (Gorbalenya et al., 2002; Venkataraman et al., 2018; Gao et al., 2020), cross-verified using the CASTp webserver. CASTp 3.0 provides dependable, inclusive, and global topological identifications and dimensions of protein designating residues' identification in the binding site pocket and its volume, cavities, and channels (Tian et al., 2018).

Ligand Selection and Ligand file Preparation

A library of 248 plant compounds was prepared, mainly consist of flavonoids, alkaloids, lactones and terpenes. Compounds were selected based on their antiviral activity against single-stranded RNA virus (Lin et al., 2014). Additionally, two nucleoside analogs, favipiravir, and remdesivir were taken as control. SMILES for the selected ligands were taken from the PubChem (https://pubchem.ncbi.nlm.nih.gov/) (**Supplementary Table S1**) and converted to pdbqt format using Open Babel software.

Molecular Docking

Molecular docking is the most critical part of computational drug designing, ensuring binding the ligand molecule to the selected protein's binding pocket in the right conformation. In the present study, PyRx virtual screening software was used in docking studies. PyRx uses autodock four and autodock vina as docking programs (Trott and Olson, 2010). A grid box was prepared to have a dimension of 120.6361 Å × 115.6029 Å × 116.6400 Å and 26.0286 Å × 44.5394 Å × 43.1279 Å in the *X*, *Y* and *Z* axis, respectively. The grid box covers almost all the active site residues. Compounds having the lowest binding energy were selected for further study. The docked protein-ligand structures were visualized in PyMol software (Lill and Danielson, 2011), and hydrogen bond interactions were studies using LigPlot (Wallace et al., 1995).

Drug Likeliness and Pharmacological Properties

The selected ligand molecules' drug likeliness properties were predicted based on the Lipinski rule (Lipinski, 2004) and Molsoft L.L.C.: Drug-Likeness (http://www.molsoft.com/mprop/) webserver. The pkCSM tool (http://biosig.unimelb.edu.au/pkcsm/prediction) was used to predict the ADMET properties of the selected ligands (Douglas et al., 2015).

Molecular Dynamics (MD) Simulation

All-atoms MD simulation was performed using Amber16, selecting ff14SB force field and TIP3P water molecules (Case et al., 2005; Maier et al., 2015) for the coordinates of RdRP and the docked complexes with drug molecules, Tellimagrandin I, SaikosaponinB2, Hesperidin, and (-)-Epigallocatechin Gallate. A GAFFs force field is used to parameterize all selected ligands (Wang et al., 2006). A cubic simulation box was prepared to keep the protein at the center with an edge distance of 10 Å, and the explicit TIP3P water molecules were padding around the protein (Jorgensen et al., 1983). The counter-ions ($Na + Cl^{-}$) were added to neutralize the simulation box. Particle Mesh Ewald (PME), a cut-off of 14 Å, was applied for the electrostatic interactions, and a cut-off of about 12 Å was used to manage the Vander Waals forces (Essmann et al., 1995). The SHAKE algorithm was applied to constrain H-bonds (Ryckaert et al., 1977). The prepared systems' energy minimization was performed in three stages, each of 10,000 steps of steepest descent (SD) and conjugate gradient (CG) to relax the system. Further, each simulation system was gradually heated from 50 to 300 K in six steps, followed by 10,000 steps of SD and CG minimization. Under the NVT ensemble condition, each system is equilibrated for 1 ns? Finally, all five systems were submitted for the production run under NPT ensemble condition for 100 ns with a time step of 2 fs?

MD Trajectory Analysis and MM-GBSA Assay

From the obtained MD trajectories, using the cpptraj tool available in Amber16, the structural order parameters (RMSD, R_g, RMSF, and SASA) were computed to analyze the structural stability of RdRP and binding complexes with drug molecules, Tellimagrandin I (-)-Epigallocatechin Gallate, SaikosaponinB2, and Hesperidin, respectively. The binding free energy of protein-ligand complexes was estimated utilizing the Molecular Mechanics/Generalized Born Surface Area (MM/GBSA) method, taking the structural ensembles from the last 20 ns trajectory (Wang et al., 2019; Kumar et al., 2021). The binding free energy components can be represented according to the equations:

$$\Delta G = G_{comp} - \left(G_{rec} + G_{lig}\right), \quad (1)$$

where ΔG represents the binding free energy of the receptor-ligand system, G_{comp} denotes the free energy of receptor complexed with ligand and, G_{rec} and G_{lig} define the individual free energy of receptor and ligand, respectively. The binding free energy of each of these was calculated using the MMPBSA. py script (Amber16). The bonded and non-bonded energy terms, electrostatic interactions, and van der Waals energies are defined by molecular mechanics energy (EMM). The polar solvation free energies (G_{SOL-GB}) and nonpolar solvation free energies (G_{SURF}) are calculated from the solvent-accessible surface area, and ($G_{SOL} = G_{SOL-GO} + G_{SCRF}$) using the generalized Born approach.

RESULTS

Homology Modeling, Energy Minimization and Model Validation

The degree of sequence similarity between the template and the query amino acid sequence dramatically determines the generated models' solidity (Azam et al., 2014). Here, the PDB ID- 6m71.1 A having a sequence similarity of 100%, was selected as a template. SWISS-MODEL web server computed a ligand and co-factor free model with an excellent GMQE (Global Model Quality Estimation) score of 0.86 and QMEAN Z-scores −1.52 (Waterhouse et al., 2018). The RdRp model structure was downloaded, and the Ramachandran plot was further used to validate the model via PROCHECK (Laskowski et al., 1993). The predicted model had 100% residues in favored, additionally allowed, and generously allowed regions (**Supplementary Figure S1**).

YASARA Energy minimization webserver was used to enhance the modeled structure's stereochemistry (**Supplementary Figure S2**). RdRp structure was further evaluated through ProSa. The z-score was −12.9 (**Supplementary Figure S3A),** and ProSa designated energy plots (**Supplementary Figure S3B**) showed an excellent structure.

Binding Site Prediction

Binding site residues or binding pockets were anticipated through a literature survey (Gorbalenya et al., 2002; Gao et al., 2020; Venkataraman et al., 2018) and a CASTp web server. The superimposed residues were considered as binding site residues **(Supplementary Figure S4A,S4B).** This structurally conserved RdRp core plays a vital role in viral RdRp enzymatic function and shows an excellent drug target (Shu

TABLE 1 | Binding energy values (kcal/mol) and interactions of the ligand with the key residue of RNA dependent DNA polymerase of SARS-CoV-2 evaluated by PyRx docking.

Ligand molecules	Binding energy (Kcal/mol)	Key residues interactions
Tellimagrandin I	−9.6	Asp617 Tyr618 Cys621 Asp622 Arg623
SaikosaponinB2	−8.9	Lys620 Arg623
Hesperidin	−8.6	Lys620 Asp622 Arg623
(-)-Epigallocatechin gallate	−8.1	Asp617 Asp622 Cys621
Remdesivir	−6.9	–
Favipiravir	−5.7	–

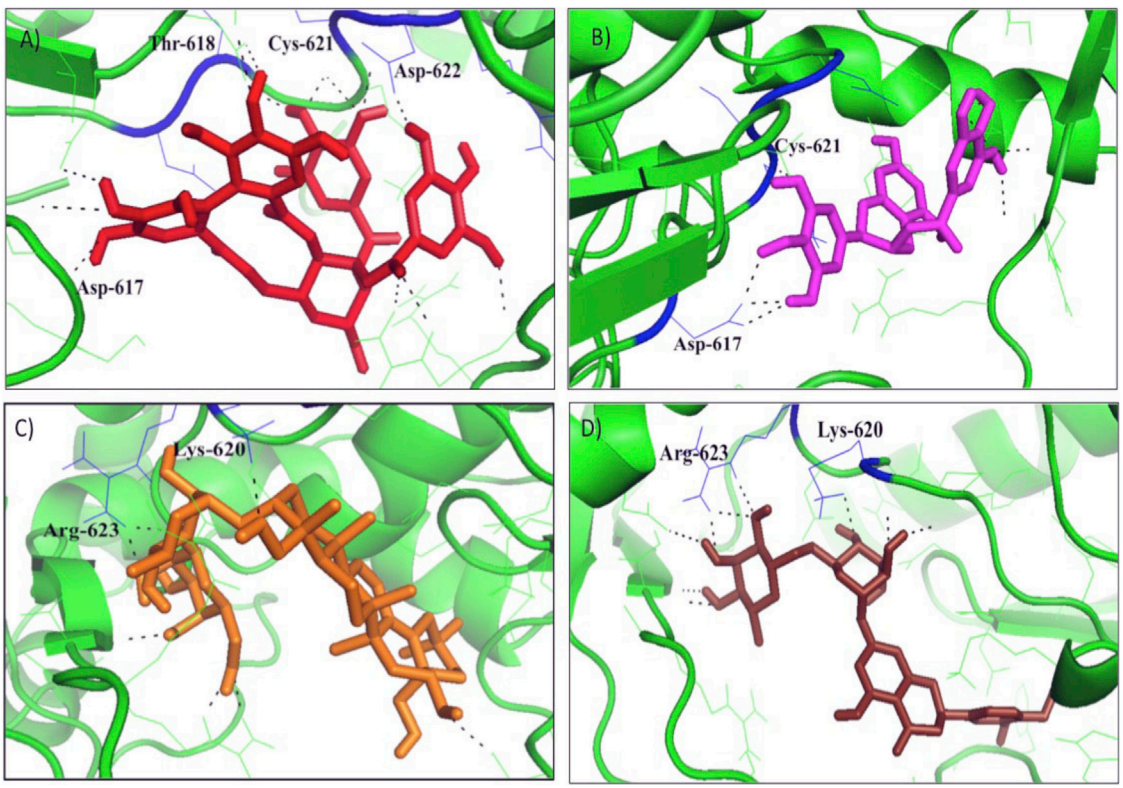

FIGURE 1 | The docking results of **(A)** Tellimagrandin I **(B)** (-)-Epigallocatechin Gallate **(C)** SaikosaponinB2, and **(D)** Hesperidin inside binding pocket of RNA dependent DNA polymerase (RdRp) of the SARS-CoV-2. Hydrogen bonded interactions are shown as black dotted lines.

and Gong, 2016). The palm region ranging from 582–628 amino acids, was considered a binding site for further studies (**Supplementary Figure S4A,S4B**).

Molecular Docking and Interaction Study

The Plant compounds, composed of 248 molecules, were docked against the SARS-CoV-2 RdRp protein using PyRx software. To some extent, all the molecules interacted with the binding site of the target protein. However, out of 248 molecules, four molecules, namely Tellimagrandin I, SaikosaponinB2, Hesperidin, and (-)-Epigallocatechin Gallate, showed the best docking score of −9.6 kcal/mol, −8.9 kcal/mol, −8.6 kcal/mol, and −8.1 kcal/mol, respectively (**Table 1**). Two nucleoside analogs, namely favipiravir, and remdesivir, were taken as a control and docked against the RdRp

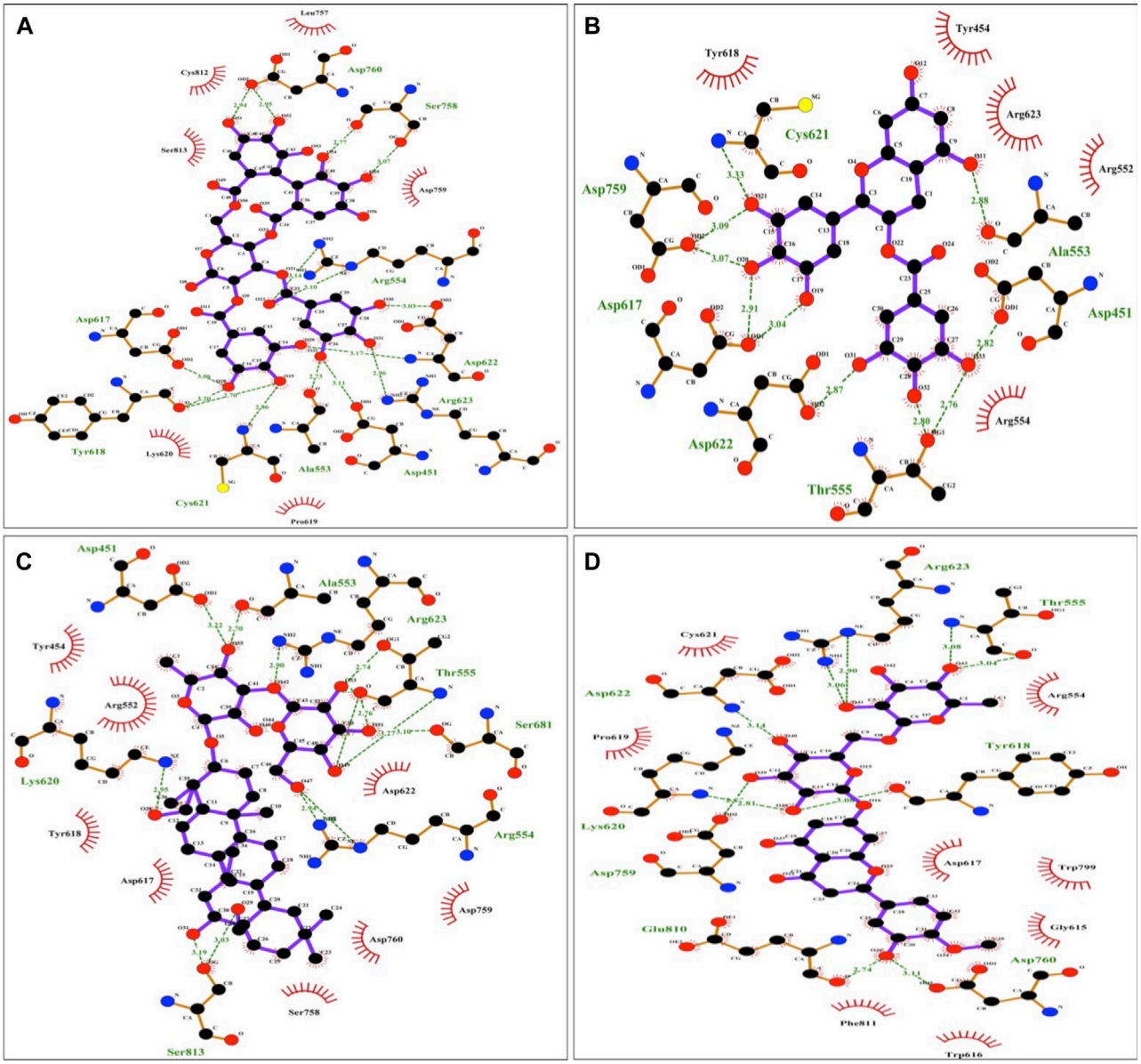

FIGURE 2 | Diagrammatic sketch illustrating the interactions between **(A)** Tellimagrandin I **(B)** (-)-Epigallocatechin Gallate **(C)** SaikosaponinB2 **(D)** Hesperidin and RNA dependent DNA polymerase of the SARS-CoV-2 by Ligplot. Ligand is shown in purple and: green dashed lines indicate hydrogen bonds with distance in angstrom (Å), spoked red arcs indicate hydrophobic contacts, atoms are shown in black for carbon, blue for nitrogen, red represents oxygen, green represents fluorine, and yellow represents sulfur.

protein with the same grid dimension used for the target protein and showed −5.7 and −6.9 kcal/mol docking score, respectively (**Table 1**).

The protein-ligand interaction was visualized using PyMol software, and the best positions were selected (**Figures 1A–D**). LigPlot analysis revealed the hydrogen bond interaction between the targeted protein and ligand molecules (**Figures 2A–D**). It was noticeable that our four selected molecules formed strong H-bond interaction commonly with the amino acid residues-ASP 617, ASP 618, LYS 620, ASP 622, and ARG 623 exhibiting a great affinity between them.

The docking and interaction pattern of the top four ligand molecules shows that they are capable of binding with the catalytic palm region of the protein, thus inhibiting the activity of RdRp and blocking the viral replication and transcription. This study unlocked the door for the proposed molecules for further pharmacokinetic analysis.

Pharmacokinetics Studies

Selected ligands were subjected to pharmacokinetics, including Lipinski rule 5, Drug likeness and ADMET analysis.

TABLE 2 | Absorption and distribution profile of the Tellimagrandin I, SaikosaponinB2, Hesperidin, and (-)-Epigallocatechin Gallate by pKCSM tool.

Compounds/ Ligands	Water solubility log mol/L	Caco2 permeability log 10^{-6} cm/s	Human intestinal absorption (%)	P-glycoprotein substrate	P-glycoprotein I inhibitor	P-glycoprotein II inhibitor	VDss (log L/kg)	Fraction unbound (human)
Tellimagrandin I	−2.892	−1.605	61.586	Yes	Yes	Yes	0.112	0.353
SaikosaponinB2	−2.482	0.237	25.425	Yes	Yes	No	−0.35	0.343
Hesperidin	−3.014	0.505	31.481	Yes	No	No	0.996	0.101
(-)-Epigallocatechin gallate	−2.894	−1.521	47.395	Yes	No	Yes	0.806	0.215

Result Obtained from the Lipinski rule of five are listed in **Supplementary Table S2** (-)-Epigallocatechin Gallate satisfied all the Lipinski rule parameters. Whereas other molecules violate the Lipinski rule, previous studies suggest that saikosaponinB2 and tellimagrandin I have been known to have inhibitory activity against coronavirus 229 E and HCV, respectively (Cheng et al., 2006; Tamura et al., 2010). Again, the Hesperidin has antiviral activity against rotavirus (Bae et al., 2000). While (-)-Epigallocatechin Gallate was found effective against SARS-CoV-2 (Singh et al., 2020). However, all four molecules show favorable drug-likeness properties (**Supplementary Table S2** and **Supplementary Figures S5A–D**).

pkCSM web tool was used to predict the ADMET properties of the selected molecules.

Absorption: Absorption is mainly calculated on account of water solubility, Caco2 permeability, human intestinal absorption, skin permeability, and whether the molecule is a P-glycoprotein substrate or inhibitor (Azam et al., 2014; Bhowmik et al., 2020; Sinha et al., 2020). The water solubility of the compound reflects at 25°C. All the selected molecules are moderately soluble in the water (**Table 2**). Caco2 permeability and human intestinal absorption determine the ultimate bioavailability; a drug having a value of more than 0.90 is considered readily permeable (Azam et al., 2014; Bhowmik et al., 2020; Sinha et al., 2020). All the ligands molecules show good permeability (**Table 2**).

The human intestine is the primary site where drugs usually get absorbed. Hydrophilic molecules are easily absorbed. A molecule with more than 30% absorbency is considered readily absorbed (Azam et al., 2014; Bhowmik et al., 2020; Sinha et al., 2020). Tellimagrandin I is found to be highly absorbed in the human intestine (**Table 2**). All the selected molecules are substrates for P-glycoprotein. Other than Hesperidin, all the molecules are either P-glycoprotein I or P-glycoprotein II inhibitors (**Table 2**). Thus, selected molecules could regulate P-glycoprotein's physiological function in the distribution of drugs.

Distribution: In the pKCSM tool, distribution is calculated in the following mentioned parameters - Human volume of distribution, human fraction unbound in plasma, blood-brain barrier, and central nervous system permeability. The volume of distribution is a theoretical volume that defines the drug's overall dose, which needs to assort identically across to give a similar blood plasma concentration. The higher the VDss value, the more of a drug is distributed in tissue rather than plasma. More extensive tissue distribution is desirable for antibiotics and antivirals (Bhowmik et al., 2020; Sinha et al., 2020). VDss is considered low if the log VDss value is lower than −0.15, while the value higher than 0.45 is considered high (Bhowmik et al., 2020; Sinha et al., 2020). Among all the molecules**, hesperidin** shows the highest value, followed by **(-)Epigallocatechin Gallate, Tellimagrandin I, and SaikosaponinB2,** respectively (**Table 2**). Most plasma drugs will occur in symmetry in between unbound or bound states concerning serum proteins. The drug's effectiveness may be stirred by a limit to which it binds to the blood's proteins; as more can bind, it can transverse cellular membrane (Bhowmik et al., 2020; Sinha et al., 2020). Fraction unbound to human plasma should lie between 0.02 and 1.0 (Sinha et al., 2020). All the compounds show a good value (**Table 2**).

Metabolism: Metabolism of a drug depends upon the molecule to be a Cytochrome P450 substrate or inhibitor. All the selected molecules are **non-inhibitor** of any cytochrome enzyme, which indicates that they will be metabolized by the enzyme's action, suggesting that they will not be hampered through the body's biological transformation (**Supplementary Table S3**).

Excretion: Excretion is calculated with total clearance and whether the molecule is a renal OCT2 substrate. Organic cation transporter 2 (OCT2) is a renal uptake transporter that deposits and clears drugs from the kidney (Sinha et al., 2020). Only **Tellimagrandin I** acts as a substrate for Renal OCT2, while other drugs are removed via a different route. All the selected molecules show total clearance less than log(CLtot) 1 ml/min/kg (**Table 3**).

Toxicity: The AMES test showing a negative value indicates that it is non-mutagenic and non-carcinogenic. None of the selected ligand molecules shows positive AMES results (**Table 3**). The Maximum recommended tolerance dose (MRTD) provides an estimate of the toxic dose in humans. MRTD less than or equal to log 0.477 (mg/kg/day) is considered low (Sinha et al., 2020). All the compounds have low toxicity to humans (**Table 3**). **hERG** (human ether-a-go-go gene) is responsible for blocking potassium channels (Sinha et al., 2020). All the selected ligands are non-inhibitor of **hERG** and do not induce hepatotoxicity and non-skin sensitive (**Table 3**).

A molecule with a high oral rat acute toxicity (LD50) value is less lethal than the lower LD50 value (Bhowmik et al., 2020; Sinha et al., 2020). For a given compound, the LD50 is the amount that causes the death of 50% of the test animals (Bhowmik et al., 2020; Sinha et al., 2020). All the selected ligands showed high oral rat acute toxicity (LD50) value (**Table 3**). The lethal concentration

TABLE 3 | Excretion and toxicity profile of the Tellimagrandin I, SaikosaponinB2, Hesperidin, and (-)-Epigallocatechin Gallate by pKCSM tool.

Compounds	Total clearance log ml/min/kg	Renal OCT2 substrate	AMES toxicity	Max. Tolerated dose (human)	Oral rat acute toxicity (LD50)	hERG inhibitor	Hepatotoxicity	Skin sensitization	Minnow toxicity
Tellimagrandin I	0.177	Yes	No	0.438	2.482	No	No	No	13.101
SaikosaponinB2	0.223	No	No	−2.178	2.959	No	No	No	1.934
Hesperidin	0.211	No	No	0.525	2.506	No	No	No	7.131
(-)-Epigallocatechin gallate	0.292	No	No	0.441	2.522	No	No	No	7.713

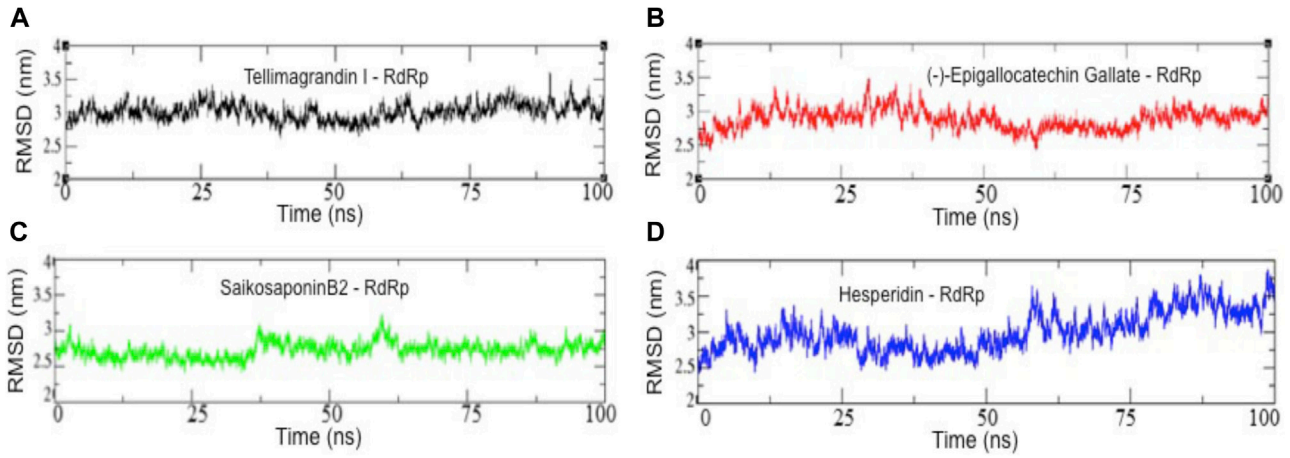

FIGURE 3 | Backbone root mean square deviation (C^{α}-RMSD) results of all four complexes. RMSD values of RdRp-Tellimagrandin I **(A)**, RdRp-(-)-Epigallocatechin Gallate **(B)**, RdRp-SaikosaponinB2 **(C)**, and RdRp-Hesperidin **(D)**. Molecular dynamic simulations were conducted for 100 ns?

values (LC50) represent a molecule's concentration necessary to cause 50% of Fathead Minnows' death. For a given compound, if the log LC50 < 0.5 mM (log LC50 < −0.3), then it is regarded as high acute toxic (Bhowmik et al., 2020; Sinha et al., 2020), all the compounds shows good score indicating that they are less toxic (**Table 3**).

MD Simulation

To determine RdRp docked complexes' conformation stability with drug molecules, Tellimagrandin I, SaikosaponinB2, Hesperidin, and (-)-Epigallocatechin Gallate, we computed the backbone root mean square deviation (C^{α}-RMSD), as shown in **Figure 3**. The result shows that the RMSD trajectory of RdRp-Tellimagrandin I quickly attains equilibrium during 0–5 ns and remains steady with RMSD value 3.0 ± 0.2 Å at the end of simulation at 100 ns (**Figure 3A**). Similarly, the RMSD plot of the RdRp-SaikosaponinB2 complex shows a relatively stable structure during ~0–37 ns with RMSD ~2.57 Å. With slight drift, RMSD increase to ~3.0 Å at ~37 ns, which settles at ~65 ns, and a stable equilibrium is continued for the remaining period of simulation (**Figure 3C**). However, RdRp-(-)-Epigallocatechin Gallate's plot shows a gradual increase in RMSD during ~0–35 ns, which slowly attains equilibrium at ~50 ns and remains consistent around RMSD value ~3.0 Å till 100 ns (**Figure 3B**). The conformational dynamics of RdRp-Hesperidin also shows an initial increase in RMSD up to ~25 ns? The structure remains stable with RMSD ~2.80 Å at ~25–60 ns. Further increase in RMSD can be noticed due to several small drifts that settle at ~85 ns, and the simulation ends with an increase in RMSD ~3.50 Å (**Figure 3D**).

To examine the structural compactness and integrity of RdRp-drug bound complexes, the radius of gyration (R_g) is calculated for each system (Nygaard et al., 2017; Prakash et al., 2018a). **Figure 4** shows that the structure of RdRp-Tellimagrandin I is stabilized around R_g value 31.25 Å, and we can see only the minor perturbations with small drifts of ~0.20 Å at 0–25 ns, but it remains stable for the remaining period of simulation (**Figure 4A**). The R_g plot of RdRp-SaikosaponinB2 shows a slight drop down in trajectory during 0–25; after that, a drift of ~0.70 Å can be seen at ~25–30 ns, which settles gradually at ~60 ns, and the structure remains stable for the period of 100 ns (**Figure 4C**). Whereas the conformational dynamics of RdRp-(-)-Epigallocatechin Gallate and RdRp-Hesperidin shows less perturbed structure throughout the simulation period with R_g value 31.25 Å (**Figures 4B,D** respectively).

We also analyzed the root mean square fluctuation (RMSF) plots of all four complexes (**Figure 5**). The residues belonging to stable secondary conformations (α-helix and β-sheet) show a

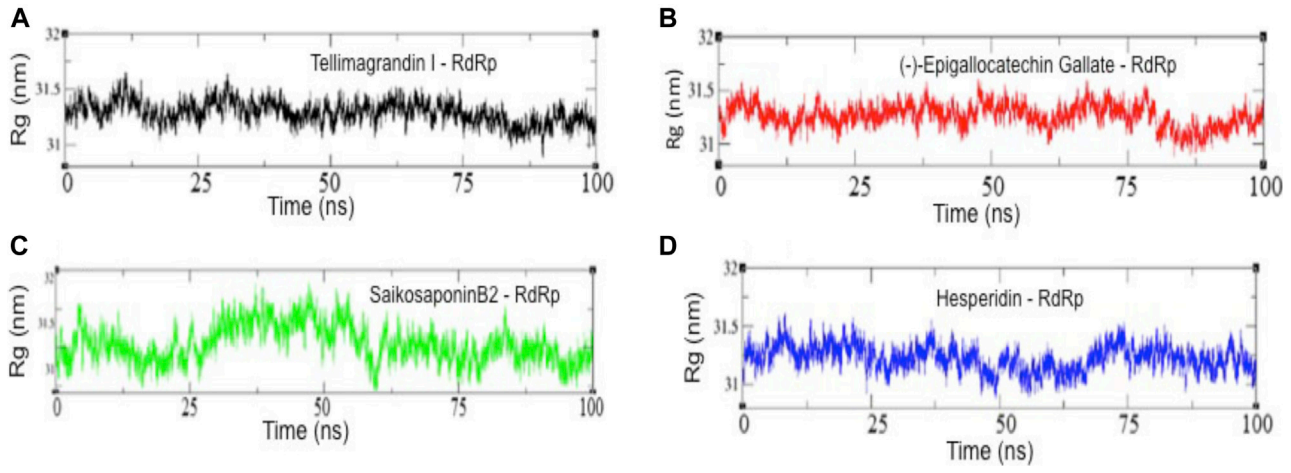

FIGURE 4 | The radius of gyration (R_g) results of all four complexes. Rg values of RdRp-Tellimagrandin I **(A)**, RdRp-(-)-Epigallocatechin Gallate **(B)**, RdRp-SaikosaponinB2 **(C)**, and RdRp-Hesperidin **(D)**. Molecular dynamic simulations were conducted for 100 ns?

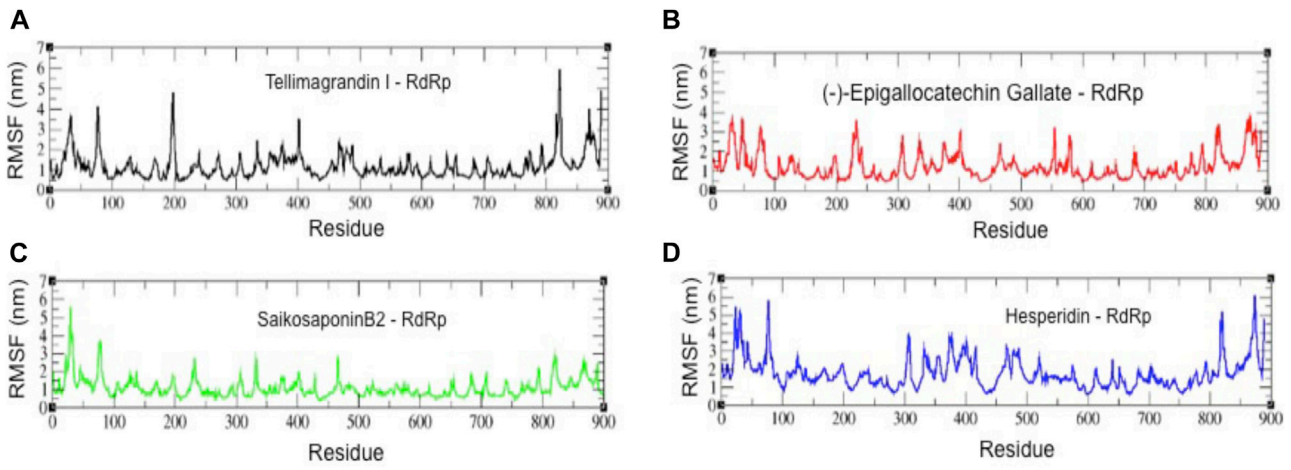

FIGURE 5 | The root mean square fluctuation (RMSF) plots of all four complexes. RMSF plots of RdRp-Tellimagrandin I **(A)**, RdRp-(-)-Epigallocatechin Gallate **(B)**, RdRp-SaikosaponinB2 **(C)**, and RdRp-Hesperidin **(D)**. Molecular dynamic simulations were conducted for 100 ns?

lower degree of residual fluctuations, whereas the residues belonging to the terminal (N-and C-terminal) and loop regions have a high degree of fluctuations. The RMSF plots of RdRp-Tellimagrandin I, RdRp-(-)-Epigallocatechin Gallate, and RdRp-SaikosaponinB2 represent typical pattern profiles that the amino acid residues belonging to termini (N-and C-terminal) and loops have average atomic fluctuation >1.5 Å (**Figures 5A–C** respectively). In contrast, the conformational dynamics of stable secondary structure, α-helices, and β-sheets remain stable during the simulation, providing elegance evidence of the stable molecular interactions with ligands. However, the plot of RdRp-Hesperidin shows that along with the regions belonging to loops, the residues 300–400 also having comparatively higher average fluctuations >2.0 Å (**Figure 5D**). This result indicates the loosely bounded conformation of Hesperidin with RdRp.

We also examine the solvent-accessible surface area (SASA) of RdRp-inhibitor complexes, which provides the conformational concerning solvent around the protein (**Figure 6**). Results show a slight change or rather no change in the conformational dynamics of RdRp-Tellimagrandin I, RdRp-(-)-Epigallocatechin Gallate, and RdRp-SaikosaponinB2, which are converged around SASA values ~150 $Å^2$, respectively (**Figures 6A–C** respectively). However, the plot of RdRp-Hesperidin shows an increase in SASA value ~80 $Å^2$ during 0–5 ns, but it remains consistent up to 55 ns with the average fluctuation of ~25–30 $Å^2$ (Figure). However, the sharp drift of ~50 $Å^2$ can be seen at ~60 ns, which gradually dropped at ~75 ns, and the structure remains stable for ~75–100 ns (**Figure 6D**).

Thus, the combined results of structural order parameters highlighted the more stable structural dynamics of RdRp

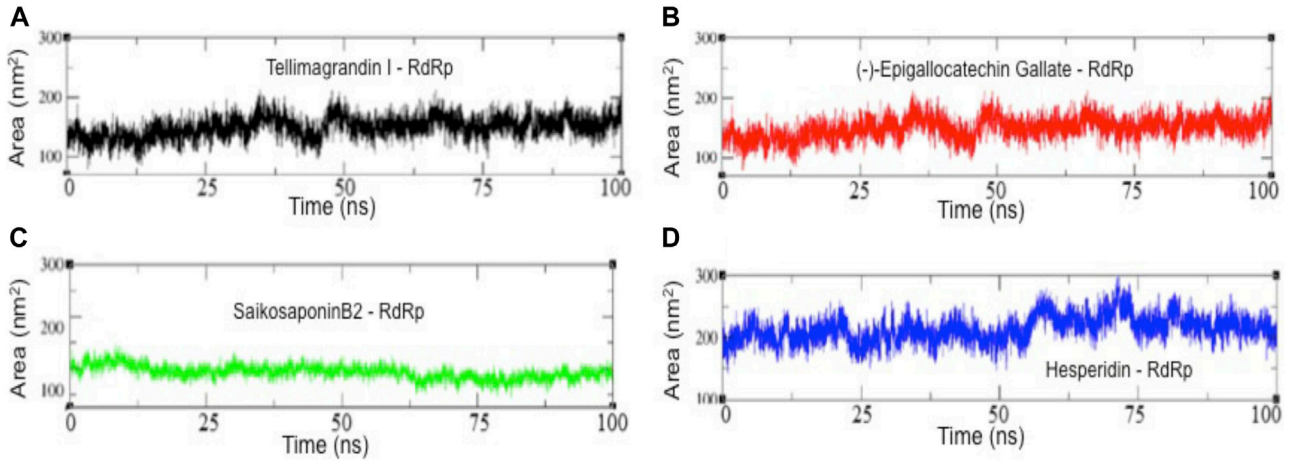

FIGURE 6 | The solvent-accessible surface area (SASA) results of all four complexes. SASA plots of RdRp-Tellimagrandin I **(A)**, RdRp-(-)-Epigallocatechin Gallate **(B)**, RdRp-SaikosaponinB2 **(C)**, and RdRp-Hesperidin **(D)**. Molecular dynamic simulations were conducted for 100 ns?

TABLE 4 | Binding free energy (kcal/mol) approximation of drug molecules (Tellimagrandin I, SaikosaponinB2, Hesperidin, and (-)-Epigallocatechin Gallate) against RNA dependent RNA polymerase (RdRp).

Compounds	$\Delta G_{binding}$	ΔE_{vdW}	$\Delta E_{electrostatic}$	ΔE_{GB}	ΔE_{SURF}	ΔG_{gas}	ΔG_{solv}
Tellimagrandin I	−32.43 ± 3.06	−48.45 ± 2.65	−12.64 ± 4.14	34.41 ± 3.94	−5.75 ± 0.19	−61.10 ± 4.88	28.66 ± 3.93
SaikosaponinB2	−42.43 ± 3.25	−64.57 ± 2.33	−26.24 ± 3.16	56.38 ± 6.15	−7.99 ± 0.23	−90.81 ± 7.52	48.38 ± 6.11
Hesperidin	−22.72 ± 3.64	−37.35 ± 2.64	−24.56 ± 5.70	44.06 ± 5.04	−4.87 ± 0.29	−61.91 ± 6.26	39.19 ± 4.96
(-)-Epigallocatechin gallate	−24.17 ± 2.73	−39.95 ± 2.18	−4.96 ± 0.23	25.97 ± 5.95	−5.23 ± 0.36	−44.91 ± 6.76	20.73 ± 3.80

complexed with Tellimagrandin I, SaikosaponinB2, and (-)-Epigallocatechin Gallate as compared to Hesperidin.

MM-GBSA Assay

Finally, to evaluate the molecular binding of drug molecules with RdRp, the quantitative assessment of binding free energy ($\Delta G_{binding}$) was carried out using MM-GBSA (Genheden and Ryde, 2015; Wang et al., 2019) on the conformational ensemble of protein-ligand complexes. Considering the convergence of MM/GBSA free energy estimates, only the last 20 ns of data were used for the analysis (Genheden and Ryde, 2015; Wang et al., 2019; Kumar et al., 2021). Results revealed that the binding affinities ($\Delta G_{binding}$) of the selected drug molecules against RdRp range from −42.43 to −22.72 kcal/mol (**Table 4**). The non-bonded terms van der Waals energies (ΔE_{vdW}) are relatively more negative than the others from −64.57 to −37.35 kcal/mol, indicating that all four compounds have good hydrophobic contacts at the active site of RdRp (**Table 4**). However, the bonded terms electrostatic interactions ($\Delta E_{electrostatic}$) ranges between −26.24 to −4.96 kcal/mol, which shows less contribution energy component, electrostatic in the relative stabilities of ligands (**Table 4**). Furthermore, the polar solvation energies (ΔE_{GB}) act against the complexation, neutralized by bonded and non-bonded interactions. We noticed the higher contribution of $\Delta E_{electrostatic}$ = −26.24 kcal/mol and lower $\Delta E_{electrostatic}$ = −4.96 kcal/mol for drug molecules, SaikosaponinB2 and (-)-Epigallocatechin Gallate, respectively (**Table 4**). However, the higher contribution of ΔE_{vdW} = −39.95 kcal/mol results in the more favorable binding of (-)-Epigallocatechin Gallate, as compared to Hesperidin (ΔE_{vdW} = −37.35) (**Table 4**). Among the four compounds, SaikosaponinB2 shows the best binding affinity ($\Delta G_{binding}$ = −42.43 kcal/mol) for RdRp, whereas the least activity is noticed for the drug molecule, Hesperidin (−22.72 kcal/mol) (**Table 4**).

DISCUSSIONS

In this present study, RNA dependent RNA polymerase was taken as a drug target as this protein is essential for viral replication and transcription of SARS-CoV-2. The conserved RdRp catalytic motifs (A–E), the palm regions were taken as active sites. Plant products, mainly flavonoids, alkaloids, lactones, and terpenes, were considered during the investigation as inhibitors against the target protein. It has been earlier noted that natural products have traditionally provided the pharmaceutical industries with many vital leads to discover new drugs. Many compounds were isolated from a plant having an anti-viral activity (Lin et al., 1999; Cheng et al., 2004; Chang et al., 2005).

In this study, 248 natural compounds as ligands were selected. Four ligands possess an excellent binding affinity toward the target protein's active site depicting the lowest binding energy

(**Table 1**), demonstrating their potentiality as inhibitors for SARS-CoV-2. The compound Tellimagrandin I depicted the best docking score of -9.6 kcal/mol (**Table 1**). The Druglike properties of the selected ligands were evaluated based on Lipinski parameters. Other than (-)-Epigallocatechin Gallate, all molecules violate the Lipinski rule as they have higher molecular weight. As a rule, it does not predict if a compound is pharmacologically active, and the already established antiviral activity in the previous study cannot be overlooked (Lin et al., 2014). Generally, a molecule showing a negative drug score is not considered a promising drug candidate; all four selected molecules show a favorable/positive drug score (**Supplementary Table S2** and **Supplementary Figures S5A–S5D**); additionally, SaikosaponinB2 possess antiviral activity against HCOV-229 E (Cheng et al., 2006) and possesses a high activity with an IC50 value of 1.7 μmol/L (Cheng et al., 2006). Therefore, SaikosaponinB2 can be considered a potent inhibitor against COVID-19.

In the present study, hesperidin showed good drug scores, as shown in **Supplementary Table S2** and **Supplementary Figure S5D**. This compound changes the immune system response by regulating interferons during influenza A virus infection and shows antiviral activity against influenza A virus (Randall and Goodbourn, 2008). This compound also exhibits antioxidant, anti-inflammatory, and lipid-lowering properties (Li and Schluesener, 2017) (-)-Epigallocatechin Gallate is one of the selected molecules favoring all the Lipinski rules with a good drug score (**Supplementary Table S2** and **Supplementary Figure S5B**) (-)-Epigallocatechin Gallate had antiviral activity against the Hepatitis C virus with IC50 value 5 μg/L (Calland et al., 2012), Enterovirus 71 (Ho et al., 2009), and Zika virus (Carneiro et al., 2016). This polyphenol has antioxidant properties. Tellimagrandin I obtained from *Rosea rugosa* showed the highest binding affinity toward the target protein and possessed an excellent drug score (**Supplementary Table S2** and **Supplementary Figure S5A**). Tellimagrandin I compound is also reported to have antiviral activity against the Hepatitis C virus (Tamura et al., 2010). Hence, Hesperidin (-)-Epigallocatechin Gallate, and Tellimagrandin I can also be considered potential drug candidates against SARS-CoV-2 RdRp protein.

In comparison, the two nucleoside analogs-favipiravir and remdesivir currently being evaluated in clinical trials for the treatment of COVID-19 scored lower −5.7 and −6.9 kcal/mol respectively against the RdRp (**Table 1**), thus enunciating the possibility of our proposed molecules to be a potent inhibitor against the SARS-CoV-19 RdRp protein.

The ligand-binding directly induced the structural changes needed to be accounted for the proteins to compute their binding free energies reliably, so we have followed this procedure.

A drug molecule's efficacy depends on the spatial binding at the target protein's active site and the protein-ligand complex's structural stability (Luthra et al., 2009; Mishra et al., 2018; Majewski et al., 2019; Wang et al., 2020). Structure-based virtual screening is a reliable strategy to identify a potential inhibitor in the drug development process (Meng et al., 2011; Agrawal et al., 2019). The molecular docking using AutoDock allows our compounds to interact with our query protein in a single rigid conformation upon which score based ranking is determined. (Forli et al., 2016; Sulimov et al., 2019). Thus, to understand the protein-ligand molecular interactions, MD simulation can provide a comprehensive insight into protein-ligand interactions' structural stability and dynamic (Luthra et al., 2009; Prakash and Luthra, 2012; Wang et al., 2013; Panda et al., 2020). Thus, to determine the conformational dynamics and stability of protein-ligand complexes, MD simulations were carried out for 100 ns at the 300 K.

The structural order parameters evaluate the molecular stability of protein-ligand complexes. **Figures 3A–D** suggests that out of four complexes, the structure of RdRp-Tellimagrandin I and RdRp-(-)-Epigallocatechin Gallate quickly attain a stable equilibrium, and the RMSD trajectory observed consistent till the simulation ends at 100 ns? RMSD plot of RdRp-SaikosaponinB2 observed equilibrated around ~2.7 Å, but the small drifts at ~37 ns and ~65 ns suggested the structural adjustment to accommodate the ligand at the active site protein, respectively (**Figures 3A–C** respectively). However, the structure of RdRp-Hesperidin shows a continuous rise in RMSD during the initial ~0–25 ns and remains stable for ~25–65 ns? A further slight increase in RMSD of ~0.7 Å indicates relatively less stable conformational dynamics of complex structure with Hesperidin (**Figure 3D**).

Further, the structural compactness of RdRp-drug complexes determines by R_g analyses suggest the stable molecular interaction with all four compounds, which are stabilized in between the range of 31.25–33.50 Å (**Figures 4A–D**). However, the drifts of 0.20–0.40 Å can be seen during the initial stages of simulation in the R_g trajectory of Tellimagrandin I and SaikosaponinB2, which indicated the structural perturbation to accommodate the ligands. The average atomic fluctuations measured through RMSF plots suggest that all four RdRp-drug complexes show similar spatial binding patterns, which indicates that all four compounds remain well accommodated at the binding pocket of RdRp with favorable molecular interactions (**Figures 5A–D**). The hydrophobic interactions play a crucial role in determining the protein conformational dynamics, which ensure the structural stability of molecular interactions (Prakash et al., 2018b; Banerjee and Bagchi, 2020). Thus, we also investigated the SASA plots of all four complexes, suggesting no considerable changes in the conformational dynamics of Tellimagrandin I (-)-Epigallocatechin Gallate, and SaikosaponinB2 stabilized around SASA values 150 $Å^2$, respectively (**Figures 6A–C** respectively). Whereas large deviation in SASA value approximately ~50–80 $Å^2$ reveals a relatively less stable structure of RdRp- Hesperidin complex (**Figure 6D**).

We further applied MM/GBSA free energy calculations to assess the thermodynamics stability of the RdRp complexed with drug molecules in terms of the binding free energy (Wang et al., 2019; Kumar et al., 2020). The MM/GBSA free energy calculation summarized in **Table 4** provided clear evidence that the drug molecules were spatially stable at the active site of RdRp by van der Waals (ΔE_{vdW}) and electrostatic interactions ($\Delta E_{electrostatic}$). Although the energy components, ΔE_{GB}, act against the

complexation, Van der Waals and electrostatic interactions mostly neutralize it. We can observe the more favorable molecular action of SaikosaponinB2 ($\Delta G_{binding}$ = −42.43 kcal/mol), suggesting it as a potential candidate against RdRp in therapy against COVID-19 (**Table 4**).

CONCLUSION

The present study explored the ligands' impacts, namely, Tellimagrandin I, SaikosaponinB2, Hesperidin (-)-Epigallocatechin Gallate's molecular interactions and analyzed them as prospective drug candidates against the SARS-COV-2 RdRp protein. The screened molecules showed excellent docking scores, excellent pharmacokinetic profiles, MD simulation, and MM/GBSA profile. Moreover, these molecules cohere affirmatively with the predetermined amino acid residues present in the core palm region of the RdRp protein, thus inhibiting the viral gene replication and transcription. The ADMET results revealed excellent bioavailability and enzymatic inhibitory effect. Though the proposed molecules already have good IC50 values against different viruses, a further experimental analysis must be carried ahead to inspect its efficacy against the SARS-CoV-2. The binding free energy estimation using MM/PBSA assays revealed that selected-inhibitors: SaikosaponinB2, Tellimagrandin I, and (-)-Epigallocatechin Gallate possess better binding free energy and molecular affinity as compared to Hesperidin. Therefore, we proposed that selected molecules might be used as lead molecules in COVID-19 therapy.

The pharmacological profiling, docking analysis, MD simulation, MD trajectory, and MM/GBSA studies evaluated Saikosaponin B2 as a potent prospective drug candidate against the SARS-CoV-2 RdRp proteins that might inhibit duplication of COVID-19 virus, resulting in mitigating the disastrous global effects of the COVID-19 pandemic.

DATA AVAILABILITY STATEMENT

The original contributions presented in the study are included in the article/**Supplementary Material**, further inquiries can be directed to the corresponding author.

AUTHOR CONTRIBUTIONS

SS, RN, PV, AP, and DK carried out the experiment, wrote the manuscript, and contributed to the analysis of the results. DK supervised the project and conceived the original idea.

FUNDING

The lab is supported by the Science and Engineering Research Board, India (FILE NO. ECR/2015//000155) and the Department of Biotechnology (India) (order no: BT/PR16224/NER/95/176/2015 and BT/PR24504/NER/95/746/2017) to Diwakar Kumar. Satabdi Saha recognizes the financial support from the Inspire Fellowship (IF180806). Rajat Nandi received funding from the DBT grant (order no: BT/PR24504/NER/95/746/2017).

SUPPLEMENTARY MATERIAL

The Supplementary Material for this article can be found online at: https://www.frontiersin.org/articles/10.3389/fphar.2021.634047/full#supplementary-material.

REFERENCES

Agrawal, P., Singh, H., Srivastava, H. K., Singh, S., Kishore, G., and Raghava, G. P. S. (2019). Benchmarking of different molecular docking methods for protein-peptide docking. *BMC Bioinformatics*. 19, 426. doi:10.1186/s12859-018-2449-y

Azam, S. S., Sarfaraz, S., and Abro, A. (2014). Comparative modeling and virtual screening for the identification of novel inhibitors for myo-inositol-1-phosphate synthase. *Mol. Biol. Rep*. 41 (8), 5039–5052. doi:10.1007/s11033-014-3370-8

Bae, E. A., Han, M. J., Lee, M., and Kim, D. H. (2000). *In Vitro* inhibitory effect of some flavonoids on rotavirus infectivity. *Biol Pharm. Bull*. 23 (9), 1122–1124. doi:10.1248/bpb.23.1122

Banerjee, P., and Bagchi, B. (2020). Dynamical control by water at a molecular level in protein dimer association and dissociation. *Proc. Natl. Acad. Sci*. 117 (5), 2302–2308. doi:10.1073/pnas.1908379117

Bhowmik, D., Nandi, R., Jagadeesan, R., Kumar, N., Prakash, A., and Kumar, D. (2020). Identification of potential inhibitors against SARS-CoV-2 by targeting proteins responsible for envelope formation and virion assembly using docking based virtual screening, and pharmacokinetics approaches. *Infect. Genet. Evol*. 84, 104451. doi:10.1016/j.meegid.2020.104451

Calland, N., Albecka, A., Belouzard, S., Wychowski, C., Duverlie, G., Descamps, V., et al. (2012). (-)-Epigallocatechin-3-gallate is a new inhibitor of hepatitis C virus entry. *Hepatology*. 55 (3), 720–729. doi:10.1002/hep.24803

Carneiro, B. M., Batista, M. N., Braga, A. C. S., Nogueira, M. L., and Rahal, P. (2016). The green tea molecule EGCG inhibits Zika virus entry. *Virology*. 496, 215–218. doi:10.1016/j.virol.2016.06.012

Case, D. A., Cheatham, T. E., Darden, T., Gohlke, H., Luo, R., Merz, K. M., et al. (2005). The Amber biomolecular simulation programs. *J. Comput. Chem*. 26 (16), 1668–1688. doi:10.1002/jcc.20290

Chang, J. S., Liu, H. W., Wang, K. C., Chen, M. C., Chiang, L. C., Hua, Y. C., et al. (2005). Ethanol extract of Polygonum cuspidatum inhibits hepatitis B virus in a stable HBV-producing cell line inhibits hepatitis B virus in a stable HBV-producing cell line. *Antivir. Res*. 66 (1), 29–34. doi:10.1016/j.antiviral.2004.12.006

Cheng, H. Y., Lin, T. C., Yang, C. M., Wang, K. C., Lin, L. T., and Lin, C. C. (2004). Putranjivain A from *Euphorbia* jolkini inhibits both virus entry and late stage replication of herpes simplex virus type 2 *in vitro* inhibits both virus entry and late stage replication of herpes simplex virus type 2. *J. Antimicrob. Chemother*. 53 (4), 577–583. doi:10.1093/jac/dkh136

Cheng, P. W., Ng, L. T., Chiang, L. C., and Lin, C. C. (2006). Antiviral effects of saikosaponins on human coronavirus 229E *in vitro*. *Clin. Exp. Pharmacol. Physiol*. 33 (7), 612–616. doi:10.1111/j.1440-1681.2006.04415.x

Doublié, S., and Ellenberger, T. (1998). The mechanism of action of T7 DNA polymerase. *Curr. Opin. Struct. Biol*. 8 (6), 704–712. doi:10.1016/s0959-440x(98)80089-4

Douglas, E. V., Blundell, T. L., and David, B. A. (2015). pkCSM: predicting small-molecule pharmacokinetic and toxicity properties using graph-based signature. *J. Med. Chem*. 58 (9), 4066–4072. doi:10.1021/acs.jmedchem.5b00104

Elfiky, A. A., and Ismail, A. M. (2018). Molecular docking revealed the binding of nucleotide/side inhibitors to Zika viral polymerase solved structures. *SAR QSAR Environ. Res*. 29 (5), 409–418. doi:10.1080/1062936X/2018.1454981

Elfiky, A. A., and Azzam, E. B. (2020). Novel Guanosine Derivatives against MERS CoV polymerase: an in silico perspective. *J. Biomol. Struct. Dyn*., 1–12. doi:10.1080/07391102/2020.1758789

Essmann, U., Perera, L., Berkowitz, M. L., Darden, T., Lee, H., and Pedersen, L. G. (1995). A smooth particle mesh Ewald method. *J. Chem. Phys*. 103, 8577–8593 doi:10.1063/1.470117

Forli, S., Huey, R., Pique, M. E., Sanner, M. F., Goodsell, D. S., and Olson, A. J. (2016). Computational protein-ligand docking and virtual drug screening with the AutoDock suite. *Nat. Protoc*. 11 (5), 905–919. doi:10.1038/nprot.2016.051

Gao, Y., Yan, L., Huang, Y., Liu, F., Zhao, Y., Cao, L., et al. (2020). Structure of the RNA-dependent RNA polymerase from COVID-19 virus. *Science*. 368 (6492), 779–782. doi:10.1126/science.abb7498

Genheden, S., and Ryde, U. (2015). The MM/PBSA and MM/GBSA methods to estimate ligand-binding affinities. *Expert Opin. Drug Discov*. 10 (5), 449–461. doi:10.1517/17460441.2015.1032936

Gorbalenya, A. E., Pringle, F. M., Zeddam, J. L., Luke, B. T., Cameron, C. E., Kalmakoff, J., et al. (2002). The palm subdomain-based active site is internally permuted in viral RNA-dependent RNA polymerases of an ancient lineage. *J. Mol. Biol*. 324 (1), 47–62. doi:10.1016/s0022-2836(02)01033-1

Ho, H. Y., Cheng, M. L., Weng, S. F., Leu, Y. L., and Chiu, D. T. (2009). Antiviral effect of epigallocatechin gallate on enterovirus 71. *J. Agric. Food Chem*. 57 (14), 6140–6147. doi:10.1021/jf901128u

Ibrahim, I. M., Abdelmalek, D. H., Elshahat, M. E., and Elfiky, A. A. (2020). COVID-19 Spike-host cell receptor GRP78 binding site prediction. *J. Infect*. 80 (5), 554–562. doi:10.1016/j.jinf.2020.02.026

Jorgensen, W. L., Chandrasekhar, J., Madura, J. D., Impey, R. W., and Klein, M. L. (1983). Comparison of simple potential functions for simulating liquid water. *J. Chem. Phys*. 79, 926–935. doi:10.1063/1.445869

Krieger, E., Joo, K., Lee, J., Lee, J., Raman, S., Thompson, J., et al. (2009). Improving physical realism, stereochemistry, and side-chain accuracy in homology modeling: four approaches that performed well in CASP8. *Proteins*. 77 (Suppl. 9), 114–122. doi:10.1002/prot.22570

Kumar, N., Srivastava, R., Prakash, A., and Lynn, A. M. (2020). Structure-based virtual screening, molecular dynamics simulation and MM-PBSA toward identifying the inhibitors for two-component regulatory system protein NarL of *Mycobacterium Tuberculosis*. *J. Biomol. Struct. Dyn*. 38, 3396–3410. doi:10.1080/07391102.2019.1657499

Laskowski, R. A., MacArthur, M. W., Moss, D. S., and Thornton, J. M. (1993). PROCHECK: a program to check the stereo chemical quality of protein structures. *J. Appl. Crystallogr*. 26 (2), 283–291. doi:10.1107/S0021889892009944

Li, C., and Schluesener, H. (2017). Health-promoting effects of the citrus flavanone hesperidin. *Crit. Rev. Food Sci. Nutr*. 57 (3), 613–631. doi:10.1080/10408398.2014.906382

Lill, M. A., and Danielson, M. L. (2011). Computer-aided drug design platform using PyMOL. *J. Comput. Aided Mol. Des*. 25 (1), 13–19. doi:10.1007/s10822-010-9395-8

Lin, L. T., Hsu, W. C., and Lin, C. C. (2014). Antiviral natural products and herbal medicines. *J. Tradit Complement. Med*. 4 (1), 24–35. doi:10.4103/2225-4110.124335

Lin, Y. M., Flavin, M. T., Schure, R., Chen, F. C., Sidwell, R., Barnard, D. L., et al. (1999). Antiviral activities of biflavonoids. *Planta Med*. 65 (2), 120–125. doi:10.1055/s-1999-13971

Lipinski, C. A. (2014). Lead- and drug-like compounds: the rule-of-five revolution. *Drug Discov. Today Technol*. 1 (4), 337–341. doi:10.1016/j.ddtec.2004.11.007

Luthra, P. M., Kumar, R., and Prakash, A. (2009). Demethoxycurcumin induces Bcl-2 mediated G2/M arrest and apoptosis in human glioma U87 cells. *Biochem. Biophys. Res. Commun*. 384 (4), 420–425. doi:10.1016/j.bbrc.2009.04.149

Lythgoe, M. P., and Middleton, P. (2020). Ongoing clinical trials for the management of the COVID-19 pandemic. *Trends Pharmacol. Sci*. 41 (6), 363–382. doi:10.1016/j.tips.2020.03.006

Maier, J. A., Martinez, C., Kasavajhala, K., Wickstrom, L., Hauser, K. E., and Simmerling, C. (2015). ff14SB: improving the accuracy of protein side chain and backbone parameters from ff99SB. *J. Chem. Theor. Comput*. 11 (8), 3696–3713. doi:10.1021/acs.jctc.5b00255

Majewski, M., Ruiz-Carmona, S., and Barril, X. (2019). An investigation of structural stability in protein-ligand complexes reveals the balance between order and disorder. *Commun. Chem*. 2, 110. doi:10.1038/s42004-019-0205-5

Meng, X. Y., Zhang, H. X., Mezei, M., and Cui, M. (2011). Molecular docking: a powerful approach for structure-based drug discovery. *Curr. Comput. Aided Drug Des*. 7 (2), 146–157. doi:10.2174/157340911795677602

Mishra, C. B., Kumari, S., Prakash, A., Yadav, R., Tiwari, A. K., Pandey, P., et al. (2018). Discovery of novel Methylsulfonyl phenyl derivatives as potent human Cyclooxygenase-2 inhibitors with effective anticonvulsant action: design, synthesis, in-silico, *in-vitro* and *in-vivo* evaluation. *Eur. J. Med. Chem*. 151, 520–532. doi:10.1016/j.ejmech.2018.04.007

Niranjan Kumar, N., Srivastava, R., Prakash, A., and Lynn, A. M. (2021). Virtual screening and free energy estimation for identifying *Mycobacterium tuberculosis* flavoenzyme DprE1 inhibitors. *J. Mol. Graph Model*. 102, 107770. doi:10.1016/j.jmgm.2020.107770

Nygaard, M., Kragelund, B. B., Papaleo, E., and Lindorff-Larsen, K. (2017). An efficient method for estimating the hydrodynamic radius of disordered protein conformations. *Biophys. J*. 113 (3), 550–557. doi:10.1016/j.bpj.2017.06.042

Panda, P. K., Arul, M. N., Patel, P., Verma, S. K., Luo, W., Rubahn, H. G., et al. (2020). Structure-based drug designing and immunoinformatics approach for SARS-CoV-2. *Sci. Adv*. 6 (28), eabb8097. doi:10.1126/sciadv.abb8097

Prakash, A., Dixit, G., Meena, N. K., Singh, R., Vishwakarma, P., Mishra, S., et al. (2018a). Elucidation of stable intermediates in urea-induced unfolding pathway of human carbonic anhydrase IX. *J. Biomol. Struct. Dyn*. 36 (9), 2391–2406. doi:10.1080/07391102.2017.1355847

Prakash, A., and Luthra, P. M. (2012). Insilico study of the A(2A)R-D (2)R kinetics and interfacial contact surface for heteromerization. *Amino Acids*. 43, 1451–1464. doi:10.1007/s00726-012-1218-x

Prakash, A., Kumar, V., Meena, N. K., and Lynn, A. M. (2018b). Elucidation of the structural stability and dynamics of heterogeneous intermediate ensembles in unfolding pathway of the N-terminal domain of TDP-43. *RSC Adv*. 8, 19835–19845. doi:10.1039/C8RA03368D

Randall, R. E., and Goodbourn, S. (2008). Interferons and viruses: an interplay between induction, signalling, antiviral responses and virus countermeasures. *J. Gen. Virol*. 89 (Pt 1), 1–47. doi:10.1099/vir.0.83391-0

Ryckaert, J. P., Ciccotti, G., and Berendsen, H. J. C. (1977). Numerical integration of the cartesian equations of motion of a system with constraints: molecular dynamics of n-alkanes. *J. Comput. Phys*. 23, 327–341. doi:10.1016/0021-9991(77)90098-5

Shu, B., and Gong, P. (2016). Structural basis of viral RNA-dependent RNA polymerase catalysis and translocation. *Proc. Natl. Acad. Sci. USA*. 113 (28), E4005–E4014. doi:10.1073/pnas.1602591113

Singh, S., Fulbabu, S. k., Sonawane, A., Kar, P., and Sadhukhan, S. (2020). Plant-derived natural polyphenols as potential antiviral drugs against SARS-CoV-2 via RNA-dependent RNA polymerase (RdRp) inhibition: an in-silico analysis. *J. Biomol. Struct. Dyn*. 28 (7), 1–16. doi:10.1080/07391102.2020.1796810

Sinha, M., Jagadeesan, R., Kumar, N., Saha, S., Kothandan, G., and Kumar, D. (2020). In-silico studies on Myo inositol-1-phosphate synthase of Leishmania donovani in search of anti-leishmaniasis. *J. Biomol. Struct. Dyn*., 1–14. doi:10.1080/07391102.2020.1847194

Sulimov, V. B., Kutov, D. C., and Sulimov, A. V. (2019). Advances in docking. *Curr. Med. Chem*. 26 (42), 7555–7580. doi:10.2174/0929867325666180904115000

Tamura, S., Yang, G. M., Yasueda, N., Matsuura, Y., Komoda, Y., and Murakami, N. (2010). Tellimagrandin I, HCV invasion inhibitor from rosae rugosae flos. *Bioorg. Med. Chem. Lett*. 20 (5), 1598–1600. doi:10.1016/j.bmcl.2010.01.084

Tian, W., Chen, C., Lei, X., Zhao, J., and Liang, J. (2018). CASTp 3.0: computed atlas of surface topography of proteins. *Nucleic Acids Res*. 46(W1), W363–W367. doi:10.1093/nar/gky473

Trott, O., and Olson, A. J. (2010). AutoDock Vina: improving the speed and accuracy of docking with a new scoring function, efficient optimization, and multithreading. *J. Comput. Chem*. 31 (2), 455–461. doi:10.1002/jcc.21334

Venkataraman, S., Prasad, B. V. L. S., and Selvarajan, R. (2018). RNA dependent RNA polymerases: insights from structure, function and evolution. *Viruses*. 10 (2), 76. doi:10.3390/v10020076

Wallace, A. C., Laskowski, R. A., and Thornton, J. M. (1995). LIGPLOT: a program to generate schematic diagrams of protein-ligand interactions. *Protein Eng.* 8 (2), 127–134. doi:10.1093/protein/8.2.127

Walls, A. C., Park, Y. J., Tortorici, M. A., Wall, A., McGuire, A. T., and Veesler, D. (2020). Structure, function, and antigenicity of the SARS-CoV-2 spike glycoprotein. *Cell.* 181 (2), 281–e6. doi:10.1016/j.cell.2020.02.058

Wang, D. D., Ou-Yang, L., Xie, H., Zhu, M., and Yan, H. (2020). Predicting the impacts of mutations on protein-ligand binding affinity based on molecular dynamics simulations and machine learning methods. *Comput. Struct. Biotechnol. J.* 18, 439–454. doi:10.1016/j.csbj.2020.02.007

Wang, E., Sun, H., Wang, J., Wang, Z., Liu, H., Zhang, J. Z. H., et al. (2019). End-point binding free energy calculation with MM/PBSA and MM/GBSA: strategies and applications in drug design. *Chem. Rev.* 119 (16), 9478–9508. doi:10.1021/acs.chemrev.9b00055

Wang, F., Sambandan, D., Halder, R., Wang, J., Batt, S. M., Weinrick, B., et al. (2013). Identification of a small molecule with activity against drug-resistant and persistent *tuberculosis*. *Proc. Natl. Acad. Sci. United States.* 110 (27), E2510–E2517. doi:10.1073/pnas.1309171110

Wang, J., Wang, W., Kollman, P. A., and Case, D. A. (2006). Automatic atom type and bond type perception in molecular mechanical calculations. *J. Mol. Graph Model.* 25 (2), 247–260. doi:10.1016/j.jmgm.2005.12.005

Waterhouse, A., Bertoni, M., Bienert, S., Studer, G., Tauriello, G., Gumienny, R., et al. (2018). SWISS-MODEL: homology modelling of protein structures and complexes. *Nucleic Acids Res.* 46 (W1), W296–W303. doi:10.1093/nar/gky427

Wiederstein, M., and Sippl, M. J. (2007). ProSA-web: interactive web service for the recognition of errors in three-dimensional structures of proteins. *Nucleic Acids Res.* 35, W407–W410. doi:10.1093/nar/gkm290

Zhou, P., Yang, X. L., Wang, X. G., Hu, B., Zhang, L., Zhang, W., et al. (2020). A pneumonia outbreak associated with a new coronavirus of probable bat origin. *Nature.* 579 (7798), 270–273. doi:10.1038/s41586-020-2012-7

Conflict of Interest: The authors declare that the research was conducted in the absence of any commercial or financial relationships that could be construed as a potential conflict of interest.

frontiers in Pharmacology

ORIGINAL RESEARCH
published: 12 April 2021
doi: 10.3389/fphar.2021.619373

Phytoconstituents, *In Vitro* Anti-Infective Activity of *Buddleja indica* Lam., and *In Silico* Evaluation of its SARS-CoV-2 Inhibitory Potential

Fadia S. Youssef[1], *Ahmed E. Altyar*[2], *Abdelsattar M. Omar*[3,4]* *and Mohamed L. Ashour*[1,5]*

[1]Department of Pharmacognosy, Faculty of Pharmacy, Ain Shams University, Cairo, Egypt, [2]Department of Pharmacy Practice, Faculty of Pharmacy, King Abdulaziz University, Jeddah, Saudi Arabia, [3]Department of Pharmaceutical Chemistry, Faculty of Pharmacy, King Abdulaziz University, Jeddah, Saudi Arabia, [4]Department of Pharmaceutical Chemistry, Faculty of Pharmacy, Al-Azhar University, Cairo, Egypt, [5]Department of Pharmaceutical Sciences, Pharmacy Program, Batterjee Medical College, Jeddah, Saudi Arabia

Phytochemical investigation of *Buddleja indica* Lam. leaves methanol extract (BIT) resulted in the isolation of six known compounds for the first time from the plant, namely, *p*-hydroxybenzoic acid 1), caffeic acid 2), quercetin 3-O-β-D glucoside-7-O-α-L-rhamnoside 3), kaempferol 3-O-β-D glucoside-7-O-α-L-rhamnoside 4), quercetin 7-O-β-D glucoside 5) and kaempferol 6). BIT extract showed potent antibacterial activity with MIC values ranging between 0.48 and 1.95 μg/ml with *Bacillus subtilis* was the most susceptible to the BIT effect. It showed a notable antimycobacterial and anti-*Helicobacter pylori* activity with MIC values of 100 and 80 μg/ml, respectively. Vesicular stomatitis virus (VSV) was more sensitive to the antiviral activity of BIT comparable to herpes simplex virus type 1 (HSV-1), showing 48.38 and 41.85% inhibition of the viral replication at a dose of 50 μg/ml for VSV and HSV-1, respectively. *In silico* molecular docking of the isolated compounds revealed that caffeic acid 2) showed the highest fitting within the active sites of DNA-gyrase, topoisomerase IV, and SARS-CoV-2 M^{Pro}. Quercetin 7-O-β-D glucoside 5) revealed the best fitting in dihydrofolate reductase active site with Δ G value equals −36.53 Kcal/mol. Kaempferol 6) exhibited the highest fitting towards β-lactamase, SARS-CoV-2PL^{pro}, and SARS-CoV-2 $3CL^{pro}$ active sites. Thus, *B. indica* Lam. can be considered as a future source of cheap, substantially safe, and credible antibacterial, antifungal, and antiviral candidate of natural origin that could effectively participate in solving the problem of COVID-19 pandemic. These findings provide a scientific consolidation for the ethnomedicinal uses of *Buddleja indica* Lam. as a topical antiseptic.

Keywords: antimicrobial, antiviral, *Buddleia indica*, COVID-19, molecular modeling, phytoconstituents, Scrophulariaceae

OPEN ACCESS

Edited by:
Vijay Kumar Prajapati,
Central University of Rajasthan, India

Reviewed by:
Arry Yanuar,
University of Indonesia, Indonesia
Md Bashir Uddin,
Sylhet Agricultural University, Bangladesh

***Correspondence:**
Abdelsattar M. Omar
asmansour@kau.edu.sa
Mohamed L. Ashour
ashour@pharma.asu.edu.eg

Specialty section:
This article was submitted to Ethnopharmacology, a section of the journal Frontiers in Pharmacology

Received: *20 October 2020*
Accepted: *03 February 2021*
Published: *12 April 2021*

Citation:
Youssef FS, Altyar AE, Omar AM and Ashour ML (2021) Phytoconstituents, In Vitro Anti-Infective Activity of Buddleja indica Lam., and In Silico Evaluation of its SARS-CoV-2 Inhibitory Potential. Front. Pharmacol. 12:619373. doi: 10.3389/fphar.2021.619373

INTRODUCTION

In spite of the great progress in the therapeutic strategies for the alleviation of many human health disorders, infectious diseases due to bacteria, fungi, and viruses still constitute a major challenge to public health (Youssef et al., 2014; Ayoub et al., 2015). Recently, in late December 2019, a novel coronavirus strain impacted people in Wuhan, China, and they suffered from pneumonia and this virus was named severe

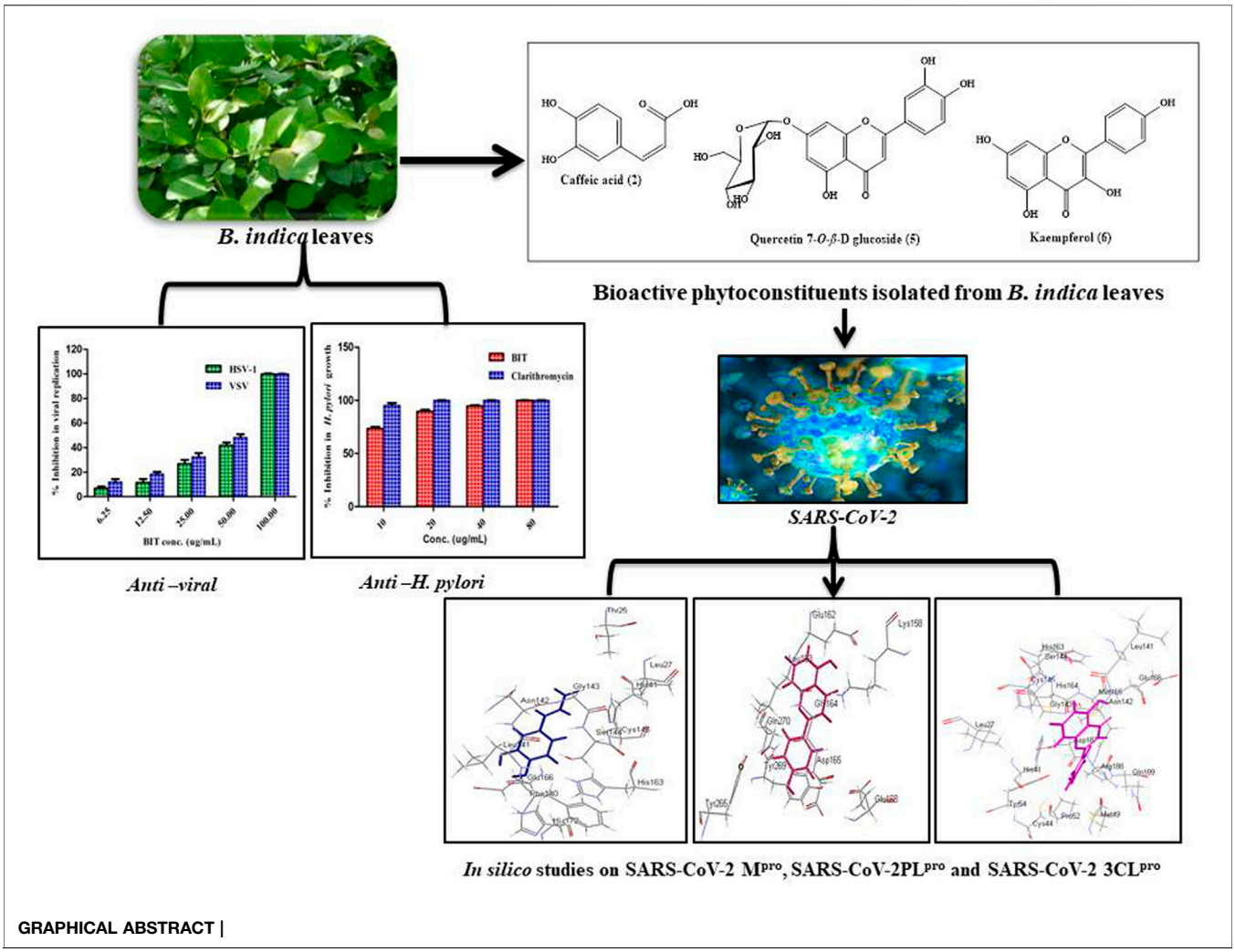

GRAPHICAL ABSTRACT |

acute respiratory syndrome–related coronavirus (SARS-CoV-2), resulting in a lethal respiratory disorder. People experiencing severe COVID-19 suffered from cytokine storm syndrome with concomitant secondary hemophagocytic, hyperinflammation, lymphohistiocytosis, hyperferritinemia, cytopenias, and acute respiratory distress syndrome. Hence, combating this pandemic and other infectious agents is of high necessity that demands the rapid discovery of effective drug entities (Mehta et al., 2020; Munnink et al., 2020). Plant kingdom constitutes an everlasting source of bioactive compounds that turn out to be relatively safe and widely acceptable by a large category of patients compared to synthetic drugs (Ashour et al., 2018; Thabet et al., 2018a).

Buddleja (Buddleia) has recently been included in the Scrophulariaceae family. It comprises about 100 species growing natively in Africa, South and North America, and Asia; meanwhile, a considerable number of the species were cultivated all over the globe, especially in central Europe and New Zealand. The *Buddleja* genus is known for possessing several biological activities represented mainly by antiviral, antimicrobial, antipyretic, antioxidant, immunosuppressive, hepatoprotective, antihypertensive, analgesic, and antipyretic activities. This is undoubtedly owing to its richness with various secondary metabolites exemplified mainly by phenylpropanoids, flavonoids, and iridoid glucosides (Youssef et al., 2018; Youssef et al., 2019).

Buddleja indica Lam. is an ornamental evergreen shrub of African, mainly Madagascan, origin. In spite of the popularity of the *Buddleja* genus in many medicinal uses, nothing was found in the literature concerning the biological activity or the phytoconstituents of *B. indica* Lam. except for its antioxidant and hepatoprotective potential (Youssef et al., 2019). It is noteworthy to mention that many members of the *Buddleja* genus were traditionally used as topical antiseptics without any scientific consolidation.

This study aimed to identify the secondary metabolites of *B. indica* Lam. leaves methanol extract using different techniques. The antimicrobial activity against a panel of bacteria and fungi, the antimycobacterial, anti-*Helicobacter pylori*, and antiviral potential will be assessed using *in vitro* studies for the first time. Furthermore, the prospect of its utilization to alleviate the COVID-19 pandemic, which has recently attacked the world resulting in many deaths, will be evaluated using *in silico* studies. This will be performed using Discovery Studio

software, aiming to explore its probable mode of action and exact behavior with the binding site of major *Coronavirus* proteins, if any. This will be done in hope of finding new natural resources that can be safely incorporated into pharmaceutical dosage forms aiming to solve this crisis.

MATERIALS AND METHODS

Plant Material

B. indica Lam. was purchased from El-Orman Botanical Garden, Giza, Egypt, in 2019. Identification and authentication of the plant were kindly performed by Mrs. Theresa Labib, Consultant of Plant Taxonomy at the Ministry of Agriculture, Giza, Egypt. The voucher specimen of the plant was given a voucher number of PHG-P-BI-163 and kept at Pharmacognosy Department, Faculty of Pharmacy, Ain Shams University, Egypt.

General Experimental Procedures

NMR spectral measurements were recorded on a Varian AS 500 MHz spectrometer. Polyamide 6 S (Fluka Analytical, Germany) and silica gel (60–120 mesh, Merck) were used for column chromatography (CC). Monitoring of CC fractions was done on precoated aluminum sheets [silica 60 F254, 0.25 mm (Merck, Darmstadt, Germany)], and detection was achieved using UV light at two different λ, 254 and 366 nm, that were concomitantly sprayed with 1% vanillin-sulfuric acid reagent and heated for 5–10 min at 105°C. HPLC (Knauer, Germany) supplied with semipreparative column Kromasil 100-5 C18 in addition to UV detector (K-2501) was used for further purification of the semipure fractions. All the solvents used are of high analytical grades, whereas those for HPLC analysis are of HPLC grade (Sigma-Aldrich (St. Louis, MO, United States).

Preparation of *Buddleja indica* Lam. Leaf Extract

The air-dried leaves of *B. indica* Lam. (500 g) were coarsely ground and then macerated in 5 L of distilled methanol with subsequent filtration and this process was repeated three times till exhaustion. The collected filtrate was subsequently evaporated under reduced pressure at a temperature not exceeding 45°C and then lyophilized to give 120 g of dried total methanol extract (BIT).

Isolation of Secondary Metabolites

About 105 g of the lyophilized extract was solubilized in 70% distilled methanol followed by fractionation using *n*-hexane, dichloromethane, and ethyl acetate successively to give 21.93, 8.32, and 27 g residue, respectively, with about 49.2 g remaining hydroalcoholic fraction. A 25 g of the ethyl acetate fraction was solubilized in the least amount of water and chromatographed over a polyamide S column chromatography and eluted with H_2O/MeOH of decreasing polarity till reaching 100% MeOH. Similar fractions were pooled together after being monitored using TLC on silica gel 254 sheets that resulted in ten major fractions. Fraction III eluted with 30% methanol was further chromatographed on silica gel column using CH_2Cl_2: CH_3OH of increasing polarity to give eight fractions. Fraction III-5 was subjected to preparative TLC using CH_2Cl_2: CH_3OH (8:2) to yield compound 1) (2 mg) and compound 2) (3.5 mg). Fraction IV eluted with 40% methanol was further chromatographed on a silica gel column. Similar fractions were pooled together after being monitored by TLC on silica gel 254 sheets to give sixty fractions. Fraction IV-44 was subjected to preparative HPLC using gradient elution using acetonitrile: water solvent system with a flow rate of 4 ml/min. This process resulted in the isolation of compound 3) (2.5 mg) and compound 4) (1 mg). However, fraction V, eluted with 50% methanol, was further chromatographed on silica gel column and similar fractions were pooled together after being monitored by TLC on silica gel 254 sheets to give 18 fractions. Fraction V-4 was subjected to preparative TLC using CH_2Cl_2: CH_3OH (9:1) to yield compound 5) (2 mg). Regarding fraction VIII, it was eluted with 80% methanol and was further chromatographed on silica gel column using CH_2Cl_2: CH_3OH of increasing polarity to give ten fractions. Fraction VIII-1 was subjected to preparative TLC using CH_2Cl_2: CH_3OH (9:1) to yield compound 6) (1.5 mg). A scheme representing the isolation of compounds (1–6) from *B. indica* Lam. total methanol leaves extract is shown in (**Supplementary Figure S1**) in the supplementary data.

Spectroscopic Data of Compounds (1–6)

The spectral data of all the previously isolated compounds (1–6) included 1D and 2D NMR. The compounds were defined as *p*-hydroxybenzoic acid 1) (Ariga et al., 2015), caffeic acid 2) (Jeong et al., 2011), quercetin 3-O-*β*-D-glucoside-7-O-α-L-rhamnoside 3) (Gaind et al., 1981), kaempferol 3-O-*β*-D glucoside-7-O-α-L-rhamnoside 4) (Gaind et al., 1981), quercetin 7-O-*β*-D glucoside 5) (Gansukh et al., 2016), and kaempferol 6) (Hadizadeh et al., 2003). NMR spectral data were supplied in the supplementary data in **Supplementary Figures S2–S19**.

BIOLOGICAL ASSESSMENTS

Assessment of the Antimicrobial Activity

Microbial Strains

BIT was investigated vs. a panel of microorganisms comprising standard Gram-positive bacteria, *Staphylococcus aureus* (ATCC 29213) and *Bacillus subtilis* (ATCC 6051); Gram-negative bacteria, *Pseudomonas aeruginosa* (ATCC 12525) and *Escherichia coli* (ATCC 25922); fungi, *Aspergillus fumigatus* (ATCC 1022), *Geotrichum candidum* (ATCC 12784), *Candida albicans* (ATCC 90028), and *Syncephalastrum racemosum* (ATCC 14831), at Al-Azhar University, Nasr City, Cairo, Egypt.

Determination of the Mean Inhibition Zones

Mean inhibition zones for the antibacterial potential were measured employing the previously described method by Damyanova et al. (Damyanova et al., 2000). Ampicillin and streptomycin were used as antibacterial standards at a concentration of 30 μg/ml. Meanwhile, the mean inhibition

zones for the antifungal activity were determined using the method previously adopted by Rathore et al. (Rathore et al., 2000), in which clotrimazole and itraconazole at a concentration of 30 µg/ml were used as the positive controls.

Determination of the Minimum Inhibitory Concentration

MIC values of BIT vs. all the examined bacterial and fungal strains were determined using the agar plate method. Nutrient agar was used for bacterial strains, whereas Sabouraud dextrose agar was employed for fungi. The respective agar media were heated in the autoclave for 25 min at 121°C and allowed to cool to 45°C. Twofold serial dilutions of the tested sample were added to the medium immediately before being poured into the Petri dishes. DMSO was used as the negative control. The culture of each organism in the nutrient broth (beef extract 5 g/L and peptone 10 g/L, pH = 7.0) for bacteria and Sabouraud dextrose broth for fungi was diluted with sterile distilled water to 10^5–10^6 CFU/mL. A loop of each suspension was inoculated in the appropriate medium with the sample or the control added. After inoculation, the plates were incubated at 37°C for 24 h for bacteria and at 30°C for three to four days for fungi. The MIC was considered to be the lowest concentration that completely inhibited the visible growth of a microorganism compared with the control (Rahman et al., 2001). Each test was performed in triplicate and both streptomycin and clotrimazole were used as positive controls.

Assessment of the Antimycobacterial Activity

The antimycobacterial potential of BIT was determined by the microplate Alamar blue assay (MABA). The used *M. tuberculosis* strain (RCMB 010126) was obtained from the culture collection of the Regional Center for Mycology and Biotechnology (RCMB), Al-Azhar University (Cairo, Egypt). This was performed as previously described and isoniazid was used as a standard drug (Gamal El-Din et al., 2018). Percent inhibition was defined as 1—(mean of test well/mean of B wells) × 100, whereas MIC was defined as the lowest concentration of drug that prevented this change in color.

Assessment of the Anti-*Helicobacter pylori* Activity

The anti-*Helicobacter pylori* effectiveness of BIT was determined using *Helicobacter pylori* ATCC 43504 following the NCCLS guidelines (1998) and as previously described (Gamal El-Din et al., 2018). Clarithromycin was used as a positive control. Inhibition (%) was computed as follows: [(Initial control absorbance-final absorbance)/(Initial control absorbance)] × 100.

Assessment of the Antiviral Activity

Cell Cultures

Vero cells (CCL-81) (Vero African green monkey kidney cells) were maintained in DMEM complete media with a high glucose level of 0.45% (L-glutamine supplemented with 10% heat-inactivated fetal bovine serum (FBS), 100 U/mL penicillin, and 100 U/ml streptomycin). Cells were cultured in 10 cm cell culture dishes (Cellstar) at 37°C in a humidified atmosphere of 5% CO_2. The cells were maintained as "monolayer culture" by serial subculturing. All experiments were performed with cells in the logarithmic growth phase under strict aseptic conditions in a biosafety level 2 lab using a biological safety cabinet level 2 (Ashour et al., 2014).

Cytotoxicity and Cell Proliferation MTT Assay

Cytotoxicity was evaluated by applying the MTT cell viability assay (Van de Loosdrecht et al., 1991; Thabet et al., 2018b). Briefly, this assay depends on the conversion of MTT (3-(4,5-dimethylthiazol-2-yl)-2,5-diphenyltetrazolium bromide) by the viable cells from the yellow color to purple formazan compound. Vero cells (CCL-81) about 2×10^4 cell/well in the exponential phase were seeded in a 96-well plate and they were cultivated for 24 h and then incubated with various concentrations of the serially diluted tested sample (stock solution 1 mg/ml) at 37°C for 24 h followed by their incubation with 0.5 mg/ml MTT for 4 h. The formed formazan compound was solubilized in 200 µL DMSO and the absorbance was measured at 570 nm. The cell viability rate (%) of three independent experiments was calculated by the following formula (Youssef et al., 2016):

The Plaque Reduction Assay

The antiviral activity was determined by a plaque reduction assay (Abou-Karam & Shier, 1990). Briefly, a confluent layer of Vero cells (CCL-81) was obtained by culturing the cells for 24 h in 0.5% CO_2 at 37°C. The cells were inoculated separately with herpes simplex virus type 1 (HSV-1) (ATCC VR 1493) or vesicular stomatitis virus (VSV) (ATCC VR 1283) (1×10^{-1}–10^{-7}/ml) and incubated at 37°C for 1 h. The infected cell cultures (2×10^3 PFU) were washed and overlaid with DMEM containing five concentrations of BIT (6.25, 12.5, 25, 50, and 100 µg/ml) for 1 h at room temperature. Each concentration was performed in three replicates and cultures were overlaid with nutrient agarose (DMEM 2x/1.8% agarose [v/v]) containing 25 mM $MgCl_2$. After 72 h incubation, cells were fixed with 10% formaldehyde in phosphate buffer, pH = 7.3, for 1 h, and stained with 0.5% crystal violet in 20% ethanol. The plaques were counted and the percentage of viral inhibition was calculated as $[1-(V_d/V_c)] \times 100$, where V_d and V_c refer to the number of plaques in the presence and absence of the tested sample, respectively. Acyclovir was employed as a positive control. The viral strains HSV-1 and VSV are available at VACSERA, Giza, Egypt. Biosafety level II was strictly followed; all equipment, vials, viral cultures, stocks, and potentially infectious materials were properly decontaminated via autoclaving prior to disposal. In addition, protective clothing was worn during preparation to prevent contamination and to guard against harm (World Health Organization, 2004).

In Silico Molecular Docking Studies

Molecular modeling studies were performed for the isolated phytoconstituents within the active centers incorporated in the occurrence of bacterial infection and antibiotic resistance development such as DNA-gyrase (PDB ID 4Z2D; 3.38 A°);

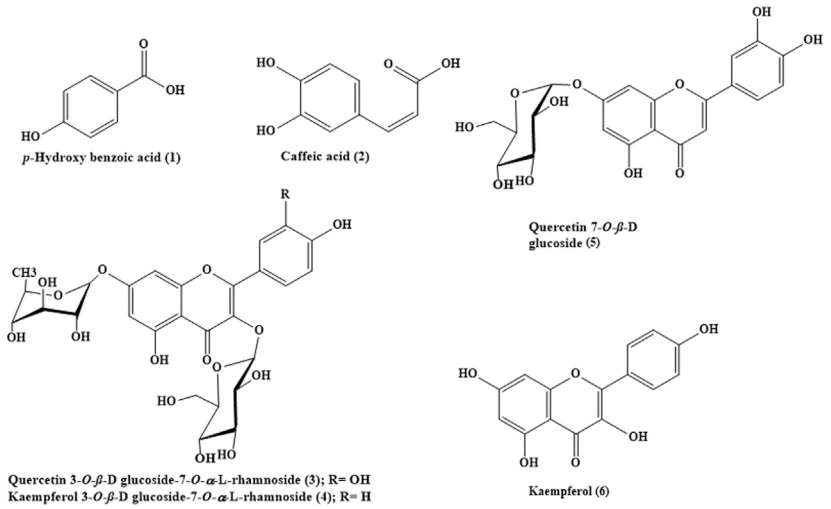

FIGURE 1 | The chemical structures of phenolic compounds isolated from *B. indica* leaves.

TABLE 1 | Mean inhibition zones of BIT against different pathogens determined by the agar diffusion method.

Microorganisms		Diameter of inhibition zone (mm)				
		BIT (50 mg/ml)	Ampicillin (30 µg/ml)	Streptomycin (30 µg/ml)	Itraconazole (30 µg/ml)	Clotrimazole (30 µg/ml)
Gram (+)						
	Staphylococcus aureus (ATCC 29213)	24.3 ± 0.02	30.1 ± 0.06	28.1 ± 0.07	NT	NT
	Bacillus subtilis (ATCC 6051)	25.7 ± 0.20	31.6 ± 0.05	29.7 ± 0.06	NT	NT
Gram (-)						
	Pseudomonas aeruginosa (ATCC 12525)	21.7 ± 0.04	28.3 ± 0.08	25.2 ± 0.09	NT	NT
	Escherichia coli (ATCC 25922)	24.9 ± 0.07	33.1 ± 0.09	29.7 ± 0.07	NT	NT
Fungi						
	Aspergillus fumigatus (ATCC 1022)	24.3 ± 0.04	NT	NT	27.4 ± 0.05	26.3 ± 0.08
	Geotrichum candidum (ATCC 12784)	21.5 ± 0.09	NT	NT	24.2 ± 0.09	23.2 ± 0.03
	Candida albicans (ATCC 90028)	19.4 ± 0.01	NT	NT	25.2 ± 0.07	20.8 ± 0.02
	Syncephalastrum racemosum (ATCC 14831)	17.5 ± 0.07	NT	NT	23.9 ± 0.04	21.4 ± 0.05

Data are measured in triplicate (n = 3) and presented as means ± SD. Well diameter: 6.0 mm (100 µL was tested). NT: not tested.

topoisomerase IV (PDB ID 4Z3O; 3.44 A°); dihydrofolate reductase (PDB ID 4KM2; 1.4 A°); β-lactamase (PDB ID 3NBL; 2.0 A°). Additionally, the main target proteins required to prohibit COVID-19 replication, that is the main protease SARS-CoV-2 M^{Pro} (PDB ID: 6LZE; 1.50 A°), SARS-CoV-2 papain-like protease (PL^{pro}) (PDB ID: 4OW0; 2.10 A°), and 3-chymotrypsin-like protease SARS-CoV-2 $3CL^{pro}$ (PDB ID: 6M2N; 2.20 A°), were tested using Discovery Studio 4.5 (Accelrys Inc., San Diego, CA, USA) applying C-Docker protocol using both pH-based and rule-based methods that were chosen during the preparation of the ligand as an option in the software prior to performing the docking experiments as previously described (Ashour et al., 2018; Janibekov et al., 2018; Thabet et al., 2018). It is noteworthy to highlight that in the pH-based method, docking takes place under conditions that mimic the interaction in the physiological medium, whereas in the rule-based method, docking takes place regarding the functional groups only. The free binding energies (ΔG) were calculated in Kcal/mol using the following equation:

$$\Delta G_{binding} = E_{complex} - \left(E_{protein} + E_{ligand}\right).$$

Here, $\Delta G_{binding}$ is the ligand–protein interaction binding energy, $E_{complex}$ is the potential energy for the complex of protein bound with the ligand, $E_{protein}$ is the potential energy of protein alone, and E_{ligand} is the potential energy for the ligand alone.

Moreover, the validation of molecular docking was performed for all the carried docking experiments via comparing the alignment of the best docking poses for the lead compound that varies according to the targeted enzyme with the lead conformer cocrystallized with the respective enzyme. RMSD (Root-Mean-Square Deviation) value is used to confirm the validity of the docking experiment and indicates the ability to predict the binding mode of novel ligands.

TABLE 2 | Minimum inhibitory concentrations (MICs) of BIT against different pathogens determined by the agar plate method.

Microorganisms		Minimum inhibitory concentration (MIC) (μg/ml)			
		BIT	Ampicillin	Streptomycin	Clotrimazole
Gram (+)					
	Staphylococcus aureus (ATCC 29213)	0.97	0.16	0.24	NT
	Bacillus subtilis (ATCC 6051)	0.48	0.08	0.12	NT
Gram (-)					
	Pseudomonas aeruginosa (ATCC 12525)	1.95	0.24	0.48	NT
	Escherichia coli (ATCC 25922)	0.97	0.06	0.12	NT
Fungi					
	Aspergillus fumigatus (ATCC 1022)	0.97	NT	NT	0.12
	Geotrichum candidum (ATCC 12784)	1.95	NT	NT	0.48
	Candida albicans (ATCC 90028)	3.9	NT	NT	0.97
	Syncephalastrum racemosum (ATCC 14831)	7.8	NT	NT	0.48

NT: Not tested.

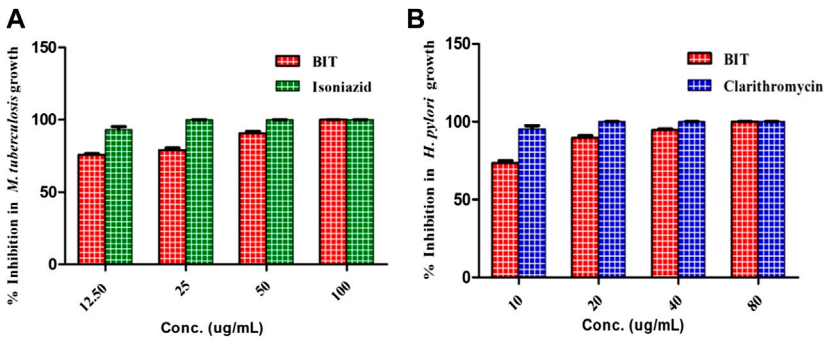

FIGURE 2 | Effect of BIT and isoniazid different concentrations on the *M. tuberculosis* **(A)** and effect of different BIT concentrations and clarithromycin on *H. pylori* growth **(B)**.

Statistical Analysis

All the measurements were done in triplicate in three independent times. Data were expressed as the mean ± SD. Graphs were constructed by GraphPad Prism® 5.1 (GraphPad Software, Inc., CA, United States). The p value < 0.05 was considered a significance difference between comparison groups.

RESULTS AND DISCUSSION

Phytochemical Characterization

Phytochemical investigation of *B. indica* Lam. leaves methanol extract resulted in the isolation and structural elucidation of six known polyphenolic compounds, which were the first to be isolated from the plant. They belong mainly to phenolic acids and flavonoids, which were fully elucidated and identified via comparing their 1D and 2D NMR data with what was previously reported in the literature. They were defined as *p*-hydroxybenzoic acid 1) (Ariga et al., 2015), caffeic acid 2) (Jeong et al., 2011), quercetin 3-O-β-D-glucoside-7-O-α-L-rhamnoside 3) (Gaind et al., 1981), kaempferol 3-O-β-D glucoside-7-O-α-L-rhamnoside 4) (Gaind et al., 1981), quercetin 7-O-β-D glucoside 5) (Gansukh et al., 2016), and kaempferol 6) (Hadizadeh et al., 2003). A scheme showing the compounds isolated from *B. indica* Lam. leaves is illustrated in **Figure 1**. It is noteworthy to mention that *p*-hydroxybenzoic acid, buddlenoid B, 2′-O-benzoyl aucubin, buddlejoside A, kaempferol-7-O-α-L-rhamnopyranoside, 6-acetylaucubin, gmelinoside F and gmelinoside H, isorhamnetin 7-O-α-L-rhamnopyranoside, catalpol 6-O-[4-methoxy-E-cinnamoyl-(3)-α-L-rhamnopyranoside, and acacetin-7-galactoside were previously determined by the authors from the plant extract using LC-ESI-MS (Youssef et al., 2019).

The Antimicrobial, Antimycobacterial, and Anti-*Helicobacter pylori* Activity

The antibacterial activity of BIT was evaluated *in vitro* using the agar well diffusion method against different standard Gram-positive and Gram-negative bacteria via measuring the mean inhibition zones and determining the MICs. The values for the mean inhibition zones were illustrated in **Table 1**. BIT extract showed potent antibacterial activity against the tested Gram-positive and Gram-negative bacterial strains with MIC values ranging between 0.48 and 1.95 μg/ml. *Bacillus subtilis* was the

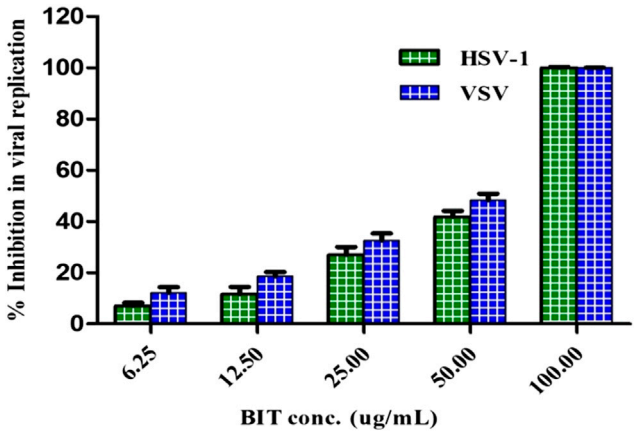

FIGURE 3 | Effect of BIT different concentrations on HSV-1 and VSV growth using direct plaque reduction assay.

most susceptible to the BIT effect, followed by *Staphylococcus aureus* and *Escherichia coli* displaying MICs of 0.48 μg/ml for the former and 0.97 μg/ml for the latter two (**Table 2**).

Moreover, BIT extract was screened *in vitro* for its antifungal activity against various fungi on Sabourad dextrose agar plates. Then, the diameter of the inhibition zone (in mm) (**Table 1**) and the minimum inhibitory concentration (MIC) values were calculated. The extract showed a powerful inhibition against nearly all of the tested organisms, as evidenced by its MIC values approaching that of the clotrimazole, the standard antifungal agent. It is worthy of mentioning that BIT is highly effective against *Aspergillus fumigatus* followed by *Geotrichum candidum* and *Candida albicans* with MICs of 0.97, 1.95, and 3.9 μg/ml, respectively. Additionally, *Syncephalastrum racemosum* was moderately sensitive to the antimicrobial effect of BIT with a MIC value of 7.8 μg/ml (**Table 2**).

Additionally, BIT extract showed substantial antimycobacterial activity against *M. tuberculosis,* exhibiting a MIC value of 100 μg/ml. It is noteworthy to mention that BIT extract and isoniazid showed 75.8 and 93.24% inhibition to *M. tuberculosis* growth at 12.5 μg/ml, respectively (**Figure 2A**). On the other hand, BIT extract also proved a notable activity against *Helicobacter pylori* growth with a MIC value of 80 μg/ml with respect to the positive control, clarithromycin, that showed a MIC value of 20 μg/ml. Furthermore, the extract showed 73.4% inhibition to *Helicobacter pylori* growth at 10 μg/ml compared to 95.37% inhibition shown by the positive control at the same concentration (**Figure 2A**).

Various extracts and isolated compounds from many *Buddleja* species were previously reported to possess a prominent antimicrobial activity. The methanol extracts of the leaves and stems of *B. saligna* produced effective inhibition to various Gram-positive and some Gram-negative microbial strains (Adedapo et al., 2009). Additionally, *B. saligna* hexane fraction showed a considerable bactericidal potency against *Mycobacterium tuberculosis* using bioautography and this could be explained in virtue of its DNA polymerase inhibitory activity (Bamuamba et al., 2008). In addition, *B. cordata* stem bark extract exhibited a notable antimycobacterial activity (Acevedo et al., 2000). Moreover, *B. globosa* and *B. cordata* leaves were reputed as potent antibacterial agents vs. *Staphylococcus aureus* and *Escherichia coli* due to the presence of various polyphenolic compounds as verbascoside that displayed MIC at a value of 1 μM (Guillermo Avila et al., 1999). However, the lipophilic, chloroform, extract of *B. globosa* stem bark displayed a potent antifungal activity with MIC of 125 μg/ml against *Epidermophyton floccosum, Trichophyton interdigitale*, and *Trichophyton rubrum* owing to the existence of terpenoid compounds, namely, buddlejone and buddledins A and B (Mensah et al., 2000). Furthermore, *B. perfoliata* Kunth that was popular in folk medicine for the alleviation of digestive tract disorder showed *in vitro* anti-*H. pylori* activity with MIC values for the aqueous and methanol extracts of its aerial parts of 500 and 62.5 μg/ml, respectively (Castillo-Juárez et al., 2009). In addition, *p*-hydroxybenzoic acid and caffeic acid were reported to possess a prominent antifungal and antibacterial activity vs. a wide array of bacteria and fungi (Manuja et al., 2013).

The Antiviral Activity

The antiviral activity was assessed using the plaque reduction assay on Vero cells (CCL-81). The BIT extract lacks measurable cytotoxicity on Vero cells at the selected doses with IC_{50} of 251.47 μg/mL as shown by the MTT assay. However, BIT showed notable antiviral activity in a dose-dependent manner against VSV and HSV-1, as demonstrated in **Figure 3**. Meanwhile, VSV was more sensitive to the antiviral activity of the BIT comparable to HSV-1, showing 48.38 and 41.85% inhibition of the viral replication at a dose of 50 μg/ml for VSV and HSV-1, respectively, with IC_{50} equaling 52.2 and 58.6 μg/ml for VSV and HSV-1, respectively, whereas acyclovir, the standard antiviral, demonstrated IC $_{50}$ values of 2.21 and 1.49 μg/ml for VSV and HSV-1, respectively (**Supplementary Table S1**). It is noteworthy to mention that few reports were found considering the antiviral activity of various *Buddleja* species in which *B. cordobensis* essential oil showed modest activity against dengue virus type 2, herpes simplex virus type 1, and Junin virus (Duschatzky et al., 2005). However, compounds isolated from BIT showed antiviral activity. Caffeic acid isolated from BIT revealed potent anti-HBV, anti-HSV, and/or ADV activities in addition to the prohibition of human coronavirus NL63 (Chiang et al., 2002; Wang et al., 2009; Langland et al., 2018; Weng et al., 2019) caused by inhibition of viral DNA replication, antigen production, and reduction of virus level in the serum (Wang et al., 2009). Furthermore, quercetin 7-O-*β*-D-glucoside exhibited potent inhibitory potential vs. influenza A and B viruses via reducing ROS autophagy production and prohibiting viral RNA polymerase by occupying m7GTP on PB2 protein of the virus (Gansukh et al., 2016). In addition, kaempferol and its derivatives, particularly with rhamnose glycoside, strongly prohibited the 3a channel protein of SARS coronavirus and thus act as good candidates for 3a channel proteins of coronaviruses (Schwarz et al., 2014).

TABLE 3 | Free binding energies (ΔG) in Kcal/mol of compounds isolated from *B. indica* Lam. leaves in the active sites of enzymes involved in the occurrence of bacterial infections and resistance using *in silico* studies.

Compounds	DNA–gyrase		Topoisomerase IV		Dihydrofolate reductase		β–lactamase	
	pH	Rule	pH	Rule	pH	Rule	pH	Rule
p–Hydroxy benzoic acid **(1)**	−13.34	−13.79	−18.37	−18.40	−15.83	−15.67	−35.98	−35.00
Caffeic acid **(2)**	−20.45	−20.45	−25.65	−25.65	−35.61	−35.61	−46.74	−46.74
Quercetin 3–O– β–D–glucoside–7–O– α–L–rhamnoside **(3)**	12.97	12.63	13.36	16.17	2.35	3.68	−16.33	−0.96
Kaempferol 3–O–β–D–glucoside–7–O– α–L–rhamnoside **(4)**	15.28	15.28	16.74	16.74	0.79	7.94	−1.78	−1.78
Quercetin 7–O– β–D glucoside **(5)**	−6.16	−13.24	−15.68	−11.43	−36.53	−18.94	−37.09	−24.16
Kaempferol **(6)**	−17.92	−21.44	−23.61	−20.94	−35.66	−27.85	−46.92	−30.08
Levofloxacin	−9.90	−9.90	ND	ND	ND	ND	ND	ND
Moxifloxacin	ND	ND	−10.22	−10.22	ND	ND	ND	ND
Trimethoprim	ND	ND	ND	ND	−28.90	−28.90	ND	ND
Cefuroxime	ND	ND	ND	ND	ND	ND	−61.76	−61.76

FD: fail to dock; ND: not done.

TABLE 4 | Free binding energies (ΔG) in Kcal/mol of compounds isolated from *B. indica* Lam. leaves in the active sites of specific proteins that serve as the main targets for SARS-CoV-2 eradication employing *in silico* studies.

Compounds	SARS-CoV-2 M^{Pro}		SARS-CoV-2PL^{pro}		SARS-CoV-2 $3CL^{pro}$	
	pH	Rule	pH	Rule	pH	Rule
p-Hydroxy benzoic acid **(1)**	−21.95	−21.00	−21.07	−20.99	−20.78	−17.10
Caffeic acid **(2)**	−28.13	−28.13	−26.79	−26.79	−28.53	−28.53
Quercetin 3-O-β-D-glucoside-7-O-α-L-rhamnoside **(3)**	−3.75	−1.70	13.91	20.96	−2.18686	8.05
Kaempferol 3-O-β-D-glucoside-7-O-α-L-rhamnoside **(4)**	7.71	8.61	34.88	34.88	11.13	12.29
Quercetin 7-O-β-D glucoside **(5)**	−19.76	−19.52	−11.40	−11.83	−22.86	−19.62
Kaempferol **(6)**	−27.84	−25.84	−28.61	−26.27	−32.77	−31.76
SARS-CoV-2 M^{Pro} ligand (FHR/PRD_002347)	−4.60	−4.60	ND	ND	ND	ND
SARS-CoV-2 PL^{pro} ligand S88	ND	ND	−22.53	−22.53	ND	ND
SARS-CoV-2 $3CL^{pr}$ ligand 3WL	ND	ND	ND	ND	−34.66	−34.66

ND: not done.

In Silico Molecular Docking Studies

In silico molecular docking of the isolated compounds was performed on crucial proteins incorporated into the growth and replication of microbes and SARS-CoV-2 in the hope of finding promising candidates to fight infection and to solve the COVID-19 pandemic. In this study, four proteins were selected as they are critical for the survival, replication, and development of bacterial resistance, namely, DNA-gyrase (PDB ID 4Z2D; 3.38 A°); topoisomerase IV (PDB ID 4Z3O; 3.44 A°); dihydrofolate reductase (PDB ID 4KM2; 1.4 A°); β-lactamase (PDB ID 3NBL; 2.0 A°). Additionally, three crucial proteins for SARS-CoV-2, which represent ideal targets to prohibit viral replication, namely, main protease SARS-CoV-2 M^{Pro} (PDB ID: 6LZE; 1.50 A°), SARS-CoV-2 papain-like protease SARS-CoV-2PL^{pro}) (PDB ID: 4OW0; 2.10 A°), and 3-chymotrypsin-like protease SARS-CoV-2 $3CL^{pro}$ (PDB ID: 6M2N; 2.20 A°), were also examined using Discovery Studio 4.5 applying C-Docker protocol employing both pH-based and rule-based experiments in an effort to search for entities that could act as leads that may help in solving this crisis.

Results of the validation experiments revealed a good alignment between the best-docked poses of the lead compound, with the lead conformer cocrystallized with the respective enzymes showing RMSD values of 1.53, 1.05, 1.70, 2.00, 1.71, 2.10, and 2.30 A° for DNA-gyrase, topoisomerase IV, dihydrofolate reductase, β-lactamase, SARS-CoV-2 M^{Pro}, SARS-CoV-2PL^{pro}, and SARS-CoV-2 $3CL^{pro}$, respectively, confirming the validity of the experiment. Figures showing the alignment between the best-docked poses of the lead compound with the lead conformer cocrystallized with the respective enzymes were displayed in **Supplementary Figure S20**.

Employing pH-based docking that mimics the interaction in the physiological medium, results illustrated in **Table 3** and **Table 4** revealed that caffeic acid 2) showed the highest fitting within the active sites of DNA-gyrase, topoisomerase IV, and SARS-CoV-2 M^{Pro} displaying ΔG of -20.45, -25.65, and -28.13 Kcal/mol, respectively, showing superior activity to levofloxacin, moxifloxacin, and SARS-CoV-2 M^{Pro} ligand (FHR/PRD_002347) with free binding energies equal to -9.9, -10.22, and -4.60 kcal/mol, respectively. Meanwhile, quercetin 7-O-β-D-glucoside 5) revealed the best fitting in dihydrofolate reductase active site with ΔG value equal to −36.53 Kcal/mol exceeding that of trimethoprim that showed Δ G of -28.90 kcal/mol. Furthermore, kaempferol 6) exhibited

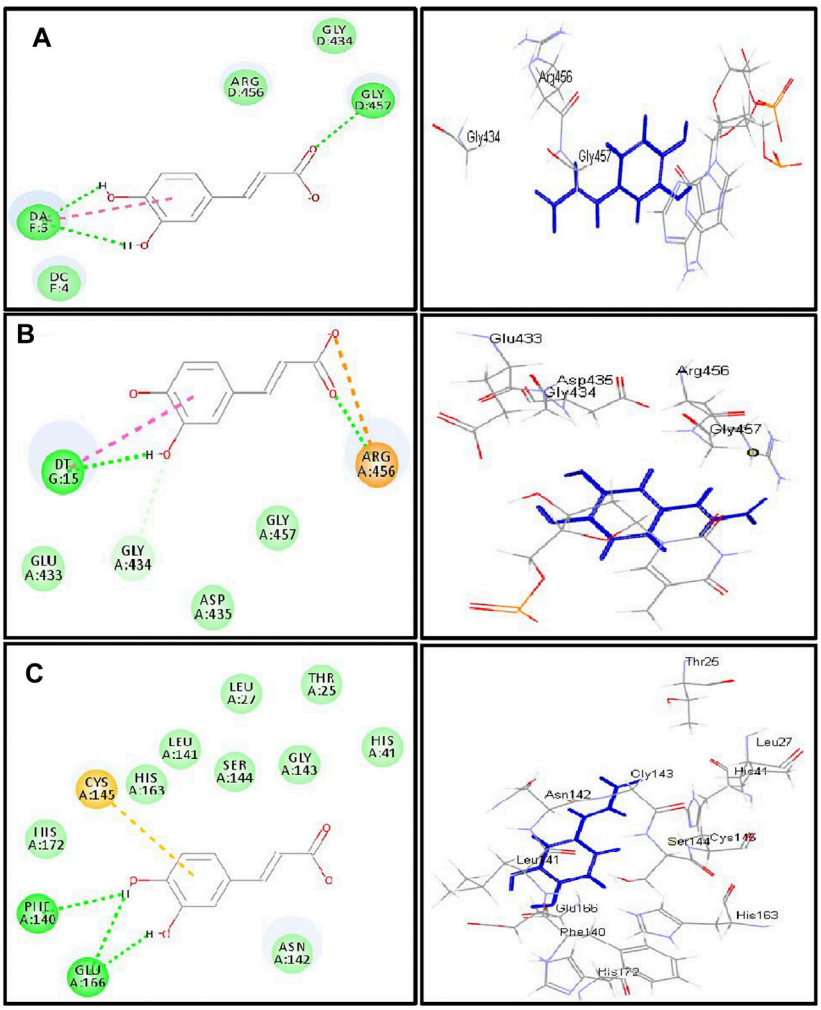

FIGURE 4 | 2D and 3D binding modes of caffeic acid in the active centers of **(A)** DNA-gyrase, **(B)** topoisomerase IV, and **(C)** SARS-CoV-2 M^{Pro}; dotted green lines indicate H-bonds; dotted light green lines indicate C-H-bonds; dotted purple lines indicate π-bonds; dotted orange bonds indicate salt bridge formation.

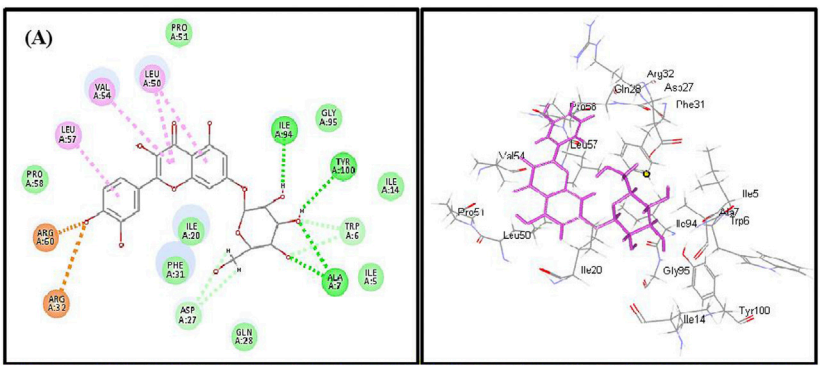

FIGURE 5 | 2D and 3D binding modes of quercetin 7-O-*β-D*-glucoside in dihydrofolate reductase active sites; dotted green lines indicate H-bonds; dotted light green lines indicate C-H-bonds; dotted purple lines indicate π-bonds; dotted orange bonds indicate salt bridge formation.

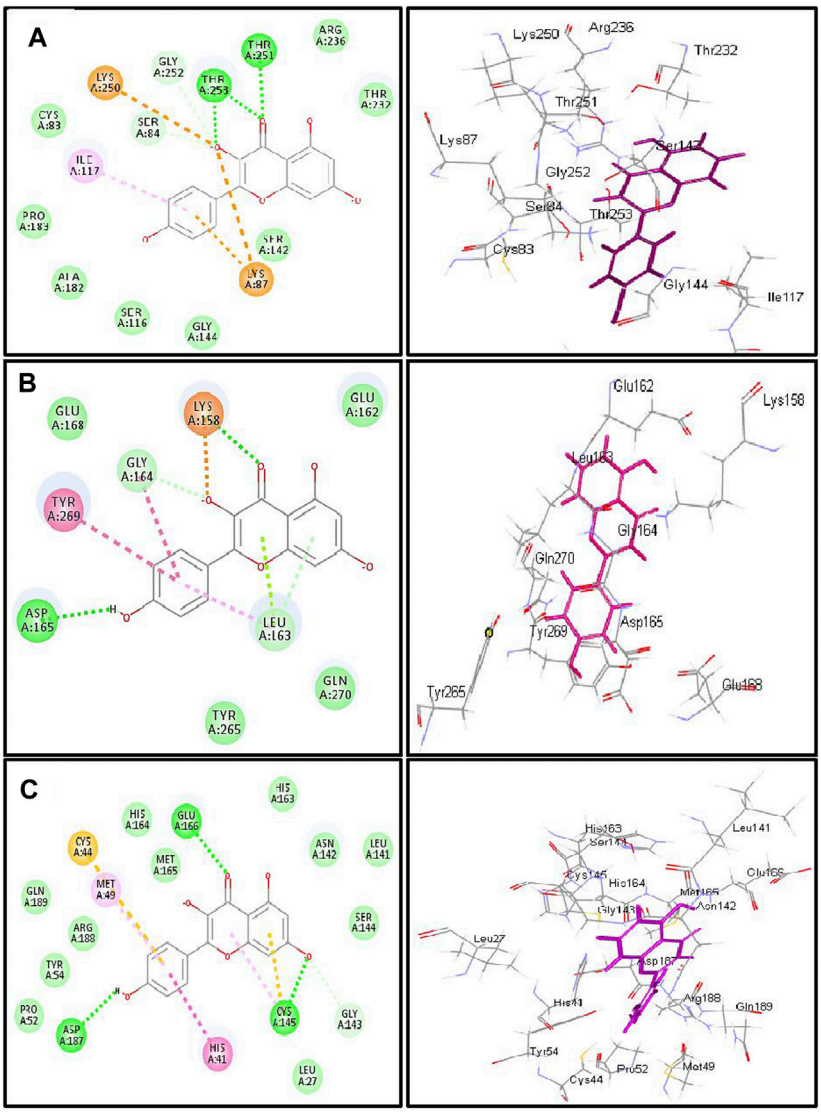

FIGURE 6 | 2D and 3D binding modes of kaempferol in the active centers of (A) β-lactamase (B) SARS-CoV-2PLpro and (C) SARS-CoV-2 3CLpro; dotted green lines indicate H-bonds; dotted light green lines indicate C-H-bonds; dotted purple lines indicate π-bonds; dotted orange bonds indicate salt bridge formation.

the highest fitting towards *β*-lactamase, SARS-CoV-2PL^{pro}, and SARS-CoV-2 3CL^{pro} active sites with free binding energies equal to −46.92, −28.61, and −32.77 Kcal/mol, respectively, approaching in this aspect cefuroxime, main SARS-CoV-2 PL^{pro} ligand S88, and main SARS-CoV-2 3CL^{pr} ligand 3WL that exerted free binding energies equal to −61.76, −22.53, and −34.66 Kcal/mol, respectively. 2D and 3D binding modes of compounds showing the highest fitting score within SARS-CoV-2 M^{Pro}, SARS-CoV-2PL^{pro}, and SARS-CoV-2 3CL^{pro} are illustrated in **Figures 4–6**.

The firm binding of caffeic acid at the active site of DNA-gyrase could be explained by virtue of the formation of three H-bonds, one π-π bond, and Van der Waals interactions with the amino acid residues existing at the active site. Similarly, the formation of two H-bonds, one π-π bond, C-H bond, and many Van der Waals interactions with amino acid existing at the active site of topoisomerase IV explained the tight binding of caffeic acid to its active center. Regarding the SARS-CoV-2 coronavirus, caffeic acid revealed a strong binding to main protease (SARS-CoV-2 M^{Pro}) that is interpreted by the formation of three conventional H-bonds with Phe 140, Glu 166, and π-sulfur interaction with Cys 145 together with many Van der Waals interactions (**Figure 4**). Meanwhile, DNA-gyrase ligand (levofloxacin) forms H-bonds and salt bridges with Lys 415 and Arg 456 in addition to the formation of π-alkyl interaction with Arg 456 and C-H bond with Glu 474 and Glu 475. Regarding topoisomerase IV ligand (moxifloxacin), it forms three H-bonds, π-π bond, and alkyl-alkyl interaction with Arg 456, C-H bond, and many Van der Waals interactions with the amino acid residues at the active site. However, SARS-CoV-2 M^{Pro} ligand

(FHR/PRD_002347; (~{N}-[(2~{S})-3-cyclohexyl-1-oxidanylidene-1-[[(2~{S})-1-oxidanylidene-3-[(3~{S})-2-oxidanylidenepyrrolidin-3-yl]propan-2-yl]amino]propan-2-yl]-1~{H}-indole-2-carboxamide) revealed the formation of H-bond with Glu 166 and C-H bonds with His 164, His 41, Asn 142, π-alkyl interaction with Pro 168 and alkyl-alkyl interaction with Cys 145, and many Van der Waals interactions (**Supplementary Figure S21**).

Quercetin 7-O-*β*-D-glucoside revealed the highest fitting to dihydrofolate reductase owing to the formation of three H-bonds with Ile 94, Tyr 100, and Ala7 and four π-alkyl interactions with Leu 57, Val 54, Leu 50, and C-H bonds with Asp 27 and Trp 6 and the formation of two attractive charges with Arg 960 and Arg 32 (**Figure 5**). However, dihydrofolate reductase ligand (trimethoprim) forms three H-bonds with Ala 7, Ile 94, and π-alkyl interaction with Leu 50 and Ile 20 and C-H bonds with Asp 27, Trp 6, and Tyr 100 (**Supplementary Figure S22**).

Kaempferol showed an excellent fitting with the active site of *β*-lactamase due to the formation of H-bonds with Thr 253 and Thr 251, π-alkyl interaction with Ile 117, and C-H bonds with Gly 252 and Ser 84 together with the formation of π-cation and attractive charges with Lys 87 and Lys 250. In terms of SARS-CoV-2PL^{pro} and SARS-CoV-2 3CL^{pro}, it forms a considerable number of bonds with the former represented by one H-bond with Asp 165, π-π bond with Tyr 269, amide–π bond with Gly 164, a salt bridge with Lys 158, π-lone pair bond with Leu 163, C-H bond with Gly 164, and π-donor H-bond with Leu 163. Meanwhile, it forms with SARS-CoV-2 3CL^{pro} three H-bonds with Glu 166, Asp 187, and Cys 145, π-π bond with His 41, π-alkyl bond with Met 49, π-sulfur bond with Cys 44 and Cys 145, and many Van der Waals interactions (**Figure 6**). *β*-Lactamase ligand (cefuroxime) forms five H-bonds with Lys 87, Ser 84, Ser 142, Thr 253, and Ile 117 in addition to three C-H bonds with Pro 183 and Gly 52 together with the formation of two attractive charges with Arg 236 and Lys 250. Regarding SARS-CoV-2PL^{pro} ligand S88 (N-[(3-fluorophenyl) methyl]-1-[(1R)-1-naphthalen-1-ylethyl]piperidine-4-carboxamid, it forms H-bonds with Tyr 269 and Lys 158, alkyl-alkyl interactions with Pro 249 and Tyr 265, π-alkyl interactions with Pro248 and Pro 249, π-π interactions with Tyr 269, C-H bonds with Gln 276, Tyr274, and Asp 165, in addition to the formation of the bond between Leu 163 and the halogen (Fluorine). SARS-CoV-2 3CL^{pro} ligand 3WL (5,6,7-trihydroxy-2-phenyl-4H-chromen-4-one) forms H-bonds with Leu 141, Ser144, Cys 145, and Gly 143, π-π bond with His 41, π-alkyl bond with Met 49 in addition to π-sulfur bond with Cys 145, C-H bonds with His 163 and Asn 142, and many Van der Waals interactions (**Supplementary Figure S23**). Interaction of all the metabolites with the different amino acid residues via the formation of various bonds with the active sites of proteins was illustrated in **Supplementary Figures S24–S30**.

CONCLUSION

The antimicrobial and antiviral properties of the methanol leaf extract of *Buddleja indica* Lam (Scrophulariaceae) were studied. The plant showed potent antimicrobial antituberculous, anti-*Helicobacter pylori*, and antiviral activity owing to its richness with polyphenolic compounds represented mainly by phenolic acids and flavonoids. Molecular modeling showed that caffeic acid, quercetin 7-O-*β*-D-glucoside, and kaempferol showed the highest fitting score in proteins implicated in the incidence of bacterial infection and the occurrence and progression of SARS-CoV-2 that triggered the COVID-19 pandemic. Thus, it can be considered as a future source of cheap, substantially safe, and credible antibacterial, antifungal, and antiviral candidate of natural origin. Besides, these findings provide a scientific consolidation in support of the ethnomedicinal uses of many *Buddleja* species as a topical antiseptic. However, future clinical trials are warranted for further assuring the activity as an antibacterial agent and in solving the COVID-19 crises for the whole extract and its isolated compounds as well.

DATA AVAILABILITY STATEMENT

The original contributions presented in the study are included in the article/**Supplementary Material**; further inquiries can be directed to the corresponding authors.

AUTHOR CONTRIBUTIONS

FY collected the plant and isolated and identified the compounds, interpreted the biological activities, conducted molecular modeling, and wrote the manuscript; AA and AO revised the manuscript; MA supervised the study and revised the whole manuscript.

FUNDING

This project was funded by the Deanship of Scientific Research (DSR) at King Abdulaziz University, Jeddah, Saudi Arabia, under Grant no. FP-64-42. The authors, therefore, acknowledge with thanks DSR for technical and financial support.

SUPPLEMENTARY MATERIAL

The Supplementary Material for this article can be found online at: https://www.frontiersin.org/articles/10.3389/fphar.2021.619373/full#supplementary-material.

REFERENCES

Abou-Karam, M., and Shier, W. T. (1990). A simplified plaque reduction assay for antiviral agents from plants. Demonstration of frequent occurrence of antiviral activity in higher plants. *J. Nat. Prod.* 53, 340–344. doi:10.1021/np50068a011

Acevedo, L., Martínez, E., Castañeda, P., Franzblau, S., Timmermann, B., Linares, E., et al. (2000). New phenylethanoids from *Buddleja cordata* subsp. cordata. *Planta Med.* 66, 257–261. doi:10.1055/s-2000-8570

Adedapo, A. A., Jimoh, F. O., Koduru, S., Masika, P. J., and Afolayan, A. J. (2009). Assessment of the medicinal potentials of the methanol extracts of the leaves and stems of *Buddleja saligna*. *BMC Complement. Altern. Med.* 9, 21. doi:10.1186/1472-6882-9-21

Ariga, G., Nandibewoor, S., and Chimatadar, S. (2015). Oxidative degradation of antibacterial drug, methylparaben, by MnVII in perchloric acid medium: a kinetic and mechanistic approach. *J. Indian Chem. Soc.* 92, 1–10.

Ashour, M. L., El-Readi, M. Z., Hamoud, R., Eid, S. Y., El Ahmady, S. H., Nibret, E., et al. (2014). Anti-infective and cytotoxic properties of *Bupleurum marginatum*. *Chin. Med.* 9, 1–10. doi:10.1186/1749-8546-9-4

Ashour, M. L., Youssef, F. S., Gad, H. A., El-Readi, M. Z., Bouzabata, A., Abuzeid, R. M., et al. (2018). Evidence for the anti-inflammatory activity of Bupleurum marginatum (Apiaceae) extracts using *in vitro* and *in vivo* experiments supported by virtual screening. *J. Pharm. Pharmacol.* 70, 952–963. doi:10.1111/jphp.12904

Ayoub, I. M., Youssef, F. S., El-Shazly, M., Ashour, M. L., Singab, A. N. B., and Wink, M. (2015). Volatile constituents of *Dietes bicolor* (Iridaceae) and their antimicrobial activity. *Z. für Naturforsch.C* 70, 217–225. doi:10.1515/znc-2015-0164

Bamuamba, K., Gammon, D. W., Meyers, P., Dijoux-Franca, M.-G., and Scott, G. (2008). Anti-mycobacterial activity of five plant species used as traditional medicines in the Western Cape Province (South Africa). *J. Ethnopharmacology* 117 (2), 385–390. doi:10.1016/j.jep.2008.02.007

Castillo-Juárez, I., González, V., Jaime-Aguilar, H., Martínez, G., Linares, E., Bye, R., et al. (2009). Anti-*Helicobacter pylori* activity of plants used in Mexican traditional medicine for gastrointestinal disorders. *J. Ethnopharmacology* 122, 402–405. doi:10.1016/j.jep.2008.12.021

Chiang, L. C., Chiang, W., Chang, M. Y., Ng, L. T., and Lin, C. C. (2002). Antiviral activity of *Plantago major* extracts and related compounds *in vitro*. *Antiviral Res.* 55, 53–62. doi:10.1016/s0166-3542(02)00007-4

Damyanova, S., Gomez, L. M., Bañares, M. A., and Fierro, J. L. G. (2000). Thermal behavior of 12-Molybdophosphoric acid supported on zirconium-loaded silica. *Chem. Mater.* 12, 501–510. doi:10.1021/cm9911316

Duschatzky, C. B., Possetto, M. L., Talarico, L. B., García, C. C., Michis, F., Almeida, N. V., et al. (2005). Evaluation of chemical and antiviral properties of essential oils from South American plants. *Antivir. Chem. Chemother.* 16, 247–251. doi:10.1177/095632020501600404

Gaind, K. N., Gaind, K. N., Singla, A. K., and Wallace, J. W. (1981). Flavonoid glycosides of *Kalanchoe spathulata*. *Phytochemistry* 20, 530–531. doi:10.1016/s0031-9422(00)84187-4

Gamal El-Din, M. I., Youssef, F. S., Ashour, M. L., Eldahshan, O. A., and Singab, A. N. B. (2018). Comparative analysis of volatile constituents of *Pachira aquatica* Aubl. and *Pachira glabra* Pasq., their anti-Mycobacterial and *anti-Helicobacter pylori* activities and their metabolic discrimination using chemometrics. *J. Essent. Oil Bearing Plants* 21, 1550–1567. doi:10.1080/0972060x.2019.1571950

Gansukh, E., Kazibwe, Z., Pandurangan, M., Judy, G., and Kim, D. H. (2016). Probing the impact of quercetin-7-*O*-glucoside on influenza virus replication influence. *Phytomedicine* 23, 958–967. doi:10.1016/j.phymed.2016.06.001

Guillermo Avila, J., de Liverant, J. G., Martínez, A., Martínez, G., Muñoz, J. L., Arciniegas, A., et al. (1999). Mode of action of *Buddleja cordata* verbascoside against *Staphylococcus aureus*. *J. Ethnopharmacology* 66, 75–78. doi:10.1016/s0378-8741(98)00203-7

Hadizadeh, F., Khalili, N., Hosseinzadeh, H., and Khair-Aldine, R. (2003). Kaempferol from saffron petals. *Chem.Preprint Arch.* 2, 234–239.

Janibekov, A. A., Youssef, F. S., Ashour, M. L., and Mamadalieva, N. Z. (2018). New flavonoid glycosides from two *Astragalus* species (Fabaceae) and validation of their antihyperglycaemic activity using molecular modelling and *in vitro* studies. *Ind. Crops Prod.* 118, 142–148. doi:10.1016/j.indcrop.2018.03.034

Jeong, C. H., Jeong, H. R., Choi, G. N., Kim, D. O., Lee, U., and Heo, H. J. (2011). Neuroprotective and anti-oxidant effects of caffeic acid isolated from *Erigeron annuus* leaf. *Chin. Med.* 6, 1–9. doi:10.1186/1749-8546-6-25

Langland, J., Jacobs, B., Wagner, C. E., Ruiz, G., and Cahill, T. M. (2018). Antiviral activity of metal chelates of caffeic acid and similar compounds towards *herpes simplex*, VSV-Ebola pseudotyped and vaccinia viruses. *Antiviral Res.* 160, 143–150. doi:10.1016/j.antiviral.2018.10.021

Manuja, R., Sachdeva, S., Jain, A., and Chaudhary, J. (2013). A comprehensive review on biological activities of *p*-hydroxy benzoic acid and its derivatives. *Int. J. Pharm. Sci. Rev. Res.* 22, 109–115.

Mehta, P., McAuley, D. F., Brown, M., Sanchez, E., Tattersall, R. S., Manson, J. J., et al. (2020). COVID-19: consider cytokine storm syndromes and immunosuppression. *The Lancet* 395, 1033. doi:10.1016/S0140-6736(20)30628-0

Mensah, A. Y., Houghton, P. J., Bloomfield, S., Vlietinck, A., and Vanden Berghe, D. (2000). Known and novel terpenes fromBuddleja globosaDisplaying selective antifungal activity against dermatophytes. *J. Nat. Prod.* 63 (9), 1210–1213. doi:10.1021/np0001023

Munnink, B. B. O., Nieuwenhuijse, D. F., Stein, M., O'Toole, Á., Haverkate, M., Mollers, M., et al. (2020). Rapid SARS-CoV-2 whole-genome sequencing and analysis for informed public health decision-making in The Netherlands. *Nat. Med.* 26, 1–6. doi:10.1038/s41591-020-0997-y

Rahman, A.-U., Choudhary, M. I., and Thomsen, W. J. (2001). *Bioassay techniques for drug development*. Netherlands: Harwood Academic Publishers.

Rathore, H., Mittal, S., and Kumar, S. (2000). Synthesis, characterization and antifungal activities of 3d-transition metal complexes of 1-acetylpiperazinyldithiocarbamate, M (acpdtc) 2. Pestic. Res. J . 12, 103–107.

Schwarz, S., Sauter, D., Wang, K., Zhang, R., Sun, B., Karioti, A., et al. (2014). Kaempferol derivatives as antiviral drugs against the 3a channel protein of coronavirus. *Planta Med.* 80, 177. doi:10.1055/s-0033-1360277

Thabet, A. A., Youssef, F. S., El-Shazly, M., El-Beshbishy, H. A., and Singab, A. N. B. (2018a). Validation of the antihyperglycaemic and hepatoprotective activity of the flavonoid rich fraction of *Brachychiton rupestris* using *in vivo* experimental models and molecular modelling. *Food Chem. Toxicol.* 114, 302–310. doi:10.1016/j.fct.2018.02.054

Thabet, A. A., Youssef, F. S., Korinek, M., Chang, F.-R., Wu, Y.-C., Chen, B.-H., et al. (2018b). Study of the anti-allergic and anti-inflammatory activity of *Brachychiton rupestris* and *Brachychiton discolor* leaves (Malvaceae) using *in vitro* models. *BMC Complement. Altern. Med.* 18 (1), 299. doi:10.1186/s12906-018-2359-6

Van de Loosdrecht, A. A., Nennie, E., Ossenkoppele, G. J., Beelen, R. H. J., and Langenhuijsen, M. M. A. C. (1991). Cell mediated cytotoxicity against U 937 cells by human monocytes and macrophages in a modified colorimetric MTT assay. *J. Immunological Methods* 141 (1), 15–22. doi:10.1016/0022-1759(91)90205-t

Wang, G. F., Shi, L. P., Ren, Y. D., Liu, Q. F., Liu, H. F., Zhang, R. J., et al. (2009). Anti-hepatitis B virus activity of chlorogenic acid, quinic acid and caffeic acid *in vivo* and *in vitro*. *Antiviral Res.* 83, 186–190. doi:10.1016/j.antiviral.2009.05.002

Weng, J. R., Lin, C. S., Lai, H. C., Lin, Y. P., Wang, C. Y., Tsai, Y. C., et al. (2019). Antiviral activity of *Sambucus* FormosanaNakai ethanol extract and related phenolic acid constituents against human coronavirus NL63. *Virus. Res.* 273, 197767. doi:10.1016/j.virusres.2019.197767

World Health Organization (2004). *Laboratory biosafety manual*. 3rd Edn. Switzerland: World Health Organization press.

Youssef, F. S., Ashour, M. L., El-Beshbishy, H. A., Singab, A. N. B., and Wink, M. (2019). Metabolic profiling of *Buddleia indica* leaves using LC/MS and evidence of their antioxidant and hepatoprotective activity using different *in vitro* and *in vivo* Experimental models. *Antioxidants* 8 (9), 412. doi:10.3390/antiox8090412

Youssef, F. S., Ashour, M. L., Sobeh, M., El-Beshbishy, H. A., Singab, A. N., and Wink, M. (2016). *Eremophila* maculata-Isolation of a rare naturally-occurring lignan glycoside and the hepatoprotective activity of the leaf extract. *Phytomedicine* 23, 1484–1493. doi:10.1016/j.phymed.2016.08.006

Youssef, F. S., Ashour, M. L., and Wink, M. (2018). Morphological, anatomical, genetical and high performance thin layer chromatography profiling of *Buddleia indica* (Scrophulariaceae). *Flora* 246–247, 83–95. doi:10.1016/j.flora.2018.07.007

Youssef, F. S., Hamoud, R., Ashour, M. L., Singab, A. N., and Wink, M. (2014). Volatile oils from the aerial parts of Eremophila maculataand their antimicrobial activity. *Chem. Biodiversity* 11, 831–841. doi:10.1002/cbdv.201300366

Conflict of Interest: The authors declare that the research was conducted in the absence of any commercial or financial relationships that could be construed as a potential conflict of interest.

frontiers in Pharmacology

ORIGINAL RESEARCH
published: 19 April 2021
doi: 10.3389/fphar.2021.635510

Giloy Ghanvati (*Tinospora cordifolia* (Willd.) Hook. f. and Thomson) Reversed SARS-CoV-2 Viral Spike-Protein Induced Disease Phenotype in the Xenotransplant Model of Humanized Zebrafish

Acharya Balkrishna[1,2], *Lakshmipathi Khandrika*[1] *and Anurag Varshney*[1,2]*

[1]*Drug Discovery and Development Division, Patanjali Research Institute, Haridwar, India,* [2]*Department of Allied and Applied Sciences, University of Patanjali, Patanjali Yog Peeth, Haridwar, India*

OPEN ACCESS

Edited by:
Vijay Kumar Prajapati,
Central University of Rajasthan, India

Reviewed by:
Binay Chaubey,
University of Gdansk, Poland
Rohit Sharma,
Banaras Hindu University, India

***Correspondence:**
Anurag Varshney
anurag@prft.co.in

Specialty section:
This article was submitted to Ethnopharmacology, a section of the journal Frontiers in Pharmacology

Received: *30 November 2020*
Accepted: *26 February 2021*
Published: *19 April 2021*

Citation:
*Balkrishna A, Khandrika L and Varshney A (2021) Giloy Ghanvati (*Tinospora cordifolia *(Willd.) Hook. f. and Thomson) Reversed SARS-CoV-2 Viral Spike-Protein Induced Disease Phenotype in the Xenotransplant Model of Humanized Zebrafish. Front. Pharmacol. 12:635510. doi: 10.3389/fphar.2021.635510*

The current Severe Acute Respiratory Syndrome disease caused by Coronavirus-2 (SARS-CoV-2) has been a serious strain on the healthcare infrastructure mainly due to the lack of a reliable treatment option. Alternate therapies aimed at symptomatic relief are currently prescribed along with artificial ventilation to relieve distress. Traditional medicine in the form of Ayurveda has been used since ancient times as a holistic treatment option rather than targeted therapy. The practice of Ayurveda has several potent herbal alternatives for chronic cough, inflammation, and respiratory distress which are often seen in the SARS-CoV-2 infection. In this study we have used the aqueous extracts of *Tinospora cordifolia* (willd.) Hook. f. and Thomson in the form of Giloy Ghanvati, as a means of treatment to the SARS-CoV-2 spike-protein induced disease phenotype in a humanized zebrafish model. The introduction of spike-protein in the swim bladder transplanted with human lung epithelial cells (A549), caused an infiltration of pro-inflammatory immune cells such as granulocytes and macrophages into the swim bladder. There was also an increased systemic damage as exemplified by renal tissue damage and increased behavioral fever in the disease induction group. These features were reversed in the treatment group, fed with three different dosages of Giloy Ghanvati. The resultant changes in the disease phenotype were comparable to the group that were given the reference compound, Dexamethasone. These findings correlated well with various phyto-compounds detected in the Giloy Ghanvati and their reported roles in the viral disease phenotype amelioration.

Keywords: tinopsora cordifolia, ayurved, viral disease, SARS–CoV–2, inflamation, zebrafish, xenotranplantation, giloy ghanvati

INTRODUCTION

Herbal medicine in the form of Ayurveda, is a well-documented and widely accepted traditional medical system in India. The use of traditional and complementary medicine is often seen in chronic illness and a general improvement of wellness (Hankey, 2010; Balkrishna, 2015). During recent times, the use of herbal based formulations has been on the rise in the direct treatment of infectious diseases. WHO has also been encouraging the research and development of traditional medicine in areas that are convergent with the modern medicine to help tackle the unique challenges posed in the 21st century (WHO, 2019).

Tinospora cordifolia (willd.) Hook. f. and Thomson is a climbing shrub that is widely distributed throughout the tropical and subtropical regions of Asia, Africa, and Australia. The different members of this family are a rich source of polysaccharides, terpenes, and alkaloids that have demonstrated activity as anti-inflammatory (Tiwari et al., 2014), immune-stimulatory including phagocytosis (Sharma et al., 2012), anti-diabetic (Sharma et al., 2013), anti-oxidant (Imtiyaj Khan et al., 2011) among others (Panchabhai et al., 2008). Compounds belonging to different classes such as Sesquiterpenes, Phenylpropanoids, and alkaloids were isolated and identified from various water and solvent fractions (Kapil and Sharma, 1997; Cho et al., 2001). Though not much work has been done to demonstrate anti-viral activity of this plant, aqueous extract of the stems of *T. cordifolia* was shown to augment the immune protective response of a commercially available Infectious Bursal disease vaccine in chicks (Sachan et al., 2019). In-silico studies using Berberine, Isocolumbin, Magnoflorine, and Tinocordiside showed high binding affinity for the surface glycoprotein, receptor binding domain, RNA dependent RNA polymerase, and main protease of SARS-CoV-2 virus (Sagar and Kumar, 2020).

The SARS-CoV-2 virus modality has been thoroughly investigated and the accumulation of pro-inflammatory cytokines and immune cells in the target tissue has been shown to be the main culprit for large scale systemic disease (Abebe et al., 2020; Inciardi et al., 2020). The robust inflammatory response as a result of viral entry, has been shown to be associated with a greater risk of long term multi-organ damage and adverse outcomes. As of today, there is no effective and recommended therapy for the novel virus; clinical management consists mainly of supportive care and symptomatic relief.

Since, the SARS-CoV-2 infection targets multiple organs, a holistic approach that can alleviate multiple symptoms may be the ideal answer to the current crisis. Ayurveda system of medicine is based on restoring balance to the body rather than just treating the source of the disease. Therapies typically are formulations that include complex herbal mixtures, minerals and metals or their bhasmas (ash, mineral salts treated with herbal concoctions and fried in metallic containers) (Meulenbeld, 1999; Liu et al., 2019). *T. cordifolia* has been prescribed in ayurveda for infective conditions, sporadic fever, skin diseases, urinary disorders, and eye diseases (Chi et al., 2016).

Giloy Ghanvati is the aqueous extracts of *T. cordifolia* that has been manufactured in the form of tablets by Patanjali Ayurveda Limited, Haridwar, India. In the current study, we have used a humanized zebrafish model for determining the effect of Giloy Ghanvati in reversing the inflammation, and tissue damage caused by the induction of SARS-CoV-2 spike protein.

Zebrafish (*Danio rerio*) has been a reliable model for infectious diseases and studying the immune function in response to the introduction of human viruses (Sullivan and Kim, 2008; Van Dycke et al., 2019). The similarities in the immune cells, cytokines, and the presence of various receptors that are required for host-pathogen interactions makes the correlation of zebrafish research to humans, very much relevant (Targen et al., 2020). Xeno-transplantation was achieved by introducing human lung epithelial A549 cells into the swim bladder of the fish (Shen et al., 2020).

We demonstrate the pro-inflammatory changes and tissue damage induced by SARS-CoV-2 spike-protein induction in the zebrafish and show the rescue of the disease pathology upon treatment with Giloy Ghanvati through morphological examination of the swim bladder and kidney, quantitate the immune cell infiltration through cytology, and finally show the restoration of behavioral fever and mortality induced by the spike protein.

MATERIALS AND METHODS

Chemicals and Reagents

Recombinant spike-protein of SARS-CoV-2 virus was procured from Bioss Antibodies (Woburn, MA, United States). Giloy Ghanvati (made of the extracts of *Tinospora cordifolia* (willd.) Hook. f. and Thomson) tablets were sourced from Patanjali Ayurveda Limited (Haridwar, Uttarakhand, India), with batch number AAI20/557 and expiry date of May 2022. All other chemicals and reagents used in the study were at least of an analytical grade and procured from Sigma-Aldrich India Limited (Bengaluru, Karnataka, India).

HPLC Analysis of Giloy Ghanvati

Preparation of Samples

Giloy Ghanvati is available as tablets and for this analysis, the tablets were finely powdered and 0.5 gm powder was diluted with 10 ml methanol: water (70:30) and sonicated for 30 min. The extract was centrifuged at 8000 rpm for 5 min at 4°C and filtered using 0.45 µm nylon filter. This was labeled as a working solution and was used for the analysis of Cordifolioside A, Palmatine and Beta-Ecdysone. The working solution was further diluted to 10 times with same solvent as above and used for the analysis of Magnoflorine.

Standards used for comparative analysis were dissolved in methanol to get the desired concentrations. Palmatine hydrochloride hyrate (Potency-97.0%) and Magnoflorine (Potency-99.0%) were procured from Sigma-Aldrich (St. Louis, MO, United States), Cordifolioside A (Potency-98.6%, ChemFaces, Wuhan, Hubei Province, China), and Beta-Ecdysone (Potency-99.0%, Tokyo Chemical Industries, Tokyo, Japan) were used as standards.

TABLE 1 | Inclusion criteria for model zebrafish in the study.

Gender	Male and female
Age	1 year
Body weight	0.5 g
Body length	25–30 mm
No. of fish per group	24
No. of fish per tank	12
Tank capacity	6 L

Zebrafish Husbandry

Standard protocols for zebrafish rearing and maintenance were followed. Fish were bred and reared in a fish rearing facility under guidelines from the Committee for the Purpose of Control and Supervision of Experiments on Animals (CPCSEA), India. Wild-Type *Danio rerio* were maintained in freshwater at a temperature of 27°C (±1°C) at a stocking density of two fish per liter water. The general characteristics of the fish used in the study are listed in **Table 1**. The tanks were under an automated photoperiod of 14-h light and 10-h dark (Westerfield, 1993; Avdesh et al., 2012; Aleström et al., 2020). Water and housing standards were maintained according to ethical standards and were overseen by the institutional animal ethics committee (vide protocol number: Go062020/IAEC). Feeding was on a 24-h cycle and each fish was given commercially available dry feed (TetraBit, Spectrum Brands Pet LLC, Blacksburg, VA, United States) according to their body weight at 5 mg per Gram.

Cell Culture

Human lung alveolar epithelial cells (A549) were procured from ATCC (Licensed repository in India at National Center for Cell Sciences, NCCS, Pune, Maharashtra, India). Cells were cultured in Dulbecco's Modified Eagle's Medium (DMEM, High Glucose) supplemented with 10% (v/v) Fetal Bovine Serum and 1% (v/v) Penicillin-Streptomycin solution (Invitrogen Life Technologies, Carlsbad, CA, United States). Stock cells frozen under liquid nitrogen were passaged at least twice before using for xeno-transplantation. Culture at about 70% confluent and at the third passage was used in the study.

Anesthesia for Xeno-Transplantation and Disease Induction

Water at a temperature lower than that is used for regular zebrafish maintenance was utilized as a means of anesthesia for the zebrafish (Chen et al., 2014; Oskay et al., 2018). Two different anesthesia tanks were set-up to maintain a constant temperature of 17 and 12°C. Changes to the operculum movement was used as a measure to determine the effect of cold water for anesthetization. The fish from the respective clutches were individually transferred to the 17°C tank and when the operculum movement was reduced visibly, the fish was transferred to the 12°C tank. The lack of a response to caudal fin touch was taken as a confirmation of complete anesthetization of the fish. After this, each fish was transferred to a stage for injection of either the human lung epithelial cells or the SARS-CoV-2 spike-protein for disease induction.

Humanized Zebrafish Model Preparation

A549 cells (1×10^2) were resuspended in a minimal volume of PBS at pH 7.4, to be used for generating the zebrafish xenograft model. Cells were injected intramuscularly along the midline at the junction of the trunk and caudal regions of experimental fish. After cell transplantation, the fish were observed for a period of 7 days to ensure that no changes to the physiology of the fish occurred due to the procedure. A few of the fish were sacrificed on the seventh day and the swim bladder was dissected out. Cytological smears of the bladder were stained with Hematoxylin-Eosin to confirm the A549 cell attachment to the swim bladder epithelium of the xeno-transplanted zebrafish (**Figure 1**). These fish were labeled as the "Humanized Zebrafish" or "HZF" group. Equal number of healthy fish were also injected with the same volume of PBS at pH 7.4 and were labeled as the "Normal control" group (**Figure 1**).

Induction of Disease Phenotype using Recombinant Spike-Protein of Sars-Cov-2

Once the A549 cells were successfully transplanted in the zebrafish, SARS-CoV-2 recombinant spike protein was injected into the swim bladder at the site of xenotransplant. Recombinant spike-protein of the SARS-CoV-2 virus was resuspended at a concentration of 1 μg/μL in PBS at pH 7.4. This was further diluted to a working concentration of 1 ng/μL by diluting 1 μL of the stock solution (1 μg/μL) in a final volume of 1 ml. This working solution was used to induce disease phenotype by injecting 2.8 ng (2.8 μL of the 1 ng/μL working solution) into the site of A549 cell xenograft, at the junction of the trunk and caudal regions along the midline. This group was labeled as the "Humanized zebrafish with SARS-CoV-2 Spike protein" or "HZF-SARS-CoV-2-S" (**Figure 1**).

Dosing of Zebrafish with Either the Reference Drug or Giloy Ghanvati

Each tablet of Giloy Ghanvati contains 500 mg of Giloy stem extract powder mixed with 78 mg of excipients. Microcrystalline Cellulose (MCC, 30 mg), Magnesium Stearate (1 mg), Erosil (8 mg), Talcum (6 mg), Gum acacia (28 mg), and Hydroxypropyl methylcellulose (HPMC, 5 mg) form the excipients to give a tablet of 578 mg total weight.

Three different doses of Giloy Ghanvati (GG) were used in the study at 0.2X, 1X, and 5X of human equivalent doses. The human dosage of GG was –2 gm/day according to the manufacturer's license sheet and the translational dosages were calculated following the principles approved by USFDA (Sharma and McNeill, 2009). Dexamethasone was used as a reference drug and this was used at 1X. The translational doses were calculated to be 80 ng/kg/day for study reference drug, Dexamethasone and 6, 28, and 142 μg/kg/day for GG (**Figure 1**).

Fish were dosed orally with feed infused with the standard and test compounds at the desired dosages. For this, known quantity

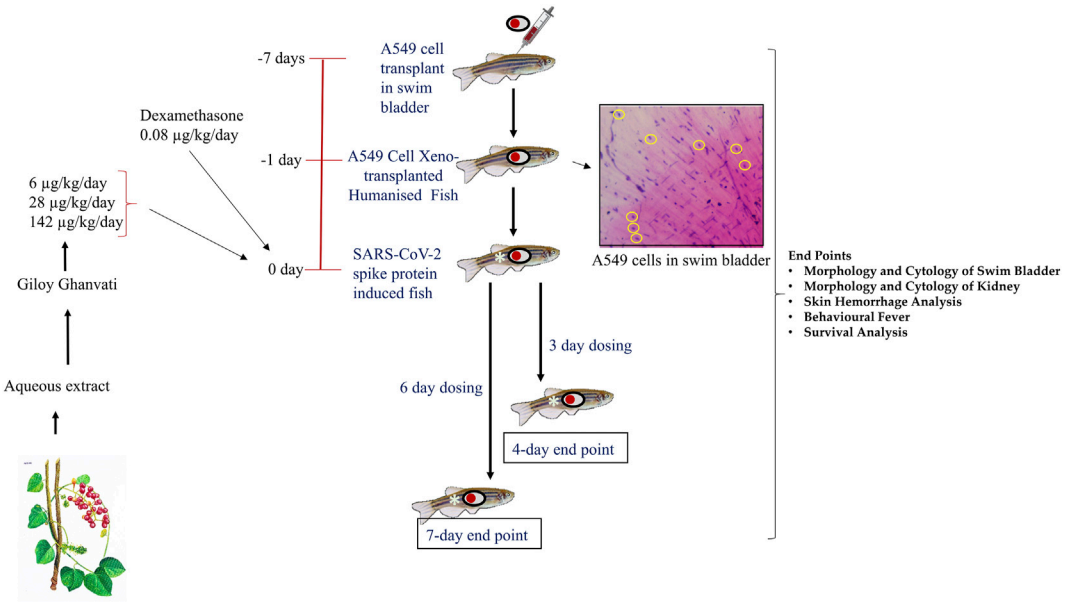

FIGURE 1 | Schematic representing the study design depicting timeline for xenotransplantation, induction with spike-protein of SARS-CoV-2 and treatment with Giloy Ghanvati (GG) and Dexamethasone as a reference drug. The inset shows the hematoxylin-eosin staining of swim bladder cytological smear. The transplanted A549 cells are highlighted in yellow circles.

of compounds for a 2.5 mg pellet was mixed with the commercially available feed and then extruded into pellets. The GG tablets (*T. cordifolia*) were crushed into a fine powder with a mortar and pestle under liquid nitrogen to prevent moisture accumulation. Each fish isolated from the groups and was fed individually with the required number of pellets per day. The normal control group was fed with the unmodified feed under similar conditions.

End-points for Screening

Two time points were chosen for the dosing, in one part of the study, the fish were dosed for 3 days and terminated on the fourth day. This time point was referred to as 4 days. In another part, the fish were dosed for 6 days and then terminated on the seventh day; this time point was referred to as 7 days (**Figure 1**). In a parallel experiment, 24 fish in each of the groups, Normal control, HZF, Disease control, Dexamethasone (1 dose) and Giloy Ghanvati (GG) treatments (3 doses) were studied for survival analysis. Mortality, if any, was recorded daily and then plotted by using Kaplan-Meier curve.

Assessment of Behavioral Fever

Behavioral fever is a reflection of the internal body temperature in fish. Since zebrafish is an ectotherm and there is no regulation of the body temperature, the fish moves to an environment that matches the body temperature. To determine the changes to behavior and assess behavioral fever, interconnected tanks with each chamber at a different temperature (23, 29, and 37°C) were used. The temperature of each compartment is automatically maintained and the time spent by each fish in the individual temperature chambers is recorded over a period of 180 s. Behavioral fever was assessed at the end of the study period and if the fish spend more time in the higher temperature chamber, it was recorded as the presence of a fever.

Euthanization and Dissection

Fish were euthanized using hypothermal shock at 4°C (Matthews and Varga, 2012). A temperature controlled cooling bath was attached to the euthanasia tank and each fish was individually transferred to the tanks. Cessation of vital signs such as operculum movement, heartbeat, and righting of the equilibrium was considered as a successful euthanization.

The fish was transferred to a stage and dissected through a ventral incision in the skin from the lower jaw to the vent. Care was taken to follow all the institutional animal ethics committee's guidelines for proper dissection protocol. The intestine was removed carefully without disturbing the swim bladder which is connected to the esophagus. The gonads were removed carefully and discarded.

Dissection of Swim Bladder for Morphological and Cytological Analysis

The swim bladder is located ventral to the kidneys and is a gas filled chamber with two distinct compartments (Menke et al., 2011). The posterior lobe is connected to the esophagus through a pneumatic duct. After isolation of the intact swim bladder it was immediately transferred to a beaker with PBS at pH 7.4. The bladder was gently washed once and observed under a stereomicroscope at ×1 magnification (Labomed CM4, Labomed Inc., Los Angeles, CA, United States). The images were captured using a camera attachment with the microscope at 14 MP resolution under transmitted light.

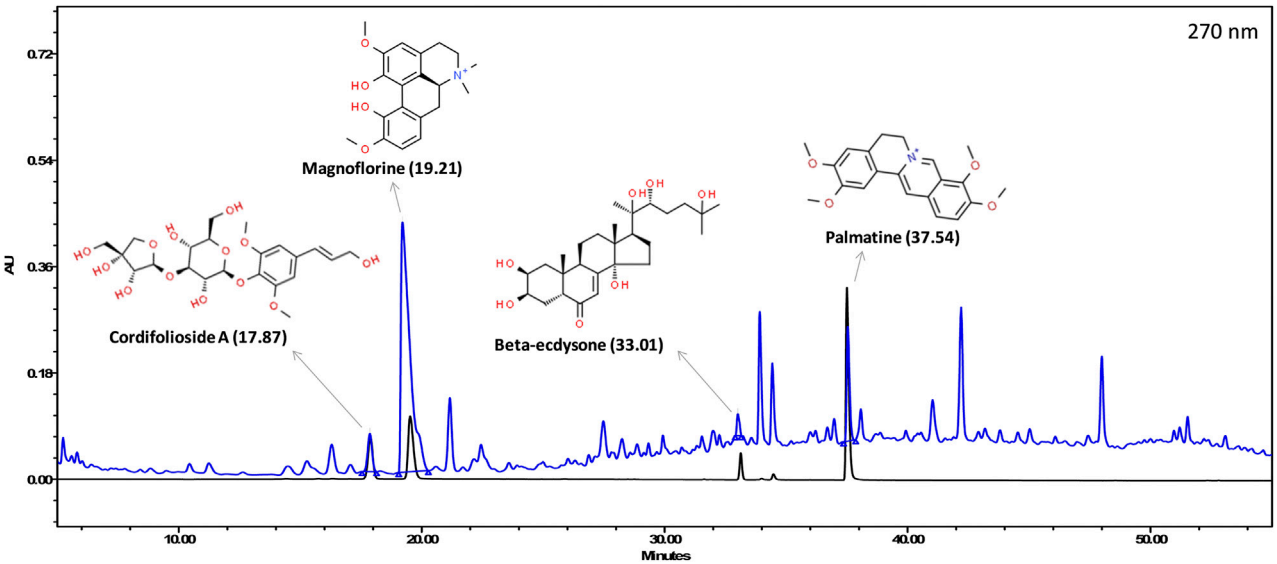

FIGURE 2 | HPLC profile showing an overlap of Giloy Ghanvati aqueous extract (blue chromatogram) and a mixture of standards (black chromatogram). The structures of the phyto-compounds and their retention time are depicted.

Cytology slides were prepared from whole swim bladder necropsy and were stained with Hematoxylin and eosin. Stained sections were imaged at ×20 magnification using Labomed light microscope (Labomed Inc., Los Angeles, CA, United States) and recorded with a camera attached to the microscope.

Morphological and Cytological Observation of Kidney

The zebrafish kidney has three morphologically distinct regions called the head, trunk (or saddle), and the tail. It is present ventral to the vertebral column (Menke et al., 2011). For dissecting the kidney, the fish was pinned with its ventral side up to expose the organ attached to the dorsal body wall. The morphological features of the kidney were imaged under transmitted light using a Labomed CM4 stereomicroscope at ×1 magnification.

Hematoxylin-Eosin stained cytological smears were used to determine necrotic and degenerative changes in the kidney. The stained sections were observed at ×20 objective magnification using a Labomed light microscope. Images were captured using a camera attachment to the microscope.

Detection of Clinical Signs of Skin Hemorrhage

Euthanized fish were washed once in PBS at pH 7.4, and patted dry with a paper towel. The fish were transferred to a stage and photographed using a Digital Single Lens Reflex camera under reflected light (Nikon D3100, Nikon Corporation, Chiyoda, Japan).

Data Analysis

All data points are represented as mean with Standard Deviation (S.D.) and displayed graphically using GraphPad Prism (Version 7.04, GraphPad Software Inc., San Diego, CA, United States). All statistical analysis was carried out by Two-Way ANOVA with Tukey's multiple comparison for determining significance. A p-value less than 0.05 was considered to be significant.

RESULTS

The various phyto-compounds of Giloy Ghanvati (GG) were analyzed using a Shodex C18-4E column as described in the methods section. Four constituents were identified based on the retention time and comparison with appropriate standards (**Figure 2**). Cordifolioside A (1.62 μg/mg dry weight of GG), Magnoflorine (11.00 μg/mg), β-Ecdysone (1.75 μg/mg), and Palmatine (1.08 μg/mg) were the main phyto-compounds detected, whereas any others present were below the detection limits. The concentration of Magnoflorine in the GG samples was higher, therefore its peak on the HPLC chromatogram appeared broader, and possibly merged with the peak of another unidentified compound.

Giloy Ghanvati Reversed SARS-CoV-2 Spike-Protein Induced Edema and Inflammatory Cell Infiltration in Swim Bladder

The swim bladder is a two lobed buoyancy organ which is filled with air when the fish takes a gulp of air through the mouth. The lobes are connected by a wide ductus communicans and they pulsate rhythmically. The inner gas gland is enveloped by a mesothelial tunica externa and is made up of epithelial cells, a smooth muscle layer, and a submucosal layer where most of the vasculature resides.

At the 4-days time point, the anterior lobe (AL) and the posterior (PL) of the swim bladder in both the normal control and the humanized zebrafish control (HZF) groups showed normal

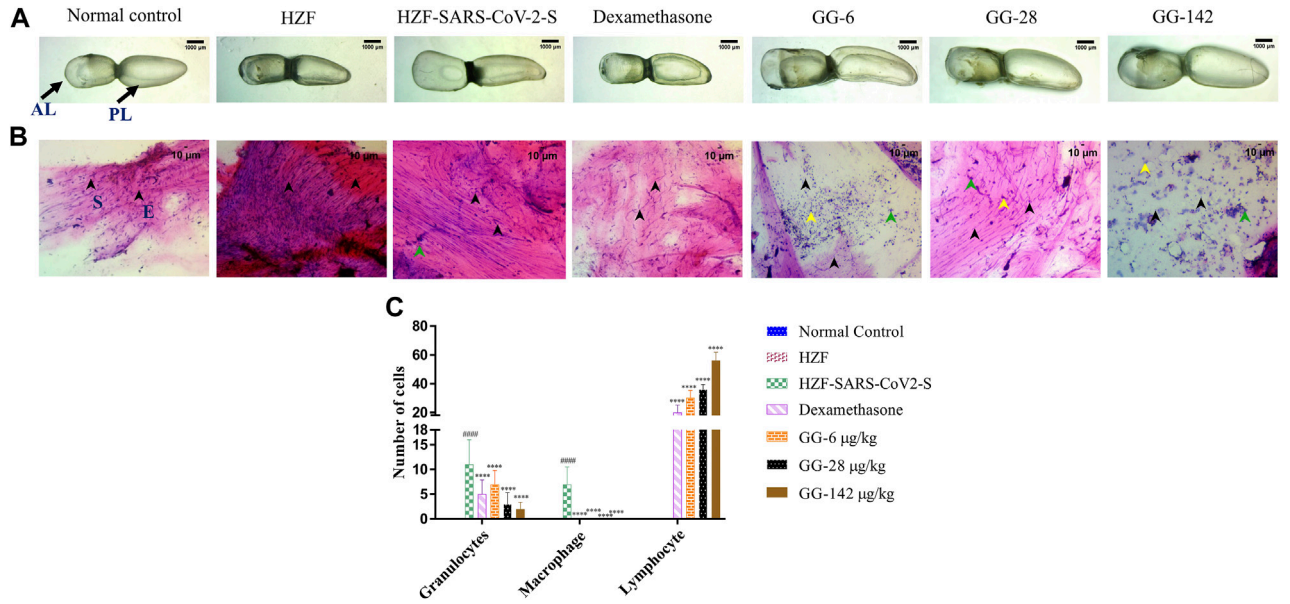

FIGURE 3 | 4-days time point to determine changes in morphology, cytology, and immune cell infiltration in the swim bladder. **(A)** Morphological changes in swim bladder with SARS-CoV-2 spike-protein induction, and treatment with Dexamethasone and Giloy Ghanvati (GG) at different concentrations (6, 28, and 142 µg/kg/day) at the 4-days time point. Images depict lateral view with the anterior lobe (AL) and posterior lobe (PL) marked. Images were taken at ×1 magnification. **(B)**. Hematoxylin-Eosin stained cytology smears of whole swim bladder. Images were captured at ×20 objective magnification. Normal cell nuclei depicted by black arrowheads; E-Epithelial cells, and S- Smooth muscle cells. Green arrowheads show granulocytes and the yellow arrowheads show lymphocytes. **(C)** Quantitative estimation of immune cell infiltrates in the swim bladder. Data points are depicted as mean ± S.D. analyzed by Two-Way ANOVA followed by Tukey's multiple comparisons test. $n = 24$, (####) $p < 0.0001$ compared to normal control, (****) $p < 0.0001$ compared to disease control.

appearance in size, shape, and color with continuous tunica externa and mesothelial lining of smooth muscle (**Figure 3A**). The disease control group (HZF-SARS-CoV-2-S) in contrast, had an inflated anterior lobe in comparison to the posterior lobe suggesting an accumulation of edematous gas. Treatment with Dexamethasone, showed the reversal of the edematous appearance and restoration of the size and shape to that seen in the normal control group. Treatment with the lowest concentration (6 µg/kg/day) of GG powdered tablet was not enough to rescue the phenotypic changes seen with the induction using SARS-CoV-2 spike protein. The anterior lobe was inflated with a discontinuous tunica externa and mesothelial lining of smooth muscle. Both the higher dilutions (28 and 142 µg/kg/day) in contrast, showed restoration of the swim bladder morphology to near normal condition as seen in the normal control group.

Cytological smears were prepared from whole mounts of the swim bladder and stained with Hematoxylin-Eosin to determine the different cell types present in the swim bladder and to quantitate the immune cell infiltration in response to the SARS-CoV-2 spike protein. The different cell types present were identified as squamous epithelium with spherical nuclei, columnar epithelium with oval nuclei, and smooth muscle cells with elongated nuclei and densely staining eosinophilic collagen. The normal control and HZF group showed normal distribution of epithelial (E, denoted by black arrowhead) and smooth muscle cells (S) as shown in **Figure 3B**. The disease control group showed an increase in the number of immune cells inside the swim bladder, as shown in a representative cytology image showing the presence of granulocytes (green arrowhead). Quantitative estimation of immune cell infiltrates showed a significantly higher ($p < 0.0001$) number of macrophages and granulocytes in the SARS-CoV-2 spike-protein induction models compared to the normal control (**Figure 1C**). Lymphocytes were conspicuously absent in the disease control model.

Treatment with Dexamethasone at 80 ng/kg/day significantly reduced the number of granulocytes with undetectable macrophage count. Conversely, the number of lymphocytes was significantly higher ($p < 0.0001$) suggesting a protective effect of dexamethasone. GG at a lower concentration of 0.2X relative to the human dose, showed a significantly lower number of granulocytes and an absence of macrophages when compared to the disease control. The number of lymphocytes was significantly higher ($p < 0.0001$) in comparison to both the disease control as well as the group treated with Dexamethasone. A dose dependent decrease in the number of granulocytes was observed at the 4 days time point, with increase in the concentration of GG given. Similarly, a dose dependent increase in the number of lymphocytes was also observed.

At the 7 days time point, the swim bladder dissected from the disease control group, showed much higher levels of edema with even a few of the swim bladders collapsing structurally (**Figure 4A**). The representative bladder showed in the figure, had swollen lobes and a collapsed ductus communicans due to an increase in pressure within the lobes. Treatment with Dexamethasone reversed some of the edematous gas accumulation but not completely as could be seen in the collapsed anterior lobe of the swim bladder. The GG treated

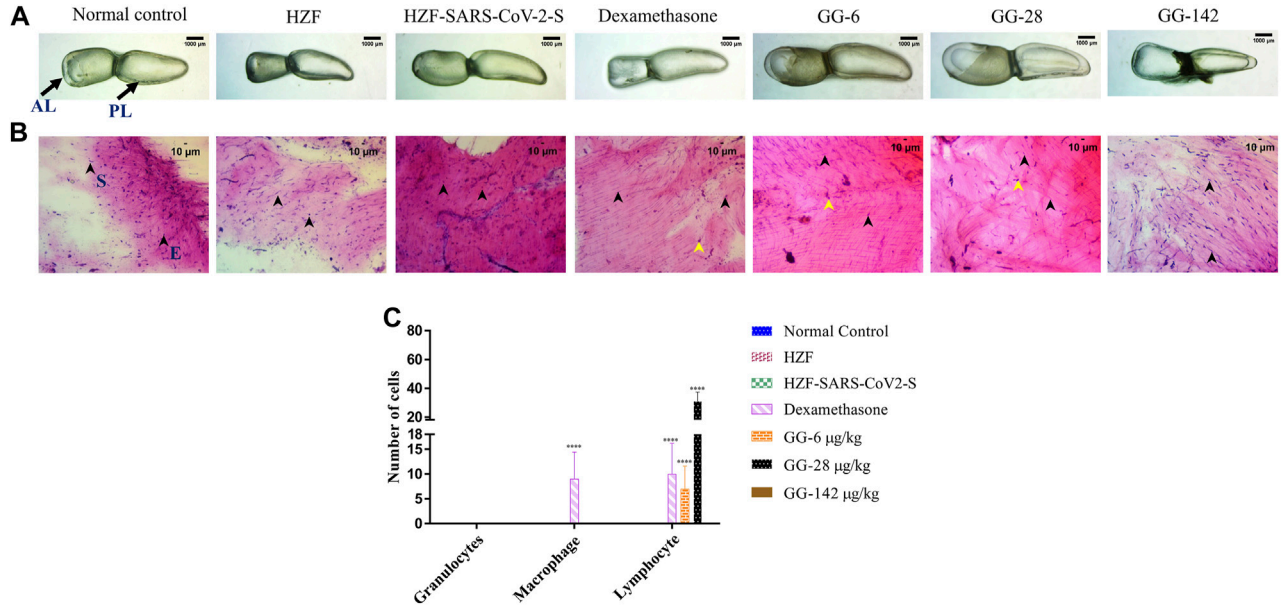

FIGURE 4 | Comparison of changes in swim bladder morphology, cytology, and immune cell infiltrates at 7-days time point. **(A)** Morphological changes in swim bladder with SARS-CoV-2 spike-protein induction, and treatment with Dexamethasone and Giloy Ghanvati (GG) at different concentrations (6, 28, and 142 µg/kg/day) compared to the normal control and humanized zebrafish. Images depict lateral view with the anterior lobe (AL) and posterior lobe (PL) marked. Images were taken at ×1 magnification. **(B)**. Hematoxylin-Eosin stained cytology smears of whole swim bladder captured using ×20 objective magnification. Normal cell nuclei depicted by black arrowheads; E- Epithelial cells, and S- Smooth muscle cells. Yellow arrowheads in the images show lymphocytes. **(C)** Quantitative estimation of immune cell infiltrates in the swim bladder. Data points are depicted as mean ± S.D. analyzed by Two-Way ANOVA followed by Tukey's multiple comparisons test. (****) $p < 0.0001$ compared to disease control, $n = 24$.

groups on the other hand showed a reversal of the edematous appearance and the swim bladder morphology was comparable to the normal and HZF control groups.

Cytological examination of the swim bladder showed normal distribution of the smooth muscle and epithelial cells in both the normal control and the HZF group (**Figure 4B**). The HZF group also showed the presence of the transplanted A549 cells in addition to the normal swim bladder cells. Surprisingly, the disease control group also did not show the presence of any immune cell infiltration at the 7-days time point. This could be a result of the disease being self-limiting after several days of induction with the spike protein. Dexamethasone treatment showed a significantly higher ($p < 0.0001$) presence of macrophages and lymphocytes in comparison to the disease control group (**Figure 4C**). Macrophages could not be detected in any of the 3 GG treatment groups, while a significant increase in the number of lymphocytes was detected upon treatment with 6 and 28 µg/kg/day. In contrast, the highest concentration (142 µg/kg/day) of GG did not show the presence of lymphocytes.

Recovery of Renal Damage Due to SARS-CoV-2 Spike-Protein by Giloy Ghanvati

The kidney is attached to the parenchymal layer in the dorsal wall of the body cavity. Three distinct regions could be identified in the kidney called the head, trunk (or saddle), and tail, extending from the anterior to the posterior of the body. The head of the kidney is packed with the mesonephric nephrons with glomerular tufts followed by proximal and distal tubules segments. The mesonephros (middle kidney) appears highly pigmented with melanocytes that are distributed throughout the kidney from head to tail.

The kidney in both the normal control and the HZF groups showed normal morphology with well-defined internal arrangements (**Figure 5A**). The Spike-protein induction group showed a loss of tubular segments and increased vascular degeneration, and a slightly larger trunk suggesting inflammation accompanied by increased necrosis. Treatment with Dexamethasone showed a densely packed arborized kidney architecture and an overall appearance similar to the kidney seen in the normal control group. Treatment with GG at all three different concentrations did not show phenotype rescue at the 4-days time point. A loss in melanocyte pigmentation and disorganized tubular segments were seen with an increase in necrosis was observed in the GG treatment groups which suggested that there was no recovery from disease phenotype at this point.

Cytological observation showed that the renal tissue from both normal control and HZF groups, had a normal pathology with evenly distributed glomerulocytes. Hematoxylin and Eosin staining revealed arborized tubular network with epithelial and mesangial cells (labeled with black arrowheads in the image) clearly visible throughout the section (**Figure 5B**). The disease control group in contrast, showed a disorganized cellular

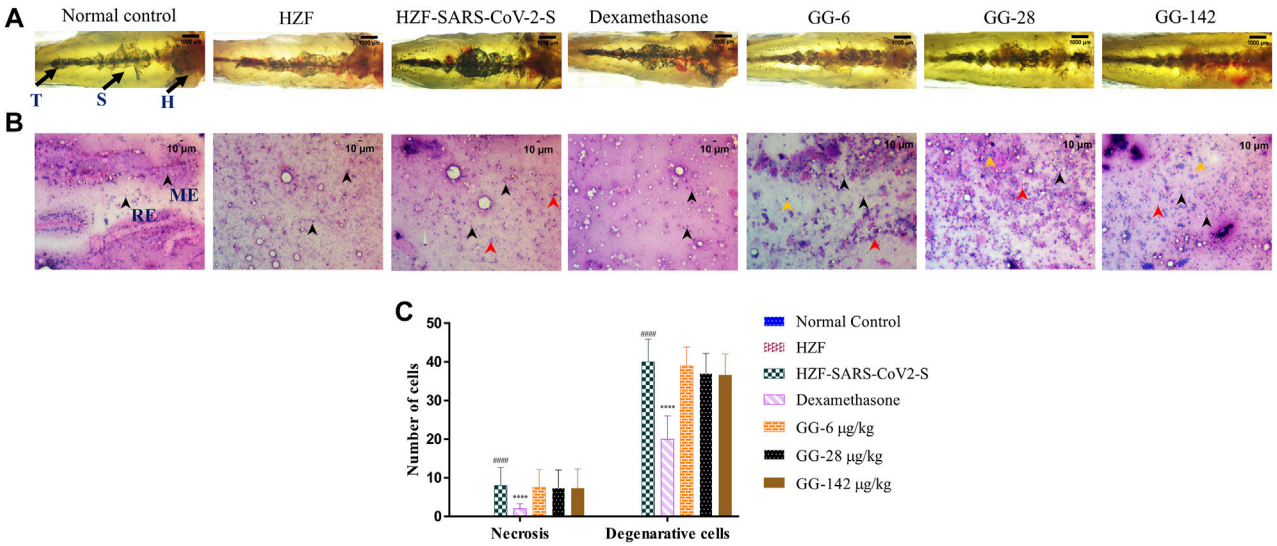

FIGURE 5 | Changes to the structure, cytology, and quantitation of necrotic and degenerative cells at 4-days time point. **(A)** Structural examination of the kidney at 1X using transmitted light. Melanocytes appear as dark pigmented granules. The three regions of the kidney Head (H), Trunk or Saddle (S), and Tail (T) extend from the anterior to the posterior of the body. **(B)** Cytological examination of hematoxylin-eosin stained smears of kidney tissue imaged at ×20 objective magnification. Black arrowheads depict nuclei of normal cells, yellow show degenerative cells while red show necrotic cells. **(C)** Quantitation of kidney damage as assessed by the presence of degenerative and necrotic cells in cytological smears. Data points represent mean ± S.D. analyzed by Two-Way ANOVA followed by Tukey's multiple comparisons test. (****) $p < 0.0001$ compared to disease control, n = 24.

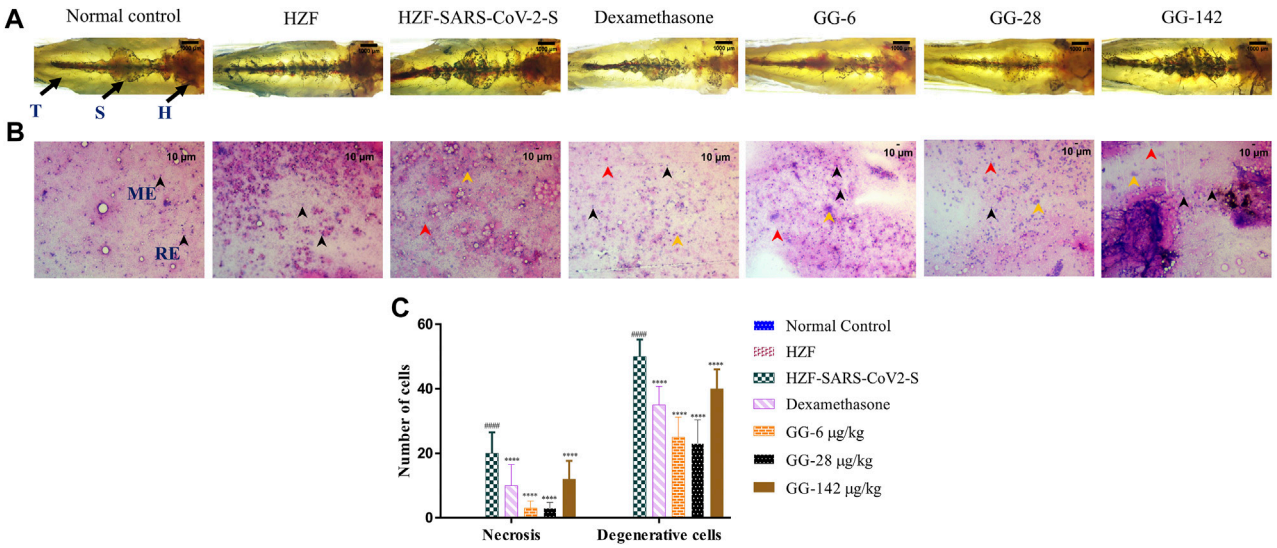

FIGURE 6 | 7-days time point showing changes to kidney morphology, cytology, and quantitative analysis of damage. **(A)** Structural examination of the kidney at 1X using transmitted light. Granular appearance shows the presence of melanocytes. **(B)** Cytological examination of hematoxylin-eosin stained smears of kidney tissue imaged at ×20 objective magnification. Black arrowheads depict nuclei of normal cells, yellow show degenerative cells while red show necrotic cells. **(C)** Quantitation of kidney damage as assessed by the presence of degenerative and necrotic cells in cytological smears. Data points represent mean ± S.D. analyzed by Two-Way ANOVA followed by Tukey's multiple comparisons test (****) $p < 0.0001$ compared to disease control, $n = 24$.

arrangements reminiscent of tubular necrosis. This was identified by increased erythrocyte aggregation, renal epithelial cells that are mostly basophilic with mildly stained nucleus suggesting increased number of degenerative (Yellow arrowheads) and necrotic cells (marked by red arrowheads). Treatment with Dexamethasone showed a very low distribution of necrotic and degenerative cells, and a normal distribution of epithelial podocytes. Quantitative estimation of the number of necrotic and

degenerative cells showed a significant reduction ($p < 0.0001$) compared to the disease control group (**Figure 5C**).

At the 4 days time point, all the three doses of GG showed the presence of degenerative and necrotic cells. The quantitative estimation showed a slight reduction in the number of the respective cells in comparison to the disease control but this was not statistically significant. There was a dose dependent reduction to a very limited extent suggesting that treatment with GG did indeed have a rescue effect but perhaps to a limited extent.

Kidney morphology at 7 days time point showed normal appearance in both the normal control and the HZF control group. The kidney dissected from the disease control group showed a loss of tubular segments and increased degeneration of the kidney tissue compared to the normal control group (**Figure 6A**). The Dexamethasone treatment group showed structural anomalies with a disorganized glomerular tufts and melanocyte pigmentation. Treatment with GG also did not show a complete recovery from the damage induced by the presence of the SARS-CoV-2 spike protein, seen in the decreased melanocyte pigmentation and highly disorganized tubular architecture.

Cytological examination of the kidney from the disease control group (7 days time point) revealed a higher presence of degenerative and necrotic renal epithelial cells that have a mildly stained nucleus and a basophilic cytoplasm (**Figure 6B**). Dexamethasone treatment group showed a moderate distribution of necrotic and degenerative cells. The numbers of these cells were significantly lower ($p < 0.0001$) than that seen in the disease control group (**Figure 6C**). The GG treatment groups showed a gradual rescue of cytological features, wherein the lower concentrations (6 and 28 μg/kg/day) showed a dose dependent reduction in the number of both the degenerative and necrotic cells. This reduction was statistically significant compared to the disease control group. The highest concentration of GG (142 μg/kg/day) however, showed an increase in the damage to the kidney architecture with disorganized renal epithelial cells. Though there was an increase in the number of degenerative and necrotic cells in this group compared to the lower concentrations, it was still significantly lower ($p < 0.0001$) than that of the disease control group (**Figure 6C**). The number of necrotic cells was comparable in both the Dexamethasone and the highest GG concentration groups.

SARS-CoV-2 Spike-Protein Induced Skin Hemorrhage Was Ameliorated By Treatment With Giloy Ghanvati

Skin hemorrhage, one of the clinical signs of vascular dysfunction, was not detectable in both the normal control and the HZF groups. Representative image from the disease control group at the 4 days time point, showed the presence of hemorrhagic regions near the pectoral and anal fins (**Figure 7A**). All the fish in this group were detected with skin hemorrhage in one of the regions near the dorsal, pectoral, anal or caudal fin. Treatment with Dexamethasone and three different concentrations of Giloy Ghanvati reversed the skin hemorrhage and the fish showed unblemished skin under reflected light.

Representative image of the fish from the disease control group at the 7-days time point showed the presence of skin hemorrhage at the anal fin region (**Figure 7B**). The different treatment groups with either Dexamethasone or GG showed a complete reversal of the clinical signs of skin hemorrhage as shown by the representative images.

Treatment with Giloy Ghanvati Reversed the Abnormal Behavioral Fever Induced by SARS-CoV-2 Spike-Protein

Behavioral fever is a measure of the internal body temperature of the fish and is determined by the time spent (in seconds) at three different temperatures 23, 29, and 37°C. At the 3 days time point, the normal control and HZF group fish spent a larger part of the recorded duration at 29°C which is the normal physiological temperature (**Figure 8A**). Disease control group were observed to spend most of their time at 37°C indicating a change in their physiological body temperature suggestive of behavioral fever. The mean time recorded by this group at the higher temperature was significantly higher than that seen in either the normal control or the HZF group (**Table 2**). The fish from Dexamethasone treatment group spent most of their time at 37°C but the average time was significantly less ($p < 0.0001$) compared to the disease control group. The time spent at 29°C was also comparatively higher than the disease control group and was statistically significant.

The average time spent by all the 3 GG treatment groups at 37°C, was higher than the time spent at 29°C, respectively. However, when compared to the disease control group, the time spent by each of the different treatment groups at 37°C was significantly lower ($p < 0.0001$). There was a dose dependent increase in the time spent at 29°C when treated with GG.

Fish from the Dexamethasone group, at the 7-days time point, showed comparable time spent at all the three temperature chambers (**Figure 8B**; **Table 2**). This suggests that this group of fish is recovering from behavioral fever. Treatment with low doses of GG (6 and 28 μg/kg/day) did not have much effect on the behavioral fever as the fish spent more time at 37°C compared to 29°C. However, the average time spent by these groups at 37°C was significantly lower than that of the disease control group. GG at 142 μg/kg/day was able to reverse the behavioral fever phenotype as the fish spent significantly more ($p < 0.0001$) time at 29°C compared to 37°C (**Table 2**).

Giloy Ghanvati Reversed SARS-CoV-2 Spike-Protein Induced Mortality

Mortality in the study groups was recorded daily and the percent survival was calculated in a parallel experiment which was observed for 10 days. As expected the normal control and the HZF group showed 100% survival, whereas the disease control group had only 80% survival (**Figure 9**). Treatment with Dexamethasone restored the survival of that group comparable

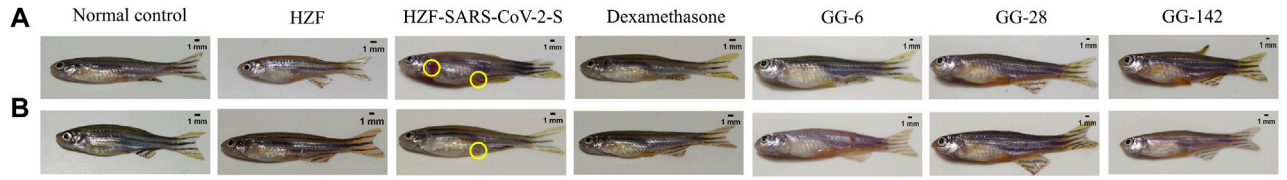

FIGURE 7 | Whole body images were captured under reflected light without any magnification. Regions of skin hemorrhage are marked with yellow circles. **(A)** 4-days time point, **(B)** 7-days time point.

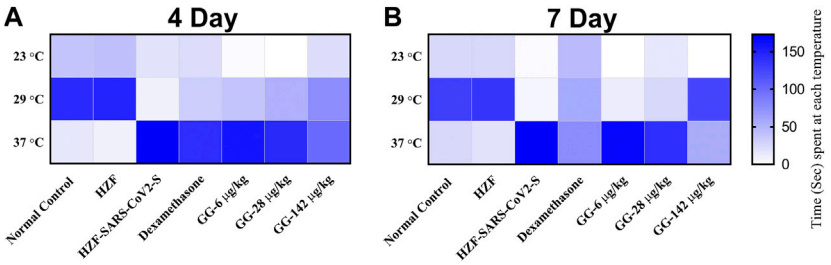

FIGURE 8 | Heat map showing changes to body temperature of zebrafish as assessed by behavioral fever. The mean time spent by individual fish in each of the three temperature chambers (23, 29, and 37°C), is shown. Increase in color intensity shows longer time spent at a particular temperature.

TABLE 2 | Changes to body temperature as assessed by behavioral fever. Time spent (in seconds) by individual fish in three different temperature chambers (23, 29, and 37°C). Data is shown as mean ± S.D. of 24 individuals, analyzed by Two-Way ANOVA followed by Tukey's multiple comparison test (#) denotes $p < 0.0001$ compared to the normal control (*) denotes $p < 0.0001$ compared to disease control, and (a) denotes $p < 0.0001$ when compared to 37°C.

Study groups	4th day time point			7th day time point		
	23°C	29°C	37°C	23°C	29°C	37°C
Normal control	35.58 ± 3.0	129.63 ± 1.4	14.92 ± 2.7	24.13 ± 0.7	130.00 ± 0.8	25.88 ± 0.7
HZF	37.79 ± 1.5	134.00 ± 1.5	8.21 ± 2.0	25.88 ± 1.3	135.75 ± 1.5	18.38 ± 1.3
HZF-SARS-CoV-2	15.96 ± 1.6#	7.04 ± 1.3#	157.08 ± 1.6#	2.38 ± 1.1#	4.75 ± 1.3#	172.88 ± 1.3#
Dexamethasone	21.13 ± 2.3*	30.46 ± 2.3*	128.29 ± 1.9*	45.54 ± 1.6*	57.54 ±2.0*	76.92 ± 2.1*
GG-6 µg/kg	1.21 ± 2.1*	36.17 ± 2.6*	142.63 ± 2.3*	0.00*	11.92 ± 1.9*	168.08 ±1.9*
GG-28 µg/kg	0.58 ± 1.2*	48.46 ± 1.9*	130.96 ± 2.1*	14.25 ± 1.8*	25.13 ± 1.8*	140.63 ± 1.9*
GG-142 µg/kg	20.17 ± 4.5*	69.92 ± 3.5*	89.92 ± 4.2*	0.00*	123.96 ±2.0*/a	56.04 ± 2.0*

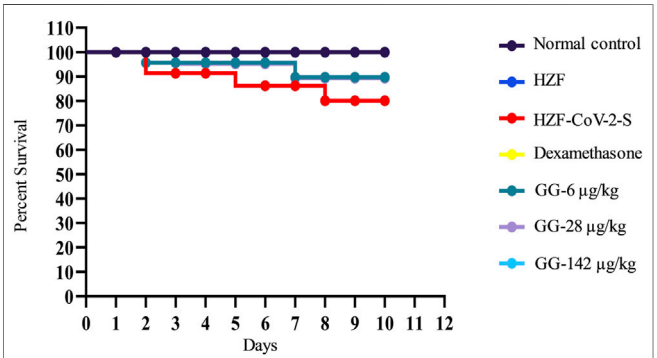

FIGURE 9 | Mortality in the different study groups was recorded every day for 10 days in a parallel experiment. Survival analysis is presented as Kaplan-Meier curve.

to the normal control. In the GG treatment groups, 100% survival was seen only with the highest concentration, whereas both 6 and 28 µg/kg/day showed 89% survival.

DISCUSSION

In this study, we used a formulation tablet named Giloy Ghanvati (GG) which is prepared from an aqueous extract from *Tinospora cordifolia* (willd.) Hook. f. and Thomson. *T. cordifolia* belongs to a group of medicinal plants used for the treatment of many different conditions including cold and fever (Chi et al., 2016). Cordifolioside A was reported to have immune-modulatory effects and an increase in the phagocytic activity of neutrophils was attributed to the synergistic effect of various phyto-compounds isolated from *T. cordifolia* (Giloy) (Sharma

et al., 2012). In our study we identified Cordifolioside A, Palmatine, β-Ecdysone, and Magnoflorine from GG, in HPLC analysis.

Magnoflorine is a member of the aprophine derivatives of isoquinoline alkaloids, and is very widely distributed in the plant kingdom. The compound has been shown to have a widely varying pharmacological effects including anti-inflammatory and immunomodulatory activities (Sharma et al., 2012; Wang et al., 2019). Though the mode of action is not fully known, *in vitro* and *in vivo* studies showed improved phagocytic activity of macrophages (Ahmad et al., 2016; Ahmad et al., 2018). Cordifolioside A is a phenylpropene disaccharide and has been shown to have immune-stimulatory activity in mice challenged with sheep RBCs, as measured by antibody production (Maurya et al., 1996). Macrophage cell line when treated with Cordifolioside A showed increased activity of NADH-oxidase, NADPH-oxidase and myeloperoxidase, all three of which are signs of macrophage activation (More and Pai, 2012).

Beta-Ecdysone and other ecdysteroids appear in many plants as protection agents against herbivorous insects and are purported to have medicinal value (Dinan et al., 2001). Phytoecdysteoids have been identified in more than 100 plant families and plants are capable of biosynthesis of these from mevalonic acid, unlike insects (Adler and Grebenok, 1995). The most commonly found phytoecdysteroid is 20-hydroxyecdysone (beta-ecdysone) and has also been identified in *T. cordifolia* (Abiramasundari et al., 2018) and has been demonstrated to induce osteogenic transformation. They have been shown to have immunomodulatory activity wherein the concentration of antibody forming B cells in the spleen of mice immunized with sheep RBC was higher (Sakhibov et al., 1989). Recent studies by LaFont et al. (LaFont et al., 2020) suggest a beneficial effect of ecdysone on the Renin-Angiotensin system. This could be especially beneficial in the SARS-CoV-2 infection as the ACE-2 receptor is also involved in the proper maintenance of the Renin-Angiotensin System.

The final compound detected in our study was Palmatine, an isoquinoline alkaloid, that is present in a wide variety of plants (Tarabasz and Kukula-Koch, 2020). The anti-inflammatory activity of this compound may be due to its activity in suppressing COX-2 and also as a prostaglandin biosynthesis suppressor (Küpeli et al., 2002). It has also been shown to inhibit Respiratory Syncytial Virus (RSV) (Lee et al., 2017), through the induction of Type 1 Interferon and its associated signaling pathways. It was also found to be prophylactic in mice.

The xeno-transplant model was used to replicate the human responses by introducing A549 cells into the swim bladder. The fish were observed for a period of 7 days and no changes in the normal behavior of the xeno-transplanted fish. During the experimental period, behavioral fever was used as a measure of fever associated with inflammation or an immune response to the presence of foreign cells and the lack of any changes suggested that there was no adverse effect due to the presence of these cells. Studies by Shen et al. (Shen et al., 2020) showed that the A549 cells colonize well even within the larvae of zebrafish and do not cause any untoward developmental changes in the larvae.

In our study, we identified increased infiltration of granulocytes and macrophages in swim bladder of the SARS-CoV-2 spike-protein induction group. There was a significant reduction in the number of granulocytes in all the 3GG treatment groups (6, 28, and 142 μg/kg/day), and showed dose dependency with an increase in concentration. Surprisingly, macrophages were not detected in either the Dexamethasone or GG treatment groups. Studies in rats (Koppada et al., 2009), were able to show that *T. cordifolia* extract was able to not only downregulate the production of various inflammatory mediators but also activate lymphocytes and increased humoral response in Mozambique *Tilapia* (Sudhakaran et al., 2006). It can be speculated that the decreased number of macrophages in the GG treatment groups could be a result of increased T cell and B cell response than macrophages. This could be corroborated by the significant dose dependent increase in the number of lymphocytes seen in the GG treatment groups.

The production of pro-inflammatory milieu at the site of SARS-CoV-2 spike-protein introduction was reflected in the morphological changes in the swim bladder. The bladder was inflamed and in some cases structurally collapsed due to edema, which is a response to the presence of pro-inflammatory cytokines and immune cells. This change in the morphology was not fully recovered upon treatment with Dexamethasone even at the 7-days time point. Treatment with GG at two different concentrations (28 and 142 μg/kg/day) was able to reverse the swim bladder changes at the 4-days time point itself. This suggested that GG is very effective in reducing the pro-inflammatory milieu seen in the presence of SARS-CoV-2 spike protein. These results are in line with our previous results using a tri-herbal formulation containing *T. cordifolia* ((Balkrishna et al., 2020).

The reduction in the pro-inflammatory cell infiltrates can be attributed to the reduction in the pro-inflammatory cytokines by GG. Studies have shown that Magnoflorine reduced LPS induced expression of TNF-α, IL-6, and IL-1β, in mice, in a dose dependent manner (Guo et al., 2018). In addition, Palmatine was also shown to inhibit these cytokines in Endometrial Epithelial Cells (gEEG) (Yan et al., 2017). These studies provide a mechanistic insight into the action of GG in reducing pro-inflammatory responses seen with the SARS-CoV-2 spike protein.

The "cytokine storm" syndrome is known to cause systemic shock and multi-organ failure in severe cases, when left untreated (Mokhtari et al., 2020). Acute kidney injury was seen in about 29% of the severe cases. ACE2 receptor which is needed for successful viral entry into cells is expressed on almost all the cell types seen in the kidney such as the proximal tubule epithelium, endothelium of glomerulus, and podocytes (Gheblawi et al., 2020). The Renin-Angiotensin system which plays a key role in maintaining proper kidney function is known to be activated via the ACE2 receptor and interference in this due to SARS-CoV-2 binding to the ACE2 receptor can induce injury to the resident renal cells (Ingraham et al., 2020).

Loss of tubular segments and vascular degeneration was observed in the disease control and was much more severe in the 7-days time point compared to the 4-days time point. Treatment with GG reduced the renal cell necrosis and the

number of degenerative cells in a dose dependent manner at the 4-days time point. However, treatment with 142 μg/kg/day GG showed higher number of necrotic and degenerative cells at the 7-days time point compared to the lower doses at the same point. The number of either type of cells was comparable to the Dexamethasone treatment group and was significantly lower than that seen in the disease control group. Ethanolic extracts of *T. cordifolia* containing Palmatine, in addition to other phyto-compounds, showed protection against nephrotoxicity induced by either aflatoxin-b (1) (Sharma and Gupta, 2011) or gentamicin (Khaksari et al., 2019). It has been shown to have these protective effects due to its powerful anti-oxidant activity.

Apart from the gross cytological and morphological changes seen in various organs of the disease control fish, the disease control showed a clear preference for water at 37°C. This behavior fever is a reflection of the body temperature and showed that the disease control fish had a high fever. Treatment with Dexamethasone for did not reverse the behavioral fever at the 4-days time point while there was a trend toward normalization at the 7-days time point. Lower concentrations of GG also did not reverse the behavioral fever even at the 7-days time point but treatment with 142 μg/kg/day totally reversed the behavioral fever showing that the highest dose given for 6 days (7-days time point) was able to rescue the SARS-CoV-2 spike-protein induced disease phenotype. The mortality seen with SARS-CoV-2 spike-protein was completely reversed with the highest dose of GG but lower doses (6 and 28 μg/kg/day) could only rescue mortality to 89% over a period of 10 days.

CONCLUSION

The present study shows the pharmacological effects of the aqueous extracts of *Tinospora cordifolia* (willd.) Hook. f. and Thomson in the form of Giloy Ghanvati (GG) tablets against SARS-CoV-2 spike-protein induced disease phenotype in a humanized zebrafish model. Treatment with GG reversed the pro-inflammatory cell infiltration in the swim bladder and also rescued the tubule damage and necrosis seen in the kidney. SARS-CoV-2 spike-protein induced fish demonstrated behavioral fever indicative of higher body temperature and this was reversed upon treatment with the test formulation. Taken together, the morphological, cytological, and behavioral changes observed with induction of SARS-CoV-2 spike-protein were rescued to near normal levels with GG treatment.

DATA AVAILABILITY STATEMENT

The raw data supporting the conclusion of this article will be made available to the scientific community upon request.

ETHICS STATEMENT

The animal study was reviewed and approved by the Institutional Ethics Committee of Pentagrit Research (vide with the approval number 223/Go062020/IAEC).

AUTHOR CONTRIBUTIONS

AB. provided broad direction for the study, identified and prepared the test formulations, generated resources and gave final approval for the manuscript; LK. performed data curing and wrote the manuscript; AV. conceptualized and supervised overall studies, generated resources, critically reviewed and finally approved the manuscript. All authors have read and agreed to the published version of the manuscript.

FUNDING

This research received no external funding. This presented work has been conducted using internal research funds from Patanjali Research Foundation Trust, Hardwar, India.

ACKNOWLEDGMENTS

We appreciate the zebrafish test facilities and experimentations at our CRO partner, Pentagrit Labs, Chennai, India. We thank Jyotish Shrivastava and Meenu Tomer for phytochemical analysis. We extend our gratitude to Priyanka Kandpal, Tarun Rajput, Gagan Kumar, and Lalit Mohan for their swift administrative supports.

REFERENCES

Abebe, E. C., Dejenie, T. A., Shiferaw, M. Y., and Malik, T. (2020). The newly emerged COVID-19 disease: a systemic review. *Virol. J.* 17 (1), 96. doi:10.1186/s12985-020-01363-5

Abiramasundari, G., Mohan Gowda, C. M., and Sreepriya, M. (2018). Selective Estrogen Receptor Modulator and prostimulatory effects of phytoestrogen β-ecdysone in *Tinospora cordifolia* on osteoblast cells. *J. Ayurveda Integr. Med.* 9 (3), 161–168. doi:10.1016/j.jaim.2017.04.003

Adler, J. H., and Grebenok, R. J. (1995). Biosynthesis and distribution of insect-molting hormones in plants-A review. *Lipids* 30, 257–262. doi:10.1007/BF02537830

Ahmad, W., Jantan, I., Kumolosasi, E., and Bukhari, S. N. A. (2016). Standardized extract of Tinospora crispa stimulates innate and adaptive immune responses in Balb/c mice. *Food Funct.* 7 (3), 1380–1389. doi:10.1039/C5FO01531F

Ahmad, W., Jantan, I., Kumolosasi, E., Haque, M. A., and Bukhari, S. N. A. (2018). Immunomodulatory effects of Tinospora crispa extract and its major compounds on the immune functions of RAW 264.7 macrophages. *Int. Immunopharmacol.* 60, 141–151. doi:10.1016/j.intimp.2018.04.046

Aleström, P., D'Angelo, L., Midtlyng, P. J., Schorderet, D. F., Schulte-Merker, S., Sohm, F., et al. (2020). Zebrafish: housing and husbandry recommendations. *Lab. Anim.* 54 (3), 213–224. doi:10.1177/0023677219869037

Avdesh, A., Chen, M., Martin-Iverson, M. T., Mondal, A., Ong, D., Rainey-Smith, S., et al. (2012). Regular care and maintenance of a zebrafish (*Danio rerio*) laboratory: an introduction. *J Vis Exp.* 69, 4196. doi:10.3791/4196

Balkrishna, A. (2015). *A practical approach to the science of ayurveda: a comprehensive guide for healthy living*. New Delhi: Lotus Press.

Balkrishna, A., Solleti, S. K., Verma, S., and Varshney, A. (2020). Application of humanized zebrafish model in the suppression of SARS-CoV-2 spike protein induced pathology by tri-herbal medicine coronil via cytokine modulation. *Molecules* 25 (21), 5091. doi:10.3390/molecules25215091

Chen, K., Wang, C.-Q., Fan, Y.-Q., Xie, Y.-S., Yin, Z.-F., Xu, Z.-J., et al. (2014). The evaluation of rapid cooling as an anesthetic method for the zebrafish. *Zebrafish* 11 (1), 71–75. doi:10.1089/zeb.2012.0858

Chi, S., She, G., Han, D., Wang, W., Liu, Z., and Liu, B. (2016). GenusTinospora: Ethnopharmacology, phytochemistry, and Pharmacology. *J. Evid.Based Integr. Med.* 1–32. doi:10.1155/2016/9232593

Cho, J. Y., Nam, K. H., Kim, A. R., Park, J., Yoo, E. S., Baik, K. U., et al. (2001). *In-vitro* and *in-vivo* immunomodulatory effects of syringin. *J. Pharm. Pharmacol.* 53 (9), 1287–1294. doi:10.1211/0022357011776577

Dinan, L., Savchenko, T., and Whiting, P. (2001). On the distribution of phytoecdysteroids in plants. *Cell. Mol. Life Sci.* 58 (9), 1121–1132. doi:10.1007/PL00000926

Gheblawi, M., Wang, K., Viveiros, A., Nguyen, Q., Zhong, J.-C., Turner, A. J., et al. (2020). Angiotensin-converting enzyme 2: SARS-CoV-2 receptor and regulator of the renin-angiotensin system. *Circ. Res.* 126 (10), 1456–1474. doi:10.1161/CIRCRESAHA.120.317015

Guo, S., Jiang, K., Wu, H., Yang, C., Yang, Y., Yang, J., et al. (2018). Magnoflorine ameliorates lipopolysaccharide-induced Acute lung injury via suppressing NF-κB and MAPK activation. *Front. Pharmacol.* 9, 982. doi:10.3389/fphar.2018.00982

Hankey, A. (2010). Ayurveda and the battle against chronic disease: an opportunity for Ayurveda to go mainstream?. *J. Ayurveda Integr. Med.* 1 (1), 9. doi:10.4103/0975-9476.59819

Imtiyaj Khan, M., Sri Harsha, P. S. C., Giridhar, P., and Ravishankar, G. A. (2011). Pigment identification, antioxidant activity, and nutrient composition of*Tinospora cordifolia*(willd.) Miers ex Hook. f & Thoms fruit. *Int. J. Food Sci. Nutr.* 62 (3), 239–249. doi:10.3109/09637486.2010.529069

Inciardi, R. M., Solomon, S. D., Ridker, P. M., and Metra, M. (2020). Coronavirus 2019 disease (COVID-19), systemic inflammation, and cardiovascular disease. *Jaha* 9 (16), e017756. doi:10.1161/JAHA.120.017756

Ingraham, N. E., Barakat, A. G., Reilkoff, R., Bezdicek, T., Schacker, T., Chipman, J. G., et al. (2020). Understanding the renin-angiotensin-aldosterone-SARS-CoV axis: a comprehensive review. *Eur. Respir. J.* 56, 2000912. doi:10.1183/13993003.00912-2020

Kapil, A., and Sharma, S. (1997). Immunopotentiating compounds from *Tinospora cordifolia*. *J. Ethnopharmacol.* 58 (2), 89–95. doi:10.1016/S0378-8741(97)00086-X

Khaksari, M., Esmaili, S., Abedloo, R., and Khastar, H. (2019). Palmatine ameliorates nephrotoxicity and hepatotoxicity induced by gentamicin in rats. *Arch. Physiol. Biochem.* 1, 1. doi:10.1080/13813455.2019.1633354

Koppada, R., Norozian, F. M., Torbati, D., Kalomiris, S., Ramachandran, C., and Totapally, B. R. (2009). Physiological effects of a novel immune stimulator drug, (1,4)-α-d-glucan, in rats. *Basic Clin. Pharmacol. Toxicol.* 105 (4), 217–221. doi:10.1111/j.1742-7843.2009.00383.x

Küpeli, E., Koşar, M., Yeşilada, E., and Başer, K. H. C. (2002). A comparative study on the anti-inflammatory, antinociceptive and antipyretic effects of isoquinoline alkaloids from the roots of Turkish Berberis species. *Life Sci.* 72 (6), 645–657. doi:10.1016/S0024-3205(02)02200-2

LaFont, R., Raynal, S., Serova, M., Didry-Barca, B., Guibout, L., Latil, M., et al. (2020). 20-Hydroxyecdysone activates the protective arm of the renin angiotensin system via Mas receptor. *bioRxiv*. doi:10.1101/2020.04.08.032607

Lee, B.-H., Chathuranga, K., Uddin, M. B., Weeratunga, P., Kim, M. S., Cho, W.-K., et al. (2017). Coptidis Rhizoma extract inhibits replication of respiratory syncytial virus *in vitro* and *in vivo* by inducing antiviral state. *J. Microbiol.* 55 (6), 488. doi:10.1007/s12275-017-7088-x

Liu, J., Zhang, F., Ravikanth, V., Olajide, O. A., Li, C., and Wei, L.-X. (2019). Chemical compositions of metals in bhasmas and Tibetan zuotai are a major determinant of their therapeutic effects and toxicity. *Evid.Based Complement. Alternat. Med.* (4), 1–3. doi:10.1155/2019/1697804

Matthews, M., and Varga, Z. M. (2012). Anesthesia and euthanasia in zebrafish. *ILAR J.* 53 (2), 192–204. doi:10.1093/ilar.53.2.192

Maurya, R., Wazir, V., Kapil, A., and Kapil, R. S. (1996). Cordifoliosides A and B, two new phenylpropene disaccharides from*Tinospora cordifolia*possessing immunostimulant activity. *Nat. Product. Lett.* 8 (1), 7–10. doi:10.1080/10575639608043231

Menke, A. L., Spitsbergen, J. M., Wolterbeek, A. P. M., and Woutersen, R. A. (2011). Normal anatomy and histology of the adult zebrafish. *Toxicol. Pathol.* 39 (5), 759–775. doi:10.1177/0192623311409597

Meulenbeld, G. J. (1999). "Introduction," In *A History of Indian medical literature*. Groningen: (Egbert Forsten).

Mokhtari, T., Hassani, F., Ghaffari, N., Ebrahimi, B., Yarahmadi, A., and Hassanzadeh, G. (2020). COVID-19 and multiorgan failure: a narrative review on potential mechanisms. *J. Mol. Hist.* 51 (6), 613–628. doi:10.1007/s10735-020-09915-3

More, P., and Pai, K. (2012). In vitroNADH-oxidase, NADPH-oxidase and myeloperoxidase activity of macrophages after*Tinospora cordifolia*(guduchi) treatment. *Immunopharmacol. Immunotoxicol.* 34 (3), 368–372. doi:10.3109/08923973.2011.606324

Oskay, Y., Çetin, B., Şerifoğlu, N., Arslan-Ergül, A., and Adams, M. M. (2018). A novel, low-cost anesthesia and injection system for zebrafish researchers. *Zebrafish* 15 (2), 85–95. doi:10.1089/zeb.2017.1513

Panchabhai, T. S., Kulkarni, U. P., and Rege, N. N. (2008). Validation of therapeutic claims of*Tinospora cordifolia*: a review. *Phytother. Res.* 22 (4), 425–441. doi:10.1002/ptr.2347

Sachan, S., Dhama, K., Latheef, S. K., Samad, H. A., Mariappan, A. K., Munuswamy, P., et al. (2019). Immunomodulatory potential of *Tinospora cordifolia* and CpG ODN (TLR21 agonist) against the very virulent, infectious bursal disease virus in SPF chicks. *Vaccines (Basel)* 7 (3):106. doi:10.3390/vaccines7030106

Sagar, V., and Kumar, A. H. (2020). *Efficacy of natural compounds from* Tinospora cordifolia *against SARS-CoV-2 protease, surface glycoprotein and RNA polymerase*. Research Square. doi:10.21203/rs.3.rs-27375/v1

Sharma, R., Kumar, V., Galib, R., Prajapati, P., Ravishankar, B., and Ashok, B. (2013). Evaluation of hypoglycaemic and anti-hyperglycaemic activities of Guduchi Ghana in Swiss albino mice. *Int. J. Green. Pharm.* 7 (2), 145. doi:10.4103/0973-8258.116397

Sharma, U., Bala, M., Kumar, N., Singh, B., Munshi, R. K., and Bhalerao, S. (2012). Immunomodulatory active compounds from *Tinospora cordifolia*. *J. Ethnopharmacol.* 141 (3), 918–926. doi:10.1016/j.jep.2012.03.027

Sharma, V., and Gupta, R. (2011). Ameliorative effects of *Tinospora cordifolia* root extract on histopathological and biochemical changes induced by Aflatoxin-B1in mice kidney. *Toxicol. Int.* 18 (2), 94. doi:10.4103/0971-6580.84259

Sharma, V., and McNeill, J. H. (2009). To scale or not to scale: the principles of dose extrapolation. *Br. J. Pharmacol.* 157 (6), 907–921. doi:10.1111/j.1476-5381.2009.00267.x

Shen, W., Pu, J., Sun, J., Tan, B., Wang, W., Wang, L., et al. (2020). Zebrafish xenograft model of human lung cancer for studying the function of LINC00152 in cell proliferation and invasion. *Cancer Cel Int* 20 (1), 376. doi:10.1186/s12935-020-01460-z

Sudhakaran, D. S., Srirekha, P., Devasree, L. D., Premsingh, S., and Michael, R. D. (2006). Immunostimulatory effect of *Tinospora cordifolia* Miers leaf extract in *Oreochromis mossambicus*. *Indian J. Exp. Biol.* 44 (9), 726–732. Available at: http://www.ncbi.nlm.nih.gov/pubmed/16999027.

Sullivan, C., and Kim, C. H. (2008). Zebrafish as a model for infectious disease and immune function. *Fish Shellfish Immunol.* 25 (4), 341–350. doi:10.1016/j.fsi.2008.05.005

Tarabasz, D., and Kukula-Koch, W. (2020). Palmatine: a review of pharmacological properties and pharmacokinetics. *Phytother. Res.* 34 (1), 33–50. doi:10.1002/ptr.6504

Targen, S., Kaya, T., Avci, M. E., Gunes, D., Keskus, A. G., and Konu, O. (2020). ZenoFishDb v1.1: a database for xenotransplantation studies in zebrafish. *Zebrafish* 17 (5), 305–318. doi:10.1089/zeb.2020.1869

Tiwari, M., Dwivedi, U. N., and Kakkar, P. (2014). *Tinospora cordifolia* extract modulates COX-2, iNOS, ICAM-1, pro-inflammatory cytokines and redox status in murine model of asthma. *J. Ethnopharmacol.* 153 (2), 326–337. doi:10.1016/j.jep.2014.01.031

Van Dycke, J., Ny, A., Conceição-Neto, N., Maes, J., Hosmillo, M., Cuvry, A., et al. (2019). A robust human norovirus replication model in zebrafish larvae. *PLOS Pathog.* 15 (9), e1008009. doi:10.1371/journal.ppat.1008009

Wang, L.-J., Jiang, Z.-M., Xiao, P.-T., Sun, J.-B., Bi, Z.-M., and Liu, E.-H. (2019). Identification of anti-inflammatory components in Sinomenii Caulis based on

spectrum-effect relationship and chemometric methods. *J. Pharm. Biomed. Anal.* 167, 38–48. doi:10.1016/j.jpba.2019.01.047

Westerfield, M. (1993). *The zebrafish book. A guide for the laboratory use of zebrafish (*Danio rerio*)*. 4th ed. Eugene: University of Oregon Press.

Who (2019). *WHO global report on traditional and complementary medicine 2019*. Geneva. World Health Organization.

Yan, B., Wang, D., Dong, S., Cheng, Z., Na, L., Sang, M., et al. (2017). Palmatine inhibits TRIF-dependent NF-κB pathway against inflammation induced by LPS in goat endometrial epithelial cells. *Int. Immunopharmacol.* 45, 194–200. doi:10.1016/j.intimp.2017.02.004

Conflict of Interest: The Giloy Ghanvati (Tinospora cordifolia (willd.) Hook.f. & Thomson) was sourced by Patanjali Ayurved Ltd, Haridwar, Uttarakhand, India. AB is an honorary trustee in Divya Yog Mandir Trust, Haridwar, India. In addition, he holds an honorary managerial position in Patanjali Ayurved Ltd., Haridwar, India. Other than providing the test formulation, Patanjali Ayurved Ltd was not involved in any aspect of research reported in this study.

All remaining authors declare that the research was conducted in the absence of any commercial or financial relationships that could be construed as a potential conflict of interest.

frontiers in Pharmacology

REVIEW
published: 26 April 2021
doi: 10.3389/fphar.2021.658273

Phytochemicals as Potential Therapeutics for SARS-CoV-2–Induced Cardiovascular Complications: Thrombosis and Platelet Perspective

*Samir K. Beura, Abhishek R. Panigrahi, Pooja Yadav and Sunil K. Singh**

Department of Zoology, School of Basic and Applied Sciences, Central University of Punjab, Bathinda, India

After gaining entry through ACE2 aided by TMPRSS2, the SARS-CoV-2 causes serious complications of the cardiovascular system leading to myocarditis and other myocardial injuries apart from causing lung, kidney and brain dysfunctions. Here in this review, we are going to divulge the cellular and immunological mechanisms behind the cardiovascular, thrombotic and platelet impairments that are caused in COVID-19. In addition, we also propose the significance of various anti-platelet and anti-thrombotic phytochemicals in the treatment of COVID-19. The virus induces many immune-modulatory cytokines and chemokines which help in the intravascular coagulation and create a pro-thrombotic environment along with pulmonary embolism and thrombocytopenia. Different types of innate and adaptive immune cells and their granular contents regulate the pathophysiology of SARS-CoV-2 induced endothelial and platelet dysfunctions which correlate the involvement of platelets with myocardial injury and intravascular thrombi directly or indirectly. Hence, by exploiting the natural bioactive compounds from medicinal plants and inhibiting the platelet mediated thrombus formation can be beneficial for the treatment of SARS-CoV-2 infection.

Keywords: SARS-CoV-2, ACE2, thrombosis, platelet, myocardial injury, cytokine storm, phytochemical

OPEN ACCESS

Edited by:
Vijay Kumar Prajapati,
Central University of Rajasthan, India

Reviewed by:
Gagan Flora,
The University of Iowa, United States
Rajanish Giri,
Indian Institute of Technology Mandi, India

****Correspondence:***
Sunil K. Singh
sunil.singh@cup.edu.in

Specialty section:
This article was submitted to Ethnopharmacology, a section of the journal Frontiers in Pharmacology

Received: *25 January 2021*
Accepted: *25 March 2021*
Published: *26 April 2021*

Citation:
Beura SK, Panigrahi AR, Yadav P and Singh SK (2021) Phytochemicals as Potential Therapeutics for SARS-CoV-2–Induced Cardiovascular Complications: Thrombosis and Platelet Perspective. Front. Pharmacol. 12:658273. doi: 10.3389/fphar.2021.658273

INTRODUCTION

The coronavirus disease 2019 (COVID-19) is a severe acute respiratory syndrome coronavirus 2 (SARS-CoV-2) caused disease that has reported a total of 119,222,995 infections and 2,644,461 deaths worldwide (as per the WHO report till March 15, 2021). The SARS-CoV-2 belongs to the genus Betacoronavirus, which is closely related to other recent past viruses of this group like severe acute respiratory syndrome coronavirus (SARS-CoV) and Middle East respiratory syndrome coronavirus (MERS-CoV) (Gao et al., 2020). The SARS-CoV-2 gains entry into the host cell primarily by the interaction of viral spike (S) glycoprotein with a host cell receptor that is, angiotensin converting enzyme 2 (ACE2), aided by the priming of S protein by a serine protease that is, transmembrane protease serine 2 (TMPRSS2) (Hoffmann et al., 2020b). Due to the abundance of ACE2 receptors in major tissues like pulmonary tissues, cardiac tissues, and associated endothelial tissues, there are more chances of developing viral-induced complications such as myocardial injuries and acute coronary injuries (Clerkin et al., 2020). The elevated concentration of immunomodulatory molecules like interleukins (IL-2 and IL-7), interferon

TABLE 1 | List of different key molecules and major complications due to cardiovascular, thrombogenic, and platelet impairments in COVID-19.

	Cardiovascular events	Thrombogenic events	Platelet events
Key molecules	Troponin T (TnT) C-reactive protein (CRP) Pro-brain natriuretic Peptide (BNP) Creatine kinase (CK) D-dimer Procalcitonin Ferritin IL-6 TNF-α IFN-γ	vWF TF ADAMTS-13 Fibrinogen Fibrinogen degradation Products (FDPs) D-dimer IL-6 TNF-α	IFN-I Platelet α-granular contents Platelet dense-granular contents Extracellular vesicle (EV)
Major complications	Acute myocardial injury Acute myocarditis Myocardial infarction (MI) Fulminant myocarditis (FM) Tachy/brady arrhythmia	Venous thromboembolism (VTE) Disseminated intravascular Coagulation (DIC) Thrombotic Microangiopathy (TMA) Intravascular micro/macro Thrombosis (IMT) Blood hypercoagulability Endocardial thrombosis	Thrombocytopenia Platelet hyperactivation Platelet–fibrin–microthrombi (PFM)

TABLE 2 | List of different phytochemicals having effect on platelet functions and thrombosis, which could have potential roles in the treatment of COVID-19.

Phytochemicals	Species name	Mechanism of action	References
Curcumin	*Curcuma longa* L.	Inhibits ADP, PAF, collagen, and AA-induced platelet activation and aggregation	Kim and Park (2019), Mohd Nor et al. (2016), Soni et al. (2020), Babaei et al. (2020)
Berberine	*Berberis vulgaris* L.	Inhibits platelet by Ca^{2+} mobilization and AA metabolism	Mohd Nor et al. (2016), Kim et al. (2019), Zhang BY et al. (2020)
Magnolol	*Magnolia officinalis* (Rehder and E.H.Wilson)	Inhibits platelet activation and aggregation by inhibiting intracellular Ca^{2+} mobilization and thromboxane formation	Mohd Nor et al. (2016), Lin et al. (2015)
Quercetin	*Allium cepa* L	Inhibits platelet *via* regulation of cAMP/PLA2 pathway and downregulation of intracellular Ca^{2+} mobilization and COX-1	El Haouari and Rosado (2016), Biancatelli et al. (2020)
Andrographolide	*Andrographis paniculata* (Burm.f.) Nees	Inhibits thrombin/collagen-induced platelet aggregation through cGMP/PKG/p38MAPK pathway	El Haouari and Rosado (2016), Enmozhi et al. (2020)
Rutaecarpine	*Tetradium ruticarpum* (A.Juss.) T.G.Hartley	Inhibits of platelet function by inhibiting PLC mediated TXA2 attenuation and downregulation of intracellular Ca^{2+} mobilization	El Haouari and Rosado (2016)
Gingerol	*Zingiber officinale* Roscoe	Inhibits AA-induced platelet activation and aggregation	Mohd Nor et al. (2016), Rathinavel et al. (2020)
Baicalin	*Scutellaria baicalensis* Georgi	Inhibited thrombin production, thrombin catalyzed fibrin polymerization, and platelet functions	Lee et al. (2015), Su et al. (2020)

(IFN-γ), G-CSF, MCP-1, MIP-1α, and tumor necrosis factor (TNF-α) (**Table 1**) in plasma is found in COVID-19 patients suggesting the cytokine storm–induced inflammation causing cardiac as well as pulmonary injuries (Mehta et al., 2020). This cytokine storm augments the expression of adhesion molecules which not only activates the endothelial cells inducing vascular inflammation but also causes inflammatory cell infiltration (e.g., macrophages). The dysregulation of cytokines causes vascular endothelial dysfunction, thus creating a procoagulant and prothrombotic environment leading to microvascular thrombi formation, which may lead to multi-organ failure (Liu et al., 2020). Foremost, the clinical results suggest that elevated concentration of circulating D-dimer and other cardiac enzymes, reflecting vascular thrombosis with fibrinolysis, also contribute to pulmonary intravascular coagulopathy as a result of decreased platelet counts (McGonagle et al., 2020). Recent reports hypothesize that the decreased platelet count might be an outcome of the following three mechanisms that is, virus-induced cytokine-mediated destruction of bone marrow resident platelet progenitor cells (low platelet production), dysregulated cytokine-induced platelet destruction, or by microthrombi-induced platelet consumption (Xu et al., 2020). Based upon the viral-mediated inflammatory responses and diagnosis, there are many conventional drug trials ongoing which target the viral structural and nonstructural proteins, in addition to targeting ACE2 and other cytokines (Sanders et al., 2020). It has been earlier reported that the plant metabolites like alkaloids, terpenoids, flavonoids, and lignins (**Table 2**) have shown their antiviral effects against rotavirus, influenza virus, dengue virus, hepatitis virus, and MERS-CoV as well as SARS-CoV (Swain et al., 2020) (Ghildiyal et al., 2020).

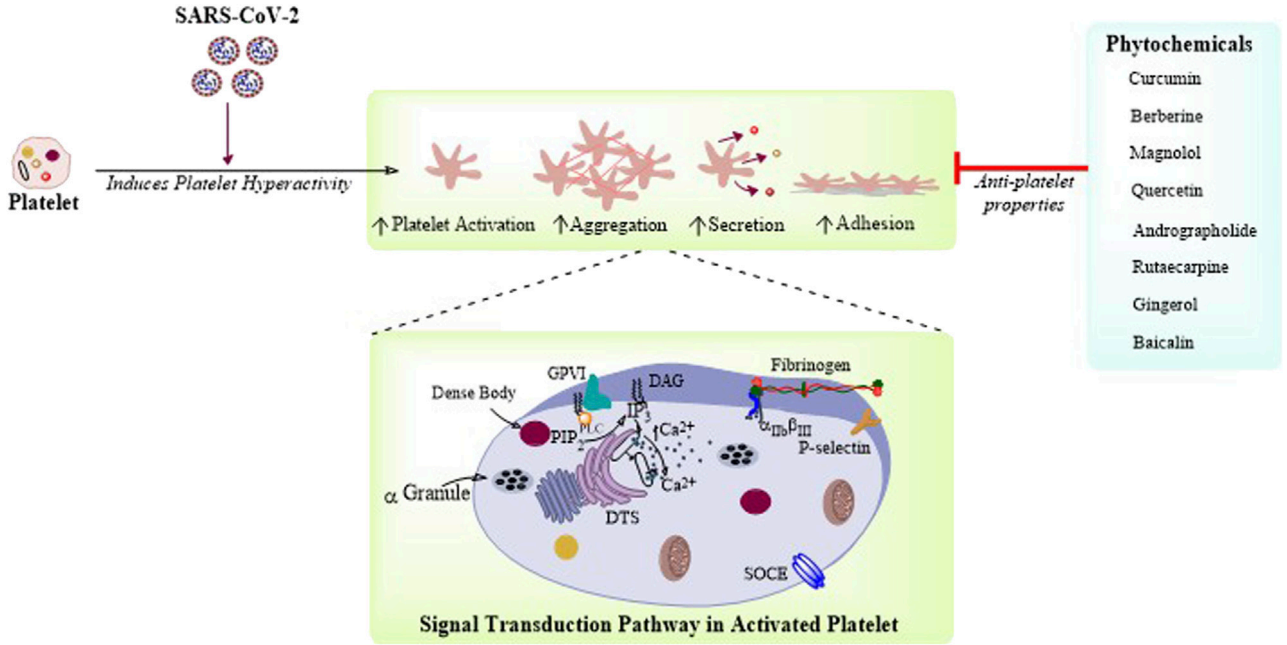

FIGURE 1 | Phytochemicals targeting platelet function and thrombosis: Platelet function is governed by intracellular Ca^{2+} signaling resulting in platelet adhesion, activation, aggregation, and secretion. SARS-CoV-2 is demonstrated here to cause increased platelet activation, secretion, and aggregation. There are few phytochemicals which are reported to have antiplatelet activity and could be potential therapeutic candidates for the treatment of COVID-19.

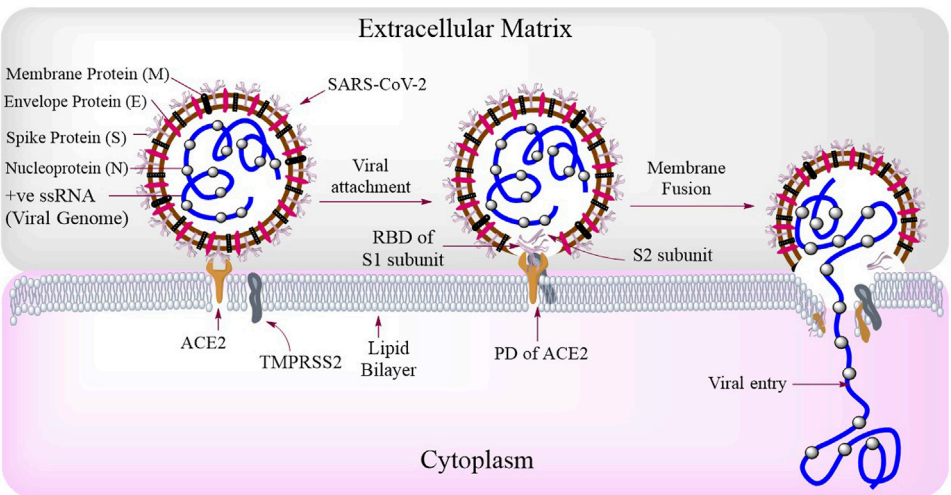

FIGURE 2 | SARS-CoV-2 structure and routes of entry: SARS-CoV-2 consists of Spike protein (S) membrane protein (M), envelope protein (E), nucleoprotein (N), and the viral genome (+ve ssRNA). Among these, the S protein is most important and is made up of two types of subunits that is, S1 (for binding with host receptor) and S2 (for viral fusion) subunits. During viral attachment, the receptor-binding domain (RBD) of S1 interacts with the peptidase domain (PD) of ACE2. The entry and fusion of this virus is aided by a transmembrane serine protease, TMPRSS2.

These herbal plants through their bioactive compounds can target viral replication and viral entry (**Figure 1**) (via ACE2 and TMPRSS2), and could be potentially effective against virus-induced complications (Benarba and Pandiella, 2020). Considering all these evidences, the use of traditional herbal plants could be promising either alone or in combination against COVID-19.

Here in this review, we are going to overview the effects of SARS-CoV-2 on thrombosis and cardiovascular complications, considering the virology of SARS-CoV-2 and its route of entry. We also highlight the potential therapeutic effects of phytochemicals which possess inhibitory action against platelet function and thrombus formation in order to counter SARS-CoV-2–induced COVID-19.

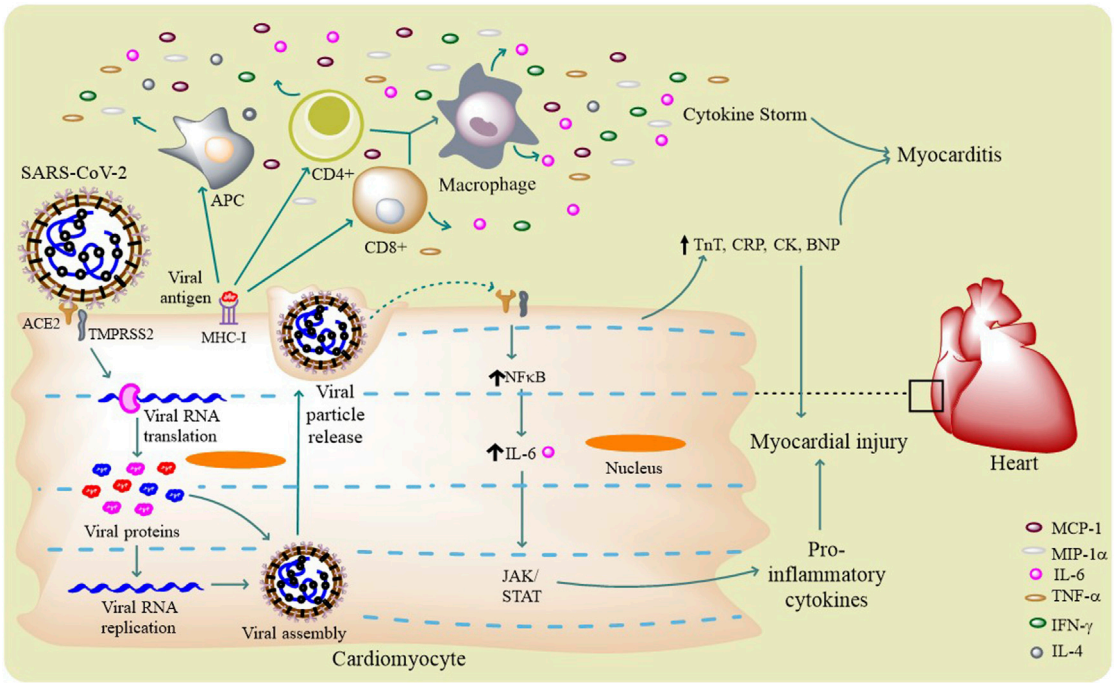

FIGURE 3 | SARS-CoV-2 life cycle and cardiovascular complications: SARS-CoV-2 infects a host cell through ACE2 and TMPRSS2, and through its intracellular life cycle it produces a number of new virions. The virus activates different innate and adaptive immune cells (APCs and T cells) to release certain pro-inflammatory molecules like IL-6, IFN-γ, TNF-α, and MCP-1 that results in cytokine storm. This surge in immunomodulatory molecules mediates the occurrence myocarditis. Virus itself can induce the host cell to produce pro-inflammatory cytokines through IL-6–mediated JAK/STAT and NF-κB pathways. Few circulating biomarker proteins like TnT, CRP, CK, and BNP can potentially cause myocardial injury.

STRUCTURE AND LIFE CYCLE OF SARS-COV-2

So far, seven human coronavirus strains have been identified including HCoV-229E, HCoV-OC43, HCoV-NL63, HCoV-HKU1, SARS-CoV, MERS-CoV, and SARS-CoV-2, where the first four causes mild common cold whereas the last three causes severe respiratory syndromes (Xu et al., 2020). Among these last three, SARS-CoV-2–causing COVID-19 is the most lethal one. The genome of SARS-CoV-2 consists of 29,903 bp long positive single-stranded RNA (+ve ssRNA). Each SARS-CoV-2 virion is approximately 50–200 nm in diameter (Ibrahim et al., 2020). Like other coronaviruses, SARS-CoV-2 has four structural proteins that is, S (spike), E (envelope), M (membrane), and N (nucleocapsid) proteins; the N protein holds the RNA genome and the S, E, and M proteins in together forms the viral structure **(Figure 2)**. Apart from these, the genome of this virus also expresses polyproteins, nucleoproteins and membrane proteins that is, RNA polymerase, 3-chymotrypsin-like protease, papain-like protease, helicase, glycoprotein, and accessory proteins (Shereen et al., 2020).

A matured full length spike (S) protein consists of two functional subunits which are responsible for two major functions separately that is, the S_1 subunit; for binding to the host cell receptor and the S_2 subunit; for the fusion of viral and cellular membranes (Walls et al., 2020). Between these two subunits, the viral S_1 protein has receptor-binding domain (RBD) which binds to the peptidase domain (PD) of host cellular receptor ACE2 **(Figure 2)** to facilitate the entry of the virus as seen in case of SARS-CoV (Yan et al., 2020). The spike protein of the virus needs the help of another protein from host cell called transmembrane protease serine 2 (TMPRSS2), for priming of S protein to expose its fusion region to bind with ACE2 (Hoffmann et al., 2020a). The endosomal protease, cathepsin L (CTSL) and Basigin (BSG)/CD147 are also reported to be essential for spike protein processing and viral entry into the host cells (Colaco et al., 2020). After attachment, the viral membrane fuses with the host cell membrane, aided by the S2 subunit of SARS-CoV-2 spike protein. After the fusion of virus and host cell membranes, the viral + ve ssRNA undergoes translation to produce viral replicase polyproteins (PP1a and PP1ab), which are RNA-dependent RNA polymerases (RdRp). The viral RNA polymerases then produce a number of relevant sub-genomic mRNAs, which are further translated into viral proteins **(Figure 3)**. The viral proteins and genomes assemble in ER and Golgi and bud through the ER-Golgi intermediate compartment (ERGIC) to release new virions outside (Shereen et al., 2020).

THE ROUTES OF SARS-COV-2 ENTRY: ACE2 AND TMPRSS2

As it has been discussed about the structure of SARS-CoV-2 earlier, it is now well elucidated about the basic protein molecules

which this virus uses as its receptor(s) to get inside a host cell. In humans, this virus uses two key receptor molecules that is, ACE2 and TMPRSS2 **(Figure 2)** to get the ticket of entry (Hoffmann et al., 2020b). ACE2 is a type I integral membrane glycoprotein of 805 amino acid residues length and functions as a zinc metalloenzyme and carboxypeptidase, found on chromosome X. The genes coded on this chromosome could bring an insight about the gender bias considering the fact that men have only one X chromosome, hence, there is increased fatality for SARS-CoV-2 infection in men as compared to women (Li Y et al., 2020). ACE2 is located abundantly on the surface of the endothelium, kidney, lungs, heart, and intestine (Tikellis et al., 2011). It is a major component of the renin-angiotensin system (RAS), where angiotensinogen is cleaved into a decapeptide, angiotensin I (Ang I) by renin. Then, Ang I can further be cleaved into vasoconstricting octapeptide, angiotensin II (Ang II) by ACE. Then, both Ang I and Ang II can be processed by ACE2 to produce Ang 1–9 and Ang 1–7, respectively. Ang 1–7 peptide, can bind with a G protein-coupled receptor (GPCR) called "Mas" to mediate its vasodilating and vasoprotective effects (Kuba et al., 2013). Here in this way, ACE2 not only antagonizes the effect of Ang II, thus decreasing the blood pressure and inflammation, but also regulates electrolyte balance and cardiovascular homeostasis (Oudit et al., 2003). The *in vivo* studies have demonstrated that ACE, Ang II, and Ang II type 1 (AT1) receptor together functions as lung injury–promoting factors, but the mechanism is still to be deciphered, while the antagonizing regulation of Ang II levels by ACE2 functions as protecting agent against acute and chronic lung injury (Kuba et al., 2013). ACE2 can also cleave a number of other peptides including des-Arg9-bradykinin (DABK), apelin, neurotensin, dynorphin A, and ghrelin (Mughal and O'Rourke, 2018). So in short, an ACE2 comprises an N-terminal peptidase domain (PD) that cleaves Ang I into Ang 1–9, which is further processed into Ang 1–7 and a C-terminal collectrin-like domain (CPD), ending with a 40 amino acid long single transmembrane intracellular segment (Yan et al., 2020).

Similarly, TMPRSS2 is a multidomain type II transmembrane serine protease of 492 amino acid residues length and is found on chromosome 21. TMPRSS2 is expressed predominantly in human prostates, colon, lung, kidney, liver, and pancreas, and it is noticed to be upregulated in prostate cancer. TMPRSS2 can bind and activate protease-activated receptor 2 (PAR2), a GPCR in tumors (Meyer et al., 2013). TMPRSS2 can also cleave and trim the spike proteins of viruses for membrane fusion and entry into different cells especially in the case of SARS-CoV entry into type II pneumocytes aided by ACE2 (Heurich et al., 2014).

SARS-COV-2–INDUCED CARDIOVASCULAR COMPLICATIONS

The coronaviruses are not generally restricted to the lungs and associated tissues, but have the potential to invade other organs and tissues, out of which the cardiovascular system, especially the heart and associated blood vessels are most affected. It had been earlier reported that SARS-CoV causes acute myocarditis and other cardiovascular diseases (CVDs) as it takes the help of host ACE2 to get entry (Kuba et al., 2006). Acute myocardial injury, hypotension, tachycardia, bradycardia, cardiomegaly, arrhythmia, and cardiac arrest–like conditions were prevalent in SARS (Xiong et al., 2020). Similarly, MERS-CoV also caused CVDs, where the plasma levels of troponin I and serum creatinine were reported to be elevated (Alhogbani, 2016), (Badawi and Ryoo, 2016). Like SARS-CoV, SARS-CoV-2 also uses this same ACE2 as its receptor for fusion and entry into the host cell. Heart is one of the major sites, where ACE2 is found, thus the virus has a direct impact on the heart also. ACE2 is localized in cardiac endothelial cells, the smooth muscle cells of myocardial vessels, and in cardiac myocytes. This is why there are more number of cardiac complications which are observed in case of COVID-19 (Kuster et al., 2020).

The binding of SARS-CoV-2 with ACE2 can result in the alteration(s) of ACE2 signaling pathways that might lead to acute myocardial injury (Zheng et al., 2020). The myocardial injury is supposed to be manifested by the increase in cardiac troponin I, median creatine kinase (CK) **(Figure 3),** and ACE2-induced cytokine signaling (Kochi et al., 2020). The increased troponin levels are speculated to be possible either by the binding of SARS-CoV-2 to endothelial ACE2–causing coronary microvascular ischemia or due to the virus-induced cytokine storm that induces inflammatory proteins resulting in myocarditis. Studies have reported the high circulatory levels of pro-inflammatory cytokines in patients with severe/critical COVID-19 resulting in acute systemic inflammation of the heart and other organs (Gupta et al., 2020). The presence of viral mRNA in heart and myocardial localizations of coronavirus particles (outside of cardiomyocytes) are evident in a SARS-CoV-2 infected patient suggesting the direct infection the myocardium (Nishiga et al., 2020). The *in vitro* studies have also confirmed this direct infection of cardiomyocytes by SARS-CoV-2 (Bojkova et al., 2020).

Understanding about the mechanism behind cardiac inflammation suggests that cytokine release syndrome (CRS) is evident in COVID-19 condition, but another similar phenomenon also exists in many cancer patients. In cancer many cytokines, more notably, IL-6 was found to be elevated along with ACE2, demonstrating a possible insight of cancer-like surge of cytokines (Gupta et al., 2020). Moreover, the same cytokine (i.e., IL-6) is also seen to be increased in COVID-19 patients (Chen et al., 2020b). Comorbidities are reported to be present, with hypertension being the most common, followed by diabetes and coronary heart diseases. It was recently reported that patients with high plasma troponin T (TnT) levels also possess higher leukocyte counts, lower lymphocyte counts, higher levels of D-dimer, C-reactive protein (CRP), procalcitonin, and N-terminal pro-brain natriuretic peptides (BNPs) (**Table 1**), leading to myocardial injury (**Figure 3**) (Guo et al., 2020).

Systemic inflammation and increased shear stress due to increased coronary blood flow can mediate the precipitation of ruptured plaques inside the artery. Platelets generally cover up this ruptured area by clot formation, thus further narrowing the artery diameter, resulting in acute myocardial infarction (MI). Both tachy- and brady-arrhythmias are known to occur in

COVID-19 (Bansal, 2020). Due to dysregulated cytokines, there are probabilities for the development of atherosclerotic plaques in SARS-CoV-2 infected patients. The atherosclerotic condition may arise due to elevated concentrations of plasma IL-1β, IL-6, and TNF-α, thus inducing plaque rupture and luminal thrombosis (Vinciguerra et al., 2020). Recent studies have suggested about the infiltration of myocardium by interstitial mononuclear inflammatory cells along with elevated concentrations of Th1 cell response–related cytokines that is, IFN-γ, inducible protein 10 (IP-10), IL-1β, and MCP-1 as well as Th2 cell response–related cytokines that is, IL-10 and IL-4 in COVID-19 autopsy results. These results suggest the possibility of occurrence of SARS-CoV-2–induced fulminant myocarditis (FM) (Chen et al., 2020b).

SARS-COV-2–INDUCED THROMBOTIC COMPLICATIONS

A report of SARS-CoV-2–induced fibrinous pulmonary thrombi is recently noticed in many patients, along with cardiovascular complications in COVID-19 (Dolhnikoff et al., 2020). Thrombosis refers to the formation of a blood clot inside the blood vessel, which can be an outcome of normal response to injury or due to pathological conditions (i.e., infection or inflammation). Blood platelets along with endothelial cells and coagulation proteins are the pivotal mediators of thrombosis (Koupenova-Zamor et al., 2017). There are basically two types of thrombosis that is, arterial thrombosis that often results in stroke and myocardial infarction (MI), and venous thrombosis which causes venous thromboembolism (VTE) and pulmonary embolism (PE). Arterial thrombi generally form around the ruptured plaques and are rich in platelets, whereas the venous thrombi are rich in fibrin and RBCs (Koupenova-Zamor et al., 2017), (Klatt et al., 2018). Thrombogenic events include ischemic stroke, pulmonary embolism, deep venous thrombosis (DVT), mesenteric ischemia, and acute coronary syndrome, which occur as a result of major complications of certain pathological conditions, such as hypertension, atherosclerosis, and diabetes mellitus (DM) (Fraga-Silva et al., 2009). As we know the SARS virus uses ACE2 as its entry receptor into a cell, ACE2 also plays a major role in the virus-induced thrombogenic events. Contrastingly, it has been reported that thrombus formation is attenuated by the activation of ACE2 and this ACE2 also decreases platelet adhesion to the blood vessels (Fraga-Silva et al., 2009).

Generally, the pro-atherosclerotic Ang II is converted into antiatherosclerotic Ang 1–7 by the help of ACE2 (Wang et al., 2020). Moreover, ACE2 is thought to be responsible for DABK degradation, which is a pro-inflammatory bradykinin that can cause microvascular leakage (Madeddu, 2020). An increase in reactive oxygen species (ROS) and a decrease in endothelium-derived nitric oxide (EDNO) are characteristic features of endothelial dysfunction. Recently, it has been documented that there is a protective RAS signaling axis which is composed of ACE2, Ang 1–7, and Mas receptors, and these molecules together augments the vascular functioning (Fraga-Silva et al., 2013). Many cardiovascular protective molecules through this ACE2-mediated axis are generated that is, NO and Akt phosphorylation, resulting in vasodilation and it also decreases the chance of thrombosis (Rabelo et al., 2011).

In SARS patients, the concentration of D-dimer and prolonged thromboplastin time (PTT) are seen to be elevated according to recent reports. In some other cases, the marantic valvular vegetation (associated with occipital lobe, kidney, spleen, and heart), pulmonary thromboembolism (PTE), and venous thrombosis–like conditions were documented (Ng et al., 2005). Hypofibrinolysis and hypercoagulation were also noticed in SARS patients earlier (Sun et al., 2014). Swelling, proliferation and apoptosis of vascular endothelial cells, inflammatory cell infiltration, edema, and fibrinoid necrosis were also observed in blood vessels of different organs and tissues like muscle, lungs, heart, kidney, adrenal gland, liver, brain, and GI tract of these patients. Moreover, there were evidences for micro circulations of soft tissues around lungs, kidney, and spleen eventually leading to the formation of venous thrombi (Xiang-Hua et al., 2010).

Like SARS patients, the VTE rates are elevated in SARS-CoV-2 infection along with the elevated fibrinogen concentration and high prothrombotic intravascular coagulation (Cavalcanti et al., 2020). The occurrence of cerebral venous thromboses is also reported in COVID-19 patients indicating the possibility of cerebrovascular diseases. The presence of anti–β2-glycoprotein-I IgA and IgG antibodies and anticardiolipin IgA antibodies were also observed in COVID-19 patients. The incidence of elevated prothrombin time and the increased partial thromboplastin time was evident. Reports suggest that thrombocytopenia, leukocytosis, and endothelial injuries were also noticed in these patients (Zhang Y et al., 2020), (Chen et al., 2020a). The concentration of inflammatory cytokines like IL-6 and TNF-α was seen to be elevated causing a prothrombotic condition aided by upregulated tissue factors (TF). But contrastingly, the imbalance in the regulation of antithrombin III, plasminogen activator inhibitor type 1 (PAI-1), and protein C during inflammation and sepsis actually augments an anticoagulated state in case of SARS-CoV-2 infections (Atri et al., 2020). The alteration of fibrinogen and fibrinogen degradation products (FDP) (**Table 1**) may create the coagulation abnormalities in COVID-19 (Fei et al., 2020).

These coagulation abnormalities may lead to decreased ADAMTS-13 resulting in aggregation of uncleaved von Willebrand factor (vWF) multimers followed by the deposits of microvascular platelet thrombi, indicating the complications of both disseminated intravascular coagulation (DIC) and/or thrombotic microangiopathy (TMA) (**Figure 4**) (Levi and Thachil, 2020). The vWF maintains normal hemostasis by mediating platelet–platelet interaction and platelet–blood vessel interaction, but under endothelial injury it can be released into blood circulation as vWF multimers. At the same time, ADAMTS-13, being a metalloprotease in blood circulation can cleave these thrombogenic multimers to ensure an antithrombotic condition (Morici et al., 2020).

In short, the overall coagulopathy observations in COVID-19 patients result in the occurrence of macrovascular thromboses

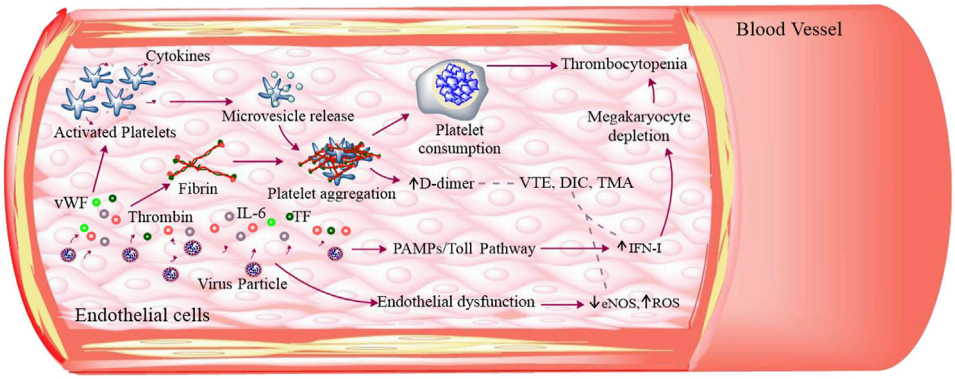

FIGURE 4 | SARS-CoV-2–induced thromboses and platelet dysfunction: SARS-CoV-2 infection caused endothelial dysfunction that releases ROS, IL-6, TF, and vWF. These molecules along with thrombin can activate platelets. The activated platelets adhere, aggregate, and secrete its granular (α and dense granules) contents as well as extracellular vesicles. The aggregated platelets induce high platelet consumption and IFN-I through Toll pathway inhibiting magakaryocyte to produce platelets, thus leading to low platelet production. All these cumulatively results in thrombocytopenia. The fibrinogen degradation produces D-dimer and other thrombogenic molecules that result in venous thromboembolism (VTE), disseminated intravascular coagulation (DIC), and thrombotic microangiopathy (TMA).

(consisting of RBCs, WBCs, platelets and fibrin) and microvascular thromboses (consisting of platelet and fibrin) in venules, arterioles, and capillaries in all major organs (Becker, 2020). Reports suggest the occurrence of blood hypercoagulability among hospitalized COVID-19 patients (Terpos et al., 2020). The minimal evidences of microangiopathy, endocardial thrombi, viral particles in adipocytes, intravascular megakaryocytes, and an unusual abundance of platelets in the spleen were also observed in SARS-CoV-2 infected patients (Becker, 2020). But, in essence the SARS-CoV-2–induced COVID-19 is a severe prothrombotic disease predominantly (Arachchillage et al., 2020). In addition, many patients who were receiving antithrombotic therapy for thrombotic diseases may have the risk to develop COVID-19 (Bikdeli et al., 2020).

Recent investigations have deduced the role of exosomal non-coding RNAs such as miR-424 and miR-103a, where the former is associated with hypercoagulability and the latter is linked with deep vein thrombosis, although the governing mechanisms is undefined in COVID-19 (Gambardella et al., 2020).

ROLE OF PLATELETS IN COVID-19

Whenever, the coronavirus-induced thrombosis is noticed, there comes a scenario of virus–platelet interaction. After RBC, platelets are the second most abundant cells found in the blood. Normal platelet counts range from 150,000 to 450,000 platelets/microliter in a healthy person (Izak and Bussel, 2014). There often arises a condition called as thrombocytopenia, in which a significant decrease in the platelet count occurs. This drop in platelet count can occur because of low platelet production, high platelet destruction, and high platelet consumption. Viruses often prefer platelets as their host cells and interact with them for invading the body immunity. The virus attachment occurs *via* different receptors present on platelets like lectins, integrins, and Toll-like receptors (TLRs), causing thrombocytopenia (Assinger, 2014). The release of the alpha and dense-granular contents is often observed from virus-stimulated platelets. These contents are reported to have stimulatory effects on immune cells against viral invasion (Pryzdial et al., 2017).

If coronaviruses are specifically observed, especially SARS-CoV, then thrombocytopenia, lymphopenia, and leukopenia-like conditions are often noticeable. The major reason behind these conditions is the site of viral infection, which are lung tissues and pulmonary endothelial cells. During infection, the damaged cells here cause platelet activation, aggregation and entrapment, resulting in thrombus formation as well as platelet and megakaryocyte consumption (Yang et al., 2004). Many studies suggest that thrombocytopenia, due to SARS-CoV, might have occurred due to platelet consumption (*via* direct viral infection of megakaryocytes and platelets), apoptosis and growth inhibition, natural immune damage of megakaryocytes and platelets, induction of low grade disseminated intravascular coagulopathy (DIC), or due to increased D-dimer (Yang et al., 2005). Like SARS-CoV, MERS-CoV infected persons also show thrombocytopenia (Ko et al., 2016).

There is a strong correlation between the platelet count and mortality of COVID-19 patients (Yang et al., 2020). Later it has been well elucidated from a study including 1799 COVID-19 patients that the viral infection causes a similar decrease in platelet count. It was later proposed that platelet was largely consumed through endothelial damage–mediated platelet activation, aggregation, and thrombosis in addition to abnormal hematopoiesis and alteration of pulmonary capillary bed, considering the fact that lung is the site of platelet release (Lippi et al., 2020). Viral infection often results in overproduction of interferon, which generally possesses antiviral activity. However, type I interferons have the potential ability to inhibit megakaryocytes, resulting in impaired platelet production. More importantly, the lungs may be the sites of platelet release from mature megakaryocytes (Yang et al., 2005). Viral infection, oxygen toxicity, and/or continuing high-pressure, in general,

induce lung damage. The damaged lung tissue and pulmonary endothelial cells were supposed to result in platelet activation, aggregation, and entrapment in the lungs, and thrombi formation at the site of injury causing the rapid consumption of platelets and megakaryocytes (Yang et al., 2005).

There have been numerous instances where decreased platelet count (thrombocytopenia) was observed in patients affected by SARS-CoV-2 (**Figure 4**; Atri et al., 2020; Yin et al., 2020; Hedrich, 2020). Recent case studies have revealed the role of megakaryocyte in this disease pathogenesis, where megakaryocytes were reported to be associated with the formation of platelet-fibrin-microthrombi that were found inside the cardiac microvasculature and other organs (Rapkiewicz et al., 2020). A novel study demonstrated the presence of SARS-CoV-2 specific RNA coding for RdRp, E (Zaid et al., 2020b), and N1 (Manne et al., 2020) in platelets, but the mechanism of entry of these viral factors is still unknown. The above finding leads to the speculation of cellular internalization of viral particle(s) by platelets. In addition to this, an elevated number of phosphatidylserine (PE)-exposed extracellular vesicles (EVs) suggesting coagulopahy (**Table 1**) along with α- and dense-granular contents (**Figure 4**) of platelets were observed to be released in SARS-CoV-2 infected patients (Zaid et al., 2020b). Moreover, an increased secretion of platelet granular contents that is, PF4 (Platelet Factor 4) from alpha granules and 5-HT (serotonin) from dense granules was observed in COVID-19 patients, indicating the platelet activation. PF4 is considered as a major regulator of T cell development, whereas 5-HT is a weak platelet agonist. If 5-HT is accompanied by other agonists like ADP, it can result in platelet aggregation (Koupenova and Freedman, 2020). The platelets also secreted more soluble CD40L and IL-1β in response to low thrombin treatment, suggesting hyperactivated platelets in SARS-CoV-2 infections in a recent study (Zaid et al., 2020a). But for now, platelets do not have ACE2 receptors for viral binding directly (Battinelli, 2020), hence, a lot about platelet–SARS-CoV-2 interaction has to be elucidated in the near future.

The hyperactivated platelets mediate platelet adherence, aggregation, and secretion (of platelet proteins and few inflammatory cytokines) in COVID-19 suggesting the fact that these platelets are supposed to take part in thrombo-inflammation (Zaid et al., 2020b). This increased platelet activation and aggregation could be manifested by elevated MAPK pathway and generation of thromboxane (TXA) (Manne et al., 2020). Recently, it has been reported that critically affected COVID-19 patients exhibit increased platelet activation and platelet–monocyte aggregation. This platelet–monocyte interaction is responsible for TF expression in the monocytes through P-selectin– and integrin αIIb/β3-dependent signaling (Hottz et al., 2020). There were a number of evidences which suggest that SARS-CoV-2 can directly interact with platelets, thus potentially modulating their thrombotic and inflammatory functions (McFadyen et al., 2020). In future studies, we can hopefully get more clear mechanistic ideas about SARS-CoV-2–induced platelet's structural and functional abnormalities.

ROLE OF IMMUNOMODULATORY MOLECULES IN COVID-19

Whenever a virus enters a host cell, its antigenic factors are supposed to be presented by antigen presenting cells (APCs) in order to elicit an immune reaction, which is required as body's natural antiviral approach. Major histocompatibility complexes (MHC-I and II) along with mannose binding lectins (MBLs) are required for antigen presentation which is proven in the case of SARS-CoV (Li X et al., 2020). In general, these viruses adopt some striking approaches for immune evasion. It was well illustrated in case of SARS-CoV and MERS-CoV that these viruses can replicate inside a pattern recognition receptor (PRR)–deprived double membrane vesicle to avoid host defense (Li X et al., 2020).

The coronavirus infections are manifested upon inflammation in different organs and tissues. For these inflammations to take place, cytokines and chemokines play vital roles leading to immunopathology. In COVID-19 patients, the pro-inflammatory cytokines like IL-1, IL-2, IL-6, IL-7, IL-10, IP-10, and TNFα as well as chemokines like IL-8 are found in higher concentrations. The abundance of these immunomodulatory molecules creates cytokine storm, which in turn initiates viral sepsis and inflammation-induced lung and cardiovascular injuries (Qin et al., 2020). By the help of these cytokines and chemokines, the monocytes and T lymphocytes are attracted from the blood to the site of infection and this infiltration of lymphocytes causes lymphopenia and an elevated neutrophil–lymphocyte ratio in COVID-19 patients (Tay et al., 2020).

Apart from these, macrophage inflammatory protein (MIP)-1α, monocyte chemoattractant protein (MCP)-1, C-reactive protein (CRP), G-CSF, procalcitonin, and ferritin were noticed in COVID-19 patients. These are the major inflammatory molecules which can cause myocardial injury (Akhmerov and Marbán, 2020). The presence of C5b-9 (membrane attack complex or MAC), C4d, and mannose binding lectin (MBL)–associated serine protease (MASP-2) were also observed during recent studies, where MAC can mediate microvascular endothelial cell injury and other microthrombotic syndromes (Magro et al., 2020). Hence, the evidences of hyperactivated complement system were observed in recent SARS-CoV-2 infected patients and previous MERS-CoV and SARS-CoV infected ones (Fletcher-Sandersjöö and Bellander, 2020). Recent evidence suggests that acute respiratory distress syndrome (ARDS) is manifested by a number of risk factors, out of which hyaluronan (HA) is important in case of SARS infected patients. The elevated levels of cytokines like TNF-α and Il-1 were noticed in COVID-19 patients. These cytokines have the strong potential to induce the enzyme(s) responsible for HA production and HA-synthase-2 (HAS2) in case of fibroblasts, EpCAM+ alveolar epithelial cells, and CD31+ endothelial cells (Shi et al., 2020). DM is suggested as a potential risk for developing COVID-19 due to elevated concentration of plasma furin (a protease that cleaves S1 and S2 subunits of SARS-CoV-2 spike (S) protein) (Muniyappa and Gubbi, 2020).

In severely affected patients, the activated CD8+ T cells, CD4+ T cells, follicular helper T cells (T_{FH}), antibody secreting cells (ASCs), and the antibodies like IgM and IgG were reportedly detected (Thevarajan et al., 2020). But at the same time, the number of helper T cells, suppressor T cells, and regulatory T cells were found to be decreased significantly. SARS-CoV-2 is also associated with increased leukocyte counts, decreased basophil, eosinophil and monocyte counts (Qin et al., 2020). The presence of CCL2 and CCL7 (potent chemokines for the recruitment of monocytes) were noticed to be enriched in bronchoalveolar fluid (BALF) from severe COVID-19 patients (Merad and Martin, 2020). Researchers suggest that the antiviral response is generally induced first by the innate immune cells, by recognizing the pathogen associated molecular patterns (PAMPs) of coronavirus, through TLR-3 and TLR-7, endosomal RNA receptors, cytosolic RNA sensor, and RIG-I/MDA5 (Prompetchara et al., 2020). These recognition events stimulate the downstream NF-κB and IRF3-mediated signaling cascades, inducing the first line of viral defense, the interferon (IFN-I) and other pro-inflammatory cytokine production. Then, the IFN type-I, through JAK-STAT pathway, complexed with IRF9 can induce the expression of IFN-stimulated genes (ISGs) (Prompetchara et al., 2020). It is evident that the SARS-CoV and MERS-CoV interfere with these signaling, leading to the production of IFNs, thus evading the immune system in many ways. As the SARS-CoV-2 uses the same receptor which SARS-CoV uses, the pattern of immunopathology was speculated to be the same. If we take a look at the adaptive immune responses, the T cell response in SARS-CoV suggests that $CD8^+$ T cell responses were more of greater magnitude than that of $CD4^+$ T cells (Prompetchara et al., 2020). Recent findings also suggest that patients with COVID-19 exhibit elevated levels of neutrophil extracellular traps (NETs) in blood serum (McFadyen et al., 2020). NETs are considered to be very important in platelet aspect as NETs can induce platelet activation *via* TLRs, thus activating the integrin receptor αIIbβ3 that can cause platelet aggregation and granule secretion. Hence, NETs are significant in linking thrombosis, coagulation, and inflammation both in microvascular (local) and macrovascular (systemic) aspects (Ortega-Paz et al., 2020). Many immunological factors and enzymes can be the targets for the development of drugs for COVID-19 (Russell et al., 2020).

ANTIPLATELET AND ANTITHROMBOTIC EFFECTS OF PHYTOCHEMICALS IN COVID-19

The recent emergence of new variants of SARS-CoV-2 has enforced the use of bioactive components of herbal plants called as phytochemicals. Phytochemicals are the plant derived primary or secondary compounds having health benefits. There are different classes of phytochemicals for example, alkaloids, flavonoids, terpenoids, phenols, and tannins, which possess anti-infection and antioxidant activities (Majnooni et al., 2020). The purified phytochemicals from natural plants were reported to have potential therapeutic effects against coronavirus that is, the herbal extracts from medicinal plants like *Cibotium barometz* (L.) J. Sm.; *Senna tora* (L.) Roxb.; *Dioscorea polystachya* Turcz.; *Gentiana scabra* Bunge; *Taxillus chinensis* (DC.) Danser; and many others were earlier described to inhibit the replication of SARS-CoV genome (Chojnacka et al., 2020). In addition, the Indian ayurvedic herb that is, Ashwagandha (*Withania somnifera* (L.) Dunal)-derived Withaferin A (Wi A), a bioactive withanolide, and Withanone (Wi-N) were reported to have inhibitory activities against human papillomavirus (HPV) and influenza viruses which can potentially downregulate the expression of TMPRSS2, thus predicting their action to block SARS-CoV-2 entry (Kumar et al., 2020).

Here in this section, we will discuss only those phytochemicals which have antiplatelet and antithrombotic effects, and can be potentially used for the treatment of COVID-19 (**Table 2**). As it is already known that cardiovascular complications arise from the impairment of platelet function(s) resulting in platelet hyperactivation and aggregation, causing thrombus formation inside blood vessels (Elisa Hirsch et al., 2017). The following are few phytochemicals which target platelet adhesion, activation, aggregation, and secretion (**Figure 1**). *Curcuma longa* L. or turmeric is used as an antiviral herb in many areas and is reported to possess anti-inflammatory, antipyretic, and anti-nociceptive properties (Kim and Park, 2019). Curcumin, an active constituent of this plant has various cellular and molecular effects, that is, it inhibits cellular apoptosis, used as an antioxidant, and an ant-tumor and antifibrotic compound. Moreover, this compound has been reported to inhibit ADP, platelet activation factor (PAF), and collagen and arachidonic acid (AA)–induced platelet activation and aggregation (Mohd Nor et al., 2016). Curcumin shows inhibitory effects on TLR, NF-κB, COX, TGF-b1, PAI-1 Cas-3, cytokines, and chemokines. It has been implicated that curcumin has the potential ability to inhibit SARS-CoV and SARS-CoV-2 enzymes, in addition to the evidence of curcumin-mediated inhibition of TMPRSS2 (Soni et al., 2020). Recent reports suggest that curcumin can also be used for the treatment of COVID-19 (Babaei et al., 2020). Similarly, *Berberis vulgaris L.* is also used as an antimicrobial herb and possesses antipyretic as well as antiemetic properties. Berberine is an active constituent of this plant and has been reported to inhibit platelet adhesion and aggregation (Mohd Nor et al., 2016). Berberine inhibits platelet by regulating Ca^{2+} mobilization and arachidonic acid metabolism (Kim et al., 2019). A recent study has revealed that berberine can be effective against SARS-CoV-2, considering the fact that it might be effective in reducing the serum levels of inflammatory molecules to restrict cytokine storm. It has been demonstrated that berberine is effective against influenza by reducing the release oxygen radicals and inhibiting inflammatory injury in mice (Zhang Y et al., 2020). Another plant, *Magnolia officinalis* (Rehder and E.H.Wilson) is used as an anticancer and antipyretic herb. Magnolol is a bioactive constituent of this plant and has proven to inhibit platelet activation and aggregation by inhibiting intracellular Ca^{2+}

mobilization and thromboxane formation (Mohd Nor et al., 2016). Magnolol is reported to reduce pro-inflammatory cytokines, ROS production, the expression of iNOS and COX-2, and NF-κB activation in lungs (Lin et al., 2015). Quercetin from *Allium cepa* L. is reported to have antiplatelet activity *via* elevation of cAMP level and attenuation of PLA2 and TXA2 level through downregulation of intracellular Ca^{2+} mobilization and COX-1 (El Haouari and Rosado, 2016). Hence, quercetin in combination with ascorbic acid is speculated to be used for the treatment of COVID-19 (Biancatelli et al., 2020). Andrographolide from *Andrographis paniculata* (Burm.f.) Nees was previously demonstrated to inhibit thrombin-induced platelet aggregation. This compound inhibits platelet aggregation through the upregulation of cGMP/PKG followed by downregulation of p38MAPK/ERK2/NF-κB pathway. Moreover, the compound also attenuated collagen-mediated platelet aggregation through the activation of eNOS/NO/cGMP cascade and eventual inhibition of PI3K/Akt/p38MAPK pathway (El Haouari and Rosado, 2016). A recent research demonstrated that andrographolide can be a potential inhibitor for SARS-CoV-2 main protease in an *in silico* study (Enmozhi et al., 2020). Rutaecarpine from *Tetradium ruticarpum* (A.Juss.) T.G.Hartley was reported to have antiplatelet activity possibly due to inhibition of PLC resulting in TXA2 attenuation and downregulation of intracellular Ca^{2+} mobilization (El Haouari and Rosado, 2016). In addition, the *Ginkgo biloba* L. extract inhibited platelet function by inhibiting the production of TXA2, and activated the production of cAMP which ultimately reduced platelet intracellular Ca^{2+} levels (El Haouari and Rosado, 2016). The extract of *Carthamus tinctorius* L. is reported to have antithrombotic activity as it increases activated partial thromboplastin time (APTT), plasma thrombin time (PTT), and prothrombin time (PT). A phytochemical named gingerol from *Zingiber officinale* Roscoe has also been reported to have antiplatelet activity as it inhibits AA-induced platelet activation and aggregation probably through inhibition of COX-1 (Mohd Nor et al., 2016). It has been recently reported that 6-gingerol has good pharmacokinetic properties and could be a promising phytochemical against SARS-CoV-2 through *in silico* studies (Rathinavel et al., 2020). Baicalin from *Scutellaria baicalensis* Georgi has been demonstrated to inhibit thrombin catalyzed fibrin polymerization and platelet functions. It also inhibited the FXa and thrombin productions, and also decreased TNF-α–induced PAI-1 production (Lee et al., 2015). Baicalin is recently reported to be a novel inhibitor of 3CL protease of SARS-CoV-2 (Su et al., 2020). There are some bioactive phytochemicals like Magnolol and Rutaecarpine whose antiplatelet effects are well elucidated (El Haouari and Rosado, 2016), (Mohd Nor et al., 2016), but their therapeutic potential against SARS-CoV-2 is still to be experimentally validated. Besides, there are other phytochemicals which are not illustrated here having antiplatelet and antithrombotic activities and their potential efficacy is still to be proven against COVID-19. Thus, *in vitro* and *in vivo* studies are still needed for the evaluation of pharmacokinetic properties and deleterious potential of these phytochemicals in COVID-19.

CONCLUSION

The SARS-CoV-2 is not always restricted only to the lungs and associated tissues, but it can invade other organs and tissues, out of which the heart is affected most. Severe respiratory distress and lung associated complications were initially thought to be the main cause of COVID-19 related deaths. Later on, detailed research and the discovery of many biomarkers of cardiac injury and its related complications were also found to be associated with the high fatality rate in COVID-19 patients. The detection of anti–β-2 glycoprotein IgA and IgG antibodies along with anticardiolipin IgA in SARS-CoV-2 infected patients shows inappropriate blood clot formation leading to cardiovascular complication. Thrombocytopenia, endothelial dysfunction, thromboembolism (**Table 1**) and leukocytosis were some of the underlying causes of the severe acute illness in COVID-19 patients. Platelet is an essential innate immune cell which responds to the SARS-CoV-2 infection. Viral infection–induced lung tissue damage can result in platelet activation, aggregation, entrapment in the lungs, and thrombi formation at the site of injury. Reduced platelet count was associated with their direct consumption during viral infection, increased number of D-dimers from fibrinolysis, high levels of type I interferon, and DIC.

The virus-induced cytokine storm causes severe inflammation in the lung tissues and increases the risk of cardiovascular tissue damage. Platelets were also reported as carriers for viral antigens that can respond to infection by secreting cytokines, granular contents, and EVs. Briefly, thrombocytopenia or low platelet count is associated with abnormal coagulation function(s), severe disease manifestation, and increased mortality in patients with COVID-19. In future, experiments in this aspect can bring insights for other roles of platelet in SARS-CoV-2 infection too. Hence, specific consideration ought to be given to cardiovascular insurance during the treatment for COVID-19. There are a number of conventional drug and vaccine trials going on for the treatment of COVID-19, but the natural bioactive compounds were earlier proven to be effective against SARS-family viruses. Phytochemicals are the natural bioactive components of herbal plants that were reported to have various cardioprotective activities, including the inhibition of platelet adhesion, activation, aggregation, and secretion, thus reducing the possibility of thrombus formation and vascular occlusion (**Figure 1**). These phytochemicals in general can target the platelet intracellular Ca^{2+} mobilization, thromboxane synthesis, and phospholipases–mediated MAPK pathways resulting in the downregulation of platelet functions. Hence, such phytochemicals could be advantageous and effective in the treatment of COVID-19. Further *in vitro* and *in vivo* studies on the efficacy of these phytochemicals will validate their effectiveness in COVID-19–induced thrombotic and cardiovascular complications.

AUTHOR CONTRIBUTIONS

SS and SB designed the study. SB, AP, and PY researched data for the article and contributed to discussions of its content. SB and AP drew all figures. SB and AP wrote the manuscript and reviewed. SS and PY edited the manuscript before submission.

ACKNOWLEDGMENTS

SB and PY are the recipients of research fellowships from Council of Scientific and Industrial Research (CSIR) and University Grants Commission (UGC), New Delhi, respectively. AP is highly thankful to the Department of Science and Technology (DST) [DST/NM/NB/2018/40 (G)], Government of India, for providing a research fellowship.

REFERENCES

Akhmerov, A., and Marbán, E. (2020). COVID-19 and the heart. *Circ. Res.* 126, 1443–1455. doi:10.1161/circresaha.120.317055

Alhogbani, T. (2016). Acute myocarditis associated with novel Middle East respiratory syndrome coronavirus. *Ann. Saudi Med.* 36, 78–80. doi:10.5144/0256-4947.2016.78

Arachchillage, D. J., Remmington, C., Rosenberg, A., Xu, T., Passariello, M., Hall, D., et al. (2020). Anticoagulation with argatroban in patients with acute antithrombin deficiency in severe COVID-19. *Br. J. Haematol.* 190, e286–8. doi:10.1111/bjh.16927

Assinger, A. (2014). Platelets and infection - an emerging role of platelets in viral infection. *Front. Immunol.* 5, 649. doi:10.3389/fimmu.2014.00649

Atri, D., Siddiqi, H. K., Lang, J. P., Nauffal, V., Morrow, D. A., and Bohula, E. A. (2020). COVID-19 for the cardiologist. *JACC* 5, 518–536. doi:10.1016/j.jacbts.2020.04.002

Babaei, F., Nassiri-Asl, M., and Hosseinzadeh, H. (2020). Curcumin (a constituent of turmeric): new treatment option against COVID-19. *Food Sci. Nutr.* 8, 5215–5227. doi:10.1002/fsn3.1858

Badawi, A., and Ryoo, S. G. (2016). Prevalence of comorbidities in the Middle East respiratory syndrome coronavirus (MERS-CoV): a systematic review and meta-analysis. *Int. J. Infect. Dis.* 49, 129–133. doi:10.1016/j.ijid.2016.06.015

Bansal, M. (2020). Cardiovascular disease and COVID-19. *Diabetes Metab. Syndr.* 14 (3), 247–250. doi:10.1016/j.dsx.2020.03.013

Battinelli, E. M. (2020). COVID-19 concerns aggregate around platelets. *J. Am. Soc. Hematol.* 136, 1221–1223. doi:10.1182/blood.2020007805

Becker, R. C. (2020). COVID-19 update: covid-19-associated coagulopathy. *J. Thromb. Thrombolysis* 50, 54–14. doi:10.1007/s11239-020-02134-3

Benarba, B., and Pandiella, A. (2020). Medicinal plants as sources of active molecules against COVID-19. *Front. Pharmacol.* 11, 1189. doi:10.3389/fphar.2020.01189

Biancatelli, R. M. L. C., Berrill, M., Catravas, J. D., and Marik, P. E. (2020). Quercetina e vitamina C: una terapia sperimentale e sinergica per la prevenzione e il trattamento della mala: a correlata alla SARS-CoV-2 (COVID-19).

Bikdeli, B., Madhavan, M. V., Jimenez, D., Chuich, T., Dreyfus, I., Driggin, E., et al. (2020). COVID-19 and thrombotic or thromboembolic disease: implications for prevention, antithrombotic therapy, and follow-up. *J. Am. Coll. Cardiol.* 75, 2950–2973. doi:10.1016/j.jacc.2020.04.031

Bojkova, D., Wagner, J., Shumliakivska, M., Aslan, G., Saleem, U., Hansen, A., et al. (2020). SARS-CoV-2 infects and induces cytotoxic effects in human cardiomyocytes. *Cardiovasc. Res.* 116 (14), 2207–2215. doi:10.1093/cvr/cvaa267

Cavalcanti, D. D., Raz, E., Shapiro, M., Dehkharghani, S., Yaghi, S., Lillemoe, K., et al. (2020). Cerebral venous thrombosis associated with COVID-19. *AJNR Am. J. Neuroradiol.* 41 (8), 1370–1376. doi:10.3174/ajnr.A6644

Chen, C., Chen, C., Yan, J. T., Zhou, N., Zhao, J. P., and Wang, D. W. (2020a). Analysis of myocardial injury in patients with COVID-19 and association between concomitant cardiovascular diseases and severity of COVID-19. *Zhonghua Xin Xue Guan Bing Za Zhi* 48, E008. doi:10.3760/cma.j.cn112148-20200225-00123

Chen, C., Li, H., Hang, W., and Wang, D. W. (2020b). Cardiac injuries in coronavirus disease 2019 (COVID-19). *J. Mol. Cell. Cardiol.* 145, 25–29. doi:10.1016/j.yjmcc.2020.06.002

Chojnacka, K., Witek-Krowiak, A., Skrzypczak, D., Mikula, K., and Młynarz, P. (2020). Phytochemicals containing biologically active polyphenols as an effective agent against Covid-19-inducing coronavirus. *J. Funct. Foods* 73, 104146. doi:10.1016/j.jff.2020.104146

Clerkin, K. J., Fried, J. A., Raikhelkar, J., Sayer, G., Griffin, J. M., Masoumi, A., et al. (2020). COVID-19 and cardiovascular disease. *Circulation* 141, 1648–1655. doi:10.1161/circulationaha.120.046941

Colaco, S., Chhabria, K., Singh, N., Bhide, A., Singh, D., Singh, A., et al. (2020). Expression of SARS-CoV-2 receptor ACE2 and the spike protein processing enzymes in developing human embryos. arXiv:2004.04935.

Dolhnikoff, M., Duarte-Neto, A. N., de Almeida Monteiro, R. A., Ferraz da Silva, L. F., Pierre de Oliveira, E., Nascimento Saldiva, P. H., et al. (2020). Pathological evidence of pulmonary thrombotic phenomena in severe COVID-19. *J. Thromb. Haemost.* 18(6):1517–1519. doi:10.1111/jth.14844

El Haouari, M., and Rosado, J. A. (2016). Medicinal plants with antiplatelet activity. *Phytother. Res.* 30, 1059–1071. doi:10.1002/ptr.5619

Enmozhi, S. K., Raja, K., Sebastine, I., and Joseph, J. (2020). Andrographolide as a potential inhibitor of SARS-CoV-2 main protease: an in silico approach. *J. Biomol. Struct. Dyn.* 1, 1–7. doi:10.1080/07391102.2020.1760136

Fei, Y., Tang, N., Liu, H., and Cao, W. (2020). Coagulation dysfunction. *Arch. Pathol. Lab. Med.* 144, 1223. doi:10.5858/arpa.2020-0324-SA

Fletcher-Sandersjöö, A., and Bellander, B.-M. (2020). Is COVID-19 associated thrombosis caused by overactivation of the complement cascade? A literature review. *Thromb. Res.* 194, 36–41. doi:10.1016/j.thromres.2020.06.027

Fraga-Silva, R. A., Costa-Fraga, F. P., Murça, T. M., Moraes, P. L., Martins Lima, A., Lautner, R. Q., et al. (2013). Angiotensin-converting enzyme 2 activation improves endothelial function. *Hypertension* 61, 1233–1238. doi:10.1161/hypertensionaha.111.00627

Fraga-Silva, R. A., Sorg, B. S., Wankhede, M., deDeugd, C., Ferreira, A. J., Jun, Y., et al. (2009). ACE2 activation promotes antithrombotic activity. *Mol. Med.* 16 (5–6), 210–215. doi:10.2119/molmed.2009.00160

Gambardella, J., Sardu, C., Morelli, M. B., Messina, V., Marfella, R., Maggi, P., et al. (2020). Abstract 221: exosomal microRNAs drive tromboembolism in covid-19. *Circulation* 142, A221. doi:10.1161/circ.142.suppl_4.221

Gao, Y., Yan, L., Huang, Y., Liu, F., Zhao, Y., Cao, L., et al. (2020). Structure of the RNA-dependent RNA polymerase from COVID-19 virus. *Science* 368, 779–782. doi:10.1126/science.abb7498

Ghildiyal, R., Prakash, V., Chaudhary, V. K., Gupta, V., and Gabrani, R. (2016). "Phytochemicals as antiviral agents: recent updates," in *Plant-derived bioactives*. Editor M. Swamy (Singapore: Springer). doi:10.1007/978-981-15-1761-7_122

Guo, T., Fan, Y., Chen, M., Wu, X., Zhang, L., He, T., et al. (2020). Cardiovascular implications of fatal outcomes of patients with coronavirus disease 2019 (COVID-19). *JAMA Cardiol.* 5 (7), 811–818. doi:10.1001/jamacardio.2020.1017

Gupta, A. K., Jneid, H., Addison, D., Ardehali, H., Boehme, A. K., Borgaonkar, S., et al. (2020). Current perspectives on Coronavirus 2019 (COVID-19) and cardiovascular disease: a white paper by the JAHA editors. *J. Am. Heart Assoc.* 9, e017013. doi:10.1161/jaha.120.017013

Hedrich, C. M. (2020). COVID-19 - considerations for the paediatric rheumatologist. *Clin. Immunol.* 214, 108420. doi:10.1016/j.clim.2020.108420

Heurich, A., Hofmann-Winkler, H., Gierer, S., Liepold, T., Jahn, O., and Pöhlmann, S. (2014). TMPRSS2 and ADAM17 cleave ACE2 differentially and only proteolysis by TMPRSS2 augments entry driven by the severe acute respiratory syndrome coronavirus spike protein. *J. Virol.* 88, 1293–1307. doi:10.1128/jvi.02202-13

Hirsch, G. E., Nazario Viecili, P. R., de Almeida, A. S., Nascimento, S., Porto, F. G., Otero, J., et al. (2017). Natural products with antiplatelet action. *Cpd* 23, 1228–1246. doi:10.2174/1381612823666161123151611

Hoffmann, M., Kleine-Weber, H., Krüger, N., Mueller, M. A., Drosten, C., and Pöhlmann, S. (2020a). The novel coronavirus 2019 (2019-nCoV) uses the SARS-coronavirus receptor ACE2 and the cellular protease TMPRSS2 for entry into target cells. *BioRxiv*.

Hoffmann, M., Kleine-Weber, H., Schroeder, S., Krüger, N., Herrler, T., Erichsen, S., et al. (2020b). SARS-CoV-2 cell entry depends on ACE2 and TMPRSS2 and is blocked by a clinically proven protease inhibitor. *Cell* 181, 271–280.e8. doi:10.1016/j.cell.2020.02.052

Hottz, E. D., Azevedo-Quintanilha, I. G., Palhinha, L., Teixeira, L., Barreto, E. A., Pão, C. R. R., et al. (2020). Platelet activation and platelet-monocyte aggregates formation trigger tissue factor expression in severe COVID-19 patients. *Blood* 136 (11), 1330–1341. doi:10.1182/blood.2020007252

Ibrahim, I. M., Abdelmalek, D. H., Elshahat, M. E., and Elfiky, A. A. (2020). COVID-19 spike-host cell receptor GRP78 binding site prediction. *J. Infect.* 80, 554–562. doi:10.1016/j.jinf.2020.02.026

Izak, M., and Bussel, J. B. (2014). Management of thrombocytopenia. *F1000Prime Rep.* 6, 45. doi:10.12703/P6-45

Kim, K., Do, H. J., Oh, T. W., Kim, K.-Y., Kim, T. H., Ma, J. Y., et al. (2019). Antiplatelet and antithrombotic activity of a traditional medicine, hwangryunhaedok-tang. *Front. Pharmacol.* 9, 1502. doi:10.3389/fphar.2018.01502

Kim, K., and Park, K.-I. (2019). A review of antiplatelet activity of traditional medicinal herbs on integrative medicine studies. *Evid. Based Complement. Alternat. Med.* 2019, 7125162. doi:10.1155/2019/7125162

Klatt, C., Krüger, I., Zey, S., Krott, K.-J., Spelleken, M., Gowert, N. S., et al. (2018). Platelet-RBC interaction mediated by FasL/FasR induces procoagulant activity important for thrombosis. *J. Clin. Invest.* 128, 3906–3925. doi:10.1172/jci92077

Ko, J.-H., Park, G. E., Lee, J. Y., Lee, J. Y., Cho, S. Y., Ha, Y. E., et al. (2016). Predictive factors for pneumonia development and progression to respiratory failure in MERS-CoV infected patients. *J. Infect.* 73, 468–475. doi:10.1016/j.jinf.2016.08.005

Kochi, A. N., Tagliari, A. P., Forleo, G. B., Fassini, G. M., and Tondo, C. (2020). Cardiac and arrhythmic complications in patients with COVID-19. *J. Cardiovasc. Electrophysiol.* 31 (5), 1003–1008. doi:10.1111/jce.14479

Koupenova, M., and Freedman, J. E. (2020). Platelets and COVID-19: inflammation, hyperactivation and additional questions. *Circ. Res.* 127 (11), 1419–1421. doi:10.1161/CIRCRESAHA.120.318218

Koupenova-Zamor, M., Kehrel, B. E., Corkrey, H. A., and Freedman, J. E. (2017). Thrombosis and platelets: an update. *Eur. Heart J.* 38 (11), 785–791. doi:10.1093/eurheartj/ehw550

Kuba, K., Imai, Y., and Penninger, J. M. (2013). Multiple functions of angiotensin-converting enzyme 2 and its relevance in cardiovascular diseases. *Circ. J.* 77, 301–308. doi:10.1253/circj.cj-12-1544

Kuba, K., Imai, Y., Rao, S., Jiang, C., and Penninger, J. M. (2006). Lessons from SARS: control of acute lung failure by the SARS receptor ACE2. *J. Mol. Med.* 84, 814–820. doi:10.1007/s00109-006-0094-9

Kumar, V., Dhanjal, J. K., Bhargava, P., Kaul, A., Wang, J., Zhang, H., et al. (2020). Withanone and withaferin-A are predicted to interact with transmembrane protease serine 2 (TMPRSS2) and block entry of SARS-CoV-2 into cells. *J. Biomol. Struct. Dyn.*, 1–13. doi:10.1080/07391102.2020.1775704

Kuster, G. M., Pfister, O., Burkard, T., Zhou, Q., Twerenbold, R., Haaf, P., et al. (2020). SARS-CoV2: should inhibitors of the renin–angiotensin system be withdrawn in patients with COVID-19? *Eur. Heart J.* 41 (19), 1801–1803. doi:10.1093/eurheartj/ehaa235

Lee, W., Ku, S.-K., and Bae, J.-S. (2015). Antiplatelet, anticoagulant, and profibrinolytic activities of baicalin. *Arch. Pharm. Res.* 38, 893–903. doi:10.1007/s12272-014-0410-9

Levi, M., and Thachil, J. (2020). Coronavirus disease 2019 coagulopathy: disseminated intravascular coagulation and thrombotic microangiopathy-either, neither, or both. *Semin. Thromb. Hemost.* 46, 781. doi:10.1055/s-0040-1712156

Li, X., Geng, M., Peng, Y., Meng, L., and Lu, S. (2020). Molecular immune pathogenesis and diagnosis of COVID-19. *J. Pharm. Anal.* 10, 102–108. doi:10.1016/j.jpha.2020.03.001

Li, Y., Jerkic, M., Slutsky, A. S., and Zhang, H. (2020). Molecular mechanisms of sex bias differences in COVID-19 mortality. *Crit. Care* 24, 1–6. doi:10.1186/s13054-020-03118-8

Lin, M.-H., Chen, M.-C., Chen, T.-H., Chang, H.-Y., and Chou, T.-C. (2015). Magnolol ameliorates lipopolysaccharide-induced acute lung injury in rats through PPAR-γ-dependent inhibition of NF-kB activation. *Int. Immunopharmacol.* 28, 270–278. doi:10.1016/j.intimp.2015.05.051

Lippi, G., Plebani, M., and Henry, B. M. (2020). Thrombocytopenia is associated with severe coronavirus disease 2019 (COVID-19) infections: a meta-analysis. *Clin. Chim. Acta* 506, 145–148. doi:10.1016/j.cca.2020.03.022

Liu, P. P., Blet, A., Smyth, D., and Li, H. (2020). The science underlying COVID-19. *Circulation* 142, 68. doi:10.1161/circulationaha.120.047549

Madeddu, P. (2020). Cardiovascular complications of COVID-19: evidence, misconceptions, and new opportunities. *Vasc. Biol.* 2 (1), E3–E6. doi:10.1530/VB-20-0008

Magro, C., Mulvey, J. J., Berlin, D., Nuovo, G., Salvatore, S., Harp, J., et al. (2020). Complement associated microvascular injury and thrombosis in the pathogenesis of severe COVID-19 infection: a report of five cases. *Transl. Res.* 220 (20), 1–13. doi:10.1016/j.trsl.2020.04.007

Majnooni, M. B., Fakhri, S., Shokoohinia, Y., Kiyani, N., Stage, K., Mohammadi, P., et al. (2020). Phytochemicals: potential therapeutic interventions against coronavirus-associated lung injury. *Front. Pharmacol.* 11, 1744. doi:10.3389/fphar.2020.588467

Manne, B. K., Denorme, F., Middleton, E. A., Portier, I., Rowley, J. W., Stubben, C., et al. (2020). Platelet gene expression and function in patients with COVID-19. *Blood* 136, 1317. doi:10.1182/blood.2020007214

McFadyen, J. D., Stevens, H., and Peter, K. J. C. (2020). The emerging threat of (micro) thrombosis in COVID-19 and its therapeutic implications. *Circ. Res.* 127 (4), 571–587. doi:10.1161/CIRCRESAHA.120.317447

McGonagle, D., O'Donnell, J. S., Sharif, K., Emery, P., and Bridgewood, C. (2020). Immune mechanisms of pulmonary intravascular coagulopathy in COVID-19 pneumonia. *Lancet Rheumatol.* 2 (7), e437–e445. doi:10.1016/S2665-9913(20)30121-1

Mehta, P., McAuley, D. F., Brown, M., Sanchez, E., Tattersall, R. S., and Manson, J. J. (2020). COVID-19: consider cytokine storm syndromes and immunosuppression. *Lancet* 395, 1033–1034. doi:10.1016/s0140-6736(20)30628-0

Merad, M., and Martin, J. C. (2020). Pathological inflammation in patients with COVID-19: a key role for monocytes and macrophages. *Nat. Rev. Immunol.* 20, 355–358. doi:10.1038/s41577-020-0331-4

Meyer, D., Sielaff, F., Hammami, M., Böttcher-Friebertshäuser, E., Garten, W., and Steinmetzer, T. (2013). Identification of the first synthetic inhibitors of the type II transmembrane serine protease TMPRSS2 suitable for inhibition of influenza virus activation. *Biochem. J.* 452, 331–343. doi:10.1042/bj20130101

Mohd Nor, N. H., Othman, F., Mohd Tohit, E. R., and Md Noor, S. (2016). Medicinal herbals with antiplatelet properties benefit in coronary atherothrombotic diseases. *Thrombosis* 2016, 5952910. doi:10.1155/2016/5952910

Morici, N., Bottiroli, M., Fumagalli, R., Marini, C., and Cattaneo, M. (2020). Role of von Willebrand factor and ADAMTS-13 in the pathogenesis of thrombi in SARS-CoV-2 infection: time to rethink. *Thromb. Haemost.* 120, 1339. doi:10.1055/s-0040-1713400

Mughal, A., and O'Rourke, S. T. (2018). Vascular effects of apelin: mechanisms and therapeutic potential. *Pharmacol. Ther.* 190, 139–147. doi:10.1016/j.pharmthera.2018.05.013

Muniyappa, R., and Gubbi, S. (2020). COVID-19 pandemic, coronaviruses, and diabetes mellitus. *Am. J. Physiol.-Endocrinol. Metab.* 318, E736–E741. doi:10.1152/ajpendo.00124.2020

Ng, K. H. L., Wu, A. K. L., Cheng, V. C. C., Tang, B. S. F., Chan, C. Y., Yung, C. Y., et al. (2005). Pulmonary artery thrombosis in a patient with severe acute respiratory syndrome. *Postgrad. Med. J.* 81, e3. doi:10.1136/pgmj.2004.030049

Nishiga, M., Wang, D. W., Han, Y., Lewis, D. B., and Wu, J. C. (2020). COVID-19 and cardiovascular disease: from basic mechanisms to clinical perspectives, *Nat. Rev. Cardiol.* 17 (9), 543–558. doi:10.1038/s41569-020-0413-9

Ortega-Paz, L., Capodanno, D., Montalescot, G., and Angiolillo, D. J. (2020). COVID-19 associated thrombosis and coagulopathy: review of the pathophysiology and implications for antithrombotic management. *J. Am. Heart Assoc.* 10 (3), e019650. doi:10.1161/JAHA.120.019650

Oudit, G. Y., Crackower, M. A., Backx, P. H., and Penninger, J. M. (2003). The role of ACE2 in cardiovascular physiology. *Trends Cardiovasc. Med.* 13, 93–101. doi:10.1016/s1050-1738(02)00233-5

Prompetchara, E., Ketloy, C., and Palaga, T. (2020). Immune responses in COVID-19 and potential vaccines: lessons learned from SARS and MERS epidemic. *Asian Pac. J. Allergy Immunol.* 38, 1–9. doi:10.12932/ap-200220-0772

Pryzdial, E. L. G., Lin, B. H., and Sutherland, M. R. (2017). "Virus–platelet associations," in *Platelets in Thrombotic and Non-Thrombotic Disorders: pathophysiology, Pharmacology and Therapeutics: an Update*. Editors P. Gresele, N. S. Kleiman, J. A. Lopez, and C. P. Page (Cham: Springer International Publishing), 1085–1102.

Qin, C., Zhou, L., Hu, Z., Zhang, S., Yang, S., Tao, Y., et al. (2020). Dysregulation of immune response in patients with coronavirus 2019 (COVID-19) in Wuhan, China. *Clin. Infect. Dis.* 71, 762–768. doi:10.1093/cid/ciaa248

Rabelo, L. A., Alenina, N., and Bader, M. (2011). ACE2-angiotensin-(1-7)-Mas axis and oxidative stress in cardiovascular disease. *Hypertens. Res.* 34, 154–160. doi:10.1038/hr.2010.235

Rapkiewicz, A. V., Mai, X., Carsons, S. E., Pittaluga, S., Kleiner, D. E., Berger, J. S., et al. (2020). Megakaryocytes and platelet-fibrin thrombi characterize multi-organ thrombosis at autopsy in COVID-19: a case series. *EClinicalMedicine* 24, 100434. doi:10.1016/j.eclinm.2020.100434

Rathinavel, T., Palanisamy, M., Palanisamy, S., Subramanian, A., and Thangaswamy, S. (2020). Phytochemical 6-gingerol–a promising drug of choice for COVID-19. *Int. J. Adv. Sci. Eng.* 6 (4), 1482–1489. doi:10.29294/IJASE.6.4.2020.1482-1489

Russell, B., Moss, C., George, G., Santaolalla, A., Cope, A., Papa, S., et al. (2020). Associations between immune-suppressive and stimulating drugs and novel COVID-19-a systematic review of current evidence. *ecancer* 14, 1022. doi:10.3332/ecancer.2020.1022

Sanders, J. M., Monogue, M. L., Jodlowski, T. Z., and Cutrell, J. B. (2020). Pharmacologic treatments for coronavirus disease 2019 (COVID-19): a review. *Jama* 323, 1824–1836. doi:10.1001/jama.2020.6019

Shereen, M. A., Khan, S., Kazmi, A., Bashir, N., and Siddique, R. (2020). COVID-19 infection: emergence, transmission, and characteristics of human coronaviruses. *J. Adv. Res.* 24, 91–98. doi:10.1016/j.jare.2020.03.005

Shi, Y., Wang, Y., Shao, C., Huang, J., Gan, J., Huang, X., et al. (2020). COVID-19 infection: the perspectives on immune responses. *Cell Death Differ.* 27, 1451–1454. doi:10.1038/s41418-020-0530-3

Soni, V. K., Mehta, A., Ratre, Y. K., Tiwari, A. K., Amit, A., Singh, R. P., et al. (2020). Curcumin, a traditional spice component, can hold the promise against COVID-19? *Eur. J. Pharmacol.* 886, 173551. doi:10.1016/j.ejphar.2020.173551

Su, H., Yao, S., Zhao, W., Li, M., Liu, J., Shang, W., et al. (2020). Discovery of baicalin and baicalein as novel, natural product inhibitors of SARS-CoV-2 3CL protease *in vitro*. *bioRxiv*. doi:10.2210/pdb6m2n/pdb

Sun, W., Li, Z., Shi, Z., Wang, B., Gao, F., Yang, Y., et al. (2014). Relationship between post-SARS osteonecrosis and PAI-1 4G/5G gene polymorphisms. *Eur. J. Orthop. Surg. Traumatol.* 24, 525–529. doi:10.1007/s00590-013-1223-0

Swain, S. S., Panda, S. K., and Luyten, W. (2020). Phytochemicals against SARS-CoV as potential drug leads. *Biomed. J.* S2319–4170 (20), 30229–30238. doi:10.1016/j.bj.2020.12.002

Tay, M. Z., Poh, C. M., Rénia, L., MacAry, P. A., and Ng, L. F. P. (2020). The trinity of COVID-19: immunity, inflammation and intervention. *Nat. Rev. Immunol.* 20, 363–374. doi:10.1038/s41577-020-0311-8

Terpos, E., Ntanasis-Stathopoulos, I., Elalamy, I., Kastritis, E., Sergentanis, T. N., Politou, M., et al. (2020). Hematological findings and complications of COVID-19. *Am. J. Hematol.* 95, 834. doi:10.1002/ajh.25829

Thevarajan, I., Nguyen, T. H. O., Koutsakos, M., Druce, J., Caly, L., van de Sandt, C. E., et al. (2020). Breadth of concomitant immune responses prior to patient recovery: a case report of non-severe COVID-19. *Nat. Med.* 26, 453–455. doi:10.1038/s41591-020-0819-2

Tikellis, C., Bernardi, S., and Burns, W. C. (2011). Angiotensin-converting enzyme 2 is a key modulator of the renin-angiotensin system in cardiovascular and renal disease. *Curr. Opin. Nephrol. Hypertens.* 20, 62–68. doi:10.1097/MNH.0b013e328341164a

Vinciguerra, M., Romiti, S., and Greco, E. (2020). Atherosclerosis as pathogenetic substrate for Sars-Cov2 cytokine storm. *J. Clin. Med.* 9 (7), 2095. doi:10.3390/jcm9072095

Walls, A. C., Park, Y.-J., Tortorici, M. A., Wall, A., McGuire, A. T., and Veesler, D. (2020). Structure, function, and antigenicity of the SARS-CoV-2 spike glycoprotein. *Cell* 181, 281–292.e6. doi:10.1016/j.cell.2020.02.058

Wang, J., Hajizadeh, N., Moore, E. E., McIntyre, R. C., Moore, P. K., Veress, L. A., et al. (2020). Tissue plasminogen activator (tPA) treatment for COVID-19 associated acute respiratory distress syndrome (ARDS): a case series. *J. Thromb. Haemost.* 18, 1752–1755. doi:10.1111/jth.14828

Xiang-Hua, Y., Le-Min, W., Ai-Bin, L., Zhu, G., Riquan, L., Xu-You, Z., et al. (2010). Severe acute respiratory syndrome and venous thromboembolism in multiple organs. *Am. J. Respir. Crit. Care Med.* 182, 436–437. doi:10.1164/ajrccm.182.3.436

Xiong, T.-Y., Redwood, S., Prendergast, B., and Chen, M. (2020). Coronaviruses and the cardiovascular system: acute and long-term implications. *Eur. Heart J.* 41 (19), 1798–1800. doi:10.1093/eurheartj/ehaa231

Xu, P., Zhou, Q., and Xu, J. (2020). Mechanism of thrombocytopenia in COVID-19 patients. *Ann. Hematol.* 99, 1205–1208. doi:10.1007/s00277-020-04019-0

Yan, R., Zhang, Y., Li, Y., Xia, L., Guo, Y., and Zhou, Q. (2020). Structural basis for the recognition of SARS-CoV-2 by full-length human ACE2. *Science* 367, 1444–1448. doi:10.1126/science.abb2762

Yang, M., Li, C. K., Li, K., Hon, K. L., Ng, M. H., Chan, P. K., et al. (2004). Hematological findings in SARS patients and possible mechanisms (review). *Int. J. Mol. Med.* 14, 311–315. doi:10.3892/ijmm.14.2.311

Yang, M., Ng, M. H., and Li, C. K. (2005). Thrombocytopenia in patients with severe acute respiratory syndrome (review). *Hematology* 10, 101–105. doi:10.1080/10245330400026170

Yang, X., Yang, Q., Wang, Y., Wu, Y., Xu, J., Yu, Y., et al. (2020). Thrombocytopenia and its association with mortality in patients with COVID-19. *J. Thromb. Haemost.* 18, 1469–1472. doi:10.1111/jth.14848

Yin, S., Huang, M., Li, D., and Tang, N. (2020). Difference of coagulation features between severe pneumonia induced by SARS-CoV2 and non-SARS-CoV2. *J. Thromb. Thrombolysis*, 1–4. doi:10.1007/s11239-020-02105-8

Zaid, Y., Puhm, F., Allaeys, I., Naya, A., Oudghiri, M., Khalki, L., et al. (2020b). Platelets can contain SARS-CoV-2 RNA and are hyperactivated in COVID-19. *Circ. Res.* 127 (11), 1404–1418. doi:10.1161/CIRCRESAHA.120.317703

Zaid, Y., Puhm, F., Allaeys, I., Naya, A., Oudghiri, M., Khalki, L., et al. (2020a). Platelets can associate with SARS-Cov-2 RNA and are hyperactivated in COVID-19. *Circ. Res.* 127, 1404–1418. doi:10.1161/circresaha.120.317703

Zhang, B. Y., Chen, M., Chen, X. C., Cao, K., You, Y., Qian, Y. J., et al. (2020). Berberine reduces circulating inflammatory mediators in patients with severe COVID-19. *Br. J. Surg.* 108 (1), e9–e11. doi:10.1093/bjs/znaa021

Zhang, Y., Xiao, M., Zhang, S., Xia, P., Cao, W., Jiang, W., et al. (2020). Coagulopathy and antiphospholipid antibodies in patients with covid-19. *N. Engl. J. Med.* 382, e38. doi:10.1056/NEJMc2007575

Zheng, Y.-Y., Ma, Y.-T., Zhang, J.-Y., and Xie, X. (2020). COVID-19 and the cardiovascular system. *Nat. Rev. Cardiol.* 17, 259–260. doi:10.1038/s41569-020-0360-5

Conflict of Interest: The authors declare that the research was conducted in the absence of any commercial or financial relationships that could be construed as a potential conflict of interest.

frontiers in Pharmacology

REVIEW
published: 03 May 2021
doi: 10.3389/fphar.2021.629935

Natural Products Modulating Angiotensin Converting Enzyme 2 (ACE2) as Potential COVID-19 Therapies

Murtala Bello Abubakar[1,2], Dawoud Usman[1,2], Gaber El-Saber Batiha[3]*, Natália Cruz-Martins[4,5,6]*, Ibrahim Malami[2,7], Kasimu Ghandi Ibrahim[1,2], Bilyaminu Abubakar[2,8], Muhammad Bashir Bello[2,9], Aliyu Muhammad[10], Siew Hua Gan[11], Aliyu Ibrahim Dabai[2,12], M Alblihed[13], Arabinda Ghosh[14], Reem H. Badr[15], Devarajan Thangadurai[16] and Mustapha Umar Imam[2,17]*

[1]Department of Physiology, Faculty of Basic Medical Sciences, College of Health Sciences, Usmanu Danfodiyo University, Sokoto, Nigeria, [2]Centre for Advanced Medical Research and Training, Usmanu Danfodiyo University, Sokoto, Nigeria, [3]Department of Pharmacology and Therapeutics, Faculty of Veterinary Medicine, Damanhour University, Damanhour, Egypt, [4]Faculty of Medicine, University of Porto, Porto, Portugal, [5]Institute for Research and Innovation in Health (i3S), University of Porto, Porto, Portugal, [6]Laboratory of Neuropsychophysiology, Faculty of Psychology and Education Sciences, University of Porto, Porto, Portugal, [7]Department of Pharmacognosy and Ethnopharmacy, Faculty of Pharmaceutical Sciences, Usmanu Danfodiyo University, Sokoto, Nigeria, [8]Department of Pharmacology and Toxicology, Faculty of Pharmaceutical Sciences, Usmanu Danfodiyo University, Sokoto, Nigeria, [9]Department of Veterinary Microbiology, Faculty of Veterinary Medicine, Usmanu Danfodiyo University, Sokoto, Nigeria, [10]Department of Biochemistry, Faculty of Life Sciences, Ahmadu Bello University, Zaria, Kaduna Sate, Nigeria, [11]School of Pharmacy, Monash University Malaysia, Bandar Sunway, Malaysia, [12]Department of Microbiology, Usmanu Danfodiyo University, Sokoto, Nigeria, [13]Department of Microbiology, College of Medicine, Taif University, Taif, Saudi Arabia, [14]Microbiology Division, Department of Botany, Gauhati University, Guwahati, India, [15]Department of Botany and Microbiology, Faculty of Science, Alexandria University, Alexandria, Egypt, [16]Department of Botany, Karnatak University, Dharwad, India, [17]Department of Medical Biochemistry, Faculty of Basic Medical Sciences, College of Health Sciences, Usmanu Danfodiyo University, Sokoto, Nigeria*

OPEN ACCESS

Edited by:
Anirban Mandal, Mrinalini Datta Mahavidyapith, India

Reviewed by:
Francis-Alfred Unuagbe Attah, University of Ilorin, Nigeria
Chun Yang, Nanjing Medical University, China

***Correspondence:**
Murtala Bello Abubakar
murtala.bello@udusok.edu.ng
Gaber El-Saber Batiha
gaberbatiha@gmail.com
Natália Cruz-Martins
ncmartins@med.up.pt

Specialty section:
This article was submitted to Ethnopharmacology, a section of the journal Frontiers in Pharmacology

Received: *16 November 2020*
Accepted: *08 March 2021*
Published: *03 May 2021*

Citation:
Abubakar MB, Usman D, El-Saber Batiha G, Cruz-Martins N, Malami I, Ibrahim KG, Abubakar B, Bello MB, Muhammad A, Gan SH, Dabai AI, Alblihed M, Ghosh A, Badr RH, Thangadurai D and Imam MU (2021) Natural Products Modulating Angiotensin Converting Enzyme 2 (ACE2) as Potential COVID-19 Therapies. Front. Pharmacol. 12:629935. doi: 10.3389/fphar.2021.629935

The 2019 coronavirus disease (COVID-19) is a potentially fatal multisystemic infection caused by the severe acute respiratory syndrome coronavirus-2 (SARS-CoV-2). Currently, viable therapeutic options that are cost effective, safe and readily available are desired, but lacking. Nevertheless, the pandemic is noticeably of lesser burden in African and Asian regions, where the use of traditional herbs predominates, with such relationship warranting a closer look at ethnomedicine. From a molecular viewpoint, the interaction of SARS-CoV-2 with angiotensin converting enzyme 2 (ACE2) is the crucial first phase of COVID-19 pathogenesis. Here, we review plants with medicinal properties which may be implicated in mitigation of viral invasion either via direct or indirect modulation of ACE2 activity to ameliorate COVID-19. Selected ethnomedicinal plants containing bioactive compounds which may prevent and mitigate the fusion and entry of the SARS-CoV-2 by modulating ACE2-associated up and downstream events are highlighted. Through further experimentation, these plants could be supported for ethnobotanical use and the phytomedicinal ligands could be potentially developed into single or

Abbreviations: ACE2, Angiotensin converting enzyme two; ADME/T, Absorption, Distribution, Metabolism, Excretion/and Toxicity; DPP4, Dipeptidyl peptidase four; mAb, monoclonal antibody; NA, not available; PK, Pharmacokinetic; S-RBD, Spike glycoprotein receptor binding domain; TMPRSS2, Transmembrane protease serine two; Wi-A, Withaferine-A; Wi-N, Withanone.

combined preventive therapeutics for COVID-19. This will benefit researchers actively looking for solutions from plant bioresources and help lessen the burden of COVID-19 across the globe.

Keywords: medicinal plants, renin-angiotensin-system, COVID-19, ACE2, SARS-CoV-2.

INTRODUCTION

By the end of December 2020, less than a year after it was declared an outbreak, the severe acute respiratory syndrome coronavirus-2 (SARS-CoV-2) had infected over 80 million people and claimed almost two million lives (European Center for Disease Prevention and Control, 2020). This places its mortality score over a thousand-fold greater than that of its homolog, the 2002/2003 SARS-CoV (WHO, 2004; de Wit et al., 2016). To date (30th, January. 2021), based on a MEDLINE search, due to its severity, over 90,000 papers (and possibly more) have addressed the 2019 coronavirus disease (COVID-19). COVID-19 develops after SARS-CoV-2 gains entry into host cells by binding to angiotensin converting enzyme 2 (ACE2) receptors (Hoffmann et al., 2020). This crucial first step initiates a cascade of events that results in a vicious cycle of virion to cell infection and replication that includes attachment, penetration, uncoating, translation, replication, assembly and release. The fusion to ACE2 receptor and internalization causes down-regulation of the ACE2 receptor, halting its traditional protective functions over the renin-angiotensin system (RAS) and potentiating the pathophysiological sequelae of COVID-19 (Verdecchia et al., 2020).

In this way, finding solutions to COVID-19 is at the core of solving this global pandemic. At present, available pharmaceuticals face numerous limitations in the treatment of COVID-19. The challenges range from safety and side effects to poor efficacy which warrants the search for better treatment modalities (Gupta and Misra, 2020; Nittari et al., 2020). Like with SARS-CoV, persistent complications, such as lung damage, make preventive strategies the best option (Kuba et al., 2005). In this pursuit, the development of vaccines and therapeutic approaches conceptually linked to ACE2 rank high for preventing COVID-19 (Bourgonje et al., 2020). Vaccines are either undergoing trials (with some concerns) or facing issues of distribution, acceptance or storage, and are a long shot from herd immunity. Meanwhile, in the search for ACE2-centered therapeutics, scientists have uncovered an ACE2 receptor decoy called human recombinant ACE2 (hrsACE2; APN01) (Monteil et al., 2020). These synthetic approaches may prove expensive and may take longer to verify across people and conditions.

Natural products with some degree of biological benefits are regarded as bioactive compounds. Phytochemicals include a broad spectrum of plant bioactive compounds which are majorly proven to be safe. In recent times, these phytochemicals obtained from herbs have gained prominence in ethnomedicine as attractive choices for antiviral therapies (Utomo et al., 2020). Some polyphenols, a subset of phytochemicals, have been suggested to inhibit the fusion and entry of SARS-CoV-2 (Paraiso et al., 2020). So far, reports indicate that most African countries bear lesser COVID-19 burden compared to some Northern and Western nations of the globe (**Figure 1**). To explain this, several reasons have been proposed, including demography, climate, genetic variations, cross immunity, and antimalarial usage (Lalaoui et al., 2020).

The African and Asian regions are famous for their ethnomedicinal herbs (**Figure 2**) and a close comparison reveals a previously unseen correlation between countries having no ethnomedicinal policies and a higher burden of

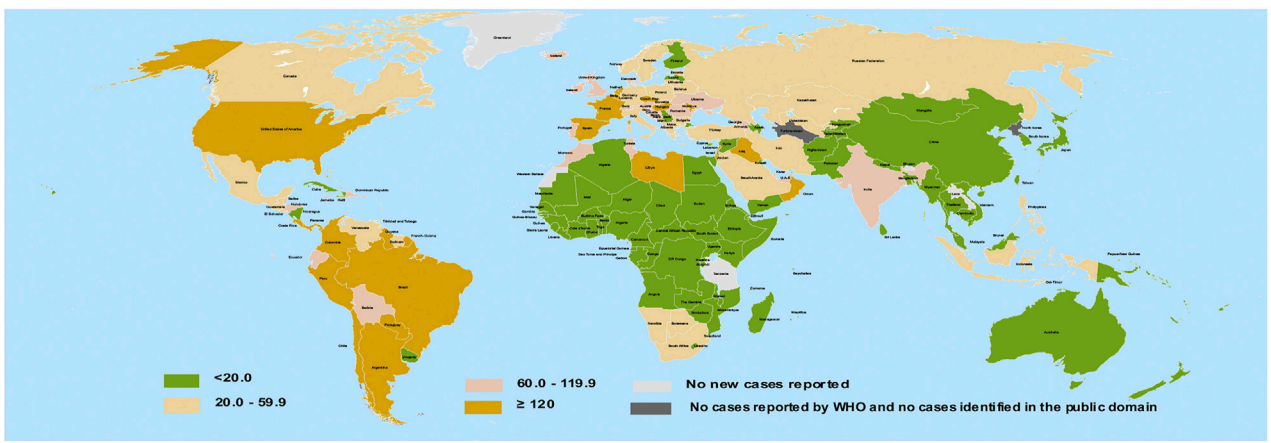

FIGURE 1 | Geographical distribution of COVID-19 infection per 100,000 of population across 14-days. Redrawn from source: European Center for disease Prevention and Control (ECDC). Data for September 26, 2020 (European Center for disease Prevention and Control, 2020).

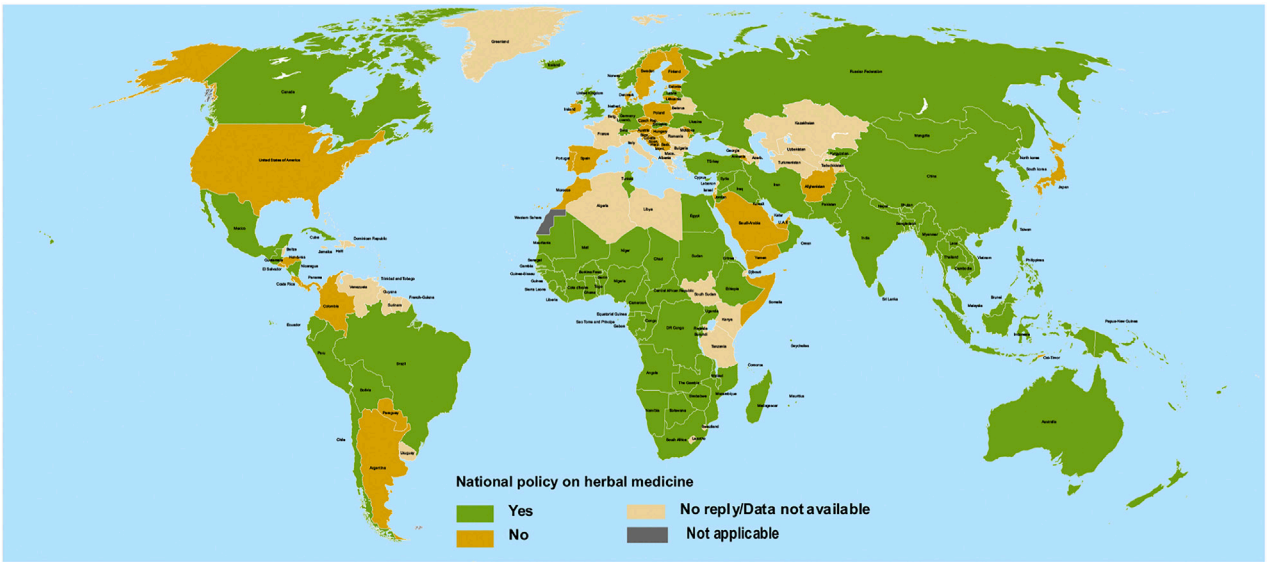

FIGURE 2 | Geographical national level policy for herbal medicines among 194 countries. Redrawn from source: WHO Global Report on Traditional and Complimentary Medicine (WHO, 2019).

COVID-19 (compare **Figures 1**, **2**). Ethnomedicinal policies are developed following the demanding use of ethnomedicines. In turn, these policies offer goals and objectives to governments for the development and support of ethnomedicines and may include guideline principles related to safety and efficacy (Oyebode et al., 2016; WHO, 2019). The uniform rise in incidence of COVID-19 in regions of lower ethnomedicinal policies hints to a possible link between ethnomedicinal use and COVID-19 incidence. Despite the number of reasons put forward to explain the relatively mild emergence of COVID-19 in regions like Africa compared to America and Europe (Lalaoui et al., 2020), no involvement of ethnomedicinal use has been suggested until now. Possibly, ethnomedicinal plants contain bioactive compounds that contribute to prevent or mitigate SARS-CoV-2 invasion via interactions with ACE2-mediated viral tropism (fusion and entry).

Given the global burden and challenge posed by the pandemic and the urgent need for the rapid development of efficient, safe, cost-effective, and readily available prevention and treatment modalities, we turned to phytomedicine. Following the spike of converging evidences, we sought to review evidences related to ACE2 that may suggest the use of phytochemical remedies. Here, we also take a closer look at the SARS-CoV-2 and the indirect phytomedicinal targeting of ACE2 mediated tropism. This aims to provide an indirect evidence for the use of ACE2 interactive phytochemicals, singly or combined, for preventing and mitigating COVID-19, its symptoms and clinical co-morbidities. Notably, the influence of ethnomedicines on ACE2 modulation is not an exclusive factor in determining the rate of spread of COVID-19, but a highlight that identifies what logical next steps can be developed based on existing research. This will benefit investigators in quest for remedies from phytomedicine.

Morphology and Genomic Organization of SARS-CoV-2

Coronaviruses are taxonomically grouped into the order of Nidovirales, family Coronaviridae and subfamily Orthocoronavirinae. The subfamily is further divided into alpha, beta, delta, and gamma coronavirus genera. The beta coronavirus genus comprises SARS-CoV, MERS-CoV and the recently emerged SARS-CoV-2 (Chen et al., 2020c). Morphologically, all coronaviruses are enveloped with crown-like particles enclosing a positive sense RNA genome (**Figure 3**). The lipid bilayer envelope which surrounds the viral particle is derived from the host cell membrane, and embeds three structural proteins, namely: 1) membrane (M), 2) envelope (E), and spike (S) glycoproteins. The other viral structural protein, nucleoprotein (N), is internally located and intimately associated with the viral genomic RNA (Kumar et al., 2020b).

The SARS-CoV-2 genomic RNA has approximately 30 kb in size and is made up of 13–15 (12 functional) open reading frames (ORFs) that are arranged in 5–3′ order of appearance. The first ORF from the 5′ end comprises approximately 67% of the genome and encodes several non-structural proteins. On the other hand, the remaining ORFs encode both accessory and structural proteins, including the major S, E, M, and N proteins (Naqvi et al., 2020). The M and E proteins are required for virus morphogenesis, assembly and budding, while the S glycoprotein is a fusion viral protein comprised of two subunits; S1 and S2. The S1 subunit is made up of signal peptide, N-terminal domain (NTD) and a receptor-binding domain (RBD) (Watanabe et al., 2020). The S2 subunit contains two heptad-repeat regions known as HR-N and HR-C, which form the coiled-coil structures surrounded by the protein ectodomain. Importantly, the S protein in its native

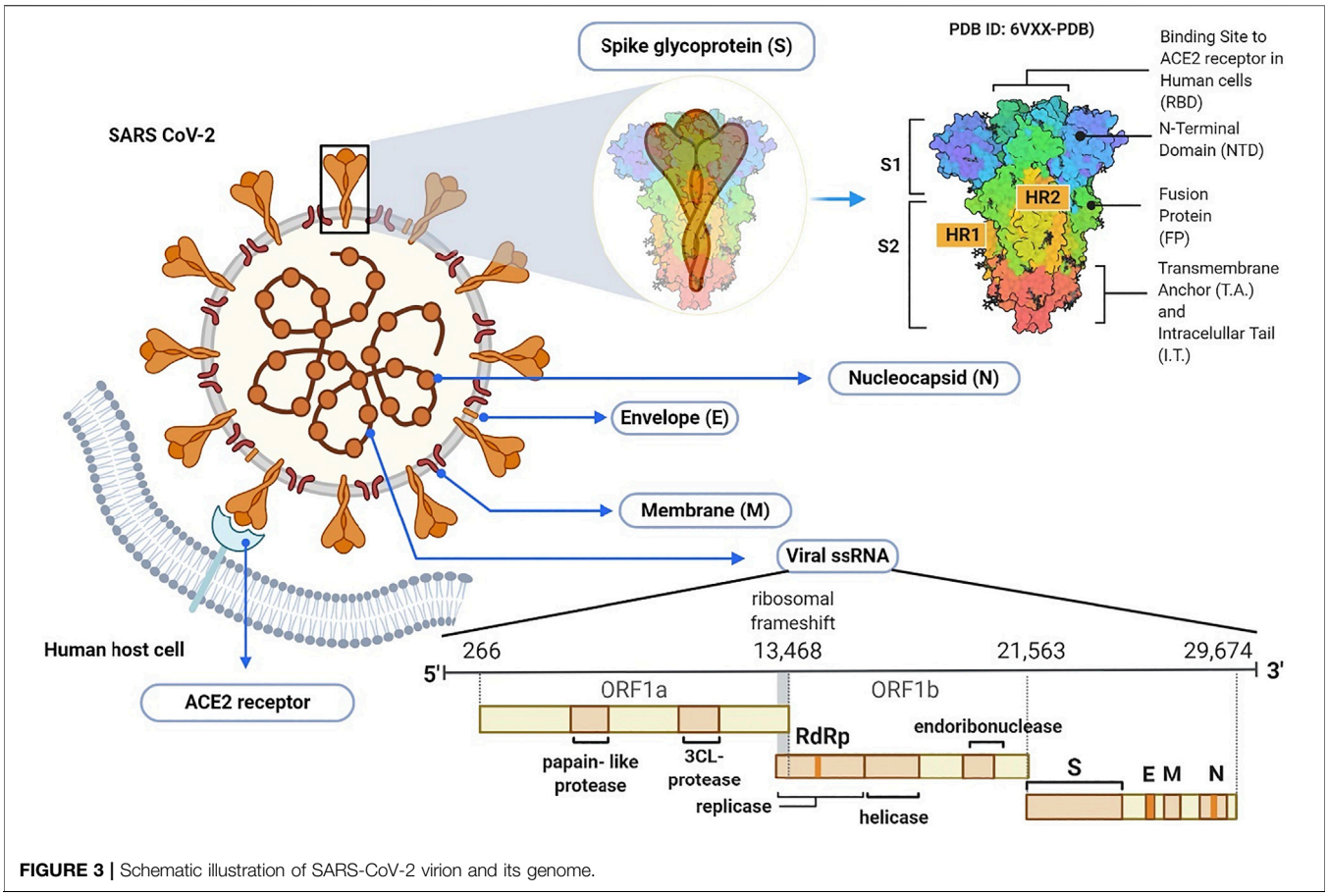

FIGURE 3 | Schematic illustration of SARS-CoV-2 virion and its genome.

form is coated with polysaccharide molecules, a property that partly enables SARS-CoV-2 to evade surveillance of the host immune system during entry (Shah et al., 2020).

Pathophysiology of COVID-19

Although coronaviruses target the respiratory tract, they can also affect the gastrointestinal (GI) tract, kidney, central nervous (CNS) and cardiovascular (CV) systems (Peiris et al., 2003; To et al., 2004). Their systemic effects manifest as lesions and multiple organ dysfunctions especially in immunocompromized patients and the elderly with already existing history of chronic ailments like cancer, CNS disorders, and diabetes. Similarly, the organs that are predominantly affected by SARS-CoV-2 express high levels of ACE2, meaning that such organs, due to ACE2, have high affinity to SARS-CoV-2 reception (Letko et al., 2020). The ACE2 can catalyze the hydrolysis of angiotensin II (a vasoconstrictor peptide) into angiotensin (1–7) which is a vasodilator that lowers the blood pressure (Verdecchia et al., 2020). Eventually, the invasion of SARS-CoV-2 deviates the ACE2 functionality, causing increase in blood pressure, disruption of blood vessels, and inflammation of organs (Letko et al., 2020).

Notably, the SARS-CoV-2 preferentially targets the respiratory tract. Alveolar type II cells (AT2) of the lungs express high levels of ACE2, making them the primal targets of SARS-CoV-2 (Verdecchia et al., 2020). In the native alveoli, oxygen is essentially absorbed, whereas carbon (IV) oxide is released. However, due to the presence of SARS-CoV-2, ACE2 is prevented from modulating the protein angiotensin II (ANG II), thereby causing further damage to the blood vessels of the lungs, overall preventing oxygen and carbon (IV) oxide exchange. The resultant effect is difficulty in breathing and improper functioning of the lungs, which worsen the damaging effect to the lung parenchyma, ending up in bronchitis, edema, alveolar collapse and acute respiratory distress syndrome (Huang et al., 2020; Tan et al., 2021).

Should the invasion continue, the virus may gradually infiltrate and infect the circulating immune cells which carry it to other organs like the digestive tract, (i.e. stomach, duodenum, colon, and ileum) displaying inflammatory changes by attacking the epithelial cells of the mucous membrane of ileum and colon (Shi et al., 2005). In a broad view, ACE2 is expressed in abundance within the small intestine. Autopsy under high-resolution electron microscopy has shown that the virus replicates rapidly in intestinal tissue, thereby preventing the ACE2 from carrying out its functions in amino-acid balance, intestinal inflammatory response, homeostasis of the intestinal microbiota and regulatory expression of antimicrobial peptides. Consequently, a secondary infection by bacteria may also affect the weakened intestine, since ACE2 has been hindered from

regulating the intestinal microbiota (Wang et al., 2020a). Due to low movement of bowels, an early sign of digestive tract invasion by SARS-CoV-2 could be diarrhea.

Circulating coronavirus in the blood stream can migrate to the heart and affect the cardiac tissue (Hamming et al., 2004). Accordingly, underlying cardiac injury elevates the risk of disease severity in COVID-19 due to heightened risks of myocarditis (To et al., 2004; Chen et al., 2020a). Kidney dysfunction is also a common feature of COVID-19 (Li et al., 2020c), as evidenced by reports of increased blood urea nitrogen, serum creatine and urea (Fan et al., 2020; Yang et al., 2020b). Urinary system failure, genital invasion and possibly death are also possible outcomes (Fan et al., 2020; Zhang et al., 2020b).

The most detrimental of all possibilities is damage to the CNS, when the SARS-CoV-2 nucleic acid contaminates the cerebrospinal fluid of the spinal cord and brain stem. Using the neuronal pathway, i.e., motor and sensory neurons, it streams via the nerves of the olfactory lobe of the nasal cavity to the brain. In fact, the use of motor proteins, kinesins and dynein, prominent to these neuronal pathways is essential for viral migration. The olfactory lobe, a part of the brain that translates smell responses, is the starting point of dysfunction. This partly explains the early signs of inability to smell, i.e. anosmia (Sun and Guan, 2020; Wu et al., 2020). Additionally, since the brain stem controls vital functions including blood pressure, heart beat and reflex actions like respiration, viral perforation of the brain stem eventually results in multiple organ dysfunctions. The development of intracranial infection may result in confusion, headache and epilepsy. Also, more serious complications, such as obstruction of cerebral blood flow, brain swelling, and coma could also occur. These are mostly mediated by interleukins (such as IL-6, IL-12, IL-15) and tumour-necrosis factor (TNF) in the brain, indicating an inflammatory response (Li et al., 2020b; Wu et al., 2020).

Notably, several organs could also deviate from proper functioning, such as the spleen and liver, but those highlighted above are the most susceptible. Furthermore, aside factors such as patient's age, patient's immune system, early diagnosis and treatment, the level of ACE2 expression also affects the COVID-19 pathophysiology. These pathophysiological features of COVID-19 as highlighted, could be quite detrimental and chronic; therefore, necessitating the need for more research into effective therapies for the prevention and/or treatment of COVID-19.

COVID-19 and ACE2

One of the key signaling pathways that acts as a homeostatic regulator for the cardiovascular system is the RAS. Irrespective of an individual's health status, RAS maintains a dynamic control of vascular function. This is achieved through different regulatory components and effector peptides such as the carboxypeptidase, ACE2, which converts angiotensin II to a vasodilator, angiotensin (1–7) through the ACE2/Ang one to seven axis (Donoghue et al., 2000; Tikellis and Thomas, 2012). ACE2 counteracts the effect of ACE/RAS pathway (de Kloet et al., 2010). ACE2 is an integral membrane protein present in the lungs, liver, heart, kidney, and endothelium (Donoghue et al., 2000). More importantly, ACE2 receptors are abundant in the epithelial cells of the surfaces of the nostrils, mouth, and lungs (Chen et al., 2020b). Sequence analysis demonstrated that ACE and ACE2 have over a 40% homology of their respective amino acids (Donoghue et al., 2000). The 40 kb ACE2 gene located on chromosome Xp22 consists of 18 exons and 20 introns and codes for a protein of 805 amino acids (Turner et al., 2002; Marian, 2013).

Unlike other coronaviruses that explore several receptors, like aminopeptidase N and dipeptidyl peptidase four in addition to ACE2 in gaining entry into cells during infection, SARS-CoV-2 exploits only the ACE2 protein for cell entry and subsequent viral replication (Zhou et al., 2020). The N-terminal region of the ACE2 receptor is anchored by the spike glycoprotein (S1) of SARS-CoV-2. Following receptor binding, SARS-CoV-2 employs some of the host proteases for spike protein priming. These include cathepsin L, cathepsin B, trypsin, factor X, elastase, furin, and transmembrane protease serine 2 (TMPRSS2) (Gheblawi et al., 2020). Being the major point-of-entry for SARS-CoV-2, the ACE2 protein expression on respiratory epithelial cell surfaces is critical for the pathogenesis of COVID-19 in individuals exposed to the virus. The vulnerability of the lungs to SARS-CoV-2 infection is premised on two facts; the large surface area of the lungs and the vast expression of ACE2 proteins on the type 2 pneumocytes of the alveoli in the lungs (Zhao et al., 2020). It is also noteworthy to state that the GI tract, especially the small intestine and colon could be critical points of entry since previous studies have demonstrated a high expression of ACE2 in these organs (Hamming et al., 2004; Li et al., 2020a). Also, the multiple organ failure in individuals with complicated COVID-19 could be linked to the vast distribution of ACE2 receptors in these organs (Guan et al., 2020; Huang et al., 2020) indicating the important roles of ACE2.

ACE2 as a Therapeutic Target

Though, a focus on the ACE2 activity accompanying COVID-19 may be considered commonplace, it is arguably one of the significant direct/indirect targets for therapeutics in COVID-19. ACE2 physiology is important in hypertension, cardiac, kidney, and lung physiology (Tikellis and Thomas, 2012). The apparent relevance of ACE2 physiology in COVID-19 has come in two ways, both supporting immense clinical focus on its modulation: 1) as a receptor for SARS COV2 (ClinicalTrials.gov identifiers: NCT04335136) and 2) as an enzyme for the generation of ANG 1–7 (ClinicalTrials.gov identifiers: NCT04311177, NCT04312009, NCT04338009, NCT04338009, NCT04394117, and NCT04394117) (Bhalla et al., 2020). The unfortunate neglect of ACE2 therapeutic potential (and lessons learned) following SARS-CoV outbreak strongly necessitated and still advocates for the recent efforts to develop ACE2-centered therapeutics for the current SARS COV2 (Bhalla et al., 2020). Thus, efforts (till date) to find an ACE2-centered therapeutic are re-emerging with a steep focus after its rediscovery as a receptor for SARS COV 2 (Hoffmann et al., 2020).

To date, ACE2 receptor is the major known entry point for SARS-CoV-2 into human cells. The virus uses its spike protein in attaching to ACE2 receptor of susceptible cells. This would mean

TABLE 1 | Some natural bioactive compounds shown to modulate ACE2 prior to the COVID-19 era.

Natural products	Bioactive compound	Method of assessment	References
Flavonoids	Naringenin apigenin	*In vivo*	(Sui et al., 2010; Wang et al., 2019)
	Baicalin	*In vivo*	(Wei et al., 2015)
Steroids and steroids glycosides	Ginsenoside Rg3	*In vivo*	(Liu et al., 2019)
Coumarins	Osthole	*In vivo*	(Shi et al., 2013; Hao and Liu, 2016)
Alkaloids	Nicotianamine	*In vitro*	(Takahashi et al., 2015)
	Emodin	*In vitro*	(Ho et al., 2007)

that a COVID-19 vaccine could be developed based on the spike protein sub-unit of SARS-CoV-2. In this regard, Tan and Colleagues have recently described a new vaccine candidate immunogenic against SARS-CoV-2 spike RBD, with demonstrated stability at ambient temperature; reducing cold-chain dependence (Tan et al., 2021). Alternatively, the development of small molecules or antibodies that are competitive antagonists for ACE2 receptor have been explored (Glasgow et al., 2020). These agents have shown superior neutralizing efficiency to convalescent sera (Glasgow et al., 2020; Tan et al., 2021).

Furthermore, Kuba and colleagues demonstrated that a downregulation of ACE2 protein by SARS-CoV leads to severe lung injury in laboratory mice (Kuba et al., 2005). By implication, this could mean that excessive administration of soluble ACE2 proteins would not only counteract the scenario of cell viral entry but also maintain the physiological activity of ACE2, including protection against lung injury via negative RAS regulation (Imai et al., 2005; Yu et al., 2016). This is the basis for recombinant ACE2 decoys (Monteil et al., 2020). Based on the clinical trials done so far, ACE2 protein that is synthesized through recombinant DNA technology, has shown to be efficacy in healthy and ARDS patients (Haschke et al., 2013; Khan et al., 2017). Recombinant ACE2 sequesters circulating viruses, thereby preventing the interaction between SARS-CoV-2 spike and endogenous ACE2 proteins. This effect allows endogenous ACE2 protein to negatively regulate the RAS, thereby preventing tissue injury as seen in COVID-19 (Zhang et al., 2020a). Notably, the oral delivery of ACE2 and Ang-(1–7) bioencapsulated in plant cells has been explored in non-COVID-19 disease states and may represent an innovative therapeutic strategy for COVID-19 (Shil et al., 2014). Additionally, the administration of Ang one to seven receptor agonists, like AVE 0991, has also been demonstrated to exert cardio-renal and pulmonary protective effects (Gheblawi et al., 2020).

Despite these efforts, the current absence of any approved ACE2-centered therapeutic (to reduce SARS-CoV-2 transmission, COVID-19 progression or halt cardiovascular complications) hints to the need for research in this respect (Bhalla et al., 2020). This is the reason why recent investigations are still ongoing toward developing an ACE2 interactive therapeutic (Esparza et al., 2020; Yahalom-Ronen et al., 2020) and much more brainstorming is needed.

Natural Products and ACE2

Natural products have for long been considered as important sources of therapeutic agents. These agents are remarkably low molecular weight molecules capable of eliciting enzyme activities due to their complex nature (Malami et al., 2016). The secondary bioactive agents/plant metabolites, which are able to reduce or wholly inhibit enzyme catalytic activities, can be used as ACE2 modulators. Available evidence from previous studies supports the inhibitory properties of natural products toward ACE2 enzyme activity. Moreover, these natural products are considerably used in traditional medicine and are extensively found as part of the human diet. Here, we describe some of the common natural products that have been previously reported with ACE2 modulatory activity prior to the COVID-19 era (**Table 1**).

Flavonoids are widely found in a variety of fruits and vegetables, including citrus fruits and tomatoes (Tutunchi et al., 2020). Among the different classes of natural products combined, flavonoids represent the largest group of ACE2 inhibitors. In fact, several studies have previously implicated some flavonoids to possess inhibitory properties against ACE2 activity. For instance, a previous *in vivo* study showed that apigenin upregulates the expression of the ACE2 gene in spontaneously hypertensive rats (Sui et al., 2010). Wei and co-workers also demonstrated that baicalin, a natural flavone, attenuates angiotensin-II induced endothelial dysfunction by modulating ACE2 expression both at mRNA and protein levels (Wei et al., 2015). Naringenin, a flavanone found in grape fruit, can also attenuate hypertensive reno-vascular damage *in vivo* by downregulating the ACE2 expression (Wang et al., 2019). These reports highlight a potential of flavonoids in mitigating SARS-CoV-2 viral infection via modulation of ACE2. Notably, as is highlighted later in this review, flavonoids like naringenin, naringin, nobiletin, hesperidin, hesperetin, neo-hesperidin, pinocembrin, quercetin, myricetin, and kaempferol have shown potential ACE2 binding affinity toward the residues that contact S protein of SARS-CoV-2 (Chen and Du, 2020; Cheng et al., 2020; Güler et al., 2020; Ngwa et al., 2020; Omar et al., 2020; Yang et al., 2020a).

Another class of natural products with ACE2 modulatory properties are the steroids and steroid glycosides. Ginsenosides are naturally occurring steroid glycosides commonly found in ginseng rhizome. An *in vivo* study demonstrated that ginsenoside Rg3, a tetracyclic triterpenoid saponin, induces the upregulation of ACE2 levels and attenuates Ang II-mediated renal injury (Liu et al., 2019). Following the outbreak of SARS-CoV-2, a recent

TABLE 2 | Functional foods known to modulate ACE2.

Functional food	Bioactive compound	Method of assessment	References
Fatty acids	Omega- FA 3	*In vivo*	(Gupte, 2011; Ulu et al., 2013)
Food-derived peptides			
Soybeans egg-white *Spirulina platensis* (blue-green algae)	Nicotianamine peptide LY peptide RALP peptide GHS peptide IRW peptide IQP peptide VEP	*In vitro*, *in vivo*	(Majumder et al., 2015; Takahashi et al., 2015; Zheng et al., 2017; He et al., 2019; Liao, 2019; Liao et al., 2019)

GHS, Gly His-Ser; IQP, Ile-Gln-Pro; IRW, Ile-Arg-Trp; LY, Leu-Tyr; RALP, Arg-Ala-Leu-Pro; VEP, Val-Glu-Pro.

virtual screening revealed that the steroid, arundoin, and some steroid glycosides (azukisaponin I, 20(S),24(R)-ocotillol and ginsenoside Rg6) can modulate ACE2 activity (Zi et al., 2020). In this study, the bioactive compounds demonstrated promising activity with a lower percentage inhibition based on an ACE2 kinase inhibition assay. Additionally, glycyrrhizin, another steroid glycoside found in the roots *Glycyrrhiza glabra* L., has been predicted to latch on to ACE2 with an estimated binding energy of −9 kcal mol^{-1}, potentially preventing viral entry (Chen and Du, 2020).

Furthermore, coumarins, which are naturally occurring phenolic compounds, have also shown ACE2 modulatory properties. An *in vitro* and *in vivo* study showed that the prenylated coumarin, osthole, mitigates inflammation and acute lung injury in mice by preventing ACE2 and Ang (1–7) down-regulation, resulting in a lowered release of proinflammatory cytokines (TNF-α and IL-6) (Shi et al., 2013). This protective influence of osthole was proposed to occur due to the counter effects ACE2/Ang (1–7) has over the ACE/AngII axis, and was confirmed by an abrogation effect following the use of an ACE2 inhibitor (Shi et al., 2013). In a related study, Hao and Liu demonstrated that osthole attenuates pulmonary fibrosis and inhibits lung inflammation by modulating ACE2 in rat models of bleomycin-induced pulmonary fibrosis (Hao and Liu, 2016).

With regards to alkaloids, a recent study has highlighted that cepharanthine, a naturally occurring alkaloid¸ can bind to spike protein and inhibit the viral interaction with ACE2 protein *in silico* (Ohashi et al., 2020). In another study, the non-proteinogenic alkaloid, nicotianamine, exhibited a similar effect on ACE2 (Chen and Du, 2020), which agrees with a previous *in vitro* demonstration by Takahashi et al. (2015). Also, evidence had shown that a natural anthraquinone, emodin, significantly inhibits the infectivity of S protein-pseudotyped retrovirus to Vero E6 cells by binding to ACE2 protein and blocking the SARS-CoV S protein from binding to ACE2 at a 50% minimum inhibitory concentration (IC_{50}) of 200 μM (Ho et al., 2007).

Functional Foods and ACE2

Apart from providing nutrients and energy, functional foods also modulate the body's physiological functions (Nicoletti, 2012). The potentially numerous health benefits of functional foods to humans have been explored (Muhammad et al., 2018). Among the several important beneficial effects of functional foods include their potential to prevent and treat COVID-19. Here, we present functional foods that have been shown to modulate ACE2 (**Table 2**).

Fatty Acids (FA)

Naturally occurring fatty acids have been previously reported to have health benefits in several disease states. Omega-3 FA, fixed oils, oils obtained from nuts, coconut, soy, sesame, and fruits are common sources of naturally occurring FA. Omega-3 FA are a class of polyunsaturated fatty acids (PUFA) that are known to have beneficial effects in the prevention and management of various diseases (Muhammad et al., 2018). The two major biologically active types of omega-3 FA are eicosapentaenoic acid and docosahexaenoic acid (DHA) (Daak et al., 2020). The ACE2 activities of these bioactive agents have been demonstrated in previous studies. Ulu and co-workers have shown that diet rich in omega-3 FA attenuated inflammation in angiotensin-II dependent hypertension by up-regulating the ACE2 activity (Ulu et al., 2013). In another study, Gupte. (2011) revealed that omega-3 FA upregulated the expression of ACE2 mRNA in adipocytes (Gupte, 2011). As we shall discuss, following the emergence of COVID-19, several essential oils from functional foods have also been identified as ACE2 modulators (Senthil Kumar et al., 2020; Thuy et al., 2020).

Food-Derived Peptides

Previous indications suggest food-derived bioactive peptides can regulate the body's physiological functions. These food-derived peptides have been demonstrated to exert potential health benefits to humans and thus serve as functional foods. In relation to this, soy proteins isolated from soybeans (*Glycine max* L.) were demonstrated to have ACE2 inhibitory properties (**Table 2**). In the first ACE2 inhibitory study using food products, Takahashi et al. (2015) demonstrated the ACE2 inhibitory activity of soybean (*Glycine max* L.) and its isolated bioactive protein. In their study, the bioactive protein, nicotianamine, intensely inhibited the ACE2 activity at 84 nM concentration. Similarly, bioactive peptides from rapeseed, Leu-Tyr (LY), Arg-Ala-Leu-Pro (RALP) and Gly His-Ser (GHS), have been shown to modulate the ACE2 activity in spontaneously hypertensive rats (He et al., 2019). In this study, ACE2 expression markedly increased following oral administration of the peptides (30 mg/kg) both at the gene and protein levels. A related study had also demonstrated that administration of bioactive peptides (10 mg/kg/day) from blue-green algae, *Spirulina platensis (Arthrospira platensis)*, upregulates the expression of ACE2 in spontaneously hypertensive rats (Zheng et al., 2017). The fact that

these specific peptides modulate ACE2 expression and subsequent activity hints to their bioactivity. However, the pharmacokinetics and mechanisms behind these physiological effects remain largely unknown and may require extensive investigations before becoming practically applicable. Additionally, food components interact with peptides in different ways that may affect the availability of peptides within the matrix (Chakrabarti et al., 2018). As such, to recommend foods rich in ACE2 modulatory peptides, further research is needed to determine the release, stability and mechanisms of bioactive peptides following normal digestion. Furthermore, hydrolysates from pre-digestion when subjected to normal digestion may produce different peptide sets (Chakrabarti et al., 2018). In this case, investigations are needed to demonstrate if the identified physiological effects are abolished, unabolished or changed.

Furthermore, evidences have indicated that the egg-white-derived antihypertensive peptide Ile-Arg-Trp induces the expression of ACE2 and decreases proinflammatory gene expression in mesenteric arteries of spontaneously hypertensive rats (Majumder et al., 2015). A similar *in vivo* study had further demonstrated that the tripeptide IRW elicits vasorelaxation and abolishes vascular inflammation by increasing the levels of circulatory ACE2 and Ang (1–7), potentiating its protective activity. (Liao et al., 2019). Notably, IRW is less-susceptible to peptide modifications by digestive enzymes (Bejjani and Wu, 2013). Findings from these studies demonstrate the previously established beneficial effects of food-derived proteins and other components in modulating ACE2 activity that subsequently influences the body physiology in a way that could antagonize the development of COVID-19. Though these peptides for intake may be largely acceptable due to natural source, a minimal tissue bioavailability of most peptides limits theirs use as therapeutic agents (Campos et al., 2011). To address this, approaches like microencapsulation, use of enzyme inhibitors, may be needed to achieve effective oral delivery. Further *in vivo* studies are also needed to understand the immune response to peptides and human trials may become necessary to validate efficacy. However, the production of such synthetic bioactive peptides faces limitations in expense and requires newer low-cost innovations.

Phytomedicinal Plants, COVID-19 and the Effects on ACE2

At this time, several claims have been made on herbal-based traditional medicines or phytomedicines as remedies to COVID-19. These herbs and products include COVID organics (Madagascar), claims on *Andrographis paniculata* (Burm.f.) Nees, *Tinospora crispa* (L.) Hook. f. and Thomson, and *Gymnanthemum amygdalinum* (Delile) Sch. Bip (DR-Congo), turmeric (*Curcuma longa* L.), a Sri Lankan herbal drink, and some Tanzanian claims about recipes from lemon grass, ginger, and neem leaves. Notably, like synthetic agents for COVID-19 such as remdesivir, dexamethasone and chloroquine, some of these herbs and products are recently being supported by preliminary evidence and have been suggested for further empirical assessments (Borkotoky and Banerjee, 2020; Enmozhi et al., 2020; Rakib et al., 2020). With a focus on identifying and supporting the development of plant products having some level of scientific evidence in the context of ACE2-centered SARS-CoV-2 fusion-entry, we describe three classes of phytomedicinal agents, based on the target used to modulate viral tropism (virion fusion and entry) along the Spike-RBD/TMPRSS2/ACE2 axis. These phytomedicinal agents include those that may 1) interfere with host cell surface proteins (ACE-2 receptor and TMPRSS2 protease), 2) interface with viral spike glycoprotein, or 3) interrupt spike-RBD/ACE2 interaction **(Figure 4).**

The Spike-RBD/TMPRSS2/ACE2 Axis

The SARS-CoV-2 fusion and entry, which is characteristic of COVID-19, marks a phytomedicinal target for COVID-19 therapy. Following SARS-CoV-2 spike-RBD attachment to the host cell ACE2 receptor, the membrane bound activator protease, TMPRSS2, cleaves the viral spike protein and facilitates its fusion with the host cell membrane (Hoffmann et al., 2020). This constitutes the Spike-RBD/TMPRSS2/ACE2 axis and the cleavage (or priming) that occurs at the junction between subunit one and two of the spike protein precedes internalization. The Spike-RBD/TMPRSS2/ACE2 axis presents several interventional targets for natural products at the 1) receptor binding motif (RBM) of the receptor binding domain (RBD) of the spike glycoprotein, 2) ACE2 receptor active site that recognizes the RBD and 4) TMPRSS2 protease (**Figure 5**).

Interference With ACE2 Activity–ACE2

Several plant products have shown potential in interfering with the activity of ACE2 (Chen and Du, 2020; Joshi et al., 2020; Poochi et al., 2020). For example, the essential oils from *Allium sativum L* (garlic), *Ammoides pusilla (Brot.) Breistr.*, *Melaleuca cajuputi Maton* and *Sm. ex R. Powell* (cajeput) and *Piper* spp (pepper) like *Piper nigrum L.* and *Piper retrofractum Vahl,* can potentially latch onto ACE2 and competitively inhibit viral binding and entry (Abdelli et al., 2020; Gutierrez-Villagomez et al., 2020; My et al., 2020; Thuy et al., 2020). These inhibitory effects have been attributed to the presence of certain ligands (**Table 3**). For instance, Senthil Kumar et al. (2020) demonstrated that essential oils from geranium and lemon prove to be effective against ACE2 by downregulating its mRNA and protein expressions in epithelial cells. Further gas chromatography mass spectrometry (GC-MS) analysis identified citronellol, geraniol and neryl acetate in geranium oils, and limonene in lemon oils as the major ligands (particularly citronellol and limonene) responsible for the downregulation of ACE2 expression in HT-29 cells. Same ligands were also identified to inhibit TMPRSS2 (Senthil Kumar et al., 2020). Notably, not all ligands that bind with ACE2 inhibit its enzymatic activity (Williamson and Kerimi, 2020). The fact that some of these essential oils bear several molecules with binding capacity hints to some possible synergistic effect that may account for the overall efficacy of essential oils. Interestingly, some of these interactive ligands can be synthesized (Gutekunst et al., 2012; Liu et al.,

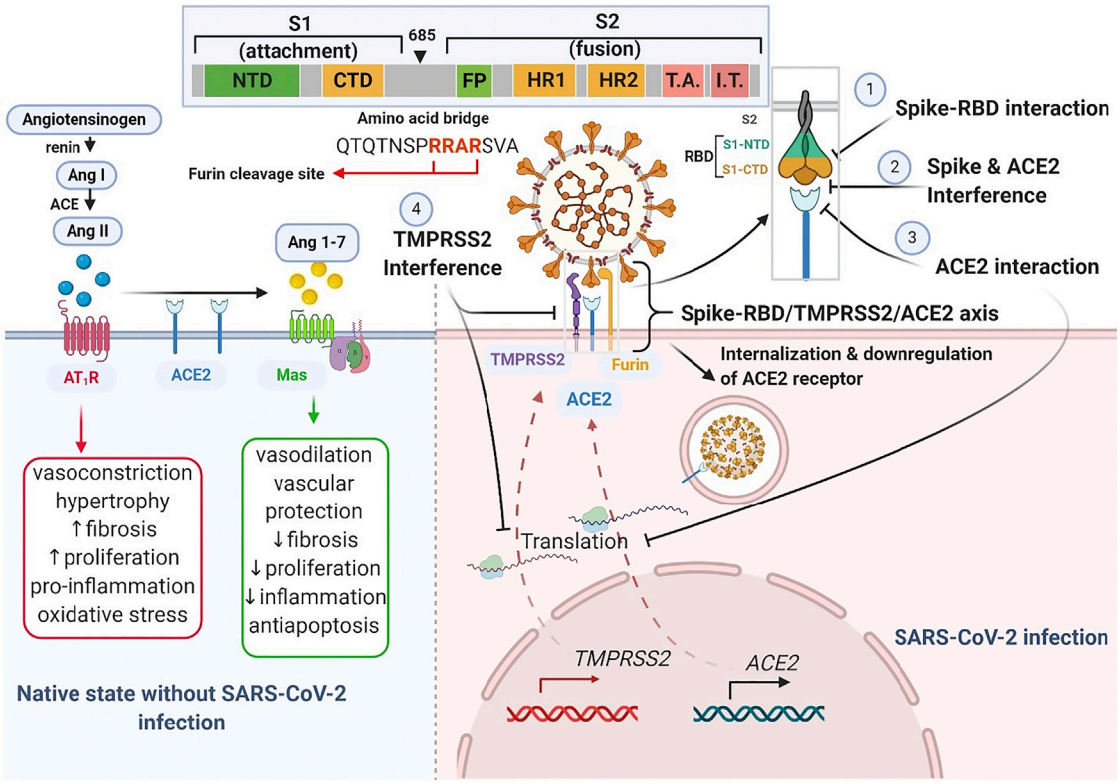

FIGURE 4 | Schematic drawing of Spike-RBD/TMPRSS2/ACE2 axis. The left half illustrates the native counter-interaction between the RAS pathway and ACE2. The right half highlights four targets of phytomedicine against the Spike-RBD/TMPRSS2/ACE2 axis following SARS-CoV-2 infection. The inset shows the furin cleavage site (-RRAR-) of a spike glycoprotein.

2012), indicating a vastly unexplored potential. Additionally, in a novel attempt, Rattanapisit and co-workers used a plant expression system (*Nicotiana benthamiana* Domin) to develop and characterize the rapid production of recombinant RBD as a biopharmaceutical capable of neutralizing viral entry by specifically binding to ACE2 (Rattanapisit et al., 2020). Such use of plants as platforms for recombinant protein production, offers benefit over animal-based platforms in terms of cost and is also advantaged in its flexibility, rapid scalability and safety. The recombinant RBD possibly exhibit *in vivo* neutralization activity similar to recently developed capsid-like particle-based vaccines against SARS-CoV-2 invasion (Fougeroux et al., 2021), and may represent another turning point for COVID-19 therapeutics.

Interference With ACE-2 Activity - ACE2 and Angiotensin

ACE2 is known to counter the vasoconstrictive and other detrimental effects of the Angiotensin-1/ACE/Angiotensin-II/AT-1 Receptor axis which is a component of the RAS. ACE2 converts angiotensin-1 and -II into angiotensin one to seven, which acts on Mas receptors. This shunt represents the renin angiotensin system suppressive axis called "ACE2/Ang 1–7/Mas receptor axis," which produces vasodilatory and other beneficial effects that represent the protective effect of ACE2 on the body (Furuhashi et al., 2020). As stated earlier, the fusion of SARS-CoV-2 to ACE2 and its subsequent entry downregulates the levels of ACE2 thereby potentiating the detrimental activity of RAS. This makes the RAS an important marker to look at when testing possible COVID-19 therapies. Currently, a Tomeka® Prevention Trial (TPT) is underway in DR Congo to assess the effect of using Tomeka® regimen for COVID-19 on markers of the RAS such as angiotensin-II and -(1–7) (ClinicalTrials.gov identifier: NCT04537585). Tomeka® is an herbal mixture made from soy (from soybean; *Glycine* max L.), sorghum (*Sorghum bicolor* L.), maze (*Zea mays* L.) and mushrooms (*Agaricus bisporus* L.). Nicotianamine had been highlighted as the bioactive phytoconstituent of soy responsible for its potent inhibition of ACE2 (**Figure 5**) and it was hence, called "soybean ACE2 inhibitor - ACE2iSB" (Chen and Du, 2020).

Interface With the Viral Spike Glycoprotein and Its RBD

For COVID-19, it is more logical to find phytomedicinal agents that specifically target the interaction of RBD at the Spike/ACE2 complex and not particular to ACE2. This caution

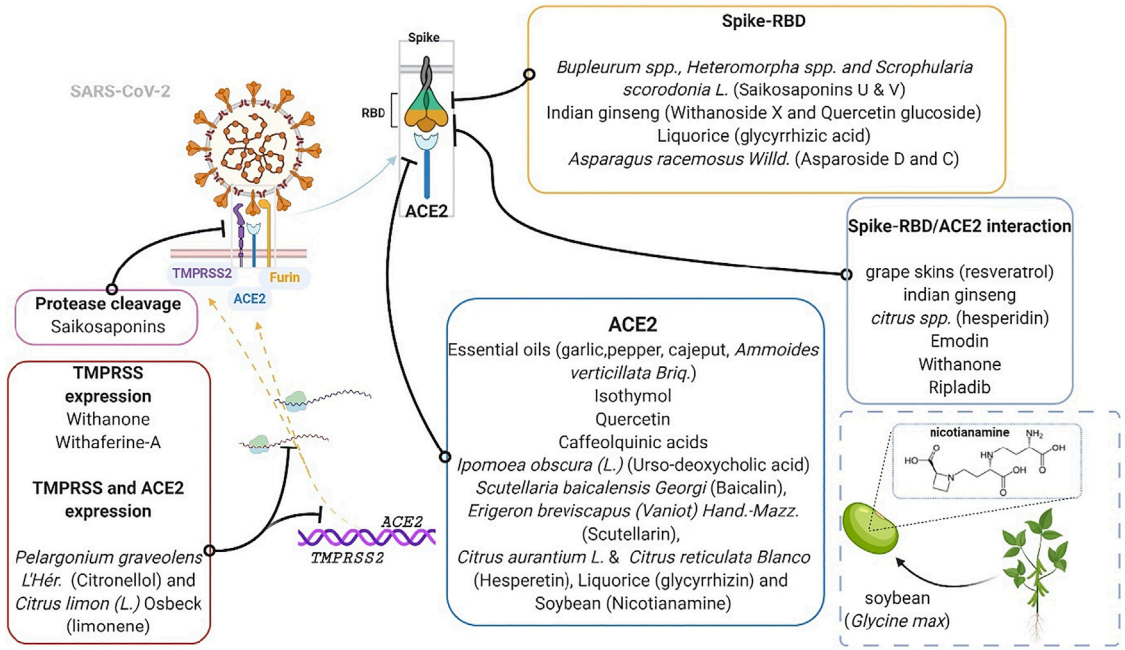

FIGURE 5 | Plants and plant products that modulate entry of SARS-CoV-2. The inset shows nicotianamine derived from soy, a product of soybean (*Glycine* max L.). ACE2, Angiotensin converting enzyme two; RBD, receptor binding domain; TMPRSS2, transmembrane protease serine 2. Phytomedicinal targets of the Spike-RBD/TMPRSS2/ACE2 axis.

is because agents solely targeting ACE2 may interfere with ACE2 enzyme activity and its complex protective functions (Kai and Kai, 2020). Natural products with significant RBD binding affinity compared to ACE2 can dominate over ACE2 in latching onto RBD, thereby blocking viral attachment, fusion and entry.

Preliminary data based on molecular docking analyses predict several natural plant products as RBD interface binding compounds (Chikhale et al., 2020a; Chikhale et al., 2020b; Sinha et al., 2020a; Sinha et al., 2020b; **Table 3**). Most data come from "conceivable therapeutics" through *in silico* molecular analysis of available structural macromolecules. An advantage to the preliminary *in silico* screening of substances is that pharmacokinetic properties, such as safety could be easily established, shifting priority to the *in vitro* confirmation of efficacy. Thus, preliminary evidences necessitate further *in vitro* and *in vivo* investigations. Notably, Wang and co-workers have recently identified AXL, a transmembrane tyrosine-protein kinase, as a supportive pulmonary entry receptor for the SARS-CoV-2 which may also interact with the spike glycoprotein, but at its NTD region (Wang et al., 2021). This represents another potential target for plant based therapeutic investigations.

Interrupting the Spike-RBD/ACE2 Interaction

Studies suggest that 1) resveratrol from grape skins, 2) ripladib from the leaf extracts of the native bryoni, and 3) withanone from Indian ginseng, can selectively bind and inhibit both RBD and ACE2 (Alexpandi et al., 2020; Balkrishna et al., 2020; Wahedi et al., 2020). These ligands can potentially inhibit the Spike-RBD/TMPRSS2/ACE2 axis simultaneously at the RBD and ACE2. Moreover, multiple ligand activity on the said axis indicates a higher likelihood of getting some potent alternative for COVID-19. Ho et al. (2007), in an *in vitro* study, established that emodin, from *Rheum* sp. and *Polygonium* sp. abolish the interaction between 2002/2003 SARS-CoV spike protein and ACE2 in a dose-dependent manner. Given the level of homology between the two coronaviruses, an investigation into the influence of emodin against the interaction of the SARS-CoV-2 spike and ACE2 is necessary.

Notably, the components of some plants may differ based on the plant part used (Kumar et al., 2020a). For instance, the *Citrus* spp. peel represents the most abundant store of hesperidin, another possibly potent inhibitor of the RBD and ACE2 interaction (Utomo et al., 2020). Consequently, the hesperidin ligand is currently scheduled for a randomized double-blind controlled trial in Egypt (ClinicalTrials.gov identifier: NCT04452799) (Haggag et al., 2020; Okasha, 2020). Knowledge of such should guide research and may afford some better protection against SARS-CoV-2 invasion.

Interfering With the Host Membrane Enzymes; TMPRSS2, Furin and ADAM-17

The protease cleavage site between the S1/S2 subunits of the spike protein bears an arginine-arginine-alanine-arginine (RRAR) sequence (Wang et al., 2020b) (as shown in **Figure 4**). What

TABLE 3 | Plant derivatives with potential effect on the Spike-RBD/TMPRSS2/ACE2 axis.

Target	Plant (bioactive phytoconstituent/ product)	Study type	Efficacious dose(s)	Biological test	Mechanistic effect	Findings	References	Comment
Interfere with ACE2 activity	*Nicotiana benthamiana* domin (recombinant RBD)	*In silico and In vitro* (vero E6 cells)	NA	Recombinant mAb RBD production in a plant expression system. Neutralization efficiency against positive sera	Binds to ACE2	Specific binding to the SARS-CoV-2 receptor and its neutralization	Rattanapisit et al. (2020)	Suggested consideration of this plant derived recombinant RBD for the development of vaccines and viral detection/diagnostic reagents
	Pelargonium graveolens L'Hér. (Citronellol) and *Citrus* × *limon* (L.) osbeck (Limonene)[a]	*In vitro* (HT-29 cell line)	50 μg/ml geranium oil and 25 μg/ml lemon oil	Gene expression profile (mRNA and protein)	Downregulates the expression of ACE2 and TMPRSS2	Significant inhibition of ACE2 and TMPRSS2 in epithelial cells to protect against SARS-CoV-2 invasion	Senthil Kumar et al. (2020)	Citronellol and limonene were the most potent of eight ACE2 inhibitory oil extracts and had dose dependent effects
	Momordica dioica roxb. ex willd (catechin, quercetin, hederagenin and oleanolic acid)	*In silico and In vitro*	NA	Molecular docking and *in silico* ADME predictions methods	Docking to ACE2	The constituent bioactive flavonoids (catechin and quercetin) and triterpenoids (hederagenin and oleanolic acid) inhibit ACE2 and DPP4 receptors	Sakshi et al. (2021)	Constituent flavonoids have better affinities than standard remdesivir, favipiravir and hydroxychloroquine
	Valeriana jatamansi jones ex roxb. (Hesperidin), *Oroxylum indicum* (L.) kurz (chrysin), *Rheum australe* D.Don (emodin)	*In silico*	NA	Molecular docking and molecular dynamics	Allosterically binds to ACE2 and can also destabilize spike-ACE2 interaction	Ligands (especially hesperidin) triggers conformational changes that causes spike-ACE2 fragment to be unstable	Basu et al. (2020)	Spike inhibitory capacity similar to that of docked chloroquine and hydroxychloroquine
	Artemisia absinthium L. (anabsinthin, absinthin, dicaffeoylquinic acids), *Syzygium aromaticum* (L.) merr. and L.M.Perry (3-0-caffeoylquinic), *Phaseolus vulgaris* L. (quercetin 3-glucuronide-7-glucoside, quercetin 3-vicianoside, isosakuranetin 7-O-neohesperidoside) and *Inula helenium* L. (Quercetin-7-O-galactoside, 3,5-dicaffeoylquinic acid, 3,4,5-tricaffeoylquinic acid)	*In silico*	NA	Molecular modeling/ docking and dynamic simulations	High affinity binding to pocket of the active site of ACE2	Ligands could inhibit viral fusion	Joshi et al. (2020)	Compounds demonstrated good intestinal and brain permeability. Also showed no carcinogenic tendency
	Allium sativum L. (diallyl tetrasulfide and	*In silico*	N/A	Molecular modeling/ docking	Binds to ACE2 receptor	Could inhibit viral entry and infectivity	Thuy et al. (2020)	Ligands are the two most potent of seventeen inhibitors of

(Continued on following page)

TABLE 3 | (*Continued*) Plant derivatives with potential effect on the Spike-RBD/TMPRSS2/ACE2 axis.

Target	Plant (bioactive phytoconstituent/ product)	Study type	Efficacious dose(s)	Biological test	Mechanistic effect	Findings	References	Comment
	trisulfide, 2-propenyl propyl)[a]							ACE2 gotten from essential oil of plant
	Piper sp. (pipercyclobutanamide B, a and nigramide Q) like *Piper nigrum* L. and *Piper retrofractum* vahl	*In silico*	NA	Molecular modeling/ docking and dynamic simulations	Docks closely to active site of ACE2	These dimeric piperamides of essential oil could possibly inhibit ACE2 mediated entry of SARS CoV2	Gutierrez-Villagomez et al. (2020)	Exhibit potential drug likeness based on ADME. Pipercyclobutanamide B (most potent) docked along duct to ACE2 active site
	Ipomoea obscura (L.) ker gawl. (Urso-deoxycholic acid)[a]	*In silico*	N/A	Molecular modeling/ docking	Bind to ACE2 receptor	Could inhibit viral entry and infectivity	Poochi et al. (2020)	This is the most potent of five possibly bioactive ACE2 inhibitors from ethanolic extract of the plant
	Ammoides verticillata (desf.) briq. -From Algeria (isothymol)	*In silico*	NA	Molecular modeling/ docking	Binds to ACE2 receptor	High affinity and can inhibit ACE2 better than captopril and chloroquine drugs	Abdelli et al. (2020)	Suggest oil is one of the richest natural sources of isothymol. Good ADMET
	Melaleuca cajuputi maton & sm. ex R. Powell (terpineol, guaiol and linalool)[a]	*In silico*	NA	Molecular modeling/ docking and dynamic simulations	Latch to the active site of ACE2	Lots of convergence points and the inhibitory intensity of these compounds on ACE2 could prevent viral invasion	My et al. (2020)	Out of ten inhibitory substances, these three have the most potent effect on ACE2. Guaiol is also present in guaiacum and cypress pine oils
	Scutellaria baicalensis georgi (baicalin), *Erigeron breviscapus* (vaniot) hand-mazz. (Scutellarin), *Citrus* × *aurantium* L. *and Citrus reticulata* blanco (hesperetin), liquorice; *Glycyrrhiza uralensis* fisch. ex DC. (glycyrrhizin) and soybean; *Glycine* max (L.) merr. (Nicotianamine)	*In silico*	NA	Molecular modeling/ docking and dynamic simulations	Latch to the active site of ACE2	Potential to bind ACE2 and hinder viral entry	Chen and Du (2020)	Nicotianamine is "soybean ACE2 inhibitor" (ACE2iSB)
	Gancao*: Glycyrrhiza* spp. and chaihu*: Bupleurum* spp. (glyasperin F and isorhamnetin)	*In silico*	NA	Molecular docking	Bind to ACE2	Latch onto site 1 and site 2 of ACE2	Ren et al. (2020)	Suggest the ligands, glyasperin F and isorhamnetin, account for strong binding affinity
Interface with the viral spike glycoprotein and its RBD	Liquorice; *Glycyrrhiza glabra* L. (glycyrrhizic acid)	*In silico*	NA	Molecular modeling/ docking and dynamic simulations	Bind to cavity of prefusion spike glycoprotein	High binding affinity to spike protein may block viral fusion to ACE2	Sinha et al. (2020a)	High protein-ligand stability. Most potent of six interactive ligands
	Bupleurum spp., *Heteromorpha* spp. *and Scrophularia scorodonia* L.	*In silico*	NA	Molecular modeling/ docking and dynamic simulations	Binds to RBD and cleavage site of the spike glycoprotein	May inhibit viral entry by interfering with virion-receptor binding and	Sinha et al. (2020b)	Out of 23 saikosaponins, had the most potent latching affinity to active site of

(Continued on following page)

TABLE 3 | (*Continued*) Plant derivatives with potential effect on the Spike-RBD/TMPRSS2/ACE2 axis.

Target	Plant (bioactive phytoconstituent/ product)	Study type	Efficacious dose(s)	Biological test	Mechanistic effect	Findings	References	Comment
	(saikosaponins U and V)[a]					protease cleavage		spike glycoprotein (i.e. RBD)
	Indian ginseng: *Withania somnifera* (L.) dunal (withanoside X and quercetin glucoside)[a]	*In silico*	NA	Molecular modeling/ docking and dynamic simulations	Binds receptor binding domain of prefusion spike protein from SARS-CoV-2	Favourable interaction with receptor binding motif (RBM) of RBD to block viral fusion	Chikhale et al. (2020a)	Ligands were potent (out of 17) inhibitors of SARS-CoV-2 spike glycoprotein
	Asparagus racemosus willd. (Asparoside D and C)	*In silico*	NA	Molecular modeling/ docking and dynamic simulations	Bind to spike RBD	Good affinity and stable docking of spike RBD	Chikhale et al. (2020b)	Higher binding affinity than remdesivir (standard drug)
Interrupting the spike-rbd/ace2 interaction	*Withania somnifera* (L.) dunal (withanone)	*In silico*	NA	Molecular modeling/ docking	Interrupts at the junction between ACE2 receptor and viral S-RBD	Decreased binding free energies, destabilized salt bridges, hence blocks and weaken SARS CoV2 entry and infectivity	Balkrishna et al. (2020)	Suggest plant as first choice herb in curbing COVID-19
	Diplocyclos palmatus (L.) leaf extract (ripladib)	*In silico*	NA	Molecular modeling/ docking	Interrupts at the RBD of Spike-ACE2 complex	Predicted strong binding at RBD interface to block Spike-ACE2 interactions and viral entry	Alexpandi et al. (2020)	ADMET analysis indicate good pharmacokinetic properties
	Citrus spp. (hesperidin)	*In silico*	NA	Molecular modeling/ docking	Binds to both RBD and ACE2 receptor	The flavonoid can possibly interrupt RBD/ ACE2 interface to abrogate entry	Utomo et al. (2020)	The peel of Citrus sp. represents the most abundant methoxy flavonoid (hesperidin) store of the plant
	Grape skin: *Vitis vinifera* L. (resveratrol)	*In silico*	NA	Molecular modeling/ docking and dynamic simulations	Bind tightly and interfere with viral S protein/ ACE2 receptor complex	Highly stable binding and selectivity to viral protein/ ACE2 receptor complex. Disrupts the spike protein	Wahedi et al. (2020)	Most potent of four stilbene-based natural compounds
Interfere with the host membrane protease	*Aframomum melegueta* K.Schum. (quercetin, apigenin)	*In silico and In vitro*	30, 10, 3, 1, 0.3 mg/L. From fruit (with seed)	Docking. *In vitro* inhibition of recombinant soluble human furin. Immuno-blotting	Disrupts spike glycoprotein/ receptor interaction by inhibiting furin cleavage	Metabolites inhibited furin dependent pre-glycoprotein processing by possibly blocking furin recognition site	Omotuyi et al. (2020)	Suggested bioactive influence of flavonoids (like quercetin, apigenin). Good ADMET sores
	Withania somnifera (L.) dunal (withanone and Withaferine-A)	*In silico*	NA	Molecular modeling/ docking	Binds to TMPRSS2 catalytic site (Wi-N > Wi-A), alters allosteric site and also downregulates	Predicted multiple action in blocking SARS CoV2 cell entry and propagation by	Kumar et al. (2020c)	Possible drug-able agents for prevention and therapeutics

(Continued on following page)

TABLE 3 | (*Continued*) Plant derivatives with potential effect on the Spike-RBD/TMPRSS2/ACE2 axis.

Target	Plant (bioactive phytoconstituent/ product)	Study type	Efficacious dose(s)	Biological test	Mechanistic effect	Findings	References	Comment
					TMPRSS2 transcription	inhibiting TMPRSS2		

[a]*These compounds were found to be the most potent of several others.*

Abbreviations: *ACE2, Angiotensin converting enzyme two; ADME/T, Absorption, Distribution, Metabolism, Excretion/and Toxicity; DPP4, Dipeptidyl peptidase four; mAb, monoclonal antibody; NA, not available; PK, Pharmacokinetic; S-RBD, Spike glycoprotein receptor binding domain; TMPRSS2, Transmembrane protease serine two; Wi-A, Withaferine-A; Wi-N, Withanone.*

is now known is that furin, a proprotein convertase enzyme, performs cumulative role with TMPRSS2 by pre-activating this site, aiding viral entry (Bestle et al., 2020; Shang et al., 2020). One molecular simulation study suggests that saikosaponins interact significantly with the arginine residues of the cleavage site to prevent S1/S2 protein cleavage, hindering the virion-cell fusion and viral entry (Sinha et al., 2020b). Indeed, the furin pre-activation of spike protein facilitates viral entry particularly in cells with low levels of expressed TMPRSS2 (Lippi et al., 2020; Shang et al., 2020). Omotuyi et al. (2020) demonstrated in a conformational and *in vitro* study, that processed fruit (with seed) from *Aframomum melegueta* K.Schum., an African resource, and its secondary metabolites mitigates SARS-CoV-2 entry by inhibiting furin. Indeed, some proteinaceous plant products (peptides) and metabolites (flavonoids such as rutin, naringin, methylhesperidin and baikalin), have exhibited anti-protease potencies and have been implicated for disease treatment (Majumdar et al., 2010; Hellinger and Gruber, 2019). In addition, ADAM-17, a membrane metallopeptidase opposes viral entry by cleaving off the extracellular domain of ACE2 receptor. The ACE2 domain that is shed off retains some enzyme activity and can convert angiotensin II to angiotensin 1–7 (Palau et al., 2020; Williamson and Kerimi, 2020). Hence, a closer look into the ability of plant-based ligands to upregulate ADAM-17 represents a potential angle for exploration, which may achieve satisfactory outcomes.

SAFETY

Phytomedicinal agents investigated against the Spike-RBD/TMPRSS2/ACE2 axis have displayed beneficial pharmacokinetic properties when subjected to *in silico* analysis of Absorption, Distribution, Metabolism, Excretion and Toxicity (ADMET) (Abdelli et al., 2020; Alexpandi et al., 2020; Gutierrez-Villagomez et al., 2020). These preliminary findings hint to their safety and drug-like potential. However, in view of the limitation of virtual screening, further *in vitro and in vivo* experiments are needed to verify results and provide experimental basis for the research and development/promotion of natural antiviral drugs/nutrition. The cytotoxic status of a plant is also an important safety concern. An *in vitro* study showed that geranium and lemon essential oils inhibited the expression of ACE2 and TMPRSS2 at mRNA and protein levels with no cytotoxic effects on human cell (Senthil Kumar et al., 2020). Additionally, most plant products highlighted are very promising agents keeping in view their pre-reported biological benefits. Thus, further experiments are warranted based on previous research findings and the reported biological safety of these natural compounds. Moreover, these natural compounds may be synthesized and made readily available for immediate testing.

Formalizing the Use of COVID-19 Phytomedicines

Following the wide use of phytomedicines as alternatives for preventing and treating COVID-19 in Africa, the Africa Center for disease Control and Prevention (Africa CDC) recommended the development of state-based herbal registries. The mobilization of funds, technical research support and proper communication for the development of such proclaimed remedies have also been emphasized (Africa CDC, 2020). These activities can help guide the establishment of botanical assets in the management of COVID-19.

Similar to what was introduced during the 2002/2003 SARS-COV outbreak, a Chinese traditional medicine program challenged its experts with the development of preventive and treatment strategies for COVID-19. A similar global effort to introduce scientifically backed herbal remedies to combat COVID-19 alongside conventional treatment will prove helpful. Though these herbals are promising options in decreasing virion entry and the course of infection, caution must be established and tests must be conducted to avoid toxic and non-efficacious regimens. Undeniably, clinically proven therapeutics remain the gold standard for treatment. As such, efforts to engage preliminary and pre-clinically supported herbs of minimal side effects and cost with randomized controlled trials should be considered.

CONCLUSIONS AND FUTURE PERSPECTIVES

Natural products are of prominence and have been adopted for traditional use across many African and Asian countries. Aside policies and a bundle of other factors, the relatively lesser COVID-19 burden observed in regions of Africa and Asia could be influenced by certain potentiators of self-care such

as cost of medication, interest, beliefs, dissatisfaction in synthetic medications and taking responsibility of one's health, which push toward ethnobotanical use for COVID-19; a scenario where "the kitchen cabinet becomes thy medicine cabinet." Of concern, the undeniably increasing demand for plant products is occurring globally at a time threatened by plant extinctions; particularly of wild plants due to excess harvest, habitat degradation, specie invasion, low growth, low abundance, and/or susceptibility to disease. This coupled with the fact that at least one potential drug candidate is lost biennially emphasizes the need for conservation and resource management strategies (Chen et al., 2016). This is most possible given the current state of biotechnology and must be considered particularly in developing countries where about 80% of the populace adopt herbal products for basic healthcare (Moyo et al., 2015; Chen et al., 2016). The overall indicators show that a number of plants and their products possess multimodal influence on viral tropism. Beside the use of plant decoctions, some phytoconstituents previously highlighted, indicate potentially mitigating effects against viral entry by directly or indirectly modulating the ACE2 activity at the Spike-RBD/TMPRSS2/ACE2 axis. This perspective has implications for traditional medicine (TM) and we believe will support and inform ongoing and upcoming investigations on the management of COVID-19. More so, some of the highlighted ligands have been tested in the past and documented to be beneficial across comorbidities which may accompany COVID-19. Perhaps, this lightens the need for further studies before clinical trials. Other benefits including availability, affordability and safety, support the development of these phytomedicinal therapies; a step toward attaining the third united nations sustainable developmental goal - "good health and wellbeing for all."

AUTHOR CONTRIBUTIONS

All authors contributed equally to this work. All have read and agree with the submission of this manuscript.

ACKNOWLEDGMENTS

We appreciate the support and resource provided by staff and postgraduate members of the Center for Advanced Medical Research and Training (CAMRET), Usmanu Danfodiyo University, Sokoto, Nigeria. DU acknowledges the postgraduate scholarship awarded to him (CAMRET/2019/MSc/SCH003) by CAMRET. NC-M. acknowledges the Portuguese Foundation for Science and Technology under the Horizon 2020 Program (PTDC/PSI-GER/28076/2017). The work was also supported by Taif University Researchers Supporting Program (Project number: TURSP-2020/93), Taif University, Saudi Arabia.

REFERENCES

Abdelli, I., Hassani, F., Bekkel Brikci, S., and Ghalem, S. (2020). In silico study the inhibition of angiotensin converting enzyme 2 receptor of COVID-19 by Ammoides verticillata components harvested from Western Algeria. *J. Biomol. Struct. Dyn.*, 1–14. doi:10.1080/07391102.2020.1763199

Africa, C. D. C. (2020). Statement on herbal remedies and medicines for prevention and treatment of COVID-19. Africa centres for disease control and prevention: african union Available from: https://africacdc.org/download/statement-on-herbal-remedies-and-medicines-for-prevention-and-treatment-of-covid-19-2/ (Accessed October 11, 2020).

Alexpandi, R., De Mesquita, J. F., Pandian, S. K., and Ravi, A. V. (2020). Quinolines-based SARS-CoV-2 3CLpro and RdRp inhibitors and spike-RBD-ACE2 inhibitor for drug-repurposing against COVID-19: an in silico analysis. *Front. Microbiol.* 11. doi:10.3389/fmicb.2020.01796

Balkrishna, A., Pokhrel, S., Singh, J., and Varshney, A. (2020). Withanone from Withania somnifera may inhibit novel Coronavirus (COVID-19) entry by disrupting interactions between viral S-protein receptor binding domain and host ACE2 receptor. *Res. Square* .doi:10.21203/rs.3.rs-17806/v1

Basu, A., Sarkar, A., and Maulik, U. (2020). Molecular docking study of potential phytochemicals and their effects on the complex of SARS-CoV2 spike protein and human ACE2. *Sci. Rep.* 10 (1), 17699. doi:10.1038/s41598-020-74715-4

Bejjani, S., and Wu, J. (2013). Transport of IRW, an ovotransferrin-derived antihypertensive peptide, in human intestinal epithelial caco-2 cells. *J. Agric. Food Chem.* 61 (7), 1487–1492. doi:10.1021/jf302904t

Bestle, D., Heindl, M. R., Limburg, H., Van Lam van, T., Pilgram, O., Moulton, H., et al. (2020). TMPRSS2 and furin are both essential for proteolytic activation of SARS-CoV-2 in human airway cells. *Life Sci. alliance* 3 (9). doi:10.26508/lsa.202000786

Bhalla, V., Blish, C. A., and South, A. M. (2020). A historical perspective on ACE2 in the COVID-19 era. *J. Hum. Hypertens.* doi:10.1038/s41371-020-00459-3

Borkotoky, S., and Banerjee, M. (2020). A computational prediction of SARS-CoV-2 structural protein inhibitors from Azadirachta indica (Neem). *J. Biomol. Struct. Dyn.* 1-17 doi:10.1080/07391102.2020.1774419

Bourgonje, A. R., Abdulle, A. E., Timens, W., Hillebrands, J. L., Navis, G. J., Gordijn, S. J., et al. (2020). Angiotensin-converting enzyme 2 (ACE2), SARS-CoV -2 and the pathophysiology of coronavirus disease 2019 (COVID -19). *J. Pathol.* 251 (3), 228–248. doi:10.1002/path.5471

Campos, M., Guerrero, L., Betancur, D., and Hernandez-Escalante, V. (2011). Bioavailability of bioactive peptides. *Food Rev. Int.* 27, 213–226. doi:10.1080/87559129.2011.563395

Chakrabarti, S., Guha, S., and Majumder, K. (2018). Food-derived bioactive peptides in human health: challenges and opportunities. *Nutrients* 10 (11), 1738. doi:10.3390/nu10111738

Chen, H., and Du, Q. (2020). *Potential natural compounds for preventing SARS-CoV-2 (2019-nCoV) infection*. doi:10.20944/preprints202001.0358.v3

Chen, L., Li, X., Chen, M., Feng, Y., and Xiong, C. (2020a). The ACE2 expression in human heart indicates new potential mechanism of heart injury among patients infected with SARS-CoV-2. *Cardiovasc. Res.* 116 (6), 1097–1100. doi:10.1093/cvr/cvaa078

Chen, S. L., Yu, H., Luo, H. M., Wu, Q., Li, C. F., and Steinmetz, A. (2016). Conservation and sustainable use of medicinal plants: problems, progress, and prospects. *Chin. Med.* 11, 37. doi:10.1186/s13020-016-0108-7

Chen, Y., Guo, Y., Pan, Y., and Zhao, Z. J. (2020b). Structure analysis of the receptor binding of 2019-nCoV. *Biochem. Biophysical Res. Commun.* 525 (1), 135–140. doi:10.1016/j.bbrc.2020.02.071

Chen, Y., Liu, Q., and Guo, D. (2020c). Emerging coronaviruses: genome structure, replication, and pathogenesis. *J. Med. Virol.* 92 (4), 418–423. doi:10.1002/jmv.25681

Cheng, L., Zheng, W., Li, M., Huang, J., Bao, S., Xu, Q., et al. (2020). *Citrus fruits are rich in flavonoids for immunoregulation and potential targeting ACE2*. Preprints

Chikhale, R. V., Gurav, S. S., Patil, R. B., Sinha, S. K., Prasad, S. K., Shakya, A., et al. (2020a). Sars-cov-2 host entry and replication inhibitors from Indian ginseng:

an in-silico approach. *J. Biomol. Struct. Dyn.*, 1–12 .doi:10.1080/07391102.2020.1778539

Chikhale, R. V., Sinha, S. K., Patil, R. B., Prasad, S. K., Shakya, A., Gurav, N., et al. (2020b). In-silico investigation of phytochemicals from *Asparagus racemosus* as plausible antiviral agent in COVID-19. *J. Biomol. Struct. Dyn.*, 1–15 .doi:10.1080/07391102.2020.1784289

Daak, A. A., Lopez-Toledano, M. A., and Heeney, M. M. (2020). Biochemical and therapeutic effects of omega-3 fatty acids in sickle cell disease. *Complement. Therapies Med.* 52. 102482. doi:10.1016/j.ctim.2020.102482

de Kloet, A. D., Krause, E. G., and Woods, S. C. (2010). The renin angiotensin system and the metabolic syndrome. *Physiol. Behav.* 100 (5), 525–534. doi:10.1016/j.physbeh.2010.03.018

de Wit, E., van Doremalen, N., Falzarano, D., and Munster, V. J. (2016). SARS and MERS: recent insights into emerging coronaviruses. *Nat. Rev. Microbiol.* 14 (8), 523–534. doi:10.1038/nrmicro.2016.81

Donoghue, M., Hsieh, F., Baronas, E., Godbout, K., Gosselin, M., Stagliano, N., et al. (2000). A novel angiotensin-converting enzyme-related carboxypeptidase (ACE2) converts angiotensin I to angiotensin 1-9. *Circ. Res.* 87 (5), e1–e9. doi:10.1161/01.res.87.5.e1

Enmozhi, S. K., Raja, K., Sebastine, I., and Joseph, J. (2020). Andrographolide as a potential inhibitor of SARS-CoV-2 main protease: an in silico approach. *J. Biomol. Struct. Dyn.* 1-7 doi:10.1080/07391102.2020.1760136

Esparza, T. J., Martin, N. P., Anderson, G. P., Goldman, E. R., and Brody, D. L. (2020). High affinity nanobodies block SARS-CoV-2 spike receptor binding domain interaction with human angiotensin converting enzyme. *Sci. Rep.* 10 (1), 22370. doi:10.1038/s41598-020-79036-0

European Centre for Disease Prevention and Control (2020). COVID-19 situation update worldwide, as of 26 September 2020 Available from: https://www.ecdc.europa.eu/en/geographical-distribution-2019-ncov-cases (Accessed September 26, 2020).

Fan, C., Li, K., Ding, Y., Lu, W. L., and Wang, J. (2020). ACE2 expression in kidney and testis may cause kidney and testis damage after 2019-nCoV infection. *medRxiv* doi:10.1101/2020.02.12.20022418

Fougeroux, C., Goksøyr, L., Idorn, M., Soroka, V., Myeni, S. K., Dagil, R., et al. (2021). Capsid-like particles decorated with the SARS-CoV-2 receptor-binding domain elicit strong virus neutralization activity. *Nat. Commun.* 12 (1), 324. doi:10.1038/s41467-020-20251-8

Furuhashi, M., Moniwa, N., Takizawa, H., Ura, N., and Shimamoto, K. (2020). Potential differential effects of renin-angiotensin system inhibitors on SARS-CoV-2 infection and lung injury in COVID-19. *Hypertens. Res.* 43 (8), 837–840. doi:10.1038/s41440-020-0478-1

Gheblawi, M., Wang, K., Viveiros, A., Nguyen, Q., Zhong, J.-C., Turner, A. J., et al. (2020). Angiotensin-converting enzyme 2: SARS-CoV-2 receptor and regulator of the renin-angiotensin system. *Circ. Res.* 126 (10), 1456–1474. doi:10.1161/circresaha.120.317015

Glasgow, A., Glasgow, J., Limonta, D., Solomon, P., Lui, I., Zhang, Y., et al. (2020). Engineered ACE2 receptor traps potently neutralize SARS-CoV-2. *Proc. Natl. Acad. Sci. USA* 117 (45), 28046. doi:10.1073/pnas.2016093117

Guan, W.-j., Ni, Z.-y., Hu, Y., Liang, W.-h., Ou, C.-q., He, J.-x., et al. (2020). Clinical characteristics of coronavirus disease 2019 in China. *N. Engl. J. Med.* 382 (18), 1708–1720. doi:10.1056/nejmoa2002032

Güler, H. I., Tatar, G., Yildiz, O., Belduz, A. O., and Kolayli, S. (2020). Investigation of potential inhibitor properties of ethanolic propolis extracts against ACE-II receptors for COVID-19 treatment by Molecular Docking Study. *ScienceOpen Preprints*. doi:10.35206/jan.762734

Gupta, R., and Misra, A. (2020). Contentious issues and evolving concepts in the clinical presentation and management of patients with COVID-19 infectionwith reference to use of therapeutic and other drugs used in Co-morbid diseases (Hypertension, diabetes etc). *Diabetes Metab. Syndr. Clin. Res. Rev.* 14 (3), 251–254. doi:10.1016/j.dsx.2020.03.012

Gupte, M. (2011). *Role of angiotensin converting enzyme 2 (ACE2) in obesity -associated hypertension*. Lexington, Kentucky: University of Kentucky Doctoral Dissertations. Available from: https://uknowledge.uky.edu/gradschool_diss/37 (Accessed October 28, 2020).

Gutekunst, W. R., Gianatassio, R., and Baran, P. S. (2012). Sequential C sp 3-H arylation and olefination: total synthesis of the proposed structure of pipercyclobutanamide A. *Angew. Chem. Int. Ed.* 51 (30), 7507–7510. doi:10.1002/anie.201203897

Gutierrez-Villagomez, J. M., Campos-García, T., Molina-Torres, J., López, M. G., and Vázquez-Martínez, J. (2020). Alkamides and piperamides as potential antivirals against the severe acute respiratory syndrome coronavirus 2 (SARS-CoV-2). *J. Phys. Chem. Lett.* 11 (19), 8008–8016. doi:10.1021/acs.jpclett.0c01685

Haggag, Y. A., El-Ashmawy, N. E., and Okasha, K. M. (2020). Is hesperidin essential for prophylaxis and treatment of COVID-19 Infection?. *Med. Hypotheses* 144, 109957. doi:10.1016/j.mehy.2020.109957

Hamming, I., Timens, W., Bulthuis, M., Lely, A., Navis, G., and van Goor, H. (2004). Tissue distribution of ACE2 protein, the functional receptor for SARS coronavirus. A first step in understanding SARS pathogenesis. *J. Pathol.* 203 (2), 631–637. doi:10.1002/path.1570

Hao, Y., and Liu, Y. (2016). Osthole alleviates bleomycin-induced pulmonary fibrosis via modulating angiotensin-converting enzyme 2/angiotensin-(1-7) *Axis* and decreasing inflammation responses in rats. *Biol. Pharm. Bull.* 39 (4), 457–465. doi:10.1248/bpb.b15-00358

Haschke, M., Schuster, M., Poglitsch, M., Loibner, H., Salzberg, M., Bruggisser, M., et al. (2013). Pharmacokinetics and pharmacodynamics of recombinant human angiotensin-converting enzyme 2 in healthy human subjects. *Clin. Pharmacokinet.* 52 (9), 783–792. doi:10.1007/s40262-013-0072-7

He, R., Yang, Y.-J., Wang, Z., Xing, C.-R., Yuan, J., Wang, L.-F., et al. (2019). Rapeseed protein-derived peptides, LY, RALP, and GHS, modulates key enzymes and intermediate products of renin-angiotensin system pathway in spontaneously hypertensive rat. *NPJ Sci. Food* 3, 1. doi:10.1038/s41538-018-0033-5

Hellinger, R., and Gruber, C. W. (2019). Peptide-based protease inhibitors from plants. *Drug Discov. Today* 24 (9), 1877–1889. doi:10.1016/j.drudis.2019.05.026

Ho, T., Wu, S., Chen, J., Li, C., and Hsiang, C. (2007). Emodin blocks the SARS coronavirus spike protein and angiotensin-converting enzyme 2 interaction. *Antivir. Res.* 74 (2), 92–101. doi:10.1016/j.antiviral.2006.04.014

Hoffmann, M., Kleine-Weber, H., Schroeder, S., Krüger, N., Herrler, T., Erichsen, S., et al. (2020). SARS-CoV-2 cell entry depends on ACE2 and TMPRSS2 and is blocked by a clinically proven protease inhibitor. *Cell* 181 (2), 271–280. doi:10.1016/j.cell.2020.02.052

Huang, C., Wang, Y., Li, X., Ren, L., Zhao, J., Hu, Y., et al. (2020). Clinical features of patients infected with 2019 novel coronavirus in Wuhan, China. *The Lancet* 395 (10223), 497–506. doi:10.1016/s0140-6736(20)30183-5

Imai, Y., Kuba, K., Rao, S., Huan, Y., Guo, F., Guan, B., et al. (2005). Angiotensin-converting enzyme 2 protects from severe acute lung failure. *Nature* 436 (7047), 112–116. doi:10.1038/nature03712

Joshi, T., Joshi, T., Sharma, P., Mathpal, S., Pundir, H., Bhatt, V., et al. (2020). In silico screening of natural compounds against COVID-19 by targeting Mpro and ACE2 using molecular docking. *Eur. Rev. Med. Pharmacol. Sci.* 24 (8), 4529–4536. doi:10.26355/eurrev_202004_21036

Kai, H., and Kai, M. (2020). Interactions of coronaviruses with ACE2, angiotensin II, and RAS inhibitors-lessons from available evidence and insights into COVID-19. *Hypertens. Res.* 43 (7), 648–654. doi:10.1038/s41440-020-0455-8

Khan, A., Benthin, C., Zeno, B., Albertson, T. E., Boyd, J., Christie, J. D., et al. (2017). A pilot clinical trial of recombinant human angiotensin-converting enzyme 2 in acute respiratory distress syndrome. *Crit. Care (London, England)* 21 (1), 234. doi:10.1186/s13054-017-1823-x

Kuba, K., Imai, Y., Rao, S., Gao, H., Guo, F., Guan, B., et al. (2005). A crucial role of angiotensin converting enzyme 2 (ACE2) in SARS coronavirus-induced lung injury. *Nat. Med.* 11 (8), 875–879. doi:10.1038/nm1267

Kumar, B. K., Sekhar, K. V. G. C., Kunjiappan, S., Jamalis, J., Balaña-Fouce, R., Tekwani, B. L., et al. (2020a). Druggable targets of SARS-CoV-2 and treatment opportunities for COVID-19. *Bioorg. Chem.* 104,.104269. doi:10.1016/j.bioorg.2020.104269

Kumar, S., Nyodu, R., Maurya, V. K., and Saxena, S. K. (2020b). "Morphology, genome organization, replication, and pathogenesis of severe acute respiratory syndrome coronavirus 2 (SARS-CoV-2)," in *Coronavirus disease 2019 (COVID-19): epidemiology, pathogenesis, diagnosis, and therapeutics*. Editor S. K. Saxena (Singapore: Springer Singapore), 23–31.

Kumar, V., Dhanjal, J. K., Bhargava, P., Kaul, A., Wang, J., Zhang, H., et al. (2020c). Withanone and Withaferin-A are predicted to interact with transmembrane protease serine 2 (TMPRSS2) and block entry of SARS-

CoV-2 into cells. *J. Biomol. Struct. Dyn.*, 1–13. doi:10.1080/07391102.2020.1775704

Lalaoui, R., Bakour, S., Raoult, D., Verger, P., Sokhna, C., Devaux, C., et al. (2020). What could explain the late emergence of COVID-19 in Africa?. *New Microbes New Infect.* 38, 100760. doi:10.1016/j.nmni.2020.100760

Letko, M., Marzi, A., and Munster, V. (2020). Functional assessment of cell entry and receptor usage for SARS-CoV-2 and other lineage B betacoronaviruses. *Nat. Microbiol.* 5 (4), 562–569. doi:10.1038/s41564-020-0688-y

Li, M. Y., Li, L., Zhang, Y., and Wang, X. S. (2020a). Expression of the SARS-CoV-2 cell receptor gene ACE2 in a wide variety of human tissues. *Infect. Dis. poverty* 9 (1), 45. doi:10.1186/s40249-020-00662-x

Li, Y. C., Bai, W. Z., and Hashikawa, T. (2020b). The neuroinvasive potential of SARS-CoV2 may play a role in the respiratory failure of COVID-19 patients. *J. Med. Virol.* 92 (6), 552–555. doi:10.1002/jmv.25728

Li, Z., Wu, M., Guo, J., Yao, J., Liao, X., Song, S., et al. (2020c). Caution on kidney dysfunctions of 2019-nCoV patients. *MedRxiv*. doi:10.1101/2020.02.08.20021212

Liao, W., Fan, H., Davidge, S. T., and Wu, J. (2019). Egg white-derived antihypertensive peptide IRW (Ile-Arg-Trp) reduces blood pressure in spontaneously hypertensive rats via the ACE2/ang (1-7)/mas receptor *Axis. Mol. Nutr. Food Res.* 63 (9), e1900063. doi:10.1002/mnfr.201900063

Liao, W. (2019). Food protein-derived peptides targeting angiotensin converting enzyme 2. Education and research archive (ERA). Edmonton, Alberta: University of Alberta (Accessed October 15, 2020). doi:10.7939/r3-4v2n-7x45

Lippi, G., Lavie, C. J., Henry, B. M., and Sanchis-Gomar, F. (2020). Do genetic polymorphisms in angiotensin converting enzyme 2 (ACE2) gene play a role in coronavirus disease 2019 (COVID-19)? *Clin. Chem. Lab. Med. (Cclm)*, 1 doi:10.1515/cclm-2020-0727

Liu, H., Jiang, Y., Li, M., Yu, X., Sui, D., and Fu, L. (2019). Ginsenoside Rg3 attenuates angiotensin II-mediated renal injury in rats and mice by upregulating angiotensin-converting enzyme 2 in the renal tissue. *Evidence-Based Complement. Altern. Med.* doi:10.1155/2019/6741057

Liu, R., Zhang, M., Wyche, T. P., Winston-McPherson, G. N., Bugni, T. S., and Tang, W. (2012). Stereoselective preparation of cyclobutanes with four different substituents: total synthesis and structural revision of pipercyclobutanamide A and piperchabamide G. *Angew. Chem. Int. Ed.* 51 (30), 7503–7506. doi:10.1002/anie.201203379

Majumdar, S., Mohanta, B. C., Chowdhury, D. R., Banik, R., Dinda, B., and Basak, A. (2010). Proprotein convertase inhibitory activities of flavonoids isolated from Oroxylum indicum. *Cmc* 17 (19), 2049–2058. doi:10.2174/092986710791233643

Majumder, K., Liang, G., Chen, Y., Guan, L., Davidge, S. T., and Wu, J. (2015). Egg ovotransferrin-derived ACE inhibitory peptide IRW increases ACE2 but decreases proinflammatory genes expression in mesenteric artery of spontaneously hypertensive rats. *Mol. Nutr. Food Res.* 59 (9), 1735–1744. doi:10.1002/mnfr.201500050

Malami, I., Abdul, A. B., Abdullah, R., Bt Kassim, N. K., Waziri, P., and Christopher Etti, I. (2016). *Silico discovery of potential uridine-cytidine kinase 2 inhibitors from the rhizome of alpinia mutica*, *Molecules (Basel, Switzerland)*,21, 417 doi:10.3390/molecules21040417

Marian, A. J. (2013). The discovery of the ACE2 gene. *Circ. Res.* 112 (10), 1307–1309. doi:10.1161/circresaha.113.301271

Monteil, V., Kwon, H., Prado, P., Hagelkrüys, A., Wimmer, R. A., Stahl, M., et al. (2020). Inhibition of SARS-CoV-2 infections in engineered human tissues using clinical-grade soluble human ACE2. *Cell* 181 (4), 905–913. doi:10.1016/j.cell.2020.04.004

Moyo, M., Aremu, A. O., and Van Staden, J. (2015). Medicinal plants: an invaluable, dwindling resource in sub-Saharan Africa. *J. Ethnopharmacology* 174, 595–606. doi:10.1016/j.jep.2015.04.034

Muhammad, A., Mada, S. B., Malami., I., Forcados, G. E., Erukainure, O. L., and Sani, H. (2018). Postmenopausal osteoporosis and breast cancer: the biochemical links and beneficial effects of functional foods. *Biomed. Pharmacother. = Biomedecine pharmacotherapie* 107, 571–582 .doi:10.1016/j.biopha.2018.08.018

My, T. T. A., Loan, H. T. P., Hai, N. T. T., Hieu, L. T., Hoa, T. T., Thuy, B. T. P., et al. (2020). Evaluation of the inhibitory activities of COVID-19 of Melaleuca cajuputi oil using docking simulation. *ChemistrySelect* 5 (21), 6312–6320. doi:10.1002/slct.202000822

Naqvi, A. A. T., Fatima, K., Mohammad, T., Fatima, U., Singh, I. K., Singh, A., et al. (2020). Insights into SARS-CoV-2 genome, structure, evolution, pathogenesis and therapies: structural genomics approach. *Biochim. Biophys. Acta (Bba) - Mol. Basis Dis.* 1866 (10), 165878. doi:10.1016/j.bbadis.2020.165878

Ngwa, W., Kumar, R., Thompson, D., Lyerly, W., Moore, R., Reid, T.-E., et al. (2020). Potential of flavonoid-inspired phytomedicines against COVID-19. *Molecules* 25 (11), 2707. doi:10.3390/molecules25112707

Nicoletti, M. (2012). Nutraceuticals and botanicals: overview and perspectives. *Int. J. Food Sci. Nutr.* 63 (Suppl. 1 2)–6. doi:10.3109/09637486.2011.628012

Nittari, G., Pallotta, G., Amenta, F., and Tayebati, S. K. (2020). Current pharmacological treatments for SARS-CoV-2: a narrative review. *Eur. J. Pharmacol.* 882, 173328. doi:10.1016/j.ejphar.2020.173328

Ohashi, H., Watashi, K., Saso, W., Shionoya, K., Iwanami, S., Hirokawa, T., et al. (2020). Multidrug treatment with nelfinavir and cepharanthine against COVID-19. *bioRxiv* doi:10.1101/2020.04.14.039925

Okasha, K. M. (2020). Hesperidin and diosmin for treatment of COVID-19. Available from: https://clinicaltrials.gov/show/NCT04452799 (Accessed October 28, 2020).

Omar, S., Bouziane, I., Bouslama, Z., and Djemel, A. (2020). (ACE2) from natural products: quercetin, hispidulin, and cirsimaritin exhibited better potential inhibition than hydroxy-chloroquine against COVID-19 main protease active site and ACE2. *Chemrxiv. Preprint.In-silico identification of potent inhibitors of COVID-19 main protease (Mpro) and angiotensin converting enzyme 2* doi:10.26434/chemrxiv.12181404.v1

Omotuyi, I. O., Nash, O., Ajiboye, B. O., Olumekun, V. O., Oyinloye, B. E., Osuntokun, O. T., et al. (2020). Aframomum melegueta K.Schum. secondary metabolites exhibit polypharmacology against SARS-CoV-2 drug targets: *in vitro* validation of furin inhibition.*Phytotherapy research : ptr* doi:10.1002/ptr.6843

Oyebode, O., Kandala, N.-B., Chilton, P. J., and Lilford, R. J. (2016). Use of traditional medicine in middle-income countries: a WHO-SAGE study. *Health Policy Plan.* 31 (8), 984–991. doi:10.1093/heapol/czw022

Palau, V., Riera, M., and Soler, M. J. (2020). ADAM17 inhibition may exert a protective effect on COVID-19. *Nephrol. Dial. Transpl.* 35 (6), 1071–1072. doi:10.1093/ndt/gfaa093

Paraiso, I. L., Revel, J. S., and Stevens, J. F. (2020). Potential use of polyphenols in the battle against COVID-19. *Curr. Opin. Food Sci.* 32, 149. doi:10.1016/j.cofs.2020.08.004

Peiris, J. S. M., Yuen, K. Y., Osterhaus, A. D. M. E., and Stöhr, K. (2003). The severe acute respiratory syndrome. *N. Engl. J. Med.* 349 (25), 2431–2441. doi:10.1056/nejmra032498

Poochi, S. P., Easwaran, M., Balasubramanian, B., Anbuselvam, M., Meyyazhagan, A., Park, S., et al. (2020). Employing bioactive compounds derived from *Ipomoea* obscura (L.) to evaluate potential inhibitor for SARS-CoV-2 main protease and ACE2 protein. *Food Front.* doi:10.1002/fft2.29

Rakib, A., Paul, A., Chy, M. N. U., Sami, S. A., Baral, S. K., Majumder, M., et al. (2020). Biochemical and computational approach of selected phytocompounds from Tinospora crispa in the management of COVID-19. *Molecules* 25 (17), 3936. doi:10.3390/molecules25173936

Rattanapisit, K., Shanmugaraj, B., Manopwisedjaroen, S., Purwono, P. B., Siriwattananon, K., Khorattanakulchai, N., et al. (2020). Rapid production of SARS-CoV-2 receptor binding domain (RBD) and spike specific monoclonal antibody CR3022 in Nicotiana benthamiana. *Sci. Rep.* 10 (1), 17698. doi:10.1038/s41598-020-74904-1

Ren, X., Shao, X.-X., Li, X.-X., Jia, X.-H., Song, T., Zhou, W.-Y., et al. (2020). Identifying potential treatments of COVID-19 from Traditional Chinese Medicine (TCM) by using a data-driven approach. *J. Ethnopharmacology* 258, 112932. doi:10.1016/j.jep.2020.112932

Sakshi, C., Harikrishnan, A., Jayaraman, S., Choudhury, A. R., and Veena, V. (2021). Predictive medicinal metabolites from Momordica dioica against comorbidity related proteins of SARS-CoV-2 infections. *J. Biomol. Struct. Dyn.*, 1–14. doi:10.1080/07391102.2020.1868340

Senthil Kumar, K. J., Gokila Vani, M., Wang, C. S., Chen, C. C., Chen, Y. C., Lu, L. P., et al. (2020). *Geranium* and lemon essential oils and their active compounds downregulate angiotensin-converting enzyme 2 (ACE2), a SARS-CoV-2 spike receptor-binding domain, *Plants (Basel, Switzerland)* Epithelial cells, 9 doi:10.3390/plants9060770

Shah, V. K., Firmal, P., Alam, A., Ganguly, D., and Chattopadhyay, S. (2020). Overview of immune response during SARS-CoV-2 infection: lessons from the past. *Front. Immunol.* 11. doi:10.3389/fimmu.2020.01949

Shang, J., Wan, Y., Luo, C., Ye, G., Geng, Q., Auerbach, A., et al. (2020). Cell entry mechanisms of SARS-CoV-2. *Proc. Natl. Acad. Sci. USA* 117 (21), 11727–11734. doi:10.1073/pnas.2003138117

Shi, X., Gong, E., Gao, D., Zhang, B., Zheng, J., Gao, Z., et al. (2005). Severe acute respiratory syndrome associated coronavirus is detected in intestinal tissues of fatal cases. *Am. J. Gastroenterol.* 100 (1), 169–176. doi:10.1111/j.1572-0241.2005.40377.x

Shi, Y., Zhang, B., Chen, X.-J., Xu, D.-Q., Wang, Y.-X., Dong, H.-Y., et al. (2013). Osthole protects lipopolysaccharide-induced acute lung injury in mice by preventing down-regulation of angiotensin-converting enzyme 2. *Eur. J. Pharm. Sci.* 48 (4-5), 819–824. doi:10.1016/j.ejps.2012.12.031

Shil, P. K., Kwon, K.-C., Zhu, P., Verma, A., Daniell, H., and Li, Q. (2014). Oral delivery of ACE2/Ang-(1-7) bioencapsulated in plant cells protects against experimental uveitis and autoimmune uveoretinitis. *Mol. Ther.* 22 (12), 2069–2082. doi:10.1038/mt.2014.179

Sinha, S. K., Prasad, S. K., Islam, M. A., Gurav, S. S., Patil, R. B., AlFaris, N. A., et al. (2020a). Identification of bioactive compounds from *Glycyrrhiza* glabra as possible inhibitor of SARS-CoV-2 spike glycoprotein and non-structural protein-15: a pharmacoinformatics study. *J. Biomol. Struct. Dyn.*, 1–15. doi:10.1080/07391102.2020.1779132

Sinha, S. K., Shakya, A., Prasad, S. K., Singh, S., Gurav, N. S., Prasad, R. S., et al. (2020b). An in-silico evaluation of different Saikosaponins for their potency against SARS-CoV-2 using NSP15 and fusion spike glycoprotein as targets. *J. Biomol. Struct. Dyn.*, 1–12. doi:10.1080/07391102.2020.1762741

Sui, H., Yu, Q., Zhi, Y., Geng, G., Liu, H., and Xu, H. (2010). [Effects of apigenin on the expression of angiotensin-converting enzyme 2 in kidney in spontaneously hypertensive rats]. *Wei Sheng Yan Jiu* 39 (6), 693–700.

Sun, T., and Guan, J. (2020). Novel coronavirus and the central nervous system. *Eur. J. Neurol.* doi:10.1111/ene.14227

Takahashi, S., Yoshiya, T., Yoshizawa-Kumagaye, K., and Sugiyama, T. (2015). Nicotianamine is a novel angiotensin-converting enzyme 2 inhibitor in soybean. *Biomed. Res.* 36 (3), 219–224. doi:10.2220/biomedres.36.219

Tan, T. K., Rijal, P., Rahikainen, R., Keeble, A. H., Schimanski, L., Hussain, S., et al. (2021). A COVID-19 vaccine candidate using SpyCatcher multimerization of the SARS-CoV-2 spike protein receptor-binding domain induces potent neutralising antibody responses. *Nat. Commun.* 12 (1), 542. doi:10.1038/s41467-020-20654-7

Thuy, B. T. P., My, T. T. A., Hai, N. T. T., Hieu, L. T., Hoa, T. T., Thi Phuong Loan, H., et al. (2020). Investigation into SARS-CoV-2 resistance of compounds in garlic essential oil. *ACS omega* 5 (14), 8312–8320. doi:10.1021/acsomega.0c00772

Tikellis, C., and Thomas, M. C. (2012). Angiotensin-converting enzyme 2 (ACE2) is a key modulator of the renin angiotensin system in health and disease. *Int. J. Pept.* 2012, 256294. doi:10.1155/2012/256294

To, K., Tong, J. H., Chan, P. K., Au, F. W., Chim, S. S., Allen Chan, K., et al. (2004). Tissue and cellular tropism of the coronavirus associated with severe acute respiratory syndrome: an *in-situ* hybridization study of fatal cases. *J. Pathol.* 202 (2), 157–163. doi:10.1002/path.1510

Turner, A. J., Tipnis, S. R., Guy, J. L., Rice, G. I., and Hooper, N. M. (2002). ACEH/ACE2 is a novel mammalian metallocarboxypeptidase and a homologue of angiotensin-converting enzyme insensitive to ACE inhibitors. *Can. J. Physiol. Pharmacol.* 80 (4), 346–353. doi:10.1139/y02-021

Tutunchi, H., Naeini, F., Ostadrahimi, A., and Hosseinzadeh-Attar, M. J. (2020). Naringenin, a flavanone with antiviral and anti-inflammatory effects: a promising treatment strategy against COVID -19. *Phytotherapy Res.* 34, 3137. doi:10.1002/ptr.6781

Ulu, A., Harris, T. R., Morisseau, C., Miyabe, C., Inoue, H., Schuster, G., et al. (2013). Anti-inflammatory effects of ω-3 polyunsaturated fatty acids and soluble epoxide hydrolase inhibitors in angiotensin-II-dependent hypertension. *J. Cardiovasc. Pharmacol.* 62 (3), 285–297. doi:10.1097/fjc.0b013e318298e460

Utomo, R. Y., Ikawati, M., and Meiyanto, E. (2020). Revealing the potency of citrus and galangal constituents to halt SARS-CoV-2 infection. *Preprints*, 2020030214. doi:10.20944/preprints202003.0214.v1

Verdecchia, P., Cavallini, C., Spanevello, A., and Angeli, F. (2020). The pivotal link between ACE2 deficiency and SARS-CoV-2 infection. *Eur. J. Intern. Med.* 76, 14–20. doi:10.1016/j.ejim.2020.04.037

Wahedi, H. M., Ahmad, S., and Abbasi, S. W. (2020). Stilbene-based natural compounds as promising drug candidates against COVID-19. *J. Biomol. Struct. Dyn.* 1-10 doi:10.1080/07391102.2020.1762743

Wang, J., Zhao, S., Liu, M., Zhao, Z., Xu, Y., Wang, P., et al. (2020a). ACE2 expression by colonic epithelial cells is associated with viral infection, immunity and energy metabolism. *medRxiv*. doi:10.1101/2020.02.05.20020545

Wang, Q., Qiu, Y., Li, J.-Y., Zhou, Z.-J., Liao, C.-H., and Ge, X.-Y. (2020b). A unique protease cleavage site predicted in the spike protein of the novel pneumonia coronavirus (2019-nCoV) potentially related to viral transmissibility. *Virol. Sin.* 35 (3), 337–339. doi:10.1007/s12250-020-00212-7

Wang, S., Qiu, Z., Hou, Y., Deng, X., Xu, W., Zheng, T., et al. (2021). AXL is a candidate receptor for SARS-CoV-2 that promotes infection of pulmonary and bronchial epithelial cells. *Cel Res.* doi:10.1038/s41422-020-00460-y

Wang, Z., Wang, S., Zhao, J., Yu, C., Hu, Y., Tu, Y., et al. (2019). Naringenin ameliorates renovascular hypertensive renal damage by normalizing the balance of renin-angiotensin system components in rats. *Int. J. Med. Sci.* 16 (5), 644–653. doi:10.7150/ijms.31075

Watanabe, Y., Allen, J. D., Wrapp, D., McLellan, J. S., and Crispin, M. (2020). Site-specific glycan analysis of the SARS-CoV-2 spike. *Science (New York, N.Y.)* 369 (6501), 330–333 .doi:10.1126/science.abb9983

Wei, X., Zhu, X., Hu, N., Zhang, X., Sun, T., Xu, J., et al. (2015). Baicalin attenuates angiotensin II-induced endothelial dysfunction. *Biochem. Biophysical Res. Commun.* 465 (1), 101–107. doi:10.1016/j.bbrc.2015.07.138

WHO (2004). *Summary of probable SARS cases with onset of illness from 1 November 2002 to 31 July 2003 (Based on data as of the 31 December 2003)* World Health Organisation (WHO). Available from: https://www.who.int/csr/sars/country/table2004_04_21/en/ (Accessed September 30, 2020).

WHO (2019). *WHO global report on traditional and complimentary medicine 2019*. Geneva: World Health Organization. Available from: https://apps.who.int/iris/handle/10665/312342 (Accessed.September 30, 2020).

Williamson, G., and Kerimi, A. (2020). Testing of natural products in clinical trials targeting the SARS-CoV-2 (Covid-19) viral spike protein-angiotensin converting enzyme-2 (ACE2) interaction. *Biochem. Pharmacol.* 178, 114123. doi:10.1016/j.bcp.2020.114123

Wu, Y., Xu, X., Chen, Z., Duan, J., Hashimoto, K., Yang, L., et al. (2020). Nervous system involvement after infection with COVID-19 and other coronaviruses. *Brain Behav. Immun.* 87, 18–22. doi:10.1016/j.bbi.2020.03.031

Yahalom-Ronen, Y., Tamir, H., Melamed, S., Politi, B., Shifman, O., Achdout, H., et al. (2020). A single dose of recombinant VSV-ΔG-spike vaccine provides protection against SARS-CoV-2 challenge. *Nat. Commun.* 11 (1), 6402. doi:10.1038/s41467-020-20228-7

Yang, L., Li, Y.-T., Miao, J., Wang, L., Fu, H., Li, Q., et al. (2020a). Network pharmacology studies on the effect of Chai-Ling decoction in coronavirus disease 2019. *Traditional Med. Res.* 5 (3), 145–159.

Yang, X., Yu, Y., Xu, J., Shu, H., Xia, J. a., Liu, H., et al. (2020b). Clinical course and outcomes of critically ill patients with SARS-CoV-2 pneumonia in Wuhan, China: a single-centered, retrospective, observational study. *Lancet Respir. Med.* 8 (5), 475–481. doi:10.1016/s2213-2600(20)30079-5

Yu, L., Yuan, K., Phuong, H. T. A., Park, B. M., and Kim, S. H. (2016). Angiotensin-(1-5), an active mediator of renin-angiotensin system, stimulates ANP secretion via Mas receptor. *Peptides* 86, 33–41. doi:10.1016/j.peptides.2016.09.009

Zhang, H., Penninger, J. M., Li, Y., Zhong, N., and Slutsky, A. S. (2020a). Angiotensin-converting enzyme 2 (ACE2) as a SARS-CoV-2 receptor: molecular mechanisms and potential therapeutic target. *Intensive Care Med.* 46 (4), 586–590. doi:10.1007/s00134-020-05985-9

Zhang, Y., Geng, X., Tan, Y., Li, Q., Xu, C., Xu, J., et al. (2020b). New understanding of the damage of SARS-CoV-2 infection outside the respiratory system. *Biomed. Pharmacother.* 127, 110195. doi:10.1016/j.biopha.2020.110195

Zhao, Y., Zhao, Z., Wang, Y., Zhou, Y., Ma, Y., and Zuo, W. (2020). Single-cell RNA expression profiling of ACE2, the receptor of SARS-CoV-2. *bioRxiv* .doi:10.1101/2020.01.26.919985

Zheng, J., Wang, J., Pan, H., Wu, H., Ren, D., and Lu, J. (2017). Effects of IQP, VEP and Spirulina platensis hydrolysates on the local kidney renin angiotensin system in spontaneously hypertensive rats. *Mol. Med. Rep.* 16 (6), 8485–8492. doi:10.3892/mmr.2017.7602

Zhou, P., Yang, X.-L., Wang, X.-G., Hu, B., Zhang, L., Zhang, W., et al. (2020). A pneumonia outbreak associated with a new coronavirus of probable bat origin. *Nature* 579 (7798), 270–273. doi:10.1038/s41586-020-2012-7

Zi, C.-T., Zhang, N., Yang, L., Wang, L.-X., Wu, Y.-L., Su, Y.-S., et al. (2020). Discovery of a potent angiotensin converting enzyme 2 inhibitor from Chinese medicinal and edible plant via docking-based virtual screening. *Research square*. doi:10.21203/rs.3.rs-32515/v1

Conflict of Interest: The authors declare that the research was conducted in the absence of any commercial or financial relationships that could be construed as a potential conflict of interest.

frontiers in Pharmacology

REVIEW
published: 28 May 2021
doi: 10.3389/fphar.2021.671498

Traditional Herbal Medicines, Bioactive Metabolites, and Plant Products Against COVID-19: Update on Clinical Trials and Mechanism of Actions

Safaet Alam[1†], *Md. Moklesur Rahman Sarker*[1,2*†], *Sadia Afrin*[3], *Fahmida Tasnim Richi*[3], *Chao Zhao*[4†], *Jin-Rong Zhou*[5†] *and Isa Naina Mohamed*[6*†]

[1]Department of Pharmacy, State University of Bangladesh, Dhaka, Bangladesh, [2]Pharmacology and Toxicology Research Division, Health Med Science Research Limited, Dhaka, Bangladesh, [3]Department of Pharmacy, Faculty of Pharmacy, University of Dhaka, Dhaka, Bangladesh, [4]College of Food Science, Fujian Agriculture and Forestry University, Fuzhou, China, [5]Nutrition/Metabolism Laboratory, Beth Israel Deaconess Medical Center, Harvard Medical School, Boston, MA, United States, [6]Pharmacology Department, Medical Faculty, Universiti Kebangsaan Malaysia (The National University of Malaysia), Kuala Lumpur, Malaysia

SARS-CoV-2 is the latest worldwide pandemic declared by the World Health Organization and there is no established anti-COVID-19 drug to combat this notorious situation except some recently approved vaccines. By affecting the global public health sector, this viral infection has created a disastrous situation associated with high morbidity and mortality rates along with remarkable cases of hospitalization because of its tendency to be high infective. These challenges forced researchers and leading pharmaceutical companies to find and develop cures for this novel strain of coronavirus. Besides, plants have a proven history of being notable wellsprings of potential drugs, including antiviral, antibacterial, and anticancer therapies. As a continuation of this approach, plant-based preparations and bioactive metabolites along with a notable number of traditional medicines, bioactive phytochemicals, traditional Chinese medicines, nutraceuticals, Ayurvedic preparations, and other plant-based products are being explored as possible therapeutics against COVID-19. Moreover, the unavailability of effective medicines against COVID-19 has driven researchers and members of the pharmaceutical, herbal, and related industries to conduct extensive investigations of plant-based products, especially those that have already shown antiviral properties. Even the recent invention of several vaccines has not eliminated doubts about safety and efficacy. As a consequence, many limited, unregulated clinical trials involving conventional mono- and poly-herbal therapies are being conducted in various areas of the world. Of the many clinical trials to establish such agents as credentialed sources of anti-COVID-19 medications, only a few have reached the landmark of completion. In this review, we have highlighted and focused on plant-based anti-COVID-19 clinical trials found in several scientific and authenticated databases. The aim is to allow researchers and innovators to identify promising and prospective anti-COVID-19 agents in clinical trials (either completed or recruiting) to establish them as novel therapies to address this unwanted pandemic.

Keywords: anti-COVID-19, phytomedicine, antiviral, traditional Chinese medicine, Ayurved medicine, phytochemicals, anti-infective, bioactive metabolites

OPEN ACCESS

Edited by:
Banasri Hazra,
Jadavpur University, India

Reviewed by:
Chandrabose Selvaraj,
Alagappa University, India
Jen-Tsung Chen,
National University of Kaohsiung, Taiwan

***Correspondence:**
Md. Moklesur Rahman Sarker
moklesur2002@yahoo.com
dr.moklesur2014@gmail.com
prof.moklesur@sub.edu.bd
Isa Naina Mohamed
isanaina@ppukm.ukm.edu.my

†***ORCID:***
Safaet alam
orcid.org/0000-0002-1831-2278
Md. Moklesur Rahman Sarker
orcid.org/0000-0001-9795-0608
Chao Zhao
orcid.org/0000-0003-1096-632X
Jin-Rong Zhou
orcid.org/0000-0002-6745-9495
Isa Naina Mohamed
orcid.org/0000-0001-8891-2423

Specialty section:
This article was submitted to Ethnopharmacology, a section of the journal Frontiers in Pharmacology

Received: *23 February 2021*
Accepted: *06 May 2021*
Published: *28 May 2021*

Citation:
Alam S, Sarker MMR, Afrin S, Richi FT, Zhao C, Zhou J-R and Mohamed IN (2021) Traditional Herbal Medicines, Bioactive Metabolites, and Plant Products Against COVID-19: Update on Clinical Trials and Mechanism of Actions. Front. Pharmacol. 12:671498. doi: 10.3389/fphar.2021.671498

INTRODUCTION

Coronavirus disease 2019 (COVID-19), caused by a newly identified strain of coronavirus, came under scrutiny in early December 2019 after an outbreak of pneumonia appeared in the city of Wuhan, Hubei Province, Central China (Abd El-Aziz and Stockand 2020; Li et al., 2020; Ludwig and Zarbock, 2020). Severe acute respiratory syndrome coronavirus (SARS-CoV) in 2002 and Middle East Respiratory Syndrome Corona Virus (MERS-CoV) in 2012 imposing critical menaces to humankind. Now, coronavirus has registered its third appearance in 2019 as a novel strain of coronavirus, SARS-CoV-2 which is extremely pathogenic and denominated as SARS-CoV-2 (Ludwig and Zarbock, 2020). SARS-CoV-2 has spread very quickly in several countries, with 109, 594, 835 confirmed cases of infection and about 2,424,060 deaths worldwide as of February 18, 2021, according to the WHO Coronavirus disease (COVID-19) Dashboard (Lai et al., 2020; Li et al., 2020; WHO, 2021). The WHO Director-General announced the COVID-19 epidemic to be a public health emergency of global significance on January 30, 2020. on February 11, 2020, the epidemic of the 2019-novel coronavirus disease (2019-nCoV) was given a new label. This was followed by the announcement of the COVID-19 outbreak as a global pandemic in March 2020 (Abd El-Aziz and Stockand, 2020; Guo et al., 2020; Ludwig and Zarbock, 2020). SARS-CoV-2 is a beta-coronavirus with enveloped and non-segmented positive-sense RNA (Guo et al., 2020). Like SARS-CoV, it uses the same receptor, angiotensin-converting enzyme 2 (ACE2) to infect humans, primarily through the respiratory system (Guo et al., 2020; Ludwig and Zarbock, 2020). Four essential structural proteins have been are identified as major drug targets in the virus: the glycoprotein of the surface spike (S), the membrane (M) protein, the glycoprotein of the small envelope (E), and the nucleocapsid (N) (Ludwig and Zarbock, 2020; Sarkar et al., 2020). Thus, finding effective and reliable therapeutic options for SARS-CoV-2 has become an unparalleled concern for researchers (Sarkar et al., 2020). Plant products may a wonderful gateway to the discovery and development of anti-COVID-19 therapeutics (**Figure 1**).

People across the world, especially from Asian regions like India, China and Japan, and some African nations have used plants as medicaments since the ancient era (Hoareau and DaSilva, 1999). Folkloric use of these plants among tribal people is mostly because of their profound availability and comparatively low cost (Jahan and Ahmet, 2020). Even in the modern era, plants are still very promising therapeutic sources to treat complications like pain, oxidative stress, cancer, diarrhea, depression, fever, and thrombosis, along with infectious diseases. This gives us hope that drugs can be developed to exert anti-COVID-19 efficacy from phyto wellsprings through several mechanism of actions (**Figure 2**) (Andrighetti-Fröhner et al., 2005; Alam et al., 2020; Jahan and Ahmet, 2020; Yang et al., 2020; Emon et al., 2021). The secondary metabolites alkaloids, flavonoids, polyphenols, tannins, lignins, coumarins, terpenoids, and stilbenes from medicinal plants are claimed to be efficacious in ameliorating infections from pathogenic microorganisms owing to its ability to arrest viral protein and enzymatic activities by binding with them, preventing viral penetration into and replication in the host cells (McCutcheon et al., 1995; Semple et al., 1998; Jahan and Ahmet, 2020). Consequently, several reports have suggested the possibility of inhibitory actions of plant-derived bioactive compounds against this novel strain of coronavirus, SARS-CoV-2 (Jahan and Ahmet, 2020).

Herbal medicines have also helped to mitigate the effects of contagious diseases like SARS-CoV. Evidence reinforces the view that herbal medicine may well be efficacious in managing and reducing the risk of COVID-19 as well. The National Health Commission of China has authorized the use of herbal medicine as an alternative remedy for COVID-19 in conjunction with Western medicine, and has released several recommendations on herbal therapy (Ang et al., 2020). Many doctors and researchers have indeed begun to use herbal medicines in human trials against SARS-CoV-2. Since many botanical drugs show antiviral efficacy, the use of herbal remedies for therapeutic purposes should not be underestimated. Currently, well-known herbal medicines with antiviral function are being used as supplementary treatments to suppress SARS-CoV-2 outbreaks, since conventional treatments are still not well flourished (Panyod et al., 2020). Traditional Chinese medicines (TCM) also have a rich history and many years of experience in the treatment and regulation of communicable diseases. They act by optimizing body immunity to pathogenic factors, balancing the immune response, reducing hyper-inflammatory states, and fostering body repair. Earlier TCM therapies have been found to prevent diseases from progressing to risky and critical conditions, which also has had efficacy in reducing the mortality rate. Giving new prospects for COVID-19 treatment, a set of current clinical findings have shown that TCM can play an important role in the treatment and prevention of COVID-19 (Ren et al., 2020). Ayurveda, which is of Indian origin, is another classical medical philosophy. It puts greater prominence on building body strength and the power of the mind. For respiratory disorders, different treatment options such as steam inhalation, immunomodulators, herbal infusions, and gargling hot water are used in Ayurveda, which also gives us hope in this pandemic situation (Golechha, 2020).

In the absence of specific evidence-based therapy against SARS-CoV-2, some researchers have shifted toward plant-based therapies, as many drugs are plant materials or their derivatives (Silveira et al., 2020). Despite the development of vaccines in recent days, extensive multi-site clinical studies are still required to ensure actual efficacy and safety (Silveira et al., 2020). Thus, notable importance is given to the discovery of potential anti-COVID-19 natural products and herbal medicines as records of plant-based therapeutics displayed promising efficacy against several viruses by strengthening the immune system (Huang J. et al., 2020; Zhang et al., 2020).

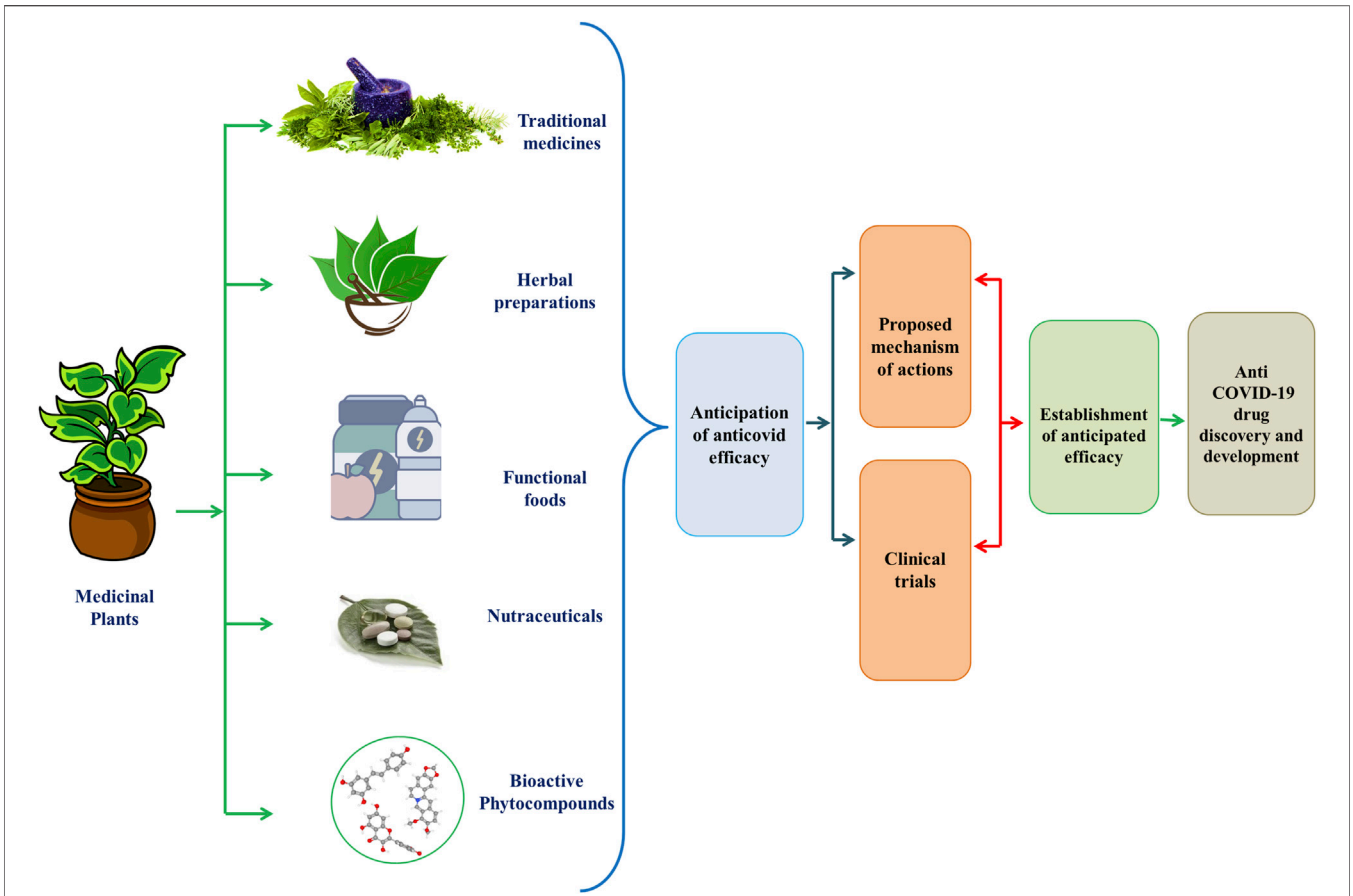

FIGURE 1 | Graphical Abstract of Phytomedicines/Herbal Medicines/Bioactive compounds/Functional Foods/Nutraceuticals for the development of anti-COVID-19 therapies.

Thus, in this study, we report on clinical studies with completed and/or recruiting status that are exploring the efficacy and safety of traditional medicines, isolated compounds, functional foods, nutraceuticals, herbal preparations, and other plant-based products like those used in Chinese medicines and Ayurved, used against SARS-CoV-2. The aim of those studies is to facilitate the use of such materials as remedial and preventive therapies against COVID-19 and to draw the attention of drug developers in this field while new synthetic drugs are still under investigation and have not provided satisfactory results (Panyod et al., 2020).

Article Search Strategy and Methodology

To summarize the findings regarding plant-based products and traditional medicines with completed and/or recruiting clinical trial status; a literature search was conducted using PubMed, Web of Science, Scopus, ScienceDirect, Wiley Online Library, Google Scholar, and CNKI Scholar databases. There was also a search for clinical trials on the ClinicalTrials.gov website (https://www.clinicaltrials.gov/) because of its authenticity. The keywords used in the searches included5 "COVID-19," "SARS-CoV-2," "phytomedicines," "bioactive compounds," "Ayurved medicine," "traditional Chinese medicine," "herbal medicine," "anti-COVID-19," "plant-based medicine" and "clinical trials". Only articles reporting completed and/or recruiting clinical studies and/or mechanisms of actions were included in the final review. There were 475 papers and clinical trials initially identified. After eliminating titles and abstracts related to clinical trials and/or mechanisms of action, 140 unique articles and clinical trials were identified that met the criteria and purpose of this review (**Figure 3**).

Completed Clinical Trials of Phyto-Based Promising Preparations (Bioactive Metabolites/Traditional Medicines/Plant Extracts/Nutraceuticals/Functional Foods/ Chinese Medicines/Ayurved Medicines/ Plant Based Other Preparations)

Clinical Studies of Bioactive Metabolites to Treat COVID-19

Colchicine

Colchicine is a lipid-soluble, tricyclic alkaloid with bioavailability that ranges from 24 to 88% and a long terminal half-life ranging

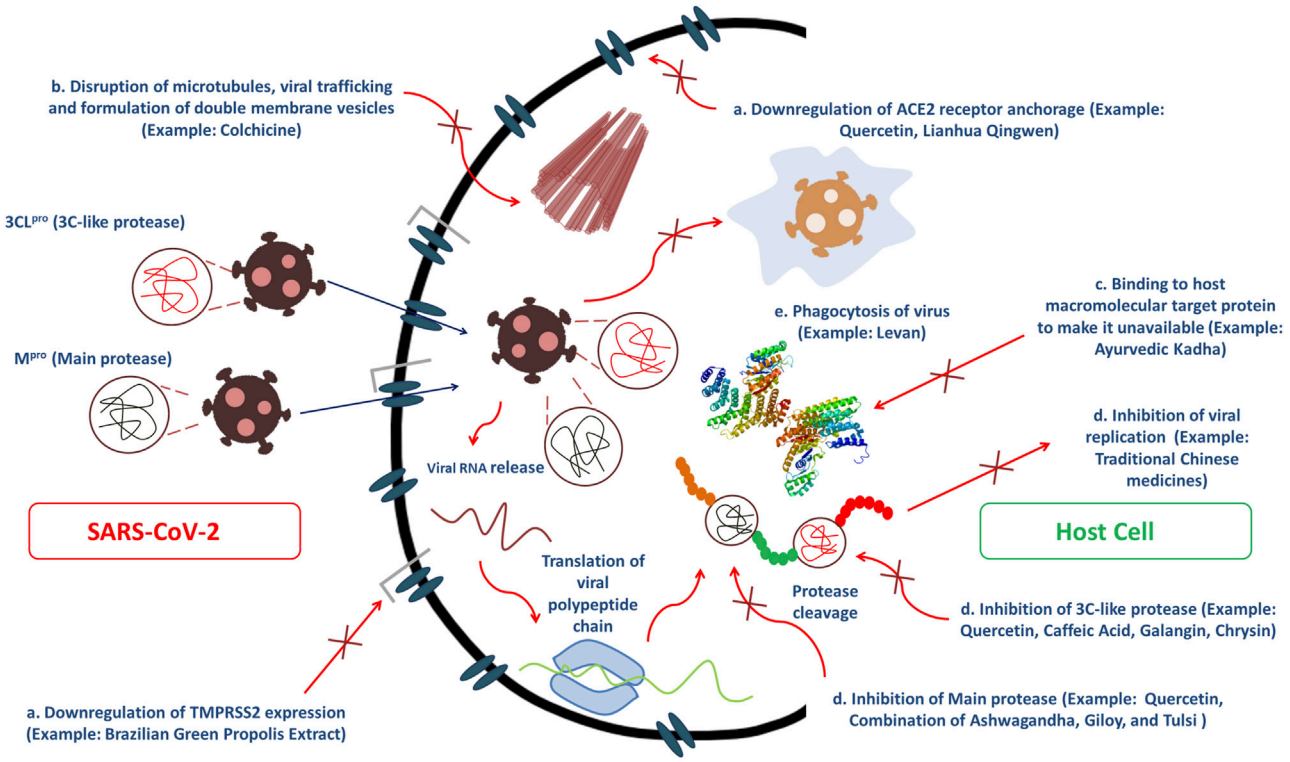

FIGURE 2 | Several modes of bioactive phytoconstituents and traditional herbal medicines to exert anti-COVID-19 efficacy including **(A)** inhibition of main protease and 3C-like protease, **(B)** Disruption of microtubules, viral trafficking and formulation of double membrane vesicles, **(C)** Binding affinity toward host macromolecular target protein to make it unavailable and **(D)** Downregulation of ACE2 receptor anchorage and TMPRSS2 expression which ultimately causes inhibition of viral replication.

from 20 to 40 h (Slobodnick et al., 2015). While the therapeutic activities of colchicine have been known for centuries, the medication was first approved by the United States Food and Drug Administration (FDA) in 2009 (Slobodnick et al., 2015). Even before FDA approval, researchers have worked to expand the spectrum of clinical uses of colchicine from gout and Mediterranean family fever (Slobodnick et al., 2015). Besides, colchicine is also being tested against COVID-19 infection because of its ability to interfere with the inflammatory immune response. For instance, it inhibits the chemotaxis of inflammatory leukocytes particularly neutrophils and monocytes. Then it also compromises their adhesion to endothelial cells by inhibiting the expression of the adhesion molecule E-selectin, consequently preventing them from migrating to inflamed tissue. The plant metabolites have also been associated with a reduction in the production of superoxide free radicals, a decline in tumor necrosis factor and the deactivation of the NLRP3 inflammasome (Montealegre-Gómez et al., 2020; Schlesinger et al., 2020). In particular, colchicine tends to reduce the release of cytokines to manage inflammatory activity (Di Lorenzo et al., 2020).

By arresting SARS-CoV-2 replication through disrupting microtubules, which are climacteric for viral trafficking and the formation of double-membrane vesicles, colchicine could be efficacious against SARS-CoV-2 infection (Perricone et al., 2020). Colchicine is a microtubule disassembling agent since it inhibits the polymerization of tubulin protein, which has a deleterious effect on microtubule polymerization (Montealegre-Gómez et al., 2020). When colchicine binds to β-tubulin subunit due to its strong affinity, the αβ-tubulin heterodimeric subunits lose their straight conformation, culminating in curved tubulin heterodimers as a consequence of which a microtubule polymer with a different morphology emerges (Montealegre-Gómez et al., 2020; Schlesinger et al., 2020). As the cytoskeleton's most essential element is microtubules, colchicine interferes with several cellular functions which are greatly conditioned upon cytoskeleton (Montealegre-Gómez et al., 2020). It explains the antiviral efficacy of colchicine as some viruses, particularly Coronaviruses, rely on microtubules and the cytoskeleton for their entry into the cell, replication and transcription of the viral genome. As per hypothesis colchicine can prevent coronavirus from entering the cell because entry requires the spike protein to interact with cytoskeletal proteins, specifically tubulin. Colchicine can further interfere with coronavirus replication, since microtubules are critical for the development of double-membrane vesicles in affected cells, as well as the transfer and assembly of spike proteins into virions, all of which are key steps in the viral replication (Schlesinger et al., 2020).

The use of 0.5 mg of colchicine per day during the early infection stage (phase 1) of COVID-19 is appropriate because the host has sufficient immunity and it will prevent the disease from progressing to phase 2 and/or 3. But in the pulmonary phase

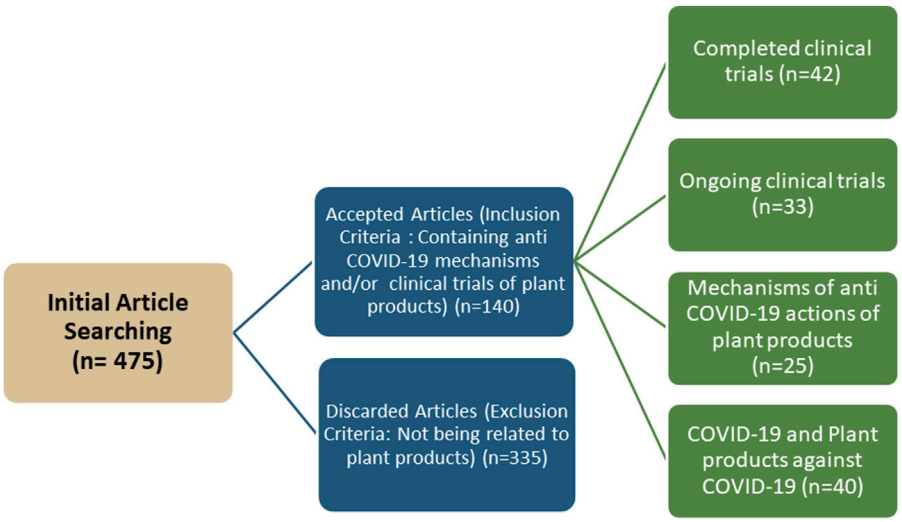

FIGURE 3 | Flowchart for article search, screening and selection in literature review.

(phase 2), it would be reasonable to use 0.5 mg of colchicine (bid) as the patient's immune system has become weakened. The most critical phase is 3, which is characterized by cytokine storms that culminate in a systemic hyper inflammatory condition that can lead to multiple organ failure and ultimately, death in the patient. Attempting to control Cytokine Storms would be feasible with 0.5 mg of colchicine (qd or bid) in monotherapy or with glucocorticoids (dexamethasone) as a combination therapy (Vitiello et al., 2021).

A phase 3 randomized, double-blind, placebo-controlled clinical trial was conducted on colchicine to evaluate its candidacy for COVID-19 treatment. The triple masking (participant, care provider, and investigator) approach was coordinated by the Montreal Heart Institute (MHI) in Canada, South Africa, South America, Europe, and the United States of America. Initially, 6,000 patients who were COVID-19 positive in terms of nasopharyngeal PCR test were recruited in the clinical trial for the assessment of the effectiveness of colchicine compared to placebo (colchicine group: placebo group allocation ratio 1:1; half patients would receive colchicine while the rest half would receive placebo) for one month (NCT04322682, 2020; Montreal Heart Institute, 2020). From the recruitment, 4506 COVID-19 patients finally participated in the trial. Colchicine was given to patients (n = 2,253) at risk of complications as soon as the diagnosis of SARS-CoV-2 infection was confirmed by PCR (at the initial stage of COVID-19), which lowered the risk of development of a severe form of the disease followed by abatement of the incidence of hospitalizations compared to placebo (n = 2,253). In this contact-less COLCORONA trial (ClinicalTrials.gov Identifier: NCT04322682), patients infected with SARS-CoV-2 participated who were at least 40 years old and of either sex. They had been diagnosed with COVID-19 infection within the last day. Each patient in the treatment group received 0.5 mg colchicine orally twice daily as a primary treatment; for the first 3 days, followed by one dose daily for the next 27 days. Similarly, the placebo group received placebo tablets at the same dose and same pattern like the colchicine group. Patients who were hospitalized or under emergency consideration of being hospitalized were kept out of this trial. The trial was conducted only among patients who were staying at home (NCT04322682, 2020; Montreal Heart Institute, 2020). The outcomes revealed that colchicine alleviated the risk of death and hospitalization 21% more in the treatment group than in the placebo group. Another promising outcome of this statistically significant clinical trial was a decline in hospitalizations of 25%, the use of mechanical ventilation by 50%, and mortality by 44% among 4,159 patients who were tested positive for corona infection in nasopharyngeal PCR tests. These outcomes were accredited to colchicine as a promising oral drug for treating coronavirus-infected non-hospitalized patients (Montreal Heart Institute, 2020).

Quercetin

Quercetin comes from the Latin word "Quercetum" meaning oak forest. It belongs to the class of flavonols, and it cannot be formed in the human psyche (Lakhanpal and Rai, 2007). Quercetin is chemically 3,3′,4′5,7-pentahydroxyflavone. It is widely available in many fruits, leaves, seeds, and grains, though it generally couples with residual sugars to form quercetin glycosides (Li et al., 2016). Researchers have found that supplementation with quercetin can facilitate anti-inflammatory, antioxidant, anti-viral, and immuno-protective activities (Uchide and Toyoda, 2011;Colunga Biancatelli et al., 2020). Because of its auspicious antiviral efficacy in inhibiting polymerases, proteases, and reverse transcriptase; suppressing DNA gyrase; and binding viral capsid proteins, quercetin has been subjected to many models of viral infection (Debiaggi et al., 1990; Cushine and Lamb, 2005). Theoretically, Quercetin can be a prominent antiviral agent as it inhibits 3-chymotrypsin-like

protease (3CLpro) and papain-like protease (PLpro), which are the main druggable targets of SARS-CoV-2. In addition, quercetin has been one of the best performing ligands for the S protein: ACE2 receptor interface in structure-based drug discovery. As a consequence, it can restrict viral identification at the host cell surface and/or interrupt host-virus interactions at the receptor level and its subsequent entry into the cell (Derosa et al., 2020).

A randomized clinical trial was conducted from March 20, 2020, to July 31, 2020, on quercetin to evaluate its effectiveness (both prophylaxis and treatment) against SARS-CoV-2 as a primary treatment. It was an open-label masking approach that was coordinated for 3 months. In this randomized trial (ClinicalTrials.gov Identifier: NCT04377789) 447 participants were categorized as a no intervention (no quercetin group), a quercetin prophylaxis group, and a quercetin treatment group. Those in the quercetin prophylaxis group with no history of COVID-19 infection were given 500 mg of quercetin daily. The members of the quercetin treatment group had confirmed cases of COVID-19 and they were provided with 1,000 mg quercetin daily. Clinical data of the prevalence of COVID-19, standardized mortality rates, and morbidity rates were collected for further analysis as major aims (NCT04377789, 2020). Although the aim of this clinical trial was to evaluate the pervasiveness of quercetin in prophylaxis group and the mortality rate in treatment group (James et al., 2020), to the best of our knowledge no conspicuous outcome has been published so far in any online databases (Saeedi-Boroujeni and Mahmoudian-Sani, 2021).

Clinical Studies of Traditional Chinese medicine (TCM) to Treat COVID-19

Lianhua Qingwen

Lianhua Qingwen (LHQW), a traditional Chinese medicine, is now officially registered in the 2015 edition of Chinese Pharmacopeia (Li et al., 2020; Ling et al., 2020). The LHQW preparation is available as granules, capsule and decoction dosage forms, and was prepared by using 13 components: dried fruit of *Forsythia suspensa* (Thunb.) Vahl (known as 'lian- qiao' in China) [Oleaceae; Forsythiae fructus], dried stem or aerial part of *Ephedra sinica* Stapf from Ephedraceae family (honey-fried Herba Ephedrae which is locally known as 'zhi-ma-huang'), dried flower buds of *Lonicera japonica* Thunb. (locally known as 'jin-yin-hua) [Caprifoliaceae; Lonicerae Japonicae Flos], dried root of *Isatis indigotica* Fortune ex Lindl. (Chinese name 'ban-lan-gen') [Brassicaceae; Isatidis Radix], kernel of *Prunus arminiaca* L. (locally known as 'chao-ku-xing-ren') [Rosaceae; Semen Armeniacae Amarum], dried aerial part of *Pogostemon cablin* (Blanco) Benth. (locally known as 'guang-huo-xiang') [Labiatae; Pogostemonis Herba], dried rhizome and remnants of leaf stems of *Dtyopteris crassirhiaoma* Nakai (locally known as 'mian-ma-guanzhong' [Dryopteridaceae; Dryopteridis Crassirhizomatis Rhizoma], aerial part of *Houttuynia cordata* Thunb. (locally known as 'yu-xing-cao') [Saururaceae; Houttuyniae Herba], dried roots and rhizomes of *Rheum palmatum* L., *Rheum tanguticum* Maxim. ex Balf. and *Rheum officinale* Baill (locally known as 'da-huang') [Polygonaceae; Rhei Radix et Rhizoma], dried root and rhizome of *Glycyrrhiza uralensis* Fisch. (locally known as 'gan-cao') [Fabaceae; Glycyrrhizae Radix et Rhizoma], root and rhizome of *Rhodiola crenulata* (Hook. f. et Thoms.) H. Ohba (locally known as 'hong-jing-tian') [Crassulaceae; Rhodiolae Crenulatae Radix et Rhizoma], mineral agent Gypsum Fibrosum (known as 'shi-gao'), and L-menthol (known as 'bo-he-nao') (Chen et al., 2021; Li et al., 2021).

It displays a wide spectrum of antiviral functions, primarily because of its immunological modulation and inhibitory impact on the replication of the virus, and its inhibitory effect on the release of pro-inflammatory cytokines. Evidence suggests that LHQW has a therapeutic effect on COVID-19 because of its strong binding capacity with M^{pro} and ACE2; which are SARS-CoV-2's therapeutic targets. Thus, it can be proved to be beneficial for treating COVID-19 as a supplementary and synergetic strategy (Li L.-C. et al., 2020; Ling et al., 2020). Twelve representative components were the key constituents of LHQW, and they were evaluated as chemical markers: salidroside, chlorogenic acid, Forsythoside E, crypto-chlorogenic acid, amygdalin, sweroside, hyperin, rutin, Forsythoside A, phillyrin, rhein, and glycyrrhizic acid (Li et al., 2020; Ling et al., 2020). However, a very latest study has been conducted to establish the cause responsible for SARS-CoV-2 inhibition and core basic anti-COVID-19 mechanism of pharmacologically active ingredients of LHQW by Prof. Caisheng Wu and Prof. Yifeng Chai from the School of Pharmacy, Xiamen University. In accordance with their research work, the base of the action of LHQW against COVID-19 resides in pernicious interplay of ACE2 targeted LHQW components with ACE2 and spike (S) protein complex. Basically, by scrutinizing ACE2 bio-chromatographic stationary phase, which was drawn out via analyzing human plasma and urine after multiple administration of LHQW on the basis of HRMS and intelligent non-targeted data mining techniques, 85 components were found. Among them, only some components namely, Glycyrrhizic acid, Amygdalin, Forsythoside A, Forsythoside I, Rhein, Aloe-emodin, Neochlorogenic acid and Prunasin were manifested to have good binding affinity to ACE2 and ultimately the ACE2 inhibition was carried out by forsythoside A, forsythoside I, rhein, neochlorogenic acid and its isomers. Furthermore, computer-aided molecular docking analysis also gave proof that, these components effectively bind with the contact surface of ACE2 and S protein complex; hence, the complex is affected. And it is suspected to be the main reason for LHQW to inhibit SARS-CoV-2 (Chen et al., 2021).

Chinese medicine LHQW and its role as an adjuvant therapy in COVID-19 therapy were clinically analyzed in a retrospective study conducted from January 11 to January 30, 2020. The results were posted in the Chinese Journal of Experimental Formulas. The study was conducted on 21 members of a treatment group who received conventional treatment combined with LHQW granules, 1 bag at a time, 3 times a day. During the trial, the treatment group showed a statistically significant difference ($p < 0.05$) in the rates at which shortness of breath, sputum, fever, and cough symptoms disappeared. In addition, the duration of fever

in the treatment group was 1.5 days shorter than in the control group (Kaitao et al., 2020).

In another study, clinical data of 103 patients from January 1 to January 27, 2020, were collected. The treatment and control groups had 63 and 38 patients, respectively. In the treatment group, symptomatic therapy, conventional treatment (intervention to support nutrition), antiviral and antibacterial drug treatment were paired with LHQW granules for 10-days. LHQW granules were used as adjuvant treatment in this case. The control group received conventional therapy only. The treatment group was significantly better ($p < 0.05$) in terms of the rate of disappearance of fever, cough and fatigue, shortness of breath, and downward trend. However, between the two groups, there was no statistically significant discrepancy in the median duration of fever (Ruibing et al., 2020).

Toujie Quwen

This traditional Chinese medicine may exert antioxidant, antiviral, and anti-inflammatory effects, together with modulating the immune system. Thus, it plays a primary protective role in the lungs, through certain possible bio targets of COVID-19. Toujie Quwen (TJQW) works on EGFR (Estimated Glomerular Filtration Rate), CASP3 (Caspase 3), STAT3 (Signal transducer and activator of transcription 3), ESR1 (Estrogen Receptor 1), FPR2 (Formyl-peptide receptor-2), BCL2L1 (Bcl-2-like protein 1), BDKRB2 (B2 bradykinin receptor), MPO (Myeloperoxidase), and ACE (Angiotensin-converting enzyme) which have been identified as possible therapeutic and core pharmacological targets, most of which have been reported to be implicated in pulmonary inflammation (Huang J. et al., 2020).

Toujie Quwen (TJQW) has been formulated with a focus on utilizing heat-clearing and detoxifying botanical drugs to reduce heat and phlegm, to relax the body parts, to stabilize and retain critical energy, and to remove pathogenic factors along with spleen invigoration and dampness elimination (Huang Y. et al., 2020). TJQW contains 16 components of TCM: dried fruit of *Forsythia suspensa* (Thunb.) Vahl (known as 'lian- qiao' in China) [Oleaceae; Forsythiae fructus], edible tulip which is locally known as 'shan-ci-gu' (Tulipa gesneriana L. from Liliaceae family), *Lonicera japonica* Thunb. (Japanese honeysuckle flower, jin-yin-hua) from Caprifoliaceae family, dried root of the medicinal plant *Scutellariae baicalensis* Georgi (locally known as 'huang-qin') [Lamiaceae; Radix Scutellariae baicalensis], leaves of *Isatis indigotica* Fortune ex Lindl. (Chinese name 'da-qing-ye') [Brassicaceae; Folium Isatidis], dried roots of *Bupleurum chinense* DC. (known as 'chai-hu') [Apiaceae; Bupleurum Radix], *Artemisia apiacea* Hance (known as 'qing-hao') from Compositae family, the cast-off shell of the *Cryptotympana pustulata* Fabricius (known as 'chan-tui') [Cicadidae; Periostracum Cicadae], dried roots of *Peucedanum praeruptorum* Dunn (known as 'qian-hu') [Apiaceae; Radix Peucedani], *Fritillaria cirrhosa* D.Don (known as 'chuan-bei-mu') from Liliaceae family, *Fritillaria thunbergii* Miq. (known as 'zhe-bei-mu') also from Liliaceae family, dried sclerotium of *Wolfiporia cocos* (F.A. Wolf) Ryvarden & Gilb. (an edible medicinal mushroom known as 'fu-ling') [Polyporaceae; Poria cocos], unripe fruit of *Prunus mume* (Siebold) Siebold & Zucc.) (known as 'wu-mei') [Rosaceae; Fructus Mume], dried root of *Scrophularia ningpoensis* Hemsl. (known as 'xuan-shen') [Scrophulariaceae; Radix Scrophulariae], *Astragalus propinquus* Schischkin (known as 'huang-qi') from Fabaceae family, and root of *Pseudostellaria heterophylla* (Miq.) Pax (known as 'tai-zi-shen') [Caryophyllaceae; Radix Pseudostellariae] (Huang J. et al., 2020). The bioactive metabolites in TJQW, such as umbelliprenin, quercetin, kaempferol, luteolin, praeruptorin E, stigmasterol, and oroxylin A, have possible anti-inflammatory and antiviral activities and may be effective against SARS-CoV-2 infection (Huang Y. et al., 2020).

A clinical trial was conducted to evaluate the effectiveness of TJQW granules as an adjuvant therapy in combination with Arbidol against SARS-CoV-2 and the impact on the expression of specific T cells. A total of 73 patients diagnosed with COVID-19 were randomly divided into the treatment group (37 cases) and control group (36 cases). Upregulation of the lymphocyte count and downregulation of C-reactive protein (CRP) and a reduced TCM syndrome score were observed in the treatment group. The discrepancy in results between the treatment and control group was statistically significant ($p < 0.05$). In contrast to the control group, there was a statistically significant increase in the number of CD4+/CD8+ cells in the treatment group (Xiaoxia et al., 2020).

Shufeng Jiedu

In traditional Chinese medicine, Shufeng Jiedu capsule (SFJDC), is often used to cure influenza, and is now suggested for the management of COVID-19 infections (Chen et al., 2020). SFJDC is a popular formulation prepared from—the root and rhizome of *Polygonum cuspidatum* Sieb. et Zucc (known as 'hu-zhang') [Polygonaceae; Polygoni Cuspidati Rhizoma et Radix], dried fruit of *Forsythia suspensa* (Thunb.) Vahl (known as 'lian-qiao') [Oleaceae; Forsythiae Fructus], root of *Isatis indigotica* Fort. (known as 'ban-lan-gen') [Brassicaceae; Isatidis Radix], dried root of *Bupleurum chinense* DC. (known as 'chai-hu') [Apiaceae; Bupleuri Radix], Herba Patriniae which is scientifically known as *Patrinia scabiosaefolia* Link and locally known as 'bai-jiang-cao' from Caprifoliaceae family, 'ma-bian-cao' (*Verbena officinalis* L. from Verbenaceae family), dried roots of *Phragmites communis* Trinius (locally known as 'lu-gen') [Poaceae; Phragmitis Rhizoma], and dried root and rhizome of *Glycyrrhiza uralensis* Fisch. (locally known as 'gan-cao') [Fabaceae; Glycyrrhizae Radix et Rhizoma] (Chen et al., 2020).

To study the effectiveness of SFJDC as an adjuvant therapy together with Arbidol to treat uncomplicated COVID-19, 200 patients were divided into an observation group and a control group of 100 each (Qi et al., 2020). For two weeks, the observation group was given 2.08 g of Shufeng Jiedu capsule and 0.2 g Arbidol three times a day while the control group was given only 0.2 g Arbidol (tid) (Liu et al., 2020; Qi et al., 2020; Sun et al., 2020). Compared to the control group, the chest CT condition, the white blood cell count, and lymphocytes percentage were significantly improved in the observation group ($p < 0.05$). The fevers in the observation group were shorter than in the control group. Also, the observation group's overall success rate was 88%, compared to 75% for the control group (Qi et al., 2020).

Clinical data for 70 patients who were clinically diagnosed with COVID-19 in Bozhou People's Hospital and who received care from January 31, 2020, to February 11, 2020, were compiled and analyzed to determine the efficacy of SFJDC as an adjuvant therapy together with Arbidol Hydrochloride to treat COVID-19 (Qi et al., 2020). Thirty patients received only 0.2 g Arbidol hydrochloride capsules, and the other 40 patients received the combination of two drugs: 2.08 g of Shufeng Jiedu capsule and 0.2 g Arbidol three times a day (Liu et al., 2020; Qi et al., 2020; Sun et al., 2020). The negative conversion time was slightly shorter for the group that received both drugs compared to the other group. Also, the latter group had a statistically significant difference in antipyretic duration, dry cough disappearance period, nasal congestion, runny nose, pharyngeal distress, fatigue, diarrhea, and negative conversion time for the novel coronavirus compared to the former group ($p < 0.05$) (Qu et al., 2020).

Qingfei Touxie Fuzheng Recipe

Qingfei Touxie Fuzheng is a traditional Chinese medicine. Studies suggest that using this recipe in conjunction with Western medicine was more successful for treating COVID-19 than using Western medicine alone. The likely mechanism is the upregulation of antiviral factors and the downregulation of pro-inflammatory factors (Ding et al., 2020).

To examine the therapeutic effectiveness of the Qingfei Touxie Fuzheng recipe as an adjuvant therapy to treat COVID-19, clinical data on 100 patients were collected (Ding et al., 2020). The 51 patients in the treatment group received a course of antiviral and anti-infection-based Western medicine namely recombinant human interferon α1b for injection (5 million U, bid) or ribavirin (0.5 g, bid) along with the Qingfei Touxie Fuzheng recipe (150 mL, bid) and the control group only received aforementioned western medicine (Ding et al., 2020; Liu et al., 2020; Sun et al., 2020). The levels of ESR, CRP, and IL-6 were substantially reduced in the treatment group relative to the control group, and the discrepancy was statistically significant ($p < 0.05$). Also, in alleviating clinical manifestations of fever, cough, expectoration, chest tightness, and shortness of breath; facilitating the absorption of pulmonary lesions; and improving oxygenation, the results for the treatment group were considerably better than those for the control group (Ding et al., 2020).

Other Traditional Chinese Formulations

The following clinical trials were completed, and data were collected from the literature and/or ClinicalTrials.gov but the names of the products were not available:

Clinical data of 67 patients were obtained to examine the effectiveness of combining traditional Chinese and Western medicine in the treatment of non-critical COVID-19 patients receiving traditional Chinese as adjuvant therapy. Of the 67 patients, 18 were in the Western medicine group, and 49 were in the integrated traditional Chinese and Western medicine group (Jia et al., 2020). The former group was given oxygen therapy, antiviral drugs, anti-inflammatory drugs, immunologic agents and other treatment to alleviate symptoms and the latter group was provided TCM decoction and Chinese patent medicine namely Shufeng Jiedu capsule, Lianhua Qingwen granule etc along with aforementioned western medicine (Jia et al., 2020; Ni et al., 2020; Wang et al., 2021). However, some critically ill patients were given anti-inflammatory medicine for immune regulation and supporting therapy of gamma globulin. The latter group was given a decoction of Chinese medicine. In terms of clinical results, the overall trajectory of the disease, antipyretic timeframe, and rate of CT improvement was not statistically different ($p < 0.05$). The latter group's dampness toxin stagnation syndrome and heat toxin blocking lung syndrome were 65.31% and 34.69% respectively. In addition, their stays in the hospital were shorter and they had fewer severe effects. No transformation from mild to chronically ill state occurred in either group during the surveillance period (Jia et al., 2020).

Clinical data from January 15 to February 8, 2020, on 52 patients with COVID-19 were obtained to examine the therapeutic efficacy of combining Chinese and Western medicine to treat SARS-CoV-2 infection in patients receiving conventional Chinese medicine as adjuvant therapy where among the 52 patients, 23 were male and 29 were female (Xia et al., 2020). The Western medicine group was given arbidol, ribavirin, alpha interferon, lopinavir/ritonavir, oseltamivir for treating viral infections as well as to prevent or treat any other viral or secondary infections moxifloxacin, levofloxacin, azithromycin, cephalosporins penicillin drugs were provided. Gamma globulin and methylprednisolone was delivered as a supplementary treatment regime, while the group treated with both Chinese and Western medicine was also given Lianhua Qingwen Granules, Ganlu Xiaodu Dan, Huoxiang Zhengqi Water, different Decoction of Shidu Yufei, Yudu Biaofei, NIaxing Shigan and varying injection of Xuebijing, Phlegm Heat Qing, Shengmai, Shenfu etc (Xia et al., 2020; An et al., 2021). For the latter group, the rate at which accompanying symptoms disappeared and the clinical cure rates were 85.3% and 91.2% respectively. In addition, the duration of clinical symptoms, mean hospital stay, time to return to normal body temperature, and score on the TCM syndrome scale for the latter group were statistically significantly lower compared to the former group (Xia et al., 2020).

In another study, 19 confirmed patients were treated with a combination of traditional Chinese (as an adjuvant) and Western medicine (antiviral and oxygen therapy) and it was reported that the fever, cough, exhaustion, and other symptoms improved substantially following treatment (Zhongqian et al., 2020; Zhou et al., 2020). Hospitalization lasted 16.36 ± 4.95 days, no patient became extremely ill, and the rate of effectiveness of the combination approaches was 100% (Zhongqian et al., 2020).

According to Ruibing et al., 2020, another clinical study was conducted on 103 patients' data were collected between January 1 and January 27, 2020, to determine the efficacy of integrated Chinese and western medicine in patients who received LHQW granules as adjuvant (Ruibing et al., 2020). The treatment group had 63 patients, and the control group had 38. In the former group, symptomatic therapy and medicine to relieve cough and asthma, conventional treatment (intervention to support nutrition), glucocorticoid and antiviral, antibacterial, immunomodulatory drug treatment were paired with LHQW granules for 10-days (Ruibing et al., 2020; Zhou et al., 2020). The

latter group received previously-mentioned conventional therapy only. The treatment group was significantly better in the disappearance rates for fever, cough, and fatigue, and shortness of breath had a downward trend ($p < 0.05$). However, the difference in the median duration of fever was not statistically significant (Ruibing et al., 2020).

In another study, to evaluate the efficacy of conventional Chinese medicine against SARS-CoV-2 as primary therapy, 30 patients diagnosed with COVID-19 in February 2020 were arbitrarily categorized into three groups of 10 cases each. Group A was the placebo group; Group B was handled with conventional Chinese medicine and fumigation; and Group C received traditional Chinese medicine along with fumigation and absorption in conjunction with a rich level of vitamin C. In groups B and C, the degree of recovery from the disease state and the elimination of weakness, coughing, sore throat, and chest tightness were better than in group A. Moreover, the outcomes for group C were better than those of group B (Wang et al., 2020).

Based on a clinical study by Tan et al. (2020), clinical data on 50 hospitalized patients with confirmed and suspected cases of COVID-19 were obtained to examine the therapeutic efficacy of traditional Chinese medicine as an adjuvant therapy in treating pneumonia from the novel coronavirus (Tan et al., 2020). They received discrete TCM syndrome differentiation therapy (Chinese decoction along with antiviral drugs, anti-inflammatory agents, oxygen therapy and glucocorticoid) (Tan et al., 2020; Zhou et al., 2020) and their rates for being clinically cured, effective, or totally effective were 46.00, 52.00, and 98.00% respectively. In addition, fever, sweating, fatigue, discomfort in the body, tightness in the chest, shortness of breath, and other signs also diminished at a greater pace (Tan et al., 2020).

In another study, clinical data on 103 patients from January 27, 2020, to March 1, 2020, were gathered. Of the 103 patients, 51 were in the treatment group and 52 were in the control group. The former group was given a combination of traditional Chinese and Western medicine with the former acting as an adjuvant. The latter group received conventional treatment (antiviral, and anti-inflammatory drugs, oxygen therapy, and glucocorticoid) (Meng et al., 2020; Zhou et al., 2020). Compared to the control group, the absolute value of lymphocytes, albumin content, number of cases of enhanced lung absorption, and cure rate improved significantly, while CRP and the mortality rate declined substantially in the treatment group (Meng et al., 2020).

Besides, in another study, clinical data on 23 hospitalized COVID-19 patients who were 23–72 years old were examined to determine the therapeutic efficacy of a combination of traditional Chinese and Western medicine (antiviral and anti-inflammatory drugs, oxygen therapy and glucocorticoid) with the former acting as an adjuvant to treat SARS-CoV-2. Of the 23 patients, 10 were male and 13 were female (Zhou et al., 2020; Zhu et al., 2020). Clinical symptoms of fever, sputum, chest tightness, and asthma digestive tract symptoms were recorded as 78.3, 26.1, 26.1, and 8.7% respectively. Hematological tests revealed that the overall number of white blood cells was normal. However, 16 patients reported low lymphocytes, and two patients were observed to have an irregular liver function. Triglycerides and cholesterol levels were elevated and CRP was reduced at discharge. Chest CT scans confirmed that there were several shades of ground glass under the pleura. The condition was exacerbated by interstitial thickening. Antiviral, anti-infective, and oxygen inhalation therapies were used to cure all cases. Non-invasive ventilation was provided to only one critical patient. After obtaining the negative results of the nucleic acid screening, all patients were released (Zhu et al., 2020).

These trials of patented traditional Chinese medicines were conducted to ensure safety and efficacy in treating SARS-CoV-2 infection, although the exact formulations or recipes are not publicly available.

Clinical Studies of Ayurvedic Medicine to Treat COVID-19

Ayurvedic Kadha

Ayurvedic medicine and its extracts have been used for a very long time in the prevention and cure of viral maladies. Ayurvedic Kadha is prepared from using several Indian botanical drugs including 'tulsi' (*Ocimum sanctum* L. from Lamiaceae family), 'haldi' (*Curcuma longa* L. from Zingiberaceae family), 'giloy' (*Tinospora cordifolia* (Lour.) Merr. from Menispermaceae family), 'black pepper' (*Piper nigrum* L. belonging to Piperaceae family), 'ginger' (*Zingiber officinale* Roscoe from Zingiberaceae family), 'clove' (*Syzygium aromaticum* (L.) Merr. & L.M.Perry from Myrtaceae family), 'cardamom' (*Elettaria cardamomum* (L.) Maton from Zingiberaceae family), 'lemon' (*Citrus limon* (L.) Osbeck from Rutaceae family) and 'ashwagandha' (*Withania somnifera* (L.) Dunal from Solanaceae family) (Maurya and Sharma, 2020). Preparing Kadha (decoction) for oral intake is a significant Ayurvedic procedure for amplifying the effect of pharmacological agents in botanical drugs. Kadha is an ancient type of medicine made by combining botanical drugs and spices. The Indian government suggested the use of Kadha during the COVID-19 epidemic to enhance immunity and promote healing (Maurya and Sharma, 2020). The Ayurvedic Kadha-based phytochemicals have a strong binding affinity with the various viral and host macromolecular target proteins. This suggests that they can exert antiviral efficacy by regulating viral replication and proliferation in host cells. (Maurya and Sharma, 2020).

An observational study (ClinicalTrials.gov Identifier: NCT04387643) with 52 participants was conducted for the 30 days between March 1, 2020, and April 2, 2020. The aim was to assess the efficacy of Ayurvedic kadha as a primary therapy to protect healthcare workers during the COVID-19 pandemic. After the study period, their physical and psychological health, their ability to cope with distress, and their capacity for self-help were evaluated (NCT04387643, 2020).

Guduchi Ghan Vati

Tinospora cordifolia (Lour.) Merr., locally known as "Guduchi" or "Giloe" is a large, deciduous, and glabrous climbing shrub from the Menispermaceae family. It is available throughout the tropical regions in India and China, and it has a notable history in folkloric use (Upadhyay et al., 2010; Patgiri et al., 2014). An aqueous extract of *T. cordifolia* is used to prepare the popular Ayurvedic formulation,

Guduchi GhanVati, which is listed in the Ayurvedic Pharmacopoeia of India. With a wide spectrum of pharmacological activities, Guduchi Ghan Vati, traditional Indian medicine, is generally prescribed as an immunomodulatory and antioxidant agent (Upadhyay et al., 2010; Patgiri et al., 2014). In recent studies, Guduchi GhanVati was also found to be effective against SARS-CoV-2 (Kumar et al., 2020a; Kumar et al., 2020b).

Clinical data from May 12 to June 15, 2020, was collected on 91 participants between 18 and 75 years of age. The aim was to evaluate the efficacy of Ayurveda (Guduchi GhanVati-extract of *Tinospora cordifolia*) as a primary therapy to manage confirmed COVID-19 patients who were asymptomatic to mildly symptomatic. In this trial (ClinicalTrials.gov: Identifier: NCT04480398), participants were divided into two groups. The Ayurvedic group comprised 40 individuals who were given two tablets (500 mg each) of Guduchi Ghan Vati (extract of *Tinospora cordifolia*) orally twice each day after a meal for 28 days. The control group of 51 individuals was provided with conventional and standard therapy (NCT04480398, 2020). The results showed a reduction of 11.7% in symptoms in the control group after an average of 1.8 days and none developed any exaggerated symptoms in the Ayurveda group. The Ayurvedic group's virologic clearance at day 7 and at day 14 was 97.5% and 100% respectively, while for the control group it was 15.6% and 82.3% respectively. The differences were statistically significant. The average stay in the hospital for the Ayurvedic group was 6.4 days; for the control group, it was 12.8 days (Kumar et al., 2020a; Kumar et al., 2020b).

An open-label single-arm feasibility trial was conducted to assess the efficacy of Guduchi Ghan Vati (an aqueous extract of *Tinospora cordifolia*) as a primary therapy to manage COVID-19 infection in 46 asymptomatic patients. Only 40 patients completed the 14-days trial period. All the patients were provided with two tablets (1,000 mg) 2 times a day for 14 days, but there was no control group. After the treatments, no one showed COVID-19 symptoms. Viral clearance was 32.5% and 95%, on day 3 and day 7, respectively. Data for day 14 revealed all respondents' test reports were negative (Kumar et al., 2020a; Kumar et al., 2020b).

Combination of Ashwagandha, Giloy, and Tulsi

Withania somnifera (L.) Dunal from Solanaceae family (locally known as 'ashwagandha'), *Tinospora cordifolia* (Lour.) Merr. from Menispermaceae family (locally known as 'giloy') and *Ocimum sanctum* L. from Lamiaceae family (locally known as 'tulsi') are notable herbal plants used in the Ayurvedic treatment system. All these immunomodulator plants have displayed promising immunity-boosting efficacy against infection, which has drawn the attention of researchers to assess their anti-COVID-19 activity (Shree et al., 2020). Bioactive metabolites of Ashwagandha, Giloy, and Tulsi were predicted to show prominent efficacy against SARS-CoV-2 infection in recent studies. An in-silico study revealed that this formulation can arrest the main protease (Mpro or 3Clpro) of a novel strain of coronavirus because of phytochemicals like somniferin, isorientin 4′-O-glucoside 2″-O-p-hydroxybenzoate, withanoside V, tinocordiside, somniferine, and vicenin. ADME/T profiling also showed its safety and drug-like activity (Shree et al., 2020).

A community-based participatory study was conducted to evaluate the effectiveness of Ayurveda intervention as supportive care for patients with mild to moderate COVID-19. Patients with severe cases were excluded from this study. In this open-label approach (ClinicalTrials.gov Identifier: NCT04716647), 28 people with confirmed infections with SARS-CoV-2 participated from October 9, 2020, to December 18, 2020. As primary therapy, they were given oral tablets of Ashwagandha, Giloy, and Tulsi. Based on age, weight, and the severity of symptoms, patients were given between 250 mg and 5 g of Ashwagandha, between 500 mg and 1 g of Giloy, and between 500 mg and 1 g of Tulsi. Then clinical recovery time, the number of patients whose nasopharyngeal swab test converted to negative in the study period, and other clinical outcome data were gathered for evaluation (NCT04716647, 2020). The gain from Ayurveda was better for relief of symptoms, so cline recovery within seven days was proposed. Although there was no control group, a statistically significant disparity was found by data triangulation from different normal treatments. The Ayurvedic procedure can have a positive impact, particularly for people suffering from mild to moderate symptoms of COVID-19 (Kulkarni et al., 2021).

Tinospora cordifolia and Piper longum

Tinospora cordifolia (Lour.) Merr. from Menispermaceae family is a plant found in regions of India and China. In traditional Ayurvedic medicine, it is used in the formulation of Guduchi Ghan Vati (Upadhyay et al., 2010; Patgiri et al., 2014). It can also be coadministered with *Piper longum* L. (from Piperaceae family), another popular medicinal plant used in the Ayurvedic system. *P. longum* is locally known as "Pippali" and "Indian Long Pepper." Pippali is a traditional Ayurvedic complementary ingredient that enhances the bioavailability and absorption of the other active components, and *P. longum* itself possesses notable antiviral activity (Pandey et al., 2013; Priya and Kumari, 2017).

A placebo-controlled, randomized trial (ClinicalTrials.gov Identifier: NCT04621903) was conducted from October 8 to October 27, 2020, to evaluate the efficiency and safety of an Ayurvedic combination (Guduchi and Pipli) as a primary treatment for 28 asymptomatic to mildly symptomatic patients who were confirmed patients of COVID-19. The participants were given Guduchi (*Tinospora Cordifolia*; 300 mg) and Pipli (*Piper Longum* 75 mg) twice daily (NCT04621903, 2020). By day 3 after treatment, 71.1% of the patients in the treatment group recovered, and 50% of the placebo group recovered. By day 7, 100% of patients in the treatment group recovered, but only 60% of the control group recovered. The recovery response rate in the treatment group was higher than the control group. The probability of delayed healing process from infection in the treatment group was significantly decreased by 40% (Devpura et al., 2021).

Other Ayurvedic Formulations Without Products/Ingredients Named

An open-label clinical trial (ClinicalTrials.gov Identifier: NCT04345549) was conducted on Ayurveda as a primary

therapy to evaluate its efficacy as supportive care in self-management for flu-like symptoms of COVID-19 for people in self-isolation. In total 18 patients participated from February 26, 2020, to March 30, 2020. People with known hypersensitivity to any Ayurveda botanical drugs were excluded from the study. All the participants were instructed to self-isolate for 7 days and to practice grooming and self-care according to the prescribed directives. Participants were also recommended to use plants, lifestyle, and yoga to implement Ayurveda therapy. In line with Ayurveda, individuals were recommended to gargle with warm water, practice steam inhalation, take paracetamol to control body temperature, and drink plenty of fluids with ginger, lemon, turmeric, or honey, and relax both body and mind. They were also advised to practice yoga breathing. After the treatment, data on the duration of fever and the score for the severity of influenza symptoms were collected and analyzed to determine the efficacy of this approach as supportive care (NCT04345549, 2020).

A non-randomized single-blinded trial (ClinicalTrials.gov Identifier: NCT04351542) was conducted on Ayurveda as a primary therapy and supportive care for flu-like illness during the COVID-19 pandemic. This trial started on March 6, 2020, with 32 participants and ended primarily on April 6, 2020. People were divided into an Ayurveda care group and an active comparator (usual care) group. Participants from the former group were given individualized Ayurveda treatment, and usual care was recommended for the latter group. After the study, the duration of the fever, the score for the severity of symptoms, and reported improvement of patients were observed and further analyzed and compared to determine the suitability of Ayurveda as supportive care for flu-like symptoms during COVID-19 (NCT04351542, 2020).

The Ayurvedic medicine was conducted in the hope of ensuring safety and efficacy against COVID-19 infection, but the precise intervention was not disclosed by the respective researcher groups.

Clinical Studies of Herbal Medicine and Functional Foods to Treat COVID-19

Fuzheng Huayu Capsule/Tablet

The Fuzheng Huayu capsule or tablet is a patented Chinese herbal medicine formulated after decades of laboratory and clinical study by the Institute of Liver disease, Shanghai University of Traditional Chinese Medicine. The Shanghai Modern Pharmaceutical Company developed composite capsules that are prescribed for treating a wide spectrum of hepatic disorders (Shi et al., 2020; Wu et al., 2020). The herbal extraction combines six Chinese herbal medicines: fruits of *Schisandra chinensis* (Turcz.) Baill. (known as 'wu-wei-zi') [Schisandraceae; Fructus Schisandra chinensis], *Paecilomyces hepiali* Chen & Dai from Trichocomaceae family (locally known as 'chong-cao'), root and rhizome of *Salviae miltiorrhizae* Bunge (Chinese name 'dan-shen') [Lamiaceae; Salviae Miltiorrhizae Radix et Rhizoma], *Pinus armandii* Franch. from Pinaceae family (known as 'song-hua-feng'), seed of *Prunus persica* (L.) Batsch (known as 'tao-ren') [Rosaceae; Semen Persicae], and *Gynostemma pentaphyllum* (Thunb.) Makino from Cucurbitaceae family (known as 'jiao-gu-lan') (Shi et al., 2020; Wu et al., 2020). In treating chronic liver disorders, an FZHY capsule can ameliorate the complications caused by viral hepatitis B and C, which gives a ray of hope about its antiviral efficacy (Chen et al., 2019).

A phase 4 case-controlled, non-randomized, open-label clinical trial was conducted from February 1, 2020, to April 15, 2020, to assess the impact of Fuzheng Huayu as a primary therapy on lung inflammation in 66 patients with severe SARS-CoV-2 pneumonia and to diminish the advancing rate to severe type. In this trial (ClinicalTrials.gov Identifier: NCT04645407), 66 persons were divided into two groups: those that received Fuzheng Huayu and the control group. For 14 days, those in the experimental group were given Fuzheng Huayu tablets 0.4 g/tablet, 1.6 g/time, 3 times/day after meals, in addition to conventional therapy. The control group was given only conventional therapy. The patients were monitored for improvement in chest CT, remission or progression of critical illness, the clinical remission of respiratory symptoms. They were given routine blood tests as well as tests of CRP level, procalcitonin level, and oxygen saturation, and the data were analyzed to find primary and secondary outcomes (NCT04645407, 2020).

Cretan IAMA

Since the Bronze Age, the island of Crete has been noted for its use of herbal medicine. Previous studies have revealed the antioxidant function of certain plants from Crete. In addition, recent research on Cretan herbal wellsprings done by the University of Crete in collaboration with the University of Leiden, Netherlands, has led to a new formula (Lionis, 2015). Olvos Science SA has recently introduced an over-the-counter drug in Greece produced as soft-gel capsules (Lionis, 2015). "Cretan IAMA" is a combination of essential oils extracted from three aromatic botanical drugs from Lamiaceae family: Coridothymus capitatus (*Thymus capitatus* (L.) Hoffmanns. & Link, *Salvia fruticosa* Mill., and *Origanum dictamnus* L. in a fixed ratio and dissolved in extra virgin oil. This formulation acts synergistically to promote the natural increase in the body's defense mechanism (Lionis, 2015).

A phase 3, single-arm, open-label small interventional proof-of-concept (POC) study (ClinicalTrials.gov Identifier: NCT04705753) was conducted on Cretan IAMA (CAPeo) to test its therapeutic efficacy as a primary treatment for resolving the frequency and duration of symptoms and their intensity in patients. The study was conducted from April 1, 2020, to October 15, 2020. Twenty participants received Cretan IAMA soft gels at 1 ml per day as a dietary supplement (NCT04705753, 2020).

Nigella sativa and Honey

Nigella sativa L. is a popular herbal plant with ethnomedicinal importance from the Ranunculaceae family. It is commonly known as "Black Cumin" or by its local name, "Kalojira" (Forouzanfar et al., 2014). *N. sativa* has been traditionally used for over 2000 years in Middle Eastern folklore medicines and traditional Arabian herbal medicines (Forouzanfar et al., 2014). In previous studies, researchers discovered its anti-COVID-19 efficacy by decreasing SARS-CoV replication in cell cultures (Ulasli et al., 2014). Moreover, an *in silico* study revealed that notable compounds like thymoquinone α-hederin and nigelledine possess a greater affinity for multiple

SARS-CoV-2 enzymes and proteins. The energy complex scores of those compounds are even higher than those for hydroxychloroquine, chloroquine, and Favipiravir, which have shown some anti-SARS-CoV-2 efficacy (Ashraf et al., 2020). Besides, because of the overlapping pharmacological profiles of honey and *N. sativa*, it is believed that this combination can reduce the severity of disease and control viral replication. Honey mixed with *N. sativa* has already shown remarkable potential for treating several other diseases. This gives researchers a ray of hope to use this combination in the current pandemic (Ameen et al., 2011; Bhatti et al., 2016; Moghimipour et al., 2019)

Bacillus subtilis, isolated from honey, produces a very promising antiviral component known as levan (β-2,6-fructan) that functions against many pathogenic respiratory RNA viruses. By facilitating the aggregation of cells and viruses, levan amplifies the phagocytosis procedure. Another proposed mechanism of antiviral activity in honey is through the nitric oxide pathway. Studies have shown that honey raised the concentration of NO at the cellular level. In turn, this neurotransmitter shuts off viral protease enzymes by blocking their capability for viral polyprotein cleavage. As a consequence, viral RNA synthesis is occluded at a very early stage. Then, viral replication, the accumulation of viral protein, and the release of the virus from infected cells are hampered sequentially. Whether NO can express antiviral activity against SARS-CoV-2 or simply prevent the progression of the disease is still uncertain. Caffeic acid, phenethyl ester (CAPE), galangin, and chrysin are natural phenolic chemical compounds from honey. They have a strong ability to inhibit the viral 3-chymotrypsin-like cysteine protease (3CLpro), the enzyme responsible for the cleavage of the viral polyprotein pp1a and pp1ab. Then, nonstructural proteins (nsps) and RNA-dependent RNA polymerase (RdRp) cannot form as pp1a and pp1ab. The polyprotein cleavage process is interrupted, which ensures that replication of structural protein RNA; viral RNA synthesis, and virion assembly do not occur. In that way, SARS-CoV-2 replication will eventually be halted (Al-Hatamleh et al., 2020).

The molecular docking system also found that nigellidine and α-hederin of *N. sativa* might be active SARS-CoV-2 inhibitor compounds because they exhibit the most binding affinity with SARS-CoV-2 molecular targets 6LU7 and 2GTB, which are protease and peptidase respectively. They might also induce an antiviral cellular response by raising the number of CD4 cells (Ulasli et al., 2014; Koshak and Koshak, 2020).

A phase 3 randomized, placebo-controlled, open-label, add-on, cohort, adaptive, investigator-initiated interventional trial was conducted from April 30, 2020, to August 30, 2020 on honey and *Nigella sativa* to evaluate their role as a co-therapy in treating COVID-19. A triple masking approach ensures that the care provider, the investigator, and the outcomes assessor do not know who is receiving the drug and who is receiving a placebo. In this study (ClinicalTrials.gov Identifier: NCT04347382), 313 confirmed COVID-19 patients were divided into an experimental group and a placebo comparator group (who received standard medical care). The former group was given 80 mg per kg per day of *N. sativa* seed as powder which was ground and put into a capsule and natural honey 1 gm per kg per day for a maximum of 14 days. The latter group was given an empty capsule with 250 ml of distilled water and conventional therapy, which includes supportive medical care and antibacterial or antiviral if advised. After the treatment, clinical data for the two groups were collected and analyzed. They included the number of days between the last positive result for a COVID-19 PCR test and a negative result, the severity of symptom progression, the duration of hospital stays, clinical grade status, the 30-days mortality rate, duration of fever, and oxygen saturation at room air (NCT04347382, 2020). A lower clinical score was observed in the honey and nigella group. By day 6, 63.6% of patients with moderate COVID-19 infection resumed their normal activity, while only 28% of severe cases could do so. Alleviation of disease symptoms, substantially earlier viral clearance, and a considerable reduction in mortality among severe patients were observed in the honey and nigella group compared to the control group. No adverse effects from honey and Nigella sativa were observed in the treatment group (Ashraf et al., 2020)

Brazilian Green Propolis Extract (EPP-AF)

Propolis is a resinous component from plant exudates created by honey bees. It's been used in traditional herbal medicine since ancient times and is frequently used as a supplement for the immune system and healthcare. A few categories of propolis, such as Brazilian green propolis, are thoroughly appreciated for their therapeutic potential. Propolis is produced primarily by bees from substances that they gather from particular plants, such as *Baccharis dracunculifolia* DC. from Asteraceae family (Berretta et al., 2020).

Depending on the plant species in each location, the formulation of propolis differs. Some of the most typical propolis constituents are myricetin, caffeic acid phenethyl ester, hesperetin and pinocembrin, hesperetin, limonin, quercetin, and kaempferol (Berretta et al., 2020). The extract of propolis and some of its components help to reduce viral replication. They also exert inhibitory effects on the signaling pathways of ACE2, TMPRSS2, and PAK1 that are very relevant targets of the SARS-CoV-2. By reducing TMPRSS2 expression and ACE2 anchorage, propolis hampered the entry of the virus into the cell (Berretta et al., 2020). In the understanding of the existing urgency triggered by the COVID-19 pandemic and insufficient therapeutic possibilities, propolis was proposed as an effective, convenient, and possibly relevant therapeutic alternative, easily accessible as an organic nutrient and dietary supplement (Berretta et al., 2020).

A phase 3, randomized, open, pilot clinical study (ClinicalTrials.gov Identifier: NCT04480593) was conducted on Brazilian green propolis extract (EPP-AF) with hospitalized COVID-19 patients. It ran from June 2, 2020, to August 30, 2020, and its aim was to evaluate the candidacy of this extract as an adjuvant therapy option along with standard treatment including antibiotics or antivirals, vasopressor support, corticosteroids etc. against SARS-CoV-2 infection. In this single (outcomes-assessor) masking approach, 120 patients were randomly separated into three categories. The control group received standard conventional treatment. The first experimental group received 400 mg per day green propolis extract (EPP-AF) and conventional treatment. A second experimental group received 800 mg per day EPP-AF and conventional treatment. After the treatment, oxygen therapy dependency time, hospitalization time, the occurrence of side effects, the rate and severity of acute kidney injury, the need for renal replacement therapy, the need for vasopressor and ICU, invasive oxygenation

TABLE 1 | Ongoing clinical trials of several plants, functional foods, and plant based products including bioactive phytocompounds, traditional medicines, nutraceuticals and similar other preparations against SARS-CoV-2 infection.

No	Drugs	Therapy type	Phase	Participant numbers	Intervention	Outcomes	ClinicalTrials.Gov Identifier	References
1	Fuzheng Huayu Tablet	Primary therapy	Phase II	160 participants	0.4 g/tablet, 1.6 g/time, 3 times/day	The improvement proportion of pulmonary fibrosis, Blood oxygen saturation, Clinical symptom score, The 6-min walk distance	NCT04279197	NCT04279197 (2020)
2	Natural honey	Adjuvant therapy	Phase III	1,000 participants	Natural honey supplement 1 gm/kg/day divided into 2–3 doses for 14 days	Rate of recovery from positive to negative swaps, fever to normal temperature in days, Resolution of lung inflammation in CT or X ray, 30 days mortality rate, number of days till reaching negative swab results	NCT04323345	NCT04323345 (2020)
3	Anluohuaxian	Primary therapy	Not applicable	750 participants	Six grams each time, twice a day	Changes in high-resolution computer tomography of the lung, Change in 6-min walking distance, Changes in vital capacity of the lung	NCT04334265	NCT04334265 (2020)
4	Escin	Adjuvant therapy	Phase II, Phase III	120 participants	Oral admisntration of standard therapy and Escin tablet for 12 days (40 mg thrice a day)	Determination of mortality rate, the differences in oxygen intake methods, time of hospitalization (days), time of hospitalization in intensive care units, pulmonary function	NCT04322344	NCT04322344 (2020)
5	*Caesalpinia spinosa* (Molina) Kuntze extract (P2Et) (Fabaceae)	Adjuvant therapy	Phase II, Phase III	100 participants	P2Et active extract capsule equivalent to 250 mg of P2Et every 12 h for 14 days + Standard care	The efficacy of P2Et in reducing the length of hospital stay of patients with clinical suspicion or confirmed case of COVID-19	NCT04410510	NCT04410510 (2020)
6	*Nigella sativa* L. (Ranunculaceae)	Primary therapy	Phase II	200 participants	Nigella sativa Black seed oil in 500 mg capsules	Determination of proportion of patients who are clinically recovered, normalization of chest radiograph, rate of complications	NCT04401202	NCT04401202 (2020)
7	Essential oil	Primary therapy	Not applicable	65 participants	Essential oil Blend 5 drops of on a tester strip	Determination of State Trait Anxiety Scale (STAI-S) at 15 min	NCT04495842	NCT04495842 (2020)
8	Plant polyphenol	Primary therapy	Phase II	200 participants	Both plant polyphenols and placebo is introduced individually along with vitamin D3 10,000 IU	Reduction rate of hospitalization at 21 days from enrollment	NCT04400890	NCT04400890 (2020)
9	Silymarin	Adjuvant therapy	Phase III	50 participants	Silymarin oral 420 mg/day in 3 divided doses	Time to clinical improvement, clinical outcome, duration of mechanical ventilation, hospitalization, virologic response	NCT04394208	NCT04394208 (2020)
10	ArtemiC (curcumin, artemisinin, vitamin C, and Boswellia serrata)	Adjuvant therapy	Phase II	50 participants	ArtemiC will be sprayed orally twice a day for the first 2 days in the treatment period	Time to clinical improvement, Time to negative COVID-19 PCR	NCT04382040	NCT04382040 (2020)

(Continued on following page)

TABLE 1 | (*Continued*) Ongoing clinical trials of several plants, functional foods, and plant based products including bioactive phytocompounds, traditional medicines, nutraceuticals and similar other preparations against SARS-CoV-2 infection.

No	Drugs	Therapy type	Phase	Participant numbers	Intervention	Outcomes	ClinicalTrials.Gov Identifier	References
11	Medicinal cannabis (*Cannabis sativa* L. from Cannabaceae family)	Primary therapy	Phase II	200,000 participants	Cannabis, medical	Treatment of COVID-19, treatment of symptoms	NCT03944447	NCT03944447 (2020)
12	Jing-Guan-Fang (JGF)	Primary therapy	Not applicable	300 participants	Jing-Guan-Fang (JGF)	The number of COVID-19 patients after this preventive treatment	NCT04388644	NCT04388644 (2020)
13	Licorice extract	Adjuvant therapy	Not applicable	70 participants	Licorice capsules; 250 mg standardized extract (25% Glycyrrhizin—62.5 mg) for 10 days	Increased number of people recovering from COVID-19	NCT04487964	NCT04487964 (2020)
14	Iota-Carrageenan	Primary therapy	Phase IV	400 participants	A nasal spray with Iota-Carrageenan or placebo 4 times a day	Progression to a more severe disease state, defined as need for oxygen therapy, lasting of disease, incidence of COVID-19 disease onset in the first week after treatment	NCT04521322	NCT04521322 (2020)
15	Acai palm berry extract (*Euterpe oleracea* Mart. from Arecaceae family)	Primary therapy	Phase II	480 participants	One capsule (520 mg) of Açaí Palm Berry every 8 h for a total of 3 capsules a day for 30 days	7-point ordinal symptom scale, need for mechanical ventilation, need for hospitalization	NCT04404218	NCT04404218 (2020)
16	QuadraMune™ (Composed of four natural ingredients)	Primary therapy	Not applicable	500 participants	Two pills of QuadraMune (TM) daily for 12 weeks	Prevention of COVID-19	NCT04421391	NCT04421391 (2020)
17	Phenolic monoterpenes + colchicine	Adjuvant therapy	Phase II	200 participants	Colchicine along with phenolic monoterpenes added to standard treatment in patients with COVID-19 infection	Improvement in clinical, radiological and laboratory manifestations will be estimated in treated group compared to control one	NCT04392141	NCT04392141 (2020)
18	Cannabidol	Primary therapy	Phase I, Phase II	400 participants	Oral administration of Cannabidiol (150 mg twice daily) for 14 days	Evaluation of the impact of Cannabidol on the cytokine profile with severe and critically COVID-19 infected people along with safety and efficacy profile	NCT04731116	NCT04731116 (2020)
19	Resistant Starch	Primary therapy	Phase II, Phase III	1,500 participants	Twenty grams for 14 days in a twice daily pattern where nonresistant starch was used in the same amount as placebo	Determination of hospitalization rate for COVID-19 associated complications	NCT04342689	NCT04342689 (2020)
20	Colchicine	Adjuvant therapy	Phase III	102 participants	An preliminary dose of 1.5 mg followed by 0.5 mg twice daily during the next 7 days and 0.5 mg once daily until the completion of 14 days treatment	Assessment of changes in the patients' clinical status through the 7 points ordinal scale WHO R&D Blueprint expert group along with IL-6 concentrations	NCT04667780	NCT04667780 (2020)
		Primary therapy	Phase II	70 participants	Initial dose of 1.2 mg followed by 0.6 mg after 2 h on day 1. After that 0.6 mg of two doses up to 14th day	Assessment of decreased risk of progression into ARDS requiring upraised oxygen needs, mechanical ventilation and mortality	NCT04363437	NCT04363437 (2020)

(Continued on following page)

TABLE 1 | (*Continued*) Ongoing clinical trials of several plants, functional foods, and plant based products including bioactive phytocompounds, traditional medicines, nutraceuticals and similar other preparations against SARS-CoV-2 infection.

No	Drugs	Therapy type	Phase	Participant numbers	Intervention	Outcomes	ClinicalTrials.Gov Identifier	References
21	Special Chinese medicine	Primary therapy	Not applicable	150 participants	Lung and spleen qi deficiency syndrome: 9 g French pinellia (*Pinellia ternata* (Thunb.) Makino from Araceae family), 10 g chenpi (*Citrus aurantium* L. from Rutaceae family), 15 g Codonopsis (*Codonopsis pilosula* (Franch.) Nannf. from Campanulaceae family), 30 g sunburn astragalus (*Astragalus membranaceus* (Fisch.) Bunge from Fabaceae family), 6 g *Amomum villosum* Lour. from Zingiberaceae family, and Licorice 6 g etc. Qi and Yin deficiency syndrome: root of *Salviae miltiorrhizae* Bunge 10 g, [Lamiaceae; North and south radix salviae], 15 g *Ophiopogon japonicus* (Thunb.) Ker Gawl. from Asparagaceae family, 6 g American ginseng (*Panax quinquefolius* L. from family Araliaceae family), 6 g Schisandra (*Schisandra chinensis* (Turcz.) Baill. from Schisandraceae family), 6 g gypsum l5 g, 10 g light bamboo leaves (*Bambusa vulgaris* Schrad. from Poaceae family), 10 g mulberry leaves (*Morus alba* L. from Moraceae family), 15 g reed root (*Ceanothus americanus* L. from Ramnaceae family), 15 g *Salvia miltiorrhiza* Bunge from Lamiaceae family, 6 g raw liquorice etc.	Assessment of changes in CM diagnostic pattern & clinical characteristics along with body constitution scores	NCT04544605	NCT04544605 (2020)
22	Nicotine	Primary therapy	Phase III	1,633 participants	3.5 mg: day 1 to day 3 Seven milligrams: day 4 to day 9 10.5 mg: day 10 to day 15 14 mg: day 16 to day 98 10.5 mg: Day 99 to day 105 Seven milligrams: day 106 to day 112 3.5 mg: day 113 to day 119 As Nicotine patch	Determination of COVID-19 seroconversion between week o and week 19 after randomization	NCT04583410	NCT04583410 (2020)
		Primary therapy	Phase III	220 participants	0.5 patch for day 1 and day 2, 1 patch for day 3 and day 4, 1.5 patches for day 5 and day 6 where 2 patches from day 7 to the day discharge from hospital where one patch contains 7 mg nicotine	Determination of any he unfavorable outcome on day 14	NCT04608201	NCT04608201 (2020)
		Primary therapy	Phase III	220 participants	Two patches of 7 mg/day Treatment at 14 mg/day during mechanical ventilation since after first successful extubation followed by dose decrement	Determination of inhibition of the penetration and propagation of SARS-CoV2 by nicotine	NCT04598594	NCT04598594 (2020)

(Continued on following page)

TABLE 1 | (*Continued*) Ongoing clinical trials of several plants, functional foods, and plant based products including bioactive phytocompounds, traditional medicines, nutraceuticals and similar other preparations against SARS-CoV-2 infection.

No	Drugs	Therapy type	Phase	Participant numbers	Intervention	Outcomes	ClinicalTrials.Gov Identifier	References
23	Hesperidin	Primary therapy	Phase II	216 participants	Capsules containing 0.5 gm of hesperidin in the evening and at bed time with water	Determination of proportion of subjects with COVID-19 symptoms	NCT04715932	NCT04715932 (2020)
24	Resveratrol + Zinc	Primary therapy	Phase II	60 participants	2 grams of resveratrol twice a day + Zinc picolinate 50 mg for thrice a day for 5 days	Assessment of reduction of COVID-19 viral load and its severity	NCT04542993	NCT04542993 (2020)
25	Melatonin	Primary therapy	Phase II	30 participants	Ten milligrams thrice a day dose day for 14 days	Determination of cumulative incidence of treatment-emergent adverse effects	NCT04474483	NCT04474483 (2020)
		Adjuvant therapy	Not applicable	55 participants	Nine milligrams dose of melatonin for seven to ten nights	Determination of modulation of immune system	NCT04409522	NCT04409522 (2020)
		Primary therapy	Phase II	18 participants	Maximum daily dose 500 mg per day	Determination of impact of Melatonin on mortality rate and hospital stay	NCT04568863	NCT04568863 (2020)
		Primary therapy	Not applicable	150 participants	Ten milligrams melatonin at bedtime	Electronically tracking of symptom severity	NCT04530539	NCT04530539 (2020)
		Primary therapy	Phase II, Phase III	450 participants	Two milligrams of prolonged release melatonin orally before bedtime for 12 weeks	Determination of prophylaxis efficacy of melatonin	NCT04353128	NCT04353128 (2020)

time, plasma CRP variation data were collected from all three groups, analyzed, and compared (NCT04480593, 2020).

Ongoing Clinical Trials of Promising Phyto-Based Preparations (Bioactive Metabolites, Traditional Medicines, Plant Extracts, Nutraceuticals, Functional Foods, Chinese Medicines, Ayurved Medicines, And Other Plant-Based Preparations)

There are trials of several promising and potent phyto-based formulations to treat SARS-CoV-2 infections, which are currently in the recruiting phase or in different stages. It is anticipated that these formulations will be potential sources in the discovery and development of anti-COVID-19 medicaments. This is because of their previous history of antiviral activities. Some of the promising formulations/agents are presented in **Table 1**.

CONCLUSION

Assessment of plant-based preparations including traditional medicines, bioactive compounds, and functional foods or nutraceuticals to battle the novel strain of coronavirus could provide a gigantic triumph for the distorted public health system. This expectation is based on the tremendous contributions that metabolites or herbal preparations have made in the past to address many kinds of serious ailments including infectious diseases. In this article, we have presented and discussed the data from several completed clinical trials that may yield valuable new treatments for COVID-19. They may be independent therapies or complementary or alternative medicines to manage COVID-19. Many prospective metabolites and plant-based herbal preparations in different forms of delivery led to promising outcomes in preclinical studies, and they are in various stages of clinical trials. However, to evaluate the effectiveness and safety profiles of these phytochemicals and mono- and poly-herbal formulations, it is crucial to perform extensive and more rigorous, high-quality, and evidence-based medical interventions and human trials to exploit, as far as possible, their therapeutic potential for the clinical management of COVID-19 infected patients.

AUTHOR CONTRIBUTIONS

MMRS and SAl conceptualized the research work. SAl, SAf, and FTR performed extensive literature search and collected relevant articles. SAl, SAf, and FTR wrote the manuscript draft. CZ and J-RZ critically reviewed the manuscript. SAl edited and drafted the manuscript. MMRS and INM critically evaluated and thoroughly revised the manuscript and supervised this project.

ACKNOWLEDGMENTS

The authors are thankful to the Department of Pharmacy, State University of Bangladesh, and Health Med Science Research Limited, Dhaka, Bangladesh for providing necessary supports to produce this article.

REFERENCES

Abd El-Aziz, T. M., and Stockand, J. D. (2020). Recent Progress and Challenges in Drug Development against COVID-19 Coronavirus (SARS-CoV-2) - an Update on the Status. *Infect. Genet. Evol.* 83, 104327. doi:10.1016/j.meegid.2020.104327

Al-Hatamleh, M. A. I., Hatmal, M. m. M., Sattar, K., Ahmad, S., Mustafa, M. Z., Bittencourt, M. D. C., et al. (2020). Antiviral and Immunomodulatory Effects of Phytochemicals from Honey against COVID-19: Potential Mechanisms of Action and Future Directions. *Molecules* 25 (21), 5017. doi:10.3390/molecules25215017

Alam, S., Emon, N. U., Shahriar, S., Richi, F. T., Haque, M. R., Islam, M. N., et al. (2020). Pharmacological and Computer-Aided Studies Provide New Insights into Millettia Peguensis Ali (Fabaceae). *Saudi Pharm. J.* 28, 1777–1790. doi:10.1016/j.jsps.2020.11.004

Ameen, N. M., Altubaigy, F., Jahangir, T., Mahday, I. A., Mohammed, E. A., and Musa, O. A. (2011). Effect of Nigella Sativa and Bee Honey on Pulmonary, Hepatic and Renal Function in Sudanese in Khartoum State. *J. Med. Plants Res.* 5 (31), 6857–6863. doi:10.5897/JMPR11.1357

An, X., Zhang, Y., Duan, L., Jin, D., Zhao, S., Zhou, R., et al. (2021). The Direct Evidence and Mechanism of Traditional Chinese Medicine Treatment of COVID-19. *Biomed. Pharmacother.* 137, 111267. doi:10.1016/j.biopha.2021.111267

Andrighetti-Fröhner, C. R., Sincero, T. C. M., Da Silva, A. C., Savi, L. A., Gaido, C. M., Bettega, J. M. R., et al. (2005). Antiviral Evaluation of Plants from Brazilian atlantic Tropical forest. *Fitoterapia* 76 (3-4), 374–378. doi:10.1016/j.fitote.2005.03.010

Ang, L., Song, E., Lee, H. W., and Lee, M. S. (2020). Herbal Medicine for the Treatment of Coronavirus Disease 2019 (COVID-19): a Systematic Review and Meta-Analysis of Randomized Controlled Trials. *Jcm* 9 (5), 1583. doi:10.3390/jcm9051583

Ashraf, S., Ashraf, S., Ashraf, M., Imran, M. A., Kalsoom, L., Siddiqui, U. N., et al. (2020). Honey and Nigella Sativa against COVID-19 in Pakistan (HNS-COVID-PK): A Multi-center Placebo-Controlled Randomized Clinical Trial. *medRxiv*. doi:10.1101/2020.10.30.20217364

Berretta, A. A., Silveira, M. A. D., Cóndor Capcha, J. M., and De Jong, D. (2020). Propolis and its Potential against SARS-CoV-2 Infection Mechanisms and COVID-19 Disease. *Biomed. Pharmacother.* 131, 110622. doi:10.1016/j.biopha.2020.110622

Bhatti, I., Inayat, S., Uzair, B., Menaa, F., Bakhsh, S., Khan, H., et al. (2016). Effects of Nigella Sativa (Kalonji) and Honey on Lipid Profile of Hyper Lipidemic Smokers. *IJPER* 50 (3), 376–384. doi:10.5530/ijper.50.3.9

Chen, J., Hu, Y., Chen, L., Liu, W., Mu, Y., and Liu, P. (2019). The Effect and Mechanisms of Fuzheng Huayu Formula against Chronic Liver Diseases. *Biomed. Pharmacother.* 114, 108846. doi:10.1016/j.biopha.2019.108846

Chen, X., Wu, Y., Chen, C., Gu, Y., Zhu, C., Wang, S., et al. (2021). Identifying Potential Anti-COVID-19 Pharmacological Components of Traditional Chinese Medicine Lianhuaqingwen Capsule Based on Human Exposure and ACE2 Biochromatography Screening. *Acta Pharmaceutica Sinica B* 11 (1), 222–236. doi:10.1016/j.apsb.2020.10.002

Chen, X., Yin, Y.-H., Zhang, M.-Y., Liu, J.-Y., Li, R., and Qu, Y.-Q. (2020). Investigating the Mechanism of ShuFeng JieDu Capsule for the Treatment of Novel Coronavirus Pneumonia (COVID-19) Based on Network Pharmacology. *Int. J. Med. Sci.* 17 (16), 2511–2530. doi:10.7150/ijms.46378

Colunga Biancatelli, R. M. L., Berrill, M., Catravas, J. D., and Marik, P. E. (2020). Quercetin and Vitamin C: an Experimental, Synergistic Therapy for the Prevention and Treatment of SARS-CoV-2 Related Disease (COVID-19). *Front. Immunol.* 11, 1451. doi:10.3389/fimmu.2020.01451

Cushnie, T. P. T., and Lamb, A. J. (2005). Antimicrobial Activity of Flavonoids. *Int. J. Antimicrob. Agents* 26 (5), 343–356. doi:10.1016/j.ijantimicag.2005.09.002

Debiaggi, M., Tateo, F., Pagani, L., Luini, M., and Romero, E. (1990). Effects of Propolis Flavonoids on Virus Infectivity and Replication. *Microbiologica* 13 (3), 207–213. PMID: 2125682

Derosa, G., Maffioli, P., D'Angelo, A., and Di Pierro, F. (2020). A Role for Quercetin in Coronavirus Disease 2019 (COVID-19). *Phytotherapy Res.* 35, 1230–1236. doi:10.1002/ptr.6887

Devpura, G., Tomar, B. S., Nathiya, D., Sharma, A., Bhandari, D., Haldar, S., et al. (2021). Randomized Placebo-Controlled Pilot Clinical Trial on the Efficacy of Ayurvedic Treatment Regime on COVID-19 Positive Patients. *Phytomedicine* 84, 153494. doi:10.1016/j.phymed.2021.153494

Di Lorenzo, G., Di Trolio, R., Kozlakidis, Z., Busto, G., Ingenito, C., Buonerba, L., et al. (2020). COVID 19 Therapies and Anti-cancer Drugs: A Systematic Review of Recent Literature. *Crit. Rev. oncology/hematology* 152, 102991. doi:10.1016/j.critrevonc.2020.102991

Ding, X. J., Zhang, Y., He, D. C., Zhang, M. Y., Tan, Y. J., Yu, A., et al. (2020). Clinical Effect and Mechanism of Qingfei Touxie Fuzheng Recipe in the Treatment of Novel Coronavirus Pneumonia. *Herald Med.* 39 (05), 640–644. doi:10.3870/j.issn.1004-0781.2020.05.012 Available at: http://www.yydbzz.com/CN/10.3870/j.issn.1004-0781.2020.05.012

Emon, N. U., Alam, S., Rudra, S., Riya, S. R., Paul, A., Hossen, S. M. M., et al. (2021). Antidepressant, Anxiolytic, Antipyretic, and Thrombolytic Profiling of Methanol Extract of the Aerial Part of Piper Nigrum : *In Vivo*, *In Vitro*, and In Silico Approaches. *Food Sci. Nutr.* 9, 833–846. doi:10.1002/fsn3.2047

Forouzanfar, F., Bazzaz, B. S., and Hosseinzadeh, H. (2014). Black Cumin (Nigella Sativa) and its Constituent (Thymoquinone): a Review on Antimicrobial Effects. *Iran J. Basic Med. Sci.* 17 (12), 929–938. PMID: 25859296

Golechha, M. (2020). Time to Realise the True Potential of Ayurveda against COVID-19. *Brain Behav. Immun.* 87, 130–131. doi:10.1016/j.bbi.2020.05.003

Guo, Y.-R., Cao, Q.-D., Hong, Z.-S., Tan, Y.-Y., Chen, S.-D., Jin, H.-J., et al. (2020). The Origin, Transmission and Clinical Therapies on Coronavirus Disease 2019 (COVID-19) Outbreak - an Update on the Status. *Mil. Med Res* 7 (1), 1–0. doi:10.1186/s40779-020-00240-0

Hoareau, L., and DaSilva, E. J. (1999). Medicinal Plants: a Re-emerging Health Aid. *Electron. J. Biotechnol.* 2 (2), 3–4. Available at: https://www.clinicaltrials.gov/ct2/show/NCT04480593?term=SARS-CoV2&recrs=e&draw=3 (Accessed on February 18, 2021).

Huang, J., Tao, G., Liu, J., Cai, J., Huang, Z., and Chen, J.-x. (2020a). Current Prevention of COVID-19: Natural Products and Herbal Medicine. *Front. Pharmacol.* 11, 11. doi:10.3389/fphar.2020.588508

Huang, Y., Zheng, W.-j., Ni, Y.-s., Li, M.-s., Chen, J.-k., Liu, X.-h., et al. (2020b). Therapeutic Mechanism of Toujie Quwen Granules in COVID-19 Based on Network Pharmacology. *BioData mining* 13 (1), 1–21. doi:10.1186/s13040-020-00225-8

Jahan, I., and Onay, A. (2020). Potentials of Plant-Based Substance to Inhabit and Probable Cure for the COVID-19. *Turk J. Biol.* 44 (3), 228–241. doi:10.3906/biy-2005-114

James, P. T., Ali, Z., Armitage, A. E., Bonell, A., Cerami, C., Drakesmith, H., et al. (2020). Could Nutrition Modulate COVID-19 Susceptibility and Severity of Disease? A Systematic Review. *medRxiv*. doi:10.1101/2020.10.19.20214395

Jia, S., Zongguo, Y., Chen, Y., Yujie, C., Yunfei, L., Ying, L., et al. (2020). Observation on the Clinical Efficacy of Integrated Traditional Chinese and Western Medicine in the Treatment of 49 Cases of Non-critical New Coronavirus Pneumonia in Shanghai[J]. *Shanghai J. Traditional Chin. Med.* 54 (04), 30–35. doi:10.16305/j.1007-1334.2020.04.095Available at: https://kns.cnki.net/kcms/detail/detail.aspx?doi=10.16305/j.1007-1334.2020.04.095

Kaitao, Y., Mingyu, L., and Xin, L. (2020). Retrospective Clinical Analysis of Traditional Chinese Medicine Lianhua Qingwen in Treating New Coronavirus Pneumonia [in Chinese] Chinese. *J. Exp. Trad Med. Formulae* 26, 8–12. doi:10.13422/j.cnki.syfjx.20201099 Available at: https://kns.cnki.net/kcms/detail/detail.aspx?doi=10.13422/j.cnki.syfjx.20201099

Koshak, D. A. E., and Koshak, P. E. A. (2020). Nigella Sativa L as a Potential Phytotherapy for Coronavirus Disease 2019: A Mini Review of In Silico Studies. *Curr. Ther. Res.* 93, 100602. doi:10.1016/j.curtheres.2020.100602

Kulkarni, V., Sharma, N., Modi, D., Kumar, A., Joshi, J., and Krishnamurthy, N. A Community-Based Participatory Research to Assess the Feasibility of Ayurveda Intervention in Patients with Mild-To-Moderate COVID-19. *medRxiv*. 2021, doi:10.1101/2021.01.20.21250198

Kumar, A., Prasad, G., Srivastav, S., Gautam, V. K., and Sharma, N. A Retrospective Study on Efficacy and Safety of Guduchi Ghan Vati for COVID-19 Asymptomatic Patients. *medRxiv*. 2020a, doi:10.1101/2020.07.23.20160424

Kumar, A., Prasad, G., Srivastav, S., Gautam, V. K., and Sharma, N. Efficacy and Safety of Guduchi Ghan Vati in the Management of Asymptomatic COVID-19 Infection: An Open Label Feasibility Study, *medRxiv*. 2020b, doi:10.1101/2020.09.20.20198515

Lai, C.-C., Shih, T.-P., Ko, W.-C., Tang, H.-J., and Hsueh, P.-R. (2020). Severe Acute Respiratory Syndrome Coronavirus 2 (SARS-CoV-2) and Coronavirus Disease-2019 (COVID-19): The Epidemic and the Challenges. *Int. J. Antimicrob. Agents* 55 (3), 105924. doi:10.1016/j.ijantimicag.2020.105924

Lakhanpal, P., and Rai, D. K. (2007). Quercetin: a Versatile Flavonoid. *Internet J. Med. Update* 2 (2), 22–37. doi:10.4314/ijmu.v2i2.39851

Li, H., Liu, S.-M., Yu, X.-H., Tang, S.-L., and Tang, C.-K. (2020). Coronavirus Disease 2019 (COVID-19): Current Status and Future Perspectives. *Int. J. Antimicrob. Agents* 55 (5), 105951. doi:10.1016/j.ijantimicag.2020.105951

Li, L.-C., Zhang, Z.-H., Zhou, W.-C., Chen, J., Jin, H.-Q., Fang, H.-M., et al. (2020a). Lianhua Qingwen Prescription for Coronavirus Disease 2019 (COVID-19) Treatment: Advances and Prospects. *Biomed. Pharmacother.* 130, 110641. doi:10.1016/j.biopha.2020.110641

Li, S., Zhang, J., Li, F., Mao, A., Li, Y., Zhao, C., et al. (2021). Traditional Chinese Medicine Lianhua Qingwen for Treating COVID-19. *Medicine* 100 (2), e24204. doi:10.1097/MD.0000000000024204

Li, Y., Yao, J., Han, C., Yang, J., Chaudhry, M., Wang, S., et al. (2016). Quercetin, Inflammation and Immunity. *Nutrients* 8 (3), 167. doi:10.3390/nu8030167

Ling, X. Y., Tao, J. L., Sun, X., and Yuan, B. (2020). Exploring Material Basis and Mechanism of Lianhua Qingwen Prescription against Coronavirus Based on Network Pharmacology. *Chin. Trad. Herbal Drugs*, 1723–1730. Available at: https://search.bvsalud.org/global-literature-on-novel-coronavirus-2019-ncov/resource/en/COVIDwho-379966.

Lionis, C. (2015). Evidence-based Innovative Therapeutic Medicine of Cretan Plants: Some Encouraging Specific Functions and Claims. *Hell J. Nucl. Med.* 18 Suppl 1, 145

Liu, M., Gao, Y., Yuan, Y., Yang, K., Shi, S., Zhang, J., et al. (2020). Efficacy and Safety of Integrated Traditional Chinese and Western Medicine for Corona Virus Disease 2019 (COVID-19): a Systematic Review and Meta-Analysis. *Pharmacol. Res.* 158, 104896. doi:10.1016/j.phrs.2020.104896

Ludwig, S., and Zarbock, A. (2020). Coronaviruses and SARS-CoV-2: a Brief Overview. *Anesth. Analg* 131, 93–96. doi:10.1213/ANE.0000000000004845

Maurya, D. K., and Sharma, D. (2020). Evaluation of Traditional Ayurvedic Preparation for Prevention and Management of the Novel Coronavirus (SARS-CoV-2) Using Molecular Docking Approach. *chemrxiv*. doi:10.26434/chemrxiv.1211021

McCutcheon, A. R., Roberts, T. E., Gibbons, E., Ellis, S. M., Babiuk, L. A., Hancock, R. E. W., et al. (1995). Antiviral Screening of British Columbian Medicinal Plants. *J. Ethnopharmacol.* 49 (2), 101–110. doi:10.1016/0378-8741(95)90037-3

Meng, L., Bo, J., Hongjie, X., Qian, Y., Xueqing, Z., Kun, L., et al. (2020). Analysis of Factors Affecting Death of Patients with New Coronavirus Pneumonia. 51 (6), 1450–1454. Available at: http://www.tiprpress.com/zcy/article/abstract/20200809. doi:10.7501/j.issn.02532670.2020.06.010

Moghimipour, E., Ghorbani, A., Malayeri, A., Siahpoosh, A., Khodadoost, M., Rajaeipour, M., et al. (2019). Evaluation of Nigella Sativa and Honey Combination for Treatment of Kidney Stone: a Randomized, Placebo Controlled Clinical Trial. *J. Contemp. Med. Sci.* 5 (1).

Montealegre-Gómez, G., Garavito, E., Gómez-López, A., Rojas-Villarraga, A., and Parra-Medina, R. (2020). Colchicine: A Potential Therapeutic Tool against COVID-19. Experience of 5 Patients. *Reumatología Clínica*. doi:10.1016/j.reuma.2020.05.001

Montreal Heart Institute (2020). Colchicine Reduces the Risk of COVID-19-Related Complications. Available at: https://www.globenewswire.com/news-release/2021/01/23/2163109/0/en/Colchicine-reduces-the-risk-of-COVID-19-related-complications.html (Accessed on February 14, 2021).

NCT03944447 (2020). Outcomes Mandate National Integration with Cannabis as Medicine for Prevention and Treatment of COVID-19 (OMNI-Can), ClinicalTrials.Gov. Available at: https://clinicaltrials.gov/ct2/show/NCT03944447 (Accessed on February 21, 2021).

NCT04279197 (2020). Treatment of Pulmonary Fibrosis Due to COVID-19 with Fuzheng Huayu, ClinicalTrials.Gov. Available at: https://clinicaltrials.gov/ct2/show/NCT04279197 (Accessed on February 21, 2021).

NCT04322344 (2020). Escin in Patients with Covid-19 Infection (Add-On-COV2), ClinicalTrials.Gov. Available at: https://clinicaltrials.gov/ct2/show/NCT04322344 (Accessed on February 21, 2021).

NCT04322682 (2020). Colchicine Coronavirus SARS-CoV2 Trial (COLCORONA) (COVID-19), ClinicalTrials.Gov. Available at: https://www.clinicaltrials.gov/ct2/show/NCT04322682?

NCT04323345 (2020). Efficacy of Natural Honey Treatment in Patients with Novel Coronavirus, ClinicalTrials.Gov. Available at: https://clinicaltrials.gov/ct2/show/NCT04323345 (Accessed on February 21, 2021).

NCT04334265 (2020). Efficacy and Safety of Anluohuaxian in the Treatment of Rehabilitation Patients with Corona Virus Disease 2019, ClinicalTrials.Gov. Available at: https://clinicaltrials.gov/ct2/show/NCT04334265 (Accessed on February 21, 2021).

NCT04342689 (2020). The Role of Resistant Starch in COVID-19 Infection, ClinicalTrials.Gov. Available at: https://clinicaltrials.gov/ct2/show/NCT04342689?term=starch&recrs=a&draw=2&rank=2 (Accessed on February 22, 2021).

NCT04345549 (2020). Ayurveda Self-Management for Flu like Symptoms during the COVID-19 Outbreak, ClinicalTrials.Gov. Available at: https://clinicaltrials.gov/ct2/show/ (Accessed on February 18, 2021).

NCT04347382 (2020). Honey & Nigella Sativa Trial Against COVID-19 (HNS-COVID-PK), ClinicalTrials.govNCT04347382?recrs=e&cond=SARS+CoV2&draw=2. Available at: https://www.clinicaltrials.gov/ct2/show/ (Accessed on February 18, 2021).

NCT04351542 (2020). Ayurveda for Flu Like Illness During COVID-19 Outbreak, ClinicalTrials.govNCT04351542?term=SARS-CoV2&recrs=e&draw=8. Available at: https://www.clinicaltrials.gov/ct2/show/ (Accessed on February 18, 2021).

NCT04353128 (2020). Efficacy of Melatonin in the Prophylaxis of Coronavirus Disease 2019 (COVID-19) Among Healthcare Workers. (MeCOVID), ClinicalTrials.Gov. Available at: https://clinicaltrials.gov/ct2/show/NCT04353128?term=melatonin&recrs=a&cond=Covid19&draw=2&rank=5 (Accessed on February 22, 2021).

NCT04363437 (2020). Evaluation of the Colchicine in Moderate-Severe Hospitalized Patients before ARDS to Treat COVID-19 (COMBATCOVID19), ClinicalTrials.Gov. Available at: https://clinicaltrials.gov/ct2/show/NCT04363437?recrs=a&cond=Covid19&draw=36 (Accessed on February 22, 2021).

NCT04377789 (2020). Effect of Quercetin on Prophylaxis and Treatment of COVID-19, ClinicalTrials.govNCT04377789?term=SARS-CoV2&recrs=e&draw=3. Available at: https://www.clinicaltrials.gov/ct2/show/ (Accessed on February 18, 2021).

NCT04382040 (2020). A Phase II, Controlled Clinical Study Designed to Evaluate the Effect of ArtemiC in Patients Diagnosed with COVID-19, ClinicalTrials.Gov. Available at: https://clinicaltrials.gov/ct2/show/NCT04382040 (Accessed on February 21, 2021).

NCT04387643 (2020). Protecting Health Care Workers During the COVID-19 Outbreak, ClinicalTrials.govNCT04387643?term=SARS-CoV2&recrs=e&draw=6. Available at: https://www.clinicaltrials.gov/ct2/show/ (Accessed on February 18, 2021).

NCT04388644 (2020). Survey of Satisfaction on Traditional Chinese Medicine Jing-Guan-Fang (JGF) for COVID-19 Prevention, ClinicalTrials.Gov. Available at: https://www.clinicaltrials.gov/ct2/show/NCT04388644?term=traditional+chinese+medicine&recrs=a&cond=%22Coronavirus+Infections%22&draw=2&rank=1 (Accessed on February 21, 2021).

NCT04392141 (2020). Colchicine Plus Phenolic Monoterpenes to Treat COVID-19, ClinicalTrials.Gov. Available at: https://clinicaltrials.gov/ct2/show/NCT04392141?recrs=a&cond=Covid19&draw=3&rank=78 (Accessed on February 21, 2021).

NCT04394208 (2020). Silymarin in COVID-19 Pneumonia (SCOPE), ClinicalTrials.Gov. Available at: https://clinicaltrials.gov/ct2/show/NCT04394208 (Accessed on February 21, 2021).

NCT04400890 (2020). Randomized Proof-Of-Concept Trial to Evaluate the Safety and Explore the Effectiveness of a Plant Polyphenol for COVID-19, ClinicalTrials.Gov. Available at: https://clinicaltrials.gov/ct2/show/NCT04400890 (Accessed on February 21, 2021).

NCT04401202 (2020). Nigella Sativa in COVID-19, ClinicalTrials.Gov. Available at: https://clinicaltrials.gov/ct2/show/NCT04401202 (Accessed on February 21, 2021).

NCT04404218 (2020). The Açaí Berry COVID-19 Anti-inflammation Trial (ACAI), ClinicalTrials.Gov. Available at: https://clinicaltrials.gov/ct2/show/NCT04404218 (Accessed on February 21, 2021).

NCT04409522 (2020). Evaluation of Therapeutic Effects of Melatonin by Inhibition of NLRP3 Inflammasome in COVID19 Patients, ClinicalTrials.Gov. Available at: https://clinicaltrials.gov/ct2/show/NCT04409522?term=melatonin&recrs=a&cond=Covid19&draw=2&rank=2 (Accessed on February 22, 2021).

NCT04410510 (2020). P2Et Extract in the Symptomatic Treatment of Subjects with COVID-19, ClinicalTrials.Gov. Available at: https://clinicaltrials.gov/ct2/show/NCT04410510 (Accessed on February 21, 2021).

NCT04421391 (2020). QuadraMune(TM) for Prevention of COVID-19, ClinicalTrials.Gov. Available at: https://clinicaltrials.gov/ct2/show/NCT04421391 (Accessed on February 21, 2021).

NCT04474483 (2020). Safety and Efficacy of Melatonin in Outpatients Infected with COVID-19 (COVID-19), ClinicalTrials.Gov. Available at: https://clinicaltrials.gov/ct2/show/NCT04474483?term=melatonin&recrs=a&cond=Covid19&draw=2&rank=1 (Accessed on February 22, 2021).

NCT04480398 (2020). Efficacy and Safety of Guduchi Ghan Vati for COVID-19 Asymptomatic Patients, ClinicalTrials.govNCT04480398?term=SARS-CoV2&recrs=e&draw=5. Available at: https://www.clinicaltrials.gov/ct2/show/ (Accessed on February 18, 2021).

NCT04480593, 2020. The Use of Brazilian Green Propolis Extract (EPP-AF) in Patients Affected by COVID-19. (Bee-COVID), ClinicalTrials.Gov.

NCT04487964 (2020). Complementary Intervention for COVID-19, Clinical Trials.Gov. Available at: https://clinicaltrials.gov/ct2/show/NCT04487964 (Accessed on February 21, 2021).

NCT04495842 (2020). The Effect of Aromatherapy on COVID-19-Induced Anxiety, ClinicalTrials.Gov. Available at: https://clinicaltrials.gov/ct2/show/NCT04495842 (Accessed on February 21, 2021).

NCT04521322 (2020). Efficacy of a Nasal Spray Containing Iota-Carrageenan in the Prophylaxis of COVID-19 Disease in Health Personnel Dedicated to Patients Care with COVID-19 Disease (CARR-COV-02), ClinicalTrials.Gov. Available at: https://clinicaltrials.gov/ct2/show/NCT04521322 (Accessed on February 21, 2021).

NCT04530539 (2020). The Effect of Melatonin and Vitamin C on COVID-19, ClinicalTrials.Gov. Available at: https://clinicaltrials.gov/ct2/show/NCT04530539?term=melatonin&recrs=a&cond=Covid19&draw=2&rank=4 (Accessed on February 22, 2021).

NCT04542993 (2020). Can SARS-CoV-2 Viral Load and COVID-19 Disease Severity Be Reduced by Resveratrol-Assisted Zinc Therapy (Reszinate), ClinicalTrials.Gov. Available at: https://clinicaltrials.gov/ct2/show/NCT04542993?term=resveratrol&recrs=a&draw=2&rank=9 (Accessed on February 22, 2021).

NCT04544605 (2020). Special Chinese Medicine Out-Patient Programme for Discharged COVID-19 Patients, ClinicalTrials.Gov. Available at: https://clinicaltrials.gov/ct2/show/NCT04544605?recrs=a&cond=Covid19&draw=4 (Accessed on February 21, 2021).

NCT04568863 (2020). Efficacy of Intravenous Melatonin on Mortality in Adult Patients Admitted to the Intensive Care Unit with COVID-19 (MELCOVID), ClinicalTrials.Gov. Available at: https://clinicaltrials.gov/ct2/show/NCT04568863?term=melatonin&recrs=a&cond=Covid19&draw=2&rank=3 (Accessed on February 22, 2021).

NCT04583410 (2020). Efficacy of Nicotine in Preventing COVID-19 Infection (NICOVID-PREV), ClinicalTrials.Gov. Available at: https://clinicaltrials.gov/ct2/show/NCT04583410?recrs=a&cond=Covid19&draw=19 (Accessed on February 22, 2021).

NCT04598594 (2020). Evaluation of the Evaluation of the Efficacy of Nicotine Patches in SARS-CoV2 (COVID-19) Infection in Intensive Care Unit Patients (NICOVID-REA), ClinicalTrials.Gov. Available at: https://clinicaltrials.gov/ct2/show/NCT04598594?recrs=a&cond=Covid19&draw=23 (Accessed on February 22, 2021).

NCT04608201 (2020). Evaluation of the Efficacy of Nicotine Patches in SARS-CoV2 (COVID-19) Infection in Hospitalized Patients (NICOVID), ClinicalTrials.Gov. Available at: https://clinicaltrials.gov/ct2/show/NCT04608201?recrs=a&cond=Covid19&draw=24 (Accessed on February 22, 2021).

NCT04621903 (2020). A Pilot Study on Efficacy and Safety of Ayurveda Combination in Patients with Mild-To-Moderate COVID-19, ClinicalTrials.Gov. Available at: https://clinicaltrials.gov/ct2/show/NCT04621903 (Accessed on February 18, 2021).

NCT04645407 (2020). Effects of Fuzheng Huayu Tablets on COVID-19, ClinicalTrials.Gov. Available at: https://www.clinicaltrials.gov/ct2/show/NCT04645407?term=SARS-CoV2&recrs=e&draw=8 (Accessed on February 18, 2021).

NCT04667780 (2020). Study to Investigate the Treatment Effect of Colchicine in Patients with COVID-19, ClinicalTrials.Gov. Available at: https://clinicaltrials.gov/ct2/show/NCT04667780?recrs=a&cond=Covid19&draw=12 (Accessed on February 21, 2021).

NCT04705753 (2020). Assessment of the Clinical Effectiveness of a Herbal Extract (Cretan IAMA) in Patients with Viral Respiratory Infections, Including COVID-19, in Primary Healthcare Settings, and Co-assessment of its Prophylactic Effect in People Cohabiting with These Patients (COVID-19-IAMA), ClinicalTrials.Gov. Available at: https://www.clinicaltrials.gov/ct2/show/NCT04705753?term=SARS-CoV2&recrs=e&draw=4 (Accessed on February 18, 2021).

NCT04715932 (2020). Study of Hesperidin Therapy on COVID-19 Symptoms (HESPERIDIN) (Hesperidin), ClinicalTrials.Gov. Available at: https://clinicaltrials.gov/ct2/show/NCT04715932?term=hesperidin&cond=covid19&draw=2&rank=1 (Accessed on February 22, 2021).

NCT04716647 (2020). Feasibility of Ayurveda in Patients with Mild-To-Moderate COVID-19: A Community-Based Participatory Research, ClinicalTrials.Gov. Available at: https://www.clinicaltrials.gov/ct2/show/NCT04716647?term=SARS-CoV2&recrs=e&draw=5 (Accessed on February 18, 2021).

NCT04731116 (2020). Cannabidiol Treatment for Severe and Critical Coronavirus (COVID-19) Pulmonary Infection, ClinicalTrials.Gov. Available at: https://clinicaltrials.gov/ct2/show/NCT04731116?recrs=a&cond=Covid19&draw=12 (Accessed on February 21, 2021).

Ni, L., Chen, L., Huang, X., Han, C., Xu, J., Zhang, H., et al. (2020). Combating COVID-19 with Integrated Traditional Chinese and Western Medicine in China. *Acta Pharmaceutica Sinica B* 10, 1149–1162. doi:10.1016/j.apsb.2020.06.009

Pandey, M. M., Rastogi, S., and Rawat, A. K. S. (2013). Indian Traditional Ayurvedic System of Medicine and Nutritional Supplementation. *Evidence-Based Complement. Altern. Med.* 2013, 1–12. doi:10.1155/2013/376327

Panyod, S., Ho, C.-T., and Sheen, L.-Y. (2020). Dietary Therapy and Herbal Medicine for COVID-19 Prevention: A Review and Perspective. *J. traditional Complement. Med.* 10, 420–427. doi:10.1016/j.jtcme.2020.05.004

Patgiri, B., Umretia, B., Vaishnav, P., Prajapati, P., Shukla, V., and Ravishankar, B. (2014). Anti-inflammatory Activity of Guduchi Ghana (Aqueous Extract of Tinospora Cordifolia Miers.). *Ayu* 35 (1), 108. doi:10.4103/0974-8520.141958

Perricone, C., Bartoloni, E., and Gerli, R. (2020). Colchicine, an Anti-rheumatic Agent, as a Potential Compound for the Treatment of COVID-19. *Reumatologia* 58 (5), 261. doi:10.5114/reum.2020.100088

Priya, N. C., and Kumari, P. S. (2017). Antiviral Activities and Cytotoxicity Assay of Seed Extracts of Piper Longum and Piper Nigrum on Human Cell Lines. *Int. J. Pharm. Sci. Rev. Res.* 44 (1), 197–202.

Qi, X., Yinjie, J., Sisi, W., Yang, W., Jun, A., Wuping, X., et al. (2020). Analysis of the Value of Traditional Chinese Medicine Shufeng Jiedu Capsule Combined with Arbidol in the Treatment of Mild New Coronavirus Pneumonia. *Chin. Emerg. Traditional Chin. Med.* 29, 756–758. Available at: http://med.wanfangdata.com.cn/Paper/Detail?id=PeriodicalPaper_zgzyjz202005002.

Qu, X. K., Hao, S. L., Ma, J. H., Wei, G. Y., Song, K. Y., Tang, C., et al. (2020). Observation on Clinical Effect of Shufeng Jiedu Capsule Combined with Arbidol Hydrochloride Capsule in Treatment of COVID-19, *Chin. Trad. Herbal Drugs*, 1167–1170. Available at: https://search.bvsalud.org/global-literature-on-novel-coronavirus-2019-ncov/resource/pt/COVIDwho-59635.

Ren, J. L., Zhang, A. H., and Wang, X. J. (2020). Traditional Chinese Medicine for COVID-19 Treatment. *Pharmacol. Res.* 155, 104743. doi:10.1016/j.phrs.2020.104743

Ruibing, L., Wenju, W., and Xin, L. (2020). Clinical Observation on 63 Suspected Cases of Novel Coronavirus Pneumonia Treated by Chinese Medicine Lianhua Qingwen [J/OL]. *J. Traditional Chin. Med.* 61 (8), 655–659. Available at: https://kns.cnki.net/kcms/detail/11.2166.R.20200215.1633.004.html.

Saeedi-Boroujeni, A., and Mahmoudian-Sani, M. R. (2021). Anti-inflammatory Potential of Quercetin in COVID-19 Treatment. *J. Inflamm.* 18 (1), 1–9. doi:10.1186/s12950-021-00268-6

Sarkar, C., Mondal, M., Torequl Islam, M., Martorell, M., Docea, A. O., Maroyi, A., et al. (2020). Potential Therapeutic Options for COVID-19: Current Status, Challenges, and Future Perspectives. *Front. Pharmacol.* 11, 1428. doi:10.3389/fphar.2020.572870

Schlesinger, N., Firestein, B. L., and Brunetti, L. (2020). Colchicine in COVID-19: an Old Drug, New Use. *Curr. Pharmacol. Rep.* 6 (4), 137–145. doi:10.1007/s40495-020-00225-6

Semple, S. J., Reynolds, G. D., O'leary, M. C., and Flower, R. L. (1998). Screening of Australian Medicinal Plants for Antiviral Activity. *J. ethnopharmacology* 60 (2), 163–172. doi:10.1016/S0378-8741(97)00152-9

Shi, K., Liu, Y., Wang, X., Li, Y., Zhang, Q., Hu, Y., et al. (2020). Adjuvant Fuzheng Huayu Capsule Reduces the Incidence of Hepatocellular Carcinoma in Patients with Hepatitis B-Caused Cirrhosis. *Evidence-Based Complement. Altern. Med.*, 2020. doi:10.1155/2020/8826091

Shree, P., Mishra, P., Selvaraj, C., Singh, S. K., Chaube, R., Garg, N., et al. (2020). Targeting COVID-19 (SARS-CoV-2) Main Protease through Active

Phytochemicals of Ayurvedic Medicinal Plants Withania Somnifera (Ashwagandha), Tinospora Cordifolia (Giloy) and Ocimum Sanctum (Tulsi)–A Molecular Docking Study. *J. Biomol. Struct. Dyn.*, 1–4. doi:10.1080/07391102.2020.1810778

Silveira, D., Prieto-Garcia, J. M., Boylan, F., Estrada, O., Fonseca-Bazzo, Y. M., Jamal, C. M., et al. (2020). COVID-19: Is There Evidence for the Use of Herbal Medicines as Adjuvant Symptomatic Therapy? *Front. Pharmacol.* 11, 1479. doi:10.3389/fphar.2020.581840

Slobodnick, A., Shah, B., Pillinger, M. H., and Krasnokutsky, S. (2015). Colchicine: Old and New. *Am. J. Med.* 128 (5), 461–470. doi:10.1016/j.amjmed.2014.12.010

Sun, C. Y., Sun, Y. L., and Li, X. M. (2020). The Role of Chinese Medicine in COVID-19 Pneumonia: A Systematic Review and Meta-Analysis. *Am. J. Emerg. Med.* doi:10.1016/j.ajem.2020.06.069

Tan, W., Li, S., Yiyang, C., Yakun, F., Wei, Y., Xiaozheng, D., et al. (2020). Clinical Efficacy Analysis of 50 Cases of Novel Coronavirus Pneumonia in Traditional Chinese Medicine [J], *Jilin Traditional Chin. Med.* term=SARS-CoV2&recrs=e&draw=2, 40, 281–285. doi:10.13463/j.cnki.jlzyy.2020.03.001 Available at: https://kns.cnki.net/kcms/detail/detail.aspx?doi=10.13463/j.cnki.jlzyy.2020.03.001

Uchide, N., and Toyoda, H. (2011). Antioxidant Therapy as a Potential Approach to Severe Influenza-Associated Complications. *Molecules* 16 (3), 203252. doi:10.3390/molecules16032032

Ulasli, M., Gurses, S. A., Bayraktar, R., Yumrutas, O., Oztuzcu, S., Igci, M., et al. (2014). The Effects of Nigella Sativa (Ns), Anthemis Hyalina (Ah) and Citrus Sinensis (Cs) Extracts on the Replication of Coronavirus and the Expression of TRP Genes Family. *Mol. Biol. Rep.* 41 (3), 1703–1711. doi:10.1007/s11033-014-3019-7

Upadhyay, A. K., Kumar, K., Kumar, A., and Mishra, H. S. (2010). Tinospora Cordifolia (Willd.) Hook. F. And Thoms.(Guduchi)–Validation of the Ayurvedic Pharmacology through Experimental and Clinical Studies. *Int. J. Ayurveda Res.* 1 (2), 112. doi:10.4103/0974-7788.64405

Vitiello, A., Ferrara, F., and Ferrara, F. (2021). Colchicine and SARS-CoV-2: Management of the Hyperinflammatory State. *Respir. Med.*, 106322. doi:10.1016/j.rmed.2021.106322

Wang, Y. L., Yang, X. D., Liu, Y. P., Zhang, J., Feng, Y. F., Shang, L., et al. (2020). Preliminary Clinical Effect Analysis of the Treatment of Novel Coronavirus Pneumonia by Internal Administration of Traditional Chinese Medicine Plus Fumigation and Absorption Combined with Super Dose of Vitamin C in Treating NOVID-19. *J. Xi'an Jiaotong Univ.(Med. Sci.*, 1–7. Available at: https://pesquisa.bvsalud.org/global-literature-on-novel-coronavirus-2019-ncov/resource/en/czh-424.

Wang, Z., Liu, H., Wu, M., Zhou, Y., Che, J., Zhang, S., et al. (2021). Integrated Lianhua-Qingwen and Western Medicine versus Western Medicine-Only Therapies against COVID-19: A Systematic Review and Meta-Analysis. *Researchsquare*. doi:10.21203/rs.3.rs-149782/v1

Who (2021). WHO Coronavirus Disease (COVID-19) Dashboard. Available at: https://COVID19.who.int/?gclid=Cj0KCQiA4L2BBhCvARIsAO0SBdZbO3T-KPgQ73OHj0Qvo8Eq_pVbDJcr0xKePgUsABuHCyikOhqQULDQaAtQy-EALw_wcB (Accessed on February 18, 2021).

Wu, M., Zhou, Y., Qin, S. L., Lin, L. J., Ping, J., Tao, Z., et al. (2020). Fuzheng Huayu Capsule Attenuates Hepatic Fibrosis by Inhibiting Activation of Hepatic Stellate Cells. *Evidence-Based Complement. Altern. Med.*, 2020. doi:10.1155/2020/3468791

Xia, W., An, C., Zheng, Y., Zhang, J., Huang, M., Wang, Y., et al. (2020). Clinical Study on 34 Cases of New Coronavirus Pneumonia Treated with Integrated Traditional Chinese and Western Medicine. *J. Tradit. Chin. Med.* doi:10.13288/j.11-2166/r.2020.05.002 Available at: https://kns.cnki.net/kcms/detail/detail.aspx?doi=10.13288/j.11-2166/r.2020.05.002

Xiaoxia, F., Luping, L., and Xinghua, T. (2020). Clinical Study on 37 Cases of Novel Coronavirus Pneumonia Treated with Integrated Traditional Chinese and Western Medicine[J]. *Chin. New Drugs Clin. Pharmacol.* 31 (05), 600–604. doi:10.19378/j.issn.1003-9783.2020.05.016 Available at: https://kns.cnki.net/kcms/detail/detail.aspx?doi=10.19378/j.issn.1003-9783.2020.05.016

Yang, Y., Islam, M. S., Wang, J., Li, Y., and Chen, X. (2020). Traditional Chinese Medicine in the Treatment of Patients Infected with 2019-new Coronavirus (SARS-CoV-2): a Review and Perspective. *Int. J. Biol. Sci.* 16 (10), 1708. doi:10.7150/ijbs.45538

Zhang, H. T., Huang, M. X., Liu, X., Zheng, X. C., Li, X. H., Chen, G. Q., et al. (2020). Evaluation of the Adjuvant Efficacy of Natural Herbal Medicine on COVID-19: a Retrospective Matched Case-Control Study. *Am. J. Chin. Med.* 48 (04), 779–792. doi:10.1142/S0192415X20500391

Zhongqian, H., Zhongbao, L., Shuwen, L., Hongjun, B., Changhong, W., and Jinlei, C. (2020). Observation on the Clinical Treatment of 19 Cases of Nanyang New Coronary Pneumonia (Common type)[J]. *Forum Traditional Chin. Med.* 35 (02), 22–24. doi:10.13913/j.cnki.41-1110/r.2020.02.011 Available at: https://kns.cnki.net/kcms/detail/detail.aspx?doi=10.13913/j.cnki.41-1110/r.2020.02.011

Zhou, Z., Gao, N., Wang, Y., Chang, P., Tong, Y., and Fu, S. (2020). Clinical Studies on the Treatment of Novel Coronavirus Pneumonia with Traditional Chinese Medicine—A Literature Analysis. *Front. Pharmacol.* 11, 1355. doi:10.3389/fphar.2020.560448

Zhu, M., Lv, Q. Q., Gu, M. H., Chen, Y. C., Wang, J., and Huang, Z. Q. (2020). Clinical Diagnosis and Integrated Treatment of Traditional Chinese and Western Medicine for Confirmed Patients with Coronavirus Disease 2019 in Yangzhou Area of Jiangsu Province. *J. Clin. Med. Pract.* 24 (05), 1–5. doi:10.7619/jcmp.202005001 Available at: http://jcmp.yzu.edu.cn/en/article/doi/10.7619/jcmp.202005001

Conflict of Interest: The authors declare that the research was conducted in the absence of any commercial or financial relationships that could be construed as a potential conflict of interest.

frontiers in Pharmacology

REVIEW
published: 21 June 2021
doi: 10.3389/fphar.2021.630834

Overview of Viral Pneumonia Associated With Influenza Virus, Respiratory Syncytial Virus, and Coronavirus, and Therapeutics Based on Natural Products of Medicinal Plants

Ziwei Hu[1], Jinhong Lin[1], Jintao Chen[1], Tengxi Cai[1], Lixin Xia[1], Ying Liu[1], Xun Song[1] and Zhendan He[1,2]**

[1]School of Basic Medicine, School of Pharmaceutical Sciences, Health Science Center, Shenzhen University, Shenzhen, China, [2]College of Pharmacy, Shenzhen Technology University, Shenzhen, China

OPEN ACCESS

Edited by:
Rong-Rong He,
Jinan University, China

Reviewed by:
Letizia Angiolella,
Sapienza University of Rome, Italy
Armando Caceres,
Universidad de San Carlos de Guatemala, Guatemala

***Correspondence:**
Xun Song
xsong@szu.edu.cn
Zhendan He
npcr417@126.com

Specialty section:
This article was submitted to Ethnopharmacology, a section of the journal Frontiers in Pharmacology

Received: *18 November 2020*
Accepted: *19 May 2021*
Published: *21 June 2021*

Citation:
Hu Z, Lin J, Chen J, Cai T, Xia L, Liu Y, Song X and He Z (2021) Overview of Viral Pneumonia Associated With Influenza Virus, Respiratory Syncytial Virus, and Coronavirus, and Therapeutics Based on Natural Products of Medicinal Plants. Front. Pharmacol. 12:630834. doi: 10.3389/fphar.2021.630834

Viral pneumonia has been a serious threat to global health, especially now we have dramatic challenges such as the COVID-19 pandemic. Approximately six million cases of community-acquired pneumonia occur every year, and over 20% of which need hospital admission. Influenza virus, respiratory virus, and coronavirus are the noteworthy causative agents to be investigated based on recent clinical research. Currently, anaphylactic reaction and inflammation induced by antiviral immunity can be incriminated as causative factors for clinicopathological symptoms of viral pneumonia. In this article, we illustrate the structure and related infection mechanisms of these viruses and the current status of antiviral therapies. Owing to a set of antiviral regiments with unsatisfactory clinical effects resulting from side effects, genetic mutation, and growing incidence of resistance, much attention has been paid on medicinal plants as a natural source of antiviral agents. Previous research mainly referred to herbal medicines and plant extracts with curative effects on viral infection models of influenza virus, respiratory virus, and coronavirus. This review summarizes the results of antiviral activities of various medicinal plants and their isolated substances, exclusively focusing on natural products for the treatment of the three types of pathogens that elicit pneumonia. Furthermore, we have introduced several useful screening tools to develop antiviral lead compounds.

Keywords: viral pneumonia, medicinal plants, natural compounds, influenza virus, respiratory syncytial virus, coronavirus

INTRODUCTION

Community-acquired pneumonia (CAP) is a commonly encountered lung inflammation involving the alveoli resulting from the lower respiratory tract infection that occurs in patients without recent health care exposure. CAP is responsible for the high rate of morbidity and mortality worldwide. As much as 5.6 million cases of CAP occur annually, and more than 20% of which need hospital admission (Niederman et al., 2001). According to the World Health Organization (WHO), 15% of

children under 5 years of age die from pneumonia (WHO 2020b); CAP is the eighth leading cause of death in the United States with approximately 50,000 people dying from the disease each year (CDC 2018; CDC 2019a; Heron 2019).

Recent surveys show that viruses are the major cause of CAP. A prospective study based on real time-PCR (RT-PCR) technique revealed that viral respiratory tract infections are highly prevalent among hospitalized CAP patients with immunodeficiency and low immune function (Tatarelli et al., 2019). Viral respiratory infection is common in pneumonia and is present in approximately 25% of patients with CAP. With the widespread introduction of improved diagnostic tests, at least 26 viruses associated with CAP have now been identified (Ruuskanen et al., 2011). Among viral pathogens, respiratory syncytial virus (RSV) predominantly remains the viral agent of severe CAP around the world (Ebbert and Limper, 2005; Lee et al., 2013; Mackenzie et al., 2019; Seidenberg 2019). Influenza virus (IFV) is the most common cause of viral pneumonia, following RSV, among 4,765 adults hospitalized with influenza, with 1,392 (29%) having pneumonia (Cantan et al., 2019). Recently, new pathogens discovered in patients infected with CAP, which have so far spread from China to 216 countries through rapid and frequent international air travel causing more than 0.6 million deaths worldwide, were associated with severe acute respiratory syndrome coronavirus 2 (SARS-CoV-2)–related 2019 novel coronavirus disease (COVID-19).

Currently, vaccines and antiviral agents have been developed as therapeutics to treat viral pneumonia. The two major antivirals used to treat influenza are neuraminidase (NA) inhibitors (peramivir, oseltamivir, laninamivir, and zanamivir) and M2 ion channel inhibitors (rimantadine and amantadine) and can be used to suppress the incidence of complications such as pneumonia (Moscona 2005; Gavigan and McCullers, 2019; Arabi et al., 2020). Nevertheless, M2 inhibitors are not widely used in clinical practice since only type A strain has M2 ion channel protein, While, M2 inhibitors, such as amantadine and rimantadine, doesn't work on the emergence of drug-resistance mutations in M2 proton channel (Hussain et al., 2017). A cohort study supports ribavirin therapy, which was approved by the Food and Drug Administration (FDA), as the primary treatment for infants and young children with RSV-associated pneumonia (Gomez et al., 2014). In contrast to IFV and RSV, experience with antiviral projects for coronavirus-associated CAP is scarce, with current knowledge coming mainly from case studies and surveillance data from clinical treatment.

Given that the treatment protocols of specific virus still lag behind for viral pneumonia, and short of miracle drugs, there is still a crying need for exploring new medicines to treat viral pneumonia. Natural products with antiviral efficacy, which are abundant in medicinal plants, are worth developing and utilizing as an alternative pharmacotherapy for treating CAPs. In the past,the discovery of antiviral lead compounds from various promising medicinal plants was limited because of, for one thing,a higher frequency of mutations and, for another, lack of chemical techniques for the identification of novel plant-based antiviral natural compounds. Thus far, a total of 1,073 small molecule new chemical entities (NCEs) have been approved for marketing from 1981 to 2010, among which 64% of the NCEs are identified as natural products or natural product-derived (Newman and Cragg, 2012), and it is considered that medicinal plants are still the primary sources of pharmacologically bioactive compounds for the therapeutics of viral pneumonia throughout history. In addition, challenges involved in frequent virus mutation, as well as the onset of viral resistances toward current antiviral agents, enhance an increasing interest for natural products as antiviral candidates. Nowadays, improved techniques in silico, such as high-throughput screening, molecular-docking, pharmacology network, and so on, strongly contribute to the isolation of potential drugs.

The aim of this review is to summarize the results on the antiviral activities of various isolated compounds from different kinds of plants, elucidating the latent mechanisms and potential interactions with related targets. This review will exclusively focus on natural products for the treatment of the above three important types of pathogens that elicit pneumonia, and other pathogens need not be discussed. Meanwhile, we have introduced some useful *in silico* methods to develop drugs from medicinal plants.

ETIOLOGY AND CURRENT ANTIVIRAL INTERVENTIONS

Respiratory Syncytial Virus

Human respiratory syncytial viruses (HRSVs) are deemed as highly infectious pathogens that induce acute lower respiratory tract illness (ALRTI), infecting and rendering diseases in individuals of all ages, particularly in children under 5 years and in adults over the age of 65. Since it is difficult to distinguish pneumonia and bronchiolitis clinically from radiographically, numerous epidemiological studies now follow the WHO recommendation to regard any RSV-associated ALRTI as pneumonia (Borchers et al., 2013). A recent systematic review pointed out the global number of cases of RSV pneumonia in 2015 at 33.1 million, of which 3.2 million hospital admissions and 59,600 deaths with 45% of cases occurring before 6 months of age (Shi et al., 2017a).

HRSV is a pleomorphic, enveloped, cytoplasmic virus with single-stranded, nonsegmented, and negative-sensed RNA genomes of 15.2 kb that belong to the family of Paramyxoviridae of the order *Mononeavirales*, genus *Pneumovirus*, subfamily *Pneumovirinae* (Bonnet et al., 2005; Fodha et al., 2008). Its antigen of single serotype split into two subgroups, A and B, which are further divided into 13 and 20 genotypes, respectively (Anderson et al., 1985; Pangesti et al., 2018). Both groups can spread simultaneously during outbreaks, but the proportions of A and B, as well as subtypes, vary yearly.

Therapeutic drugs for HRSV have been designed to target three major pathways of the virus cycle based on the virus structure, such as entry, replication, and transcription. The genomic RNA is associated with four nucleocapsid/polymerase proteins: nucleoprotein N, phosphoprotein P, transcription processivity factor M2-1, and the large polymerase subunit L.

Three encoded transmembrane surface glycoproteins on envelope participating in maximally efficient fusion contributed to infectivity, including the major attachment protein G, the fusion protein F, and the small hydrophobic (SH) protein, which remain the targets regarded most important for antiviral agents development.

The treatment of HRSV pneumonia is supportive. At present, two antiviral agents approved by the FDA are considered for optimal therapies to prevent and treat HRSV infection in children and infants with high risk. Ribavirin is a guanosine analog commonly administered in the form of erosolization, whereas intravenous ribavirin is not commercially available in the majority of countries. Multiple studies suggest that erosolized ribavirin mostly show its effectiveness at early stages of infection. Nevertheless, the application of erosolized ribavirin remains controversial owing to drug delivery, concerns about health risks for caregivers, as well as potential side effects (anemia, etc). Another successful agent allowed for human use known as a humanized monoclonal antibody against F glycoprotein. The clinical results of two randomized trials of prophylaxis with palivizumab provided the basis for FDA approval (Feltes et al., 2003). One carried out a 55% entire drop in hospital admission for RSV, corresponding to a relative reduction of 39% in children with CLD. Motavizumab is an investigational monoclonal antibody (mAb), another humanized IgG1 monoclonal antibody with a higher affinity compared to palivizumab, and can prevent serious diseases resulting from RSV in high-risk pediatric patients, and yet, the New Drug Application (NDA) of the MedImmune for motavizumab had been rejected by the FDA.

New and affordable therapeutic or prophylactic tools are urgent to develop due to a high economical cost of the current treatment. Furthermore, viral genetic mutations that allow for escaping bring about challenges in the development of antiviral agents. Therefore, there is an urgent necessary for patients to seek for new antiviral drugs.

Influenza Virus

Seasonal influenza-associated severe pneumonia can lead to 6–29% of substantial mortality (Oliveira et al., 2001; Murata et al., 2007; Paules and Subbarao, 2017). Influenza infection accounts for the susceptibility to pneumonia by a factor of ~100, while approximately 25% of pneumonia patients may exacerbate as continuum of the acute respiratory distress syndrome (ARDS) (Rello and Pop-Vicas, 2009; Shrestha et al., 2015). There are four pathways for IFV to trigger pneumonia, which are primary influenza pneumonia, secondary bacterial pneumonia, pneumonia due to unusual pathogens or in immunocompromised hosts, as well as deteriorations of chronic pulmonary diseases (Rothberg et al., 2008). During the 2009 pandemic, severe influenza pneumonia shapes the outcome of concurrent bacterial superinfection developed in 4–24% of cases caused by microorganisms, such as *Staphylococcus aureus*, *Chlamydia pneumoniae*, β-hemolytic *streptococci*, and *Legionella pneumophila* (Gerber et al., 1978; Miyashita and Matsushima, 2000; Johnson et al., 2008; Louie et al., 2009; Shrestha et al., 2015). Risk factors for progression to pneumonia were an absolute lymphocyte count less than 200 cells/ml besides that not receiving influenza-directed antiviral therapy (Chemaly et al., 2006). A large study examining children hospitalized with influenza from 2007 to 2015 noted that only 69% received antiviral treatment (Gavigan and McCullers, 2019).

IFV with a negative-sense, single-stranded, and segmented RNA genome belongs to the family Orthomyxoviridae, which are further classified into IFV A, B, C, and D. In previous studies, influenza A and B viruses whose highly contagious pandemic are primarily responsible for seasonally acute respiratory disease that outbreaks and spreads worldwide give rise to increased ICU admission, mortality, and a substantial economic burden. Compared with influenza B, researchers tend to be preferentially concentrated on type A, because it is generally considered the predominant type in influenza disease. However, a study elucidated that pneumonia is more likely to occur in men with a confirmed type B infection and presenting with shortness of breath (Dai et al., 2020).

Nowadays, there are 131 subtypes of A strains that have been identified in nature, based on hemagglutinin (H1-H18) and neuraminidase (N1-N11) transmembrane glycoproteins, among which A(H1N1) and A(H3N2) routinely circulate worldwide (CDC 2019b). Nevertheless, seasonal H1N1 strain had been replaced by the 2009 H1N1 pandemic strain (H1N1 pdm09), and H7N9 strain was discovered as a novel subtype in 2013. Additionally, influenza B virus is divided into two lineages: B/Yamagata and B/Victoria (Jha et al., 2020). Since the 2009 pandemic year, the primary circulating A strains have been the H1N1 pandemic strain and an H3N2 strain, whereas both the types of influenza B clades have cocirculated according to national surveillance reports (Gavigan and McCullers, 2019). The frequency of primary viral pneumonia differed among the virus-associated pneumonia subtypes (pH1N1, 80%; H3N2, 26.5%; and B, 31%) (Ishiguro et al., 2016).

In brief, two groups of antivirals are available for the treatment of influenza: the neuraminidase inhibitors (NAIs), and the virus polymerase inhibitors. Amantadine, which has been used to treat influenza for many decades, has been found to target the M2 ion channel that interferes with viral uncoating following entry into the host cell. In addition, amantadine can affect the pH regulation of vesicles involved in the transport of viral glycoproteins to the cell surface during assembly (Pinto et al., 1992). As significant rates of resistance to the adamantanes and to its 10-fold more active derivative, rimantadine, this medication is being phased out since 2005 (Monto and Arden, 1992). The hemagglutinin is a sialic acid receptor-binding molecule and mediates entry of the virus into the target cell. The neuraminidase inhibitor (and oseltamivir and zanamivir) block viruses release via cleaving the cellular-receptor sialic acid residues to which the newly formed particles are attached (Moscona 2005). If the infection is limited to one round of replication there are not enough virus particles to cause disease. However, dapivirine, an FDA-approved HIV non-nucleoside reverse transcriptase inhibitor, was found to have broad-spectrum antiviral activity against multiple strains of influenza A and B viruses (Hu et al., 2017).

Coronavirus

SARS-CoV and Middle East Respiratory Syndrome (MERS)-CoV are known as causative agents associated with high case fatality

rate, whereas the other four human coronaviruses (HCoV-NL63, HCoV-229E, HCoV-OC43, and CoV-HKU1) are mainly associated with mild, self-limiting respiratory illnesses in immunocompetent hosts. Recently, a highly contagious agent that has emerged in China, SARS-CoV-2, was incidentally discovered in the case of cluster persons with acute respiratory infection identified whose clinical features resembled those of a viral pneumonia. Together with the above coronaviruses, SARS-CoV-2 account for a global threat to public health. Coronavirus belongs to the Coronaviridae family within the order of *Nidovirale*, contains a nonsegmented, positive-sense RNA genome of approximately 30 kilobase (kb). Coronavirus has currently been subdivided into four groups—the alpha-, beta-, gamma-, delta—on the basis of phylogenetic clustering (Fehr and Perlman, 2015; Kang et al., 2020). A canonical set of four main proteins of coronavirus virions are the spike (S), membrane (M), envelope (E), and nucleocapsid (N) protein, of which the first three are located in membrane envelope and the last one found in the ribonucleoprotein. Several crystal structures have been determined for coronaviruses, and these provide attractive targets for antiviral drug design. Here, we will focus on coronaviruses infection to human host and three coronavirus SRAS, MERS, and COVID-19 are the keystone to expound.

Human Coronaviruses

Prior to 2013, HCoV strains were primarily considered possible etiological agents in CAP that replicate in the epithelial cells of the nasopharynx and induce human illnesses, not only in the common colds but also in pneumonia (Hendley et al., 1972; Kunkel and Herrler, 1993; Vabret et al., 2003). Two of human coronaviruses are classified as α-coronaviruses, HCoV-229E and HCoV-NL63, while the others are β-coronaviruses, HCoV-HKU1 and HCoV-OC43. HCoVs provide significant insights into the genetic variability and evolution among coronaviruses. HCoV-NL63 displays homology with HCoV-229E based on phylogenetic analyses (Pyrc et al., 2007). A study found that the significantly greater association of HCoVs coinfections shows a rate of severe lower respiratory tract infections greater than 60% in patients with coinfections compared to less than 10% in patients with a single infection, especially in neonates and young children, although whether the coinfection by HCoV was a factor increasing the severity of the associated viral infection remains hypothetical (Gerna et al., 2006). Most HCoV infections are not diagnosed because they cause mild, self-limited upper respiratory disease, and no specific therapy is available.

Highly Pathogenic Disease: SARS, MERS, and COVID-19

Modern society did not draw high attention to coronavirus until the SARS-CoVs outbreak. During the 2002–2003 SARS pandemic, there were 8,422 cases of SARS-CoV in 32 countries, with 916 deaths and a fatality rate of 10–15% (WHO 2003). A novel human CoV, named MERS-CoV, emerged in the Middle East in 2012, and by October 16, 2018, 2,260 confirmed cases of infection with MERS-CoV had been documented in 27 countries by the WHO and were associated with 803 deaths (WHO 2020a; Kim et al., 2021).

SARS-CoV and MERS-CoV originated from bats that infected other intermediary reservoir in closer proximity to humans. It is widely accepted that SARS-CoV stems from a number of cave-dwelling species of Chinese horseshoe bats (genus *Rhinolophus*) (Li et al., 2005a; Lau et al., 2005). Both of them are β-coronavirus that mainly invade type II pneumocytes and bronchial epithelial cells, resulting in pneumonia, but the exact mechanism of lung injury is controversial. The highly glycosylated spike protein (S) host–receptor interaction plays a major determinant of initiating virus entry into the host cells. Human angiotensin-converting enzyme 2 (ACE2) binding is a critical determinant for the host range of SARS-CoV, whereas MERS-CoV utilizes dipeptidyl peptidase 4 (DPP4) as a cellular receptor, also known as CD26 (Bang et al., 2016). This carbohydrate shield may act as a target for compounds specifically binding to sugar moieties (e.g., lectins), accordingly coating the protein and blocking the interaction with the receptor (Mbae et al., 2018).

Up to now, neither approved specific drugs nor monoclonal antibody therapies to treat these two kinds of coronavirus infections. It is well known that three cysteine proteases, papain-like protease (PL^{pro}) and 3C-like protease ($3CL^{pro}$), as well as RNA-dependent RNA polymerase (RdRp), are validated antiviral drug targets because they are the components of the coronavirus lifecycle that mediate the replicase polyproteins pp1a and pp1b (Kim et al., 2014). Although the primary functions of PL^{pro} and $3CL^{pro}$ are to process the viral polyprotein in a coordinated manner, PL^{pro} has the additional function of stripping ubiquitin and ISG15 from host-cell proteins to aid coronaviruses in their evasion of the host innate immune response. Redemsivir (GS-5734) is a promising nucleotide analogue antiviral drug developed by Gilead science (Gordon et al., 2020). The HIV protease inhibitors approved by FDA, lopinavir and ritonavir (LPV/r) compound, were thought to markedly decrease the mortality of MERS-CoV or SARS (Chan et al., 2003; De Wilde et al., 2014; Sheahan et al., 2020). HR2P peptides may target the early stage of virus entry, namely the fusion between the envelope and cell membranes, which is supported by the evidence that HR2P is a highly efficient depressor for MERS-CoV S protein-mediated cell–cell fusion and syncytium formation (Lu et al., 2014).

The virus mutation is more likely to develop severe complications from coronavirus pneumonia that requires strengthened clinical vigilance. Currently, COVID-19 has been a challenge to global public health. A novel coronavirus, named SARS-CoV-2, was discovered by deep sequencing analysis from lower respiratory tract samples. It shows that SARS-CoV-2 can bind to ACE2 receptor in humans through structural analysis (Lu et al., 2020). The future evolution, adaptation, and spread of this virus warrant urgent investigation. LPV/r is also the first anti-HIV-1 drug reported to be tried for clinical treatment of SARS-CoV-2 infection. At this time, preventive therapies for these types of novel coronaviruses are still in preclinical stages.

NATURAL PRODUCTS WITH REPORTED ACTIVITIES AGAINST VIRAL PNEUMONIA: FOCUS ON MEDICINAL PLANTS

The recent emergence of the deadly human coronavirus that causes COVID-19 is a sobering reminder that new and deadly

TABLE 1 | Medicinal plants extracts against influenza virus.

Plant species	Compound name	Extract	Strain, Subtype	Bioactivity	Assay	IC50/ EC50	SI	Positive control	References
Aloevera(L.) Burm.f.	Aloin	Purchased from SA	A/PR/8/34 (H1N1) A/WSN/33 (H1N1) A/TW/3446/02 (H3N2) B/TW/70,555/5 (influenza B) A/TW/126/09 (H1N1pdm09) A/TW/066/09 (H1N1pdm09)	Inhibited viral neuraminidase activity	Plaque	IC50: 91.83 ±18.97 μM (average value of all the tested strains)	>5.44	OTC: 25 μM	Huang et al. (2019)
Burkea africana Hook.	Oleanane-type triterpene saponins 7	Ethanol	A/Jena/8178/09 (H1N1pdm09)	Inhibited the HA (a hypothesis without verification)	CPE	IC50: 0.27 ± 0.13 μM	6	OTC: 0.064 ± 0.013 μM	Mair et al. (2018)
			A/Hong Kong/68 (H3N2)			IC50: 0.05 ± 0.02 μM	31	OTC: 0.003 ± 0.001 μM	
Bletillastriata(Thunb.) Rchb.f.	Phenanthrenes (analogs 4)	95% Ethanol	A/Sydney/5/97 (H3N2)	Inhibited matrix protein and reduced mRNA transcription; inhibited the NA	MTS	IC50: 14.6 ± 2.4 μM	5.5	OTC: 4.9 ± 0.9 μM	Shi et al. (2017a)
Canarium album (Lour.) DC.	Isocorilagin	75% Ethanol	A/Puerto Rico/8/34 (H1N1)	Interfered with replication; inhibited	MTT	IC50: 9.19 ± 1.99 μM	28.65	Peramivir: 6.48 μM	Chen et al. (2020)
			NA-H274Y (H1N1)	NA; influenced the		IC50: 4.64 ± 3.01 μM	56.75		
			A/Aichi/2/68 (H3N2)	virus release		IC50: 23.72 ± 2.51 μM	11.10		
Centipedaminima(L.) A. Braun and Asch.	Brevilin A	Supercritical fluid	A/PR/8/34 (H1N1)	Inhibited vRNA synthesis; decreased the M and NS protein expression	Plaque	EC50: 2.96 ± 1.10 μM	8	Ribavirin: 7.05 ± 1.10 μM	Zhang et al. (2019)
			A/FM/1/47 (H1N1)			EC50: 1.60 ± 1.14 μM	14	Ribavirin: 9.19 ± 1.02 μM	
			A/HongKong/498/97 (H3N2)			EC50: 3.28 ± 1.09 μM	7	Ribavirin: 10.76 ± 1.07 μM	
			A/chicken/Guangdong/ 1996 (H9N2)			EC50: 2.07 ± 1.12 μM	11	Ribavirin: 10.35 ± 1.04 μM	
Camellia sinensis (L.) Kuntze.	Theaflavin-3,3'-DG	Polyphenolic	A/PR/8/34 (H1N1)	Inhibited the NA and HA; decreased IL-6 expression	MTS	IC50:26.25 ± 6.20 μM	5.46	OTC:15.57 ± 1.73 nM	Zu et al. (2012)
			A/Sydney/5/97 (H3N2)			IC50: 10.67 ± 0.31 μM	13.43	OTC :8.88 ± 2.17 nM	
			B/Jiangsu/10/2003			IC50:42.07 ± 2.16 μM	3.41	OTC :31.60 ± 2.88 nM	
Cleistocalyx operculatus (Roxb.) Merr. and L. M. Perry	C-methylated- flavonoid	Methanol	A/PR/8/34 (H1N1)	Inhibited viral replication; affected an early stage of virus infection	Ez-Cytox	EC50: 4.9 ±0.35 μM	>24.49	Tamiflu: 2.24 ±0.15 μM	Dao et al. (2010)
Curcuma longa L.	Curcumin	Purchased from SA	A/PR/8/34 (H1N1)	Interrupted virus-cell attachment	Plaque	EC50: 0.47 ± 0.05 μM	92.5	-	Chen et al. (2020)
Dianthus superbus L.	Crude extract (quercetin and isorhamnetin were main compounds)	Butanol	A/PR/34/8 (H1N1)	Blocked viral replication	SRB	IC50: 4.97 ± 0.6 μg/ml	20.1	-	Kim et al. (2019b)
			B/LEE/40 (influenza B)			IC50:3.9 ± 0.5 μg/ml	25.4		

(Continued on following page)

TABLE 1 | (*Continued*) Medicinal plants extracts against influenza virus.

Plant species	Compound name	Extract	Strain, Subtype	Bioactivity	Assay	IC50/ EC50	SI	Positive control	References
Dianthussuperbus var.*longicalycinus*(Maxim.) F.N. Williams	Quercetin-7-O-glucoside	Methanol	A/PR/8/34 (H1N1) A/Vic/3/75 (H3N2) B/Lee/40 B/Maryland/1/59	Reduced virus-induced symptoms; blocked viral RNA polymerase PB2	SRB	IC50: 3.1 ± 0.43 μg/ml IC50: 6.61 ± 0.08 μg/ml IC50: 8.19 ± 1.14 μg/ml IC50: 5.17 ± 0.10 μg/ml	32.35 15.19 12.21 19.34	OTC: 25.4 μg/ml OTC: 22.3 μg/ml OTC: 42.2 μg/ml OTC: 35.2 μg/ml	Gansukh et al. (2016)
Embelia ribes Burm. f.	Embelin	Ethyl acetate	A/Puerto Rico/8/34 (H1N1) B/Malaysia/2506/04 (Victoria-like) A/mallard/ Pennsylvania/10218/84 (H5N2)	Prevented absorption; blocked the cell receptors	MTT	IC50: 0.3±0.1 μM IC50: 0.2±0.1 μM IC50: 0.1±0.0 μM	10 15 31	OTC: 0.16±0.01 μM OTC: 0.31±0.04 μM OTC: 0.1±0.02 μM	Hossan et al. (2018)
*Glycine*max(L.) Merr.	Daidzein Glycitein	Water	A/PR/8/34 (H1N1)	Inhibited viral adsorption and replication	MTT	IC50: 143.6 ± 78.9 μM IC50: 204.7 ± 21.0 μM	>27 >17,182	OTC: 0.628 nM	Nagai et al. (2019)
*Geraniumthunbergii*Siebold ex Lindl. and Paxton.	Geraniin	Ethanol	A/PR/8/34 (H1N1) A/Korea/33/2005 (H1N1) A/Korea/32/2005 (H3N2) B/Korea/72/2006 (influenza B)	Restricted viral replication	MTS	IC50: 27.6 μM IC50: 11.1 μM IC50: 25.8 μM IC50: 8.72 μM	-	OTC: 0.628 nM OTC: 0.338 nM OTC: 0.855 nM OTC: 10.8 nM	Choi et al. (2019)
Isatis indigotica Fortune ex Lindl.	Epiprogoitrin Progoitrin Epigoitrin Goitrin	Methanol	A/California/7/2009 (H1N1)	Disturbed viral adsorption	CCK8	IC50: 0.44 ± 0.03 μM IC50: 0.19± 0.01 μM IC50: 0.36 ± 0.02 μM IC50: 0.19± 0.02 μM	-	-	Nie et al. (2020)
Not mentioned	Berberine-piperazine derivatives (analogs BPD-13)	Sythesis	A/PR/8/34 (H1N1) A/ Vic/3/75 (H3N2) B/Lee/ 40 B/Maryland/1/5	Inhibited the NA	SRB	IC50: 35.16 ± 0.002 μg/ml IC50: 33.15 ± 0.021 μg/ml IC50: 31.35 ± 0.031 μg/ml IC50: 29.17 ± 0.081 μg/ml	110.65 117.29 123.98 133.01	OTC: 21.12 ± 0.12 μg/ml OTC: 31.75 ± 0.55 μg/ml OTC: 72.32 ± 0.066 μg/ml OTC: 65.18 ± 0.037 μg/ml	Enkhtaivan et al. (2018)
*Paeoniaalbiflora*Pall.	Pentagalloylglucose	Ethanol	A/PR/8/34 (H1N1) A/WSN/33 (H1N1) A/Hong Kong/1/68 (H3N2)	Reduced the activity of virus NA and HA	MTT	IC50: 30.6 μM IC50: 20 μM IC50: 34.8 μM	27.4 42 24 1	OTC:100 μM	Zhang et al. (2019)
Portulaca oleracea L.	Crude extract	Water	A/WSN/1933 (H1N1) A/California/07/2009 (H1N1) A/Perth/16/2009 (H3N2)	Inhibited viral attachment	MTS	EC50: 220.1μg/mL EC50: 121.6μg/mL EC50: 112.4μg/mL	36.65 66.34 71.77	-	Li et al. (2019)

(Continued on following page)

TABLE 1 | *(Continued)* Medicinal plants extracts against influenza virus.

Plant species	Compound name	Extract	Strain, Subtype	Bioactivity	Assay	IC50/ EC50	SI	Positive control	References
			A/Brisbane/10/2007 (H3N2)			EC50: 191.2μg/mL	42.19		
Rhodiola rosea L.	Kaempferol	95% Methanol	A/PR/8/34 (H1N1) A/Chicken/Korea/ MS96/96 (H9N2)	Inhibited the NA	MTT	EC50: 30.2 μM EC50: 18.5 μM	>9.93 >16.22	Tamiflu: 8.3 μM Tamiflu: 6.25 μM	Jeong et al. (2009)
*Salviaplebeia*R.Br.	Nepetin Hispidulin Rosmarinic acid methyl ester	Methanol	A/PR/8/34 (H1N1)	Inhibited the NA	MTT	EC50: 17.45 ± 0.54 μM EC50: 22.62 ± 1.79 μM EC50: 22.60 ± 2.76 μM	11.47 ± 0.37 > 8.90 ± 0.76 8.98 ± 1.23	OTC: 0.10 ± 0.02 μM	Bang et al. (2016)
Sambucus nigra L.	5,7,3′,4′-Tetra-O-methyl quercetin (±)-Dihydromyricetin	Supercritical CO2; 80% Ethanol	A/PR/8/34 (H1N1)	Bound to the viral envelope; inhibited attachment	MTT	IC50: 0.36 μM IC50: 8.7 μM	-	OTC: 0.32 μM Amantadine: 27 μM	Roschek et al. (2009)
Vitis amurensis Rupr.	Amurensin K (+)-viniferol C Trans-vitisin B	Methanol	A/California/08/2009 (H1N1) A/PR/8/34 (H1N1) H274Y mutant (Oseltamivir-resistant novel H1N1)	Suppressed the activity of influenza NA	4-MU-NANA	IC50: 14.43±1.67 μM IC50: 8.94 ± 1.06 μM IC50: 23.89 ± 2.76 μM	-	OTC: 70.88±2.90 nM OTC: 3.89±0.75 nM OTC: 12.50 ± 0.56 μM	Nguyen et al. (2011)

coronaviruses can emerge at any time and subsequently develop to become pandemics. Therefore, the continued development of therapeutic and prophylactic countermeasures to potentially deadly coronaviruses is warranted. At present, numerous bioactive constitutes targeted IFV, RSV and coronavirus have been screened and identified in the amelioration or prevention investigations of viral pneumonia. The screening procedure involves testing dilutions of the compounds against a range of viruses growing in cell cultures. Assays that a compound interferes with the proliferation of a virus might include inhibition of cytopathic effect (CPE) or of plaque formation. Selectivity and mechanism are crucial for the clinical use of antiviral drugs. Biologically, the underlying value of a compound can be assessed by the selectivity index (SI), which depends on its cytotoxic effect and antiviral activity. A compound with a low IC_{50} and a high SI is most likely to have a value as an anti-viral drug. Some cases of IC_{50} and SI values are given in **Tables 1–4**. Furthermore, the infection mechanism of these three viruses and modes of action of bioactive phytochemicals on them were shown in **Figure 1**.

Anti-Influenza Virus Agents

Recently, Nie et al. (2020) screened two pairs of enantiomers (glucosinolate isomers) isolated from *Isatis indigotica* Fortune ex Lindl. by chiral separation against influenza A virus (IAV), which among the antiviral potency of the components was in the order of progoitrin > goitrin > epigoitrin > epiprogoitrin. Elderberry (*Sambucus nigra* L.), a traditional European medicine rich in flavonoids, plays an essential role in anti-influenza and immune stimulation. Early stage of research established that two anti-influenza flavonoids isolated from elderberry fruit inhibit H1N1 infection by decreasing the ability of infecting host cells (Roschek et al., 2009). Nevertheless, quality assurance must be considered on account of unripe elderflower fruits contain a certain amount of sambunigrin, a latent toxic glycoside can release cyanide of which concentration decreases in the ripening process (Vlachojannis et al., 2010; Stuppner et al., 2020). Quercetin, a kind of natural compounds marketed as a dietary supplement, also exhibits a good performance of inhibiting virus, which frequently in daily doses of up to 1,000 mg d^{-1} exceeds usual dietary intake levels (Andres et al., 2018). An investigation carried out by Gansukh et al. elucidated that quercetin-7-O-glucoside might be useful in alleviating symptoms and pathogenesis in the host (Gansukh et al., 2016). In a later study the same team further confirmed the value to IFV of *Dianthus superbus* L. (Kim et al., 2019b). Quercetin 3-glucoside (Q3G), an analogous flavonoid obtained from the methanol extract of *D. superbus*, was the most active fraction in blocking IFV replication via a time-dependent assay (Nile et al., 2020). Specially, brevilin A and C-methylated flavonoid that were determined to be (E)-4,2′,4′-trihydroxy-6′-methoxy-3′,5′-dimethylchalcone have the similar bioactive mechanism as Q3G (Dao et al., 2010; Zhang et al., 2019).

Among plants-derived compounds, *Canarium album* (Lour.) DC. derived isocorilagin, a polyphenolic compound, showed an

TABLE 2 | Medicinal plants extracts against respiratory syncytial virus.

Plant species	Compound name	Extract	Strain, Subtype	Bioactivity	Assay	IC50/ EC50	SI	Positive control	References
Agastacherugosa(Fisch. and C.A. Mey.) Kuntze	4-Methoxycinnamaldehyde	Purchased from WAKO	Long strain	Inhibited viral attachment and internalization; increased IFN production	XTT	IC50: 0.055 μg/ml	898.2	Ribavirin : 0.3-30 μg/ ml	Wang et al. (2009)
Celastrus hindsii Benth.	2α-hydro xyabietatriene	95% Ethanol	A2 strain	Not investigated	CPE	IC50: 3.13 ± 0.90 μM	-	Ribavirin: 4.1 ± 0.66 μM	Luo et al. (2018)
	Celahin D					IC50: 1.55 ± 0.34 μM			
	Vitamin E quinone					IC50: 3.13 ± 0.43 μM			
Cimicifuga foetida L.	Cimicifugin	Purchased from Sigma-Aldrich	Long strain (in A549 cells)	Inhibited viral attachment; stimulated epithelial cells to secrete IFN-β to counteract viral infection	XTT	IC50: 5.4 μg/ ml	45.57	Ribavirin: 29.8 μg/ ml	Wang et al. (2012)
			Long strain (in HEp-2 cells)			IC50: 38.6 μg/ml	6.48	Ribavirin: 31.8 μg/ ml	
Cleistocalyx operculatus (Roxb.) Merr&L.M. Perry.	Cleistocaltones A	95% Ethanol	A2 strain	Reduced F proteins	MTT	IC50: 6.75 ± 0.75 μM	>14.81	Ribavirin: 15.00 ± 1.00 μM	Song et al. (2019)
	Cleistocaltones B					IC50: 2.81 ± 0.31 μM	9.02		
Clerodendrum trichotomum Thunb.	Acteoside	Water	rgRSV strain	Reduced replication; blocked syncytial formation	CCK8	EC50: 15.64 ± 1.07 ng/ ml	47.33	-	Chathuranga et al. (2019)
Coffea arabica L. (the source of synthetic materials)	3,4-O-dicaffeoyl-1,5-γ-quinide	Synthesis	Long strain 18537 strain	Inhibited intracellular post-entry replication step	CPE	EC50: 0.240 μM	>416	Ribavirin: 5.05 μM	Sinisi et al. (2017)
						EC50: 0.236 μM	>423		
			rgRSV strain			EC50: 0.170 μM	>588		
Commiphora gileadensis (L.) C. Chr.	Guggulsterone	Methanol	RSV B	Inhibited viral absorption	MTT	IC50: 23.31 μg/ml	10.25	-	Bouslama et al. (2019)
Delphinium ajacis L.	Ajacisine E	95% Ethanol	A2 strain	Not investigated	MTT	IC50: 10.1 ± 0.3μM	>9.9	Ribavirin: 3.1 ± 0.8 μM	Yang et al. (2017)
Euphorbia jolkinii Boiss.	Jolkinol A	Methanol	Long strain	Not investigated	CPE	IC50: 10 μM	8	Ribavirin: 6.97 μM	Huang et al. (2014)
Ficus religiosa L.	Bark crude extract	Water	A2 strain	Inhibited viral attachment	MTS	EC50: 2.23 μg/ml	84.5	Ribavirin: 6.67 μg/ ml	Cagno et al. (2015)
Forsythiasuspensa (Thunb.) Vahl.	Calceolarioside B	Ethanol	Not described	Not investigated	CPE	EC50: 3.43 μM	56.33	-	Li et al. (2014)
	Forsythoside A					EC50: 6.72 μM	34.23		
Lonicerajaponica Thunb.	Dicaffeoylquinic acid	Ethanol	Long strain	Reduced virus replication and fusion	MTS	EC50:0.068 ± 0.002 μM	>5800	Ribavirin: 3.2 μM	Ojwang et al. (2005)
Lophatherum gracile Brongn.	Isoorientin	95% ethanol	Long strain A2 strain	Triggered inflammatory reactions; inhibited replication	MTT	IC50: 3.1 ± 0.2 μg/ ml	138.7	Ribavirin: 1.6 ± 1.0 μg/ ml	Chen et al. (2019)
Narcissustazetta var.*algirus* (Pomel) Batt.	Narcissus tazetta lectin	-	Long strain	Bound to viral glycoproteins; affected the later infection phase	MTT	IC50: 2.3 μg/ ml	141.36	-	Ooi et al. (2006)
Rosmarinus officinalis L.	Carnosic acid	70% Ethanol	A2 strain (in A549 cells)	Inhibited NS2 and G protein RNA synthesis; affected viral factors	MTT	IC50: 6.51 μg/ ml	20.09	-	Shin et al. (2013)
			A2 strain (in HEp-2 cells)			IC50: 6.71 μg/ ml	-		
			B/KR strain				-		

(Continued on following page)

TABLE 2 | (*Continued*) Medicinal plants extracts against respiratory syncytial virus.

Plant species	Compound name	Extract	Strain, Subtype	Bioactivity	Assay	IC50/ EC50	SI	Positive control	References
						No numerical value			
Scheffleraheptaphylla (L.) Frodin.	3,5-Di-O-caffeoylquinic acid 3,4-Di-O-caffeoylquinic acid	60% Ethanol	Long strain	Blocked virus-cell fusion; inhibited replication cycle at the late phase	MTT	IC50: 1.16 μM IC50: 2.23 μM	1116 500	Ribavirin: 36.7	Li et al. (2005b)
Smilax glabra Roxb.	Mannose-binding lectin	Saline	Not described	Not investigated	CPE	EC50: 8.1 μM	-	Ribavirin: 12.5 μM	Ooi et al. (2006)
Wikstroemia indica (L.) C. A. Mey.	Daphnoretin	Ethanol	Long strain	Reduced the PKC pool to affect fusion; inhibited viral replication at the later infection phase	MTT	IC50: 5.87 μg/ ml	28.17	Ribavirin: 3.05 μg/ ml	Ho et al. (2010)
Wikstroemia indica (L.) C. A. Mey.	Genkwanol B Genkwanol C Stelleranol	Ethanol	Long strain	Inhibited viral replication cycle	MTT	IC50: 9.6 μM IC50: 6.6 μM IC50: 10.2 μM	11.0 21.9 15.8	Ribavirin: 21.6 μM	Huang et al. (2010)
Wikstroemia indica (L.) C.A.Mey	Sekikaic acid	Ethyl acetate	rgRSV strain A2 strain	Inhibited viral replication at a post-entry step	MTT	IC50: 5.69 μg/ ml IC50: 7.73 μg/ ml	5.46 4.02	Ribavirin: 1.20 ± 0.45 μg/ ml -	Lai et al., (2013)
Youngia japonica (L.) DC.	Dicaffeoylquinic acid	95% Ethanol	Long strain	Affected the early stage of viral replication	CPE	IC50: 0.5 μg/ ml	>200	Ribavirin: 2.5 μg/ ml	Ooi et al. (2006)

antiviral activity against diverse influenza A strains by targeting NA with low cytotoxic effects against host cells (Chen et al., 2020). Furthermore, *Canarium album* (Lour.) DC. is widely used as a medicinal and edible plant with characteristics of safe and economic. Taken together, isocorilagin promises to be a highly effective, reliable, and affordable neuraminidase inhibitor against a range of IAV strains. *Portulaca oleracea* L. water extract was able to alleviate the symptoms of pandemic IAV infection. Further mechanistic studies revealed that it clearly inhibited the virus-cells attachment and exerted good virucidal activity, significantly reducing the viral load within 10 min (Li et al., 2019). Geraniin displayed high antiviral activity against influenza A and B strains, by inhibiting NA activity following viral infection in MDCK cells (Choi et al., 2019). The OECD 423 acute oral toxicity test carried out by a team demonstrated that geraniin was safe for human consumption with the no-observed-adverse-effect level of geraniin being below 2000 mg kg^{-1}, while that of geraniin-enriched extract was more than 2000 mg kg^{-1} (Moorthy et al., 2019). Embelin are well known for their antiviral properties exhibiting a strong inhibitory effect on influenza replication, in particular the strain B, with the lowest IC_{50} value of 0.2 ± 0.1 μM (Hossan et al., 2018).

A further example of a plant-derived natural product is nepetin, a methanolic extract originated from aerial parts of *Salvia plebeia* R.Br. provides noteworthy candidates for further investigation of novel NA inhibitors in the future (Bang et al., 2016). Huang et al. (2019) conducted a study to investigate the efficacy of aloin, which is contained in *Aloe vera* (L.) Burm.f., to reduce virus load in the lungs. Yet, it is worth noting that aloin was reported to be the most toxic in all the compounds of *A. vera*, and related institutions have introduced the safety usage guideline on recommending acceptable amounts of aloin in pharmaceuticals and food (Kaparakou et al., 2021). Since 2002, the FDA has suggested that it should not exceed 10 mg L^{-1} aloin in *A. vera* products when used as food or as a dietary supplement. As part of an ongoing anti-influenza screening project on natural products, eight oligostilbenes were isolated as active principles from the methanol extract of *Vitis amurensis* Rupr. among which (+)-viniferol C and amurensin K showed the excellent antiviral activity (Nguyen et al., 2011). Daidzein and glycitein, two active compounds isolated from Glycine max (L.) Merr., demonstrated excellent antiviral activity, among which the latter was firstly reported with anti-IFV effect (Nagai et al., 2019). Different compounds derived from *Burkea africana* Hook. and *Bletilla striata* (Thunb.) Rchb.f. have been identified for their role against H3N2 strains (Shi et al., 2017b; Mair et al., 2018). Moreover, *Rhodiola rosea* L. and black tea commonly used plants as ethnomedicine in China for infectious diseases, and exhibited IFV proliferation at low concentrations (Mukhtar et al., 2008; Jeong et al., 2009; Zu et al., 2012).

It shows a natural product derivative or conjugate against IFV in the overview. The anti-influenza activities of berberine-piperazine derivatives (BPD) were evaluated in the range from 35.16 μg/ml to 90.25 μg/ml of the IC_{50} along with cytotoxicity level which was observed in the range 44.8 μg/ml to 3,890.6 μg/ml of CC_{50} toward MDCK cells (Enkhtaivan et al., 2018).

TABLE 3 | Medicinal plants extracts against coronavirus.

Plant species	Compound name	Extract	Cell lines	Strain, Subtype	Bioactivity	Assay	IC50/ EC50	SI	Positive control	References
Alnus japonica (Thunb.) Steud.	Hirsutenone	Ethanol	-	SARS-CoV	Inhibit PL^{pro}	RLRGG-AMC	IC50: 4.1±0.3 μM	-	-	Park et al. (2012a)
Artemisiacarvifolia Buch. -Ham. ex Roxb.	Arteether	Purchased from market	Vero E6	SARS-CoV-2	Reduced viral NP protein; blocked viral infection at the post-entry level; inhibited viral RNA and protein	CCK8	EC50: 31.86 ± 4.72 μM	>6.42 ± 0.95 >3.13 ± 1.14 >3.11 ± 0.12 >4.03 ± 0.15 =5.10 ± 2.08 =7.00 ± 0.76 >4.40 ±0.61	-	Cao et al. (2020)
	Artemether						EC50: 73.80 ± 26.91 μM			
	Arteminsinin						EC50: 64.45 ± 2.58 μM			
	Artmisone						EC50: 49.64 ± 1.85 μM			
	Artesunate						EC50: 12.98 ± 5.3 μM			
	Lumefantrine						EC50: 10.28 ± 1.12 μM			
	Arteannuin B						EC50: 23.17 ± 3.22 μM			
Boesenbergiarotunda (L.) Mansf.	Pandurantin A	95% EtOH	Vero E6	SARS-CoV-2	Inhibited at both pre-entry and postinfection phase	MTT	IC50: 0.81 μM	18.16	-	Kanjanasirirat et al. 2020,
	Hydroxychloroquin						IC50: 5.08 μM	>19.68		
Bupleurum chinense DC.	Saikosaponin A	Purchased from Sigma Chemical	MRC-5	HCoV-229E	Inhibited viral attachment	XTT	EC50: 8.6 ± 0.3 μM	26.6	Actinomycin D: 0.02 μM	Cheng et al. (2006)
	Saikosaponin B_2						EC50: 1.7 ± 0.1 μM	221.9		
	Saikosaponin C						EC50: 19.9 ± 0.1 μM	19.2		
	Saikosaponin D						EC50: 13.2 ± 0.3 μM	13.3		
Comus officinalis Siebold and Zucc.	Savinin Betulonic acid	Ethyl acetate	Vero E6	SARS-CoV	Inhibited PL^{pro} and $3CL^{pro}$	MTT	EC50: 1.13 μM	>667	Niclosamide: <0.1 μM	Wen et al. (2007)
							EC50: 0.63 μM	180	*Valinomycin: 1.63 μM*	
Echinaceapurpurea (L.) Moench.	Standardized preparation (caftaric acid and cichoric acid were main compounds)	65% Alcoholic	Vero E6	HCoV-299E	Interacted with virions; inhibited replication	MTT	IC50: 3.2 μg/ml	-	-	Signer et al. (2020)
Euphorbia neriifolia L.	3β-friedelanol	Ethanol	MRC-5	HcoV-229E	Induced cell death	XTT	5 μg/ml	-	0.02 μg/ml	Chang et al. (2012)
Forsythia suspensa (Thunb.) Vahl	Phillyrin	Purchased from market	Vero E6 Huh-7	SARS-CoV-2 HcoV-229E	Regulated host immune response	MTT	IC50: 63.90 μg/ml	30.66	-	Ma et al. (2020)
							IC50: 64.53 μg/ml	16.02		
Glycyrrhizauralensis Fisch.	Glycyrrhizic acid	Purchased from commercial suppliers	MASMCS 16HBE	SARS-CoV-2 S protein	Blocked the binding between the RBS and ACE2	MTT SPR	IC50: 22 μM	>4.55	-	Yu et al. (2020)
Glycyrrhiza uralensis Fisch.	Glycyrrhizin	Purchased from market	Vero E6	SARS-CoV	Induced nitrous oxide synthase and viral replication	MTT	EC50: 300±51 mg/L	>67	Pyrazofurin: 4.2 ± 0.57 mg/L 6-azauridine: 16.8 ± 2.9 mg/L	Cinatl et al. (2003)
Lithospermumerythrorhizon Siebold and Zucc.	Shikonin	Not described	Vero E6	SARS-CoV-2	Inhibited $3CL^{pro}$	CCK8	IC50:15.75 ± 8.22 μM	-	Ebselen: 0.67 ± 0.09 μM	Jin et al. (2020)
Lycorisradiata (L'Hér.) Herb.	Lycorine	Purchased from MicroSource Discovery Systems	LLC-MK2	HCoV-OC43	Suppressed viral replication	MTT	EC50: 0.15 μM	29.13	-	Shen et al. (2019)
Not mentioned	Resveratrol	Purchased from Sigma-Aldrich	Vero E6	HcoV-229E SARS-CoV-2	Not investigated	MTT	EC50: 4.6 μM	45.65	Lopinavir/ritonavir: 8.8 μM Chloroquine: 5.0 μM	Pasquereau et al. (2021)
							EC50: 10.66 μM	4.52		
Polygonum cuspidatum Siebold and Zucc.	Resveratrol	Not described	Vero E6	MERS-CoV	Prolonged cellular survival; inhibited replication targeted N; blocked NF-κB pathway	MTT	125-250 μM	-	-	Lin et al. (2017)

(Continued on following page)

TABLE 3 | (*Continued*) Medicinal plants extracts against coronavirus.

Plant species	Compound name	Extract	Cell lines	Strain, Subtype	Bioactivity	Assay	IC50/EC50	SI	Positive control	References
Psychotrialpecacuanha (Brot.) Standl.	Emetine	Purchased from MicroSource Discovery Systems	Vero E6	MERS-CoV	Inhibited viral entry and replication	MTT	EC50: 0.34 μM	9.06	-	Shen et al. (2019)
Psoralea corylifolia L.	Isobavachalcone	Ethanol	-	SARS-CoV	Inhibited PL^{pro}	Z-RLRGG-AMC	IC50: 7.3 ± 0.8 μM	-	-	Kim et al. (2014)
	Psoralidin						IC50: 4.2 ± 1.0 μM	-		
Rheumpalmatum L.	Emodin	Water	Vero E6	SARS-CoV	Inhibited the interaction of viral S protein and cell receptor ACE2	MTT	IC50: 200 μM	-	Promazine	Ho et al. (2007)
Sambucusformosana Nakai.	Caffeic acid	Purchased from Sigma-Aldrich	LLC-MK2	HcoV-NL63	Blocked viral attachment; Inhibited viral replication	MTT	IC50: 3.54 μM	>141	-	Weng et al. (2019)
Salvia miltiorrhiza Bunge.	Tanshinone I	Ethanol	-	SARS-CoV	Inhibited PL^{pro}	LXGG-AMC	IC50: 0.7 μM	-	-	Park et al. (2012b)
Stephania tetrandra S. Moore	Bis-benzylisoquinoline alkaloids-tetrandrine	Purchased from Wuhan ChemFaces Biochemical	MRC-5	HcoV-OC43	Suppressed viral replication; inhibited S and N protein	MTS	IC50: 0.33 ± 0.03 μM	40.19	-	Kim et al. (2019a)
	Fangchinoline						IC50: 1.01 ± 0.07 μM	11.46		
	Cepharanthine						IC50: 0.83 ± 0.07 μM	13.63		

Anti-Respiratory Syncytial Virus Agents

Generally rational drug use for different CAPs is summarized in **Table 2**. Many medicinal plants have been reported to treat animals and people who suffer from RSV-related pneumonia. Caffeoylquinic acids (CQAs) are a broad class of secondary metabolites that have been found in esculent and medicinal plants from various families. Accumulated evidence demonstrated that CQAs have a wide range of biological activities including antiviral effects. One such example is dicaffeoylquinic acid, respectively isolated from *Lonicera japonica* Thunb. and *Youngia japonica* (L.) DC., which produced obvious anti-RSV activity that is better than that of ribavirin (Ojwang et al., 2005; Ooi et al., 2006). A caffeoylquinic acid derivative, namely 3,5-Di-Ocaffeoylquinic acid purified from Schefflera heptaphylla, could inhibit RSV with IC50 at 1.16 μM (Li et al., 2005b). Although CQAs have increased interest for using as antiviral therapeutics, the reports of their safety pharmacological effects are limited.

4-Methoxycinnamaldehyde, an active constituent of *Agastache rugosa* (Fisch. and C.A. Mey.) Kuntze, could suppress viral entrance by interfering viral attachment (IC_{50} of 0.06 mg/ml) and internalization (IC_{50} of 0.01 mg/ml). The compound significantly increased the basal production of IFN, but not the virus-induced IFN production (Wang et al., 2009). In a later study Wang's team also found that a major compound of *Cimicifuga foetida* L., namely cimicifugin, possessed inhibitory activity against RSV through suppressing viral attachment and internalization (Wang et al., 2012). Yet for all that, the potential risk existing in administrating cimicifuga plants cannot be reckoned with, particularly the severe hepatotoxicity. It has been reported that in two cases patients developed fulminant hepatic failure due to the use of this herbal remedy (Levitsky et al., 2005; Chow et al., 2008). Therefore, safety consideration should be retained as a high priority for novel drugs cimicifuga therapeutics in the early stages of development and clinical trials (Guo et al., 2017). A compound 19 (jolkinii A) of *Euphorbia jolkinii* Boiss. displayed significant anti-RSV activity, with an IC_{50} value of 10 μM and an SI of 8.0 (Huang et al., 2014). In recent years, Chathuranga et al. (2019) also suggested that extracts of *E. jolkinii* could provide a potential source of antiviral candidate against RSV infection. In his investigation, oral inoculation with each herb extract obviously improved viral clearance in the lungs of BALB/c mice. Two novel phloroglucinol-terpenoid adducts (Cleistocaltones A and B) as the anti-RSV test compounds reduced the expression of RSV F proteins and showed IC_{50} values of 6.75 ± 0.75 μM and 2.81 ± 0.31 μM, respectively, and were isolated from the buds of *Cleistocalyx operculatus* (Roxb.) Merr. and Perry (Song et al., 2019).

A study of isoorientin provides a convincing and powerful support for the traditional use of *Lophatherum gracile* Brongn. in the RSV-related diseases treatment (Chen et al., 2019). Following the probit analysis of brine shrimp lethality assay, the LD_{50} values of isoorientin were calculated to be more than 1000 μg/ml compared to cytotoxic lignan podophyllotoxin with 2.79 μg/ml. It could be effective if isoorientin was to be treated as safe drugs, of which high LD_{50} values indicated very low general toxicity

(Kumarasamy et al., 2004). Other glycosides, such as calceolarioside B, genkwanol C, were also discovered as anti-RSV agents (Huang et al., 2010; Li et al., 2014). Bouslama et al. (2019) have put forward a number of possible mechanisms whereby guggulsterone may exert their antiviral action. They suggested that the antiviral activity in guggulsterones probably derives from the steps involving recognition and binding to specific receptors. The antiviral composition of essential acid of *Rosmarinus officinalis* L. suppressed the replication of HRSV and viral gene expression without inducing type-I interferon production or affecting cell viability in viral suspension tests (Shin et al., 2013). Two lectins, mannose-binding lectin and narcissus tazetta lectin, were isolated from *Smilax glabra* Roxb. and *Narcissus tazetta* L., respectively. Both of them have the function of broad-spectrum antivirus, including RSV and IFV. The virus was also susceptible to a crude water extract (Saponins/Carbohydrate/Tannins) from *Ficus religiosa* L. bark (Cagno et al., 2015).

Three terpenoids 2α-hydroxyabietatriene, celahin D, and vitamin E quinone showed inhibitory activity on reverse transcriptase activity with an IC_{50} of approximately 3.13 μM. In the contrast, celahin D showed the lower one compared to three compounds (Luo et al., 2018). Further isolation of *Wikstroemia indica* (L.) C.A. Mey. fraction led to a purified compound, daphnoretin. It was found to have anti-RSV activity using CPE assay, with an IC_{50} value of 5.87 mg/ml and an SI value of 28.17 (Ho et al., 2010). *W. indica* is thought to be poisonous; there are adverse effects that can be caused, including dizziness, nausea, vomiting, and diarrhea. Therefore, too much inhalation and skin contact are not allowed when processing, grinding, and decocting (Li et al., 2009). Sheng-Ma-Ge-Gen-Tang (SMGGT) has been used to treat pediatric viral infection and one of the most effective medicine herbs is *Cimicifuga foetida* L., which could be useful for preventing and managing viral infection by stimulating IFN-β (Wang et al., 2012; Feng Yeh et al., 2013).

Anti-Coronavirus Agents

There are several medicinal plants that treat for three kinds of HCoVs. Recently, the present results indicated that saikosaponin B_2 and 3β-friedelanol both have potent natural drugs against HCoV-229E *in vitro* and that their modes of action possibly involve interference in the early stages of viral replication, such as absorption and penetration of the virus (Cheng et al., 2006; Chang et al., 2012). The bis-benzylisoquinoline alkaloids tetrandrine, fangchinoline, together with cepharanthine, which are particularly high in *Stephania tetrandra* S. Moore and other related species of Menispermaceae, dramatically suppressed the replication of HCoV-OC43 and inhibited expression of protein S and N (Kim et al., 2019a). One research showed that Sambucus javanica Blume. stem ethanol extract displayed potential anti-HCoV-NL63 activity; caffeic acid could be the vital component with anti-HCoV-NL63 activity via interfering the binding interaction of HCoV-NL63 with heparan sulfate proteoglycans (co-receptor) and ACE2 (receptor) on cell surface (Weng et al., 2019).

Renowned as polyphenolic phytoalexin with a wide range of biological properties, resveratrol (3,5,4'-trans-trihydroxystilbene) administration spans a large spectrum of areas, especially the prevention and treatment of viral diseases. It has been shown, in the present study against coronavirus, that resveratrol demonstrated the important impact on anti-HCoV-229E and anti-SARS-CoV-2 compared to LPV/r and chloroquine (Pasquereau et al., 2021). In addition, cohort clinical trials that document the efficacy, safety, and pharmacokinetics provided evidence that the side effects of resveratrol are mild and sporadic compared with its overwhelming health benefits (Sedlak et al., 2018; Galiniak et al., 2019; Singh et al., 2019). Therefore, resveratrol could be a promising candidate to further use in a clinical testing in fighting COVID-19.

As a pivotal enzyme of mediating replication and transcription in coronaviruses, $3CL^{pro}$ has become a magnet for new drugs target. Shikonin exhibited promising antiviral activity by targeting $3CL^{pro}$ (Jin et al., 2020). Nevertheless, it needs to be carefully used. In an acute toxicity study, the median lethal dose (LD_{50}) was calculated to be 20 mg/kg in mice, while the median lethal concentration (LC_{50}) was 16 mg/kg in rabbits. Echinaforce®, a standardized 65% alcoholic extracted from freshly harvested *Echinacea purpurea* (L.) Moench., has been reported to inhibit enveloped respiratory viruses including influenza A and B, RSV, or parainfluenza virus through neutralization with whole virions and related proteins. In the current study, Signer et al. found that four human coronaviruses were also inhibited when exposed to Echinaforce®, among which HCoV-229E was irreversibly inactivated at 3.2 μg/ml IC_{50} (Signer et al., 2020).

Glycyrrhizic acid, a nontoxic broad-spectrum that is derived from *Glycyrrhiza uralensis* Fisch., also provides new insights into developing anti-coronavirus therapy. In light of surface plasmon resonance (SPR) assays and NanoBit assay, disrupting the interaction the binding between the S proteins RBD and ACE2 could be a mechanism of glycyrrhizic acid (ZZY-44) to exhibit virucidal activity against SARS-CoV-2 (Yu et al., 2020). The researcher has performed a high-content screening investigation for the antiviral candidates and identified that rhizomes of *Boesenbergia rotunda* (L.) Mansf. and its bioactive compound panduratin A exert the inhibitory effect against SARS-CoV-2 infection at both pre-entry and postinfection phases (Kanjanasirirat et al., 2020). Meanwhile, treatment with this compound was able to restrain viral infectivity in human airway epithelial cells.

As we all know, *Artemisia annua* L. was an ancient Chinese herb widely applied in clinical therapeutics on account of multiple pharmacological properties, particularly in antimalarial activities. Recently, a cluster of compounds derived from this plant were revealed to exhibit inhibitory effects against SARS-CoV-2. Among nine artemisinin-related constituents, arteannuin B that acted at the post-entry step of SARS-CoV-2 showed the most prominent antiviral potential with an EC_{50} of 10.28 ± 1.12 μM. Artesunate and dihydroartemisinin, which could be clinically achieved in plasma after intravenous administration, had similar EC_{50} values of 12.98 ± 5.30 μM and 13.31 ± 1.24 μM, respectively (Cao et al., 2020). There are several antiviral ingredients in *Forsythia suspensa* (Thunb.) Vahl., of which phillyrin (KD-1) is the most representative. According to

TABLE 4 | Molecular docking results of influenza virus, respiratory syncytial virus, and coronavirus.

Plant species	Compound name	Virus Type	Binding Subunit	PDB Code	Affinity (kcal/mol)	Residues	Positive(kcal/mol)	Software	References
Anethum graveolens L.	Quercetin	SARS-CoV-2	3CLpro	6LU7	−8.17 −8.47	His164, Glu166, Asp187, Gln192, Thr190	Nelfinavir : −10.72 Lopinavir : −9.41	Autodock 4.2	Khaerunnisa et al. (2020)
Allium cepa L. *Cocos nucifera* L.	Oleanolic acid Progesterone Stigmasterol Fucosterol	SARS-CoV-2	3CLpro	6W63	−9.2 −8.4 −9.4 −9.1	Cys145, Met49, Met165, Leu167, Pro168 Gly143, Gln192, Thr190, Met165 Met165, Met49, Cys44, Cys145, His41 Met49, Met165, Leu167, Pro168, His41, Cys145	Remdesivir: -7.6	AutoDock 4.2	Fitriani et al. (2020)
Camellia sinensis (L.) Kuntze.	Thearbigin Quercetin-3-O-rutinoside	SARS-CoV-2	3CLpro	6LU7	−8.5 −7.5	Glu166, Asn142, Met165, Cys145 Glu166, Leu141, Gly143, Asn142	-	ParDock	Upadhyay et al. (2020)
Chrysanthemum cinerariifolium (Trevir.) Sch.Bip.	Rutin Schaftoside Apigenin-6,8-di-C-β-D-galactoside	RSV	N	4UCC	−8.49 −8.18 −7.29	Glu128, Glu112, Arg132, Asp152, Arg150 Glu144, Arg132, Glu128, Lys110, Asp152 Arg132, Glu112, Glu128, Lys110, Lys46	1-[(2,4-dichlorophenyl) methyl] pyrazole-3,5-dicarboxylic acid: -5.95	Maestro 9.3	Kant et al. (2018)
Coffea arabica L. (the source of synthetic materials)	Berberine-piperazine derivatives	Influenza A Virus (H3N8)	NA	4WA4	−8.2	Ala432, Arg116, Arg150, Ser178, Ile221, Trp177	OTC: -6.1	AutoDock Vina	Enkhtaivan et al. (2018)
Dianthus superbus var. *monticola Makino*	Quercetin-7-O-glucoside	Influenza A Virus	PB2	4NCE	−9.1	Ser321, Ser324, Arg332, His342, Met431, Lys376, Glu361, His357, Phe323, Phe404	m^7GTP: -7.5	AutoDock Vina	Gansukh et al. (2016)
Dianthus superbus L.	Quercetin 3-rutinoside Quercetin 3-rhamnoside 7-rhamnoside Kaempferol 3-glucoside-Glucoside 7-rhamnoside	Influenza A virus (pdmH1N109)	PA	4AWM	−9.8 −9.7 −8.9	Not described	-	AutoDock Vina	Kim et al. (2019b)
Dianthus superbus L.	Quercetin 3-glucoside	Influenza A virus (H3N2)	PB2	4NCE	−8.0	Arg355, Arg332, Lys376, Ile354, Met431, Phe323, Phe363, Phe404, Asn429	GTP: -7.0	AutoDock Vina	Nile et al. (2020)
Embelia ribes Burm.f.	Embelin	Influenza A Virus (H5N2)	HA	5E30	−5.2	Glu190, Arg193, Ser227, Gly228, Tyr98, Val135	α-2,6 linked terminal sialic acids (SAs): -6.2	AutoDock Vina	Hossan et al. (2018)
Geranium thunbergia Siebold ex Lindl. & Paxton	Geraniin	Influenza A Virus (H1N1pdm09)	NA	3TI6	−9.9	Arg225, Glu227	OTC: -6.6	AutoDock Vina	Choi et al. (2019)
Glycyrrhiza uralensis Fisch	Liquiritigenin	Influenza Virus	NA	4B7N	−7.05	Arg118, Ile149, Arg368, Ser400, Ile427, Pro431, Lys432	-	AutoDock	Sathya et al. (2019)
Laminaria japonica Aresch.	Dieckol	SARS-CoV	3CLpro	2ZU5	−11.51	Thr190, His63, Ser144, Cys145, His41	-	AutoDock 3.0.5	Park et al. (2013)
Not mentioned	Quercetin-3-β-galactoside	SARS-CoV	3CLpro	1UK4	−9.24	Leu141, Asn142, Met165, Glu166, Gln189	-	DOCK4.0	Cheng et al. (2006)
Not mentioned	Aloe-emodin + (-) Epicatechin Rhein Withanolide D Withanolide A	SARS-CoV-2	3CLpro	6LU7	−7.4 −7.6 −8.1 −7.8 −7.7	Not mentioned Not mentioned Ile106, Gln110, Thr29, Thr111, Phe294, Asp295 Lys102, Phe103, Val104, Arg105, Ile106 Phe294, Thr292, Asp295, Asp153, Ser158	Nelfinabir: -8.4	Swiss Dock	Chandel et al. (2020)

(Continued on following page)

TABLE 4 | (*Continued*) Molecular docking results of influenza virus, respiratory syncytial virus, and coronavirus.

Plant species	Compound name	Virus Type	Binding Subunit	PDB Code	Affinity (kcal/mol)	Residues	Positive(kcal/mol)	Software	References
Not mentioned	Hypericin Cepharanthine	SARS-CoV	NSP12-NSP8	6NUR	−8.3 −7.9	-	Nilotinib: -8.4 Tegobuvir: -8.4	Autodock Vina	Ruan et al. (2021)
Not mentioned	Cepharanthine Hypericin Berberine	SARS-CoV-2	NSP12-NSP8	7BW4	−8.6 −8.2 −7.8	Arg215, Leu155, Val225	-	AutoDock Vina	Ruan et al. (2021)
Olea Europaea L.	Luteolin-7-glucoside	SARS-CoV-2	3CLpro	6LU7	−8.17 −8.47	Phe140, Cys145, His163, His164, Thr190	Nelfinavir : -10.72 Lopinavir : -9.41	Autodock 4.2	Khaerunnisa et al. (2020)
Radix Paeoniae Alba.	Gallic acid	Influenza A virus (H1N1)	NA	3CKZ	−5.7	Arg152, Glu227	-	AutoDock Vina	Zhang et al., 2020
Rapanea melanophloeos (L.) Mez	Quercetin-3-O-α-L-rhamnopyranoside	Influenza Virus	M2 NA	2KQT 3TI6	−10.81 −10.47	Ala30, Ile33, Val27 Asp151, Asn347, Ile149	Rimantadine: -5.51 OTC: -7.06	Glide	Mehrbod et al. (2019)
Spinacia oleracea L.	Kaempferol	SARS-CoV-2	3CLpro	6LU7	−8.58	Tyr54, His164, Glu166, Apr187, Thr190	Nelfinavir : -10.72 Lopinavir : -9.41	Autodock 4.2	Khaerunnisa et al. (2020)
Torreya nucifera (L.) Siebold and Zucc.	Amentoflavone	SARS-CoV	3CLpro	223E	−11.42	His163, Leu141, Gln189, Val186, Cys145, His41	Apigenin: -7.79	Autodock 3.0.5	Ryu et al., 2010b
*Tripterygiumwilfordii*Hook. f.	Iguesterin	SARS-CoV	3CLpro	1UK4	−9.97	Cys44, Thr25	-	Autodock 3.0.5	Ryu et al. (2010a)
Veratrumsabadilla Retz.	Sabadinine	SARS-CoV	3CLpro	Not mentioned	−11.6	His44, Cys144	-	AutoDock Vina	Toney et al. (2004)

research conducted by Yang's group, KD-1 not merely reduced replication of SARS-CoV-2 and HCoV-229E *in vitro*, but also markedly downregulated proinflammatory cytokines by the way of suppressing the NF-κB signaling pathway.

Tanshinone I, a flavonoid compound purified from the medicinal plant *Salvia miltiorrhiza* Bunge., acted as time-dependent inhibitors of PL^{pro}, and furthermore exhibited the most potent nanomolar level inhibitory activity toward deubiquitinating (IC_{50} = 0.7 μM) (Park et al., 2012b). So far, the safety of tanshinone I is still under studies, whereas tanshinone IIA was observed to show severe growth inhibition, development malformation, and cardiotoxicity at high concentrations in the zebrafish normal embryos assay (Wang et al., 2017). The same author produced other studies on SARS-CoV therapeutics, compared to the former, hirsutenone isolated from *Alnus cremastogyne* Burkill. displayed good SARS-CoV PL^{pro} inhibitory activities (Park et al., 2012a). 8â-hydroxyabieta-9(11), 13 dien-12-one, and savinin demonstrated significant activity against SARS-CoVs with higher sensitivity index of above 510 from *Cornus officinalis* Siebold and Zucc. (Wen et al., 2007). The *Rheum palmatum* L. and *Glycyrrhiza uralensis* Fisch. were found to contain flavonoid emodin and glycyrrhizin, respectively, which inhibited attachment to the host cells and induced nitrousoxide synthase (Cinatl et al., 2003; Ho et al., 2007). As for their toxicity, cohort genotoxic studies have elucidated that glycyrrhizin is neither teratogenic nor mutagenic and may have properties of anti-genotoxic under the certain conditions; nonetheless, being continuously exposed to glycyrrhizin compounds at high concentration it can produce hypermineralocorticoid-like effects in both animals and humans (Isbrucker and Burdock, 2006). Another compound emodin has been proven to possess laxative effects leading to melanosis, but only at very high doses, for example, 1–3 g/kg/d for mice (Sougiannis et al., 2021). High dose of emodin can also result in mutagenic or hepatotoxicity by blocking the UGT1A1 enzyme activity (Wang et al., 2016). Kim's group isolated two compounds against SARS-CoVs, isobavachalcone and psoralidin, displaying good SARS-CoV PL^{pro} inhibitory activities (Kim et al., 2014). Psoralidin is a nontoxic but low oral bioavailability compound (Sharifi-Rad et al., 2020).

These seem to be promising compounds from some new research on MERS-CoVs. Lin et al. (2017) found that N protein that is necessary for MERS-CoVs replication was decreased after resveratrol therapeutics. Furthermore, resveratrol could downregulate the apoptosis caused by MERS-CoVs *in vitro*. Lycorine and Emetine also showed the high activity against MERS-CoVs with low IC_{50} of 1.63 and 0.34 μM, respectively (Shen et al., 2019).

ADVANCED STRATEGIES ON SCREENING EXTRACTS AGAINST CAPS

High-throughput screening (HTS) is a fragment-based screening product of multidisciplinary integration, which is one of the most active techniques in areas of medical science in

recent years. It ties merits of efficient, generally applicable, automatic, and high specificity in a particularly computational way that is superior to the conventional method and offers a new powerful tool for candidate drugs broad-spectrum screening. There are two key features to handle compounds with HTS: miniaturization and automation. In miniaturization, it has a standard format plate and each of these wells is another experiment which even can do 1,536 experiments on a single plate. Then, HTS executes the process on the microplate with automated operating systems and analyzes and processes the experimental data via detection instrument and software algorithm. Commonly, scintillation proximity assay and fluorescence assay are widely used in screening. A quenched fluorescence resonance energy transfer assay was developed to evaluate the activity of $3CL^{pro}$ in the presence of 50,000 small drug-like molecules on a fully automated system. In secondary studies, it remained five novel molecules that exhibited inhibitory activity (IC_{50} = 0.5–7.0 μM) toward $3CL^{pro}$ through a series of virtual and experimental filters (Blanchard et al., 2004).

The screening model is also critical for HTS, especially in recognizing the interaction between drugs and molecular targets and the basic mechanism of drug. At present, these models mainly focus on receptors, channels, and various cellular responses. The majority of the HTS virology assays follow a standard paradigm, which are cell-based, phenotypic screens designed to identify antiviral compounds with a broad range of mechanisms (Wen et al., 2019; Chojnacka et al., 2020). Wen et al. (2019) have succeeded in establishing an automated plaque reduction neutralization assay to determine neutralization titers of anti-RSV antibodies that allow simultaneous titration of a large number of samples in a shorter time. This higher throughput automatic counting method proved to produce more precise and reliable titers than current methods, which greatly benefit drug/vaccine candidate screening.

A cell-based HTS assay was reported to search for inhibitors of IFV. In this study, the authors set up 293T cell lines that constitutively synthesize negative strand RNA, which expresses Gaussia luciferase upon IVA infection, for which 2000 small molecules screening and 17 compounds exhibited 90–100% inhibition of luminescence signal for a rate of 0.85% (Gao et al., 2014). Another similar study used the HTS platform based on vRNA promoter luciferase reporter plasmid to identify three medicinal plants that could significantly inhibit promoter transcription activity due to the procyanidin (Dai et al., 2012).

Virtual Screening

Virtual screening encompasses all sorts of computational techniques that allow cutting a huge virtual library to a more manageable size (Walters et al., 1998). Nowadays, a large scale of algorithms offer strategies and show their unique advantages to work out modern structure-based drug designing problems because of the diversity in both their accuracy and computational speed.

Molecular docking is one of the most extensively used computational approaches, whereby large virtual libraries of chemical compounds are shrunk in size to a manageable subset, and place of the putative "ligands" into the appropriate site that creation of a negative image of the target site, ultimately 'score' their potential complementarity to binding sites (Kuntz, 1992). Characterization of the binding behavior plays a significant role in rational design of drugs and in the elucidation of the fundamental biochemical process. Nevertheless, there still remain some awkward issues urgently needed to be addressed, especially with regard to current scoring schemes. At present, nine docking programs, namely, AutoDock, Flex, Fred, Glide, Gold, Slide, Surflex, and QXP, have been widely tested to evaluate their potency in drug discovery applications (Kellenberger et al., 2004; Kitchen et al., 2004).

Some cases of screening potential antiviral compounds with molecular docking have been summarized in **Table 4**.

Network Pharmacology

As bioinformatics moves far ahead, systems biology and pharmacology can be thought of as a promising network-based approach toward more effective drug development (Jia, et al., 2009; Schadt et al., 2009). Network pharmacology highlights a paradigm shift from the current "one target, one drug" strategy to a novel version of the "network target, multi-components" strategy (Li and Zhang, 2013). Network-based drug discovery is regarded as a potential method toward more cost-effective drug development with the rapid progress. From the perspective of systems biology, system pharmacology can map the "disease-target-drug" to the network level, and screen for the lead compound through further calculation, analysis, and modeling, observe the intervention and influence of drugs on the network.

The introduction of "networks" in drug discovery, including assessments of network topology and dynamics, provides a quantifiable description of complicate systems and its response to a variety of herbal treatments. One of the greatest strengths of pharmacological network is that facilitating the discovery of new drugs mechanism from static and dynamic aspects respectively. A visual toolbox has provided the interaction relationship that integrates various information, including drugs, genes, targets, diseases, and other information in an abstract way (Hopkins, 2008). In the network composed of multiple levels, the element components shape into nodes, and the interaction forms into the connection between nodes. Common tools widely used to analyze the necessary information include in the field of TCMID research, Cytoscape, GUESS, Pajek, and VisANT (Xue, et al., 2013; Zhou et al., 2020b). As far as research on effective drugs targeting coronavirus, Zhou et al. presented a study that prioritized 16 potential anti-SARS-CoV/SARS-CoV-2 repurposable drugs that are further validated by enrichment analyses of drug–gene signatures and CoV-induced transcriptomics data in human cell lines based on a poly-pharmacology network platform that quantifies the outcomes between the virus–host interaction and drug targets in the PPI network (Zhou et al., 2020a).

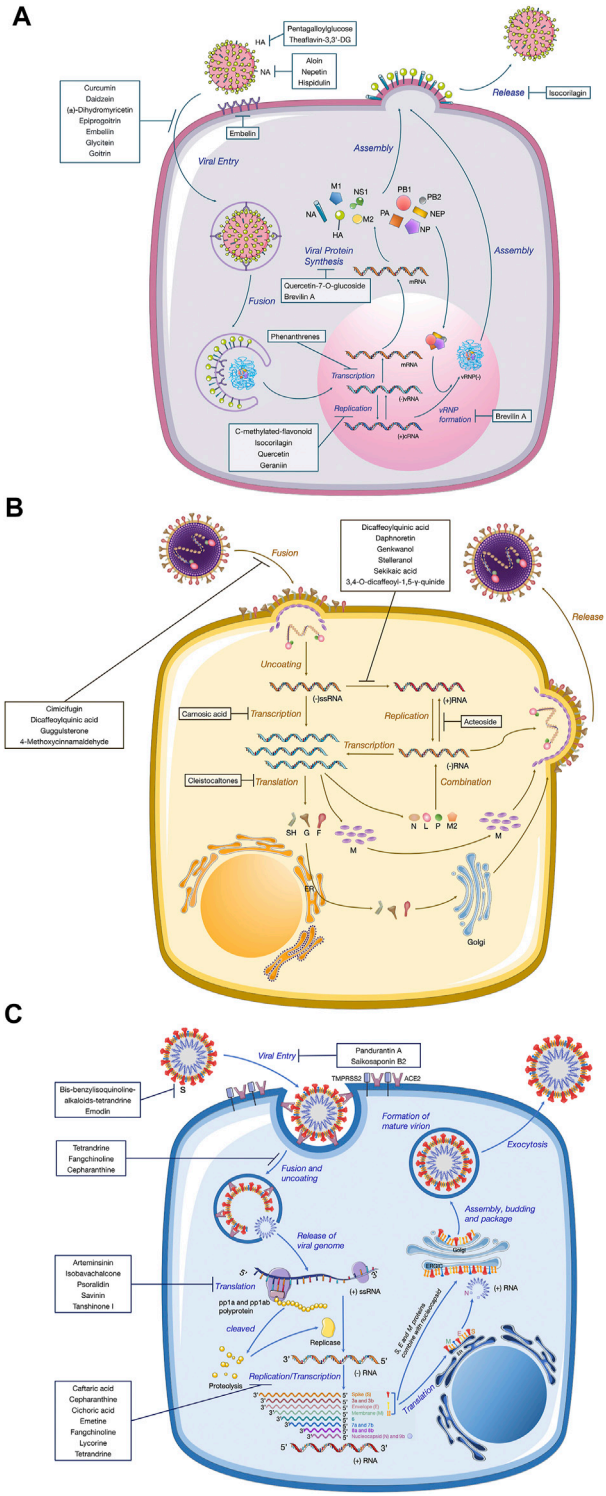

FIGURE 1 | Replication mechanisms of three different kinds of virions. A diagram of the viral lifecycle of **(A)** influenza virus, **(B)** respiratory syncytial virus, and **(C)** coronavirus, indicating where each therapeutic exerts antiviral activity. The therapeutic targets of natural products derived from medicinal plants are shown in bold.

Given the crisis in commercial translation, network pharmacology offers a new framework on how to innovate drug discovery, and thus it is an idea whose time has come, yet such strategies are at present a minority activity in the pharmaceutical industry.

CONCLUSION AND FUTURE PROSPECTS

Large cohort studies have provided direct evidence that viruses represent a common cause of CAP and three types of viruses IFVs, RSVs, and CoVs should be the most responsible for this. Vaccination is now the primary strategy for virus epidemic. Nonetheless, drug therapy is still the critical approach for CAPs in patients on account of antigenic shift. Few drugs are now approved by FDA administered during this viral infection and symptoms remission from severe CAPs. RSV infections in high-risk young children and newborns have been prevented successfully with palivizumab and Ribavirin. For IFVs, two classes of agents are internationally accredited agents for treatment, namely the adamantanes and neuraminidase inhibitors. However, the former lost their potency over time due to the rapid occurrence of drug resistances. Until now, there are no miracle drugs as therapeutic for HCoVs. The characteristics on novel coronavirus are as follows: 1) it becomes more transmissible than SARS-CoV; 2) the pathogenicity is heavier than influenza, but lighter than SARS; and 3) the detoxification time is longer. Hence, it is urgently necessary to develop target drugs to lead the response to a global public health emergency result from frequently mutational viruses like the case of SARS-CoV-2.

Naturally based pharmacotherapy plays a profound role in the treatment of viral pneumonia and, indeed, most of plant secondary metabolites and their derivatives also have a desired effect on antivirus activity. This overview used SciFinder® and PubMed to search for any article published between 2003 and 2020 that is relevant to plant-derived natural products for the prevention and treatment of viral pneumonia, in particular those caused by three types of virus that we focus on. A total of 62 types of compounds were summarized and classified in the tables. Of note, quercetins and flavonoids are phytochemicals of plant origin which have known antiviral properties to diminish the replication of many viruses like IFV and RSV.

While plaque assays are the standard tools to measure infectious virus, the methodology is time-consuming and requires experience in recognizing plaques (Wen et al., 2019). The assays are also prone to variation among analysts due to plaque recognition and manual counting errors. Here, we introduce three different advanced methods and offer a new mentality on screening antiviral drug with high effect and low toxicity. Based on HTS technology, a pharmacologically quantitative analysis is used in tandem with the established cell model to identify compounds that bind to target proteins and are thus potential new drugs. Another virtual screening method has provided a tool to enhance basic scientific research that promoted drug discovery projects, resulting in marketed pharmaceutical products. Through molecular docking, a series of

small molecules, including natural compounds, have been screened and confirmed to directly inhibit these important proteins in SARS or MERS coronavirus. Network pharmacology analysis is generally followed by molecular docking. This approach can provide information with drug–protein interaction.

Owing to the side effects of synthetic medicine, researchers turn to herbal remedies for accessible and economical treatment of viral diseases, which comparatively bear fewer chances of toxicity and resistance.

AUTHOR CONTRIBUTIONS

ZH: Writing–original draft, Writing–review and editing. XS: Writing–review and editing, funding acquisition. JL, TC, JC, and YL: Data collection and editing. ZHE: Project administration, supervision, writing–review and editing, funding acquisition.

FUNDING

This work was supported by the Natural Science Foundation of the Education Department of Guangdong Province (2020KZDZX1172), National Natural Science Foundation of China (NSFCs: 31670360, 81973293 and U1702286), Shenzhen Fundamental Research Plan (JCYJ 20170818094217688), Natural Science Foundation of SZU 860/000002110131, Shenzhen Peacock Plan Project (827/000569), and Guangdong Province Regional Joint Fund (2019B1515120029 and 2020A1515111169).

SUPPLEMENTARY MATERIAL

The Supplementary Material for this article can be found online at: https://www.frontiersin.org/articles/10.3389/fphar.2021.630834/full#supplementary-material

REFERENCES

Anderson, L. J., Hierholzer, J. C., Tsou, C., Hendry, R. M., Fernie, B. F., Stone, Y., et al. (1985). Antigenic Characterization of Respiratory Syncytial Virus Strains with Monoclonal Antibodies. *J. Infect. Dis.* 151, 626–633. doi:10.1093/infdis/151.4.626

Andres, S., Pevny, S., Ziegenhagen, R., Bakhiya, N., Schäfer, B., Hirsch-Ernst, K. I., et al. (2018). Safety Aspects of the Use of Quercetin as a Dietary Supplement. *Mol. Nutr. Food Res.* 62, 1700447. doi:10.1002/mnfr.201700447

Arabi, Y. M., Fowler, R., and Hayden, F. G. (2020). Critical Care Management of Adults with Community-Acquired Severe Respiratory Viral Infection. *Intensive Care Med.* 46, 315–328. doi:10.1007/s00134-020-05943-5

Bang, S., Quy Ha, T. K., Lee, C., Li, W., Oh, W.-K., and Shim, S. H. (2016). Antiviral Activities of Compounds from Aerial Parts of Salvia Plebeia R. Br. *J. Ethnopharmacology* 192, 398–405. doi:10.1016/j.jep.2016.09.030

Blanchard, J. E., Elowe, N. H., Huitema, C., Fortin, P. D., Cechetto, J. D., Eltis, L. D., et al. (2004). High-throughput Screening Identifies Inhibitors of the SARS Coronavirus Main Proteinase. *Chem. Biol.* 11, 1445–1453. doi:10.1016/j.chembiol.2004.08.011

Bonnet, D., Schmaltz, A. A., and Feltes, T. F. (2005). Infection by the Respiratory Syncytial Virus in Infants and Young Children at High Risk. *Cardiol. Young* 15, 256–265. doi:10.1017/s1047951105000545

Borchers, A. T., Chang, C., Gershwin, M. E., and Gershwin, L. J. (2013). Respiratory Syncytial Virus-A Comprehensive Review. *Clinic Rev. Allerg Immunol.* 45, 331–379. doi:10.1007/s12016-013-8368-9

Bouslama, L., Kouidhi, B., Alqurashi, Y. M., Chaieb, K., and Papetti, A. (2019). Virucidal Effect of Guggulsterone Isolated from Commiphora Gileadensis. *Planta Med.* 85, 1225–1232. doi:10.1055/a-1014-3303

Cagno, V., Civra, A., Kumar, R., Pradhan, S., Donalisio, M., Sinha, B. N., et al. (2015). Ficus Religiosa L. Bark Extracts Inhibit Human Rhinovirus and Respiratory Syncytial Virus Infection *In Vitro*. *J. Ethnopharmacology* 176, 252–257. doi:10.1016/j.jep.2015.10.042

Cantan, B., Luyt, C.-E., and Martin-Loeches, I. (2019). Influenza Infections and Emergent Viral Infections in Intensive Care Unit. *Semin. Respir. Crit. Care Med.* 40, 488–497. doi:10.1055/s-0039-1693497

Cao, R., Hu, H., Li, Y., Wang, X., Xu, M., Liu, J., et al. (2020). Anti-SARS-CoV-2 Potential of Artemisinins *In Vitro*. *ACS Infect. Dis.* 6, 2524–2531. doi:10.1021/acsinfecdis.0c00522

CDC (2018). Mortality in the United States, 2018. Available at: https://www.cdc.gov/nchs/products/databriefs/db355.html ((Accessed August 29, 2020).

CDC (2019a). Pneumonia Can Be Prevented-Vaccines Can Help. Available at: https://www.cdc.gov/pneumonia/prevention.html (Accessed August 29, 2020).

CDC (2019b). Types of Influenza Viruses. Available at: https://www.cdc.gov/flu/about/viruses/types.html (Accessed August 29, 2020).

Chan, K. S., Lai, S. T., Chu, C. M., Tsui, E., Tam, C. Y., Wong, M. M. L., et al. (2003). Treatment of Severe Acute Respiratory Syndrome with Lopinavir/ritonavir: a Multicentre Retrospective Matched Cohort Study. *Hong Kong Med. J.* 9, 399–406.

Chang, F.-R., Yen, C.-T., El-Shazly, M., Lin, W.-H., Yen, M.-H., Lin, K.-H., et al. (2012). Anti-human Coronavirus (Anti-HCoV) Triterpenoids from the Leaves of Euphorbia Neriifolia. *Nat. Product. Commun.* 7, 1415–1417. doi:10.1177/1934578x1200701103

Chathuranga, K., Kim, M. S., Lee, H.-C., Kim, T.-H., Kim, J.-H., Gayan Chathuranga, W. A., et al. (2019). Anti-respiratory Syncytial Virus Activity of Plantago Asiatica and Clerodendrum Trichotomum Extracts *In Vitro* and *In Vivo*. *Viruses* 11, 604. doi:10.3390/v11070604

Chemaly, R. F., Ghosh, S., Bodey, G. P., Rohatgi, N., Safdar, A., Keating, M. J., et al. (2006). Respiratory Viral Infections in Adults with Hematologic Malignancies and Human Stem Cell Transplantation Recipients. *Medicine (Baltimore)* 85, 278–287. doi:10.1097/01.md.0000232560.22098.4e

Chen, F., Yang, L., Huang, Y., Chen, Y., Sang, H., Duan, W., et al. (2020). Isocorilagin, Isolated from Canarium Album (Lour.) Raeusch, as a Potent Neuraminidase Inhibitor against Influenza A Virus. *Biochem. Biophysical Res. Commun.* 523, 183–189. doi:10.1016/j.bbrc.2019.12.043

Chen, L.-F., Zhong, Y.-L., Luo, D., Liu, Z., Tang, W., Cheng, W., et al. (2019). Antiviral Activity of Ethanol Extract of Lophatherum Gracile against Respiratory Syncytial Virus Infection. *J. Ethnopharmacology* 242, 111575. doi:10.1016/j.jep.2018.10.036

Cheng, P.-W., Ng, L.-T., Chiang, L.-C., and Lin, C.-C. (2006). Antiviral Effects of Saikosaponins on Human Coronavirus 229E *In Vitro*. *Clin. Exp. Pharmacol. Physiol.* 33, 612–616. doi:10.1111/j.1440-1681.2006.04415.x

Choi, J.-G., Kim, Y. S., Kim, J. H., and Chung, H.-S. (2019). Antiviral Activity of Ethanol Extract of Geranii Herba and its Components against Influenza Viruses via Neuraminidase Inhibition. *Sci. Rep.* 9, 12132. doi:10.1038/s41598-019-48430-8

Chojnacka, K., Witek-Krowiak, A., Skrzypczak, D., Mikula, K., and Młynarz, P. (2020). Phytochemicals Containing Biologically Active Polyphenols as an Effective Agent against Covid-19-Inducing Coronavirus. *J. Funct. Foods* 73, 104146. doi:10.1016/j.jff.2020.104146

Chow, E. C. Y., Teo, M., Ring, J. A., and Chen, J. W. (2008). Liver Failure Associated with the Use of Black Cohosh for Menopausal Symptoms. *Med. J. Aust.* 188 (7), 420–422. doi:10.5694/j.1326-5377.2008.tb01691.x

Cinatl, J., Morgenstern, B., Bauer, G., Chandra, P., Rabenau, H., and Doerr, H. (2003). Glycyrrhizin, an Active Component of Liquorice Roots, and Replication of SARS-Associated Coronavirus. *The Lancet* 361, 2045–2046. doi:10.1016/s0140-6736(03)13615-x

Dai, J., Wang, G., Li, W., Zhang, L., Yang, J., Zhao, X., et al. (2012). High-throughput Screening for Anti-influenza A Virus Drugs and Study of the Mechanism of Procyanidin on Influenza A Virus-Induced Autophagy. *J. Biomol. Screen.* 17, 605–617. doi:10.1177/1087057111435236

Dai, Z., Fan, K., Zhang, L., Yang, M., Yu, Q., Liu, L., et al. (2020). Risk Factors for Influenza B Virus-Associated Pneumonia in Adults. *Am. J. Infect. Control.* 48, 194–198. doi:10.1016/j.ajic.2019.07.010

Dao, T.-T., Tung, B.-T., Nguyen, P.-H., Thuong, P.-T., Yoo, S.-S., Kim, E.-H., et al. (2010). C-Methylated Flavonoids fromCleistocalyx Operculatusand Their Inhibitory Effects on Novel Influenza A (H1N1) Neuraminidase. *J. Nat. Prod.* 73, 1636–1642. doi:10.1021/np1002753

De Wilde, A. H., Jochmans, D., Posthuma, C. C., Zevenhoven-Dobbe, J. C., van Nieuwkoop, S., Bestebroer, T. M., et al. (2014). Screening of an FDA-Approved Compound Library Identifies Four Small-Molecule Inhibitors of Middle East Respiratory Syndrome Coronavirus Replication in Cell Culture. *Antimicrob. Agents Chemother.* 58, 4875–4884. doi:10.1128/AAC.03011-14

Ebbert, J. O., and Limper, A. H. (2005). Respiratory Syncytial Virus Pneumonitis in Immunocompromised Adults: Clinical Features and Outcome. *Respiration* 72, 263–269. doi:10.1159/000085367

Enkhtaivan, G., Kim, D. H., Park, G. S., Pandurangan, M., Nicholas, D. A., Moon, S. H., et al. (2018). Berberine-piperazine Conjugates as Potent Influenza Neuraminidase Blocker. *Int. J. Biol. Macromolecules* 119, 1204–1210. doi:10.1016/j.ijbiomac.2018.08.047

Fehr, A. R., and Perlman, S. (2015). Coronaviruses: an Overview of Their Replication and Pathogenesis. *Methods Mol. Biol.* 1282, 1–23. doi:10.1007/978-1-4939-2438-7_1

Feltes, T. F., Cabalka, A. K., Meissner, H. C., Piazza, F. M., Carlin, D. A., Top, F. H., et al.for the Cardiac Synagis Study Group (2003). Palivizumab Prophylaxis Reduces Hospitalization Due to Respiratory Syncytial Virus in Young Children with Hemodynamically Significant Congenital Heart Disease. *J. Pediatr.* 143, 532–540. doi:10.1067/s0022-3476(03)00454-2

Feng Yeh, C., Chih Wang, K., Chai Chiang, L., Shieh, D. E., Hong Yen, M., and San Chang, J. (2013). Water Extract of Licorice Had Anti-viral Activity against Human Respiratory Syncytial Virus in Human Respiratory Tract Cell Lines. *J. Ethnopharmacology* 148, 466–473. doi:10.1016/j.jep.2013.04.040

Fodha, I., Vabret, A., Bouslama, L., Leroux, M., Legrand, L., Dina, J., et al. (2008). Molecular Diversity of the Aminoterminal Region of the G Protein Gene of Human Respiratory Syncytial Virus Subgroup B. *Pathologie Biologie* 56, 50–57. doi:10.1016/j.patbio.2007.06.001

Galiniak, S., Aebisher, D., and Bartusik-Aebisher, D. (2019). Health Benefits of Resveratrol Administration. *Acta Biochim. Pol.* 66, 13–21. doi:10.18388/abp.2018_2749

Gansukh, E., Kazibwe, Z., Pandurangan, M., Judy, G., and Kim, D. H. (2016). Probing the Impact of Quercetin-7-O-Glucoside on Influenza Virus Replication Influence. *Phytomedicine* 23, 958–967. doi:10.1016/j.phymed.2016.06.001

Gao, Q., Wang, Z., Liu, Z., Li, X., Zhang, Y., Zhang, Z., et al. (2014). A Cell-Based High-Throughput Approach to Identify Inhibitors of Influenza A Virus. *Acta Pharmaceutica Sinica B* 4, 301–306. doi:10.1016/j.apsb.2014.06.005

Gavigan, P., and McCullers, J. A. (2019). Influenza. *Curr. Opin. Pediatr.* 31, 112–118. doi:10.1097/MOP.0000000000000712

Gerber, G. J., Farmer, W. C., and Fulkerson, L. L. (1978). Beta-hemolytic Streptococcal Pneumonia Following Influenza. *Jama-Journal Am. Med. Assoc.* 240, 242–243. doi:10.1001/jama.240.3.242

Gerna, G., Campanini, G., Rovida, F., Percivalle, E., Sarasini, A., Marchi, A., et al. (2006). Genetic Variability of Human Coronavirus OC43-, 229E-, and NL63-like Strains and Their Association with Lower Respiratory Tract Infections of Hospitalized Infants and Immunocompromised Patients. *J. Med. Virol.* 78, 938–949. doi:10.1002/jmv.20645

Gomez, R. S., Guisle-Marsollier, I., Bohmwald, K., Bueno, S. M., and Kalergis, A. M. (2014). Respiratory Syncytial Virus: Pathology, Therapeutic Drugs and Prophylaxis. *Immunol. Lett.* 162, 237–247. doi:10.1016/j.imlet.2014.09.006

Gordon, C. J., Tchesnokov, E. P., Feng, J. Y., Porter, D. P., and Götte, M. (2020). The Antiviral Compound Remdesivir Potently Inhibits RNA-dependent RNA Polymerase from Middle East Respiratory Syndrome Coronavirus. *J. Biol. Chem.* 295, 4773–4779. doi:10.1074/jbc.AC120.013056

Guo, Y., Yin, T., Wang, X., Zhang, F., Pan, G., Lv, H., et al. (2017). Traditional Uses, Phytochemistry, Pharmacology and Toxicology of the Genus Cimicifuga : A Review. *J. Ethnopharmacology* 209, 264–282. doi:10.1016/j.jep.2017.07.040

Hendley, J. O., Fishburne, H. B., and Gwaltney, J. M. (1972). Coronavirus Infections in Working Adults. Eight-Year Study with 229 E and OC 43. *Am. Rev. Respir. Dis.* 105, 805–811. doi:10.1164/arrd.1972.105.5.805

Heron, M. (2019). *Deaths: Leading Causes for 2017*. National Vital Statistics Reports. 68. Hyattsville, MD, USA: National Center for Health Statistics.

Ho, T., Wu, S., Chen, J., Li, C., and Hsiang, C. (2007). Emodin Blocks the SARS Coronavirus Spike Protein and Angiotensin-Converting Enzyme 2 Interaction. *Antiviral Res.* 74, 92–101. doi:10.1016/j.antiviral.2006.04.014

Ho, W.-S., Xue, J.-Y., Sun, S. S. M., Ooi, V. E. C., and Li, Y.-L. (2010). Antiviral Activity of Daphnoretin Isolated from Wikstroemia Indica. *Phytother. Res.* 24, 657–661. doi:10.1002/ptr.2935

Hopkins, A. L. (2008). Network Pharmacology: the Next Paradigm in Drug Discovery. *Nat. Chem. Biol.* 4, 682–690. doi:10.1038/nchembio.118

Hossan, M. S., Fatima, A., Rahmatullah, M., Khoo, T. J., Nissapatorn, V., Galochkina, A. V., et al. (2018). Antiviral Activity of Embelia Ribes Burm. F. Against Influenza Virus *In Vitro*. *Arch. Virol.* 163, 2121–2131. doi:10.1007/s00705-018-3842-6

Hu, Y., Zhang, J., Musharrafieh, R. G., Ma, C., Hau, R., and Wang, J. (2017). Discovery of Dapivirine, a Nonnucleoside HIV-1 Reverse Transcriptase Inhibitor, as a Broad-Spectrum Antiviral against Both Influenza A and B Viruses. *Antiviral Res.* 145, 103–113. doi:10.1016/j.antiviral.2017.07.016

Huang, C.-S., Luo, S.-H., Li, Y.-L., Li, C.-H., Hua, J., Liu, Y., et al. (2014). Antifeedant and Antiviral Diterpenoids from the Fresh Roots of Euphorbia Jolkinii. *Nat. Prod. Bioprospect.* 4, 91–100. doi:10.1007/s13659-014-0009-3

Huang, C.-T., Hung, C.-Y., Hseih, Y.-C., Chang, C.-S., Velu, A. B., He, Y.-C., et al. (2019). Effect of Aloin on Viral Neuraminidase and Hemagglutinin-specific T Cell Immunity in Acute Influenza. *Phytomedicine* 64, 152904. doi:10.1016/j.phymed.2019.152904

Huang, W., Zhang, X., Wang, Y., Ye, W., Ooi, V. E., Chung, H., et al. (2010). Antiviral Biflavonoids from Radix Wikstroemiae (Liaogewanggen). *Chin. Med.* 5, 23. doi:10.1186/1749-8546-5-23

Hussain, M., Galvin, H., Haw, T. Y., Nutsford, A., and Husain, M. (2017). Drug Resistance in Influenza A Virus: the Epidemiology and Management. *Infect. Drug Resist.* 10, 121–134. doi:10.2147/IDR.S105473

Isbrucker, R. A., and Burdock, G. A. (2006). Risk and Safety Assessment on the Consumption of Licorice Root (Glycyrrhiza sp.), its Extract and Powder as a Food Ingredient, with Emphasis on the Pharmacology and Toxicology of Glycyrrhizin. *Regul. Toxicol. Pharmacol.* 46, 167–192. doi:10.1016/j.yrtph.2006.06.002

Ishiguro, T., Takayanagi, N., Kanauchi, T., Uozumi, R., Kawate, E., Takaku, Y., et al. (2016). Clinical and Radiographic Comparison of Influenza Virus-Associated Pneumonia Among Three Viral Subtypes. *Intern. Med.* 55, 731–737. doi:10.2169/internalmedicine.55.5227

Jeong, H. J., Ryu, Y. B., Park, S.-J., Kim, J. H., Kwon, H.-J., Kim, J. H., et al. (2009). Neuraminidase Inhibitory Activities of Flavonols Isolated from Rhodiola Rosea Roots and Their *In Vitro* Anti-influenza Viral Activities. *Bioorg. Med. Chem.* 17, 6816–6823. doi:10.1016/j.bmc.2009.08.036

Jha, B. K., Pandit, R., Jha, R., and Manandhar, K. D. (2020). Overview of Seasonal Influenza and Recommended Vaccine during the 2016/2017 Season in Nepal. *Heliyon* 6, e03304. doi:10.1016/j.heliyon.2020.e03304

Jia, J., Zhu, F., Ma, X., Cao, Z. W., Li, Y. X., and Chen, Y. Z. (2009). Mechanisms of Drug Combinations: Interaction and Network Perspectives. *Nat. Rev. Drug Discov.* 8, 111–128. doi:10.1038/nrd2683

Jin, Z., Du, X., Xu, Y., Deng, Y., Liu, M., Zhao, Y., et al. (2020). Structure of Mpro from SARS-CoV-2 and Discovery of its Inhibitors. *Nature* 582, 289–293. doi:10.1038/s41586-020-2223-y

Johnson, A.-W. B. R., Osinusi, K., Aderele, W. I., Gbadero, D. A., Olaleye, O. D., and Adeyemi-Doro, F. A. B. (2008). Etiologic Agents and Outcome Determinants of Community-Acquired Pneumonia in Urban Children: a Hospital-Based Study. *J. Natl. Med. Assoc.* 100, 370–385. doi:10.1016/s0027-9684(15)31269-4

Kang, S., Peng, W., Zhu, Y., Lu, S., Zhou, M., Lin, W., et al. (2020). Recent Progress in Understanding 2019 Novel Coronavirus (SARS-CoV-2) Associated with Human Respiratory Disease: Detection, Mechanisms and Treatment. *Int. J. Antimicrob. Agents* 55, 105950. doi:10.1016/j.ijantimicag.2020.105950

Kanjanasirirat, P., Suksatu, A., Manopwisedjaroen, S., Munyoo, B., Tuchinda, P., Jearawuttanakul, K., et al. (2020). High-content Screening of Thai Medicinal Plants Reveals Boesenbergia Rotunda Extract and its Component Panduratin A as Anti-SARS-CoV-2 Agents. *Sci. Rep.* 10, 19963. doi:10.1038/s41598-020-77003-3

Kaparakou, E. H., Kanakis, C. D., Gerogianni, M., Maniati, M., Vekrellis, K., Skotti, E., et al. (2021). Quantitative Determination of Aloin, Antioxidant Activity, and

Toxicity of Aloe Vera Leaf Gel Products from Greece. *J. Sci. Food Agric.* 101, 414–423. doi:10.1002/jsfa.10650

Kellenberger, E., Rodrigo, J., Muller, P., and Rognan, D. (2004). Comparative Evaluation of Eight Docking Tools for Docking and Virtual Screening Accuracy. *Proteins* 57, 225–242. doi:10.1002/prot.20149

Kim, D. H., Park, G. S., Nile, A. S., Kwon, Y. D., Enkhtaivan, G., and Nile, S. H. (2019b). Utilization of Dianthus Superbus L and its Bioactive Compounds for Antioxidant, Anti-influenza and Toxicological Effects. *Food Chem. Toxicol.* 125, 313–321. doi:10.1016/j.fct.2019.01.013

Kim, D., Min, J., Jang, M., Lee, J., Shin, Y., Park, C., et al. (2019a). Natural Bis-Benzylisoquinoline Alkaloids-Tetrandrine, Fangchinoline, and Cepharanthine, Inhibit Human Coronavirus OC43 Infection of MRC-5 Human Lung Cells. *Biomolecules* 9, 696. doi:10.3390/biom9110696

Kim, D. W., Seo, K. H., Curtis-Long, M. J., Oh, K. Y., Oh, J.-W., Cho, J. K., et al. (2014). Phenolic Phytochemical Displaying SARS-CoV Papain-like Protease Inhibition from the Seeds of Psoralea Corylifolia. *J. Enzyme Inhib. Med. Chem.* 29, 59–63. doi:10.3109/14756366.2012.753591

Kim, J. W., Mistry, B., Shin, H. S., and Kang, S. S. (2021). Anti-biofilm Activity of N-Mannich Bases of Berberine Linking Piperazine against Listeria Monocytogenes. *Food Control* 121, 107668. doi:10.1016/j.foodcont.2020.107668

Kitchen, D. B., Decornez, H., Furr, J. R., and Bajorath, J. (2004). Docking and Scoring in Virtual Screening for Drug Discovery: Methods and Applications. *Nat. Rev. Drug Discov.* 3, 935–949. doi:10.1038/nrd1549

Kumarasamy, Y., Byres, M., Cox, P. J., Delazar, A., Jaspars, M., Nahar, L., et al. (2004). Isolation, Structure Elucidation, and Biological Activity of Flavone 6-C-Glycosides from Alliaria Petiolata. *Chem. Nat. Compd.* 40, 122–128. doi:10.1023/b:Conc.0000033926.72396.41

Künkel, F., and Herrler, G. (1993). Structural and Functional Analysis of the Surface Protein of Human Coronavirus OC43. *Virology* 195, 195–202. doi:10.1006/viro.1993.1360

Kuntz, I. D. (1992). Structure-based Strategies for Drug Design and Discovery. *Science* 257, 1078–1082. doi:10.1126/science.257.5073.1078

Lau, S. K. P., Woo, P. C. Y., Li, K. S. M., Huang, Y., Tsoi, H.-W., Wong, B. H. L., et al. (2005). Severe Acute Respiratory Syndrome Coronavirus-like Virus in Chinese Horseshoe Bats. *Proc. Natl. Acad. Sci.* 102, 14040–14045. doi:10.1073/pnas.0506735102

Lee, N., Lui, G. C. Y., Wong, K. T., Li, T. C. M., Tse, E. C. M., Chan, J. Y. C., et al. (2013). High Morbidity and Mortality in Adults Hospitalized for Respiratory Syncytial Virus Infections. *Clin. Infect. Dis.* 57, 1069–1077. doi:10.1093/cid/cit471

Levitsky, J., Alli, T. A., Wisecarver, J., and Sorrell, M. F. (2005). Fulminant Liver Failure Associated with the Use of Black Cohosh. *Dig. Dis. Sci.* 50, 538–539. doi:10.1007/s10620-005-2470-7

Li, C., Dai, Y., Zhang, S.-X., Duan, Y.-H., Liu, M.-L., Chen, L.-Y., et al. (2014). Quinoid Glycosides from Forsythia Suspensa. *Phytochemistry* 104, 105–113. doi:10.1016/j.phytochem.2014.04.010

Li, S., and Zhang, B. (2013). Traditional Chinese Medicine Network Pharmacology: Theory, Methodology and Application. *Chin. J. Nat. Medicines* 11, 110–120. doi:10.1016/s1875-5364(13)60037-0

Li, W., Shi, Z. L., Yu, M., Ren, W. Z., Smith, C., Epstein, J. H., et al. (2005a). Bats Are Natural Reservoirs of SARS-like Coronaviruses. *Science* 310, 676–679. doi:10.1126/science.1118391

Li, Y.-H., Lai, C.-Y., Su, M.-C., Cheng, J.-C., and Chang, Y.-S. (2019). Antiviral Activity of Portulaca Oleracea L. Against Influenza A Viruses. *J. Ethnopharmacology* 241, 112013. doi:10.1016/j.jep.2019.112013

Li, Y.-M., Zhu, L., Jiang, J.-G., Yang, L., and Wang, D.-Y. (2009). Bioactive Components and Pharmacological Action of Wikstroemia Indica (L.) C. A. Mey and its Clinical Application. *Curr. Pharm. Biotechnol.* 10, 743–752. doi:10.2174/138920109789978748

Li, Y., But, P. P. H., and Ooi, V. E. C. (2005b). Antiviral Activity and Mode of Action of Caffeoylquinic Acids from Schefflera Heptaphylla (L.) Frodin. *Antiviral Res.* 68, 1–9. doi:10.1016/j.antiviral.2005.06.004

Lin, S.-C., Ho, C.-T., Chuo, W.-H., Li, S., Wang, T. T., and Lin, C.-C. (2017). Effective Inhibition of MERS-CoV Infection by Resveratrol. *BMC Infect. Dis.* 17, 144. doi:10.1186/s12879-017-2253-8

Louie, J. K., Acosta, M., Winter, K., Jean, C., Gavali, S., Schechter, R., et al. (2009). Factors Associated with Death or Hospitalization Due to Pandemic 2009 Influenza A(H1N1) Infection in California. *Jama* 302, 1896–1902. doi:10.1001/jama.2009.1583

Lu, L., Liu, Q., Zhu, Y., Chan, K.-H., Qin, L., Li, Y., et al. (2014). Structure-based Discovery of Middle East Respiratory Syndrome Coronavirus Fusion Inhibitor. *Nat. Commun.* 5, 3067. doi:10.1038/ncomms4067

Lu, R., Zhao, X., Li, J., Niu, P., Yang, B., Wu, H., et al. (2020). Genomic Characterisation and Epidemiology of 2019 Novel Coronavirus: Implications for Virus Origins and Receptor Binding. *The Lancet* 395, 565–574. doi:10.1016/s0140-6736(20)30251-8

Luo, D., Xiong, S., Li, Q.-G., Jiang, L., Niu, Q.-W., He, L.-J., et al. (2018). Terpenoids from the Stems of Celastrus Hindsii and Their Anti-RSV Activities. *Fitoterapia* 130, 118–124. doi:10.1016/j.fitote.2018.08.018

Ma, Q., Li, R., Pan, W., Huang, W., Liu, B., Xie, Y., et al. (2020). Phillyrin (KD-1) Exerts Anti-viral and Anti-inflammatory Activities against Novel Coronavirus (SARS-CoV-2) and Human Coronavirus 229E (HCoV-229E) by Suppressing the Nuclear Factor Kappa B (NF-Kb) Signaling Pathway. *Phytomedicine* 78, 153296. doi:10.1016/j.phymed.2020.153296

Mackenzie, G. A., Vilane, A., Salaudeen, R., Hogerwerf, L., van den Brink, S., Wijsman, L. A., et al. (2019). Respiratory Syncytial, Parainfluenza and Influenza Virus Infection in Young Children with Acute Lower Respiratory Infection in Rural Gambia. *Sci. Rep.* 9, 17965. doi:10.1038/s41598-019-54059-4

Mair, C. E., Grienke, U., Wilhelm, A., Urban, E., Zehl, M., Schmidtke, M., et al. (2018). Anti-Influenza Triterpene Saponins from the Bark of Burkea Africana. *J. Nat. Prod.* 81, 515–523. doi:10.1021/acs.jnatprod.7b00774

Mbae, K. M., Umesha, S., and Manukumar, H. M. (2018). Therapeutic Properties of Lectins in Herbal Supplements. *Phytochem. Rev.* 17, 627–643. doi:10.1007/s11101-018-9572-2

Miyashita, N., and Matsushima, T. (2000). Chlamydia Pneumoniae Infection during an Influenza Virus A Epidemic: Preliminary Report. *J. Med. Microbiol.* 49, 391–392. doi:10.1099/0022-1317-49-4-391

Monto, A. S., and Arden, N. H. (1992). Implications of Viral Resistance to Amantadine in Control of Influenza A. *Clin. Infect. Dis.* 15, 362–367. doi:10.1093/clinids/15.2.362

Moorthy, M., Khoo, J. J., and Palanisamy, U. D. (2019). Acute Oral Toxicity of the Ellagitannin Geraniin and a Geraniin-Enriched Extract from Nephelium Lappaceum L Rind in Sprague Dawley Rats. *Heliyon* 5, e02333. doi:10.1016/j.heliyon.2019.e02333

Moscona, A. (2005). Neuraminidase Inhibitors for Influenza. *N. Engl. J. Med.* 353, 1363–1373. doi:10.1056/NEJMra050740

Mukhtar, M., Arshad, M., Ahmad, M., Pomerantz, R. J., Wigdahl, B., and Parveen, Z. (2008). Antiviral Potentials of Medicinal Plants. *Virus. Res.* 131, 111–120. doi:10.1016/j.virusres.2007.09.008

Murata, Y., Walsh, E. E., and Falsey, A. R. (2007). Pulmonary Complications of Interpandemic Influenza A in Hospitalized Adults. *J. Infect. Dis.* 195, 1029–1037. doi:10.1086/512160

Nagai, E., Iwai, M., Koketsu, R., Okuno, Y., Suzuki, Y., Morimoto, R., et al. (2019). Anti-influenza Virus Activity of Adlay tea Components. *Plant Foods Hum. Nutr.* 74, 538–543. doi:10.1007/s11130-019-00773-3

Newman, D. J., and Cragg, G. M. (2012). Natural Products as Sources of New Drugs over the 30 Years from 1981 to 2010. *J. Nat. Prod.* 75, 311–335. doi:10.1021/np200906s

Nguyen, T. N. A., Dao, T. T., Tung, B. T., Choi, H., Kim, E., Park, J., et al. (2011). Influenza A (H1N1) Neuraminidase Inhibitors from Vitis Amurensis. *Food Chem.* 124, 437–443. doi:10.1016/j.foodchem.2010.06.049

Nie, L.-x., Wu, Y.-l., Dai, Z., and Ma, S.-c. (2020). Antiviral Activity of Isatidis Radix Derived Glucosinolate Isomers and Their Breakdown Products against Influenza A *In Vitro*/ovo and Mechanism of Action. *J. Ethnopharmacology* 251, 112550. doi:10.1016/j.jep.2020.112550

Niederman, M. S., Mandell, L. A., Anzueto, A., Bass, J. B., Broughton, W. A., Campbell, G. D., et al. (2001). Guidelines for the Management of Adults with Community-Acquired Pneumonia. *Am. J. Respir. Crit. Care Med.* 163, 1730–1754. doi:10.1164/ajrccm.163.7.at1010

Nile, S. H., Kim, D. H., Nile, A., Park, G. S., Gansukh, E., and Kai, G. (2020). Probing the Effect of Quercetin 3-glucoside from Dianthus Superbus L against Influenza Virus Infection- *In Vitro* and In Silico Biochemical and Toxicological Screening. *Food Chem. Toxicol.* 135, 110985. doi:10.1016/j.fct.2019.110985

Ojwang, J. O., Wang, Y.-H., Wyde, P. R., Fischer, N. H., Schuehly, W., Appleman, J. R., et al. (2005). A Novel Inhibitor of Respiratory Syncytial Virus Isolated from Ethnobotanicals. *Antiviral Res.* 68, 163–172. doi:10.1016/j.antiviral.2005.09.003

Oliveira, E. C., Marik, P. E., and Colice, G. (2001). Influenza Pneumonia. *Chest* 119, 1717–1723. doi:10.1378/chest.119.6.1717

Ooi, L. S. M., Wang, H., He, Z., and Ooi, V. E. C. (2006). Antiviral Activities of Purified Compounds from Youngia Japonica (L.) DC (Asteraceae, Compositae). *J. Ethnopharmacology* 106, 187–191. doi:10.1016/j.jep.2005.12.028

Pangesti, K. N. A., Abd El Ghany, M., Walsh, M. G., Kesson, A. M., and Hill-Cawthorne, G. A. (2018). Molecular Epidemiology of Respiratory Syncytial Virus. *Rev. Med. Virol.* 28, e1968. doi:10.1002/rmv.1968

Park, J.-Y., Jae Jeong, H., Hoon Kim, J., Min Kim, Y., Park, S.-J., Kim, D., et al. (2012a). Diarylheptanoids from Alnus Japonica Inhibit Papain-like Protease of Severe Acute Respiratory Syndrome Coronavirus. *Biol. Pharm. Bull.* 35, 2036–2042. doi:10.1248/bpb.b12-00623

Park, J.-Y., Kim, J. H., Kim, Y. M., Jeong, H. J., Kim, D. W., Park, K. H., et al. (2012b). Tanshinones as Selective and Slow-Binding Inhibitors for SARS-CoV Cysteine Proteases. *Bioorg. Med. Chem.* 20, 5928–5935. doi:10.1016/j.bmc.2012.07.038

Pasquereau, S., Nehme, Z., Haidar Ahmad, S., Daouad, F., Van Assche, J., Wallet, C., et al. (2021). Resveratrol Inhibits HCoV-229E and SARS-CoV-2 Coronavirus Replication *In Vitro*. *Viruses* 13, 354. doi:10.3390/v13020354

Paules, C., and Subbarao, K. (2017). Influenza. *The Lancet* 390, 697–708. doi:10.1016/s0140-6736(17)30129-0

Pinto, L. H., Holsinger, L. J., and Lamb, R. A. (1992). Influenza Virus M2 Protein Has Ion Channel Activity. *Cell* 69, 517–528. doi:10.1016/0092-8674(92)90452-i

Pyrc, K., Berkhout, B., and van der Hoek, L. (2007). The Novel Human Coronaviruses NL63 and HKU1. *J. Virol.* 81, 3051–3057. doi:10.1128/JVI.01466-06

Rello, J., and Pop-Vicas, A. (2009). Clinical Review: Primary Influenza Viral Pneumonia. *Crit. Care* 13, 235. doi:10.1186/cc8183

Roschek, B., Jr., Fink, R. C., McMichael, M. D., Li, D., and Alberte, R. S. (2009). Elderberry Flavonoids Bind to and Prevent H1N1 Infection *In Vitro*. *Phytochemistry* 70, 1255–1261. doi:10.1016/j.phytochem.2009.06.003

Rothberg, M. B., Haessler, S. D., and Brown, R. B. (2008). Complications of Viral Influenza. *Am. J. Med.* 121, 258–264. doi:10.1016/j.amjmed.2007.10.040

Ruuskanen, O., Lahti, E., Jennings, L. C., and Murdoch, D. R. (2011). Viral Pneumonia. *The Lancet* 377, 1264–1275. doi:10.1016/s0140-6736(10)61459-6

Schadt, E. E., Friend, S. H., and Shaywitz, D. A. (2009). A Network View of Disease and Compound Screening. *Nat. Rev. Drug Discov.* 8, 286–295. doi:10.1038/nrd2826

Sedlak, L., Wojnar, W., Zych, M., Wyględowska-Promieńska, D., Mrukwa-Kominek, E., and Kaczmarczyk-Sedlak, I. (2018). Effect of Resveratrol, a Dietary-Derived Polyphenol, on the Oxidative Stress and Polyol Pathway in the Lens of Rats with Streptozotocin-Induced Diabetes. *Nutrients* 10, 1423. doi:10.3390/nu10101423

Seidenberg, J. (2019). Respiratorisches Synzytialvirus. *Internist* 60, 1146–1150. doi:10.1007/s00108-019-00673-3

Sharifi-Rad, J., Kamiloglu, S., Yeskaliyeva, B., Beyatli, A., Alfred, M. A., Salehi, B., et al. (2020). Pharmacological Activities of Psoralidin: a Comprehensive Review of the Molecular Mechanisms of Action. *Front. Pharmacol.* 11, 571459. doi:10.3389/fphar.2020.571459

Sheahan, T. P., Sims, A. C., Leist, S. R., Schäfer, A., Won, J., Brown, A. J., et al. (2020). Comparative Therapeutic Efficacy of Remdesivir and Combination Lopinavir, Ritonavir, and Interferon Beta against MERS-CoV. *Nat. Commun.* 11, 222. doi:10.1038/s41467-019-13940-6

Shen, L., Niu, J., Wang, C., Huang, B., Wang, W., Zhu, N., et al. (2019). High-throughput Screening and Identification of Potent Broad-Spectrum Inhibitors of Coronaviruses. *J. Virol.* 93, 15. doi:10.1128/jvi.00023-19

Shi, T., McAllister, D. A., O'Brien, K. L., Simoes, E. A. F., Madhi, S. A., Gessner, B. D., et al. (2017a). Global, Regional, and National Disease burden Estimates of Acute Lower Respiratory Infections Due to Respiratory Syncytial Virus in Young Children in 2015: a Systematic Review and Modelling Study. *Lancet* 390, 946–958. doi:10.1016/s0140-6736(17)30938-8

Shi, Y., Zhang, B., Lu, Y., Qian, C., Feng, Y., Fang, L., et al. (2017b). Antiviral Activity of Phenanthrenes from the Medicinal Plant Bletilla Striata against Influenza A Virus. *BMC Complement. Altern. Med.* 17, 273. doi:10.1186/s12906-017-1780-6

Shin, H.-B., Choi, M.-S., Ryu, B., Lee, N.-R., Kim, H.-I., Choi, H.-E., et al. (2013). Antiviral Activity of Carnosic Acid against Respiratory Syncytial Virus. *Virol. J.* 10, 303. doi:10.1186/1743-422x-10-303

Shrestha, S., Foxman, B., Berus, J., van Panhuis, W. G., Steiner, C., Viboud, C., et al. (2015). The Role of Influenza in the Epidemiology of Pneumonia. *Sci. Rep.* 5, 15314. doi:10.1038/srep15314

Signer, J., Jonsdottir, H. R., Albrich, W. C., Strasser, M., Züst, R., Ryter, S., et al. (2020). *In Vitro* virucidal Activity of Echinaforce, an Echinacea Purpurea Preparation, against Coronaviruses, Including Common Cold Coronavirus 229E and SARS-CoV-2. *Virol. J.* 17, 136. doi:10.1186/s12985-020-01401-2

Singh, A. P., Singh, R., Verma, S. S., Rai, V., Kaschula, C. H., Maiti, P., et al. (2019). Health Benefits of Resveratrol: Evidence from Clinical Studies. *Med. Res. Rev.* 39, 1851–1891. doi:10.1002/med.21565

Song, J.-G., Su, J.-C., Song, Q.-Y., Huang, R.-L., Tang, W., Hu, L.-J., et al. (2019). Cleistocaltones A and B, Antiviral Phloroglucinol-Terpenoid Adducts from Cleistocalyx Operculatus. *Org. Lett.* 21, 9579–9583. doi:10.1021/acs.orglett.9b03743

Sougiannis, A. T., Enos, R. T., VanderVeen, B. N., Velazquez, K. T., Kelly, B., McDonald, S., et al. (2021). Safety of Natural Anthraquinone Emodin: an Assessment in Mice. *BMC Pharmacol. Toxicol.* 22, 9. doi:10.1186/s40360-021-00474-1

Stuppner, S., Mayr, S., Beganovic, A., Beć, K., Grabska, J., Aufschnaiter, U., et al. (2020). Near-infrared Spectroscopy as a Rapid Screening Method for the Determination of Total Anthocyanin Content in Sambucus Fructus. *Sensors* 20, 4983. doi:10.3390/s20174983

Tatarelli, P., Magnasco, L., Borghesi, M. L., Russo, C., Marra, A., Mirabella, M., et al. (2019). Prevalence and Clinical Impact of vIral Respiratory Tract Infections in Patients Hospitalized for Community-Acquired Pneumonia: the Vircap Study. *Intern. Emerg. Med.* 15, 645–654. doi:10.1007/s11739-019-02243-9

Vabret, A., Mourez, T., Gouarin, S., Petitjean, J., and Freymuth, F. (2003). An Outbreak of Coronavirus OC43 Respiratory Infection in Normandy, France. *Clin. Infect. Dis.* 36, 985–989. doi:10.1086/374222

Vlachojannis, J. E., Cameron, M., and Chrubasik, S. (2010). A Systematic Review on the Sambuci Fructus Effect and Efficacy Profiles. *Phytother. Res.* 24, 1–8. doi:10.1002/ptr.2729

Walters, W. P., Stahl, M. T., and Murcko, M. A. (1998). Virtual Screening-An Overview. *Drug Discov. Today* 3, 160–178. doi:10.1016/s1359-6446(97)01163-x

Wang, K.-C., Chang, J.-S., Lin, L.-T., Chiang, L.-C., and Lin, C.-C. (2012). Antiviral Effect of Cimicifugin from Cimicifuga Foetida against Human Respiratory Syncytial Virus. *Am. J. Chin. Med.* 40, 1033–1045. doi:10.1142/s0192415x12500760

Wang, K. C., Chang, J. S., Chiang, L. C., and Lin, C. C. (2009). 4-Methoxycinnamaldehyde Inhibited Human Respiratory Syncytial Virus in a Human Larynx Carcinoma Cell Line. *Phytomedicine* 16, 882–886. doi:10.1016/j.phymed.2009.02.016

Wang, Q., Dai, Z., Zhang, Y. J., and Ma, S. C. (2016). [Hepatotoxicity of Emodin Based on UGT1A1 Enzyme-Mediated Bilirubin in Liver Microsomes]. *Zhongguo Zhong Yao Za Zhi* 41, 4424–4427. doi:10.4268/cjcmm20162321

Wang, T., Wang, C., Wu, Q., Zheng, K., Chen, J., Lan, Y., et al. (2017). Evaluation of Tanshinone IIA Developmental Toxicity in Zebrafish Embryos. *Molecules* 22, 660. doi:10.3390/molecules22040660

Wen, C.-C., Kuo, Y.-H., Jan, J.-T., Liang, P.-H., Wang, S.-Y., Liu, H.-G., et al. (2007). Specific Plant Terpenoids and Lignoids Possess Potent Antiviral Activities against Severe Acute Respiratory Syndrome Coronavirus. *J. Med. Chem.* 50, 4087–4095. doi:10.1021/jm070295s

Wen, Z., Citron, M., Bett, A. J., Espeseth, A. S., Vora, K. A., Zhang, L., et al. (2019). Development and Application of a Higher Throughput RSV Plaque Assay by Immunofluorescent Imaging. *J. Virol. Methods* 263, 88–95. doi:10.1016/j.jviromet.2018.10.022

Weng, J.-R., Lin, C.-S., Lai, H.-C., Lin, Y.-P., Wang, C.-Y., Tsai, Y.-C., et al. (2019). Antiviral Activity of Sambucus FormosanaNakai Ethanol Extract and Related Phenolic Acid Constituents against Human Coronavirus NL63. *Virus. Res.* 273, 197767. doi:10.1016/j.virusres.2019.197767

WHO (2003). In Communicable Disease Surveillance and Response. Available at: http://www.who.int/csr/sars/archive/2003_05_07a/en (Accessed July 29, 2020).

WHO (2020a). Middle East Respiratory Syndrome Coronavirus (MERS-CoV). Available at: https://www.who.int/health-topics/middle-east-respiratory-syndrome-coronavirus-mers#tab=tab_2 (Accessed August 9, 2020).

WHO (2020b). Pneumonia. Available at: https://www.who.int/health-topics/pneumonia#tab=tab_1 (Accessed July 22, 2020).

Xue, R., Fang, Z., Zhang, M., Yi, Z., Wen, C., and Shi, T. (2013). TCMID: Traditional Chinese Medicine Integrative Database for Herb Molecular Mechanism Analysis. *Nucleic Acids Res.* 41, D1089–D1095. doi:10.1093/nar/gks1100

Yu, S., Zhu, Y., Xu, J., Yao, G., Zhang, P., Wang, M., et al. (2021). Glycyrrhizic Acid Exerts Inhibitory Activity against the Spike Protein of SARS-CoV-2. *Phytomedicine* 85, 153364. doi:10.1016/j.phymed.2020.153364

Zhang, X., Xia, Y., Yang, L., He, J., Li, Y., and Xia, C. (2019). Brevilin A, a Sesquiterpene Lactone, Inhibits the Replication of Influenza A Virus *In Vitro* and *In Vivo*. *Viruses* 11, 835. doi:10.3390/v11090835

Zhou, Y., Hou, Y., Shen, J., Huang, Y., Martin, W., and Cheng, F. (2020a). Network-based Drug Repurposing for Novel Coronavirus 2019-nCoV/SARS-CoV-2. *Cell Discov* 6, 14. doi:10.1038/s41421-020-0153-3

Zhou, Z., Chen, B., Chen, S., Lin, M., Chen, Y., Jin, S., et al. (2020b). Applications of Network Pharmacology in Traditional Chinese Medicine Research. *Evidence-Based Complement. Altern. Med.* 2020, 1–7. doi:10.1155/2020/1646905

Zu, M., Yang, F., Zhou, W., Liu, A., Du, G., and Zheng, L. (2012). *In Vitro* anti-influenza Virus and Anti-inflammatory Activities of Theaflavin Derivatives. *Antiviral Res.* 94, 217–224. doi:10.1016/j.antiviral.2012.04.001

Conflict of Interest: The authors declare that the research was conducted in the absence of any commercial or financial relationships that could be construed as a potential conflict of interest.

frontiers in Pharmacology

MINI REVIEW
published: 25 August 2021
doi: 10.3389/fphar.2021.703837

African and Asian Medicinal Plants as a Repository for Prospective Antiviral Metabolites Against HIV-1 and SARS CoV-2: A Mini Review

Godwin Anywar[1]*, *Muhammad Akram*[2] and *Muhammad Amjad Chishti*[2]

[1]Department of Plant Sciences, Microbiology and Biotechnology, College of Natural Sciences, Makerere University, Kampala, Uganda, [2]Department of Eastern Medicine, Government College University Faisalabad, Faisalabad, Pakistan, [3]Department of Basic Clinical Sciences, Faculty of Eastern Medicine, Hamdard University, Karachi, Pakistan

Introduction: The worldwide burden of viral infections has triggered a resurgence in the search for new and more efficient antiviral drugs. Scientists are also repurposing existing natural compounds such as the antimalarial drug artemisinin from *Artemesia annua* L. as potential drug candidates for some of the emerging and re-emerging viral infections such as covid-19

Aim: The aim of this review was to analyse the existing literature to explore the actual or potential natural antiviral compounds from African and Asian medicinal plants as lead compounds in the drug discovery process.

Methods: We searched the literature on African and Asian medicinal plant species as antiviral agents for HIV-1 and the novel coronavirus (SARS-CoV-2) in various databases and search engines such as Web of Science, Google Scholar and PubMed. The search was limited to *in vitro*, *in vivo*, and clinical studies and excluded *in silico* studies.

Results: We present 16 plant species with actual or potential antiviral activity against HIV-1 and SARS-CoV-2. These plant species span the continents of Africa and Asia where they are widely used for treating several other ailments.

Conclusion: Natural compounds from plants can play a significant role in the clinical management of HIV/AIDS and the covid-19 pandemic. More research needs to be conducted to investigate the potential toxicities of the various compounds and their efficacies in clinical settings.

Keywords: medicinal plants, antiviral, COVID-19, HIV/aids, immune system, infectious diseases

OPEN ACCESS

Edited by:
Banasri Hazra,
Jadavpur University, India

Reviewed by:
Roodabeh Bahramsoltani,
Tehran University of Medical Sciences, Iran
Loh Teng Hern Tan,
Monash University Malaysia, Malaysia

***Correspondence:**
Godwin Anywar
godwinanywar@gmail.com

Specialty section:
This article was submitted to Ethnopharmacology, a section of the journal Frontiers in Pharmacology

Received: *30 April 2021*
Accepted: *10 August 2021*
Published: *25 August 2021*

Citation:
Anywar G, Akram M and Chishti MA (2021) African and Asian Medicinal Plants as a Repository for Prospective Antiviral Metabolites Against HIV-1 and SARS CoV-2: A Mini Review. Front. Pharmacol. 12:703837. doi: 10.3389/fphar.2021.703837

INTRODUCTION

The emergence and re-emergence of new infectious diseases especially of viral origin are of great concern to global public health (Louten, 2016; Mourya et al., 2019; Abrahão and de Arruda, 2020). This has reignited the search for natural compounds especially, from plants as potential sources of new drug candidates to add to the current armamentarium (Jans et al., 2020). This review focusses on HIV-1 and SARS-CoV-2, the viruses that cause AIDs and covid-19 respectively because over the last 50 years, these two viruses have caused huge pandemics globally: the HIV/AIDS pandemic and

covid-19 pandemic (Illanes-Álvarez, et al., 2021). Since the start of the HIV/AIDS pandemic in the early 80's, about 77.5 million people have become infected with HIV and over 34.7 million have succumbed to the diseases (UNAIDS, 2021). For the more recent covid-19 pandemic which begun in 2019, there have been 206,958,371 confirmed cases as of August 18, 2021 globally with 4,361,996 confirmed deaths, as of July 28, 2021 (WHO, 2021). The novel SARS-CoV-2 virus causes severe acute and fatal respiratory syndrome after gaining access to the host cells through the angiotensin-converting enzyme 2 (ACE2) co-receptors for the virus. The virus can also damage vital body organs by causing a cytokine storm (Ding et al., 2003; Hashemifesharaki and Gharibzahedi, 2020; Xu et al., 2020). Another similarity both pandemics share is causation by RNA viruses which have animal reservoirs and infections characterized by the increased synthesis of proinflammatory cytokines (Illanes-Álvarez et al., 2021).

Medicinal plants have a long history of healing many diseases. Natural compounds from plants are a rich reservoir of bioactive antiviral compounds. Recent scientific and technological advances have made it possible to easily isolate compounds from such plants with a wide range of biological activities (Martin and Ernst, 2003). Some natural products from plants contain metabolites that are key in preventing virus replication without affecting host metabolism. Such compounds are ideal candidates for the development of antiviral medicinal products with limited side effects. For instance, compounds such as 3β-friedelanol, friedelin, and epitaraxerol isolated from the ethanolic extract of *Euphorbia neriifolia* had potent anti-human coronavirus activity on human fibroblasts (MRC-5) infected cells (Chang et al., 2012). These natural plant products may additionally modify or enhance host immune responses against viruses; thus, alleviating symptoms and reducing mortality of viral infections (Kurokawa et al., 2010).

Fewer antiviral drugs are considered safe for human use than antibacterial agents mainly because viral pathogenesis is not as well understood at molecular level. Some viruses multiply and induce host cell lysis, while viruses incorporate themselves into the host chromosome and may remain dormant for years. Numerous viruses survive and thrive by hijacking the machinery of the host cell which includes different enzyme systems. Therefore, their inhibition is key to controlling viral diseases (Kurokawa et al., 2010).

Another approach that is vigorously being pursued is the repurposing of existing compounds and exploring their synergistic activity as potential drug candidates for diseases such as covid-19 (Prasad et al., 2020). Such compounds are often considered cheaper, safer, and efficacious alternatives to some of the currently available conventional drugs (Perera and Efferth, 2012). For instance, *A. annua* tea infusion is highly active against HIV-1 50% inhibitory concentration (IC_{50} = 2.0 μg/ml) but was originally used for treating malaria and fevers. Artemisinin, the main component from *A. annua* is currently the main stay for malaria treatment (Lubbe et al., 2012). Other studies are investigating the potential of already known compounds as potential candidates against SARS-CoV 2 and HIV-1. This mini-review reports on medicinal plant species and their metabolites as actual or potential antiviral candidates for HIV/AIDS and covid-19.

METHODS

We searched the literature on medicinal plant species used in Africa and Asia with scientific evidence of antiviral activity against either HIV-1 or SARS-CoV-2 or both in various databases and search engines such as Web of Science, Google Scholar and PubMed. We selected the most important plant species basing on scientific evidence from one or more studies confirming their antiviral activities. The search was limited to *in vitro*, *in vivo*, and clinical studies but excluded *in silico* studies. The search focused on English only studies conducted within the last 50 years. The selected plant species are presented in detail as follows:

RESULTS AND DISCUSSION

All the plant species selected are used in traditional medicine for treating various diseases including viral infections. Of the 16 medicinal plant species analysed, 11 were considered major because they had a larger body of scientific evidence to support their bioactivity or efficacy than the rest which were categoried as "other medicinal plant species with limited studies."**Table 1** shows a detailed breakdown of ten plant species with proven activity against SARS-CoV-2 and or HIV-1.

Acacia catechu (L.f.) Willd. Family: Fabaceae

A. catechu is a moderate size deciduous tree with a dark grayish or brown rough bark (Chopra et al., 1956). It is indigenous to India and other Asian countries, as well as East Africa (Patel et al., 2009; Sunil et al., 2019). The stem bark, aqueous and ethanol extracts of *A. catechu* caused the suppression of HIV-1 infection partly through their inhibitory effect on HIV-1 protease and partly due to the interference in interaction of viral Trans-Activator of Transcription (Tat) protein. The n-butanol fraction of *A. catechu* exhibited strong inhibitory activity against HIV proteases (IC_{50} = 12.9 μg/ml). *A. catechu* acts through various other mechanisms such as inhibition of fusion of infected cells and blocking RNA synthesis (Nutan et al., 2013). The n-butanol fraction showed a dose-dependent inhibition against HIV-$1_{NL4.3}$ infection of peripheral blood mononuclear cells (PBMC), and against HIV-1_{BaL}(R-5-tropic) as well as two different primary viral isolates of HIV-1 (Nutan et al., 2013). *A. catechu* contains various compounds such as kaempferol, quercetin, catechin, rutin, isorhamnetin, epicatechin, afzelechin, epiafzelechin, mesquitol, ophioglonin, aromadendrin and phenols (Li et al., 2010). However, the specific bioactive compounds responsible for the anti-HIV activity were not established.

Allium sativum L. Family, Amaryllidaceae

A. sativum (garlic) is a member of the onion family. It is a hardy perennial herb likely to have originated in central Asia where it

TABLE 1 | Medicinal plant species with HIV-1 and SARS-CoV-2 activities.

Plant name	Extraction solvent/ Compound extracted	Antiviral activity and type of virus/strain/viral enzyme HIV-1	SARS-CoV-2	Test model	Toxicity	Standard drug and potency/ Control	Mechanism of action	References
1. *Acacia catechu*	a) n-butanol fraction	a) IC_{50} = 12.9 μg/ml against Viral protease	ND	Enzymatic: (HIV-1 reverse transcriptase, integrase, protease, pro-viral genome integration and viral Tat protein mediated transactivation)	No cytotoxicity observed up to 100 μg/ml (CC_{50}) using $HIV_{NL4.3}$ in TZM-bl cells-based assay	Saquinavir (1 μM) 100% inhibition of HIV-1 PI	Inhibition of HIV-1 protease and interaction of viral Tat protein	Nutan et al. (2013)
	b) ethanol	b) IC_{50} = 3.6 ± 0.31 μg/ml		Cellular: $HIV\text{-}1_{NL4.3}$ $HIV\text{-}1_{BaL}$(R-5-tropic)				
	c) Water	IC_{50} = 1.8 ± 0.18 μg/ml		Cell-free virus-based assay using TZM-bl cells				
2. *Allium sativum*	Lectins (ASA and ASA1)	HIV-1	SARS-CoV Frankfurt 1 strain (CC_{50} > 100)	Vero E6 cells ATCC	IC_{50} > 100 μg/ml	Blank (infected cells incubated with medium)	Inhibits viral-cell attachment and viral reverse transcriptase in HIV-1 and infectious virus cycle of SARS-CoV-2	Tatarintsev et al. (1992), Keyaerts et al. (2007)
	Ajoene	(HIV)-1 (IIIB) EC_{50} = 0.35 μM	ND	MOLT-4 cells	IC_{50} = 1.88 μM	Dextran sulfate	Blocks HIV-1 virus-cell attachment and adsorption	Walder, et al. (1997)
3. *Ancistrocladus korupensis*	Michellamine B	HIV-1 and 2 IC_{50} = 18 μg/ml	ND	Cultured human T-lymphoblastoid cells (CEM-SS and MT-2),	ND	Uninfected, non-drug-treated cells	Inhibits replication of both HIV-1 and HIV-2, and their CPE	Manfredi et al. (1991)
	Korundamine A	EC_{50} = 2 μM		CEM-SS and MT-2			Anticytopathic activity against HIV-1	Hallock et al. (1998)
		EC_{50} = 8, l0 and 6 μM		Several resistant strains of HIV CEM-SS/OClOO MT2/A17 MT2/G9106 host cell/virus strain combinations, respectively			ND	
4. *Artemisia annua*	Ethanol leaf extract	ND	EC_{50} = 34.5 μg/ml, SI = 31	Cellular: Vero E6 cells	ND	Absorbance of uninfected cell control (100%)	Inhibits effects on virus-induced CPE in a dose dependent manner	Li et al. (2005)
			EC_{50} = 39.2 μg/ml, SI = 27	SARS-CoV-1 BJ-001 strain				
			CC_{50} = 1,053.0 (±92.8) for both	SARS-CoV-1 BJ-006 strain				
	Water infusion	IC_{50} = 2.0 μg/ml)	ND	Cellular: HIV–1	No cellular toxicity on human cells with iFIGS- and deClPhR systems	Efavirenz (a non-nucleosidic RT inhibitor in clinical use)	ND	Lubbe et al. (2012)
5. *Cullen corylifolium*	Ethanolic seed extract	ND	IC_{50} = 15 μg/ml	Enzymatic: SARS-CoV- papain-like protease (PLpro) Cellular	ND	Untreated	ND	Kim et al. (2014)

(Continued on following page)

TABLE 1 | (*Continued*) Medicinal plant species with HIV-1 and SARS-CoV-2 activities.

	6 isolated bioactive flavonoids		IC_{50} = 4.2–38.4 μM)				Dose-dependent inhibition of PLpro	
6. *Euphorbia neriifolia*	Twenty-two triterpenoids and 1 flavonoid glycoside; 3β-friedelanol, 3β-acetoxy friedelane, friedelin, and epitaraxerol	ND	ND	Cellular in MRC-5 cells (20 μL, strain 229E in the XTT assay	ND	Actinomycin D (0.02 μg/mL)	Structure-activity relationship against HCoV	Chang et. al,(2012)
7. *Mangifera indica*	Mangiferin	$HIV\text{-}1_{IIIB}$ EC_{50} = 16.90 μM SI > 140	ND	Cellular Enzymatic	Low cytotoxicity on C8166, MT-4, chronically-infected H9 cells and PBMC (CC_{50} > 1,000 μg/ml (2,369.67 μM)	IDV showed cytotoxicity on C8166 (CC_{50} value >500 μM)	Inhibits HIV-1IIIB induced syncytium formation and inhibits HIV-1 protease	Wang et al. (2011)
		MT-2 cells CC_{50} = 3.95 μ/ml IC_{50} = 125 μ/ml		MT-2 cell line	Not toxic (IC_{50} = 125 μ/ml)	Zidovuline (IC_{50} = 3.5 μ/ml)	Reduces the CPE in MT-2 cells and prevented cell death	Guha et al. (1996)
8. *Panax ginseng*	Six 300 mg/ capsules taken thrice daily	HIV-1	ND	*In vivo:* HIV-1-infected patients	ND	People without HIV-1 infection	Slows depletion of CD4 T cells and serum CD8 levels	Sung et al. (2005), Cho and Kim, (2017)
	Ginsenoside-Rb1 (100 μM)			Cellular			Prevents viral entry	Shehzad et al. (2012)
9. *Pelargonium sidoides*	Aqueous root extract	HIV-1 SI ≈ 45	ND	HIV-1 (various X4 and R5 tropic strains, and clinical isolates)	Low cytotoxicity: (CC_{50} ≤ 250 mg/ml)	Cells without virus inoculum (background) and cells exposed to virus particles in the absence of inhibitory compounds (attachment control)	Directly interferes with viral infectivity and blocks viral attachment and entry of HIV-1 particles to target cells	Helfer et al. (2014)
	Polyphenols	SI = 24	ND	ND	Low cytotoxicity: (CC_{50} ≤ 1,200 mg/ml)	ND	ND	ND
10. *Phyllanthus amarus*	Aqueous or alcohol extract	IC_{50} = 0.48–0.16 μg/ml	ND	Enzymatic HIV integrase	ND	Uninfected cells (negative control); untreated cells and a neutralizing serum (1:100 diluted) -positive control	Blocks HIV-1 attachment to cells and viral enzymes	Notka et al. (2004)
		IC_{50} = 8.17–2.53 μg/ml		Reverse transcriptase				
		IC_{50} = 21.80–6.28 μg/ml		Protease				
		IC_{50} = 2.65 μg/ml		Cellular: CD4-gp120 binding			Blocked interaction of HIV-1 gp120 and the CD4 receptor	
	Geraniin	IC_{50} = 0.48 μg/ml		Cellular: CD4-gp120 binding				
11. *Theobroma cacao*	Sodium hydroxide cocoa husk extract	HIV-1 SI = 311, 46	ND	HTLV-1-transformed T-cell lines MT-2 and MT-4	Cacao pigment was cytotoxic above 500 μg/ml to MT-2 and MT-4 cells	MOLT-4 cell and MOLT-4 cells treated with 250 μg/ml CP	Inhibits CPE of HIV-1 against HTLV-1-transformed T-cell lines MT-2 and MT-4 Inhibits syncytium	Unten et al., 1991; Sakagami et al., (2011)

(Continued on following page)

TABLE 1 | (*Continued*) Medicinal plant species with HIV-1 and SARS-CoV-2 activities.

				formation between HIV-infected and uninfected lymphoblastoid T-cell line, MOLT-4	
Cacao lignin-carbohydrate complex (LCC)	HIV-1	ND	ND	Inhibits antiviral and macrophage stimulatory activity	Sakagami et al. (2011)

CPE = Cytopathic effect; ND = Not Determined; SI = Selectivity Index.

was used as a food and medicine. Traditionally, it was used for preventing infections and the treatment of colds, influenza, bronchitis, whooping cough, gastroenteritis, dysentery and skin problems (Rivlin, 2001; Lissiman et al., 2014) and to boost immunity in people living with HIV/AIDS (Anywar et al., 2020a). *A. sativum* has a range of biological activities, including antiviral properties. It inhibits viral-cell attachment, viral reverse transcriptase, and further destruction of $CD4^T$ cells (Tatarintsev et al., 1992; Walder et al., 1997). Ajoene, a compound isolated from garlic showed dose-dependent HIV inhibition (EC_{50} = 0.35 μM). The lectins (ASA and ASA1) from garlic inhibited both HIV-1 replication and viral attachment in the later stages of infectious virus cycle of SARS-CoV (Keyaerts et al., 2007). Garlic extract inhibited angiotensin converting enzyme (ACE)2, a functional receptor for SARS-CoV Li et al. (2003) by 39.57% at a dose of 10 mg/ml Chaudhary et al. (2020) indicating its potential antiviral activity against SARS-CoV. *A. sativum* contains various other bioactive compounds including alliin, allicin, vinyldithis and flavonoids (Chavanet al., 2016; Kim et al., 2018; Baek et al., 2019; Phan et al., 2019; El-Saber Batiha et al., 2020).

Ancistrocladus korupensis D.W.Thomas and Gereau Family: Ancistrocladaceae

A. korupensis is a West African liana with the only known population limited within Korup National Park and its vicinity, in Cameroon. *A. korupensis* has antiviral activity against HIV-1 and HIV-2. Different compounds with anti-HIV activity have been isolated from its bark and leaves such as michellamine B Manfredi et al. (1991), Foster and Sork (1997) and korundamine A (Hallock et al., 1998). Michellamine B is a naturally occurring naphthylisoquinoline alkaloid that inhibits the replication of both HIV-1 and HIV-2, and their associated cytopathic effects (CPE) on cultured human T-lymphoblastoid cells (CEM-SS and MT-2), with a 50% effective concentration (CC_{50}) near 18 μg/ml (Manfredi et al., 1991). Korundamine A is also a naphthylisoquinoline alkaloid which is heterodimeric. Korundamine A exhibited anticytopathic activity against HIV-1 (EC_{50} = 2 μM) (Hallock et al., 1998). The anti-HIV activity of korundamine A is comparable to the anti-HIV activity of the michellamines. Korundamine A is also active against several resistant strains of HIV, with EC_{50} values of 8, l0 and 6 μM for the CEM-SS/OClOO, MT2/A17 and MT2/G9106 host cell/virus strain combinations, respectively (Hallock et al., 1998). Five michellamine-type dimeric naphthylisoquinoline alkaloids: michellamines A_2, A_3, A_4, B_2, and B_3, were isolated from the root bark of a related species, the Central African liana *Ancistrocladus congolensis*, along with their two known parent compounds, the michellamines A and B (Bringmann et al., 2016).

Artemisia annua L., Family Asteraceae

A. annua is a shrub, often growing over 2 m high (Ferreira et al., 1997). It is native to China and has traditionally been used to treat malaria and fevers Willcox et al. (2004), Anywar et al. (2020b) and to boost immunity in people living with HIV/AIDS (Anywar et al., 2020a). *A. annua* extracts inhibit various viruses (Efferth et al., 2008). The ethanol extracts of *A. annua* significantly inhibited the effects on virus-induced CPE in SARS-CoV. The ethanol leaf extract of *A. annua* had antiviral activity against SARS-CoV-1 BJ-001 strain (EC_{50} = 34.5) and BJ-006 strain (EC_{50} = 39.2). *A. annua* was proposed as one of the potential candidates for the development of new anti-SARS-CoV drug (Li et al., 2005). In addition, A. annua tea infusion is highly active against HIV (IC_{50} = 2.0 μg/ml) but the main component, artemisinin was inactive at 25 μg/ml (Lubbe et al., 2012). The specific phytochemical compounds responsible for its anti-HIV-1 and anti-SARS-CoV activity have not established although it contains bioactive compounds such as quercetin, polyphenols, saponins, sterols, dicaffeoylquinic acid polyaccharides (Lin et al., 2014).

Cullen corylifolium (L.) Medik. Syn *Psoralea corylifolia*, Family: Fabaceae

C. corylifolium Syn: *P. corylifolia* is a is a popular traditional medicinal herb that occurs mainly in Indonesia, Malaysia, Bangladesh, India, China, and Sri Lanka. *P. corylifolia* has well known antiviral, antioxidant, antibacterial and antidepressant activities (Chopra et al., 2013; Alam et al., 2018). *P. corylifolia* seed extract exhibited high activity against SARS-CoV-papain-like protease (PLpro) (IC_{50} = 15 μg/ml). SARS-CoV Plpro is an important enzyme in SARS virus replication (Kim et al., 2014). *P. corylifolia* contains various bioactive components (Schneiderová et al., 2013; Kim et al., 2014). All the six isolated bioactive flavonoids from *P. corylifolia*: bavachinin, neobavaisoflavone, isobavachalcone, 4′-O-methylbavachalcone, psoralidin and corylifol produced a dose-dependent inhibition of PLpro (IC_{50} = 4.2–38.4 μM) (Kim et al., 2014).

Euphorbia neriifolia L Family: Euphorbiaceae

E. neriifolia is a spiny herb native to Southeast Asia with a native range from Iran to Myanmar (Hieh et al., 1993; POWO, 2020). The herb is currently cultivated in southern Taiwan (Hieh et al., 1993). Terpenoids isolated from *E. neriifolia* exhibited a structure-activity relationship against the human coronavirus (HCoV). Twenty-three compounds (22 triterpenoids and 1 flavonoid glycoside) have been isolated from the ethanolic leaf extract of *E. neriifolia* leaves. Specifically, 3β-friedelanol exhibited more potent anti-viral activity against the corona virus (HCoV, strain 229E) than the positive control, actinomycin D (0.02 μg/ml) Chang et al. (2012) in MRC-5 cells (human fibroblasts cells).

Mangifera indica L Family: Anacardiaceae

M. indica is a medicinal and fruit tree widely used in the traditional medicine in India, and Africa (Makare et al., 2001; Anywar et al., 2020a). *M. indica* possess antiviral activities which have been attributed to the compound mangiferin, a naturally occurring gucosylxanthone (Guha et al., 1996; Wang et al., 2011). Mangiferin inhibited HIV-1_{IIIB} induced syncytium formation at non-cytotoxic concentrations, with a 50% effective concentration (EC_{50}) of 16.9 μM. Mangiferin also demonstrated antiviral activity against various laboratory-derived, clinically isolated and resistant HIV-1 strains of HIV. Mangiferin acts by inhibiting HIV proteases (Wang et al., 2011). Mangiferin reduced the CPE in MT-2 cells and prevented cell death at > 10 μ/ml with a CC_{50} of 3.95 μ/ml and a lower IC_{50} of 125 μ/ml than the standard drug zidovuline (IC_{50} of 3.5 μ/ml). Mangiferin was thus not toxic at such high concentrations compared to the standard drug (Guha et al., 1996).

Panax ginseng C.A.Mey. Family: Araliaceae

Panax ginseng is a highly valued medicinal plant that has been used for thousands of years. It is mostly cultivated in China, Korea, and Japan (Shehzad et al., 2012; 2013; Bai et al., 2018). Ginseng is a perennial herb whose rhizome is an important determinant of its quality (Choi, 2008). The consumption of Korean ginseng was shown to slow the depletion of CD4 T cells and serum CD8 levels in HIV-1-infected patients (Sung et al., 2005). A retrospective study that analyzed 252 HIV-1 patients diagnosed from 1986 to 2013 prior to the initiation of antiretroviral therapy showed that *P. ginseng* prolonged survival in HIV-1 patients. The study also showed significant correlations between the total amount of *P. ginseng* consumed and survival time ($r = 0.64$, $p < 0.0001$) and between total amount of *P. ginseng* and mean annual decrease in $CD4^+$ T-cell count in all 252 patients ($r = -0.17$, $p < 0.01$) (Cho and Kim, 2017). The ginsenoside-Rb1, which is one of the active components of *P. ginseng* (Shehzad et al., 2012), showed antiviral activity against FP-21399, a bis-azo derivative with HIV inhibition activity by preventing viral entry at 100 μM (Zhang et al., 1998). The major pharmacologically active components of ginseng root are ginsenosides which make up 2–3% of the root (Jeong et al., 2003; Shehzad et al., 2012).

Pelargonium sidoides DC. Family: Geraniaceae

P. sidoides is a popular herb whose roots are widely used in traditional medicine in South Africa for different ailments such as diarrhoea, dysentery, ear, nose, throat disorders and respiratory tract infections (Kolodziej, 2002; Brendler and van Wyk, 2008; Michaelis et al., 2011). *P. sidoides* has potent anti-HIV-1 activity. It protected PBMC and macrophages from infection with various X4 and R5 tropic HIV-1 strains, and clinical isolates by directly interfering with viral infectivity and blocking viral attachment and entry of HIV-1 particles to target cells. *P. sidoides* contains active polyphenolic compounds with low cytotoxicity (Helfer et al., 2014). However, the specific phytochemical compounds responsible for its anti-HIV-1 activity were not established.

Phyllanthus amarus Schumach. and Thonn., Family: Phyllanthaceae

Phyllanthus amarus (Syn *P. niruri*) is a small shrub that is widespread in the tropics. The aqueous or alcohol extracts of *P. amarus* extracts inhibited HIV replication both *in vivo* and *in vitro* by blocking HIV-1 attachment to cells. *P. amarus* also inhibited the HIV-1 enzymes: integrase by 0.48–0.16 μg/ml, reverse transcriptase by 8.17–2.53 μg/ml, and protease by 21.80–6.28 μg/ml. The extracts blocked the interaction of HIV-1 gp120 and the CD4 receptor with 50% inhibitory concentrations of 2.65 μg/ml for the aqueous/alcohol extract and 0.48 μg/ml for geraniin, an isolated egallotanin from the plant. Additionally, sera from human volunteers reduced HIV replication by more than 30% at a concentration of 5% *in vivo* (Notka et al., 2004). The alkaloidal extract of *P. niruri* selectively inhibited the cytopathic effects of HIV-1 on human MT-4 cells at the tested concentrations (CC_{50} = 279.85 μg/ml; EC_{50} = 20.98 μg/ml). The selectivity index (SI) (defined as CC_{50}/EC_{50}) of the extract for the viral cells was 13.34 (Naik & Juvekar, 2003). *P. amarus* contains gallotannins, and the ellagitannins: geraniin and corilagin were shown to be the most potent mediators of the anti HIV-1 activities (Notka et al., 2004).

Theobroma cacao L., Family: Malvaceae

T. Cacao is a small evergreen tree native to South America (Baliga et al., 2014). The seeds of *T. cacao* are often used in the food industry especially for chocolate making (Wickramasuriya and Dunwell, 2018). *T. cacao* has anti-HIV activity. A sodium hydroxide cocoa husk extract inhibited the CPE of HIV-1 against HTLV-1-transformed T-cell lines; MT-2 and MT-4. Furthermore, the extract also inhibited syncytium formation between HIV-infected and uninfected lymphoblastoid T-cell line, MOLT-4. The extract is thought to act by inhibiting the adsorption of the virus (Unten et al., 1991). Cacao lignin-carbohydrate complex (LCC) has also shown strong antiviral and macrophage stimulatory activity (Sakagami, et al., 2010). However, cacao mass LCC demonstrated higher anti-HIV

activity than cacao husk (Sakagami et al., 2011). The husk extract is made up of condensed or polymerized flavonoids such as catechin and anthocyanidin which are sometimes complexed with glucose (Kimura, 1979). *T. cacao* contains several bioactive compounds such theobromine, and polyphenols (Goya et al., 2016; Oyeleke, et al., 2018). However, the specific phytochemical compounds responsible for its anti-HIV-1 activity were not established.

Other Medicinal Plant Species With Limited Studies

Other plant species with promising as antiviral but with limited research are presented below.

Lindera aggregata (Sims) Kosterm. Family: Lauraceae

L. aggregata is a common herb in China and Japan. Its roots are mainly utilized for the treatment of pain, inflammation, indigestion, cold and hernia (Xiao et al., 2011; Wei et al., 2017). L. aggregata exhibited significant antiviral activity by inhibiting virus-induced CPE against the SARS-CoV strain BJ001 (EC_{50} = 88.2 ± 7.7 μg/ml) (Li et al., 2005). The specific phytochemical compounds responsible for its anti-SARS-CoV-2 activity were not established.

Lycoris radiata (L'H r.) Family; Amaryllidaceae

L. radiata is a herb native to China, Korea, Japan, and Nepal with various biological activities including: antiviral, and anti-inflammatory (Cedrón et al., 2010; Lamoral-Theys et al., 2010; Kretzing et al., 2011). The ethanolic stem extract of *L. radiata* exhibited inhibitory effects against SARS- CoV-2, which have been attributed to lycorine Li et al. (2005), the main active component (Yang et al., 2019).

Onopordum acanthium L. Family: Asteraceae

O. acanthium is a herbaceous plant native to Europe, Xinjiang and W. Himalaya in Asia, and NW. Africa (POWO, 2020). *O. acanthium* has anti-inflammatory, anti-cancer, antiviral, and antioxidant properties. *O. acanthium* was effective at inhibiting ACE-2 activity by more 80% (Sharifi et al., 2013), which could potentially be effective against SARS-CoV-2. Although the specific compounds responsible for its anti-SARS-CoV-2 activity were not established, extracts of *O. acanthium* have a wide range of bio-active components including flavonoids, triterpenoids, phenylpropanoids, sesquiterpene lactones and sterols (Csupor-Löffler et al., 2014; Abusamra et al., 2015).

Pyrrosia lingua (Thunb.) Farw., Family: Polypodiaceae

P. lingua is an epiphytic fern that mainly occurs in Korea, Japan, China, and other Asian states. *P. lingua* has antiviral, antioxidant, antibacterial and anti-cancer activities (Zheng, 1990; Fan et al., 2020). The leaves of *P. lingua* have traditionally been used to treat various viral infections. The chloroform leaf extract of *P. lingua* had antiviral activity against SARS-CoV-1 BJ-001 strain (EC_{50} = 43.2) and BJ-006 strain (EC_{50} = 40.5). *P. lingua* was proposed as one of the potential candidates for the development of new anti-SARS-CoV drugs (Li et al., 2005). Although the specific compounds responsible for its anti SARS-CoV activity were not established, *P. lingua* is known to contain several bioactive compounds such as flavonoids, chlorogenic acid, mangiferin, isomangiferin, astragaline and trifoline (Xiao et al., 2017). In separate studies, mangiferin has been shown to have potent anti-HIV-1 activities (Guha et al., 1996; Wang et al., 2011) as discussed under *M. indica*.

Trichosanthes Kirilowii Maxim., Family Cucurbitaceae

T. kirilowii is a Chinese medicinal herb with anti-HIV-1 activity (Lo et al., 2017). Trichobitacin from *T. kirilowii* suppresses HIV-1 induced formation of cell syncytia. Trichobitacin is a novel ribosome-inactivating protein that has been isolated from the roots *T. kirilowii* (Zheng et al., 2000). Trichobitacin also reduced the expression of HIV-1 p24 antigen and the number of HIV antigen positive cells in acutely HIV-1 infected culture (IC_{50} = 5 μg) (Zheng et al., 2000). According to Byers et al. (1994), clinical studies involving the use of trichosanthin to treat AIDS patients failing treatment with antiretroviral agents such as zidovudine may help to prevent loss of $CD4^+$ cells.

CONCLUSION

This review shows that 16 plant species used traditionally in Africa and Asia for treating various ailments possess *in vitro* and *in vivo* anti-HIV-1 and anti-SARS-CoV-2 activity. This affirms the potential of medicinal plants as a reservoir of potential antiviral compounds. These compounds need further investigation as potential drug candidates for HIV-1, SARS-CoV-1 and other pathogenic agents. Most of the plant species lack clinical studies to support their efficacy despite showing *in vitro* bioactivity. The potential therapeutic effects of these medicinal plants and others against SARS-CoV-2 and HIV-1 should be explored through further research, on their efficacy and safety, herbal-drug interactions, clinical trials and product development.

Only two plant species; *A. sativum* and *A. annua* showed biological activity against both HIV-1 and SARS-CoV-2. Eight of the 16 plant species plant had been tested for activity against SARS-CoV-2 whereas 10 had been tested against HIV-1. Only *P. ginseng* and *T. kirilowii* were subjected clinical trials. The rest of the plant species had only been evaluated in cellular based-assays *in vivo*.

Although the general phytochemistry of the plant species reviewed is known, it is only in a handful of cases where the specific compounds responsible for the antiviral activity was determined. The assays conducted involved the use of various extracts including crude and pure compounds as well as fractions of the extracts. The commonest extracts or solvents used were ethanol and water. The isolated pure compounds tested were geraniin from *P. amarus*, ginsenoside-Rb1 from *P. ginseng,* mangiferin from *M. indica,* six isolated bioactive flavonoids from *C. corylifolium*, michellamine B and korundamine A from *Ancistrocladus korupensis* and lectins and ajoene from *A. sativum*.

The cytotoxicity of most of the plant species was generally low where determined. However, the cytotoxicity data need to be backed by *in vitro* or *in vivo* toxicity data. This is important because be toxic and need to be thoroughly investigated to rule out or mitigate any possible harmful effects before use (Anywar et al., 2021). Medicinal plants could potentially be toxic and need to be thoroughly investigated to rule out or mitigate any possible harmful effects before use. This can be seen from the compound trichosanthin from *T. kirilowii* used to treat AIDS patients. Even though clinical studies involving the use of trichosanthin to treat AIDS patients failing treatment with antiretroviral drugs such as zidovudine may help to prevent loss of $CD4^+$ cells (Byers et al. (1994). Trichosanthin has undesirable side effects which have greatly restricted its clinical application (Zhao et al., 1999).

The plant extracts reviewed work mainly as inhibitors of the various viral enzymes involved in the virus life cycle. Although the mechanisms of action of most of the major medicinal plants were well understood, there were cases such as *Cullen corylifolium* against SARS-CoV-2, Korundamine A from *Ancistrocladus korupensis* in the different strains of HIV-1 and the water infusion *Artemisia annua* against HIV-1 where the mode of action was no determined.

Although the aspect of herb-drug interactions between the medicinal plants and conventional medicines are largely unknown, potential threats exist and need to be investigated. For instance, *P. ginseng* was found to interact with some anti-HIV drugs and change their pharmacokinetic properties. Ginsenoside Rh2, a compound from *P. ginseng* increased the accumulation and decreased the efflux of ritonavir through P-glycoprotein (P-gp) in Caco-2 cells and MDCK-MDR1 cells (Shi et al., 2013).

The potential therapeutic effects of *T. cacao* against SARS-CoV-2 should be explored through further research.

AUTHOR CONTRIBUTIONS

AG conceptualised the research idea. All the authors participated in drafting, reviewing and reading the manuscript.

ACKNOWLEDGMENTS

The authors acknowledge their individual research institutions.

REFERENCES

Abrahão, J. S., and de Arruda, L. B. (2020). Special Issue "Emerging Viruses: Surveillance, Prevention, Evolution, and Control". *Viruses* 12 (3), 306. doi:10.3390/v12030306

Abusamra, Y. A., Scuruchi, M., Habibatni, S., Maammeri, Z., Benayache, S., D'Ascola, A., et al. (2015). Evaluation of putative cytotoxic activity of crude extracts from *Onopordum acanthium* leaves and *Spartium junceum* flowers against the U-373 glioblastoma cell line. *Pak J. Pharm. Sci.* 28 (4), 1225–1232.

Alam, F., Khan, G. N., and Asad, M. H. H. B. (2018). *Psoralea corylifolia* L: Ethnobotanical, biological, and chemical aspects: A review. *Phytother Res.* 32 (4), 597–615. doi:10.1002/ptr.6006

Anywar, G., Kakudidi, E., Byamukama, R., Mukonzo, J., Schubert, A., and Oryem-Origa, H. (2020a). Indigenous traditional knowledge of medicinal plants used by herbalists in treating opportunistic infections among people living with HIV/AIDS in Uganda. *J. Ethnopharmacol*, 246, 112205. doi:10.1016/j.jep.2019.112205

Anywar, G., Kakudidi, E., Byamukama, R., Mukonzo, J., Schubert, A., and Oryem-Origa, H. (2020b). Medicinal plants used by traditional medicine practitioners to boost the immune system in people living with HIV/AIDS in Uganda. *Eur. J. Integr. Med.* 35, 101011. doi:10.1016/j.eujim.2019.101011

Anywar, G. U., Kakudidi, E. K., Byamukama, R., Mukonzo, J. K., Schubert, A., Oryem-Origa, H., et al. (2021). A review of the toxicity and phytochemistry of medicinal plant species used by herbalists in treating people living with HIV/AIDS in Uganda. *Front. Pharmacol.* 12, 435. doi:10.3389/fphar.2021.615147

Baek, S. C., Nam, K. H., Yi, S. A., Jo, M. S., Lee, K. H., Lee, Y. H., et al. (2019). Anti-adipogenic Effect of β-Carboline Alkaloids from Garlic (Allium sativum). *Foods* 8 (12), 673. doi:10.3390/foods8120673

Bai, L., Gao, J., Wei, F., Zhao, J., Wang, D., and Wei, J. (2018). Therapeutic Potential of Ginsenosides as an Adjuvant Treatment for Diabetes. *Front. Pharmacol.* 9, 423. doi:10.3389/fphar.2018.00423

Baliga, M. S., Saxena, A., Kaur, K., Kalekhan, F., Chacko, A., Venkatesh, P., et al. (2014). "Polyphenols in the Prevention of Ulcerative Colitis," in *Polyphenols in Human Health and Disease* (Massachusetts, United States: Academic Press), 655–663. doi:10.1016/b978-0-12-398456-2.00050-5

Brendler, T., and van Wyk, B. E. (2008). A historical, scientific and commercial perspective on the medicinal use of *Pelargonium sidoides* (Geraniaceae). *J. Ethnopharmacol*, 119(3), 420–433. doi:10.1016/j.jep.2008.07.037

Bringmann, G., Steinert, C., Feineis, D., Mudogo, V., Betzin, J., and Scheller, C. (2016). HIV-inhibitory michellamine-type dimeric naphthylisoquinoline alkaloids from the Central African liana *Ancistrocladus congolensis*. *Phytochemistry*, 128, 71–81. doi:10.1016/j.phytochem.2016.04.005

Byers, V. S., Levin, A. S., Malvino, A., Waites, L., Robins, R. A., and Baldwin, R. W. (1994). A phase II study of effect of addition of trichosanthin to zidovudine in patients with HIV disease and failing antiretroviral agents. *AIDS Res. Hum. Retroviruses* 10 (4), 413–420. doi:10.1089/aid.1994.10.413

Cedrón, J. C., Gutiérrez, D., Flores, N., Ravelo, A. G., and Estévez-Braun, A. (2010). Synthesis and antiplasmodial activity of lycorine derivatives. *Bioorg. Med. Chem.*, 18(13), 4694–4701. doi:10.1016/j.bmc.2010.05.023

Chang, F. R., Yen, C. T., Ei-Shazly, M., Lin, W. H., Yen, M. H., Lin, K. H., et al. (2012). Anti-human coronavirus (anti-HCoV) triterpenoids from the leaves of *Euphorbia neriifolia*. *Nat. Prod. Commun.* 7 (11), 1415–1417. doi:10.1177/1934578x1200701103

Chaudhary, N., Sabikhi, L., Hussain, S. A., and Kumar, M. H. S. (2020). A comparative study of the antioxidant and ACE inhibitory activities of selected herbal extracts. *J. Herbal Med.*, 22, 100343. doi:10.1016/j.hermed.2020.100343

Chavan, R. D., Shinde, P., Girkar, K., Madage, R., and Chowdhary, A. (2016). Assessment of anti-influenza activity and hemagglutination inhibition of *Plumbago indica* and *Allium sativum* Extracts. *Pharmacognosy Res.* 8 (2), 105–111. doi:10.4103/0974-8490.172562

Cho, Y. K., and Kim, J. E. (2017). Effect of Korean Red Ginseng intake on the survival duration of human immunodeficiency virus type 1 patients. *J. Ginseng Res.* 41 (2), 222–226. doi:10.1016/j.jgr.2016.12.006

Choi, K. T. (2008). Botanical characteristics, pharmacological effects and medicinal components of Korean Panax ginseng C A Meyer. *Acta Pharmacol. Sin* 29 (9), 1109–1118. doi:10.1111/j.1745-7254.2008.00869.x

Chopra, B., Dhingra, A. K., and Dhar, K. L. (2013). Psoralea corylifolia L. (Buguchi) - folklore to modern evidence: review. *Fitoterapia* 90, 44–56. doi:10.1016/j.fitote.2013.06.016

Chopra, R. N., Nayar, S. L., and Chopra, I. C. (1956). *Glossary of Indian medicinal plants*, Vol. 1. New Delhi: Council of Scientific & Industrial Research.

Csupor-Löffler, B., Zupkó, I., Molnár, J., Forgo, P., and Hohmann, J. (2014). Bioactivity-guided isolation of antiproliferative compounds from the roots of *Onopordum acanthium*. *Nat. Product. Commun.* 9 (3), 337–340.

Ding, Y., Wang, H., Shen, H., Li, Z., Geng, J., Han, H., et al. (2003). The clinical pathology of severe acute respiratory syndrome (SARS): a report from China. *The J. Pathol. A J. Pathological Soc. Great Britain Ireland* 200 (3), 282–289.

Efferth, T., Romero, M. R., Wolf, D. G., Stamminger, T., Marin, J. J., and Marschall, M. (2008). The antiviral activities of artemisinin and artesunate. *Clin. Infect. Dis.* 47, 804–811. doi:10.1086/591195

El-Saber Batiha, G., Magdy Beshbishy, A., G Wasef, L., Elewa, Y. H. A., A Al-Sagan, A., Abd El-Hack, M. E., et al. (2020). Chemical constituents and pharmacological activities of garlic (*Allium sativum* L.): A Review. *Nutrients* 12 (3), 872. doi:10.3390/nu12030872

Fan, Y., Feng, H., Liu, L., Zhang, Y., Xin, X., and Gao, D. (2020). Chemical components and antibacterial activity of the essential oil of six Pyrrosia species. *Chem. Biodivers*, 17(10), e2000526. doi: doi: doi:10.1002/cbdv.202000526

Ferreira, J. F. S., Simon, J. E., and Janick, J. (1997). *Artemisia annua*: botany, horticulture, pharmacology. *Horticult. Rev.* 19, 319–371.

Foster, P., and Sork, V. (1997). Population and genetic structure of the West African rain forest liana *Ancistrocladus korupensis* (Ancistrocladaceae). *Am. J. Bot.*, 84(8), 1078–1091. doi: doi: doi:10.2307/2446151

Guha, S., Ghosal, S., and Chattopadhyay, U. (1996). Antitumor, immunomodulatory and anti-HIV effect of mangiferin, a naturally occurring glucosylxanthone. *Chemotherapy* 42 (6), 443–451. doi:10.1159/000239478

Hallock, Y. F., Cardellina, J. H., Schäffer, M., Bringmann, G., François, G., and Boyd, M. R. (1998). Korundamine A, a novel HIV-inhibitory and antimalarial "hybrid" naphthylisoquinoline alkaloid heterodimer from Ancistrocladus korupensis. *Bioorg. Med. Chem. Lett.*, 8(13), 1729–1734. doi:10.1016/S0960-894X(98)00304-7

Hashemifesharaki, R., and Gharibzahedi, S. M. T. (2020). Future nutrient-dense diets rich in vitamin D: a new insight toward the reduction of adverse impacts of viral infections similar to COVID-19. *Nutrire* 45 (2), 19. doi:10.1186/s41110-020-00122-4

Helfer, M., Koppensteiner, H., Schneider, M., Rebensburg, S., Forcisi, S., Müller, C., et al. (2014). The root extract of the medicinal plant *Pelargonium sidoides* is a potent HIV-1 attachment inhibitor. *PloS one* 9 (1), e87487. doi:10.1371/journal.pone.0087487

Hieh, C. F., Chaw, S. M., and Wang, J. C. (1993). *Composite: Flora of Taiwan*. 2n Edn. (Taipei: Editorial Committee of the Flora of Taiwan), 3, 414–504.

Illanes-Álvarez, F., Márquez-Ruiz, D., Márquez-Coello, M., Cuesta-Sancho, S., and Girón-González, J. A. (2021). Similarities and differences between HIV and SARS-CoV-2. *Int. J. Med. Sci.* 18 (3), 846–851. doi:10.7150/ijms.50133

Jeong, C. S., Hyun, J. E., Kim, Y. S., and Lee, E. S. (2003). Ginsenoside Rb1: the anti-ulcer constituent from the head of Panax ginseng. *Arch. Pharm. Res.* 26 (11), 906–911. doi:10.1007/BF02980198

Keyaerts, E., Vijgen, L., Pannecouque, C., Van Damme, E., Peumans, W., Egberink, H., et al. (2007). Plant lectins are potent inhibitors of coronaviruses by interfering with two targets in the viral replication cycle. *Antivir. Res*, 75(3), 179–187. doi:10.1016/j.antiviral.2007.03.003

Kim, D. W., Seo, K. H., Curtis-Long, M. J., Oh, K. Y., Oh, J. W., Cho, J. K., et al. (2014). Phenolic phytochemical displaying SARS-CoV papain-like protease inhibition from the seeds of *Psoralea corylifolia*. *J. Enzyme Inhib. Med. Chem.* 29 (1), 59–63. doi:10.3109/14756366.2012.753591

Kim, S., Kim, D. B., Jin, W., Park, J., Yoon, W., Lee, Y., et al. (2018). Comparative studies of bioactive organosulphur compounds and antioxidant activities in garlic (*Allium sativum* L.), elephant garlic (*Allium ampeloprasum* L.) and onion (*Allium cepa* L.). *Nat. Prod. Res.* 32 (10), 1193–1197. doi:10.1080/14786419.2017.1323211

Kimura, K. (1979). Manufacturing procedure of natural pigment from cacao bean. *Jpn. Patent No. Showa* 54, 10567.

Kolodziej, H. (2002). *Pelargonium reniforme and Pelargonium sidoides: their botany, chemistry and medicinal use. Geranium and Pelargonium*. London: Taylor & Francis, 262–290.

Kretzing, S., Abraham, G., Seiwert, B., Ungemach, F. R., Krügel, U., and Regenthal, R. (2011). Dose-dependent emetic effects of the Amaryllidaceous alkaloid lycorine in beagle dogs. *Toxicon*, 57(1), 117–124. doi:10.1016/j.toxicon.2010.10.012

Kurokawa, M., Shimizu, T., Watanabe, W., and Shiraki, K. (2010). Development of new antiviral agents from natural products. *Open Antimicrob. Agents J.* 2 (1), 49–57. doi:10.2174/1876518101002020049

Lamoral-Theys, D., Decaestecker, C., Mathieu, V., Dubois, J., Kornienko, A., Kiss, R., et al. (2010). Lycorine and its derivatives for anticancer drug design. *Mini Rev. Med. Chem.* 10 (1), 41–50. doi:10.2174/138955710791112604

Li, S. Y., Chen, C., Zhang, H. Q., Guo, H. Y., Wang, H., Wang, L., et al. (2005). Identification of natural compounds with antiviral activities against SARS-associated coronavirus. *Antivir. Res* 67 (1), 18–23. doi:10.1016/j.antiviral.2005.02.007Li

Li, W., Moore, M. J., Vasilieva, N., Sui, J., Wong, S. K., Berne, M. A., et al. (2003). Angiotensin-converting enzyme 2 is a functional receptor for the SARS coronavirus. *Nature* 426 (6965), 450–454. doi:10.1038/nature02145

Li, X., Wang, H., Liu, C., and Chen, R. (2010). Chemical constituents of Acacia catechu. *Zhongguo Zhong Yao Za Zhi* 35 (11), 1425–1427.

Lissiman, E., Bhasale, A. L., and Cohen, M. (2014). Garlic for the common cold. *Cochrane Database Syst. Rev.* 2014 (11), CD006206. doi:10.1002/14651858.CD006206.pub4

Lo, H. Y., Li, T. C., Yang, T. Y., Li, C. C., Chiang, J. H., Hsiang, C. Y., et al. (2017). Hypoglycemic effects of *Trichosanthes kirilowii* and its protein constituent in diabetic mice: the involvement of insulin receptor pathway. *BMC Complement. Altern. Med.* 17, 53. doi:10.1186/s12906-017-1578-6

Louten, J. (2016). Emerging and reemerging viral diseases. *Essent. Hum. Virol.*, 291–310. doi:10.1016/B978-0-12-800947-5.00016-8

Lubbe, A., Seibert, I., Klimkait, T., and van der Kooy, F. (2012). Ethnopharmacology in overdrive: The remarkable anti-HIV activity of *Artemisia annua*. *J. Ethnopharmacol*, 141(3), 854–859. doi:10.1016/j.jep.2012.03.024

Makare, N., Bodhankar, S., and Rangari, V. (2001). Immunomodulatory activity of alcoholic extract of *Mangifera indica* L. in mice. *J. Ethnopharmacol* 78 (2-3), 133–137. doi:10.1016/s0378-8741(01)00326-9

Manfredi, K. P., Blunt, J. W., Cardellina, J. H., McMahon, J. B., Pannell, L. L., Cragg, G. M., et al. (1991). Novel alkaloids from the tropical plant *Ancistrocladus abbreviatus* inhibit cell killing by HIV-1 and HIV-2. *J. Med. Chem.* 34 (12), 3402–3405. doi:10.1021/jm00116a011

Martin, K. W., and Ernst, E. (2003). Antiviral agents from plants and herbs: a systematic review. *Antivir. Ther.* 8 (2), 77–90.

Michaelis, M., Doerr, H. W., and Cinatl, J., Jr (2011). Investigation of the influence of EPs® 7630, a herbal drug preparation from Pelargonium sidoides, on replication of a broad panel of respiratory viruses. *Phytomedicine*, 18(5), 384–386. doi:10.1016/j.phymed.2010.09.008Mourya

Mourya, D. T., Yadav, P. D., Ullas, P. T., Bhardwaj, S. D., Sahay, R. R., Chadha, M. S., et al. (2019). Emerging/re-emerging viral diseases & new viruses on the Indian horizon. *Indian J. Med. Res.* 149 (4), 447–467. doi:10.4103/ijmr.IJMR_1239_18

Naik, A. D., and Juvekar, A. R. (2003). Effects of alkaloidal extract of *Phyllanthus niruri* on HIV replication. *Indian J. Med. Sci.* 57 (9), 387–393.

Notka, F., Meier, G., and Wagner, R. (2004). Concerted inhibitory activities of *Phyllanthus amarus* on HIV replication *in vitro* and *ex vivo*. *Antivir. Res* 64 (2), 93–102. doi:10.1016/j.antiviral.2004.06.010

Nutan, M. M., Modi, M., Dezzutti, C. S., Kulshreshtha, S., Rawat, A. K., Srivastava, S. K., et al. (2013). Extracts from *Acacia catechu* suppress HIV-1 replication by inhibiting the activities of the viral protease and Tat. *Virol. J.* 10 (1), 309–317. doi:10.1186/1743-422x-10-309

Oyeleke, S. A., Ajayi, A. M., Umukoro, S., Aderibigbe, A. O., and Ademowo, O. G. (2018). Anti-inflammatory activity of *Theobroma cacao* L. stem bark ethanol extract and its fractions in experimental models. *J. Ethnopharmacol* 222, 239–248. doi:10.1016/j.jep.2018.04.050

Patel, J. D., Kumar, V., and Bhatt, S. A. (2009). Antimicrobial screening and phytochemical analysis of the resin part ofAcacia catechu. *Pharm. Biol.* 47 (1), 34–37. doi:10.1080/13880200802400527

Perera, C., and Efferth, T. (2012). Antiviral medicinal herbs and phytochemicals. *J. Pharmacogn* 3 (1), 45–48.

Phan, A. D. T., Netzel, G., Chhim, P., Netzel, M. E., and Sultanbawa, Y. (2019). Phytochemical characteristics and antimicrobial activity of Australian grown garlic (*Allium Sativum* L.) Cultivars. *Foods* 8 (9), 358. doi:10.3390/foods8090358

Plants of the world (POWO) (2020). http://powo.science.kew.org/taxon/urn:lsid:ipni.org:names:235234-1.

Prasad, A., Muthamilarasan, M., and Prasad, M. (2020). Synergistic antiviral effects against SARS-CoV-2 by plant-based molecules. *Plant Cel Rep* 39 (9), 1109–1114. doi:10.1007/s00299-020-02560-w

Rivlin, R. S. (2001). Historical perspective on the use of garlic. *J. Nutr.* 131 (3), 951S–4S. doi:10.1093/jn/131.3.951S

Sagaya Jansi, R., Khusro, A., Agastian, P., Alfarhan, A., Al-Dhabi, N. A., Arasu, M. V., et al. (2020). Emerging paradigms of viral diseases and paramount role of

natural resources as antiviral agents. *Sci. Total Environ.*, 143539. doi:10.1016/j.scitotenv.2020.143539

Sakagami, H., Kawano, M., Thet, M. M., Hashimoto, K., Satoh, K., Kanamoto, T., et al. (2011). Anti-HIV and immunomodulation activities of cacao mass lignin-carbohydrate complex. *In Vivo* 25 (2), 229–236.

Sakagami, H., Kushida, T., Oizumi, T., Nakashima, H., and Makino, T. (2010). Distribution of lignin-carbohydrate complex in plant kingdom and its functionality as alternative medicine. *Pharmacol. Ther.*, 128(1), 91–105. doi: doi: doi:10.1016/j.pharmthera.2010.05.004

Schneiderová, K., Slapetová, T., Hrabal, R., Dvořáková, H., Procházková, P., Novotná, J., et al. (2013). Tomentomimulol and mimulone B: two new C-geranylated flavonoids from Paulownia tomentosa fruits. *Nat. Prod. Res.* 27 (7), 613–618. doi:10.1080/14786419.2012.683002

Sharifi, N., Souri, E., Ziai, S. A., Amin, G., and Amanlou, M. (2013). Discovery of new angiotensin converting enzyme (ACE) inhibitors from medicinal plants to treat hypertension using an *in vitro* assay. *Daru* 21 (1), 74. doi:10.1186/2008-2231-21-74

Shehzad, O., Khan, S., Ha, I. J., Park, Y., and Kim, Y. S. (2012). Rational development of a selection model for solvent gradients in single-step separation of ginsenosides from *Panax ginseng* using high-speed counter-current chromatography. *J. Sep. Sci.* 35, 1462–1469. doi:10.1002/jssc.201200135

Shehzad, O., Kim, H. P., and Kim, Y. S. (2013). State-of-the-art separation of ginsenosides from Korean white and red ginseng by countercurrent chromatography. *Anal. Bioanal. Chem.* 405, 4523–4530. doi:10.1007/s00216-012-6609-z

Shi, J., Cao, B., Zha, W. B., Wu, X. L., Liu, L. S., Xiao, W. J., et al. (2013). Pharmacokinetic interactions between 20(S)-ginsenoside Rh2 and the HIV protease inhibitor ritonavir *in vitro* and *in vivo*. *Acta Pharmacol. Sin* 34 (10), 1349–1358. doi:10.1038/aps.2013.69

Sung, H., Kang, S. M., Lee, M. S., Kim, T. G., and Cho, Y. K. (2005). Korean red ginseng slows depletion of CD4 T cells in human immunodeficiency virus type 1-infected patients. *Clin. Diagn. Lab. Immunol.* 12 (4), 497–501. doi:10.1128/CDLI.12.4.497-501.2005

Sunil, M. A., Sunitha, V. S., Radhakrishnan, E. K., and Jyothis, M. (2019). Immunomodulatory activities of *Acacia catechu*, a traditional thirst quencher of South India. *J. Ayurveda Integr. Med.*, 10(3), 185–191. doi: doi: doi:10.1016/j.jaim.2017.10.010

Tatarintsev, A. V., Vrzhets, P. V., Ershov, D. E., Shchegolev, A. A., Turgiev, A. S., Karamov, E. V., et al. (1992). The ajoene blockade of integrin-dependent processes in an HIV-infected cell system. *Vestn Ross Akad Med. Nauk* (11–12), 6–10.

UNAIDS (2021). *Global HIV & AIDS statistics — Fact sheet*. https://www.unaids.org/sites/default/files/media_asset/UNAIDS_FactSheet_en.pdf.

Unten, S., Ushijima, H., Shimizu, H., Tsuchie, H., Kitamura, T., Moritome, N., et al. (1991). Effect of cacao husk extract on human immunodeficiency virus infection. *Lett. Appl. Microbiol.*, 13(6), 251–254. doi: doi: doi:10.1111/j.1472-765X.1991.tb00621.x

Walder, R., Kalvatchev, Z., Garzaro, D., Barrios, M., and Apitz-Castro, R. (1997). *In vitro* suppression of HIV-1 replication by ajoene [(e)-(z)-4,5,9-trithiadodeca-1,6,11-triene-9 oxide]. *Biomed. Pharmacother.*, 51(9), 397–403. doi: doi: doi:10.1016/S0753-3322(97)89433-4

Wang, R. R., Gao, Y. D., Ma, C. H., Zhang, X. J., Huang, C. G., Huang, J. F., et al. (2011). Mangiferin, an anti-HIV-1 agent targeting protease and effective against resistant strains. *Molecules* 16 (5), 4264–4277. doi:10.3390/molecules16054264

Wei, G., Chen, H., Nie, F., Ma, X., and Jiang, H. (2017). 1, 3, 6-Trihydroxy-7-Methyl-9, 10-Anthracenedione Isolated from genus Lindera with Anti-cancer Activity. *Anticancer Agents Med. Chem.* 17 (11), 1604–1607. doi:10.2174/1871520615666150914114649

WHO (2021). WHO Coronavirus (COVID-19) Dashboard. https://covid19.who.int.

Wickramasuriya, A. M., and Dunwell, J. M. (2018). Cacao biotechnology: current status and future prospects. *Plant Biotechnol. J.* 16 (1), 4–17. doi:10.1111/pbi.12848

Willcox, M., Bodeker, G., Bourdy, G., Dhingra, V., Falquet, J., Ferreira, J. F., et al. (2004). *Artemisia annua* as a traditional herbal antimalarial. *Traditional Med. plants Malar.* 4, 43–59. doi:10.1201/9780203502327-14

Xiao, M., Cao, N., Fan, J. J., Shen, Y., and Xu, Q. (2011). Studies on flavonoids from the leaves of Lindera aggregata. *Zhong Yao Cai* 34 (1), 62–64.

Xiao, W., Peng, Y., Tan, Z., Lv, Q., Chan, C. O., Yang, J., et al. (2017). Comparative evaluation of chemical profiles of *Pyrrosiae folium* originating from three pyrrosia species by HPLC-DAD combined with multivariate statistical analysis. *Molecules* 22 (12), 2122. doi:10.3390/molecules22122122

Xu, X., Chen, P., Wang, J., Feng, J., Zhou, H., Li, X., et al. (2020). Evolution of the novel coronavirus from the ongoing Wuhan outbreak and modeling of its spike protein for risk of human transmission. *Sci. China Life Sci.* 63 (3), 457–460. doi:10.1007/s11427-020-1637-5

Yang, L., Zhang, J. H., Zhang, X. L., Lao, G. J., Su, G. M., Wang, L., et al. (2019). Tandem mass tag-based quantitative proteomic analysis of lycorine treatment in highly pathogenic avian influenza H5N1 virus infection. *PeerJ* 7, e7697. doi:10.7717/peerj.7697

Zhao, J., Ben, L. H., Wu, Y. L., Hu, W., Ling, K., Xin, S. M., et al. (1999). Anti-HIV agent trichosanthin enhances the capabilities of chemokines to stimulate chemotaxis and G protein activation, and this is mediated through interaction of trichosanthin and chemokine receptors. *J. Exp. Med.* 190 (1), 101–111. doi:10.1084/jem.190.1.101

Zheng, M. (1990). Experimental study of 472 herbs with antiviral action against the herpes simplex virus. *Zhong Xi Yi Jie He Za Zhi* 10 (1), 39–41.

Zheng, Y. T., Ben, K. L., and Jin, S. W. (2000). Anti-HIV-1 activity of trichobitacin, a novel ribosome-inactivating protein. *Acta Pharmacol. Sin* 21 (2), 179–182.

Conflict of Interest: The authors declare that the research was conducted in the absence of any commercial or financial relationships that could be construed as a potential conflict of interest.

Publisher's Note: All claims expressed in this article are solely those of the authors and do not necessarily represent those of their affiliated organizations, or those of the publisher, the editors and the reviewers. Any product that may be evaluated in this article, or claim that may be made by its manufacturer, is not guaranteed or endorsed by the publisher.

frontiers in Pharmacology

ORIGINAL RESEARCH
published: 24 September 2021
doi: 10.3389/fphar.2021.707695

The Chinese Herbal Prescription JieZe-1 Inhibits Membrane Fusion and the Toll-like Receptor Signaling Pathway in a Genital Herpes Mouse Model

*Qianni Duan[1†], Tong Liu[1†], Cong Huang[1], Qingqing Shao[1], Yonggui Ma[2], Wenjia Wang[1], Tianli Liu[1], Jun Sun[3], Jianguo Fang[2], Guangying Huang[1] and Zhuo Chen[1]**

[1]Department of TCM, Institute of Integrated Traditional Chinese and Western Medicine, Tongji Hospital, Tongji Medical College, Huazhong University of Science and Technology, Wuhan, China, [2]Department of Pharmacy, Tongji Hospital, Tongji Medical College, Huazhong University of Science and Technology, Wuhan, China, [3]Department of Biochemistry and Molecular Biology, Tongji Medical College, Huazhong University of Science and Technology, Wuhan, China

OPEN ACCESS

Edited by:
Anirban Mandal,
Mrinalini Datta Mahavidyapith, India

Reviewed by:
Guang-Bo Ge,
Shanghai University of Traditional Chinese Medicine, China
Wang Ning,
Anhui University of Chinese Medicine, China

***Correspondence:**
Zhuo Chen
chenz@tjh.tjmu.edu.cn

†These authors have contributed equally to this work and share first authorship

Specialty section:
This article was submitted to Ethnopharmacology, a section of the journal Frontiers in Pharmacology

Received: 10 May 2021
Accepted: 09 September 2021
Published: 24 September 2021

Citation:
Duan Q, Liu T, Huang C, Shao Q, Ma Y, Wang W, Liu T, Sun J, Fang J, Huang G and Chen Z (2021) The Chinese Herbal Prescription JieZe-1 Inhibits Membrane Fusion and the Toll-like Receptor Signaling Pathway in a Genital Herpes Mouse Model. Front. Pharmacol. 12:707695. doi: 10.3389/fphar.2021.707695

Chinese herbal prescription JieZe-1 is effective for genital herpes with no visible adverse effects clinically. It showed an excellent anti-HSV-2 effect *in vitro*. However, its mechanism of anti-HSV-2 effect *in vivo* remains unclear. This study was designed to evaluate the anti-HSV-2 effect of JieZe-1 and berberine in a genital herpes mouse model and explore the underlying mechanism. The fingerprint of JieZe-1 was determined by high-performance liquid chromatography. First, we optimized a mouse model of genital herpes. Next, the weight, symptom score, morphological changes, viral load, membrane fusion proteins, critical proteins of the Toll-like receptor signaling pathway, cytokines, and immune cells of vaginal tissue in mice at different time points were measured. Finally, we treated the genital herpes mouse model with JieZe-1 gel (2.5, 1.5, and 0.5 g/ml) and tested the above experimental indexes at 12 h and on the 9th day after modeling. JieZe-1 improved the symptoms, weight, and histopathological damage of genital herpes mice, promoted the keratin repair of tissues, and protected organelles to maintain the typical morphology of cells. It downregulated the expression of membrane fusion proteins, critical proteins of the Toll-like receptor signaling pathway, cytokines, and immune cells. The vaginal, vulvar, and spinal cord viral load and vaginal virus shedding were also significantly reduced. In summary, JieZe-1 shows significant anti-HSV-2 efficacy *in vivo*. The mechanism is related to the inhibition of membrane fusion, the Toll-like receptor signaling pathway, inflammatory cytokines, and cellular immunity. However, berberine, the main component of JieZe-1 monarch medicine, showed no efficacy at a concentration of 891.8 μM (0.3 mg/ml).

Keywords: Chinese herbal prescription JieZe-1, genital herpes, herpes simplex virus type 2, membrane fusion, toll-like receptor signaling pathway, immune cells

Abbreviations: DCs, dendritic cells; gD, glycoprotein D; gB, glycoprotein B; gH, glycoprotein H; gL, glycoprotein L; GH, genital herpes; HPLC, High-performance liquid chromatography; HSV-2, herpes simplex virus type 2; HVEM, herpesvirus entry mediator ligand protein; ICP5, earliest virus-specific infected cell polypeptides 5; IFN-β, interferon-β; IL-6, interleukin-6; IκBα, nuclear factor-kappa-B inhibitor alpha; JZ-1, JieZe-1; MyD88, myeloid differentiation factor 88; NK cell, natural killer cell.; TLR, toll-like receptor; TNF-α, tumor necrosis factor-α; VP16, viral protein 16.

INTRODUCTION

Herpes simplex virus type 2 (HSV-2) is a linear double-stranded DNA-enveloped virus that mainly infects the skin mucosa of genital, causing genital herpes (GH) (Rubicz et al., 2011). Women of childbearing age are more susceptible to the highest infection rate (James and Kimberlin, 2015). The recognized anti-HSV-2 drugs are acyclovir, penciclovir, cidofovir, and phosphonoformic acid, which mainly work by inhibiting viral DNA replication. No new, significant, and low-toxicity clinical drugs have been identified to treat wild-type and drug-resistant strains (Schleenvoigt et al., 2018). Anti-HSV vaccine research has not yet made a breakthrough (Johnston et al., 2014). HSV-2 has infected approximately 417 million people worldwide, with 19.2 million new cases each year (Looker et al., 2015). The prevention and treatment of HSV have been significant public health issues worldwide.

The adsorption and penetration of HSV-2 into host cells begin with the binding of viral glycoprotein D (gD) to specific receptors (herpesvirus entry mediator ligand protein (HVEM), Nectin-1, Nectin-2, or 3-O-sulfated heparin sulfate) on the cell surface. GB and gH/gL heterodimers are recruited sequentially, resulting in the activation of gH/gL heterodimers. Finally, the fusion activity of gB is upregulated so that it can be directly inserted into the cell membrane through its internal fusion ring (Luo et al., 2015). The recognition of HVEM, Nectin-1, and Nectin-2 by gD triggers membrane fusion (Fu et al., 2018).

The specificity of the Toll-like receptor (TLR) signaling pathway reveals the molecular basis of the body's recognition of pathogens. After adsorption and penetration, TLR4, which resides on the cell surface, recognizes viral glycoproteins (Lagos et al., 2008). TLR3, 7, and 9, found in the cytoplasm, recognize viral nucleic acids (Paludan et al., 2011; Barber, 2013). The cytoplasmic Toll/interleukin-1 receptor (TIR) domain activates the TLR signaling pathway by interacting with TIR domain adapter myeloid differentiation factor 88 (MyD88)/TIR domain-containing adaptor protein-inducing interferon-β. The TLR signaling pathway includes the MyD88-dependent pathway (most TLRs) and the MyD88-independent pathway (TLR3 and TLR4). Nuclear factor-kappa-B inhibitor alpha (IκBα) is phosphorylated (P-IκBα), triggering its ubiquitination and subsequent degradation. Nuclear factor-kappa-B (NF-κB) is released into the nucleus and binds to cellular DNA to activate the transcription of interleukin-6 (IL-6), tumor necrosis factor-α (TNF-α), interferon-β (IFN-β), and other cytokines to exert early immune response (Dunne and O'Neill, 2003; Hayden and Ghosh, 2004; Yamamoto et al., 2004).

Immune cells are a vital part of the immune response. Natural killer cells (NK cells), dendritic cells (DCs), and other innate immune cells also play essential roles in the first line of defense against HSV-2 infection (Elboim et al., 2013). DCs produce interferon to inhibit virus replication and chemokines from attracting NK cells, which can recognize and lyse HSV-2 infected cells, as well as secrete interferon (Chen et al., 2017). DCs can also present HSV-2 antigens to activate the adaptive immune response of T lymphocytes (Retamal-Díaz A. et al., 2017). $CD4^+$ and CD8+T cells, in particular, play primary roles in clearing HSV-2 infection, preventing virus infection in neurons, and reducing latent virus copies.

By drawing lessons from the antiviral research achievements of Traditional Chinese Medicine (TCM), JieZe-1 (JZ-1), an in-hospital preparation of Tongji Hospital (Approval Number: Z20103135), was added and subtracted from Yihuang Decoction, an ancient prescription in "*Fu Qingzhu's Obstetrics and Gynecology*" during Qing dynasty of China. JZ-1 is composed of 10 herb ingredients (shown in **Table 1**) and has been widely used for lower genital tract infections with heat-damp symptoms for many years. It shows preventive and therapeutic effects on genital herpes, *Trichomonas* vaginitis, *Candida albicans* vaginitis, and drug-resistant *Ureaplasma urealyticum* infection, with little effect on the dominant vaginal flora (Wei et al., 2008; Chen et al., 2009a, Chen et al., 2009b; Chen et al., 2009c; Chen et al., 2009d; Qiao et al., 2013). JZ-1 also refers to the antiviral research results of TCM. According to the literature reported, *Phellodendron chinense* C.K.Schneid., *Ginkgo biloba* L., *Solanum nigrum* L., *Taraxacum mongolicum* Hand.-Mazz., *Thlaspi arvense* L, *Smilax glabra* Roxb., and *Paeonia* × *suffruticosa* Andrews could resist Zika virus (Robinson et al., 2018), human immunodeficiency virus (Lü et al., 2012), hepatitis C virus (Javed et al., 2011), influenza virus (He et al., 2011), respiratory syncytial virus (Li et al., 2004), HSV-1 (Ooi et al., 2004), and rabies virus (Tu et al., 2018) respectively. All the above scientific evidence gave us reason to believe that the anti-HSV-2 effect of JZ-1 is worthy of being studied. Therefore, our team has done much research on HSV-2. In previous *in vitro* experiments, JZ-1 was found to interfere with HSV-2 adsorption and penetration into host cells by significantly reducing the expression of viral proteins gB, gD, viral protein 16 (VP16), earliest virus-specific infected cell polypeptides 5 (ICP5), and ICP4, improving cell morphology and increasing cell viability (Duan et al., 2020). Furthermore, it also exerts its anti-HSV-2 effect by inducing autophagy via inhibition of the PI3K/Akt/mTOR signaling axis. Moreover, JZ-1 attenuated the increase in inflammatory cytokines that had been induced by HSV-2 infection (Shao et al., 2020). However, its anti-HSV-2 effect and mechanism of action *in vivo* remain unclear.

Based on the membrane fusion effect, combined with the regulation of the TLR signaling pathway and immune cells, this paper intends to study the molecular mechanism of JZ-1 interfering with HSV-2 infection in mice, providing scientific insights into JZ-1 against GH.

MATERIALS AND METHODS

Cell Culture and Virus Preparation

The African green monkey kidney cell line (Vero) was purchased from the China Center for Type Culture Collection (CCTCC, Wuhan, China) and cultured in Dulbecco's modified Eagle's medium (DMEM) (Thermo Scientific, Waltham, MA, United States) supplemented with 10% fetal bovine serum (FBS) (Invitrogen, Carlsbad, CA, United States). The cells were grown in monolayers, and the medium was changed to the fresh medium every 48 h. HSV-2 strain 333, originally isolated from a primary genital lesion from a patient at the Baylor College of

TABLE 1 | Composition of Chinese herbal prescription JieZe-1 (JZ-1).

Chinese name	Species name	Family	Plant part	Weight(g)	Ratio (%)	Voucher number
Huangbo	*Phellodendron chinense* C.K.Schneid.	*Rutaceae*	Bark	10	7.1	TJ-1908-318
Baiguo	*Ginkgo biloba* L.	*Ginkgoaceae*	Seed	10	7.1	TJ-1908-112
Longkui	*Solanum nigrum* L.	*Solanaceae*	Fruit, Whole Plant	30	21.4	TJ-1908-154
Pugongying	*Taraxacum mongolicum* Hand.-Mazz.	*Asteraceae*	Whole Plant	15	10.7	TJ-1908-367
Baijiangcao	*Thlaspi arvense* L.	*Brassicaceae*	Aerial Part	30	21.4	TJ-1908-349
Baixianpi	*Dictamnus dasycarpus* Turcz.	*Rutaceae*	Root Bark	10	7.1	TJ-1908-114
Tufuling	*Smilax glabra* Roxb.	*Smilacaceae*	Rhizome	15	10.8	TJ-1908-019
Mudanpi	*Paeonia* × *suffruticosa* Andrews	*Paeoniaceae*	Root Bark	10	7.1	TJ-1908-179
Bohe	*Mentha canadensis* L.	*Lamiaceae*	Aerial Part	10	7.1	TJ-1908-394
bingpian	*Dryobalanops aromatica* C.F.Gaertn.	*Dipterocarpaceae*	Crystal	0.3	0.2	TJ-1908-061

Medicine (Houston, TX, United States), was used in this study because the strain has been widely used in mouse and guinea pig studies and is pathogenic in these species (Lo et al., 2018; López-Muñoz et al., 2018). The HSV-2 strain was purchased from Guangzhou Biotest Biotechnology Development Co., Ltd. (Guangdong, China) and was propagated in Vero cells with DMEM containing 2% FBS. The cells were subjected to three freeze-thaw cycles when more than 80% of them were floating. The supernatants were stored at −80°C after centrifugation. The original HSV-2 suspension was measured by the TCID50 method and plaque assay and diluted to 1×10^6–1×10^8 TCID50/0.1 ml or 2×10^4–2×10^6 PFU/ml before use. Based on the relevant results, 1×10^7 TCID50/0.1 ml (2×10^5 PFU/ml) was chosen as the dose for follow-up experiments.

Chemicals

A phytopharmacological research should define positive controls and use preferably standard drugs from clinics, which must have been validated and used over the years (Heinrich et al., 2020). As a commonly used clinical anti-HSV-2 drug, acyclovir was used as a positive control drug in the study. The acyclovir (ACV > 99%, Hubei Wushi Pharmaceutical Co., Ltd., Anlu, China) was prepared as 133.2 mM (30 mg/ml) gels before use.

Preparation of JZ-1 Gel and Berberine Gel

Basing on the principle of scientific nomenclature for plants (Rivera et al., 2014; Heinrich et al., 2020), the full species name including authorities and family, used plant part, and the ratio of the drugs were recorded in **Table 1** through consultation with Kew Medicinal Plant Names Services (MPNS, http://mpns.kew.org/mpns-portal/). All the medicinal materials were purchased from Hubei Shengdetang Prepared Slices of Chinese Crudo Drug Co., Ltd. (Xiaogan, China), which complies with the requirements of Chinese Good Manufacturing Practices for Pharmaceutical Products certified by the People's Republic of China (**Supplementary File 2**). The quality inspection reports of medicinal materials were provided in **Supplementary File 3** (labeled in English). The plant name, batch number, locality, date, inspector's name, inspection basis, the nature of the samples, and the methodology (using TLC) for determining the identity were reported in the reports. Furthermore, the medicinal materials were also identified by the Associate Professor of Pharmacy Yonggui Ma and Professor of Pharmacy Jianguo Fang. Voucher specimens were prepared for identification and deposited in the traditional medicine collection center for Department Pharmacy of Tongji Hospital (Tongji Medical College, Huazhong University of Science and Technology). The voucher number was presented in **Table 1**. JZ-1 was prepared as described previously (Duan et al., 2020). Ethanol was selected as an extraction solvent since most components of JZ-1 are alcohol soluble. When the ethanol was recycled, the extract was concentrated to a relative density of 1.20 under 60°C. Carbomer was dissolved with ddH_2O and added to an appropriate amount of final mixed liquid, and *Dryobalanops aromatica* C.F.Gaertn. (dissolved in anhydrous ethanol) was added. Sodium hydroxide solution (5 M) was added to adjust the pH of the carbomer to form a gel. As a part of "the 10th Five-Year National Science and Technology Project" (Approval Number: 2004BA709B13-02), the procedure selection, the best preparation conditions, and stability of JZ-1 lotion and vaginal gel have been researched by our team in previous studies. JZ-1 gel showed stable efficacy in the stability test performed by our team (**Supplementary File 1**). Berberine, as the main component of the monarch drug of JZ-1, was also used in our study to determine whether it can exert the same antiviral effect as the Chinese herbal prescription JieZe-1. Berberine (HPLC ≥ 98%, Sigma-Aldrich, St Louis, MO, United States) was prepared as 891.8 μM (0.3 mg/ml) gels before use.

High-Performance Liquid Chromatography (HPLC) Analysis of JZ-1

For the analysis, the standard products were purchased from Solarbio Science & Technology Co., Ltd. (HPLC ≥ 98%, Beijing, China). D-(-)-quinic acid, trigonelline, and citric acid were prepared at 5 mg/ml with ultrapure water. Berberine, luteolin, caffeic acid, apocynin, taxifolin, and ferulic acid were prepared at 2.5 mg/ml with 50% methanol aqueous solution. Then take these solutions to make a 1,000 μl mix. The resulting solution was filtered through a 0.22 μm membrane filter before HPLC injection. HPLC was performed using an Agilent 1,260 Infinity II system (Agilent Technologies, Santa Clara, CA, United States) equipped with a DAD detector and a Welch Ultimate XB C18 (250 mm × 4.6 mm; 5 μm). The mobile phase included 0.2% phosphoric acid plus 0.4% sodium 1-heptanesulfonate (A) and methanol (B)

TABLE 2 | Improved symptom score of mice with genital HSV-2 infection.

Symptom score	Corresponding symptoms
0	Asymptomatic (no symptoms such as redness and swelling of vulva, depilation, ulcer, etc.)
0.5	Increased vaginal secretions, slightly swelled vulva, no ulcer
1	Moderate redness and swelling of vulva, no ulcer
1.5	Severe redness and swelling of vulva, perineal protrusion, no ulcer
2	Small ulcers of vulva and surrounding tissue (diameter < 5 mm)
2.5	Small ulcers of vulva and surrounding tissue (diameter < 5 mm) with redness and swelling, hair removal, pus, etc.
3	Moderate ulcer of vulva and surrounding tissue (5 mm ≤ diameter ≤ 10 mm)
3.5	Moderate ulcer of vulva and surrounding tissue (5 mm ≤ diameter ≤ 10 mm) with redness and swelling, hair removal, pus, etc.
4	Large ulcer of vulva and surrounding tissue (10 mm < diameter)
4.5	Large ulcer of vulva and surrounding tissue (10 mm < diameter). Or hind limb paralysis, lower body stiffness, loss of normal movement ability
5	Death (extreme weight loss, cold body, weak breathing, dying or death)

at a flow speed of 1.0 ml/min in the condition of a column temperature of 30°C. The detection wavelength was set at 214 nm. The reference standard sample injection volume was 10 μl. The gradient elution was as follows: 0–5 min (100–100% A, 0%–0% B), 5–60 min (100–60% A, 0%–40% B), 60–120 min (60–30% A, 40–70% B), 120–125 min (30–30% A, 70–70% B), 125–125.1 min (30–100% A, 70–0% B), 125.1–132 min (100–100% A, 0–0% B). The chromatographic data and peak area scores were collected and analyzed using ChemStation software.

Animals

All the animal experiments were carried out in a class II biosafety laboratory (BSL-2) under the Guidelines for Care and Use of Experimental Animals (Ministry of Science and Technology of China, 2011) and were approved by the Experimental Animal Ethics Committee of Tongji Medical College of Huazhong University of Science and Technology in December 2018 (IACUC Number: 840). BALB/c female mice (9 weeks, 20 ± 2 g) were purchased from Beijing Vital River Laboratory Animal Technology Co., Ltd. (Beijing, China). The mice were fed adaptively for 1 week under a 12 h light/dark cycle at 24°C with free access to water and food. The mice were randomly assigned to 10 in each group.

Modeling Method

Progesterone increases susceptibility to genital herpes infection (Kaushic et al., 2003). The mice were intramuscularly injected with 150 μl of progesterone for 5 days. On the day of modeling, after anesthesia, the mouse vagina was rubbed repeatedly 50 times and injected with 20 μl of blank gel and then 20 μl of HSV-2 suspension. The symptom score was graded as follows: 0 points, asymptomatic; 1 point, moderate swelling of the vulva; 2 points, small ulcers of the vulva (<5 mm); 3 points, moderate ulcer of the vulva (5–10 mm); 4 points, large ulcer of the vulva (>10 mm); 5 points, death. For symptoms between two levels, ±0.5 points were recorded (**Table 2**). Samples were taken from the anesthetized mice at 12 h and the 1st, 3rd, 5th, 7th, 9th, 12th, and 14th days after modeling.

Drug Administration Method

We controlled different variables to explore the drug administration method. Different concentrations of JZ-1 (0.5–2.5 g/ml) and administration cycle (9, 12, or 14 days) were used to treat mice with genital herpes. Non-anesthetized mice are active and often squeeze a part of the drug gel out. Anesthesia can significantly increase the residence time of the gel. However, frequent anesthesia can be harmful to mice. We compared the effects of anesthesia and no anesthesia on the efficacy of the drug administration. Based on the relevant results, we selected three concentration gradients, 2.5, 1.5, and 0.5 g/ml, for follow-up experiments. We administered the drug gel without anesthesia to the mice for 14 days, including 5 days before modeling and 9 days after modeling. In addition to progesterone injection, the mice were administered 20 μl of gel (JZ-1 gel, berberine gel, or blank gel) twice a day for 5 days and then were modeled using the previous method. At 12 h, half of the mice in each group were anesthetized and sampled. The other mice were given the gel twice a day in different groups and were continued to be observed. The vaginal washings were collected on day 3. On day 9, we anesthetized and sampled the remaining mice. The experimental protocol was also shown in **Figure 1**.

Virus TCID50 Detection

Vero cells were inoculated in a 96-well plate and grown in monolayers. The HSV-2 suspension was diluted 10 times and inoculated with Vero cells. The cytopathic effect (CPE) in each well was observed every day until it no longer increased. The TCID50 was calculated according to the Reed–Muench method (Reed and Muench, 1938).

Plaque Assays

Vero cells were inoculated in a 24-well plate and grown in monolayers. The HSV-2 suspension (or mouse vaginal washing filtered using a 0.22 μm aseptic filter) was diluted 10 times and inoculated with monolayer Vero cells for 2 h. The supernatant was discarded, and DMEM containing 1% methylcellulose was added to continue the culture until the number of plaques no longer increased. The cells were then

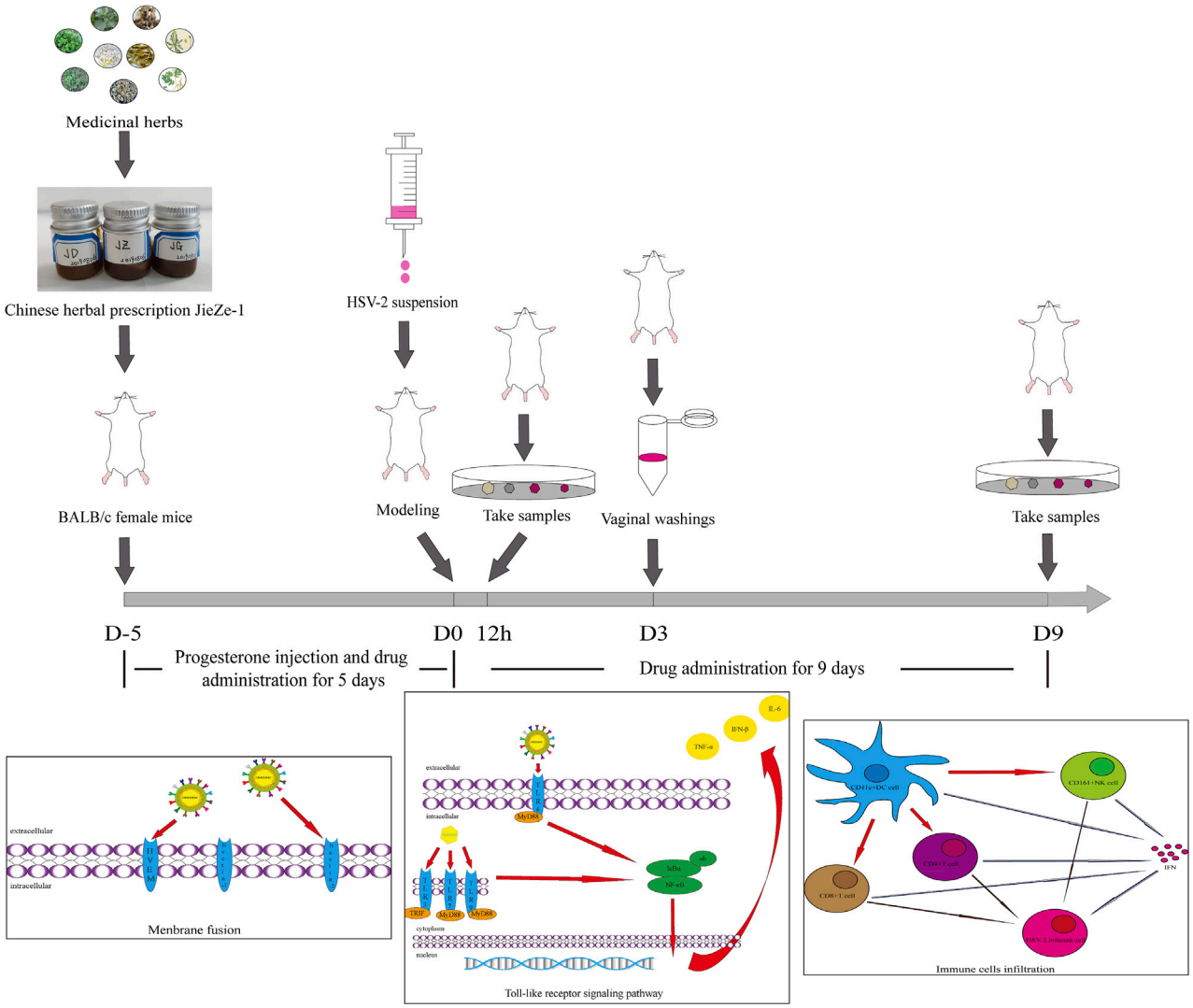

FIGURE 1 | The graphic illustration of the experiment.

fixed with paraformaldehyde and stained with crystal violet solution (Servicebio, Wuhan, China). After washing, plaque formation was observed.

Western Blotting

The vaginal and vulvar tissues were homogenized in RIPA lysis buffer with protease and phosphatase inhibitors. The concentration of total protein was determined using the BCA kit (Servicebio, Wuhan, China). The loading buffer was added to the extracts, followed by boiling for 10 min. The proteins were separated by 8–12% SDS-PAGE and transferred to a nitrocellulose membrane (Merck Millipore, Billerica, MA, United States). The membrane was sealed in skim milk and then incubated with primary antibodies against gD, ICP5, VP16, Nectin-1, Nectin-2, HVEM, TLR3, TLR9 (Abcam, Cambridge, United Kingdom), TLR4, TLR7 (Absin, Shanghai, China), MyD88 (ABclonal, Wuhan, China), IκBα, and P-IκBα (CST, Danvers, MA, United States) and secondary antibody (LI-COR, Lincoln, NE, United States). Finally, the Odyssey instrument (LI-COR, Lincoln, NE, United States) was used to acquire images on 700 or 800 nm channels.

Enzyme-Linked Immunosorbent Assay (ELISA)

IL-6, IFN-β, and TNF-α ELISA kits were purchased from Neobioscience Biological Technology Co., Ltd. (Shenzhen, China). The supernatant from the mouse vaginal tissue homogenate was extracted and evaluated using ELISA kits according to the manufacturer's protocol. In order to normalize the data, we calculated the data along with their own total protein amount to obtain a ratio.

TABLE 3 | The sequences of primers for qPCR.

Gene	Primers
HSV-2 gB forward	5'-TGCAGTTTACGTATAACCACATACAGC-3'
HSV-2 gB reverse	5'-AGCTTGCGGGCCTCGTT-3'
GAPDH forward	5'-CCTCGTCCCGTAGACAAAATG-3'
GAPDH reverse	5'-TGAGGTCAATGAAGGGGTCGT-3'

Histological Morphology and Immunohistochemistry

Vaginal and vulvar paraffin sections were stained with hematoxylin and eosin to assess the pathological changes. Immunohistochemistry was used to detect the infiltration of immune cells. Tissue sections were dewaxed, hydrated, antigen repaired, membrane permeated, and sealed. After incubating with primary antibodies against CD4, CD8, CD11c, and CD161 and secondary antibody (Servicebio, Wuhan, China) successively, the tissue sections were stained, restained, differentiated, dehydrated, cleared, sealed, and photographed for analysis.

Real-Time Quantitative PCR

Total RNA was extracted from tissues using Trizol reagent (Servicebio, Wuhan, China). The purity and concentration of the total RNA were detected by the NanoDrop 2000 system (Thermo Scientific, Waltham, MA, United States). The cDNA was synthesized by reverse transcribing 2 μg of RNA using the Hifair® II 1st Strand cDNA Synthesis Kit (Yeasen Biotech, Shanghai, China) in a Master-cycler gradient PCR apparatus (Eppendorf, Hamburg, Germany). Next, PCR was performed in a 20 μl volume containing 2 μl of cDNA, 8 μl of diluted and mixed primers, and 10 μl of SYBR Green Master Mix (Yeasen Biotech, Shanghai, China) using the LightCycler 96 System (Roche, Basel, Switzerland). The primers used are shown in **Table 3** (Namvar et al., 2005), and the relative expression of HSV-2 gB mRNA was calculated using the Log10 ($2^{-\triangle\triangle Ct}$) method.

Transmission Electron Microscope (TEM)

The vaginal and vulvar tissues of 1 mm^3 were fixed in 2.5% glutaraldehyde and 1% osmium tetroxide. After dehydrating in ethanol, the tissues were permeated with propylene oxide-epoxy resin compound and embedded with epoxy resin. The sample was then sliced using an ultra-micro slicer. Sample slices (50 nm) were stained with 1% uranyl acetate and lead citrate and then were observed and photographed by TEM (H-7000FA; Hitachi, Tokyo, Japan).

Statistical Analysis

All the data were presented as means ± standard error (SEM), and SPSS 22.0 software was used for statistical analysis. The data fitting a normal distribution was statistically analyzed using one-way ANOVA. $p < 0.05$ was regarded as statistically significant.

RESULTS

HPLC Analysis of JZ-1

The high-performance liquid chromatography results of JZ-1 are shown in **Figure 2**. The nine component chromatographic peaks in JZ-1 were confirmed, comparing the retention times and UV spectrum: D-(-)-quinic acid, citric acid, trigonelline, caffeic acid, apocynin, taxifolin, ferulic acid, luteolin, and berberine. The content of each analyte is shown in **Table 4**.

Establishment of a Mouse Model of Genital Herpes

A high virus titer leads to high mortality in mice, while a low virus titer leads to a low successful modeling rate. When the viral titer was between 1×10^6–1×10^8 TCID50/0.1 ml and 2×10^4–2×10^6 PFU/ml, a stable mouse model of genital herpes could be established with a more than 80% successful modeling rate and a less than 20% death rate (**Figures 3A, B**). The above results indicate the feasibility and stability of the modeling method of the genital herpes mouse model in this experiment. Then we recorded the changes of indexes aforesaid within 2 weeks after the establishment of the mouse model of genital herpes to gain an in-depth understanding of the disease progress. The symptom (**Figures 3C, F**) and pathological manifestations (**Figure 3G**) showed that, after HSV-2 infection, inflammation increased slightly from 12 h to day 1, and then subsided. The vaginal viral load (HSV-2 gB mRNA) increased and reached a peak from day 3 to day 5 (**Figure 3E**). The symptoms increased rapidly from day 5 and reached a peak on day 9. The vaginal mucosa began to show vacuolar degeneration and necrosis, punctate hyperemia, lymphocyte infiltration, and proliferation of capillaries. From day 9 to day 14, the symptoms were maintained at a high level. The body weight changed with symptoms, and its trend was opposite to that of the symptom score (**Figure 3D**).

Changes in the Experimental Indexes Over Time in GH Mice

At 12 h, many virions were injected into the vagina to infect vaginal epithelial cells through abraded mucosa, and the expression of gD, VP16, ICP5, HVEM, and Nectin-2 in vaginal tissue reached a peak and then showed a downward trend (**Figure 4A**), while the expression of Nectin-1 showed no significant difference over time. Therefore, we chose 12 h after modeling as the time point to explore the anti-HSV-2 membrane fusion effect of JZ-1. After adsorption and penetration, HSV-2 is recognized by TLR on the cell membrane and cytoplasm in vaginal tissue. The expression of TLR4 from 12 h, TLR3, TLR7, and TLR9 from day 3, and P-IκBα/IκBα from day 5 in the model group were significantly higher than those in the control group. TLR4 expression showed a downward trend, and TLR3, TLR7, and TLR9 showed an upward trend (**Figure 4B**). The expression of IL-6, IFN-β, and TNF-α (**Figures 4C–E**), as well as the infiltration of DCs, NK cells,

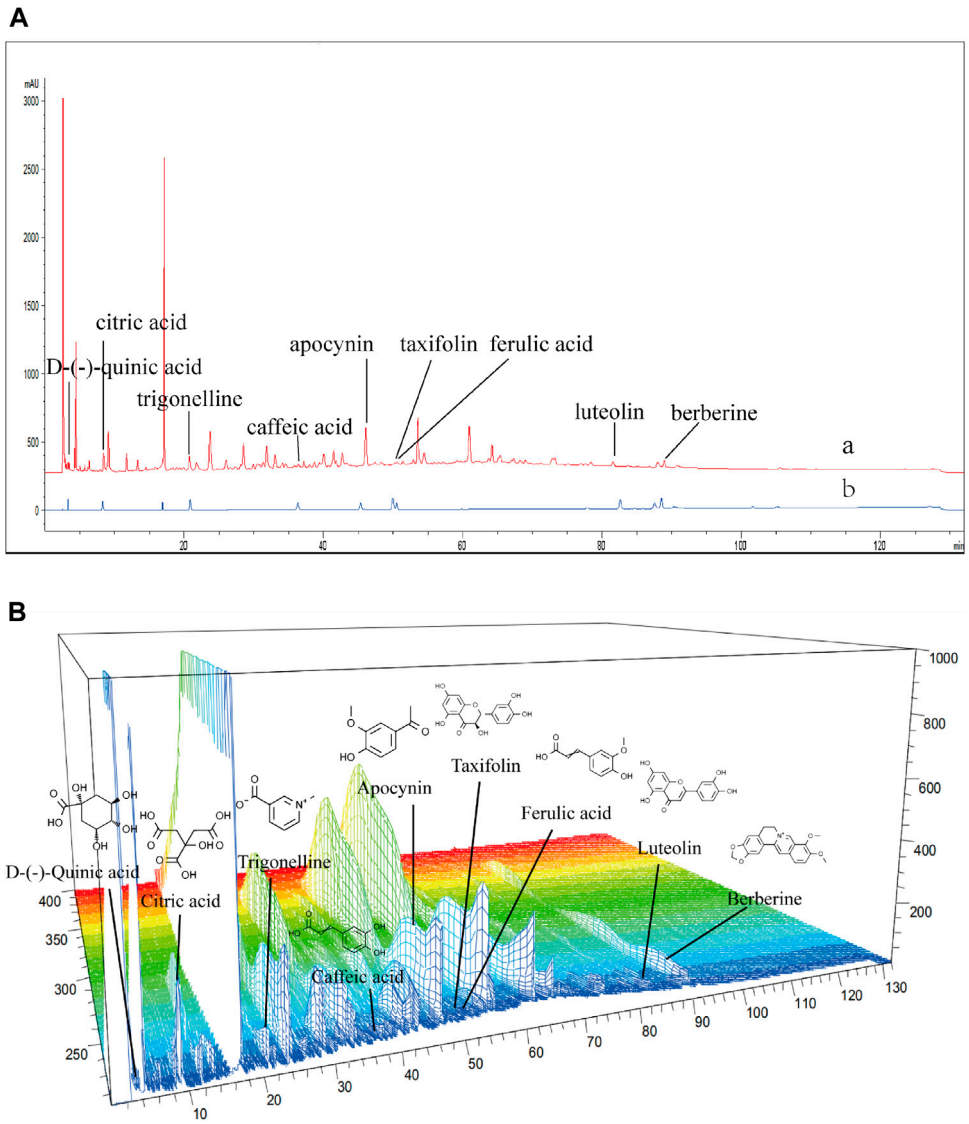

FIGURE 2 | HPLC fingerprinting of JZ-1. **(A)** HPLC fingerprint chromatograms of the JZ-1 (a) and the reference standards (b). **(B)** 3D-HPLC fingerprint chromatograms of the JZ-1.

TABLE 4 | Content of nine analytes in JZ-1.

Analyte	Content in mix (μg/ml)	Peak area in mix (mAU*s)	Peak area in JZ-1 (mAU*s)	Content in JZ-1 (μg/ml)	Content in JZ-1 (μM)
D-(-)-Quinic acid	1,250	344.86600	323.89920	1,141.42447	5,939.7
Citric acid	1,250	682.80060	1,608.82605	2,906.93432	15,130.8
Trigonelline	50	985.99890	1,610.65710	78.50905	572.4737
Caffeic acid	25	935.88611	474.04410	12.24522	67.9686
Apocynin	25	764.73834	4,783.61719	147.15459	885.5665
Taxifolin	25	1,388.26794	225.52815	3.95647	13.004
Ferulic acid	25	868.52405	398.51459	11.27769	58.0785
Luteolin	50	1,308.73914	577.26355	21.49175	75.083
Berberine	50	1,104.40137	856.66675	37.97280	112.8799

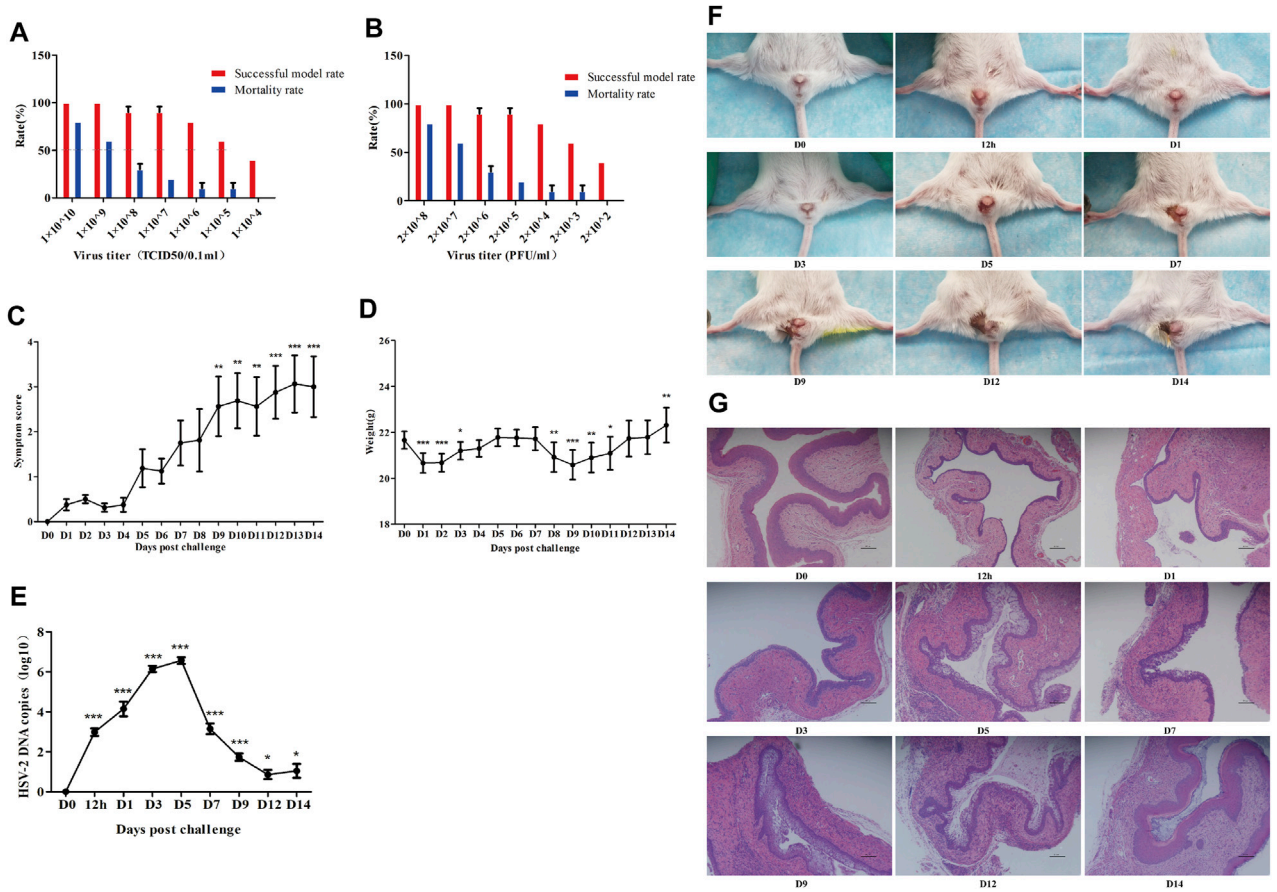

FIGURE 3 | Establishment of a mouse model of genital herpes. The model was established and optimized with multiple batches of mice. Successful model and mortality rates at different virus titers **(A, B)** were observed. Furthermore, symptoms score **(C)**, body weight **(D)**, viral load (HSV-2 gB mRNA) **(E)**, Symptom images **(F)**, vagina histomorphology (×100) **(G)** of mice at different time points after modeling were evaluated. D0: control group. 12 h: the 12 h after modeling. D1: the 1st day after modeling, et al. $^{*}p < 0.05$, $^{**}p < 0.01$, $^{***}p < 0.001$ vs. D0 group.

and T cells (**Figures 4F–I**), in the model group, were significantly higher than those in the control group. The first peak was at 12 h to day 1, decreased slightly from day 1 to day 5, and then increased again until day 14. All indicators were highly expressed on day 9, so we chose the 9th day after modeling as the time point to explore the anti-GH effect and mechanism of JZ-1 *in vivo*.

Exploration of the Effective Concentration and Administration Mode of JZ-1

An explanation of the rationale should be provided for the selection of doses, route and frequency of drug administration (Heinrich et al., 2020). We explored the method and concentration of JZ-1 administration. The body weight in the 0.5–2.5 g/ml JZ-1 groups decreased slowly from day 1 to day 12 (**Figure 5A,B**), and the vulvar symptom score in 1–2.5 g/ml JZ-1 groups were lower than those in the model group (**Figures 5C,D**). It was found that 2.5, 2, 1.5, 1, and 0.5 g/ml JZ-1 had a certain effect on maintaining the bodyweight of genital herpes mice, and the first four concentrations of JZ-1 could alleviate the vulvar symptoms of genital herpes mice. From day 13 to day 20, the bodyweight of mice in the JZ-1 groups increased significantly, and the symptom score showed a downward trend, suggesting that JZ-1 promotes the healing of genital ulcers. Comparing the trend of body weight and symptom score, the state of mice without anesthesia was better than that in mice with anesthesia (**Figures 5E,G**). JZ-1 administration for 14 days was better than that for 12 and 9 days (**Figures 5F,H**). So we selected three concentration gradients, 2.5, 1.5, and 0.5 g/ml, for follow-up experiments. By improving and prolonging the cycle of drug administration, we administered the drugs without anesthesia to the mice for 14 days, including 5 days before modeling and 9 days after modeling.

Effect of JZ-1 on GH Mice

In the model group, the vaginal mucosa of mice showed severe pathological manifestations as described previously (**Figure 6E**), and the vulvar epidermis showed discrete spongiosis, glandular atrophy, multinucleated giant cells, and cytopathic effects on day 9 (**Figure 6F**). The body weight (**Figures 6A,B**) of mice decreased. The symptom score (**Figures 6C,D**), virus titer of

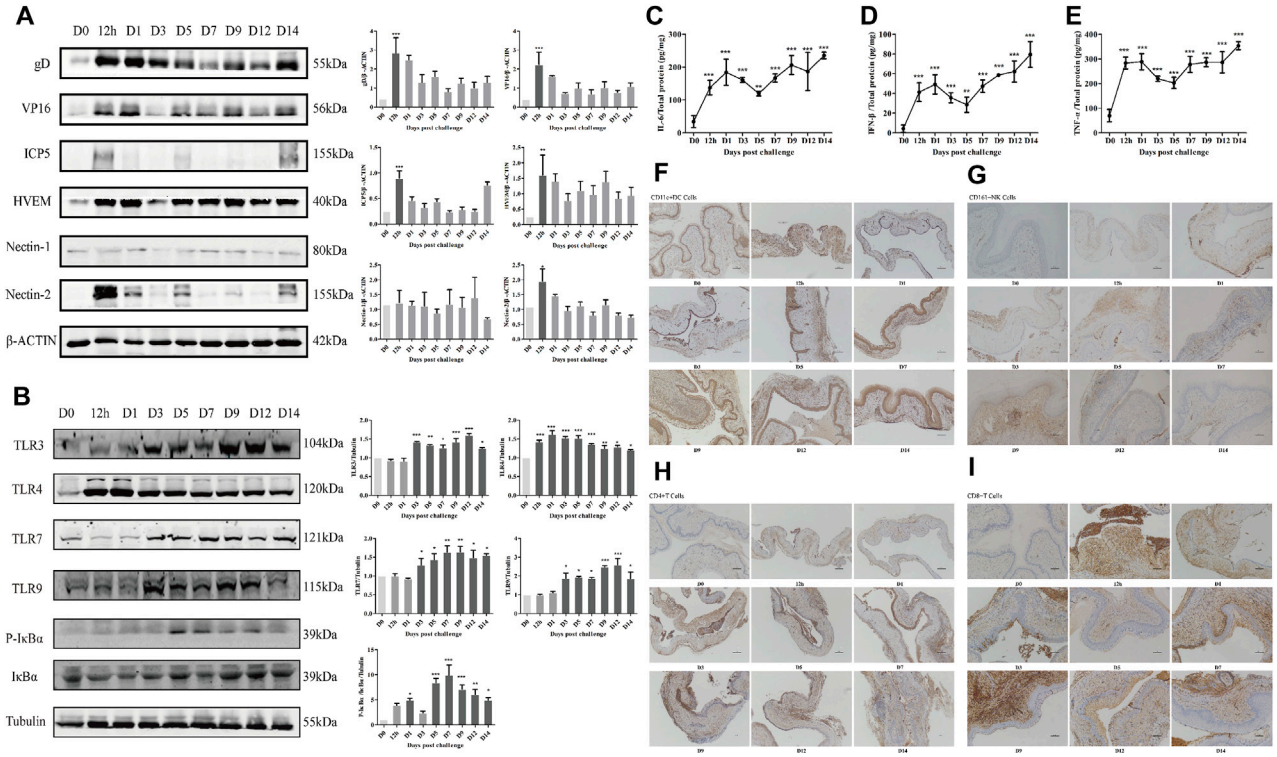

FIGURE 4 | Changes of experimental indexes in vaginal tissue at different time points after modeling in GH mice. The expression of membrane fusion-related proteins **(A)**, TLR signaling pathway-related proteins **(B)**, IL-6 **(C)**, IFN-β **(D)**, TNF-α **(E)**, and the infiltration of CD11c+DC **(F)**, CD161+NK **(G)**, CD4+T **(H)**, CD8+T **(I)** cells over time within 2 weeks after modeling were measured. $^{*}p < 0.05$, $^{**}p < 0.01$, $^{***}p < 0.001$ *vs.* D0 group.

vaginal washings (**Figure 6J**), and the viral load of the vagina (**Figure 6G**), vulva (**Figure 6H**), and spinal cord (**Figure 6I**) increased. Acyclovir and JZ-1 reversed these changes, particularly JZ-1 at 2.5 g/ml. They significantly alleviated vacuolar degeneration and necrosis of the vaginal and vulvar tissues caused by the virus, reduced the infiltration of inflammatory cells, and promoted tissue keratinization and repair.

Effect of JZ-1 on ultrastructural changes in the vaginal and vulvar tissues of GH mice

For further observation, we detected the effect of JZ-1 on ultrapathological changes of the vagina and vulvar tissues using TEM. As shown in **Figure 7**, on day 9, the perinuclear spaces of vaginal and vulvar cells in the model group were highly dilated and showed discrete spongiosis changes under TEM. The nucleus was pyknotic and deeply stained, and the chromatin was concentrated. Rough endoplasmic reticulum expansion, swelling, and degranulation could also be seen. The Golgi apparatus swelled, and the mitochondria showed high swelling, rupture, vacuolation, and lipofuscin increase. Many free ribosomes can be seen, and the lysosomes and autophagosomes increased compensatively. Many monolayer vesicles appeared in the cells, and virions were observed in the vesicles. The characteristic ultrastructural changes in the acyclovir group and JZ-1 groups were significantly fewer than those in the model group, and the acyclovir group and JZ-1 2.5 g/ml group were closest to the control group.

Effect of JZ-1 on the expression of membrane fusion-related proteins in vaginal and vulvar tissues of GH mice

First of all, we cut in from the membrane fusion in the early stage of infection. The expressions of gD, VP16, ICP5, HVEM, and Nectin-2 were increased in the model group and decreased significantly in the JZ-1 groups. At 12 h, no significant difference was found between the acyclovir and model groups (**Figure 8A**). On day 9, the expressions of gD, VP16, and ICP5 in the acyclovir group and JZ-1 groups both decreased, but the expression of HVEM and Nectin-2 only decreased in the JZ-1 group (**Figures 8B,C**). No significant change was found in the expression of Nectin-1 in all the groups. The changes in vaginal and vulvar tissues were the same.

Effect of JZ-1 on the TLR signaling pathway in the vaginal and vulvar tissues of GH mice

TLR is the molecular basis of pathogen recognition. The adsorption and penetration of HSV-2 can activate the TLR signal pathway in vaginal and vulvar tissues (Martinez-Martin and Viejo-Borbolla, 2010). On day 9, the expression of TLR3, TLR4, TLR7, TLR9, and P-IκBα/IκBα in the vaginal tissue (**Figure 9A**), TLR4, TLR7, TLR9, MyD88, and P-IκBα/IκBα in vulvar tissue (**Figure 9B**) and IL-6, IFN-β, and TNF-α in vaginal tissue (**Figures 9C–E**) were increased in the model group and decreased in the acyclovir group and JZ-1 groups, particularly in the 2.5 g/ml JZ-1 group.

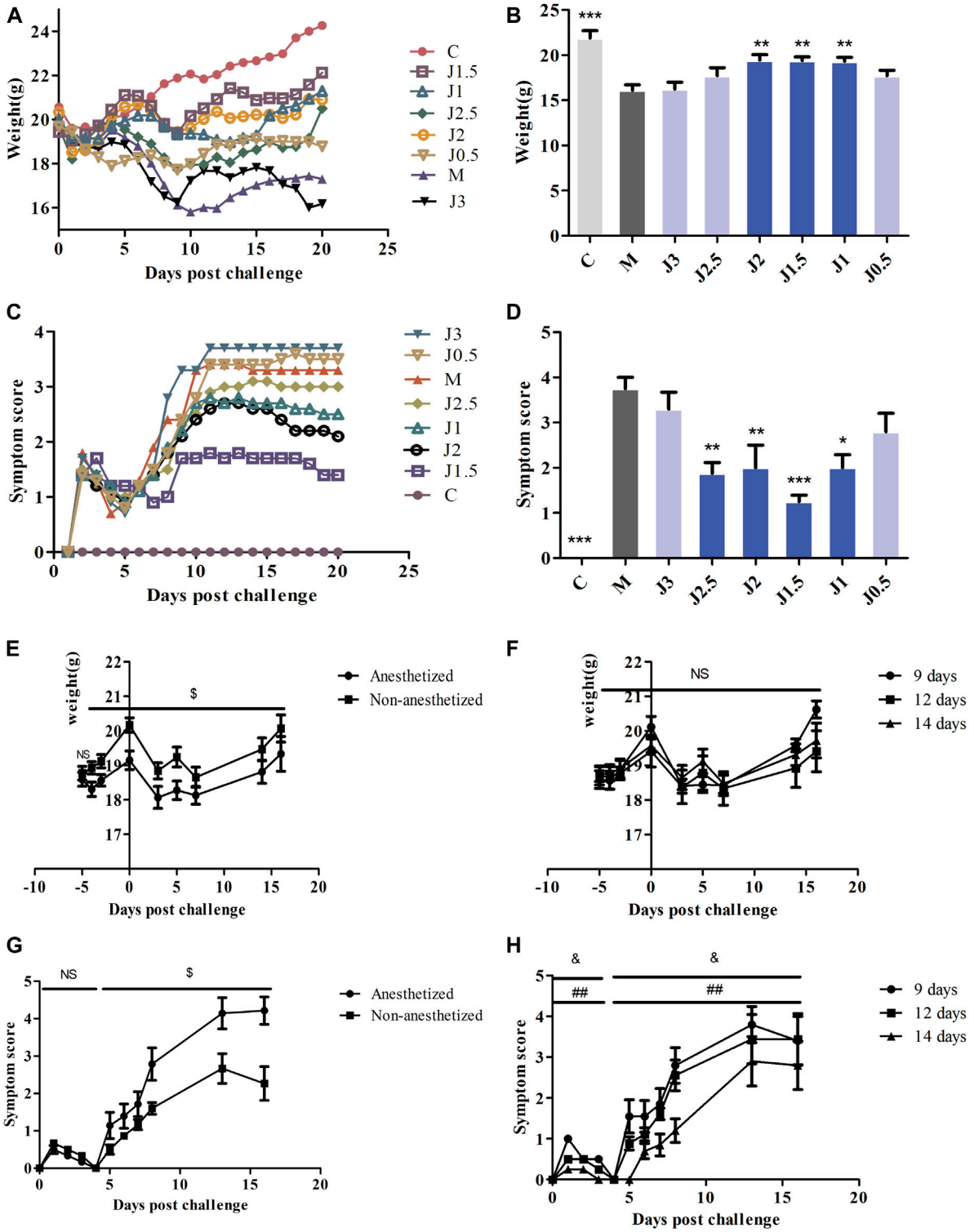

FIGURE 5 | Exploration of the effective concentration and administration mode of JZ-1. The effect of different concentrations JZ-1 on body weight **(A, B)** and symptom score **(C, D)** of GH mice was explored firstly, and the data of **(B, D)** was from day 9. Then, the effect of anesthesia and JZ-1 administration days on body weight **(E, F)** and symptom score **(G, H)** of GH mice was explored. C: control group, M: model group. J3, J2.5, J2, J1.5, J1, J0.5: 3, 2.5, 2, 1.5, 1, 0.5 g/ml JZ-1 group. 14, 12, 9 days: drug administration for 5, 3, 0 days before modeling plus 9 days after modeling. *$p < 0.05$, **$p < 0.01$, ***$p < 0.001$ *vs*. M group, $$p < 0.05$ (Anesthetized *vs*. Non-anesthetized), & $p < 0.05$ (14 days *vs*. 12 days), ##$p < 0.01$ (14 days *vs*. 9 days).

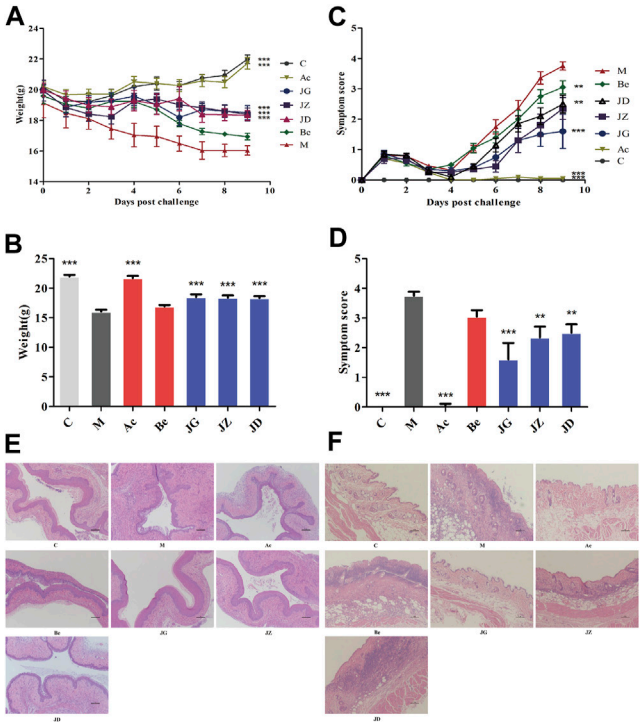

FIGURE 6 | Effect of JZ-1 on GH mice. Effect of JZ-1 on body weight **(A, B)**, symptoms score **(C, D)**, vagina **(E)** and vulva **(F)** histomorphology (×100), vagina **(G)**, vulva **(H)**, and spinal cord **(I)** viral load, virus titer of vaginal washings **(J)** of GH mice was evaluated. The data of **(B, D)** showed the statistical analysis results of body weight and symptoms score on day 9. The data of **(E-I)** was also from day 9, and **(J)** was from day 3. C, control group; M, model group; Ac, acyclovir group; Be, berberine group; JG, JZ, JD: 2.5, 1.5, and 0.5 g/ml JZ-1 group. $^{*}p < 0.05$, $^{**}p < 0.01$, $^{***}p < 0.001$ *vs.* M group.

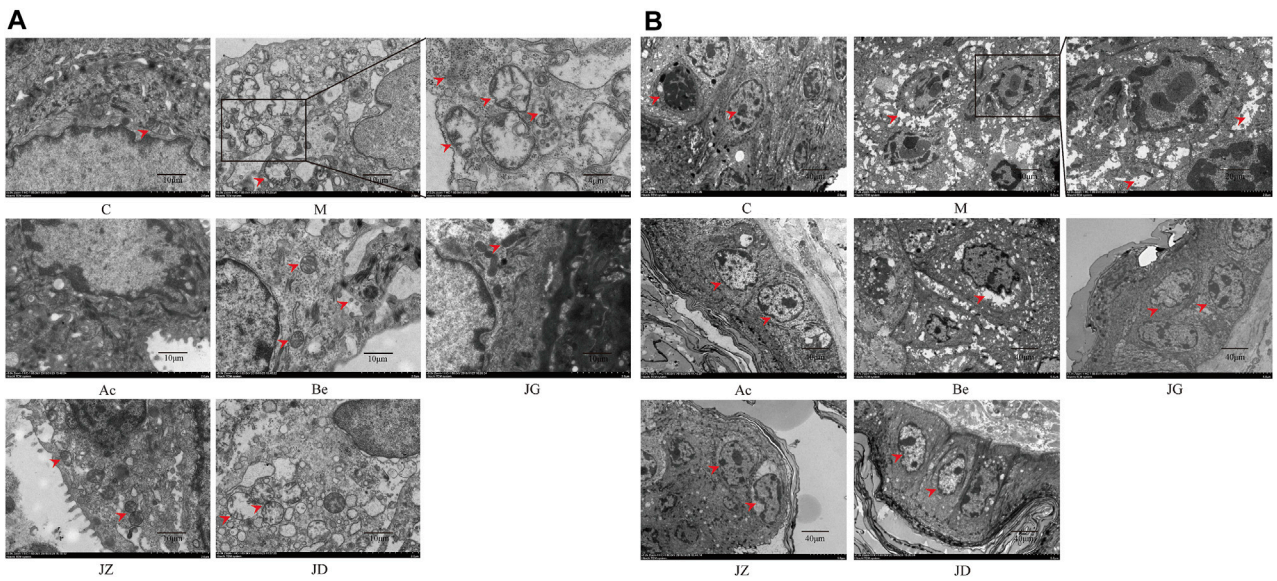

FIGURE 7 | Effect of JZ-1 on ultrapathological changes of vaginal **(A)** and vulvar **(B)** tissues in GH mice. On day 9, after modeling, the characteristic ultrapathological changes of vaginal **(A)** and vulvar **(B)** tissues in GH mice were observed by TEM. JZ-1 alleviated pyknosis and intensely staining of nuclear, reduced the concentration of chromatin, spongiosis changes of cytoplasm, and the number of lysosomes and autophagosomes. The arrows in the diagram showed the pyknosis and intensely staining of nuclear, the concentration of chromatin, spongiosis changes of cytoplasm, the lysosomes, and the autophagosomes. C, control group; M, model group; Ac, acyclovir group; Be, berberine group; JG, JZ, JD: 2.5, 1.5, and 0.5 g/ml JZ-1 group.

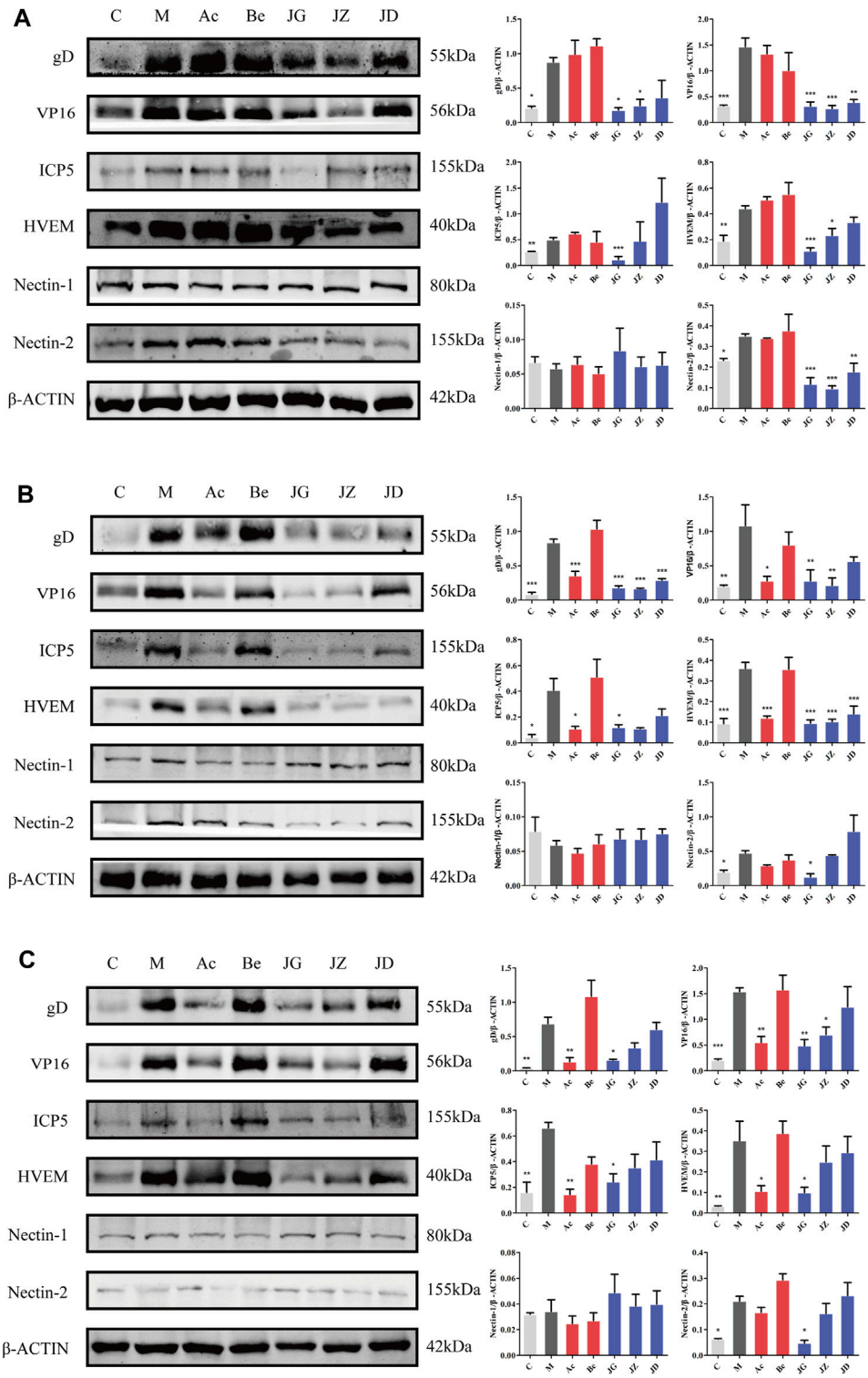

FIGURE 8 | Effect of JZ-1 on the expression of membrane fusion-related proteins in vaginal **(A, B)** and vulvar **(C)** tissues of GH mice. On 12 h **(A)** and day 9 **(B, C)** after modeling, the key proteins of membrane fusion, including gD, VP16, ICP5, HVEM, and Nectin-2, were measured by western blot. JZ-1 inhibited virus adsorption and penetration by downregulating the expression of membrane fusion-related proteins. C, control group; M, model group; Ac, acyclovir group; Be, berberine group; JG, JZ, JD: 2.5, 1.5, and 0.5 g/ml JZ-1 group. $^{*}p < 0.05$, $^{**}p < 0.01$, $^{***}p < 0.001$ *vs.* M group.

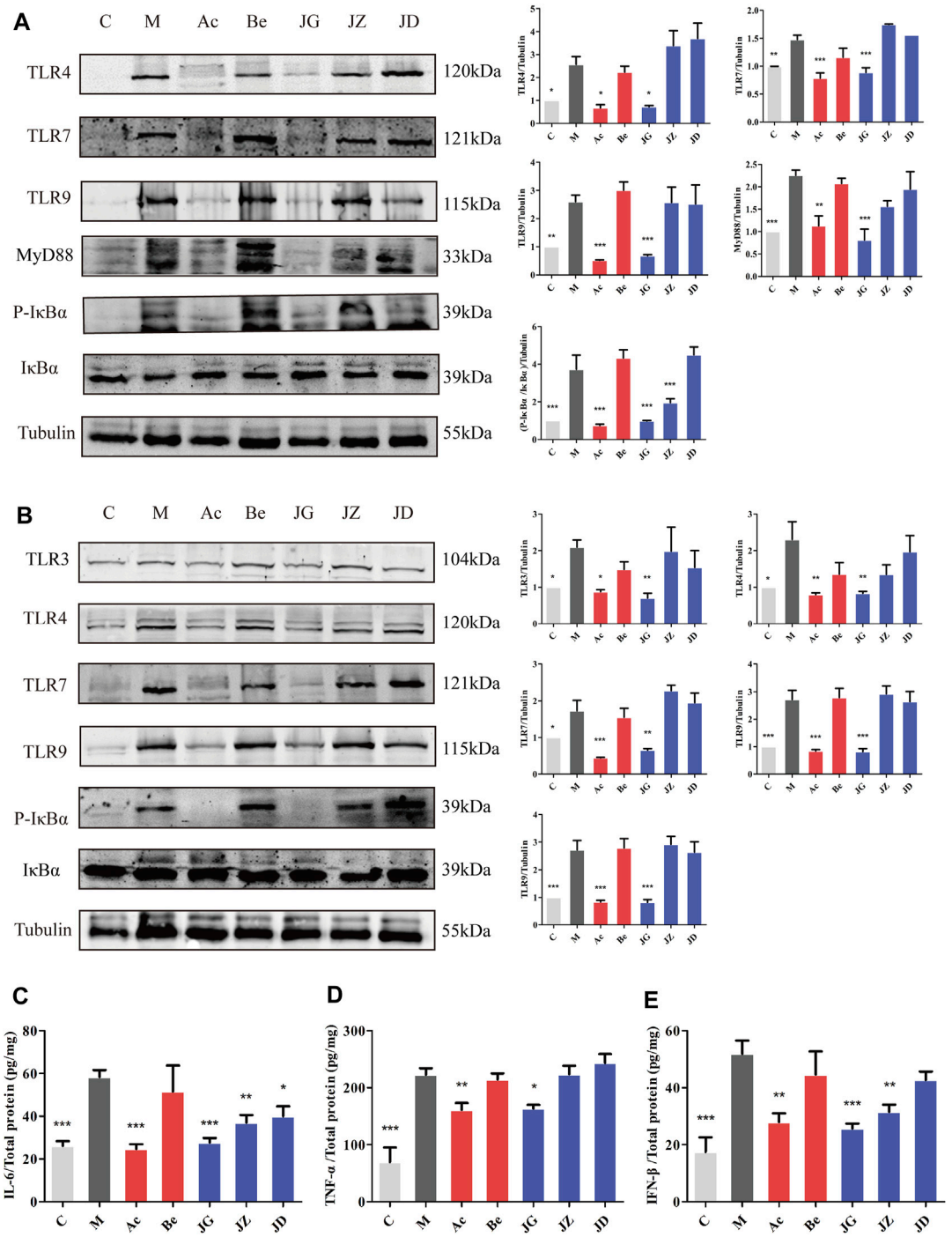

FIGURE 9 | Effect of JZ-1 on the TLR signaling pathway in vaginal **(A)** and vulvar **(B)** tissues of GH mice. On day 9 after modeling, the key proteins of the TLR signaling pathway, including TLR3, TLR4, TLR7, TLR9, MyD88, P-IκBα, and IκBα were measured by western blot. The inflammatory cytokine contents in vaginal tissue, including IL-6 **(C)**, TNF-α **(D)**, and IFN-β **(E)**, were determined by ELISA. JZ-1 downregulated the activation of the TLR signaling pathway and the expression of inflammatory cytokines. C, control group; M, model group; Ac, acyclovir group; Be, berberine group; JG, JZ, JD: 2.5, 1.5, and 0.5 g/ml JZ-1 group. $^{*}p < 0.05$, $^{**}p < 0.01$, $^{***}p < 0.001$ *vs.* M group.

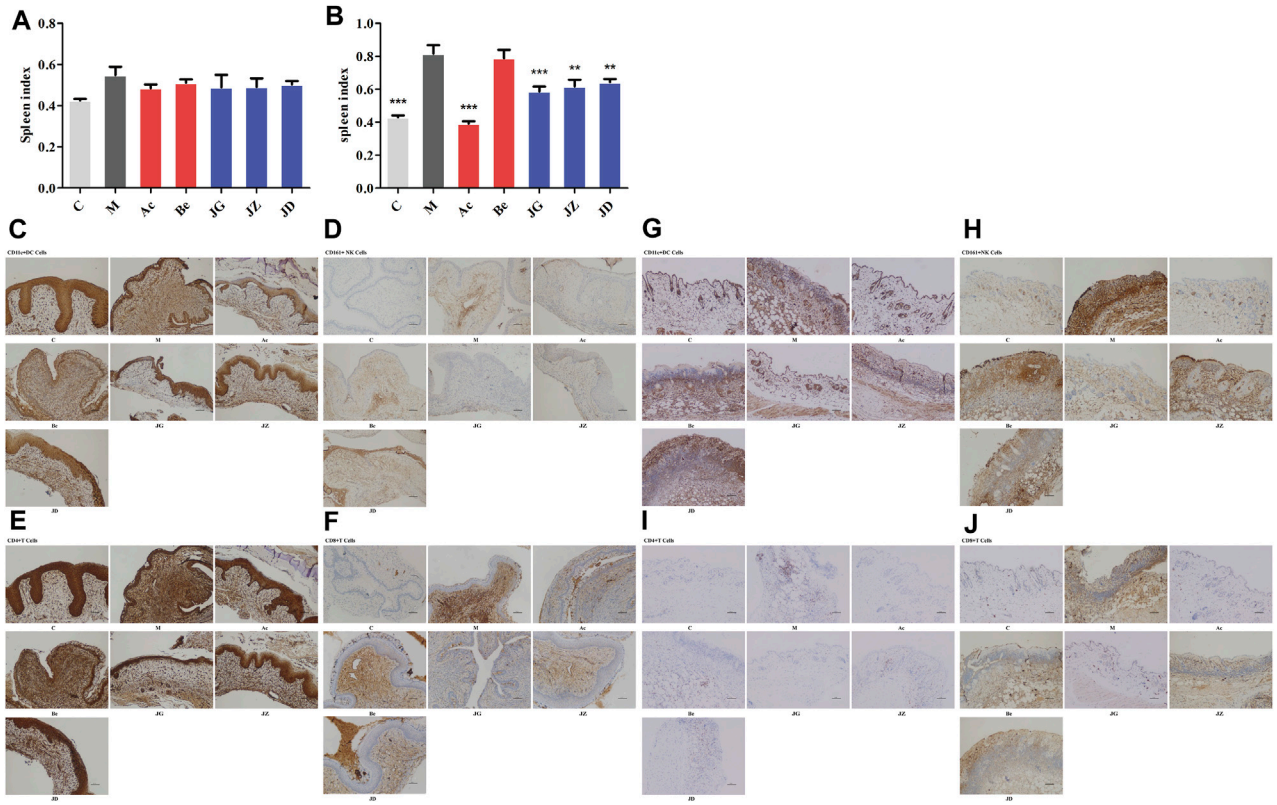

FIGURE 10 | Effect of JZ-1 on the immune response of GH mice. On 12 h **(A)** and day 9 **(B)** after modeling, the spleen index of GH mice was measured. Moreover, the immune cell infiltration in vaginal **(C–F)** and vulvar **(G–J)** tissues of GH mice on day 9 were detected by immunohistochemistry staining. JZ-1 reduced the spleen index and infiltration of immune cells. C, control group; M, model group; Ac, acyclovir group; Be, berberine group; JG, JZ, JD: 2.5, 1.5, and 0.5 g/ml JZ-1 group. $^{*}p < 0.05$, $^{**}p < 0.01$, $^{***}p < 0.001$ *vs.* M group.

Effect of JZ-1 on the Immune Response of GH Mice

The activation of the TLR signal pathway and the production of cytokines can further affect the immune cell infiltration and systemic immune response of the host (Uyangaa et al., 2014). Spleen index is one of the important indexes of immune function to some extent (Li et al., 2018). At 12 h, no significant difference was found in the spleen index among these groups (**Figure 10A**). On day 9, the spleen index (**Figure 10B**) and infiltration of immune cells (**Figures 10C–J**) in the vaginal and vulvar tissues of mice were both increased in the model group and decreased in the acyclovir and JZ-1 groups, particularly in the 2.5 g/ml JZ-1 group.

No significant difference was shown between the berberine and model groups in all the above results.

DISCUSSION

The Chinese herbal prescription Jieze-1 is used clinically for female lower reproductive tract infections diseases. *In vitro* experiments show that JZ-1 exhibits a highly effective anti-genital herpes effect (Duan et al., 2020). JZ-1 also showed a significant anti-HSV-2 effect in a mouse model of genital herpes in this study. In order to understand the anti-HSV-2 effect and mechanism of JZ-1 *in vivo*, we firstly established and optimized the GH mouse model with multiple batches of mice and recorded the changes in the target indexes over time within 2 weeks after modeling to evaluate the severity of the disease and drug efficacy accurately. HSV-2 infection is a sequential process started with the adsorption and penetration of HSV-2 into host cells (Luo et al., 2015). Then HSV-2 is recognized by Toll-like receptors and produces cytokines that regulate the systemic immune response, including immune cell infiltration (Uyangaa et al., 2014). So we chose to explore the expression of membrane fusion-related proteins, TLR signaling pathway-related proteins, cytokines, and immune cells in GH mice to study the mechanism of the anti-HSV-2 effect of JZ-1.

Firstly, the results gave us a good understanding of the pathogenesis of GH in mice. According to the results, this process can be divided into three stages. The first stage is day 0 to day 1. The modeling operation made the vaginal mucosa thin and caused acute inflammation. The expression of inflammatory factors in the vagina of mice increased. The second stage is day 1 to day 5. The acute inflammation of the vaginal tissue caused by the modeling operation will decrease slightly, resulting in a slight reduction in inflammatory factors and a slight increase in weight on day 5, which is still different from the normal state. Viral

infections in vaginal tissues continue to rise. The third stage is from day 5 to day 14. Day 5 is a turning point. On the one hand, the mouse vaginal virus load reached a peak from day 3 to day 5. The high-load virus began to destroy healthy vaginal tissue, causing visible pathological manifestations and a large amount of cytokine secretion and immune cell infiltration. The inflammation and immune response increased sharply and rapidly from day 5 and reached a peak on day 9. On the other hand, vulvar ulcers gradually developed. After adsorption and penetration, the virus migrated to the nerve sheath and resided in sensory neurons for 1–3 days (Koelle and Wald, 2000). After 4–5 days, the virus infected the surrounding neurons and returned to the out peripheral epidermis, leading to clinical vulvar primary infection syndrome (Koelle and Wald, 2000). All symptoms reached a peak on day 9. The vaginal viral load (HSV-2 gB mRNA) showed a downward trend from day 5 that may be related to the gradually activated immune response (Dai et al., 2018). The viral load reached a low point from day 12 to day 14, and the vulvar ulcer began to heal. The body weight changed with symptoms.

HSV-2 infection is started with the adsorption and penetration of HSV-2 into host cells (Luo et al., 2015). Multiple glycoproteins, such as gB, gD, gH, gL, and gJ, play essential roles in viral entry, as well as immune-modulation and immune-escape (Roller and Roizman, 1992; Retamal-Díaz et al., 2015). Studies *in vitro* have demonstrated that HSV-2 can fully adhere and penetrate host cells within 5 min of incubation with vaginal epithelial cells (Duan et al., 2020). One to 2 h after infection, the viral capsid migrates to the nucleus mediated by microtubules, dynamic proteins and releases chromatin into the nucleus (Ibáñez et al., 2018). Immediate early proteins such as ICP0, ICP4, and ICP22 were mostly produced at 4–8 h after infection (Ibáñez et al., 2018). Early proteins such as TK, ICP8, and Uracil were mostly produced at 8–12 h after infection (Ibáñez et al., 2018). Late proteins such as gD, VP16, and ICP5 were mostly produced at 12–18 h after infection (Ibáñez et al., 2018). At 20–23 h after infection, the viral structural proteins form the nucleocapsids, wrap the virus DNA to get out of the nucleus, which was further processed in the cytoplasm to form offspring virons and released to extracellular (Ibáñez et al., 2018). Thus, we selected 12 h after modeling as the early stage of GH in mice. At this time, many virions adsorbed into and penetrated vaginal cells, and the expression of membrane fusion-related proteins in vaginal tissue increased significantly. Therefore, we chose 12 h after modeling as the time point to explore the anti-HSV-2 membrane fusion effect of JZ-1.

Immune and non-immune cells express a lot of molecular sensors that detect virus components which can promote the rapid antiviral responses that inhibit viral replication and propagation (Mogensen, 2009). Once the virus comes into contact with the host cells, host receptors such as TLRs will sense these stimuli and activate the Toll-like receptor signaling pathway, resulting in the expression of inflammatory cytokines with antiviral activity (Uyangaa et al., 2014). Toll-like receptors play an important role in both HSV-2 infection *in vivo* and *in vitro*. Human TLR3-deficient CNS cells have impaired intrinsic immunity to HSV-1 (Lafaille et al., 2012). TLR2 and TLR9 synergistically control herpes simplex virus infection in the brain (Sorensen et al.). TLR4-MyD88/Mal-NF-kB axis is involved in infection of HSV-2 in human cervical epithelial cells (Liu et al., 2013). Activation of plasmacytoid dendritic cells (PDC) is caused by the involvement of nucleotide receptor-like receptors (TLRs) 7 and 9, which play a key role in antiviral immunity (Gotoh et al., 2010). Our experiments found that essential proteins of the TLRs signaling pathway were indeed involved in HSV-2 infection. We also found time-related features of the expression of each protein. TLR4 was located on the cell surface and was the first to be expressed after modeling. TLR3, TLR7, and TLR9 were located intracellular, and their expression were presented in a time-dependent manner. The phosphorylation of IκBα indicates the release of NF-κB inhibition (Hayden and Ghosh, 2004). NF-κB enters the nucleus and promotes the synthesis of cytokines such as IL-6, TNF-α, and IFN-β, which can regulate the immune response (Dunne and O'Neill, 2003; Hayden and Ghosh, 2004; Yamamoto et al., 2004). IL-6 can promote the growth and differentiation of original bone marrow-derived cells and plays a vital role in a series of processes such as the maturation, activation, proliferation, and immune regulation of immune cells (Tanaka et al., 2014). The primary role of TNF-α is to regulate the function of immune cells. It can induce chemokines and adhesion molecules, activate endothelial cells and promote T cells to produce various inflammatory factors which promote the occurrence of inflammation. In addition, natural killer (NK) can also receive signals through TNFR to amplify division, survival, and cytokine production (Aggarwal et al., 2012). IFN-β can inhibit viral growth by interfering with viral DNA replication, significantly enhance the killing activity of NK cells, and regulate T cells (Haji Abdolvahab et al., 2016). Immune cells regulated by these cytokines can further exert immune responses. NK cells are one of the innate immune cells that are capable of sensing and destroying HSV-2-infected cells (Céspedes et al., 2013). DC antigen presentation to T cells can lead to a process that involves DC-T cell interactions, resulting in the activation of T cells (Retamal-Díaz A. R. et al., 2017). T cells can regulate immune and non-immune cells, eventually killing infected cells (González et al., 2007; Tognarelli et al., 2019). Besides, NK cells, T cells, and DCs can all produce interferon to inhibit virus replication (Elboim et al., 2013). In our study, the TLRs and the infiltration of immune cells in the vagina increased significantly as the symptom score of mice reached a peak on day 9. Considering the above results, we also chose the 9th day after modeling as the time point to explore the anti-GH effect and mechanism of JZ-1 *in vivo*.

Based on the above meticulous explorations, we researched the effect of JZ-1 on HSV-2 infection and explored the underlying mechanism by examining different targets. First, weight changes and vulvar symptoms are the most intuitive indicators to evaluate the efficacy of antiviral drugs. JZ-1 and acyclovir effectively alleviate the symptoms and weight loss of GH mice, indicating JZ-1 has the same anti-HSV-2 effect as acyclovir *in vivo* experiments. The role of JZ-1 is not just improving symptoms. We measured the viral load in the vagina, vulva, and spinal cord, revealing that JZ-1 effectively inhibited the viral load. A positive

correlation exists between the spinal cord viral load and virus recurrence probability (Kollias et al., 2015). No viral load was detected in the spinal cord of GH mice 12 h after infection because the genome of HSV reaches the spinal cord 24 h after infection (Steiner et al., 1990). JZ-1 can significantly reduce the viral load of the spinal cord on day 9; whether JZ-1 can play a role in reducing the recurrence of GH or alleviating the symptoms of recurrence deserves further study. On the other hand, HSV-2 infection transmits through the intermittent release of reproductive tract shedding, with significant potential risks. The amount of vaginal viral shedding is vital in evaluating GH's infectivity (Sacks et al., 2004). The results showed that JZ-1 significantly reduces the amount of vaginal viral shedding in GH mice, suggesting the possibility of its effective reduction of cross-infection risk.

In order to confirm the anti-HSV-2 effect of JZ-1 *in vivo* from the histological level, the histopathological changes of vagina and vulva of mice were observed under hematoxylin-eosin staining and electron microscope, respectively. The results of hematoxylin-eosin staining suggested that JZ-1 could significantly alleviate the vacuolar degeneration and necrosis of vaginal and vulva tissues caused by the virus, reduce the infiltration of inflammatory cells, and promote tissue keratinization and repair. The typical morphology of organelles is essential for cells to perform normal physiological functions. Ultrastructure of cells of the genital herpes mouse model treated with JZ-1 revealed the regular appearance of organelles, suggesting the cells were protected against HSV-2 infection, a phenomenon that needs to be further explored.

In order to understand the anti-adsorption and anti-penetration effect of JZ-1, we detected the expression of membrane fusion-related proteins in the vaginal and vulva tissues of mice. By significantly downregulating the expression of membrane fusion-related proteins, JZ-1 reduces the adsorption and penetration of HSV-2. In cells with the Nectin-2 receptor, the membrane fusion of HSV-2 is mainly mediated by Nectin-2 instead of Nectin-1 (Fujimoto et al., 2017). Thus, the expression of Nectin-1 showed no difference among all the groups. Acyclovir did not change the Nectin-2 expression because it only acts on the replication stage (Field et al., 2013). The downregulation of VP16 expression, a transactivator that can promote viral gene transcription (Thompson and Sawtell, 2019), suggests that JZ-1 may also inhibit HSV-2 genome replication *in vivo*. As a member of the tumor necrosis factor receptor family, HVEM is not only expressed in vaginal epithelial cells but also in inactivated immune cells (Hu et al., 2017). The downregulation of HVEM suggests that JZ-1 not only inhibits membrane fusion but also regulates immune response.

Next, based on the Toll-like receptor signaling pathway and immune cells, we conducted our research on the immune responses. The HSV-2 of the model group fully activated the TLR signaling pathway. We first explored the expression of Toll-like receptors in the vaginal area where the virus was inoculated. Then, for the ulcer lesions of the vulva, we specifically explored the expression of TLR-MyD88 signaling pathway-related proteins. JZ-1 downregulates the pattern recognition of viruses by TLRs, inhibits the expression of the TIR domain adapter MyD88 in vulvar lesions, and reduces the phosphorylation of IκBα to inhibit NF-κB transduction into the nucleus, significantly reducing the release of cytokines such as IL-6, IFN-β, and TNF-α, and inhibiting the inflammatory response caused by the excessive immune response. So does JZ-1 further suppress the excessive immune response? We observed it by detecting the spleen index and immune cell infiltration.

In the immune system, the spleen is the largest peripheral immune organ, and the morphology of the spleen can directly affect the immune function of the body (Gu et al., 2014). At 12 h, only local inflammation caused by physical friction occurred in mice, so the spleen index among all the groups showed no difference. On day 9, the mice reached a peak of symptoms with immune dysfunction. Their body weight decreased, and the spleen enlarged compensatively, causing an increased spleen index and massive infiltration of immune cells in vaginal and vulvar tissues. JZ-1 can indeed reduce the spleen index and infiltration of NK, DC, and T cells.

JZ-1 is a traditional Chinese herbal prescription with many components. We have identified nine of them by HPLC. They were D-(-)-quinic acid, citric acid, trigonelline, caffeic acid, apocynin, taxifolin, ferulic acid, luteolin, and berberine. According to some reports, trigonelline (Ozçelik et al., 2011), apocynin (Hu et al., 2011), caffeic acid (Ikeda et al., 2011; Ozçelik et al., 2011; Utsunomiya et al., 2014), luteolin (Ojha et al., 2015; Rittà et al., 2020) and berberine (Chin et al., 2010) have anti-HSV effects. And quinic acid can resist hepatitis B virus (Wang et al., 2009) and dengue virus (Zanello et al., 2015). A disinfectant containing 0.2% citric acid can fight the foot-and-mouth disease virus (Hong et al., 2015). Taxifolin can fight hepatitis C virus (Pisonero-Vaquero et al., 2014). On the one hand, apocynin (Nam et al., 2016), trigonelline (Khalili et al., 2018), luteolin (Chen et al., 2018) inhibited Toll-like receptor-4-mediated activation of NF-κB. Ferulic acid protected against porcine parvovirus infection-induced apoptosis by suppressing the NF-κB and TLR4 (Ma et al., 2020). Berberine inhibits the expression of TNF-α, IL-6, TLR 4, and TLR 9 in the early phase of sepsis in rats (Li et al., 2015). Berberine also suppressed the viral infection-induced up-regulation of the TLR7 signaling pathway, such as TLR7, MyD88, and NF-κB (Yan et al., 2018). On the other hand, caffeic acid and ferulic acid showed the ability to enhance the killing activity of T cells and NK cells (Kilani-Jaziri et al., 2017). Citric acid plays an important role in activating dendritic cells (Ryan and O'Neill, 2017). Apocynin can inhibit cytokine production of $CD8^+$ T cells (Nam et al., 2014). Luteolin reduces the frequency of mature dendritic cells and CD4+/CD8+ T cells (Ye et al., 2019). Berberine can significantly reduce T lymphocyte and NK cell infiltration (Li et al., 2020). Meanwhile, berberine can also inhibit the maturity of dendritic cells and reduce the secretion of IL-6, IL-1β, and IL-23 by dendritic cells (Yang et al., 2013). Taken together, these chemical components of JZ-1 may function synergistically to HSV-2, Toll-like receptor pathway, and immune cells. These reports support our results.

Monarch medicine plays a significant role in Chinese herbal prescription (Xie, 2016). *Phellodendron chinense* C.K.Schneid. is the monarch medicine of JZ-1. Berberine, the identified component of JZ-1 monarch medicine (Chinese Pharmacopoeia Commission, 2020), is the primary indicator of quality control in the preparation process of JZ-1 (Ma et al., 2011). There are many reports on the antiviral and anti-inflammatory effects of berberine (Warowicka et al., 2020). It was used in our study to determine whether it can exert the same antiviral effect as the Chinese herbal prescription JieZe-1. However, 891.8 μM (0.3 mg/ml) of berberine gel showed no antiviral effect *in vivo*, suggesting that the components in the Traditional Chinese Medicine prescription are not necessarily effective. Whether it is related to the concentration or administration and whether the other components in the JZ-1 have antiviral effects are worthy of further verification. This result also suggests that the antiviral effect of the Chinese herbal prescription JieZe-1 may be exerted by the interaction of various components, reflecting the scientific implication of TCM. This is also the charm of the pharmacology of traditional Chinese herbal prescriptions.

CONCLUSION

In summary, the treatment of GH mice with JZ-1 gel improved the symptoms that have been confirmed by histopathological and cell ultrastructural analysis. JZ-1 can also reduce the vaginal, vulvar, and spinal cord viral load and vaginal virus shedding. The potential mechanism is associated with the inhibition of membrane fusion, the TLR signaling pathway, inflammatory cytokines, and cellular immunity. The above studies provide experimental evidence to reveal the effect and partial molecular mechanism of the Chinese herbal prescription JieZe-1 on anti-HSV-2 in GH mice. The anti-HSV-2 efficacy of JZ-1 is slightly less than that of acyclovir. However, it also shows preventive and therapeutic effects on multiple lower reproductive tract infectious diseases. The excellent application prospect of JZ-1 is worthy of further research and exploration.

DATA AVAILABILITY STATEMENT

The raw data supporting the conclusions of this article will be made available by the authors, without undue reservation.

ETHICS STATEMENT

The animal study was reviewed and approved by Experimental Animal Ethics Committee of Tongji Medical College of Huazhong University of Science and Technology in December 2018 (IACUC Number: 840).

AUTHOR CONTRIBUTIONS

The corresponding author ZC is in charge of the design, organization, implementation of the project, and revision of the paper. As the main executors, QD and TL contributed to the data acquisition, statistical analysis, manuscript writing, et al. CH, QS, WW, and TL provided technical help. YM and JF are in charge of drug production. JS carried out technical guidance. GH performed guidance. All authors have read and approved the final version of the manuscript. All data were generated in-house, and no paper mill was used. All authors agree to be accountable for all aspects of work, ensuring integrity and accuracy.

FUNDING

This research was supported by grants from the Natural Science Foundation of China (Nos. 81874483, 81473718, 81273787).

SUPPLEMENTARY MATERIAL

The Supplementary Material for this article can be found online at: https://www.frontiersin.org/articles/10.3389/fphar.2021.707695/full#supplementary-material

REFERENCES

Aggarwal, B. B., Gupta, S. C., and Kim, J. H. (2012). Historical Perspectives on Tumor Necrosis Factor and its Superfamily: 25 Years Later, a golden Journey. *Blood* 119, 651–665. doi:10.1182/blood-2011-04-325225

Barber, G. N. (2013). STING-dependent Cytosolic DNA Sensing Pathways. *Trends Immunol.* 35, 88–93. doi:10.1016/j.it.2013.10.010

Céspedes, P. F., Gonzalez, P. A., and Kalergis, A. M. (2013). Human Metapneumovirus Keeps Dendritic Cells from Priming Antigen-specific Naive T Cells. *Immunology* 139, 366–376. doi:10.1111/imm.12083

Chen, B., Lee, A. J., Chew, M. V., and Ashkar, A. A. (2017). NK Cells Require Antigen-specific Memory CD4+ T Cells to Mediate superior Effector Functions during HSV-2 Recall Responses *In Vitro*. *J. Leukoc. Biol.* 101, 1045–1052. doi:10.1189/jlb.4A0416-192R

Chen, C.-Y., Kao, C.-L., and Liu, C.-M. (2018). The Cancer Prevention, Anti-inflammatory and Anti-oxidation of Bioactive Phytochemicals Targeting the TLR4 Signaling Pathway. *Ijms* 19, 2729. doi:10.3390/ijms19092729

Chen, Z., Kong, X.-F., Wang, R., Ma, Y.-G., Xu, L.-J., Lu, F.-E., et al. (2009a). Investigation on Prevention Effects of Jieze No.2 on *Candida Albicans* Vaginitis. *Chin. Matern. Child Health Care China* 24, 788–790.

Chen, Z., Wang, R., Kong, X.-F., Lu, F.-E., Ma, Y.-G., and Huang, G.-Y. (2009b). The Experimental Study of Jieze No.2 on *Trichomonas* Vaginitis. *Chin. Matern. Child Health Care China* 24, 241–244.

Chen, Z., Wang, R., Ma, Y.-G., Kong, X.-F., Lu, F.-E., and Huang, G.-Y. (2009c). The Effect of Jieze No.2 Gel on *Trichomonas* Vaginitis in Rats. *Chin. Matern. Child Health Care China* 24, 644–646.

Chen, Z., Wang, R., Ma, Y.-G., Kong, X.-F., and Xiong, C.-L. (2009d). Spermicidal and Antifertility Effects of Jieze No. 2 Gel in Rabbit. *Chin. Matern. Child Health Care China* 24, 3855–3858.

Chin, L. W., Cheng, Y. W., Lin, S. S., Lai, Y. Y., Lin, L. Y., Chou, M. Y., et al. (2010). Anti-herpes Simplex Virus Effects of Berberine from Coptidis Rhizoma, a Major Component of a Chinese Herbal Medicine, Ching-Wei-San. *Arch. Virol.* 155, 1933–1941. doi:10.1007/s00705-010-0779-9

Chinese Pharmacopoeia Commission (2020). *Pharmacopoeia of the People's Republic of China*. Beijing: China medical science press.

Dai, W., Wu, Y., Bi, J., Wang, S., Li, F., Kong, W., et al. (2018). Antiviral Effects of ABMA against Herpes Simplex Virus Type 2 *In Vitro* and *In Vivo*. *Viruses* 10, 119. doi:10.3390/v10030119

Duan, Q., Liu, T., Yuan, P., Huang, C., Shao, Q., Xu, L., et al. (2020). Antiviral Effect of Chinese Herbal Prescription JieZe-1 on Adhesion and Penetration of VK2/E6E7 with Herpes Simplex Viruses Type 2. *J. Ethnopharmacol.* 249, 112405. doi:10.1016/j.jep.2019.112405

Dunne, A., and O'Neill, L. A. J. (2003). The Interleukin-1 receptor/Toll-like Receptor Superfamily: Signal Transduction during Inflammation and Host Defense. *Sci. Signaling* 2003, re3. doi:10.1126/stke.2003.171.re3

Elboim, M., Grodzovski, I., Djian, E., Wolf, D. G., and Mandelboim, O. (2013). HSV-2 Specifically Down Regulates HLA-C Expression to Render HSV-2-Infected DCs Susceptible to NK Cell Killing. *Plos Pathog.* 9, e1003226. doi:10.1371/journal.ppat.1003226

Field, H. J., Huang, M. L., Lay, E. M., Mickleburgh, I., Zimmermann, H., and Birkmann, A. (2013). Baseline Sensitivity of HSV-1 and HSV-2 Clinical Isolates and Defined Acyclovir-Resistant Strains to the Helicase-Primase Inhibitor Pritelivir. *Antivir. Res* 100, 297–299. doi:10.1016/j.antiviral.2013.08.024

Fu, X., Tao, L., Wang, P. Y., Cripe, T. P., and Zhang, X. (2018). Comparison of Infectivity and Spread between HSV-1 and HSV-2 Based Oncolytic Viruses on Tumor Cells with Different Receptor Expression Profiles. *Oncotarget* 9, 21348–21358. doi:10.18632/oncotarget.25096

Fujimoto, Y., Tomioka, Y., Ozaki, K., Takeda, K., Suyama, H., Yamamoto, S., et al. (2017). Comparison of the Antiviral Potential Among Soluble Forms of Herpes Simplex Virus Type-2 Glycoprotein D Receptors, Herpes Virus Entry Mediator A, Nectin-1 and Nectin-2, in Transgenic Mice. *J. Gen. Virol.* 98, 1815–1822. doi:10.1099/jgv.0.000804

González, P. A., Carreño, L. J., Figueroa, C. A., and Kalergis, A. M. (2007). Modulation of Immunological Synapse by Membrane-Bound and Soluble Ligands. *Cytokine Growth Factor. Rev.* 18, 19–31. doi:10.1016/j.cytogfr.2007.01.003

Gotoh, K., Tanaka, Y., Nishikimi, A., Nakamura, R., Yamada, H., Maeda, N., et al. (2010). Selective Control of Type I IFN Induction by the Rac Activator DOCK2 during TLR-Mediated Plasmacytoid Dendritic Cell Activation. *J. Exp. Med.* 207, 721–730. doi:10.1084/jem.20091776

Gu, L., Han, Y., Liu, W., Mao, Y., Li, J., and Wang, H. (2014). The Expression of IL-2 and IL-4 in CD4(+) T Cells from Mouse Lymph Nodes and Spleen during HSV-1-Induced Facial Palsy. *Inflamm. Res.* 63, 117–125. doi:10.1007/s00011-013-0680-6

Haji Abdolvahab, M., Mofrad, M. R., and Schellekens, H. (2016). Interferon Beta: from Molecular Level to Therapeutic Effects. *Int. Rev. Cell Mol Biol* 326, 343–372. doi:10.1016/bs.ircmb.2016.06.001

Hayden, M. S., and Ghosh, S. (2004). Signaling to NF-kappaB. *Genes Dev.* 18, 2195–2224. doi:10.1101/gad.1228704

He, W., Han, H., Wang, W., and Gao, B. (2011). Anti-influenza Virus Effect of Aqueous Extracts from Dandelion. *Virol. J.* 8, 538. doi:10.1186/1743-422X-8-538

Heinrich, M., Appendino, G., Efferth, T., Fürst, R., Izzo, A. A., Kayser, O., et al. (2020). Best Practice in Research - Overcoming Common Challenges in Phytopharmacological Research. *J. Ethnopharmacol.* 246, 112230. doi:10.1016/j.jep.2019.112230

Hong, J. K., Lee, K. N., You, S. H., Kim, S. M., Tark, D., Lee, H. S., et al. (2015). Inactivation of Foot-And-Mouth Disease Virus by Citric Acid and Sodium Carbonate with Deicers. *Appl. Environ. Microbiol.* 81, 7610–7614. doi:10.1128/AEM.01673-15

Hu, K., He, S., Xiao, J., Li, M., Luo, S., Zhang, M., et al. (2017). Interaction between Herpesvirus Entry Mediator and HSV-2 Glycoproteins Mediates HIV-1 Entry of HSV-2-Infected Epithelial Cells. *J. Gen. Virol.* 98, 2351–2361. doi:10.1099/jgv.0.000895

Hu, S., Sheng, W. S., Schachtele, S. J., and Lokensgard, J. R. (2011). Reactive Oxygen Species Drive Herpes Simplex Virus (HSV)-1-induced Proinflammatory Cytokine Production by Murine Microglia. *J. Neuroinflammation* 8, 123. doi:10.1186/1742-2094-8-123

Ibáñez, F. J., Farías, M. A., Gonzalez-Troncoso, M. P., Corrales, N., Duarte, L. F., Retamal-Díaz, A., et al. (2018). Experimental Dissection of the Lytic Replication Cycles of Herpes Simplex Viruses *In Vitro*. *Front. Microbiol.* 9, 2406. doi:10.3389/fmicb.2018.02406

Ikeda, K., Tsujimoto, K., Uozaki, M., Nishide, M., Suzuki, Y., Koyama, A. H., et al. (2011). Inhibition of Multiplication of Herpes Simplex Virus by Caffeic Acid. *Int. J. Mol. Med.* 28, 595–598. doi:10.3892/ijmm.2011.739

James, S. H., and Kimberlin, D. W. (2015). Neonatal Herpes Simplex Virus Infection: Epidemiology and Treatment. *Clin. Perinatol* 42, 47–viii. doi:10.1016/j.clp.2014.10.005

Javed, T., Ashfaq, U. A., Riaz, S., Rehman, S., and Riazuddin, S. (2011). In-vitro Antiviral Activity of Solanum nigrum against Hepatitis C Virus. *Virol. J.* 8, 26. doi:10.1186/1743-422X-8-26

Johnston, C., Koelle, D. M., and Wald, A. (2014). Current Status and Prospects for Development of an HSV Vaccine. *Vaccine* 32, 1553–1560. doi:10.1016/j.vaccine.2013.08.066

Kaushic, C., Ashkar, A. A., Reid, L. A., and Rosenthal, K. L. (2003). Progesterone Increases Susceptibility and Decreases Immune Responses to Genital Herpes Infection. *J. Virol.* 77, 4558–4565. doi:10.1128/jvi.77.8.4558-4565.2003

Khalili, M., Alavi, M., Esmaeil-Jamaat, E., Baluchnejadmojarad, T., and Roghani, M. (2018). Trigonelline Mitigates Lipopolysaccharide-Induced Learning and Memory Impairment in the Rat Due to its Anti-oxidative and Anti-inflammatory Effect. *Int. Immunopharmacol* 61, 355–362. doi:10.1016/j.intimp.2018.06.019

Kilani-Jaziri, S., Mokdad-Bzeouich, I., Krifa, M., Nasr, N., Ghedira, K., and Chekir-Ghedira, L. (2017). Immunomodulatory and Cellular Anti-oxidant Activities of Caffeic, Ferulic, and P-Coumaric Phenolic Acids: a Structure-Activity Relationship Study. *Drug Chem. Toxicol.* 40, 416–424. doi:10.1080/01480545.2016.1252919

Koelle, D. M., and Wald, A. (2000). Herpes Simplex Virus: the Importance of Asymptomatic Shedding. *J. Antimicrob. Chemother.* 45 Suppl T3, 1–8. doi:10.1093/jac/45.suppl_4.1

Kollias, C. M., Huneke, R. B., Wigdahl, B., and Jennings, S. R. (2015). Animal Models of Herpes Simplex Virus Immunity and Pathogenesis. *J. Neurovirol.* 21, 8–23. doi:10.1007/s13365-014-0302-2

Lafaille, F. G., Pessach, I. M., Zhang, S. Y., Ciancanelli, M. J., Herman, M., Abhyankar, A., et al. (2012). Impaired Intrinsic Immunity to HSV-1 in Human iPSC-Derived TLR3-Deficient CNS Cells. *Nature* 491, 769–773. doi:10.1038/nature11583

Lagos, D., Vart, R. J., Gratrix, F., Westrop, S. J., Emuss, V., Wong, P. P., et al. (2008). Toll-like Receptor 4 Mediates Innate Immunity to Kaposi Sarcoma Herpesvirus. *Cell Host Microbe* 4, 470–483. doi:10.1016/j.chom.2008.09.012

Li, G.-X., Wang, X.-M., Jiang, T., Gong, J.-F., Niu, L.-Y., and Li, N. (2015). Berberine Prevents Intestinal Mucosal Barrier Damage during Early Phase of Sepsis in Rat through the Toll-like Receptors Signaling Pathway. *Korean J. Physiol. Pharmacol.* 19, 1–7. doi:10.4196/kjpp.2015.19.1.1

Li, H., Feng, C., Fan, C., Yang, Y., Yang, X., Lu, H., et al. (2020). Intervention of Oncostatin M-Driven Mucosal Inflammation by Berberine Exerts Therapeutic Property in Chronic Ulcerative Colitis. *Cell Death Dis* 11, 271. doi:10.1038/s41419-020-2470-8

Li, S. S., Li, H. Y., Piao, Y. A., Liu, D. L., Tian, W. J., and Dong, Y. M. (2004). The Anti-respiratory Syncytial Virus Effect of an Active Compound (AP3) from a Chinese Medicinal Herb-Herba Patriniae *In Vitro*. *Zhonghua Liu Xing Bing Xue Za Zhi* 25, 150–153. doi:10.1016/s0197-4580(04)80675-4

Li, Y., Jiang, W., Li, Z. Z., Zhang, C., Huang, C., Yang, J., et al. (2018). Repetitive Restraint Stress Changes Spleen Immune Cell Subsets through Glucocorticoid Receptor or β-adrenergic Receptor in a Stage Dependent Manner. *Biochem. Biophys. Res. Commun.* 495, 1108–1114. doi:10.1016/j.bbrc.2017.11.148

Liu, H., Chen, K., Feng, W., Wu, X., and Li, H. (2013). TLR4-MyD88/Mal-NF-kB axis Is Involved in Infection of HSV-2 in Human Cervical Epithelial Cells. *PLoS One* 8, e80327. doi:10.1371/journal.pone.0080327

Lo, M., Zhu, J., Hansen, S. G., Carroll, T., Farr Zuend, C., Nöel-Romas, L., et al. (2019). Acute Infection and Subsequent Subclinical Reactivation of Herpes Simplex Virus 2 after Vaginal Inoculation of Rhesus Macaques. *J. Virol.* 93, e01574–18. doi:10.1128/JVI.01574-18

Looker, K. J., Magaret, A. S., Turner, K. M., Vickerman, P., Gottlieb, S. L., Newman, L. M., et al. (2015). Global Estimates of Prevalent and Incident Herpes Simplex

Virus Type 2 Infections in 2012. *PLOS ONE* 10, e114989. doi:10.1371/journal.pone.0114989

López-Muñoz, A. D., Rastrojo, A., Alcamí, A., and Dunning Hotopp, J. C. (2018). Complete Genome Sequence of Herpes Simplex Virus 2 Strain 333. *Microbiol. Resour. Announc.* 7, e00870–18. doi:10.1128/MRA.00870-18

Lü, J. M., Yan, S., Jamaluddin, S., Weakley, S. M., Liang, Z., Siwak, E. B., et al. (2012). Ginkgolic Acid Inhibits HIV Protease Activity and HIV Infection *In Vitro*. *Med. Sci. Monit.* 18, BR293–298. doi:10.12659/MSM.883261

Luo, S., Hu, K., He, S., Wang, P., Zhang, M., Huang, X., et al. (2015). Contribution of N-Linked Glycans on HSV-2 gB to Cell-Cell Fusion and Viral Entry. *Virology* 483, 72–82. doi:10.1016/j.virol.2015.04.005

Ma, X., Guo, Z., Zhang, Z., Li, X., Liu, Y., Zhao, L., et al. (2020). Ferulic Acid Protects against Porcine Parvovirus Infection-Induced Apoptosis by Suppressing the Nuclear Factor-Kb Inflammasome Axis and Toll-like Receptor 4 via Nonstructural Protein 1. *Evid. Based Complement. Alternat Med.* 2020, 3943672. doi:10.1155/2020/3943672

Ma, Y., Xie, W., Fang, J., and Chen, Z. (2011). Determination of Berberine Hydrochloride in Jieze Lotion by HPLC. *Her. Med.* 30, 1484–1486. doi:10.1002/sim.4337

Martinez-Martin, N., and Viejo-Borbolla, A. (2010). Toll-like Receptor-Mediated Recognition of Herpes Simplex Virus. *Front. Biosci. (Schol Ed.* 2, 718–729. doi:10.2741/s96

Mogensen, T. H. (2009). Pathogen Recognition and Inflammatory Signaling in Innate Immune Defenses. *Clin. Microbiol. Rev.* 22, 240–Contents. doi:10.1128/CMR.00046-08

Nam, S. J., Oh, I. S., Yoon, Y. H., Kwon, B. I., Kang, W., Kim, H. J., et al. (2014). Apocynin Regulates Cytokine Production of CD8(+) T Cells. *Clin. Exp. Med.* 14, 261–268. doi:10.1007/s10238-013-0241-x

Nam, Y. J., Kim, A., Sohn, D. S., and Lee, C. S. (2016). Apocynin Inhibits Toll-like Receptor-4-Mediated Activation of NF-Kb by Suppressing the Akt and mTOR Pathways. *Naunyn Schmiedebergs Arch. Pharmacol.* 389, 1267–1277. doi:10.1007/s00210-016-1288-5

Namvar, L., Olofsson, S., Bergström, T., and Lindh, M. (2005). Detection and Typing of Herpes Simplex Virus (HSV) in Mucocutaneous Samples by Taqman Pcr Targeting a gB Segment Homologous for HSV Types 1 and 2. *J. Clin. Microbiol.* 43, 2058–2064. doi:10.1128/JCM.43.5.2058-2064.2005

Ojha, D., Das, R., Sobia, P., Dwivedi, V., Ghosh, S., Samanta, A., et al. (2015). Pedilanthus Tithymaloides Inhibits HSV Infection by Modulating NF-Kb Signaling. *PLoS One* 10, e0139338. doi:10.1371/journal.pone.0139338

Ooi, L. S., Sun, S. S., Wang, H., and Ooi, V. E. (2004). New Mannose-Binding Lectin Isolated from the Rhizome of Sarsaparilla Smilax Glabra Roxb. (Liliaceae). *J. Agric. Food Chem.* 52, 6091–6095. doi:10.1021/jf030837o

Ozçelik, B., Kartal, M., and Orhan, I. (2011). Cytotoxicity, Antiviral and Antimicrobial Activities of Alkaloids, Flavonoids, and Phenolic Acids. *Pharm. Biol.* 49, 396–402. doi:10.3109/13880209.2010.519390

Paludan, S. R., Bowie, A. G., Horan, K. A., and Fitzgerald, K. A. (2011). Recognition of Herpesviruses by the Innate Immune System. *Nat. Rev. Immunol.* 11, 143–154. doi:10.1038/nri2937

Pisonero-Vaquero, S., García-Mediavilla, M. V., Jorquera, F., Majano, P. L., Benet, M., Jover, R., et al. (2014). Modulation of PI3K-lxrα-dependent Lipogenesis Mediated by Oxidative/nitrosative Stress Contributes to Inhibition of HCV Replication by Quercetin. *Lab. Invest.* 94, 262–274. doi:10.1038/labinvest.2013.156

Qiao, Y., Chen, Z., Ma, Y. G., Lu, F. E., Chen, S. H., and Huang, G. Y. (2013). Nonoxynol-9 Berberine Plural Gel Has Little Effect on Expression of SLPI, SP-D and Lactoferrin in Mice's Vagina. *Iran. J. Reprod. Med.* 11, 565–576.

Reed, L. J., and Muench, H. (1938). A Simple Method of Estimating Fifty Per Cent Endpoints12. *Am. J. Epidemiol.* 27, 493–497. doi:10.1093/oxfordjournals.aje.a118408

Retamal-Díaz, A., Weiss, K. A., Tognarelli, E. I., Freire, M., Bueno, S. M., Herold, B. C., et al. (2017b). US6 Gene Deletion in Herpes Simplex Virus Type 2 Enhances Dendritic Cell Function and T Cell Activation. *Front. Immunol.* 8, 1523. doi:10.3389/fimmu.2017.01523

Retamal-Díaz, A. R., Suazo, P. A., Garrido, I., Kalergis, A. M., and González, P. A. (2015). Immune Evasion by Herpes Simplex Viruses. *Rev. Chilena Infectol* 32, 58–70. doi:10.4067/S0716-10182015000200013

Retamal-Díaz, A. R., Kalergis, A. M., Bueno, S. M., and González, P. A. (2017a). A Herpes Simplex Virus Type 2 Deleted for Glycoprotein D Enables Dendritic Cells to Activate CD4+ and CD8+ T Cells. *Front. Immunol.* 8. doi:10.3389/fimmu.2017.00904

Rittà, M., Marengo, A., Civra, A., Lembo, D., Cagliero, C., Kant, K., et al. (2020). Antiviral Activity of a Arisaema Tortuosum Leaf Extract and Some of its Constituents against Herpes Simplex Virus Type 2. *Planta Med.* 86, 267–275. doi:10.1055/a-1087-8303

Rivera, D., Allkin, R., Obón, C., Alcaraz, F., Verpoorte, R., and Heinrich, M. (2014). What Is in a Name? the Need for Accurate Scientific Nomenclature for Plants. *J. Ethnopharmacol.* 152, 393–402. doi:10.1016/j.jep.2013.12.022

Robinson, C. L., Chong, A. C. N., Ashbrook, A. W., Jeng, G., Jin, J., Chen, H., et al. (2018). Male Germ Cells Support Long-Term Propagation of Zika Virus. *Nat. Commun.* 9, 2090. doi:10.1038/s41467-018-04444-w

Roller, R. J., and Roizman, B. (1992). The Herpes Simplex Virus 1 RNA Binding Protein US11 Is a Virion Component and Associates with Ribosomal 60S Subunits. *J. Virol.* 66, 3624–3632. doi:10.1128/JVI.66.6.3624-3632.1992

Rubicz, R., Leach, C. T., Kraig, E., Dhurandhar, N. V., Duggirala, R., Blangero, J., et al. (2011). Genetic Factors Influence Serological Measures of Common Infections. *Hum. Hered.* 72, 133–141. doi:10.1159/000331220

Ryan, D. G., and O'Neill, L. A. J. (2017). Krebs Cycle Rewired for Macrophage and Dendritic Cell Effector Functions. *FEBS Lett.* 591, 2992–3006. doi:10.1002/1873-3468.12744

Sacks, S. L., Griffiths, P. D., Corey, L., Cohen, C., Cunningham, A., Dusheiko, G. M., et al. (2004). HSV Shedding. *Antivir. Res* 63 (Suppl. 1), S19–S26. doi:10.1016/j.antiviral.2004.06.004

Schleenvoigt, B. T., Pletz, M. W., Deinhardt-Emmer, S., and Sauerbrei, A. (2018). Detection of a Novel Mutation Conferring Acyclovir Resistance and Consecutive Treatment Failure in an HIV-Positive Patient with Recurrent HSV-2 Infection. *J. Glob. Antimicrob. Resist.* 12, 20. doi:10.1016/j.jgar.2017.11.009

Shao, Q., Liu, T., Wang, W., Duan, Q., Liu, T., Xu, L., et al. (2020). The Chinese Herbal Prescription JZ-1 Induces Autophagy to Protect against Herpes Simplex Virus-2 in Human Vaginal Epithelial Cells by Inhibiting the PI3K/Akt/mTOR Pathway. *J. Ethnopharmacol.* 254, 112611. doi:10.1016/j.jep.2020.112611

Sørensen, L. N., Reinert, L. S., Malmgaard, L., Bartholdy, C., Thomsen, A. R., and Paludan, S. R. (2008). TLR2 and TLR9 Synergistically Control Herpes Simplex Virus Infection in the Brain. *J. Immunol.* 181, 8604–8612. doi:10.4049/jimmunol.181.12.8604

Steiner, I., Spivack, J. G., Deshmane, S. L., Ace, C. I., Preston, C. M., and Fraser, N. W. (1990). A Herpes Simplex Virus Type 1 Mutant Containing a Nontransinducing Vmw65 Protein Establishes Latent Infection *In Vivo* in the Absence of Viral Replication and Reactivates Efficiently from Explanted Trigeminal Ganglia. *J. Virol.* 64, 1630–1638. doi:10.1128/JVI.64.4.1630-1638.1990

Tanaka, T., Narazaki, M., and Kishimoto, T. (2014). IL-6 in Inflammation, Immunity, and Disease. *Cold Spring Harb Perspect. Biol.* 6, a016295. doi:10.1101/cshperspect.a016295

Thompson, R. L., and Sawtell, N. M. (2019). Targeted Promoter Replacement Reveals that Herpes Simplex Virus Type-1 and 2 Specific VP16 Promoters Direct Distinct Rates of Entry into the Lytic Program in Sensory Neurons *In Vivo*. *Front. Microbiol.* 10, 1624. doi:10.3389/fmicb.2019.01624

Tognarelli, E. I., Palomino, T. F., Corrales, N., Bueno, S. M., Kalergis, A. M., and González, P. A. (2019). Herpes Simplex Virus Evasion of Early Host Antiviral Responses. *Front. Cell. Infect. Microbiol.* 9, 127. doi:10.3389/fcimb.2019.00127

Tu, Z., Gong, W., Zhang, Y., Feng, Y., Liu, Y., and Tu, C. (2018). Inhibition of Rabies Virus by 1,2,3,4,6-Penta-O-Galloyl-β-D-Glucose Involves mTOR-dependent Autophagy. *Viruses* 10, 201. doi:10.3390/v10040201

Utsunomiya, H., Ichinose, M., Ikeda, K., Uozaki, M., Morishita, J., Kuwahara, T., et al. (2014). Inhibition by Caffeic Acid of the Influenza A Virus Multiplication *In Vitro*. *Int. J. Mol. Med.* 34, 1020–1024. doi:10.3892/ijmm.2014.1859

Uyangaa, E., Patil, A. M., and Eo, S. K. (2014). Prophylactic and Therapeutic Modulation of Innate and Adaptive Immunity against Mucosal Infection of Herpes Simplex Virus. *Immune Netw.* 14, 187–200. doi:10.4110/in.2014.14.4.187

Wang, G. F., Shi, L. P., Ren, Y. D., Liu, Q. F., Liu, H. F., Zhang, R. J., et al. (2009). Anti-hepatitis B Virus Activity of Chlorogenic Acid, Quinic Acid and Caffeic

Acid *In Vivo* and *In Vitro*. *Antivir. Res* 83, 186–190. doi:10.1016/j.antiviral.2009.05.002

Warowicka, A., Nawrot, R., and Goździcka-Józefiak, A. (2020). Antiviral Activity of Berberine. *Arch. Virol.* 165, 1935–1945. doi:10.1007/s00705-020-04706-3

Wei, H., Chen, Z., Xu, P., Ma, Y. G., Xu, L. J., and Xu, L.-J. (2008). Effect of Jieze No.1 on Cervicitis Caused by *Ureaplasma Urealyticum* and on *Ureaplasma Urealyticum In Vitro*. *Chin. J. Integr. Med.* 14, 88–93. doi:10.1007/s11655-008-0088-2

Xie, M. (2016). *Pharmacology of Traditional Chinese Medical Formulae*. Beijing: People's Medical Publishing House.

Xu, P., Chen, Z., Xu, L., and Lu, F. (2005). Spermicidal Effect of Jieze No. 1 in Combination with Nonoxynol-9 *In Vitro*. *J. Huazhong Univ. Sci. Technolog Med. Sci.* 25, 225–228. doi:10.1007/BF02873584

Yamamoto, M., Takeda, K., and Akira, S. (2004). TIR Domain-Containing Adaptors Define the Specificity of TLR Signaling. *Mol. Immunol.* 40, 861–868. doi:10.1016/j.molimm.2003.10.006

Yan, Y. Q., Fu, Y. J., Wu, S., Qin, H. Q., Zhen, X., Song, B. M., et al. (2018). Anti-influenza Activity of Berberine Improves Prognosis by Reducing Viral Replication in Mice. *Phytother Res.* 32, 2560–2567. doi:10.1002/ptr.6196

Yang, Y., Qi, J., Wang, Q., Du, L., Zhou, Y., Yu, H., et al. (2013). Berberine Suppresses Th17 and Dendritic Cell Responses. *Invest. Ophthalmol. Vis. Sci.* 54, 2516–2522. doi:10.1167/iovs.12-11217

Ye, S., Liu, H., Chen, Y., Qiu, F., Liang, C. L., Zhang, Q., et al. (2019). A Novel Immunosuppressant, Luteolin, Modulates Alloimmunity and Suppresses Murine Allograft Rejection. *J. Immunol.* 203, 3436–3446. doi:10.4049/jimmunol.1900612

Zanello, P. R., Koishi, A. C., Rezende Júnior, Cde. O., Oliveira, L. A., Pereira, A. A., de Almeida, M. V., et al. (2015). Quinic Acid Derivatives Inhibit Dengue Virus Replication *In Vitro*. *Virol. J.* 12, 223. doi:10.1186/s12985-015-0443-9

Conflict of Interest: The authors declare that the research was conducted in the absence of any commercial or financial relationships that could be construed as a potential conflict of interest.

Publisher's Note: All claims expressed in this article are solely those of the authors and do not necessarily represent those of their affiliated organizations, or those of the publisher, the editors and the reviewers. Any product that may be evaluated in this article, or claim that may be made by its manufacturer, is not guaranteed or endorsed by the publisher.

frontiers in Pharmacology

ORIGINAL RESEARCH
published: 18 November 2021
doi: 10.3389/fphar.2021.604009

Precise Investigation of the Efficacy of Multicomponent Drugs Against Pneumonia Infected With Influenza Virus

Junying Wei[1†], Jianhui Sun[1†], Jiawei Zeng[2†], Enhui Ji[1], Jing Xu[1], Chunyu Tang[3], Hairu Huo[1], Yi Zhang[1], Hongmei Li[1]* and Hongjun Yang[1]**

[1]Institute of Chinese Materia Medica, China Academy of Chinese Medical Sciences, Beijing, China, [2]Department of Clinical Laboratory, Mianyang Central Hospital, Mianyang, China, [3]Research Center of Anti-infection Chinese Medicine Engineering Technology, Yongzhou, China

OPEN ACCESS

Edited by:
Anirban Mandal,
Mrinalini Datta Mahavidyapith, India

Reviewed by:
Helen Skaltsa,
National and Kapodistrian University of Athens, Greece
LI Suyun,
Henan University of Traditional Chinese Medicine, China

***Correspondence:**
Hongjun Yang
hongjun0420@vip.sina.com
Hongmei Li
hmli@icmm.ac.cn
Junying Wei
13683350075@163.com

[†]These authors have contributed equally to this work

Specialty section:
This article was submitted to Ethnopharmacology, a section of the journal Frontiers in Pharmacology

Received: 08 September 2020
Accepted: 01 November 2021
Published: 18 November 2021

Citation:
Wei J, Sun J, Zeng J, Ji E, Xu J, Tang C, Huo H, Zhang Y, Li H and Yang H (2021) Precise Investigation of the Efficacy of Multicomponent Drugs Against Pneumonia Infected With Influenza Virus. Front. Pharmacol. 12:604009. doi: 10.3389/fphar.2021.604009

Background: Viral pneumonia is one of the most serious respiratory diseases, and multicomponent traditional Chinese medicines have been applied in the management of infected patients. As a representative TCM, HouYanQing (HYQ) oral liquid shows antiviral activity. However, the unclear mechanisms, as well as the ambiguous clinical effects, limit widespread application of this treatment. Therefore, in this study, a proteomics-based approach was utilized to precisely investigate its efficacy.

Methods: Based on the efficacy evaluation of HYQ in a mouse model of pneumonia caused by influenza A virus (H1N1) and the subsequent proteomics analysis, specific signatures regulated by HYQ treatment of viral pneumonia were identified.

Results: Experimental verifications indicate that HYQ may show distinctive effects in viral pneumonia patients, such as elevated galectin-3-binding protein and glutathione peroxidase 3 levels.

Conclusion: This study provides a precise investigation of the efficacy of a multicomponent drug against viral pneumonia and offers a promising alternative for personalized management of viral pneumonia.

Keywords: pneumonia, precise medicine, multicomponent drug, proteomics, houyanqing oral liquid

1 INTRODUCTION

Pneumonia is one of the most serious respiratory diseases, causes many deaths per year and is often caused by viruses, especially severe acute respiratory syndrome (SARS) virus (Levy et al., 2005), the 2009 pandemic influenza A (H1N1) virus (Writing Committee of the WHO Consultation on Clinical Aspects of Pandemic (H1N1) 2009 Influenza et al., 2010) and coronavirus disease 2019 (COVID-19) (Guan et al., 2020). Along with the increase in our understanding of the role of viruses in pneumonia, more findings indicate that the incidence of viral pneumonia has been underestimated (Ruuskanen et al., 2011). Thus, further studies are urgently needed that focus on the cause and pathogenesis of viral pneumonia, better management and care of patients, and identification of safer and more effective drugs, including personalized medicine for viral pneumonia patients (Schuetz et al., 2013; Rello and Perez, 2016; Gautam et al., 2018).

Multicomponent drugs represented by traditional Chinese medicine (TCM) have drawn increasing attention in viral pneumonia treatment (Wang et al., 2011; Li et al., 2015; Zhu et al., 2018; Hu et al., 2020; Li et al., 2020; Yang et al., 2020). As a typical representative, Lianhuaqingwen can affect virus morphology and exert anti-inflammatory activity *in vitro* (Li et al., 2020). Moreover, a multicenter open-label randomized controlled trial indicated that the recovery rate of patients with COVID-19 was higher in the Lianhuaqingwen treatment group than in the control group, and the median time to recovery was also shorter in the treatment group (Hu et al., 2020). Although these TCMs have shown better effects and fewer side effects in some cases, due to the characteristics of TCMs, such as multiple components and superposition effects, further investigations are needed to reveal their potential mechanisms and precise effects in the clinic (Wei et al., 2019a; Wei et al., 2019b).

In this study, we utilized a proteomics-based approach to precisely investigate the efficacy of a multicomponent drug, HouYanQing (HYQ) oral liquid, against pneumonia due to influenza virus in mice. As a traditional local medicine in Hunan Province of China, HYQ contains 4 types of herbs, *Achyranthes aspera* L. *Aster indicus* L. *Carpesium abrotanoides* L. and *Plantago depressa* Willd. in a ratio of 250:143:36:71 (Chinese Pharmacopoeia 2020). A previous study indicated that HYQ can decrease the viral load in the lungs of mice with pneumonia due to influenza virus and plays a therapeutic role in influenza A virus infection in mice (Sun et al., 2019). However, the corresponding mechanism, as well as its potential clinical application in personalized medical care of viral pneumonia, merits further investigation. This study provides a precise investigation of the efficacy of multicomponent drugs against viral pneumonia and offers a promising alternative for personalized management of viral pneumonia.

2 MATERIALS AND METHODS

2.1 Drugs and Materials

HouYanQing (HYQ) oral liquid extracts were obtained from Hunan Time Sun Pharmaceutical Co., Ltd. (Yongzhou, China. Batch 2018010908). Oseltamivir phosphate capsules were purchased from Shanghai Roche Pharmaceutical Ltd. (Shanghai, China. Batch H1035). Sequencing grade porcine trypsin and dithiothreitol (DTT) were obtained from Promega (Madison, WI, United States). Iodoacetamide (IAA) was purchased from Sigma-Aldrich Chemicals (St. Louis, Missouri, United States). All of the other chemicals were analytical grade reagents. Deionized water (R > 18.2 MΩ) used for all of the experiments was purified by using a Millipore purification system (Billerica, MA, United States).

The content of HYQ was determined based on Chinese Pharmacopoeia 2020. The sample was hydrolyzed with hydrochloric acid-ethanol for 1 h and extracted with petroleum ether (60–90°C). HPLC determinations were performed by using a SHIMADZU LC-20AT instrument (Shimadzu Corporation, Japan) equipped with Diamonsil C18 (250 mm × 4.6 mm, 5 μm) column. The mobile phase was acetonitrile (A)-Water (B) (90:10), the detection wavelength was 210 nm, the column temperature was 30 °C and the flow rate was 1 ml/min.

2.2 Animal Study

Specific-pathogen-free (SPF) male ICR mice (Charles River Laboratories, SCXK 2016–0006), 13–15 g in weight, were mildly anesthetized with ether and then infected by nasal administration of the type A influenza virus FM_1 mouse lung-adapted strain (obtained from Institute of Virology, Chinese Academy of Preventive Medicine) at a concentration of *15 LD50* (each 0.05 ml). From the day of virus infection, the infected mice were randomly divided into the treatment groups and administered high-dosage HYQ (15.6 g/kg daily, n = 24), low-dosage HYQ (3.9 g/kg daily, equivalent to a clinical dosage, n = 24), oseltamivir (40 mg/kg daily, n = 24) or water (model, n = 24) by oral administration (p.o.) twice per day for nine consecutive days. Uninfected mice were used as controls (n = 24). Both infected animals and control animals were euthanized three, six, and 9 days postinfection (eight mice were euthanized in each group at each time point). Plasma samples were collected and frozen at-20°C, and lung tissues were harvested and frozen at-80°C for the next analysis. The lung index was calculated as follows: lung index = lung weight (g)/body weight (g) *100%. All of the animal experiments were approved by the Committee on the Animal Care and Use of the Institute of Chinese Materia Medica, China Academy of Chinese Medical Sciences and were carried out in accordance with the approved guidelines. All viral experiments were performed in the ABSL-2 biosafety room.

2.3 Determination of Viral Load in Lung Tissue by Real-Time PCR (RT-PCR)

The viral load in the lung tissue of an infected mouse was determined by RT-PCR. The primers of FM_1 for RT-PCR were as follows: upstream, 5′-AAACCCAGAATGCGAATC AC-3'; downstream, 5′-GCTCAGCTTTGGGTATGAGC-3' (synthesized by Invitrogen). Briefly, total RNA was extracted using TRIzol (TaKaRa, Japan. Batch R6321) according to the manufacturer's instructions, and reverse transcription reactions were performed using the PrimeScript™ RT reagent kit (TaKaRa, Japan. Batch AK3001). The RT-PCR protocol was as follows: 95°C, 30 s; 95°C, 5 s; 60°C, 40 s; with 40 amplification cycles; 95°C, 10 s using the ABI 7500 RT-PCR machine. The assays were carried out in triplicate, and Ct values were calculated. The copy number was calculated according to the standard curve.

2.4 Proteomic Analysis

Mouse lung tissues were homogenized in PBS (KCl: 0.2 g, KH_2PO_4: 0.2 g, NaCl: 8.0 g, $Na_2HPO_4.12H_2O$: 3.9054 g, pH 7.4, 1000 ml) buffer cocktail with a tissue homogenizer (Sceintz-48, Sceintz, Ningbo, China). Then, the proteins of mouse lung tissues were lysed with 8 M urea by ultrasound, and the lysate was centrifuged at 24,000 g for 30 min at 4°C. The supernatant was collected, and the protein concentration was determined by the bicinchoninic acid assay. Three hundred

micrograms of protein was reduced by adding 0.1 M dithiothreitol for 4 h at 37°C and then alkylated by adding 0.5 M IAA for 60 min at room temperature in the dark. The protein sample was finally digested using trypsin in 50 mM ammonium bicarbonate (pH 8.0) at an enzyme:protein mass ratio of 1:50 for 24 h at 37°C.

Orbitrap Fusion (Thermo Fisher Scientific) LC-MS/MS analyses were performed on an Easy-nLC 1000 liquid chromatography system (Thermo Fisher Scientific) coupled to an Orbitrap Fusion via a nanoelectrospray ion source. Tryptic peptides were dissolved with loading buffer (acetonitrile and 0.1% formic acid), and the tryptic peptides were eluted from a 150 μm ID x 2 cm C18 trap column and separated on a homemade 150 μm ID x 12 cm column (C18, 1.9 μm, 120 Å, Dr Maisch GmbH) with a flow rate of 500 nL/min. Survey scans were acquired after an accumulation of $5e^5$ ions in the Orbitrap for m/z 300–1,400 using a resolution of 120,000 at m/z 200. The top speed data-dependent mode was selected for fragmentation in the HCD cell at a normalized collision energy of 32%, and fragment ions were then transferred into the ion trap analyzer with the AGC target at $5e^3$ and maximum injection time at 35 m. The dynamic exclusion of previously acquired precursor ions was enabled at 18 s. Spectral data were searched against the mouse protein RefSeq database (downloaded on 9–26–2018) in Proteome Discoverer1.4.1.14 suites with Mascot software (version 2.3.01, Matrix Science) to achieve a false discovery rate of <1%. The mass tolerance was set at 10 ppm for precursor ions, and it was set at 0.5 Da for the tolerance of product ions. Oxidation (M) and acetylation (Protein-N term) were chosen as variable modifications, while carbamidomethylation (C) was chosen as a fixed modification, and two missed cleavage sites for trypsin were allowed.

Intensity-based absolute quantification (iBAQ)-based protein quantification (Schwanhäusser et al., 2011; Wei et al., 2019b) was performed using in-house software. Briefly, the iBAQ intensities were obtained by dividing the protein intensities by the number of theoretical peptides, which were calculated by *in silico* protein digestion with a PERL script, and all of the fully tryptic peptides between 6 and 30 amino acids were counted, while the missed cleavages were neglected. The iBAQ value of each protein was then normalized to the total iBAQ value for all of the identified proteins to avoid possible experimental variations (Wei et al., 2014; Wei et al., 2016). Three individual samples were analyzed in each group, and the changes were identified by statistical analyses of the measured protein amounts from each individual sample (Wei et al., 2014).

2.5 Western Blot Analysis

The proteins of mouse lung tissues were extracted in ice-cold RIPA lysis buffer (Solarbio, China) by ultrasound and then determined by the enhanced bicinchoninic acid protein assay kit (Thermo, United States). Thirty micrograms of each sample was loaded on 10% SDS-PAGE gels, and protein blots were transferred onto polyvinylidene fluoride membranes (Millipore, United States). After blocking with 5% nonfat milk, the blots were incubated overnight at 4°C with the following primary antibodies: anti-glyceraldehyde-3-phosphate dehydrogenase (GAPDH, Proteintech, 10494-1-AP), anti-intercellular adhesion molecule-1 (ICAM-1, Proteintech, 16174-1-AP) and anti-transferrin (Proteintech, 17435-1-AP). Then, the membranes were washed with a mixture of Tris-buffered saline and Tween 20 (TBST) and incubated at room temperature for 1 h with a secondary antibody conjugated to horseradish peroxidase. Finally, the protein blots were visualized using an enhanced chemiluminescence kit (Millipore, United States). Three individual samples were analyzed in each group. Bar graphs are relative gray values to GAPDH. The results from each mouse were analyzed by one-way analysis of variance.

2.6 ELISA

Serum samples from the mice were centrifuged at 10,000 rpm for 10 min at 4°C. The supernatant was assayed using ELISA kits according to the manufacturer's instructions. Mouse galectin-3-binding protein (*Lgals3bp,* Cusabio, CSB-EL012888MO), mouse plasma protease C1 inhibitor (*Serping1,* Cusabio, CSB-EL021086MO), mouse glutathione peroxidase 3 (*Gpx3,* Cusabio, CSB-EL009868MO), mouse hemopexin (*Hpx,* Abcam, ab157716) and protein S100-A8 (*S100a8,* Abcam, ab263886) ELISA kits were used. Each kit consisted of a 96-well plate in which a specific antibody against a target protein was immobilized. The target protein in sera is recognized by the antibody, followed by incubation with a horseradish peroxidase-conjugated secondary antibody for colorimetric quantification. The plates were read on a microplate reader (Molecular Devices, United States) at 450 nm. The reactions were carried out in triplicate for each sample. Finally, the results were analyzed by one-way analysis of variance and were considered significant at $p < 0.05$.

3 RESULTS

3.1 Protective Effect of HYQ on the Mouse Model of Pneumonia Infected With Influenza Virus

First, the content of HYQ was determined based on Chinese Pharmacopoeia 2020. As shown in **Figure 1**, the retention time was 10.007 min for oleanolic acid and the content was 4.57 mg/g, which is in accord with Chinese Pharmacopoeia 2020. Then, the therapeutic effect of HYQ on the mouse model of pneumonia infected with influenza A virus (H1N1) was investigated at the third, sixth, and ninth days after influenza virus infection. As shown in **Figure 2A**, along with prolongation of virus infection, the lung index of the infected mice was increasingly higher than that of the control mice. At the sixth day after infection, both HYQ and oseltamivir decreased the lung index of the infected mice, and at the ninth day, the high dose of HYQ and oseltamivir remained effective. The viral load in the lung tissues of the infected mice was significantly higher than that of the other mice on the sixth day after infection (**Figure 2B**), and both high-dose HYQ and oseltamivir reduced the viral load of the infected mice, even on the ninth day. These experimental results indicate

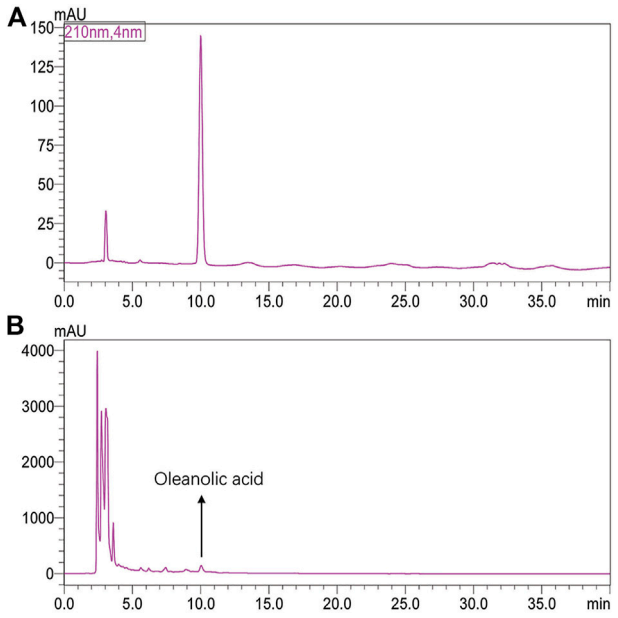

FIGURE 1 | HPLC chromatograms of the standard oleanolic acid **(A)** and HYQ Sample **(B)**.

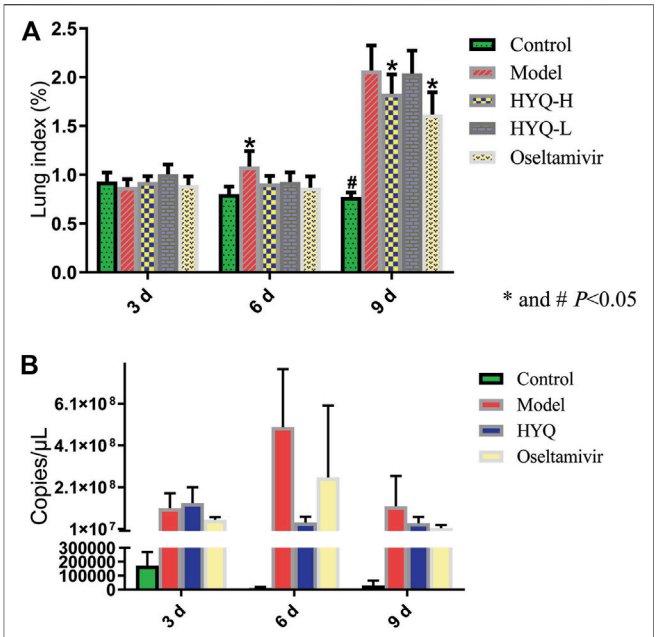

FIGURE 2 | Efficacy evaluation of HYQ against viral pneumonia in mice infected with influenza A virus (H1N1) **(A)** Lung index. HYQ-H: high-dosage HYQ. HYQ-L: low-dosage HYQ **(B)** Viral load results of the mouse lung. HYQ: high-dosage HYQ. 3, 6 and 9 days: virus infection time.

that after almost 1 week of intervention, HYQ can exert therapeutic efficacy in mice with pneumonia due to influenza virus.

3.2 Investigation of the Protein Dynamics of the HYQ-Mediated Effects on Viral Pneumonia in Mice

The protein dynamics following HYQ-mediated intervention of viral pneumonia were investigated by measuring the changes in the proteins in the mouse lung at the third and sixth days after viral infection and high-dosage HYQ administration using a high-throughput proteomics method and an accurate intensity-based absolute quantification (iBAQ)-based quantification approach (Schwanhäusser et al., 2011; Wei et al., 2014; Wei et al., 2016; Wei et al., 2019a; Wei et al., 2019b). Moreover, the iBAQ value of a protein was normalized by the total iBAQ value for all of the identified proteins to avoid possible experimental variations (Wei et al., 2014; Wei et al., 2016; Wei et al., 2019a; Wei et al., 2019b), and in each group, three individual samples were analyzed. In total, 6,208 proteins were identified (**Supplementary Table S1**). As shown in **Figure 3A**, at the third day after viral infection, compared with those in the control group, some proteins in the model group with functions such as positive regulation of apoptotic process, defense response to virus and cellular response to interferon-alpha were upregulated ($p < 0.05$), while some proteins that function in protein transport, positive regulation of T cell cytokine production and RNA splicing were downregulated ($p < 0.05$). After intervention with HYQ (**Figure 3B**), some proteins that are associated with immune system processes, defense responses to protozoans, intracellular signal transduction and others had upregulated expression levels ($p < 0.05$), while other proteins with functions such as defense responses to viruses, transforming growth factor beta receptor signaling pathways and autophagy decreased ($p < 0.05$). Furthermore, compared with the control (**Figure 3C**), HYQ administration increased the proteins that function in cellular macromolecular complex assembly and others ($p < 0.05$) and decreased the proteins associated with positive regulation of apoptotic process, cellular response to interferon-beta, defense response to virus and so on ($p < 0.05$).

Six days after virus infection, compared to those in the control (**Figure 3D**), the proteins in the infected mice with the function of positive regulation of the Wnt signaling pathway, positive regulation of the apoptotic process and innate immune response showed upregulated expression ($p < 0.05$), while the decreased proteins are involved in regulation of transcription, positive regulation of interleukin-4 production, T cell receptor signaling pathway and others ($p < 0.05$). Administration of HYQ enhanced the proteins involved in immune system process, positive regulation of cell motility, inflammatory response and so on ($p < 0.05$, **Figure 3E**), and proteins associated with adaptive immune response, T cell receptor signaling pathway and response to DNA damage stimulus were downregulated ($p < 0.05$). Additionally, compared with the control (**Figure 3F**), six-day intervention by HYQ increased the proteins that function in positive regulation of interleukin-4 production and negative regulation of viral genome replication ($p < 0.05$) while decreasing the proteins involved in apoptotic processes and cytolysis ($p < 0.05$). Therefore, the functional changes of these proteins are consistent with the effect of the drug.

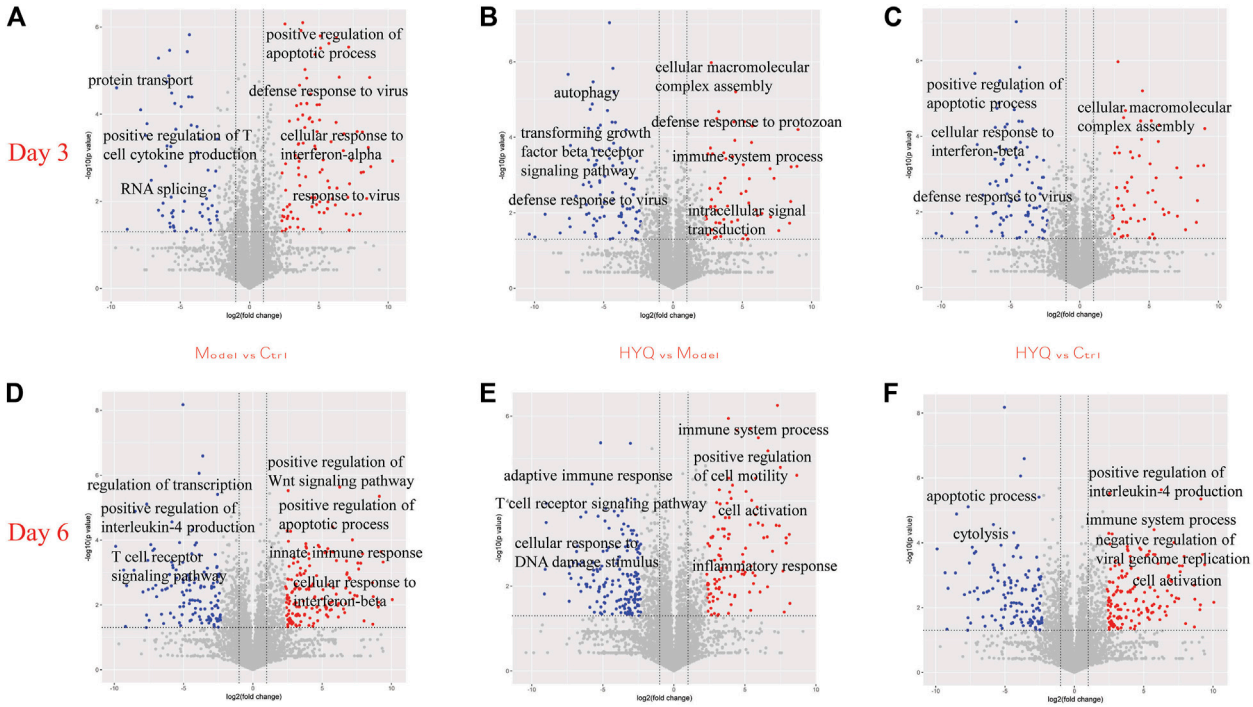

FIGURE 3 | Protein dynamics of HYQ-mediated intervention of viral pneumonia in the mouse lung at the third and sixth days after viral infection and high-dosage HYQ administration **(A)** Proteins' change at the third day after viral infection (model vs control at day 3) and the biological process or molecular function of some proteins with significantly different expression levels ($p < 0.05$) **(B)** Proteins' change at the third day after viral infection and high-dosage HYQ administration (HYQ vs model at day 3) and the biological process or molecular function of some proteins with significantly different expression levels ($p < 0.05$) **(C)** Proteins' change between high-dosage HYQ administration and control at the third day (HYQ vs control at day 3) **(D)** Model vs control at day 6 **(E)** HYQ vs model at day 6 **(F)** HYQ vs control at day 6. Ctrl: control. Days 3 and 6: virus infection time.

Based on the statistical analyses of the measured protein amounts from each individual sample in one group (Wei et al., 2014), we investigated the dynamics of some proteins at the proteomic level. These selected proteins, such as plasma protease C1 inhibitor, hemopexin, transferrin, complement factor B and complement C3, have been identified as candidate biomarkers of acute respiratory virus infection (Burke et al., 2017) or exhibited obvious fold changes during influenza infection (Kumar et al., 2014). As shown in **Figure 4**, on the third day after viral infection and HYQ administration, none of these candidate proteins were significantly different among these groups. At the sixth day, compared with those of the control group, all of these candidate proteins in the infected mice had upregulated expression levels ($p < 0.05$), and administration of HYQ decreased their expression levels ($p < 0.05$). Similarly, these changes are also consistent with the effect of the drug.

3.3 Verification of Functional Proteins in the HYQ-Mediated Effect on Viral Pneumonia in Mice

Critical functional proteins associated with the HYQ-mediated effect on viral pneumonia in mice were verified by Western blot analysis of these proteins in mouse lung tissues at the sixth day after viral infection and HYQ administration. As shown in **Figure 5**, as a highly expressed protein in inflammatory conditions (Lawson and Wolf, 2009), intercellular cell adhesion molecule-1 (ICAM-1) had upregulated expression levels in the infected mice compared with the control mice ($p < 0.05$), while both HYQ and oseltamivir decreased its expression, but the HYQ administration group had no significant difference due to the substantial variation. Transferrin was shown to be influenced by inflammation and oxidative stress (Matusiewicz et al., 2017), while both HYQ and oseltamivir can reverse the upward trend in infected mice ($p < 0.05$). Thus, these critical functional proteins were verified, which indicated that HYQ may also have an anti-inflammatory effect on the infected mice.

3.4 Investigation of the Efficacy of HYQ on Viral Pneumonia in Mice

Then, specific signatures related to the effects of HYQ against viral pneumonia were ultimately verified by ELISA-based measurements of the changes in the blood of the infected mice. As shown in **Figure 6**, on the third day after viral infection and HYQ administration, the amounts of plasma protease C1 inhibitor (*Serping1*), glutathione peroxidase 3 (*Gpx3*), hemopexin (*Hpx*) and protein S100-A8 (*S100a8*) in the infected mouse blood increased compared to that of the

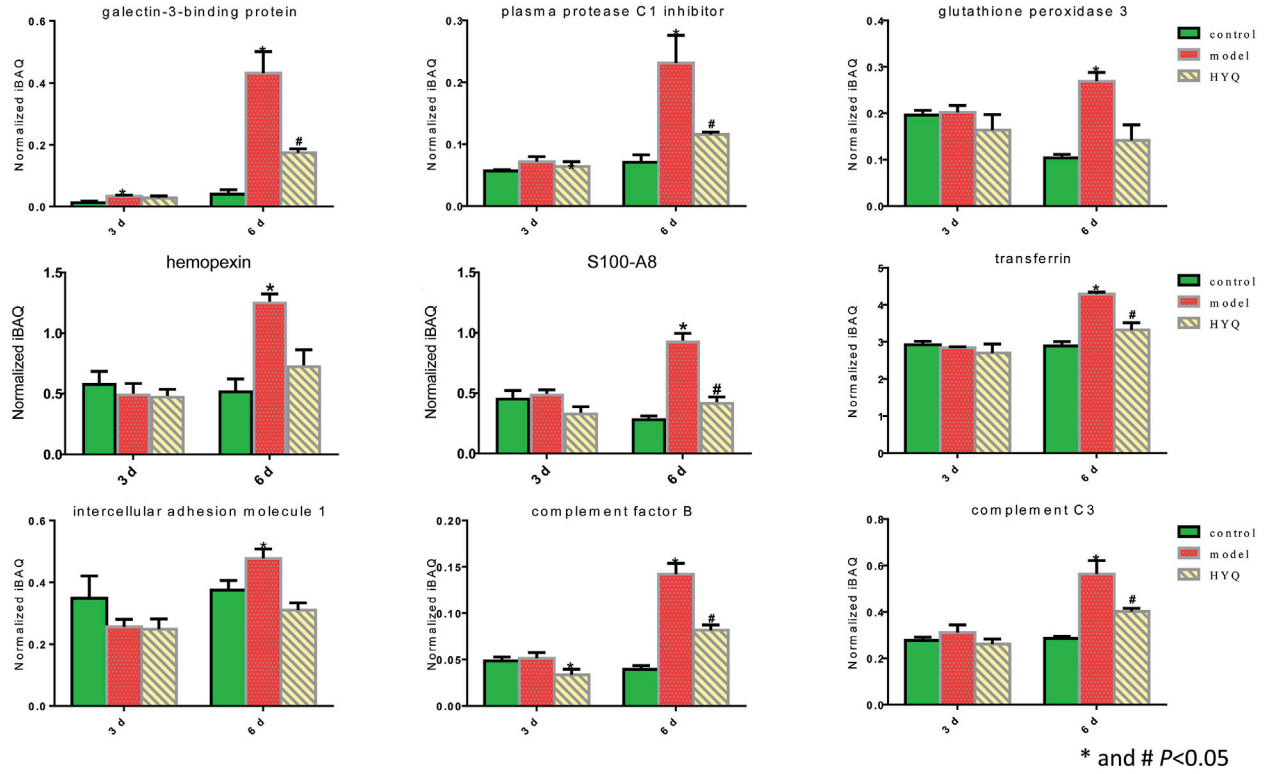

FIGURE 4 | Proteomic quantitative analysis of the candidate signatures regulated by HYQ against viral pneumonia in mouse lung. Three individual samples were analyzed in each group. The normalized iBAQ value of each protein from each individual sample was used for one-way analysis of variance; 3 and 6 days: virus infection time.

control ($p < 0.05$), and HYQ inhibited the elevations of *Serping1* and *Gpx3* compared with that of the model group ($p < 0.05$). On the sixth day, the amounts of galectin-3-binding protein (*Lgals3bp*), *Hpx* and *S100a8* in the infected mouse blood consistently increased during viral infection, whereas their expression levels in blood were all decreased by HYQ administration ($p < 0.05$). However, the expression level of *Lgals3bp* was not affected after oseltamivir administration ($p > 0.05$). Therefore, *Lgals3bp* is thought to correspond to the specific efficacy of HYQ against viral pneumonia. Moreover, oseltamivir was reported to have a potential side effect on the hepatic activities of glutathione reductase, glutathione peroxidase, and glutathione S-transferase (El-Sayed and Al-Kahtani, 2011). Thus, in some cases, HYQ may be a promising alternative treatment for viral pneumonia, and *Gpx3* may be another specific signature regulated by HYQ against viral pneumonia. Overall, HYQ may have a specific effect on viral pneumonia such as elevated *Lgals3bp* and *Gpx3* levels in the blood.

4 DISCUSSION

It was reported that a significant number of pneumonia cases are caused by viruses (Guan et al., 2020); thus, safe and effective treatment is vital to improving the quality of life of patients. Along with the increase in viral pneumonia, an increasing number of traditional Chinese medicines (TCMs) have been applied to viral pneumonia treatment due to their multiple constituents, multiple targets and good safety (Wang et al., 2011; Li et al., 2015; Zhu et al., 2018; Hu et al., 2020; Li et al., 2020; Yang et al., 2020). The HouYanQing (HYQ) oral liquid used in this study contains 4 types of herbs, which have all been safely used in local traditional medicine for many years. Experimental investigations of a mouse model of pneumonia infected with influenza A virus (H1N1) indicated that HYQ exerts good therapeutic efficacy in viral pneumonia, and proteomic investigations of the molecular function of proteins perturbed by HYQ indicated that HYQ enhances the proteins involved in immune system processes, negative regulation of viral genome replication, inflammatory responses, etc. Therefore, HYQ may be a promising alternative treatment for viral pneumonia.

However, similar to many other TCMs, the ambiguous clinical effects and unclear mechanism hinder its extensive application in the clinic. In addition, rational use of this treatment in viral pneumonia is unclear. Proteomics-based investigation of signatures associated with the specific efficacy of HYQ against viral pneumonia shed light on this issue. With the aid of the discovered biomarkers, we concluded that HYQ has a specific effect on viral pneumonia such as elevated galectin-3-binding protein (*Lgals3bp*) and glutathione peroxidase 3 (*Gpx3*) levels in blood. Therefore, in this case, this treatment can be used more effectively, and the potential side effects can be minimized.

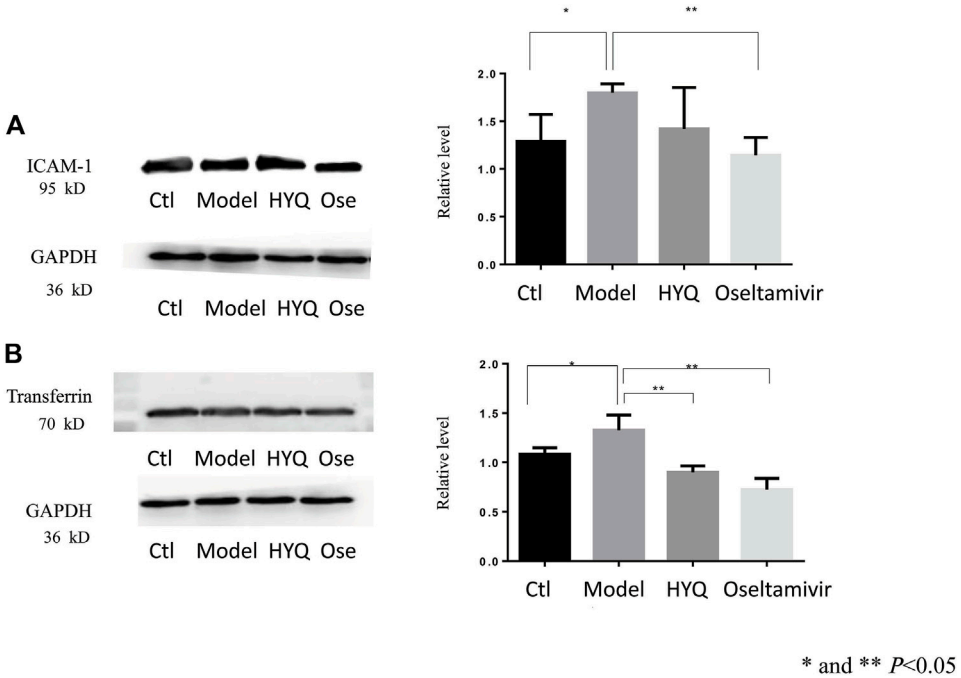

FIGURE 5 | Western blot verification of functional proteins in the HYQ-mediated effect on viral pneumonia in mouse lungs at the sixth day after infection **(A)** Image of ICAM-1 and its relative level among different groups **(B)** Image of transferrin and its relative level among different groups. Bar graphs are relative gray values to GAPDH. Three individual samples were analyzed in each group, and the results from each mouse were analyzed by one-way analysis of variance. ICAM-1: intercellular adhesion molecule-1. GAPDH: glyceraldehyde-3-phosphate dehydrogenase. Ctl: control. Ose: oseltamivir.

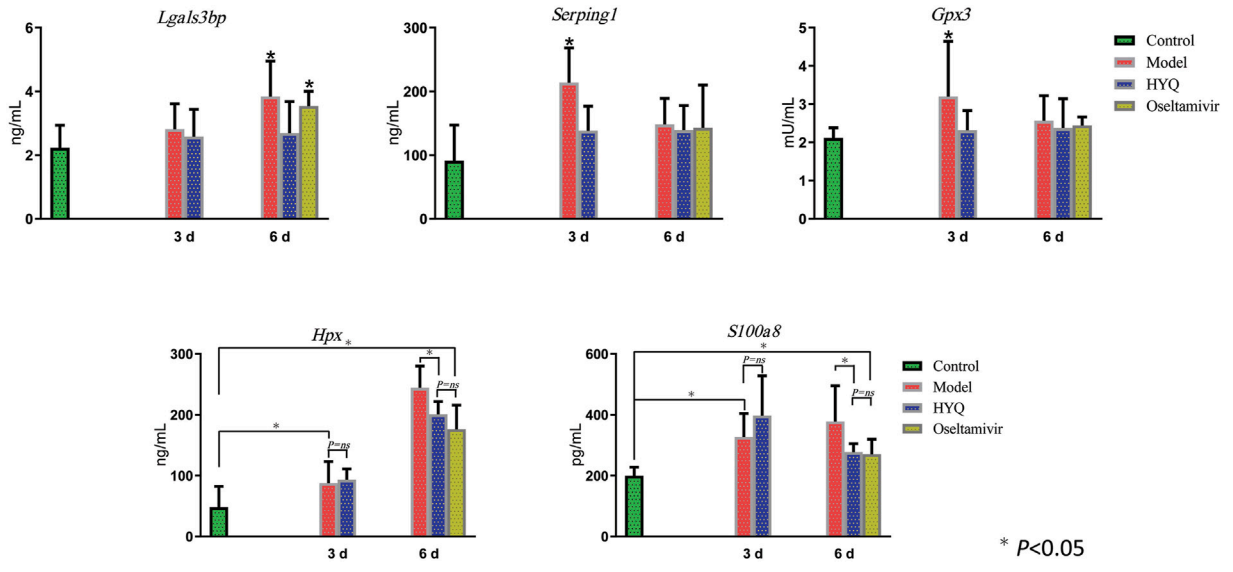

FIGURE 6 | ELISA-based verification of the candidate signatures regulated by HYQ against viral pneumonia in mouse blood. Each group contained 6 mice, and the results from each mouse were analyzed by one-way analysis of variance; 3 and 6 days: virus infection time. ns: no significance. *Lgals3bp*, galectin-3-binding protein; *Serping1*, plasma protease C1 inhibitor; *Gpx3*, glutathione peroxidase 3; *Hpx*, hemopexin; *S100a8*, protein S100-A8.

Among the signatures associated with the specific efficacy of HYQ against viral pneumonia, *Lgals3bp* promotes integrin-mediated cell adhesion and may stimulate host defense against viruses (UniProt Consortium, 2015). It was also reported that *Lgals3bp* expression is induced in viral infection and by many molecules that either mimic or are characteristic of ongoing inflammation and microbial infection, such as IFN-α, IFN-β, IFN-γ and TNF-α, and it has innate immune functions with special emphasis on viral and bacterial infections (Loimaranta et al., 2018). Although it was found that *Lgals3bp* may be a serological biomarker for acute dengue virus infection (Liu et al., 2016), acute hantavirus infection (Hepojoki et al., 2014), hepatitis C virus (HCV), human immunodeficiency virus (HIV) infection (Shaked et al., 2014; Yang et al., 2014; Rodríguez-Gallego et al., 2019), and hepatitis B virus-related hepatocellular carcinoma (Liu et al., 2017), the relationship between *Lgals3bp* and viral pneumonia is rarely investigated. *Gpx3* protects cells and enzymes from oxidative damage (UniProt Consortium, 2015) and may be involved in immune defense against pathogenic invasion (Bathige et al., 2015). Additionally, glutathione peroxidase 4 is reversibly induced by HCV to increase virion infectivity (Brault et al., 2016), and glutathione peroxidase activity could be an important prognostic factor in diabetic patients with Epstein-Barr virus infection (Dworzański et al., 2020) or as an adjuvant in the management of HIV-infected patients (Ogunro et al., 2006). Our present study indicates that HYQ can specifically regulate *Lgals3bp* and *Gpx3*, thus exerting a good protective effect against viral pneumonia.

In addition to the specific regulatory effect, as a multicomponent drug, HYQ can have multiple overlapping effects similar to other TCMs. As shown in the results, HYQ can also regulate intercellular cell adhesion molecule-1 (*Icam-1*), transferrin, plasma protease C1 inhibitor (*Serping1*), hemopexin (*Hpx*), protein S100-A8 (*S100a8*), and complement factor B and C3. In fact, transferrin, *Hpx*, and complement factor B and C3 have been identified by quantitative proteomics in a mouse model of influenza as potential markers of disease severity that can be clinically useful in humans (Kumar et al., 2014), and *Serping1* and complement factor B have been identified as candidate nasopharyngeal protein biomarkers in acute respiratory virus infection (Burke et al., 2017). Among these regulated molecules, *Serping1* plays a crucial role in regulating important physiological pathways, such as complement activation, and complement C3 plays a central role in the activation of the complement system (UniProt Consortium, 2015). As an essential element of the immune system, the complement system can be activated by some viruses, and a previous study indicated that *Serping1* and its network serve as important components of the innate immune system to restrict HIV-1 infection (Sanfilippo et al., 2017). *Hpx* has been proven to be a candidate marker for progression of fibrosis in HCV patients (Cheung et al., 2009) and a potential biomarker of respiratory syncytial virus-infected pneumonia (Wang et al., 2016). *S100a8* plays a prominent role in the regulation of inflammatory processes and the immune response (UniProt Consortium, 2015). After infection by some viruses, high expression of *S100a8* is observed, resulting in enhanced oxidative stress (Müller et al., 2017). Current experimental results showed that HYQ can also regulate these proteins and exert multiple effects on the complement system and inflammatory processes. Overall, HYQ will be a promising alternative for the safe and effective management of viral pneumonia.

5 CONCLUSION

In this study, a proteomics-based approach was utilized to precisely investigate the efficacy of a multicomponent traditional Chinese medicine, HouYanQing (HYQ) oral liquid, in a mouse model of pneumonia infected with influenza A virus (H1N1). Experimental results indicate that HYQ may show distinctive effects for viral pneumonia patients with the elevation of galectin-3-binding protein and glutathione peroxidase 3. This TCM also has multiple effects on the complement system and inflammatory processes. This study provides a precise investigation of the efficacy of a multicomponent drug against viral pneumonia and offers a promising alternative for personalized management of viral pneumonia.

DATA AVAILABILITY STATEMENT

The datasets presented in this study can be found in online repositories. The names of the repository/repositories and accession number(s) can be found in the article/ **Supplementary Material**.

ETHICS STATEMENT

The animal study was reviewed and approved by the Committee on the Animal Care and Use of the Institute of Chinese Materia Medica, China Academy of Chinese Medical Sciences.

AUTHOR CONTRIBUTIONS

JW conceived the study and wrote the manuscript JZ and CT performed the proteomics experiments. JS, HH, YZ, and HL conducted the animal study EJ and JX conducted the ELISA and Western-blot experiments HY conceived the study All authors reviewed and approved the final manuscript.

FUNDING

This work was supported by Strategic Scientific and Technological Project of Hunan Province (grant number 2016GK4050).

SUPPLEMENTARY MATERIAL

The Supplementary Material for this article can be found online at: https://www.frontiersin.org/articles/10.3389/fphar.2021.604009/full#supplementary-material

REFERENCES

Bathige, S. D., Umasuthan, N., Godahewa, G. I., Thulasitha, W. S., Whang, I., Won, S. H., et al. (2015). Two Variants of Selenium-dependent Glutathione Peroxidase from the Disk Abalone Haliotis Discus Discus: Molecular Characterization and Immune Responses to Bacterial and Viral Stresses. *Fish. Shellfish Immunol.* 45 (2), 648–655. doi:10.1016/j.fsi.2015.05.028

Brault, C., Lévy, P., Duponchel, S., Michelet, M., Sallé, A., Pécheur, E. I., et al. (2016). Glutathione Peroxidase 4 Is Reversibly Induced by HCV to Control Lipid Peroxidation and to Increase Virion Infectivity. *Gut* 65 (1), 144–154. doi:10.1136/gutjnl-2014-307904

Burke, T. W., Henao, R., Soderblom, E., Tsalik, E. L., Thompson, J. W., McClain, M. T., et al. (2017). Nasopharyngeal Protein Biomarkers of Acute Respiratory Virus Infection. *EBioMedicine* 17, 172–181. doi:10.1016/j.ebiom.2017.02.015

Cheung, K. J., Tilleman, K., Deforce, D., Colle, I., and Van Vlierberghe, H. (2009). The HCV Serum Proteome: a Search for Fibrosis Protein Markers. *J. Viral Hepat.* 16 (6), 418–429. doi:10.1111/j.1365-2893.2009.01083.x

Dworzański, J., Strycharz-Dudziak, M., Kliszczewska, E., Kiełczykowska, M., Dworzańska, A., Drop, B., et al. (2020). Glutathione Peroxidase (GPx) and Superoxide Dismutase (SOD) Activity in Patients with Diabetes Mellitus Type 2 Infected with Epstein-Barr Virus. *PLoS One* 15 (3), e0230374. doi:10.1371/journal.pone.0230374

El-Sayed, W. M., and Al-Kahtani, M. A. (2011). Potential Adverse Effects of Oseltamivir in Rats: Males Are More Vulnerable Than Females. *Can. J. Physiol. Pharmacol.* 89 (9), 623–630. doi:10.1139/y11-060

Gautam, S., Sharma, L., and Dela Cruz, C. S. (2018). Personalizing the Management of Pneumonia. *Clin. Chest Med.* 39 (4), 871–900. doi:10.1016/j.ccm.2018.08.008

Guan, W. J., Ni, Z. Y., Hu, Y., Liang, W. H., Ou, C. Q., He, J. X., et al. (2020). Clinical Characteristics of Coronavirus Disease 2019 in China. *N. Engl. J. Med.* 382 (18), 1708–1720. doi:10.1056/NEJMoa2002032

Hepojoki, J., Strandin, T., Hetzel, U., Sironen, T., Klingström, J., Sane, J., et al. (2014). Acute Hantavirus Infection Induces Galectin-3-Binding Protein. *J. Gen. Virol.* 95 (Pt 11), 2356–2364. doi:10.1099/vir.0.066837-0

Hu, K., Guan, W. J., Bi, Y., Zhang, W., Li, L. J., Zhang, B. L., et al. (2020). Efficacy and Safety of Lianhuaqingwen Capsules, a Repurposed Chinese Herb, in Patients with Coronavirus Disease 2019: A Multicenter, Prospective, Randomized Controlled Trial. *Phytomedicine* 85, 153242. doi:10.1016/j.phymed.2020.153242

Kumar, Y., Liang, C., Limmon, G. V., Liang, L., Engelward, B. P., Ooi, E. E., et al. (2014). Molecular Analysis of Serum and Bronchoalveolar Lavage in a Mouse Model of Influenza Reveals Markers of Disease Severity that Can Be Clinically Useful in Humans. *PLoS One* 9 (2), e86912. doi:10.1371/journal.pone.0086912

Lawson, C., and Wolf, S. (2009). ICAM-1 Signaling in Endothelial Cells. *Pharmacol. Rep.* 61 (1), 22–32. doi:10.1016/s1734-1140(09)70004-0

Levy, M. M., Baylor, M. S., Bernard, G. R., Fowler, R., Franks, T. J., Hayden, F. G., et al. (2005). Clinical Issues and Research in Respiratory Failure from Severe Acute Respiratory Syndrome. *Am. J. Respir. Crit. Care Med.* 171 (5), 518–526. doi:10.1164/rccm.200405-621WS

Li, H., Xu, S., Cheng, T., Tang, L., Bai, J., and Lin, M. (2015). Effects of Traditional Chinese Medicine Fu Zheng Decoction on the Immunological Function and Clinical Prognosis of the Elderly Patients with Pneumonia. *Cell Biochem Biophys* 71 (1), 473–480. doi:10.1007/s12013-014-0227-7

Li, R. F., Hou, Y. L., Huang, J. C., Pan, W. Q., Ma, Q. H., Shi, Y. X., et al. (2020). Lianhuaqingwen Exerts Anti-viral and Anti-inflammatory Activity against Novel Coronavirus (SARS-CoV-2). *Pharmacol. Res.* 156, 104761. doi:10.1016/j.phrs.2020.104761

Liu, K. T., Liu, Y. H., Chen, Y. H., Lin, C. Y., Huang, C. H., Yen, M. C., et al. (2016). Serum Galectin-9 and Galectin-3-Binding Protein in Acute Dengue Virus Infection. *Int. J. Mol. Sci.* 17 (6), 832. doi:10.3390/ijms17060832

Liu, T., Liu, D., Liu, R., Jiang, H., Yan, G., Li, W., et al. (2017). Discovering Potential Serological Biomarker for Chronic Hepatitis B Virus-Related Hepatocellular Carcinoma in Chinese Population by MAL-Associated Serum Glycoproteomics Analysis. *Sci. Rep.* 7, 38918. doi:10.1038/srep38918

Loimaranta, V., Hepojoki, J., Laaksoaho, O., and Pulliainen, A. T. (2018). Galectin-3-binding Protein: A Multitask Glycoprotein with Innate Immunity Functions in Viral and Bacterial Infections. *J. Leukoc. Biol.* 104 (4), 777–786. doi:10.1002/JLB.3VMR0118-036R

Matusiewicz, M., Neubauer, K., Lewandowska, P., Gamian, A., and Krzystek-Korpacka, M. (2017). Reduced Transferrin Levels in Active Inflammatory Bowel Disease. *Biomed. Res. Int.* 2017, 9541370. doi:10.1155/2017/9541370

Müller, I., Vogl, T., Pappritz, K., Miteva, K., Savvatis, K., Rohde, D., et al. (2017). Pathogenic Role of the Damage-Associated Molecular Patterns S100A8 and S100A9 in Coxsackievirus B3-Induced Myocarditis. *Circ. Heart Fail.* 10 (11), e004125. doi:10.1161/CIRCHEARTFAILURE.117.004125

Ogunro, P. S., Ogungbamigbe, T. O., Elemie, P. O., Egbewale, B. E., and Adewole, T. A. (2006). Plasma Selenium Concentration and Glutathione Peroxidase Activity in HIV-1/AIDS Infected Patients: a Correlation with the Disease Progression. *Niger. Postgrad. Med. J.* 13 (1), 1–5.

Rello, J., and Perez, A. (2016). Precision Medicine for the Treatment of Severe Pneumonia in Intensive Care. *Expert Rev. Respir. Med.* 10 (3), 297–316. doi:10.1586/17476348.2016.1144477

Rodríguez-Gallego, E., Tarancón-Diez, L., García, F., Del Romero, J., Benito, J. M., Alba, V., et al. (2019). Proteomic Profile Associated with Loss of Spontaneous Human Immunodeficiency Virus Type 1 Elite Control. *J. Infect. Dis.* 219 (6), 867–876. doi:10.1093/infdis/jiy599

Ruuskanen, O., Lahti, E., Jennings, L. C., and Murdoch, D. R. (2011). Viral Pneumonia. *Lancet* 377 (9773), 1264–1275. doi:10.1016/S0140-6736(10)61459-6

Sanfilippo, C., Cambria, D., Longo, A., Palumbo, M., Avola, R., Pinzone, M., et al. (2017). SERPING1 mRNA Overexpression in Monocytes from HIV+ Patients. *Inflamm. Res.* 66 (12), 1107–1116. doi:10.1007/s00011-017-1091-x

Schuetz, P., Litke, A., Albrich, W. C., and Mueller, B. (2013). Blood Biomarkers for Personalized Treatment and Patient Management Decisions in Community-Acquired Pneumonia. *Curr. Opin. Infect. Dis.* 26 (2), 159–167. doi:10.1097/QCO.0b013e32835d0bec

Schwanhäusser, B., Busse, D., Li, N., Dittmar, G., Schuchhardt, J., Wolf, J., et al. (2011). Global Quantification of Mammalian Gene Expression Control. *Nature* 473 (7347), 337–342. doi:10.1038/nature10098

Shaked, I., Hanna, D. B., Gleißner, C., Marsh, B., Plants, J., Tracy, D., et al. (2014). Macrophage Inflammatory Markers Are Associated with Subclinical Carotid Artery Disease in Women with Human Immunodeficiency Virus or Hepatitis C Virus Infection. *Arterioscler Thromb. Vasc. Biol.* 34 (5), 1085–1092. doi:10.1161/ATVBAHA.113.303153

Sun, J. H., Tang, C. Y., Huo, H. R., Li, X. Q., Wei, J. Y., Tang, D. F., et al. (2019). Protective Effect of Houyanqing Extract on Pneumonia Model in Mice Infected with Influenza Virus. *Cent. South Pharm.* 17 (8), 1229–1233. doi:10.7539/j.issn.1672-2981.2019.08.010

UniProt Consortium (2015). UniProt: a Hub for Protein Information. *Nucleic Acids Res.* 43, D204–D212. Available at: http://www.uniprot.org/. doi:10.1093/nar/gku989

Wang, Y., Wang, T., Hu, J., Ren, C., Lei, H., Hou, Y., et al. (2011). Anti-biofilm Activity of TanReQing, a Traditional Chinese Medicine Used for the Treatment of Acute Pneumonia. *J. Ethnopharmacol.* 134 (1), 165–170. doi:10.1016/j.jep.2010.11.066

Wang, X. F., Zhang, X. Y., Gao, X., Liu, X. X., and Wang, Y. H. (2016). Proteomic Profiling of a Respiratory Syncytial Virus-Infected Rat Pneumonia Model. *Jpn. J. Infect. Dis.* 69 (4), 285–292. doi:10.7883/yoken.JJID.2015.244

Wei, J., Zhang, F., Zhang, Y., Cao, C., Li, X., Li, D., et al. (2014). Proteomic Investigation of Signatures for Geniposide-Induced Hepatotoxicity. *J. Proteome Res.* 13 (12), 5724–5733. doi:10.1021/pr5007119

Wei, J., Zhang, Y., Jia, Q., Liu, M., Li, D., Zhang, Y., et al. (2016). Systematic Investigation of Transcription Factors Critical in the protection against Cerebral Ischemia by Danhong Injection. *Sci. Rep.* 6, 29823. doi:10.1038/srep29823

Wei, J., Guo, F., Zhang, M., Xian, M., Wang, T., Gao, J., et al. (2019). Signature-oriented Investigation of the Efficacy of Multicomponent Drugs against Heart Failure. *FASEB J.* 33 (2), 2187–2198. doi:10.1096/fj.201800673RR

Wei, J., Man, Q., Guo, F., Xian, M., Wang, T., Tang, C., et al. (2019). Precise and Systematic Survey of the Efficacy of Multicomponent Drugs against Functional Dyspepsia. *Sci. Rep.* 9 (1), 10713. doi:10.1038/s41598-019-47300-7

Writing Committee of the WHO Consultation on Clinical Aspects of Pandemic (H1N1) 2009 Influenza; Bautista, E., Chotpitayasunondh, T., Gao, Z., Harper, S. A., Shaw, M., Uyeki, T. M., Zaki, S. R., et al. (2010). Clinical Aspects of Pandemic 2009 Influenza A (H1N1) Virus Infection. *N. Engl. J. Med.* 362 (18), 1708–1719. doi:10.1056/NEJMra1000449

Yang, W., Zhou, J. Y., Chen, L., Ao, M., Sun, S., Aiyetan, P., et al. (2014). Glycoproteomic Analysis Identifies Human Glycoproteins Secreted from HIV Latently Infected T Cells and Reveals Their Presence in HIV+ Plasma. *Clin. Proteomics* 11 (1), 9. doi:10.1186/1559-0275-11-9

Yang, Y., Islam, M. S., Wang, J., Li, Y., and Chen, X. (2020). Traditional Chinese Medicine in the Treatment of Patients Infected with 2019-New Coronavirus (SARS-CoV-2): A Review and Perspective. *Int. J. Biol. Sci.* 16 (10), 1708–1717. doi:10.7150/ijbs.45538

Zhu, H., Lu, X., Ling, L., Li, H., Ou, Y., Shi, X., et al. (2018). Houttuynia Cordata Polysaccharides Ameliorate Pneumonia Severity and Intestinal Injury in Mice with Influenza Virus Infection. *J. Ethnopharmacol* 218, 90–99. doi:10.1016/j.jep.2018.02.016

Conflict of Interest: The authors declare that the research was conducted in the absence of any commercial or financial relationships that could be construed as a potential conflict of interest.

frontiers in Pharmacology

ORIGINAL RESEARCH
published: 21 March 2022
doi: 10.3389/fphar.2022.744439

The Traditional Chinese Medicine Formula Jing Guan Fang for Preventing SARS-CoV-2 Infection: From Clinical Observation to Basic Research

Yueh-Hsin Ping[1,2], Hsin Yeh[3], Li-Wei Chu[1], Zhi-Hu Lin[3], Yin-Chieh Hsu[3], Lie-Chwen Lin[4], Chung-Hua Hsu[1,3,5], Shu-Ling Fu[3] and Tung-Yi Lin[3,6]**

[1]Department and Institute of Pharmacology, National Yang Ming Chiao Tung University, Taipei, Taiwan, [2]Institute of Biophotonics, National Yang Ming Chiao Tung University, Taipei, Taiwan, [3]Institute of Traditional Medicine, National Yang Ming Chiao Tung University, Taipei, Taiwan, [4]National Research Institute of Chinese Medicine, Taipei, Taiwan, [5]Branch of Linsen Chinese and Kunming, Taipei City Hospital, Taipei, Taiwan, [6]Biomedical Industry Ph.D. Program, National Yang Ming Chiao Tung University, Taipei, Taiwan

OPEN ACCESS

Edited by:
Michael Heinrich,
University College London,
United Kingdom

Reviewed by:
King-Ho Cheung,
Hong Kong Baptist University, Hong Kong SAR, China
Kundlik Gadhave,
Johns Hopkins University,
United States

***Correspondence:**
Tung-Yi Lin
biotungyi@gmail.com;
tylin99@nycu.edu.tw
Shu-Ling Fu
slfu@nycu.edu.tw

Specialty section:
This article was submitted to Ethnopharmacology, a section of the journal Frontiers in Pharmacology

Received: 20 July 2021
Accepted: 17 February 2022
Published: 21 March 2022

Citation:
Ping Y-H, Yeh H, Chu L-W, Lin Z-H, Hsu Y-C, Lin L-C, Hsu C-H, Fu S-L and Lin T-Y (2022) The Traditional Chinese Medicine Formula Jing Guan Fang for Preventing SARS-CoV-2 Infection: From Clinical Observation to Basic Research. Front. Pharmacol. 13:744439. doi: 10.3389/fphar.2022.744439

COVID-19 is a global epidemic. Developing adjuvant therapies which could prevent the virus from binding to cells may impair viral infection. This study produces a traditional Chinese medicine formula, Jing Guan Fang (JGF), based on ancient medical texts, and examines the efficacy and the mechanism by which JGF prevents viral infections. JGF reduces COVID-19 like symptoms. Functional studies show that JGF inhibits the formation of syncytium and reduces the formation of viral plaque. JGF is not toxic *in vitro* and *in vivo*. Mechanistically, JGF induces lysosomal-dependent ACE2 degradation and suppresses mRNA and the protein levels of TMPRSS2 in human lung WI-38 and MRC-5 cells. Mice that inhale JGF exhibit reduced ACE2 and TMPRSS2 protein levels in lung tissues. Together, these findings suggest that JGF may improve the COVID-19 like symptoms and inhibit viral infection. Moreover, JGF may be applicable as an adjuvant preventive strategy against SARS-CoV-2 infection in addition to the use of vaccines.

Keywords: Chinese medicine decoction, Jing Guan Fang, ACE2, TMPRSS2, COVID-19, prevention

INTRODUCTION

Since December 2019, the severe acute respiratory syndrome coronavirus 2 (SARS-CoV-2) infection has caused coronavirus disease 2019 (COVID-19), which is a severe pandemic with a wide spectrum of clinical symptoms, ranging from asymptomatic infection or a mild, flu-like illness to life-threatening diseases including severe pneumonia and severe acute respiratory syndrome (SARS) (Collaborators, 2020; Guan et al., 2020; Zhu et al., 2020). Until mid-May 2021, more than 162 million COVID-19 cases were recorded worldwide. More than 3.3 million cases resulted in death tolls

Abbreviations: SARS-CoV-2, the severe acute respiratory syndrome coronavirus 2; COVID-19, the coronavirus disease 2019; MERS-CoV, middle east respiratory syndrome coronavirus; RBD, receptor binding domain; ACE2, angiotensin-converting enzyme-2; TMPRSS2, transmembrane serine protease 2; TCM, traditional Chinese medicine; JGF, jing guan fang; HPLC, high-performance liquid chromatography; FBS, fetal bovine serum; DMEM, Dulbecco's modified eagle medium; MTT, 3 (4,5-Dimethylthiazol-2-yl)-2,5-diphenyltetrazolium bromide.

(WHO, 2021). SARS-CoV-2, which is the largest positive-strand RNA virus, is a member of the Coronaviridae family which includes the severe acute respiratory syndrome coronavirus (SARS-CoV) and Middle East respiratory syndrome coronavirus (MERS-CoV) (Collaborators, 2020; Zhou et al., 2020). The RNA genome of the SARS-CoV-2 is approximately 30 K nucleotides long and encodes four structure proteins, including a spike glycoprotein (S), an envelope protein (E), a membrane protein (M), and a nucleoprotein (N) (Chen et al., 2020). The S protein is composed of two functional subunits: S1 and S2. The S1 subunit has a receptor binding domain (RBD) at the N-terminal of the S protein, which binds to a critical host receptor: the angiotensin-converting enzyme-2 (ACE2). The S2 subunit has a fusion domain at the C-terminal of the S protein that fuses viral and cellular membranes (Li, 2016; Yan et al., 2020). The SARS-CoV-2 infection begins when virus particles attach to host cells due to interactions between S1 and ACE2 (Lan et al., 2020; Walls et al., 2020; Wang et al., 2020; Wrapp et al., 2020). The S2 subunit is further cleaved by host proteases, including the transmembrane serine protease 2 (TMPRSS2) and furin, which results in the dissociation of the S1 and the S2-mediated membrane fusion process (Cheng et al., 2020; Shang et al., 2020; Li et al., 2021). The S protein must bind with ACE2 and the S protein must be proteolyzed by membrane proteases if the SARS CoV-2 and host cell membrane are to be fused so an ability to block connections between the virus and host cells is a necessary facet of anti-SARS-CoV-2 agents.

Vaccines have been developed. Development of additional strategies/adjuvant therapies to prevent frontline medical staff from contacting COVID-19 may be an important priority. Traditional Chinese medicine (TCM) is arguably the world's oldest, continually practiced medical modality. Chinese herbal medicine is an integral part of TCM dealing with natural products, that when used in combination become multi-functional. Western medicine explores a single compound and has a clear structure and anti-disease mechanism but Chinese herbal medicine is a comprehensive collection of various compounds and various functions. Some studies show that herbal medicine can reduce viral infection (Yang et al., 2020; Jan et al., 2021; Tsai et al., 2021). Chinese herbal medicine uses a cocktail-like effect to block viral infections due to their complex contents. Using clinical symptomatology, the authors' collective experience during the 2003 SARS outbreak and with reference to the ancient medical text, *WenYi Lun* (溫疫論), this study designs a TCM formula, Jing Guan Fang (JGF), to prevent viral infection. JGF consists of five commonly used herbs: *Forsythia suspensa* (Thunb.) Vahl (as the Sovereign drug; 君藥), *Scutellaria baicalensis* Georgi (as the Minister drug; 臣藥), *Bupleurum chinese* DC (as the Assistant drug; 佐藥), *Magnolia officinalis* Rehder and E.H. Wilson (as the Assistant drug; 佐藥) and *Agastache rugose* (Fisch. and C.A. Mey.) Kuntze (as the Courier drug; 使藥).

This study determines the beneficial effects of JGF in improving clinical Covid-19 like symptoms and studies how JGF affects SARS-CoV-2 spike protein/ACE2 interaction and reduces plaque formation of SARS-CoV-2. The mechanism by which JGF downregulates ACE2 and TMPRSS2 levels in lung cells *in vitro* and in lung tissues of a mouse model *in vivo* is also determined. A high-performance liquid chromatography (HPLC) fingerprint of JGF was performed to ensure authentication and standardization.

MATERIALS AND METHODS

Jing Guan Fang Preparation

JGF was formulated by our herbal medicine physicians using herbal medicine theory and clinical experience (Cheng et al., 2006; Deng et al., 2012; Law et al., 2017; Ghildiyal et al., 2020; Yang et al., 2020). The formula for JGF uses five herbs: 10 mg of *Forsythia suspensa* (30.3% of total weight), 8 mg of *Scutellaria baicalensis* (24.2% of total weight), 6 mg of *Bupleurum chinese* (18.2% of total weight), 6 mg of *Magnolia officinalis* (18.2% of total weight) and 3 mg of *Agastache rugose* (9.0% of total weight). All ingredients were purchased from a certificated pharmaceutical company (KO DA Pharmaceutical Co., Ltd. Taiwan). JGF is produced by the Branch of Linsen Chinese and Kunming, Taipei City Hospital (Taipei, Taiwan). All herbs were soaked in water and subsequently boiled for 4 h using an automatic herb boiling machine. The final product is 110 g/pack in weight and 100 ml/pack in volume. HPLC was performed to ensure the quality and standard contents of JGF (**Supplementary Figure S1**). To ensure the quality of JGF, the herbal-medicine pharmacists who participated in the study underwent training in the preparation of JGF. All JGF users were instructed how to take JGF. Non-symptomatic individuals were advised to take one dose a week and those who displayed Covid-19 like symptoms were advised to take two doses a week.

Clinical Setting and Participants

JGF was initially designed for front line staff as a complementary preventative measure against Covid-19. The formula for JGF was then made freely available to the public on 20 February 2020, in five public hospitals in the Taipei area. The clinical study was conducted from 20 February 2020 to 20 May 2020. JGF was taken by subjects as a complementary preventative strategy. A total of 2468 packs of JGF were provided to 1086 individuals, of which 396 individuals participated in the questionnaire. All participants were from the Taipei area (Taipei city and New Taipei city). The protocol was approved by the Taipei City Hospital Institutional Review Board (TCHIRB-10904015) with Clinical Trial gov. Trial registration: NCT04388644, Registered 06 April 2020 - Retrospectively registered, https://clinicaltrials.gov/ct2/show/NCT04388644.

Survey and Data Collection

Subjects filled out the online questionnaire voluntarily, or in person at the hospitals. The questionnaire recorded an individual's demographic information, symptoms prior to taking JFG, and any improvement in symptoms or adverse effects and satisfaction.

Cell Culture and Virus

BHK-21 cells and Calu-3 cells were cultured in Dulbecco's Modified Eagle Medium (DMEM, Gibco) supplemented with

10% Fetal Bovine Serum (FBS) and 1 × penicillin/streptomycin solution. Vero E6 cells were maintained in High glucose DMEM (GeneDireX) supplemented with 10% FBS. Normal human lung WI-38 VA-13 subline 2RA and MRC-5 cells were purchased from the Bioresource Collection and Research Center (BCRC, Hsinchu, Taiwan). Cells were cultured in Minimum essential medium (Eagle, Gibco) supplemented with 10% FBS, 2 mM L-glutamine, 1.5 g/L sodium bicarbonate, 0.1 mM non-essential amino acids, and 1.0 mM sodium pyruvate at 37°C under a mixture of 95% air and 5% CO_2. The SARS-CoV-2 strain 3586 (TSGH_15 GISAID accession number EPI_ISL_436100) was isolated at the Institute of Preventive Medicine, National Defense Medical Center and amplified in Vero E6 cells. The viral titer was determined using a plaque assay. SARS-CoV-2 was handled in a BSL-3 laboratory.

The Cell-Cell Fusion Assay

Calu-3, as target cells, were seeded in a 12-well plate (1×10^6 per well) and formed a single-layer of cell films for 48 h. BHK-21 cells were seeded in a 6-well plate (4×10^5 per well) and transfected with both enhanced green fluorescent protein (GFP) and Spike plasmids at a ratio of 1:5 for 24 h. GFP/Spike-coexpressing BHK cells were harvested using Cell Dissociation Buffer (Gibco) and resuspended in serum free DMEM. For Spike-mediated cell–cell fusion assays, GFP/Spike-coexpressing BHK-21 cells, as donor cells, were added to Calu-3 cells, and incubated at 4°C for 45 min to allow cell-cell binding. They were then washed with PBS and the growth medium was replaced and the cells were then incubated at 37°C for 4 h to allow cell-cell fusion. After incubation, five fields were randomly selected in each well to record the GFP-expressing cell images using an inverted fluorescence microscope (Olympus IX70). The extension area of the GFP-expressing cell images was quantified to determine the degree of cell-cell fusion using ImageJ software. The fold change in the GFP area in control terms from 0 to 4 h was delimited to 100% fusion efficiency, and the fold changes in the GFP area for various JGF treatments were normalized to the control.

$$\textit{The normalized percantage}\ (\%) = \frac{\textit{the fold change of GFP area}}{\textit{the fold change of GFP area in control}} \times 100$$

SARS-CoV-2 Plaque Formation Assay

Vero E6 cells (4×10^5/well) were seeded into 12-well plates. Before infection with SARS-CoV-2, train 3586, cells were treated with JGF (50, 100 and 200 μg/ml) for 3 h at 37°C and 5% CO_2 and were shaken occasionally. Following the JGF treatment, 50 μl SARS-CoV-2 ($2*10^3$ PFU/well) samples were added and adsorbed for 1 h at 37°C. After the absorption period, the medium was removed and 4 mL of 1.55% (v/v) methylcellulose in DMEM (2% FBS added) with JGF was added for 3 days at a temperature of 37°C in 5% CO_2. Cells were then fixed with 10% formaldehyde for 1 h at room temperature, and 0.5% (w/v) crystal violet was added into the fixed cells for at least 30 min at room temperature. SARS-CoV-2 virus (nCoV-19/Taiwan/4/2020) was obtained from Taiwan Centers of Disease Control (CDC). All experiments involving live SARS-CoV-2 were performed in CDC-approved BSL-3 and BSL-4 facilities at the Institute of Preventive Medicine in the National Defense Medical Center in accordance with requirements of the institutional biosafety committee.

Cell Viability Assay

Cells (5×10^4 cells/well) were seeded into 12-well culture plate dishes and incubated overnight. Cells were then treated with JGF (0–800 μg/ml) for 48 and 72 h. After incubation, each well was rinsed with PBS and cells that attached to the bottom of the well were fixed and stained with 1% crystal violet solution or MTT solution as described previously (Lin et al., 2017).

LDH Assay to Detect Cytotoxicity for Jing Guan Fang in BHK-21 and Calu-3 Cells

The cytotoxicity of JGF on BHK-21 and Calu-3 cells was determined using Cytotoxicity Detection Kit^{PLUS} (LDH; Merck). BHK-21 and Calu-3 cells were seeded in 96-well plates (1×10^4 cells/well). After incubation overnight at 37°C, the cells were replaced into growth medium containing various concentrations of JGF (20, 40, and 80 μg/ml), and incubated at 37°C for 24 h. The untreated cells were as the low control so they spontaneously release LDH in normal condition. Cells that were treated with lysis buffer (5 μl) for 15 min were the high control and were used to determine the maximum release of LDH in the cells. To determine the LDH activity, 100 μl of Reaction mixture (freshly prepared by mixing Catalyst and Dye solution) was added to each well and incubated for 15 min at room temperature. Multimode microplate readers (TECAN SPARK) were used to measure the absorbance of the samples at a wavelength of 490 nm. To determine the percentage of cytotoxicity, the average absorbance values for three samples and controls were calculated. These values were substituted into the equation:

$$\textit{Cytotoxicity}\ (\%) = \frac{\textit{exp. value} - \textit{low control}}{\textit{high control} - \textit{low control}} \times 100$$

Sample Preparation for Western Blotting Analysis

Cells were rinsed with cold PBS containing 1% Na_3VO_4 and harvested by scraping the cells into proteinase inhibitors and a phosphatase inhibitor cocktail (Sigma Chemical Co.) containing lysis buffer (10 mM HEPES (pH 7.9), 10 mM KCl, 0.1 mM EDTA, 0.1 mM EGTA). Whole cell lysates were centrifuged for 13,000 xg for 10 min at 4°C. The supernatant was collected as the cell extracts. The concentration of the protein from cell lysate was determined by using a Bradford assay (Bio-Rad, Hercules, CA). The cell lysate samples (30 μg) were then subjected to western blot analysis. The expression of β-actin was used as an internal control. The procedure for the Western blotting assay used the methods and procedures that were described previously (Lin et al., 2017). Antibodies against

ACE2, TMPRSS2 and actin were purchased from GeneTex (Hsinchu, Taiwan).

RNA Extraction and Quantitative Polymerase Chain Reaction

Total RNA was isolated from cells using TRIzol reagent (Invitrogen, Carlsbad, CA, United States). The cDNA synthesis used a HiScript II 1st Strand cDNA Synthesis Kit (Vazyme, JS, China). The q-PCR used a Fast SYBR Green Master Mix (Thermo Fisher Scientific) in triplicate and an Applied Biosystems Model 7000 instrument (Thermo Fisher Scientific). The data was quantitated using $2^{-\Delta Ct}$ (ΔCt = CtTarget gene-CtGAPDH; Ct: cycle number when the fluorescent value of the sample is equal to the threshold value). Primer sequences for in this study include hTMPRSS2-F: 5′-CCTCTAACTGGTGTGATGGCGT; hTMPRSS2-R: 5′-TGCCAGGACTTCCTCTGAGATG-3'. hGAPDH-F: 5′-TGGTATCGTGGAAGGACTCA-3'; and hGAPDH-R: 5′-AGTGGGTGTCGCTGTTGAAG-3'.

Animal Model

Six-to eight-month-old male C57BL/6 mice were purchased from the National Laboratory Animal Center (Taipei, Taiwan). To determine the effect of JGF on the expression of ACE2 and TMPRSS2 in various organs of mice, the mice were randomly sorted into experimental groups (n = 3). For Experiment 1, mice were fed with JGF (8 mg/mouse/day) twice. For Experiment 2, JGF was filled in a closed space using a low-temperature steam method (30–32°) and inhaled by mice. After exposure to JGF for 30 min, mice were moved to a normal environment for 10 minutes and then underwent another 30 min of exposure. Mice were sacrificed after receiving JGF for 3 h. All procedures were approved by and performed in accordance with the guidelines and regulations of the Institutional Animal Care and Use Committee (IACUC) of National Yang Ming Chiao Tung University (IACUC Approval NO: 1100511).

Statistical Analysis

Statistical differences between the experimental groups were determined using a t-test in GraphPad Prism8. A vale of $p < 0.05$ indicates a statistically significant result. The experiments were conducted three times or as indicated, and all data is expressed as mean ± SD.

RESULTS

Clinical Observation of Subjects Who Are Treated Using Jing Guan Fang

JGF was initially created in January 2020 for frontline medical staff and travelers who had returned from mainland China, Hong Kong, Macau and Singapore. This formula was then made available to the public in five public hospitals as an additional preventative measure. The clinical observation, involved 396 subjects who participated in the questionnaire. The average age of the participants was 45.9 years old, with a standard deviation of 14.1 years. The ratio of males to females is 35.1% (male) and 64.9% (female). **Table 1** summarizes the demographic and clinical characteristics for the 396 subjects who participated in the questionnaire. Sore throat was the most reported Covid-19 like symptom, with 34 subjects displaying the symptom. Cough and headache are the second and third most commonly reported Covid-19 like symptoms and a loss of taste and smell (dysgeusia) is the least commonly reported Covid-19 like symptoms. NonCovid-19 like symptoms that were reported include fatigue (n = 128), and tension (n = 102). Seven days after taking JGF, 91.2% of subjects who experienced a sore throat reported that the symptoms had improved. Improvements in non-Covid-19 like symptoms, such as fatigue (81.3%) and tension (68.6%), were also reported.

Jing Guan Fang Prevents Membrane Fusion and the Formation of Syncytium

S protein present in a cellular membrane can trigger the formation of receptor-dependent syncytia (Buchrieser et al., 2020; Cheng et al., 2020; Xia et al., 2020)so this study developed a fluorescence-based cell-cell fusion assay for which BHK cells that express both SARS-CoV-2 S protein and enhanced green fluorescent protein (GFP) act as the effectors and Calu-3 cells that express endogenous hACE2 act as targeting cells. For this assay, the binding of BHK-21 cells with Calu-3 cells indicates that SARS-CoV-2 S protein binds with the ACE2 receptor and the formation of syncytium is the results of membrane fusion. To confirm the cytotoxicity of JGF to BHK-21 and Calu-3 cells, cells were treated with various concentrations from 20 to 80 μg/ml of JGF. The treatment of Triton-100 was used as a positive control. Compared to the treatment of the control group represented the non-treatment group that served as a negative control, LDH assay depicted that JGF caused no significant amount of cell death, suggesting JGF is not cytotoxic to either BHK cells or Calu-3 cells (**Figure 1A**). The effect of JGF on the expression of the ACE-2 in Calu-3 cells was determined by Western blot assay. The results depicted the level of the ACE-2 was significantly decreased approximately 70% in the presence of 40 μg/ml of JGF treatment (**Figure 1B**). Given that the occurrence of cell-cell fusion that can be visualized as syncytium formation in the cell-cell fusion experiment, the results of confocal microscopy imaging revealed that, only in the presence of the SARS-CoV-2 S protein, DiI-labeled cellular compartments of Calu-3 cells were co-localized with GFP signals within large syncytium, suggesting that fusion of GFP-expressing BHK-21 cells with DiI-labeled Calu-3 cells (**Supplementary Figure S2**). In the cell-cell fusion assay, the fluorescence microscopy imaging revealed that the treatment of JGF can only inhibit the formation of syncytium but not the binding of BHK-21 cells with Calu-3 cells (**Figures 1C,D**). The treatment of the camostat, a pharmacological inhibitor of TMPRSS2 protease, resulting in the inhibition of syncytium formation was used as a positive control group. Moreover, the inhibition was in a dose-dependent manner, suggesting that JGF can specifically interrupt SARS-CoV-2 S-mediated membrane fusion (**Figures 1C,D**). These results suggest that JGF may potentially be used as an anti-SARS-CoV-2 agent because it suppresses membrane fusion, which is a key element of viral infection.

TABLE 1 | Demographic and clinical characteristics of the subjects with Covid-19 like symptoms.

Basic data		**All (n = 396)**
Age, years (SD)		45.9 (14.1)
Male %		35.1
Female %		64.9
Covid-19 like symptoms	Subjects displaying symptoms, persons (%)	Rate of improvement, persons/all persons (%)
Sore throat	34 (8.6)	31/34 (91.2)
Headache	25 (6.3)	19/25 (76.0)
Cough	29 (7.3)	23/29 (79.3)
Fever	13 (3.3)	11/13 (84.6)
Rhinorrhea	23 (5.8)	18/23 (78.2)
Diarrhea	24 (6.1)	18/24 (75.0)
New loss of taste or Smell	3 (0.8)	1/3 (33.3)
Associated main symptoms	Subjects displaying symptoms, persons (%)	Improving rate, persons/all persons (%)
Fatigue	128 (32.3)	104/128 (81.3)
Tension and pressure	102 (25.8)	70/102 (68.6)

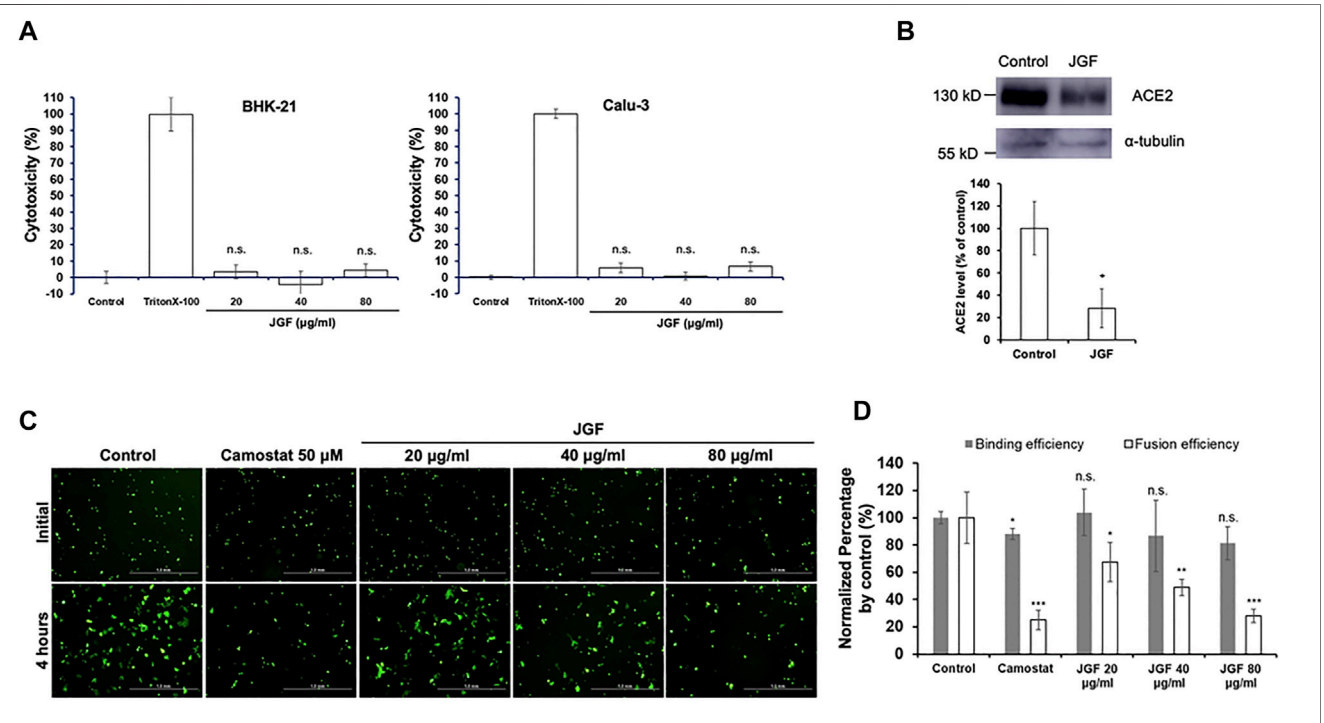

FIGURE 1 | The inhibitory activity of JGF on the interactions between SARS-CoV-2 spike (S) protein and ACE2 receptor. **(A)** Validation of the cytotoxicity of JGF. BHK-21 and Calu-3 cells were treated with indicated amounts of JGF and cell viability was examined by LDH assay. The control group represented the non-treatment group, serving as a negative control. The treatment with Triton-100 was used as a positive control. The data were presented as the mean ± SD; error bars indicated SD. n. s indicated non-significant, compared to the control group. **(B)** The expression of ACE2 in Calu-3 cells were treated with 40 μg/ml of JGF was analyzed by Western blot assay (upper panel). The level of ACE2 expression was quantified after normalization with α-tubulin. The quantification analysis from three independent experiments was shown in bottom panel. * represents $p < 0.05$. **(C)** The cell-cell fusion of SARS-CoV-2 S protein-expressing BHK cells and ACE2-expressing Calu-3 cells was visualized in the presence of indicated amounts of JGF. **(D)** The formation of syncytium was quantified for various concentrations of JGF. Compared with the control, syncytium formation was significantly inhibited after 20–80 μg/ml JGF treatments. * represents $p < 0.05$.

The Cytotoxic Effect of Jing Guan Fang on Human Fibroblast WI-38 and MRC-5 Cells

To determine the potential mechanisms by which JGF prevents SARS-CoV-2 infection, a series of *in vitro* experiments involved human lung cells. Two human lung WI-38 and MRC-5 cells were used to determine the cytotoxic effect of JGF. A crystal violet assay was used to determine the concentration at which JGF inhibits activity in human lung cells. As shown in **Figures 2A,B**, we found that JGF did not exhibit the cytotoxicity to either WI-38 or MRC-5 cells.

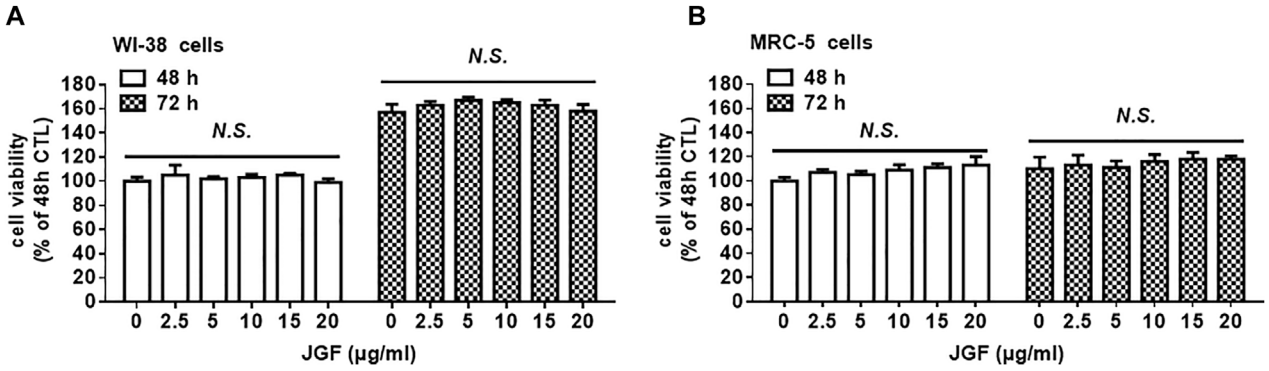

FIGURE 2 | The effect of JGF on the cell viability of lung fibroblast WI-38 and MR/C-5 cells. WI-38 **(A)** and MRC-5 **(B)** cells were treated with various low concentrations of JGF (0–20 μg/ml) for 48 and 72 h. Each group of JGF-treated samples was normalized against an untreated control. Cell viability was determined using a crystal violet assay. Data were representative of three separated experiments and were presented as the mean ± SD; error bars indicated SDs.

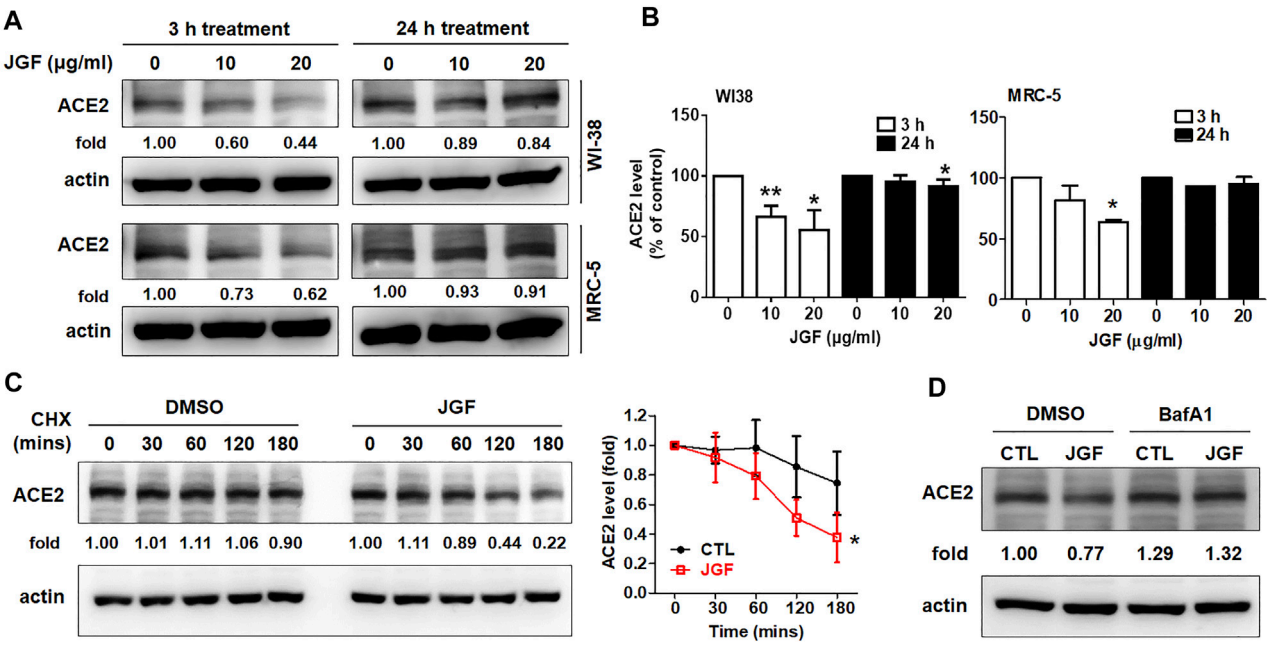

FIGURE 3 | JGF induces lysosome dependent degradation of ACE2. **(A)** WI-38 and MRC-5 cells were treated with three dosages of JGF (0–20 μg/ml) for 3 and 24 h. Western blotting was subsequently performed with whole cell lysates to detect expression of ACE2. Actin was used as the internal control. **(B)** Quantification of the intensities of the bands of ACE2 was representative of three separate determinations using ImageJ (National Institute of Mental Health, Bethesda, MD, United States). The data were presented as the mean ± SD; error bars indicated SD. Significant differences were shown (*$p < 0.05$ compared to the control group). **(C)** Time course for ACE2 degradation after the addition of cycloheximide (CHX; 100 μg/ml) in the presence or absence of JGF (10 μg/ml) for 0–180 min in WI-38 cells as analyzed by Western blotting. Right panel: The levels of ACE2 in the three-independent experiments were quantified by ImageJ and the results were presented as the mean ± SD; error bars indicate SDs. Significant differences were shown (*$p < 0.05$ compared to the control DMSO group). **(D)** WI-38 cells were pretreated with DMSO (vehicle control) or BafA1 (10 μM) for 30 min, followed by incubation with JGF (10 μg/ml) for 2 h.

Jing Guan Fang Induced Lysosome-dependent Degradation of Angiotensin-Converting Enzyme-2

We found that JGF effectively interrupted the interaction between the spike protein with the ACE2 receptor and suppressed membrane fusion, which is an essential element of viral infection (**Figure 1**). We further examined mechanisms by which JGF inhibited infection of normal human lung cells with SARS-CoV-2. Increasing evidence shows that SARS-CoV-2 infection is prevented by targeting ACE2 in lung cells to block the SARS-CoV-2 spike receptor from binding with ACE2 (Hoffmann et al., 2020). Therefore, we investigated whether JGF affected the protein levels of ACE2 in WI-38 and MRC5 cells. As shown in **Figures 3A,B**, we found that brief treatment with JGF dramatically reduced the expressions of

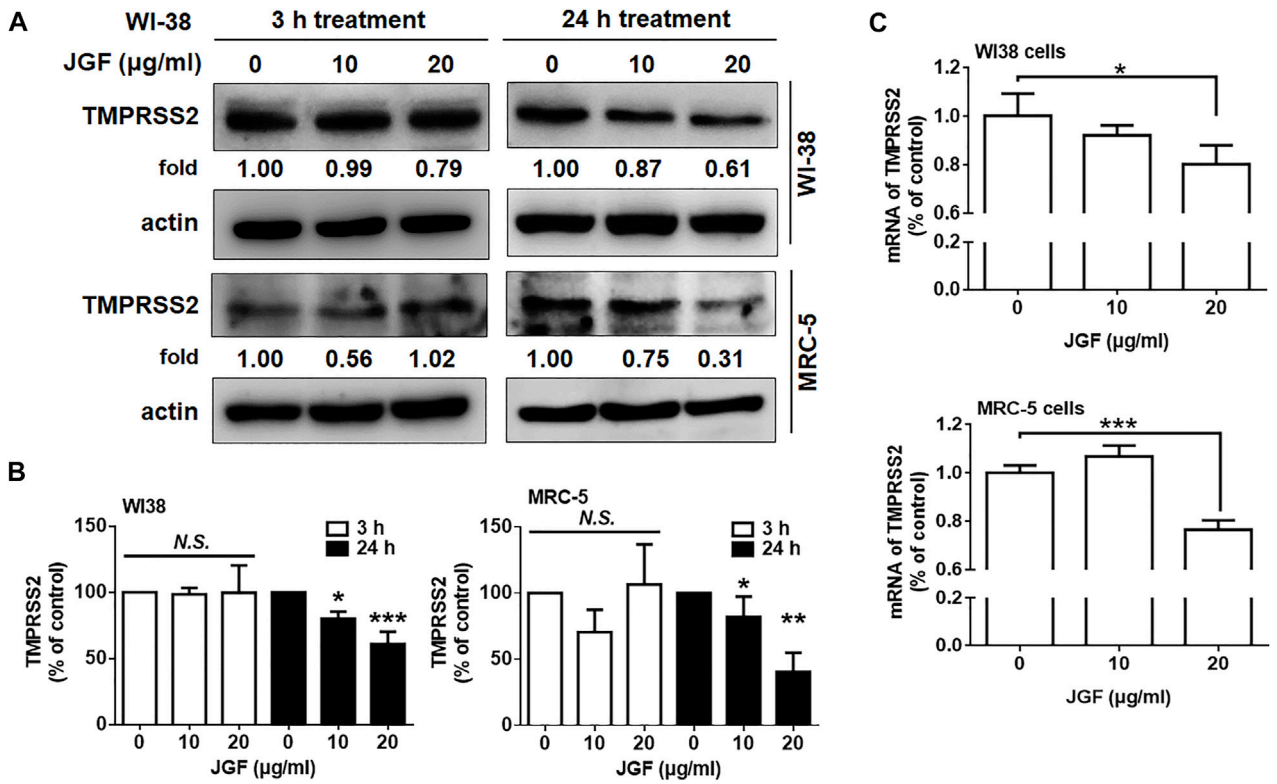

FIGURE 4 | JGF reduces TMPRSS2 levels in WI-38 cells. **(A)** WI-38 cells were treated with JGF (0–20 μg/ml) for 3 and 24 h. Western blotting was subsequently performed with whole cell lysates to detect the expression of TMPRSS2. Actin was used as the internal control. **(B)** Quantification of the intensities of the bands of TMPRSS2 was representative of three separated determinations by ImageJ. **(C)** WI-38 cells were treated with JGF (0, 10 and 20 μg/ml) for 24 h. The mRNA levels of TMPRSS2 were determined by qRT-PCR. The data was presented as the mean ± SD; error bars indicated SD. Significant differences were shown (*$p < 0.05$ compared to the control group).

ACE2 by about 40–50%, but the ACE2 level increased during JGF treatment for a longer period. These results suggested that JGF temporarily downregulates ACE2 level to reduce the infection with SARS-CoV-2. To further explore the mechanism by which JGF downregulated ACE2, we examined the Adam17 activity because ACE2 can be cleaved into extracellular soluble ACE2 and intracellular ACE2 by Adam17 (Li et al., 2021). However, JGF did not increase the activity of Adam17 or the levels of extracellular soluble ACE2 (**Supplementary Figure S3**).

These results showed that JGF significantly suppressed the total protein levels of ACE2 within a short period of time. Therefore, we further examined the mechanism by which JGF downregulated ACE2 levels. Previously, ACE2 is regulated by Ang-II type 1 receptor and E3 ligase NEDD4 to respectively induce lysosome and proteasome dependent degradation of ACE2 (Deshotels et al., 2014; Ogunlade et al., 2019). We thus examined whether JGF-induced ACE2 degradation is dependent on proteasome or lysosomal systems. Initially, we analysed the half-life of ACE2 in WI-38 cells following treatment with cycloheximide (CHX). We found that when WI-38 cells were co-treated with JGF and CHX, the level of ACE2 was dramatically downregulated in a time-dependent manner (**Figure 3C**), suggesting that JGF could induce degradation of ACE2. Next, using the lysosome inhibitor, BafA1, we found that BafA1 recovered the ACE2 level in WI38 cells after JGF treatment (**Figure 3D** and **Supplementary Figure S4**). However, MG132, which is a proteasome inhibitor, failed to rescue JGF-induced JGF degradation (**Supplementary Figure S5**). These results indicated that JGF could be used to prevent SARS-CoV-2 infection by inducing ACE2 degradation.

Jing Guan Fang Downregulates Transmembrane Serine Protease 2 Levels

It is worthy to note that TMPRSS2 is another important membrane protein for SARS-CoV-2 infection (Dong et al., 2020; Hoffmann et al., 2020). We therefore examined whether JGF affected the expression of TMPRSS2 in WI-38 cells. As shown in **Figures 4A,B**, we found that JGF did not affect the expression of TMPRSS2 within a short period of time. Interestingly, long-term treatment with JGF effectively downregulated the expression of TMPRSS2 by 40–70% (**Figure 4B**). In parallel, JGF significantly reduced mRNA of TMPRSS2 for the 24 h treatment (**Figure 4C**). These results suggested that JGF may regulate the signaling transductions which controlled the synthesis of TMPRSS2.

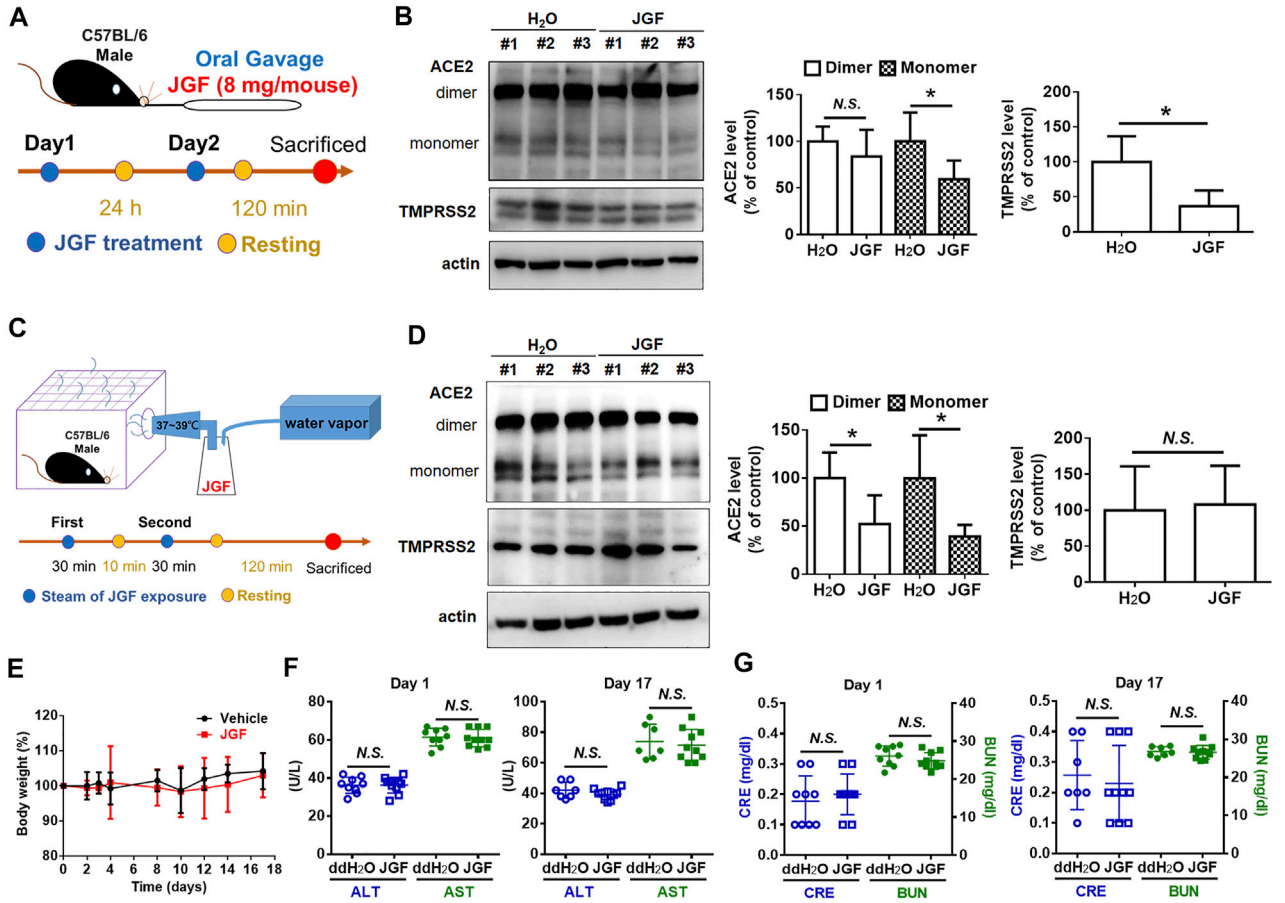

FIGURE 5 | JGF reduces ACE2 and TMPRSS2 on lung tissues of mouse model. **(A)** Scheme for mouse receiving JGF via oral gavage. **(B)** ACE2 and TMPRSS2 levels in lung tissues of mice receiving JGF via oral gavage. **(C)** Scheme for mouse receiving JGF via steam spray method. **(D)** ACE2 and TMPRSS2 levels in lung tissue of mice receiving JGF via steam spray. **(E)** The body weight changes (%) for mice receiving JGF via oral gavage every other day. **(F,G)** The AST and ALT (hepatic function; **F**) as well as BUN and Creatinine (renal function; **G**) of mice sera were analyzed on Day 1 and Day 17.

Jing Guan Fang Downregulates the Expressions of Angiotensin-Converting Enzyme-2 and Transmembrane Serine Protease 2 in Lung Tissue of Mice

It is well known that ACE2 and TMPRSS2 are expressed in human organs (Hamming et al., 2004; Hikmet et al., 2020). Specifically, ACE2 is abundantly present in the epithelia of the lung and small intestine (Hamming et al., 2004). The mRNA expressions for both ACE2 and TMPRSS2 were detected in the heart, digestive tract, kidney, and brain (Dong et al., 2020). We therefore examined the levels of ACE2 and TMPRSS2 in lung, brain, colon, and kidney tissues of mice. As shown in **Supplementary Figure S6**, we found that there were many isoforms of ACE2 and TMPRSS2 in these tissues. To determine whether JGF affected the levels of ACE2 and TMPRSS2 in lung tissue of mice, we conducted a series of *in vivo* experiments. Initially, we investigated the effect of orally ingested JGF on mice *in vivo*. Continuous feeding with JGF for 2 days effectively reduced protein levels of ACE2 and TMPRSS2 in the lungs of mice (**Figures 5A,B**). Specifically, we found that in the mice receiving the administration of JGF, the monomer of ACE levels was significantly reduced by 45%; however, the dimer form of ACE2 was not reduced in lung tissues. Surprisingly, JGF dramatically reduced protein levels of TMPRSS2 by 50% (**Figure 5B**). Moreover, in the view of traditional Chinese medicine, drugs could be absorbed through the nasal cavity by steam method, which can make the herbal medicine quickly enter the nasal cavity and lungs to address cold symptoms. We thus used the steam method to induce the mice to inhale JGF (**Figure 5C**). As shown in **Figure 5D**, we found that ACE2 was dramatically reduced by more than 50% after the mice inhale JGF; however, TMPRSS2 levels were unchanged after the short-term exposure to JGF. Alternatively, we found JGF did not affect body weight of mice (**Figure 5E**). Furthermore, to examine the degree of liver and kidney injury in mice that were fed with JGF, the AST/ALT and BUN/creatinine levels were analyzed in blood samples at the end of JGF treatment. Our results indicated neither evidence of JGF affecting liver functions nor kidney toxicity in the mouse model (**Figures 5F,G**).

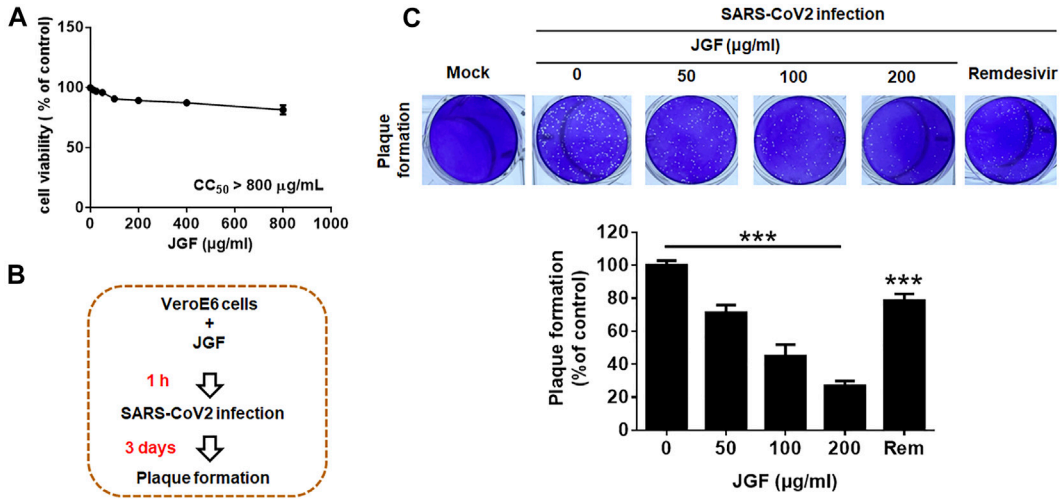

FIGURE 6 | JGF inhibits plaque formation for SARS-CoV-2 in Vero E6 cells. **(A)** Vero E6 cells were treated with various concentrations of JGF (0–800 μg/ml) for 72 h. Each group of JGF-treated samples was normalized against an untreated control. Cell viability was determined using the MTT assay. **(B)** Vero E6 cells were pre-treated with JGF (0–200 μg/ml) for 3 h and then infected with SARS-CoV-2 for 3 days **(C)** The plaque was stained with crystal violet. Data were representative of three separate experiments and were presented as the mean ± SD; error bars indicated SDs.

These results suggest that JGF may reduce infection with SARS-CoV-2 without side effect.

Jing Guan Fang inhibits the formation of plaque formation for The Severe Acute Respiratory Syndrome CoronaVirus 2 on Vero E6 cells.

The above showed that JGF can prevent viruses from infecting cells by reducing ACE2 and TMPRSS2. Therefore, we further investigated whether JGF could inhibit the viral infection and proliferation. The Vero E6 cells were chosen for investigating the SARS-CoV-2 infection. Initially, we examined the effects of JGF on cell viability of Vero E6 cells. As shown in **Figure 6A**, we found JGF did not exhibit a cytotoxic effect on Vero E6 cells even at high concentration of JGF. A cytotoxic concentration of 50 (CC_{50}) of JGF was more than 800 μg/ml. Next, virus plaque formation assay was conducted to examine the efficacy of JGF in preventing SARS-CoV-2 infection. Vero E6 cells were pretreated with JGF before SARS-CoV-2 infection (**Figure 6B**). We found that JGF dramatically inhibited plaque formation in a concentration-dependent manner compared to remdersivir (2 μM; **Figure 6C**). Specifically, JGF at 200 μg/ml dramatically reduced plaque formation of SARS-CoV-2 by 70%. Taken together, these results suggest that JGF may reduce SARS-CoV-2 infection and proliferation.

DISCUSSION

The current COVID-19 epidemic is a worldwide problem so if the viral infection can be effectively prevented, the disease rate will be reduced. This study mainly provides a scientific evidence-based view of the mechanism by which JGF reduces the infection and proliferation of SARS-CoV-2. Moreover, we demonstrated that JGF did not inhibit cell viability for normal lung cells *in vitro* and did not induce a toxic effect on liver and kidney of mice *in vivo*. The clinical observations demonstrated that JGF treatment improved the COVID-19 like symptoms. This study combines basic research and clinical observation to explore the effects of and the mechanism by which JGF prevents SARS-CoV-2 infection. Future clinical trials of the efficacy of JGF in attenuating viral infection are further evaluated.

According to the epidemiological theory of Traditional Chinese Medicine and clinical experience of SARS (Hsu et al., 2008; Lin, 2020; Hsu et al., 2006a; Hsu et al., 2006b), this study uses five common herbal medicines to formulate JGF using a specific ratio. In this study, we focused on the effects and the mechanism of the JGF formula but not individual herbal medicines because we believed that using all five herbs together may provide multifactorial effects that a single compound or herb may not be able to provide. Increasing evidence shows that these five herbal medicines exhibit anti-viral effects. Phillyrin (KD-1), which is isolated from *Forsythia suspense*, inhibits SARS-CoV-2 replication and inflammatory factors that are caused by viral infection (Ma et al., 2020). Baicalein, which is purified from *Scutellaria baicalensis* Georgi, inhibits SARS-CoV-2 replication (Huang et al., 2020). The extract from *Bupleurum chinense* DC exhibits anti-SARS-CoV-2 effects (Wu et al., 2020). Extracts from *Magnolia officinalis* and *Agastache rugose* have an anti-inflammatory effect (Seo et al., 2019; Ren et al., 2021). However, no studies show whether these herbs prevent SARS-CoV-2 infection. To examine the effect of JGF on SARS-CoV-2 infection, we initially developed a fluorescence-based cell-cell fusion assay in which BHK cells that express SARS-CoV-2-spike protein and EFGP act as the effectors, and Calu-3 cells expressing endogenous hACE2 act as targeting cells because SARS-CoV-2 cell infection depends on ACE2 and TMPRSS2 (Hoffmann et al., 2020). The results show that pretreatment with JGF of Calu-3 cells with JGF dramatically inhibits the formation of syncytium. In addition, pretreatment with JGF effectively inhibited

the formation of virus plaque for SARS-CoV-2 on Vero E6 cells. Therefore, we further examined whether JGF affected the interaction between SARS-CoV-2-spike protein and hACE2. The results for the ACE2/Spike protein interaction assay kit showed that JGF slightly interrupted the affinity of the SARS-CoV-2 spike for human ACE2 receptor in a dose-dependent manner. JGF inhibited approximately 20% of the interaction between spike and ACE2 at a concentration of 200 μg/ml (data not shown). These results suggest that JGF has a pivotal role in preventing the infection with SARS-CoV-2. Targeting on the interaction between SARS-CoV-2-spike protein and hACE2 may not reflect the main effect of JGF.

To examine the mechanism by which JGF prevented infection with SARS-CoV-2, we focused on the effects of the JGF-regulated expressions of ACE2 and TMPRSS2. Using the normal lung WI-38 2RA and MRC-5 cells, we found that JGF effectively reduced ACE2 and TMPRSS2 levels in the short and long-time treatment, respectively. Previous studies showed that ACE2 plays a pivotal role in SARS-CoV-2 cell entry (Hoffmann et al., 2020; Jia et al., 2021), so we focused on how JGF reduced ACE2 levels in normal lung cells. Soluble ACE2 (sACE2) from ACE2 cleaved by ADAM17 is used as a decoy receptor to trap spikes of virus to prevent cellular engagement for COVID-19 therapy (Monteil et al., 2020; Jia et al., 2009). However, we found that JGF did not significantly induce expression of sACE2 and activate ADAM17 **Supplementary Figure S3**. In contrast, JGF temporarily caused ACE2 to follow a lysosome-dependent degradation pathway, but long-term treatment allows the ACE2 protein would recover to its normal level. ACE2 is a multifunctional protein that controls physiological and pathological regulation (Baratchian et al., 2021; Li et al., 2020; Zipeto et al., 2020), so these results indicated that JGF does not cause long-term reduction in ACE2, which may prevent side effects that were caused by the long-term inhibition of ACE2 expression. However, TMPRSS2-mediated ACE2 cytoplasmic tail cleavage is correlated to enhanced viral uptake (Heurich et al., 2014). Interestingly, we found that long-term treatment with JGF could regulate mRNA level of TMPRSS2, leading to reduction of TMPRSS2 protein levels. The effect of JGF on the androgen receptor (AR)-mediated TMPRSS2 (Li et al., 2021) needs to be investigated in the future. Together, according to the concept of a cocktail therapy, we believed that JGF has at least two effects: the first is to temporarily induce ACE2 degradation, this study shows that JGF temporarily induces ACE2 degradation and reduces transcription of TMPRSS2. Currently, no studies show that traditional Chinese medicine reduces the expression of ACE2 and TMPRSS2 in host cells. In the future, it is needed to further identify the potential molecules of these herbs that regulate the expression of ACE2 and TMPRSS2 in host cells.

CONCLUSION

This study used TCM theory to formulate an herbal medicine formula, JGF, as an adjuvant preventive strategy against SARS-CoV-2 infection in addition to the use of vaccines. We provided the evidence and demonstrated that JGF effectively blocked the formation of syncytium and inhibited the formation of SARS-CoV-2 plaque. In addition, we identified the potential mechanisms of JGF-reduced SARS-CoV-2 invasion by induction of lysosome-dependent ACE2 degradation and the inhibition of TMPRSS2 expression. These results suggest that JGF may be a promising formula to alleviate SARS-CoV-2 infection. In Taiwan, a research group has recently developed a traditional Chinese medicine formula called NRICM101 which is mainly used for hospitalized patients with COVID-19. This medicine reduces the number of viruses and suppresses immune storms (Tsai et al., 2021). In this study, we show that JGF reduces viral infections for frontline staff who have intensive contact with infected patients. Results from the study suggest that JGF can be an useful preventative measure for frontline medical staff or people who have had high-risk exposure to COVID-19 cases.

DATA AVAILABILITY STATEMENT

The raw data supporting the conclusions of this article will be made available by the authors, without undue reservation.

ETHICS STATEMENT

The studies involving human participants were reviewed and approved by Taipei City Hospital Institutional Review Board (TCHIRB-10904015) with Clinical Trial gov. Trial registration: NCT04388644, Registered 06 April 2020 - Retrospectively registered, https://clinicaltrials.gov/ct2/show/NCT04388644. The patients/participants provided their written informed consent to participate in this study. The animal study was reviewed and approved by Institutional Animal Care and Use Committee (IACUC) of National Yang Ming Chiao Tung University (IACUC Approval NO: 1100511).

AUTHOR CONTRIBUTIONS

Y-HP and T-YL conceived and designed the study. HY, L-WC, Z-HL, Y-C-H performed the experiment. L-CL performed the finger print of JGF. C-HH designed the formula of JGF. Y-HP and T-YL analyzed the data and wrote the paper. S-LF and T-YL revised the paper. All authors read and approved the final manuscript.

FUNDING

The present work was supported by grants from the Ministry of Science and Technology, Taiwan (MOST 109-2327-B-010-005- to S-LF; MOST 109-2636-B-010-009—and MOST 110-2636-B-A49A-501 to T-YL; MOST 109-2320-B-010-034-MY3 and MOST 109-2327-B-400-004 to Y-HP) and from the National

Yang-Ming University–Far Eastern Memorial Hospital Joint Research Program (110DN04 to Y-HP).

ACKNOWLEDGMENTS

We thank Y.-F. Chin, P.-C. Liu and T.-Y. Chang (NDMC, Taiwan) for conducting the experiment of viral plaque formation. We wish to thank Anthony J. Venuti (NYCU, Taiwan) for manuscript edit. We are thankful for T.-C. Hwang and C. Huang (NYCU, Taiwan) for kindly providing reagents.

SUPPLEMENTARY MATERIAL

The Supplementary Material for this article can be found online at: https://www.frontiersin.org/articles/10.3389/fphar.2022.744439/full#supplementary-material

REFERENCES

Baratchian, M., McManus, J. M., Berk, M., Nakamura, F., Mukhopadhyay, S., Xu, W., et al. (2021). Androgen Regulation of Pulmonary AR, TMPRSS2 and ACE2 With Implications for Sex-Discordant COVID-19 Outcomes. *Sci Rep.* 11, 11130. doi:10.1038/s41598-021-90491-1

Buchrieser, J., Dufloo, J., Hubert, M., Monel, B., Planas, D., Rajah, M. M., et al. (2020). Syncytia Formation by SARS-CoV-2-Infected Cells. *EMBO J.* 39, e106267. doi:10.15252/embj.2020106267

Chen, Y., Liu, Q., and Guo, D. (2020). Emerging Coronaviruses: Genome Structure, Replication, and Pathogenesis. *J. Med. Virol.* 92, 2249–2423. doi:10.1002/jmv.26234

Cheng, P. W., Ng, L. T., Chiang, L. C., and Lin, C. C. (2006). Antiviral Effects of Saikosaponins on Human Coronavirus 229E *In Vitro*. *Clin. Exp. Pharmacol. Physiol.* 33, 612–616. doi:10.1111/j.1440-1681.2006.04415.x

Cheng, Y. W., Chao, T. L., Li, C. L., Chiu, M. F., Kao, H. C., Wang, S. H., et al. (2020). Furin Inhibitors Block SARS-CoV-2 Spike Protein Cleavage to Suppress Virus Production and Cytopathic Effects. *Cell Rep* 33, 108254. doi:10.1016/j.celrep.2020.108254

Collaborators, V. (2020). The Species Severe Acute Respiratory Syndrome-Related Coronavirus: Classifying 2019-nCoV and Naming it SARS-CoV-2. *Nat. Microbiol.* 5, 536–544. doi:10.1038/s41564-020-0695-z

Deng, Y. F., Aluko, R. E., Jin, Q., Zhang, Y., and Yuan, L. J. (2012). Inhibitory Activities of Baicalin against Renin and Angiotensin-Converting Enzyme. *Pharm. Biol.* 50, 401–406. doi:10.3109/13880209.2011.608076

Deshotels, M. R., Xia, H., Sriramula, S., Lazartigues, E., and Filipeanu, C. M. (2014). Angiotensin II Mediates Angiotensin Converting Enzyme Type 2 Internalization and Degradation through an Angiotensin II Type I Receptor-dependent Mechanism. *Hypertension* 64, 1368–1375. doi:10.1161/HYPERTENSIONAHA.114.03743

Dong, M., Zhang, J., Ma, X., Tan, J., Chen, L., Liu, S., et al. (2020). ACE2, TMPRSS2 Distribution and Extrapulmonary Organ Injury in Patients with COVID-19. *Biomed. Pharmacother.* 131, 110678. doi:10.1016/j.biopha.2020.110678

Ghildiyal, R., Prakash, V., Chaudhary, V. K., Gupta, V., and Gabrani, R. (2020). Phytochemicals as Antiviral Agents: Recent Updates. *Plant-derived Bioactives*, 279–295. doi:10.1007/978-981-15-1761-7_12

Guan, W. J., Ni, Z. Y., Hu, Y., Liang, W. H., Ou, C. Q., He, J. X., et al. (2020). Clinical Characteristics of Coronavirus Disease 2019 in China. *N. Engl. J. Med.* 382, 1708–1720. doi:10.1056/NEJMoa2002032

Hamming, I., Timens, W., Bulthuis, M. L., Lely, A. T., Navis, G., and van Goor, H. (2004). Tissue Distribution of ACE2 Protein, the Functional Receptor for SARS Coronavirus. A First Step in Understanding SARS Pathogenesis. *J. Pathol.* 203, 631–637. doi:10.1002/path.1570

Heurich, A., Hofmann-Winkler, H., Gierer, S., Liepold, T., Jahn, O., and Pöhlmann, S. (2014). TMPRSS2 and ADAM17 Cleave ACE2 Differentially and Only Proteolysis by TMPRSS2 Augments Entry Driven by the Severe Acute Respiratory Syndrome Coronavirus Spike Protein. *J. Virol.* 88, 1293–1307. doi:10.1128/JVI.02202-13

Hikmet, F., Méar, L., Edvinsson, Å., Micke, P., Uhlén, M., and Lindskog, C. (2020). The Protein Expression Profile of ACE2 in Human Tissues. *Mol. Syst. Biol.* 16, e9610. doi:10.15252/msb.20209610

Hoffmann, M., Kleine-Weber, H., Schroeder, S., Krüger, N., Herrler, T., Erichsen, S., et al. (2020). SARS-CoV-2 Cell Entry Depends on ACE2 and TMPRSS2 and Is Blocked by a Clinically Proven Protease Inhibitor. *Cell* 181, 271–e8. doi:10.1016/j.cell.2020.02.052

Hsu, C. H., Hwang, K. C., Chao, C. L., Chang, S. G., Ho, M. S., Lin, J. G., et al. (2008). An Evaluation of the Additive Effect of Natural Herbal Medicine on SARS or SARS-like Infectious Diseases in 2003: A Randomized, Double-Blind, and Controlled Pilot Study. *Evid. Based Complement. Alternat Med.* 5, 355–362. doi:10.1093/ecam/nem035

Hsu, C. H., Hwang, K. C., Chao, C. L., Chang, S. G., Ker, C. C., Chien, L. C., et al. (2006). The Lesson of Supplementary Treatment with Chinese Medicine on Severe Laboratory-Confirmed SARS Patients. *Am. J. Chin. Med.* 34, 927–935. doi:10.1142/S0192415X06004405

Hsu, C. H., HwangChangMei-Shang Ho, K. C., Chao, C. L., Chang, S. G., Ho, M. S., and Chou, P. (2006). Can Herbal Medicine Assist against Avian Flu? Learning from the Experience of Using Supplementary Treatment with Chinese Medicine on SARS or SARS-like Infectious Disease in 2003. *J. Altern. Complement. Med.* 12, 505–506. doi:10.1089/acm.2006.12.505

Huang, S., Liu, Y., Zhang, Y., Zhang, R., Zhu, C., Fan, L., et al. (2020). Baicalein Inhibits SARS-CoV-2/VSV Replication with Interfering Mitochondrial Oxidative Phosphorylation in a mPTP Dependent Manner. *Signal. Transduct Target. Ther.* 5, 266. doi:10.1038/s41392-020-00353-x

Jan, J. T., Cheng, T. R., Juang, Y. P., Ma, H. H., Wu, Y. T., Yang, W. B., et al. (2021). Identification of Existing Pharmaceuticals and Herbal Medicines as Inhibitors of SARS-CoV-2 Infection. *Proc. Natl. Acad. Sci. U S A.* 118. doi:10.1073/pnas.2021579118

Jia, H., Neptune, E., and Cui, H. (2021). Targeting ACE2 for COVID-19 Therapy: Opportunities and Challenges. *Am. J. Respir. Cel Mol Biol* 64, 416–425. doi:10.1165/rcmb.2020-0322PS

Jia, H. P., Look, D. C., Tan, P., Shi, L., Hickey, M., Gakhar, L., et al. (2009). Ectodomain Shedding of Angiotensin Converting Enzyme 2 in Human Airway Epithelia. *Am. J. Physiol. Lung Cel Mol Physiol* 297, L84–L96. doi:10.1152/ajplung.00071.2009

Lan, J., Ge, J., Yu, J., Shan, S., Zhou, H., Fan, S., et al. (2020). Structure of the SARS-CoV-2 Spike Receptor-Binding Domain Bound to the ACE2 Receptor. *Nature* 581, 215–220. doi:10.1038/s41586-020-2180-5

Law, A. H., Yang, C. L., Lau, A. S., and Chan, G. C. (2017). Antiviral Effect of Forsythoside A from Forsythia Suspensa (Thunb.) Vahl Fruit against Influenza A Virus through Reduction of Viral M1 Protein. *J. Ethnopharmacol* 209, 236–247. doi:10.1016/j.jep.2017.07.015

Li, F. (2016). Structure, Function, and Evolution of Coronavirus Spike Proteins. *Annu. Rev. Virol.* 3, 237–261. doi:10.1146/annurev-virology-110615-042301

Li, F., Han, M., Dai, P., Xu, W., He, J., Tao, X., et al. (2021). Distinct Mechanisms for TMPRSS2 Expression Explain Organ-specific Inhibition of SARS-CoV-2 Infection by Enzalutamide. *Nat. Commun.* 12, 866. doi:10.1038/s41467-021-21171-x

Li, Y., Zhou, W., Yang, L., and You, R. (2020). Physiological and Pathological Regulation of ACE2, the SARS-CoV-2 Receptor. *Pharmacol. Res.* 157, 104833. doi:10.1016/j.phrs.2020.104833

Lin, T. Y., Hsu, H. Y., Sun, W. H., Wu, T. H., and Tsao, S. M. (2017). Induction of Cbl-dependent Epidermal Growth Factor Receptor Degradation in Ling Zhi-8 Suppressed Lung Cancer. *Int. J. Cancer* 140, 2596–2607. doi:10.1002/ijc.30649

Ma, Q., Li, R., Pan, W., Huang, W., Liu, B., Xie, Y., et al. (2020). Phillyrin (KD-1) Exerts Anti-viral and Anti-inflammatory Activities against Novel Coronavirus (SARS-CoV-2) and Human Coronavirus 229E (HCoV-229E) by Suppressing the Nuclear Factor Kappa B (NF-Kb) Signaling Pathway. *Phytomedicine* 78, 153296. doi:10.1016/j.phymed.2020.153296

Monteil, V., Kwon, H., Prado, P., Hagelkrüys, A., Wimmer, R. A., Stahl, M., et al. (2020). Inhibition of SARS-CoV-2 Infections in Engineered Human Tissues Using Clinical-Grade Soluble Human ACE2. *Cell* 181, 905–e7. doi:10.1016/j.cell.2020.04.004

Ogunlade, B., Guidry, J. J., Lazartigues, E., and Filipeanu, C. (2019). ACE2 Internalization and Degradation Is Controlled by Ubiquitin Ligase NEDD4. *FASEB J.* 33, 719. doi:10.1096/fasebj.2019.33.1_supplement.719.14

Ren, W., Liang, P., Ma, Y., Sun, Q., Pu, Q., Dong, L., et al. (2021). Research Progress of Traditional Chinese Medicine against COVID-19. *Biomed. Pharmacother.* 137, 111310. doi:10.1016/j.biopha.2021.111310

Seo, Y. H., Kang, S. Y., Shin, J. S., Ryu, S. M., Lee, A. Y., Choi, G., et al. (2019). Chemical Constituents from the Aerial Parts of Agastache Rugosa and Their Inhibitory Activities on Prostaglandin E2 Production in Lipopolysaccharide-Treated RAW 264.7 Macrophages. *J. Nat. Prod.* 82, 3379–3385. doi:10.1021/acs.jnatprod.9b00697

Shang, J., Wan, Y., Luo, C., Ye, G., Geng, Q., Auerbach, A., et al. (2020). Cell Entry Mechanisms of SARS-CoV-2. *Proc. Natl. Acad. Sci. U S A.* 117, 11727–11734. doi:10.1073/pnas.2003138117

Tsai, K. C., Huang, Y. C., Liaw, C. C., Tsai, C. I., Chiou, C. T., Lin, C. J., et al. (2021). A Traditional Chinese Medicine Formula NRICM101 to Target COVID-19 through Multiple Pathways: A Bedside-To-Bench Study. *Biomed. Pharmacother.* 133, 111037. doi:10.1016/j.biopha.2020.111037

2020). Lin, w-y., War and Balance: Following Shi and Rebalancing Militant English-language Knowing Apparatuses. *Sociological Rev.* 68, 341–355.

Walls, A. C., Park, Y. J., Tortorici, M. A., Wall, A., McGuire, A. T., and Veesler, D. (2020). Structure, Function, and Antigenicity of the SARS-CoV-2 Spike Glycoprotein. *Cell* 181, 281–e6. doi:10.1016/j.cell.2020.02.058

Wang, Q., Zhang, Y., Wu, L., Niu, S., Song, C., Zhang, Z., et al. (2020). Structural and Functional Basis of SARS-CoV-2 Entry by Using Human ACE2. *Cell* 181, 894–e9. doi:10.1016/j.cell.2020.03.045

Who, Weekly. (2021). Oper. *Update COVID-19* 55.

Wrapp, D., Wang, N., Corbett, K. S., Goldsmith, J. A., Hsieh, C. L., Abiona, O., et al. (2020). Cryo-EM Structure of the 2019-nCoV Spike in the Prefusion Conformation. *Science* 367, 1260–1263. doi:10.1126/science.abb2507

Wu, J., Sun, B., Hou, L., Guan, F., Wang, L., Cheng, P., et al. (2020). Prospective: Evolution of Chinese Medicine to Treat COVID-19 Patients in China. *Front. Pharmacol.* 11, 615287. doi:10.3389/fphar.2020.615287

Xia, S., Liu, M., Wang, C., Xu, W., Lan, Q., Feng, S., et al. (2020). Inhibition of SARS-CoV-2 (Previously 2019-nCoV) Infection by a Highly Potent Pan-Coronavirus Fusion Inhibitor Targeting its Spike Protein that Harbors a High Capacity to Mediate Membrane Fusion. *Cell Res* 30, 343–355. doi:10.1038/s41422-020-0305-x

Yan, R., Zhang, Y., Li, Y., Xia, L., Guo, Y., and Zhou, Q. (2020). Structural Basis for the Recognition of SARS-CoV-2 by Full-Length Human ACE2. *Science* 367, 1444–1448. doi:10.1126/science.abb2762

Yang, Y., Islam, M. S., Wang, J., Li, Y., and Chen, X. (2020). Traditional Chinese Medicine in the Treatment of Patients Infected with 2019-New Coronavirus (SARS-CoV-2): A Review and Perspective. *Int. J. Biol. Sci.* 16, 1708–1717. doi:10.7150/ijbs.45538

Zhou, P., Yang, X. L., Wang, X. G., Hu, B., Zhang, L., Zhang, W., et al. (2020). A Pneumonia Outbreak Associated with a New Coronavirus of Probable Bat Origin. *Nature* 579, 270–273. doi:10.1038/s41586-020-2012-7

Zhu, N., Zhang, D., Wang, W., Li, X., Yang, B., Song, J., et al. (2020). A Novel Coronavirus from Patients with Pneumonia in China, 2019. *N. Engl. J. Med.* 382, 727–733. doi:10.1056/NEJMoa2001017

Zipeto, D., Palmeira, J. D. F., Argañaraz, G. A., and Argañaraz, E. R. (2020). ACE2/ADAM17/TMPRSS2 Interplay May Be the Main Risk Factor for COVID-19. *Front. Immunol.* 11, 576745. doi:10.3389/fimmu.2020.576745

Conflict of Interest: The authors declare that the research was conducted in the absence of any commercial or financial relationships that could be construed as a potential conflict of interest.

Publisher's Note: All claims expressed in this article are solely those of the authors and do not necessarily represent those of their affiliated organizations, or those of the publisher, the editors, and the reviewers. Any product that may be evaluated in this article, or claim that may be made by its manufacturer, is not guaranteed or endorsed by the publisher.

Advantages of publishing in Frontiers

OPEN ACCESS
Articles are free to read for greatest visibility and readership

FAST PUBLICATION
Around 90 days from submission to decision

HIGH QUALITY PEER-REVIEW
Rigorous, collaborative, and constructive peer-review

TRANSPARENT PEER-REVIEW
Editors and reviewers acknowledged by name on published articles

Frontiers
Avenue du Tribunal-Fédéral 34
1005 Lausanne | Switzerland

Visit us: www.frontiersin.org
Contact us: frontiersin.org/about/contact

REPRODUCIBILITY OF RESEARCH
Support open data and methods to enhance research reproducibility

DIGITAL PUBLISHING
Articles designed for optimal readership across devices

FOLLOW US
@frontiersin

IMPACT METRICS
Advanced article metrics track visibility across digital media

EXTENSIVE PROMOTION
Marketing and promotion of impactful research

LOOP RESEARCH NETWORK
Our network increases your article's readership